

# Soil Chemistry

---

*Donald L. Sparks*

*University of Delaware*

- 11 Soil Organic Matter** *Jeffrey A. Baldock and Kris Broos* ..... 11-1  
 Introduction • Composition of Soil Organic Matter • Quantifying Soil Organic Matter Content and Allocation to Fractions • Functions of Organic Matter in Soil • Factors Determining the Content of Organic Matter in Soil • Contribution of Soil Organic Matter to the Global Carbon Cycle • Summary • Acknowledgments • References
- 12 Soil Solution** *Paul Schwab* ..... 12-1  
 Basic Concepts • Sampling the Soil Solution • Thermodynamics of the Soil Solution • Interactions of Gases with the Soil Solution • Acid–Base Reactions in the Soil Solution • Formation of Soluble Complexes • Application of Thermodynamic and Equilibrium Concepts to Soil Solutions • Current Status and Future Research Directions • References
- 13 Kinetics and Mechanisms of Soil Chemical Reactions** *Donald L. Sparks* ..... 13-1  
 Introduction • Timescales of Soil Chemical Processes • Application of Chemical Kinetics to Heterogeneous Surfaces • Kinetic Models • Kinetics of Important Reactions on Soils and Soil Components • Conclusions • References
- 14 Oxidation–Reduction Phenomena** *Bruce R. James and Dominic A. Brose* ..... 14-1  
 Concepts, Principles, and Theories • Methods and Procedures • Applications of Redox Methods and Concepts to Ecological, Engineered, and Agricultural Soil Systems • Earlier Reviews and Prescient Work on Oxidation–Reduction Processes in Soils • References
- 15 Soil Colloidal Behavior** *Sabine Goldberg, Inmaculada Lebron, John C. Seaman, and Donald L. Suarez* ..... 15-1  
 Nature of Soil Colloids • Interparticle Forces • Colloidal Stability • Colloid Transport • References
- 16 Ion Exchange Phenomena** *Ian C. Bourg and Garrison Sposito* ..... 16-1  
 Introduction • Surface Charge and Ion Exchange Capacities • Ion Exchange Thermodynamics • Trends in  $^{\vee}K$  and  $^{\wedge}K$  • Ion Exchange and Chemical Speciation Models • Micro- and Nanoscale Perspectives on Ion Exchange Selectivity • References
- 17 Chemisorption and Precipitation Reactions** *Robert G. Ford* ..... 17-1  
 Introduction • Conceptual Distinctions in Chemisorption and Precipitation • Influence of Abiotic and Biotic Processes • Quantitative Descriptions of Chemisorption and Precipitation Reactions • Observations of Cation and Anion Solid-Phase Partitioning in Soils • References
- 18 Role of Abiotic Catalysis in the Transformation of Organics, Metals, Metalloids, and Other Inorganics** *Pan Ming Huang (Deceased) and A.G. Hardie* ..... 18-1  
 Introduction • Fundamentals of Catalysis • Abiotic Catalysis of Natural and Anthropogenic Organic Compounds • Abiotic Catalysis in the Transformation of Metals, Metalloids, and Other Inorganics • Role of Nanoparticles in Abiotic Catalysis • Conclusions • Acknowledgment • References
- 19 Soil pH and pH Buffering** *Paul R. Bloom and Ulf Skyllberg* ..... 19-1  
 Introduction • Definition and Determination of Soil pH • Acids and Bases in Soil Solutions • Overview of Reactions Controlling pH and pH Buffering • Buffering by Soil Organic Matter • Proton and Al Exchange in Silicate Clays • pH-Dependent Charge Buffering by Mineral Components • Buffering by Dissolution and Precipitation of Carbonates •  $H^+$  Consumption by Irreversible Weathering of Aluminous Minerals • Determination of Buffer Capacities • Soil Acidification • References

SINCE THE FIRST EDITION of the *Handbook of Soil Science* was published in 2000, many changes have taken place in the area of soil chemistry. Global environmental challenges such as climate change, water quality, nutrient management, soil contamination, ecosystem health, and energy sustainability have brought soil chemistry research to the forefront. Because these are complex challenges, they must be tackled in a highly interdisciplinary/multidisciplinary manner over a range of spatial and temporal scales. Thus, soil chemists are increasingly interacting with a wide array of scientists and engineers in multiple fields such as chemistry, biology, physics, geochemistry, engineering, economics, ecology, and environmental policy. The use of highly sophisticated analytical tools, particularly those that are in situ and synchrotron-based, and

development of advanced speciation and computational models have provided soil chemists with tools that are indispensable in understanding soil chemical reactions and processes at multiple scales. Accordingly, significant advances have been made in understanding, as never before, the chemistry of soil organic matter, soil solution and solid phase speciation, the kinetics and mechanisms of soil chemical reactions, soil colloidal chemistry, oxidation–reduction, ion exchange, adsorption and precipitation processes and complexes, abiotic catalysis, and soil acidity. Advances in these topics are comprehensively covered in the following chapters.

I am extremely grateful to the authors for their excellent contributions and to the referees who made many helpful suggestions for improvement.

11.1	Introduction .....	11-1
11.2	Composition of Soil Organic Matter .....	11-3
	Elemental Composition • Chemical/Molecular Composition • Physical Composition • Biological Composition • Defining Biologically Relevant Soil Organic Matter Fractions • Consistency between Biologically Relevant Soil Organic Matter Fractions and Pools of Carbon in Simulation Models	
11.3	Quantifying Soil Organic Matter Content and Allocation to Fractions .....	11-18
	Direct Measurement of Soil Organic Content and Component Fractions • Proximate Analyses	
11.4	Functions of Organic Matter in Soil.....	11-19
	Biochemical Functions • Physical Functions • Chemical Functions • Complexation of Inorganic Cations	
11.5	Factors Determining the Content of Organic Matter in Soil .....	11-25
	Climate • Soil Mineral Parent Materials and Products of Pedogenesis • Biota: Vegetation and Soil Organisms • Topography • Land Management Practices	
11.6	Contribution of Soil Organic Matter to the Global Carbon Cycle .....	11-36
11.7	Summary.....	11-37
	Acknowledgments.....	11-37
	References.....	11-37

Jeffrey A. Baldock  
Commonwealth Scientific and  
Industrial Research Organisation

Kris Broos  
Flemish Institute for  
Technological Research

## 11.1 Introduction

Research pertaining to the organic fraction of soils can be traced back in excess of 200 years. Achard (1786) isolated a dark amorphous precipitate upon acidification of an alkaline extract from peat. The effect of organic matter on soil N fertility (von Liebig, 1840), studies on the use of animal manures for maintaining soil fertility (Lawes, 1861), and the influence of soil and tree species on the development of humus form (Muller, 1887) all demonstrated the importance of organic matter in soil processes. The advancement of organic chemical methodologies and confirmation of the presence of various chemical structures in soil organic matter (SOM) lead to the development of theories that SOM was composed of a heterogeneous mixture of dominantly colloidal organic substances containing acidic functional groups and N. More recently, the polyphenol theory was proposed in which quinone structures of lignin and microbial origin polymerize in the presence of N-containing groups (amino acids, peptides, and proteins) to produce nitrogenous polymers (Flaig et al., 1975).

Early research pertaining to SOM has been reviewed by Stevenson (1994). While alkaline extraction of SOM is still practiced, modern analytical techniques, including solid-state  $^{13}\text{C}$  nuclear magnetic resonance ( $^{13}\text{C}$  NMR) spectroscopy, infrared (IR) spectroscopy, pyrolysis gas chromatography/mass spectroscopy (Py-GC/MS), and x-ray adsorption (XAFS), allow

selective probing of SOM chemistry within samples of whole soil. Application of these technologies avoids problems of incomplete extraction, artifact synthesis, and lack of biological significance often ascribed to alkaline extraction procedures. The combination of these techniques with SOM fractionation approaches that are capable of identifying biologically important SOM components has significantly advanced our knowledge of the organic fraction of soils and its dynamics over the last 30 years.

Despite such a long history of research and new methodological and technological advancements, many questions related to the genesis and chemical composition of SOM and its impacts on soil fertility, soil pedogenesis, and soil physical and chemical properties persist today. Many excellent texts and review papers have been written on the topic of SOM. Some of the more recent of these are given in Table 11.1. Table 11.1 is not comprehensive, but rather attempts to provide a starting point for anyone interested in understanding the nature and roles of organic matter in soils.

An examination of terms used to describe SOM and its components in the literature revealed a lack of precise and consistent definitions of what SOM is and what its various component fractions represent. Such a problem exists because of the heterogeneity of SOM with respect to its source, chemical and physical composition, diversity of function, and its dynamic character. As a result, the term SOM has been used to describe all organic

**TABLE 11.1** List of Some of the Texts and Review Articles Pertaining to the Study of SOM Released Since 1995*Texts*

- SOM management for sustainable agriculture (Lefroy et al., 1995)  
 Humic substances of soils and general theory of humification (Orlov, 1995)  
 Carbon forms and functions in forest soils (McFee and Kelly, 1995)  
 The role of nonliving organic matter in the earth's carbon cycle (Zepp and Sonntag, 1995)  
 Driven by nature: Plant litter quality and decomposition (Cadisch and Giller, 1997)  
 Soil carbon management: Economic, environmental, and societal benefits (Kimble et al., 2007)  
 Soil carbon sequestration under organic farming in the Mediterranean environment (Mainari and Caporali, 2008)

*Review articles*

- The chemical composition of SOM in classical humic compound fractions and in bulk samples—A review (Beyer, 1996)  
 Carbon in primary and secondary organo-mineral complexes (Christensen, 1996a)  
 Applications of NMR to SOM analysis—History and prospects (Preston, 1996)  
 Analytical pyrolysis and computer modeling of humic and soil particles (Schulten et al., 1998)  
 Life after death—Lignin-humic relationships reexamined (Shevchenko and Bailey, 1996)  
 Stabilization and destabilization of SOM—Mechanisms and controls (Sollins et al., 1996)  
 Soil organic carbon/SOM (Baldock and Skjemstad, 1999)  
 Role of the soil matrix and minerals in protecting natural organic materials against biological attack (Baldock and Skjemstad, 2000)  
 The supramolecular structure of humic substances: A novel understanding of humus chemistry and implications in soil science (Piccolo, 2002)  
 Indications for SOM quality in soils under different managements (von Lützow et al., 2002)  
 Importance of mechanisms and processes of the stabilization of SOM for modeling carbon turnover (Krull et al., 2003)  
 Cycling and composition of organic matter in terrestrial and marine ecosystems (Baldock et al., 2004)  
 Soil mineral-organic matter-microorganism interactions: Fundamentals and impacts (Huang, 2004)  
 The depth distribution of soil organic carbon in relation to land use and management and the potential of carbon sequestration in subsoil horizons (Lorenz and Lal, 2005)  
 Root effects on SOM decomposition (Cheng and Kuzyakov, 2005)  
 Mechanisms and regulation of organic matter stabilization in soils (Kögel-Knabner et al., 2005)  
 Labile organic matter fractions as central components of the quality of agricultural soils: An overview (Haynes, 2005)  
 Soil minerals and organic components: Impact on biological processes, human welfare, and nutrition (Haider and Guggenberger, 2005)  
 The soil carbon dioxide sink (Smith and Ineson, 2007)  
 Impacts of climate change on forest soil carbon: Principles, factors, models, uncertainties (Reichstein, 2007)  
 Composition and cycling of organic carbon in soils (Baldock, 2007)  
 An integrative approach of organic matter stabilization in temperate soils: Linking chemistry, physics, and biology (Kogel-Knabner et al., 2008a)  
 Physical carbon-sequestration mechanisms under special consideration of soil wettability (Bachmann et al., 2008)  
 Soil-carbon preservation through habitat constraints and biological limitations on decomposer activity (Ekschmitt et al., 2008)  
 Storage and stability of organic matter and fossil carbon in a luvisol and phaeozem with continuous maize cropping: A synthesis (Flessa et al., 2008)  
 Contribution of dissolved organic matter to carbon storage in forest mineral soils (Kalbitz and Kaiser, 2008)  
 Organo-mineral associations in temperate soils: Integrating biology, mineralogy, and organic matter chemistry (Kogel-Knabner et al., 2008b)  
 Comparison of two quantitative soil organic carbon models with a conceptual model using data from an agricultural long-term experiment (Ludwig et al., 2008)  
 How relevant is recalcitrance for the stabilization of organic matter in soils? (Marschner et al., 2008)  
 Stabilization mechanisms of organic matter in four temperate soils: Development and application of a conceptual model (von Lützow et al., 2008)

For additional earlier references consult Hedges and Oades (1997) and Baldock and Nelson (2000).

materials found in soil (Stevenson, 1994), all organic materials excluding charcoal (Oades, 1988), or all organic materials excluding nondecayed plant and animal tissues, their partial decomposition products, and the living soil biomass (MacCarthy et al., 1990). As suggested by MacCarthy et al. (1990), it is most important that readers establish how particular authors apply the various terms to fully understand and assess the implications of research findings. The definitions of SOM and its components to be used in this chapter have been derived from several sources (Oades, 1988; MacCarthy et al., 1990; Stevenson, 1994;

Baldock and Nelson, 2000). The term SOM is used in this work to refer to the sum of all naturally derived organic materials present, and a series of further terms are proposed to define specific components of SOM (Table 11.2).

With the advent of modern elemental analyzers, quantification of the organic fraction of a soil is now often completed by measuring the amount of organic carbon present in a soil. Although this chapter is devoted to the composition, chemistry, and functions of SOM as well as the factors that define SOM content, where particular research studies have focused on the measurement of

**TABLE 11.2** Definitions of SOM and Its Components

Component	Definition
SOM	The sum of all natural and thermally altered biologically derived organic materials found in the soil or on the soil surface irrespective of its source, whether it is living or dead, or stage of decomposition, but excluding the aboveground portion of living plants
Living components	
Phytomass	Living tissues of plant origin. Standing plant components, which are dead (e.g., standing dead trees), are included in phytomass
Microbial biomass	Organic matter associated with cells of living soil microorganisms
Faunal biomass	Organic matter associated with living soil fauna
Nonliving components	
Surface plant residues	Organic debris located on the soil surface typically dominated by pieces of plant residues (also referred to as litter)
Buried plant residues	Pieces of organic debris >2 mm found in the soil matrix collected by sieving
DOM	Water soluble organic compounds found in the soil solution, which are <0.45 $\mu\text{m}$ by definition
POM	Pieces of organic debris 53–2000 $\mu\text{m}$ in size with a recognizable cellular structure that are collected on a 53 $\mu\text{m}$ sieve after complete dispersion of a soil (typically dominated by plant residues)
HUM	Organic materials <53 $\mu\text{m}$ remaining after removal of POM and DOM
Resistant organic matter	Highly carbonized organic materials including charcoal, charred plant materials, graphite, and coal with long turnover times
Additional fractions of organic matter	
Macroorganic matter	Fragments of organic matter >20 $\mu\text{m}$ or >50 $\mu\text{m}$ contained within the soil matrix and typically isolated by sieving a dispersed soil
Light fraction	Organic materials isolated from soils by flotation of dispersed suspensions on water or heavy liquids of densities 1.5–2.0 $\text{Mg m}^{-3}$
Nonhumic biomolecules	Organic biopolymers including polysaccharides and sugars, proteins and amino acids, fats, waxes and other lipids, and lignin
Humic substances	Organic molecules with chemical structures, which do not allow them to be placed into the category of nonhumic biomolecules
Humic acid	Organic molecules soluble in alkaline solution but precipitate on acidification of the alkaline extracts
Fulvic acid	Organic molecules soluble in alkaline solution and remain soluble on acidification of the alkaline extracts
Humin	Organic materials that are insoluble in alkaline solution

soil organic carbon (SOC), the discussion will refer to the results obtained in terms of SOC and not SOM. In most instances, SOC and SOM can be used interchangeably; however, in some instances, it is more appropriate to refer to the organic fraction of soils as SOM rather than SOC. For example, when referring to the nutrient content of the soil organic fraction, it would be most appropriate to use SOM since, by definition, SOC in itself only refers to the carbon present and not the associated nutrients.

## 11.2 Composition of Soil Organic Matter

Soil organic matter is composed of a vast array of different organic residues ranging in size from simple monomeric molecules through complex polymeric compounds to pieces of plant residue >1 cm in size in agricultural systems and potentially >1 m in forests. Independent of size, individual components of SOM can exist at any point along a decomposition continuum ranging from fresh unaltered materials to highly altered materials bearing little chemical or physical similarity to their original source. Additionally, SOM can exist in a free state or be associated to varying degrees with surfaces of mineral particles or

buried within aggregations of mineral particles. Such diversity in physical and chemical properties when combined with the spatial heterogeneity of its distribution within the soil matrix at size scales ranging from micrometer to meter makes studies of SOM composition and function challenging.

Often analytical techniques are applied to the whole organic component of soils resulting in the acquisition of weighted average compositional or behavioral data. Such data may or may not provide an adequate assessment of the potential involvement of organic matter in soil processes. For example, the presence of a small amount of biologically labile organic matter could significantly alter short-term measurements of soil carbon mineralization but not be related to a measure of the total amount of organic carbon present. To better understand the nature of SOM and its roles in soil processes, various schemes have been developed to divide SOM into more homogeneous components and to subsequently conduct separate analyses on the isolated fractions.

### 11.2.1 Elemental Composition

Carbon accounts for the majority of the mass of SOM; however, oxygen, hydrogen, nitrogen, phosphorus, and sulfur can also make significant contributions. Contents of organic matter in

soils are typically quantified by measuring the gravimetric contents of organic carbon and/or total nitrogen. The traditional factor used to convert gravimetric contents of SOC into SOM is 1.72 (Equation 11.1), which assumes a carbon content of approximately 58% by weight. To obtain estimates of SOM content based on the gravimetric content of nitrogen requires the use of a C:N ratio expressed on a mass basis and typically assigned a value of 12 for agricultural soils (Equation 11.2). Spain et al. (1983) summarized the C:N ratios across 3652 surface horizons from Australian soils and obtained ratios ranging from 5 to 35 across all soil types under a variety of management strategies. Snowdon et al. (2005) obtained values ranging from 6 to 51 for Australian forest soils. Higher C:N ratios would be expected where the organic matter in a soil is dominated by less decomposed pieces of plant debris rather than well-decomposed organic matter. Conversely, where well-decomposed materials dominate, lower C:N ratios would be expected. In a review of global C:N ratios for SOM, Cleveland and Liptzin (2007) obtained values ranging from 1.7 to 25.7 when expressed on a gravimetric basis. Average gravimetric C:N ratios for the entire data set ( $n = 146$ ), grasslands ( $n = 75$ ), and forests ( $n = 55$ ) were 12.2, 11.8, and 12.4, respectively, consistent with the typically assigned gravimetric C:N ratio of 12:

$$\text{SOM (g kg}^{-1}\text{ soil)} = 1.72 \times \text{SOC (g C kg}^{-1}\text{ soil)}, \quad (11.1)$$

$$\begin{aligned} \text{SOM (g kg}^{-1}\text{ soil)} &= 1.72 \times \text{C : N ratio} \\ &\times \text{soil organic nitrogen (g N kg}^{-1}\text{ soil)}. \end{aligned} \quad (11.2)$$

Although C:N ratios have typically been expressed on a gravimetric basis for soils and plant materials, in aquatic and geochemical sciences, elemental ratios have tended to be expressed on a molar basis. Redfield (1958) recognized that marine plankton maintained an average molar C:N:P ratio of 106:16:1 similar to that in marine water. The presence of such a defined relationship for marine systems has been used to constrain marine net primary productivity (NPP) (e.g., Hecky and Kilham, 1988; Turner et al., 2003), and the recognition of defined elemental ratios in components of terrestrial systems is used to constrain nutrient dynamics within carbon and nutrient simulation models (e.g., the Century model; Parton et al., 1987, 1988). Such relationships have led to the development of the concept of ecological stoichiometry in which it is recognized that variations in molar elemental ratios fluctuate within defined boundaries based on environmental conditions and biochemical requirements of organisms. A trend toward expressing elemental ratios on a molar basis is emerging for SOM. Stevenson (1986) provided an estimate of the molar C:N:P:S ratio of SOM as 107:7.7:1:1. Cleveland and Liptzin (2007) defined average C:N:P ratios of soils obtaining values of 186:13:1 for SOM and 60:7:1 for soil microbial biomass with a tendency for grassland soils to be more nutrient rich and forest soils to be more carbon rich. Further quantification of the variance of these ratios for

different components of SOM (e.g., pieces of plant-residue and well-decomposed materials—see Section 11.1) and particular combinations of soil type and land use will aid the development of more accurate predictions of nutrient cycling and potential responses to alterations in management. In particular, improved definition of the net mineralization of nutrients (i.e., the balance between rates of gross mineralization and immobilization) and release into plant-available pools should be obtained.

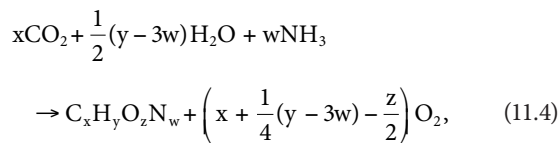
Molar ratios of carbon, oxygen, and hydrogen can also provide useful information pertaining to chemical changes that occur during decomposition, heating, or other processes where transformations of SOM take place. One useful representation of C:O:H ratios that appears underutilized in SOM studies is a van Krevelen plot (van Krevelen, 1950) in which molar H:C is plotted against molar O:C. Where the elemental composition of SOM components (biomolecules) can be defined, van Krevelen plots can be used to define the possible compositional space in which a sample must reside and whether there is a prevalence of one component over another. Additionally, the trajectory on a van Krevelen plot associated with changes induced by a process of alteration can give an indication of the associated chemical changes (e.g., dehydration, loss of CO<sub>2</sub>, or oxidation, which are all associated with different trajectories). Baldock and Smernik (2002) used a van Krevelen plot to define the extent of alteration of natural organic materials during a heating process. When using van Krevelen plots, it is essential that reliable values are obtained for the molar concentrations of O and H. For soils, the presence of hygroscopic water and alterations to soil mineral components during the heating phase of C, O, and H determinations may introduce errors in measurements of O and H concentrations.

Another useful property of SOM that can be calculated from its molar elemental composition is its oxidation state ( $C_{ox}$ ). The value of  $C_{ox}$  for a given organic molecule of the form  $C_xH_yO_zN_w$  can be calculated according to Equation 11.3 in which  $x$ ,  $y$ ,  $z$ , and  $w$  represent the molar percentages of C, H, O, and N, respectively, in the molecule or weighted average molecule in the case of SOM. The values for  $C_{ox}$  can vary from  $-4$  to  $+4$  but typically vary between  $-2.2$  and  $+3$  in organic molecules. For example, lipids, carbohydrates, and organic acids have  $C_{ox}$  values of  $-2$  to  $-1$ ,  $0$ , and  $0$  to  $+3$ , respectively (Masiello et al., 2008).  $C_{ox}$  values of SOM and its components therefore contain information pertaining to molecular composition, biochemical synthesis pathway, extent of decomposition, and diagenetic history. For example, if  $C_{ox}$  values  $< -1$  are obtained, then there is likely to be a preponderance of lipid/aliphatic structures present. Alternatively, if values  $> 1$  are obtained, then a high content of carboxylic acids is likely.  $C_{ox}$  values between  $-1$  and  $+1$  are less informative as a large range of combinations of different compounds could provide such values. However,  $C_{ox}$  values may still be used to constrain predictions of molecular composition of SOM and its components.

$C_{ox}$  is mathematically related to the oxidative ratio (OR), which defines the molar ratio of O<sub>2</sub> consumption to CO<sub>2</sub> emission during decomposition. Organic molecules having positive  $C_{ox}$  values do not need as much oxygen for complete mineralization as those with negative  $C_{ox}$  values. Based on the assumption

that net photosynthesis occurs via Equation 11.4 with all N being obtained as ammonia, the OR can be calculated from  $C_{ox}$  according to Equation 11.5. If the required N is obtained as nitrate or through biological fixation of  $N_2$ , Equations 11.6 or 11.7, respectively, should be used to calculate OR (Masiello et al., 2008). Quantification of the OR (and thus  $C_{ox}$ ) of terrestrial forms of organic matter, including that found in soils, can be used to define the fate of  $CO_2$  emitted to the atmosphere by fossil fuel burning (Randerson et al., 2006):

$$C_{ox} = \frac{2z - y + 3w}{x}, \quad (11.3)$$



$$OR = 1 - \frac{C_{ox}}{4}, \quad (11.5)$$

$$OR = 1 - \frac{C_{ox}}{4} + \frac{2w}{x}, \quad (11.6)$$

$$OR = 1 - \frac{C_{ox}}{4} + \frac{3w}{4x}. \quad (11.7)$$

## 11.2.2 Chemical/Molecular Composition

A heterogeneous chemical structure and an ability to form strong associations with soil minerals make the chemical characterization of SOM difficult. Two approaches to define the chemical/molecular composition of SOM have been used: (1) chemical extraction or degradative methodologies and (2) modern spectroscopic techniques capable of analyzing SOM in situ. With both approaches, it is essential to gain a full understanding of the methodology being used and possible deficiencies in order to assess how selective and quantitative the applied procedures are and whether there is a potential for creating artifacts. Without such an understanding, it is not possible to make appropriate interpretations of the SOM compositional data obtained.

### 11.2.2.1 Chemical Extraction and Degradative Methods

Chemical extraction and degradative methods for characterizing SOM use aqueous solutions and organic solvents to liberate SOM components with particular chemical characteristics. One of the most common approaches uses an alkaline extraction followed by acidification (Schnitzer, 2000) of the extract to isolate humic acid, fulvic acid, and humin (see Table 11.2 for definitions). These three fractions should not be considered as discrete compounds, as each will contain a multitude of different chemical structures that can be further fractionated and purified. Criticisms pertaining to the use of alkaline extraction/acid

precipitation to separate soil organic and mineral components include the following:

1. Questions related to the ability of alkaline extractable material to be representative of the composition of the unextracted and entire SOM fraction
2. The apparent lack of a relationship between the biological functioning of SOM and its alkaline extractability based on C and N isotopic tracer studies (Oades, 1995)
3. Incomplete segregation and probable mixing of SOM with different molecular compositions and susceptibilities to decomposition
4. Creation of artifacts (alteration of molecular structure) during the extraction and precipitation procedures

It is acknowledged that in early studies of SOM, separation of soil organic and mineral components was essential to allow selective characterization of the SOM, and that alkaline extraction provided such a capability. However, with the advent of more selective degradation procedures and modern analytical instrumentation that can use intact soil samples, it is suggested that the use of alkaline extractants as a means of characterizing SOM should be avoided where possible.

Many additional methods have been developed based on various extraction or degradative methods considered to be "selective" for particular molecular components of SOM. Hydrolysis with 6 M HCl or methane sulfonic acid has been used to quantify the proportion of SOM associated with proteins, amino acids, and amino sugars (e.g., Friedel and Scheller, 2002; Martens and Loeffelmann, 2003; Appuhn et al., 2004). Hydrolysis reactions with sulfuric acid have been used to quantify the allocation of SOM to carbohydrate structures (e.g., Rovira and Vallejo, 2000; Martens and Loeffelmann, 2002). The proportion of lignin in SOM has been quantified using methods that attempt to either isolate the intact lignin molecule (e.g., Tuomela et al., 2000) or quantify the monomeric species released by breaking the macromolecular structure into its component monomeric species (e.g., Baldock et al., 1997b; Chefetz et al., 2002; Leifeld and Kögel-Knabner, 2005). Various solvent-based procedures have been developed and used to quantify the presence of lipids and lipid-like organic materials in soils (e.g., Poulencard et al., 2004; Rumpel et al., 2004).

Although more specific than alkaline extraction procedures, results derived from these more specific degradation procedures should be considered as approximate due to the potential for incomplete extraction and/or nonselective action. Using a combination of extraction techniques in a "proximate analysis approach" designed to isolate and quantify klason lignin, Preston et al. (1997) demonstrated the presence of a range of nonlignin forms of carbon. Additionally, the use of degradation procedures to quantify SOM components involved in biological processes within the soil matrix may be questionable. As an example, consider a polysaccharide molecule located in a pore on the external surface of an aggregate versus the same molecule buried within a matrix of clay particles. Both polysaccharides may be broken down by a sulfuric acid digestion procedure and

detected by subsequent analyses, but the availability of these two molecules to microbial oxidation as well as their relative contribution to soil function would be expected to vary significantly.

Attempts to use chemical fractionation procedures to allocate SOM to labile and recalcitrant fractions without defined molecular composition have also been made. Hydrolysis with HCl and permanganate oxidation procedures have been proposed to offer such capabilities. With HCl hydrolysis, the proportion of carbon or nitrogen entering the hydrolysates has been considered to be indicative of the biologically labile component of SOM. Both Leavitt et al. (1996) and Paul et al. (2001) found that carbon remaining in the nonhydrolysable fraction of soil subjected to HCl hydrolysis was older than that found in the total SOC fraction prior to hydrolysis. Quantifying the proportion of SOC oxidized in permanganate solutions of increasing concentrations has also been used to define SOC fractions with different biological liabilities (Blair et al., 1995). However, the existence of strong correlations between the amounts of SOC oxidized at each permanganate concentration and total SOC (Lefroy et al., 1993) question the selectivity of this approach toward identifying differentially labile SOC components (Blair et al., 1995; Mendham et al., 2002). Furthermore, Mendham et al. (2002) showed that permanganate oxidizable SOC had little relation to the labile pool of SOC respired over a 96 day incubation period, again questioning the existence of a link between chemical and biological reactivities. The absence of a strong linkage between chemical and biological reactivities and the lack of a clear definition of the chemical nature of the SOC components attacked by each permanganate solution can limit the ability of chemical fractionation techniques to be used as proxies for biologically meaningful fractions of SOC (Baldock, 2007).

### 11.2.2.2 Chemical Characterization with Analytical Instrumentation

A variety of analytical techniques exist that can be used to characterize the chemical composition of SOM. In this chapter, four techniques that can be used to quantify the chemical nature of SOM in situ will be examined:  $^{13}\text{C}$  NMR spectroscopy, analytical pyrolysis, Fourier transform infrared spectroscopy (FTIR), and x-ray spectroscopy. Examples of the chemical information obtained by applying these analytical techniques to SOM are given in Figures 11.1 and 11.2. The forms of analytical instrumentation to be discussed are all complementary and, where possible, efforts should be made to utilize combinations of these methods to confirm and provide additional insight into the chemical composition of SOM.

#### 11.2.2.2.1 Solid-State Nuclear Magnetic Resonance Spectroscopy

Solid-state  $^{13}\text{C}$  NMR spectroscopy can be used to define the chemical environment around individual carbon atoms in an intact soil sample. The only pretreatments required are drying and then grinding to ensure homogeneity. A typical cross polarization  $^{13}\text{C}$  NMR spectrum for a soil is presented in Figure 11.1a. Organic carbon found in different chemical environments can be differentiated on the basis of chemical shift (expressed in

units of parts per million of the applied magnetic field). Duncan (1987) has presented a comprehensive review of the chemical shift values associated with different types of carbon. Solid-state  $^{13}\text{C}$  NMR spectra acquired for SOM are typically divided into chemical shift regions indicative of the major chemical forms that individual carbon atoms can take Figure 11.1a. Integration of the signal intensity within each region provides a quantitative indication of the amount of each form of carbon present in a sample, provided signal acquisition from all forms of carbon in a sample is quantitative. Methods now exist to define the level of quantitative detection of carbon within solid-state  $^{13}\text{C}$  NMR analyses of SOM (Smernik and Oades, 2000a, 2000b); however, adoption has been limited.  $^{13}\text{C}$  NMR detection efficiencies can be improved by the application of hydrofluoric acid (HF) pretreatments to concentrate carbon and remove paramagnetic species (Skjemstad et al., 1994; Schmidt and Gleixner, 2005).

Although the distribution of  $^{13}\text{C}$  NMR signal intensity within various chemical shift regions has been used to infer the molecular composition of organic matter in a sample,  $^{13}\text{C}$  NMR gives no direct information pertaining how the different types of carbon present in a sample are arranged into molecules. For example, the presence of signal intensity in the O-alkyl region (65–105 ppm) is often ascribed to carbohydrates. However, three of the 11–12 carbons found in lignin monomers will also resonate within the O-alkyl chemical shift region as will some carbon associated with proteins and lipid/wax materials. To extend the level of molecular information obtained from the application of NMR to natural organic materials, molecular mixing models have been defined (e.g., Hedges et al., 2002; Baldock et al., 2004; Nelson and Baldock, 2005). In this approach, it is assumed that the organic carbon present in a sample can be described as a mixture of biomolecules (endmembers) with defined representative chemical structures. The molecular composition of  $^{13}\text{C}$  NMR observable organic carbon is then estimated by defining the mixture of endmembers that minimizes the sum of squares of differences between predicted and measured distributions of  $^{13}\text{C}$  NMR signal intensity. Baldock et al. (2004) and Nelson and Baldock (2005) have used this approach to estimate the molecular composition and elemental stoichiometry of organic materials found in a range of terrestrial and aquatic systems.

Solid-state NMR has also been used to characterize the chemical composition of organic N in soils (Knicker et al., 1993; Clinton et al., 1995; Knicker and Skjemstad, 2000); however, the low NMR sensitivity and natural abundance of the  $^{15}\text{N}$  nucleus make the acquisition of spectra with adequate signal-to-noise ratios difficult. The majority of organic N present in soils is thought to reside in protein (amide) or heterocyclic compounds. In most  $^{15}\text{N}$  NMR studies, signals originating from amide structures dominate the acquired spectra, with heterocyclic N structures being detected as a small shoulder on the amide resonance (Mahieu et al., 2000). To improve spectral quality,  $^{15}\text{N}$ -labeled plant materials have been used in decomposition and composting experiments (e.g., Knicker and Lüdemann, 1995) with the majority of N again being allocated to amide structures. However, the typical use of short contact times ( $\leq 1$  ms) and high-field spectrometers ( $\geq 300$  MHz) have been found to discriminate against nonprotonated heterocyclic N



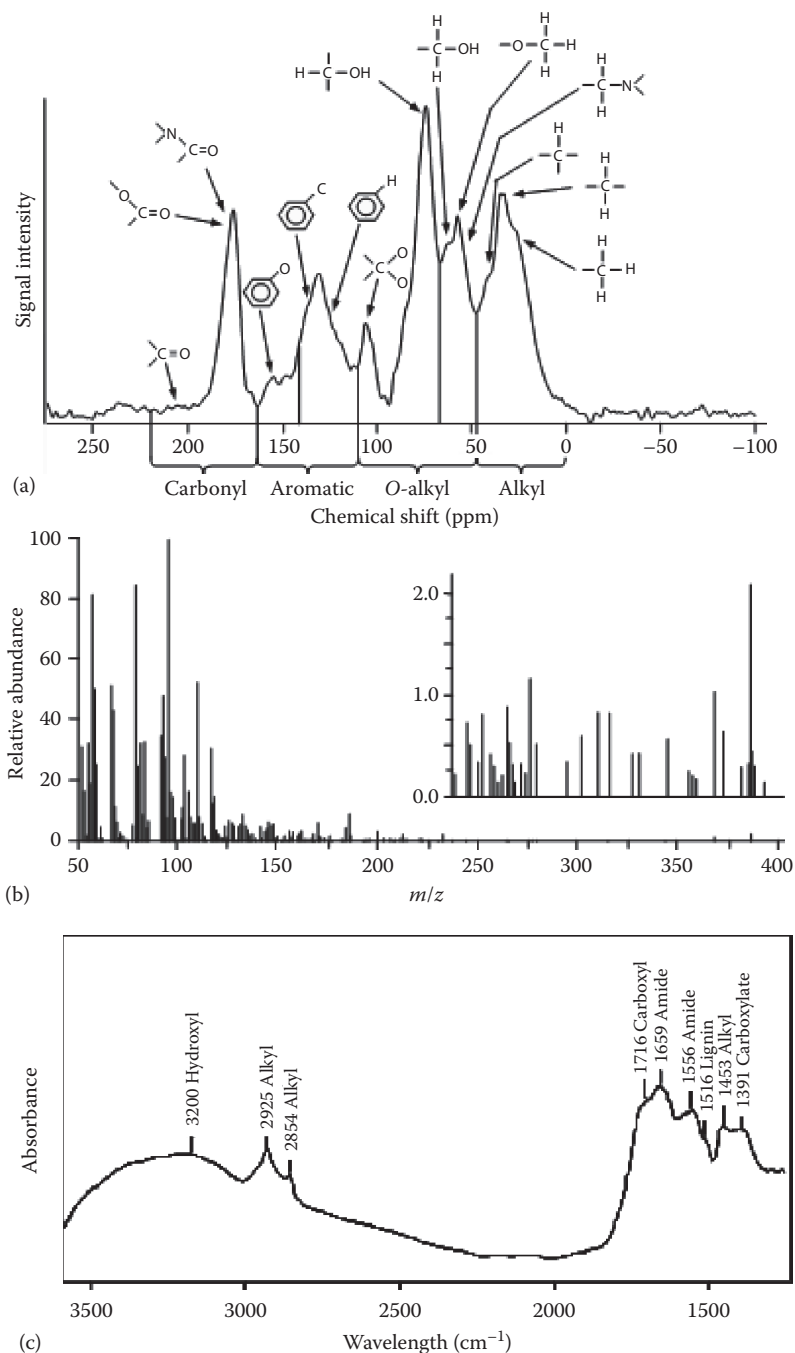


**FIGURE 11.1** Examples of the data obtained from (a) a solid-state  $^{13}\text{C}$  NMR analysis of soil humus, (b) a pyrolysis-field ionization mass spectrum of a humic acid (Schulten, 1987), and (c) a diffuse reflectance FTIR spectrum acquired for the 0–2.5 cm layer of a mineral soil ( $52\text{ g C kg}^{-1}$ ) after subtraction of mineral-derived signals.

(Keleman et al., 2002). Smernik and Baldock (2005) applied a spin counting technique to  $^{15}\text{N}$  NMR analyses of clay-associated organic matter and found that although the major form of N present was amide, up to half or more of the organic N present must have resided in a form that was insensitive to  $^{15}\text{N}$  NMR, potentially heterocyclic N. Careful consideration of  $^{15}\text{N}$  pulse programs and the use of spin counting techniques are required to obtain  $^{15}\text{N}$  NMR results that are indicative of all N present in a sample of soil.

The  $^{31}\text{P}$  nucleus is well suited to NMR due to its high natural abundance and relative NMR sensitivity.  $^{31}\text{P}$  NMR analyses have been performed on solutions extracted from soils and on solid whole soils (see Toor et al., 2006). Solution-state  $^{31}\text{P}$  NMR offers improved resolution and thus identification and quantification of P species; however, it suffers from the requirement to extract P-containing materials into solution and thus may not allow characterization of all P in a sample. Solid-state  $^{31}\text{P}$  NMR can be

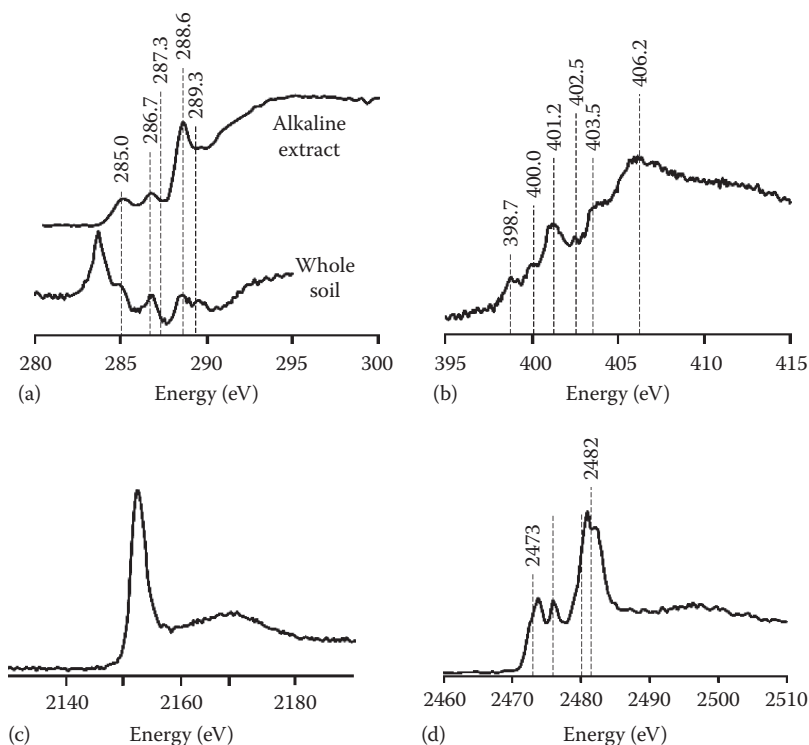


**FIGURE 11.2** (a) Carbon K-edge XANES spectra acquired for the alkaline extractable organic carbon from a forest soil in western Kenya (Lehmann et al., 2008) and a whole soil from Elstow (Gillespie et al., 2009). (b) Nitrogen K-edge XANES spectrum acquired for a whole soil from Elstow (Gillespie et al., 2009). (c) Phosphorus K-edge XANES spectrum for topsoil from a German peat (Kruse and Leinweber, 2008). (d) Sulfur K-edge XANES spectrum acquired for whole soil taken from a podzol O horizon (Prietz et al., 2007).

used to analyze a whole undisturbed sample without extraction; however, the association of soil P with Fe or Mn can render it invisible to  $^{31}\text{P}$  NMR. Organic phosphates tend to remain unresolved and appear as a broad resonance between +1 and -1 ppm due to the wide variety of organic phosphate forms (e.g., phospholipids, nucleic acids, metabolic products) and their limited mobility. In solution-state  $^{31}\text{P}$  NMR, rapid tumbling of extracted organic P-containing molecules leads to sharper signals. Toor et al. (2006) concluded that solution-state  $^{31}\text{P}$  NMR is useful for characterizing the chemical composition of soil organic P, while solid-state  $^{13}\text{P}$  NMR is more suited to the study of inorganic P components of soils.

#### 11.2.2.2 Analytical Pyrolysis Mass Spectrometry

Analytical pyrolysis characterizes the chemical composition of products of controlled pyrolysis of a sample to obtain information pertaining to the nature of the organic matter present in the sample. The application of this technique to the analysis of organic matter in whole soils and soil extracts is given by Schnitzer and Schulten (1995). Several different approaches to using analytical pyrolysis exist including off-line pyrolysis, pyrolysis mass spectrometry, derivatization pyrolysis mass spectrometry, and Py-GC/MS. A detailed description of each technique is presented by Schulten and Leinweber (1996). In pyrolysis mass spectrometry, the mass/charge ratio ( $m/z$ ) is used to differentiate

the pyrolysis products released during a rapid (Curie-point) or controlled heating of a sample. Several methods of ionization are available to promote the movement of pyrolysis products through the mass spectrometer: field ionization (FI), chemical ionization (CI), fast atom bombardment (FAB), and laser ionization (LI). Irrespective of the method of ionization used, distinctive patterns of pyrolysis products are produced (Figure 11.1b). After normalization of the  $m/z$  peak intensities, a qualitative assessment of the chemical nature of the organic C in a soil sample can be obtained. Incorporation of a gas chromatograph between the pyrolysis chamber and the mass spectrometer can further aid in the separation of similar pyrolysis fragments prior to detection and analysis by the mass spectrometer.

A cautionary note regarding the comparison of different  $m/z$  signal intensities is required. First, the intensities observed at any single  $m/z$  value may result from multiple pyrolysis fragments if they have the same  $m/z$  ratio. Second, the volatilization of different types of pyrolysis fragments varies (e.g., in pyrolysis FI MS, volatilization decreases with increasing polarity of the fragments). As a result, differences in signal intensities at various  $m/z$  values do not necessarily correlate with contents of the parent molecules present in the original soil samples. It is appropriate, however, to utilize variations in a given  $m/z$  signal intensity between samples run under a constant set of analytical conditions to infer compositional differences.

### 11.2.2.2.3 Fourier Transform Infrared Spectroscopy

FTIR can be used to determine the type of the atoms to which C is bound as well as the nature of the bond. Detailed identification of chemical structure is therefore possible. However, the application of FTIR to characterize the composition of SOM in whole soils is limited by two factors: the low organic matter content of most mineral soils and the presence of significant signals from soil mineral components. The use of “difference spectra” (spectrum of an untreated sample minus that of a pretreated sample) may provide more useful data. Subtraction of an FTIR spectrum obtained for a sample heated to 350°C to remove all organic matter from the FTIR spectrum obtained for the original soil can provide an indication of the nature of the organic components removed, provided no significant alteration to soil mineral components occurred during the heating process. Where significant alterations to soil mineralogy also occur on heating these changes will also be included in the difference spectrum. Figure 11.1c provides an example of a difference spectrum obtained for a soil.

### 11.2.2.2.4 X-Ray Absorption Spectroscopy

X-ray absorption spectroscopy (XAS) allows collection of atomic scale chemical information. A summary of the fundamentals of XAS techniques is given by Schulze and Bertsch (1995). In XAS, x-rays are absorbed by an atom at defined energies. In response, a higher-energy electron replaces the ejected electron, and excess energy is released in the form of fluorescence. The energy at which fluorescence occurs is characteristic for each electron within an atom and can be used to provide chemical information about a given type of atom (C, N, P, or S). XAS spectra are typically divided into two regions: the near-edge and extended region. X-ray absorption near-edge structure (XANES) spectroscopy examines the region before the absorption edge to around 100 eV past the edge. XANES spectra can also be referred to as near-edge x-ray absorption fine structure (NEXAFS) spectra. XANES spectra are sensitive to the oxidation state of the atom being examined. Resonances are identified by comparison with spectra acquired for standard compounds. In the extended region of x-ray absorption spectra, NEXAFS spectra provide information on coordination number, identity of nearest neighbors, and bond distances for the element being examined. XAS has been used to examine the chemical nature of organic C, N, P, and S found in soils (Figure 11.2).

Solomon et al. (2009) performed C K-edge XANES analysis of a suit of known organic C compounds indicative of those found in soil (carbohydrates, amino sugars, amino acids, phenols, quinine, benzenepolycarboxylic acid, and markers for black C). The acquired spectra showed distinct features and resonance positions for each form of carbon in the known compounds. Lehmann et al. (2008) provided the following broad classifications for XANES C resonances for alkaline extractable SOC: aromatic carbon ring structures (284–286 eV), phenolic/pyrimidine or imidazole carbon (286.4–287.4 eV), aliphatic carbon (287.3–287.8 eV), and carboxylic/amide carbon (288–289 eV). Working with whole soils (Figure 11.2a), Gillespie et al. (2009) identified

additional resonances and used XANES to quantify differences between bulk and rhizosphere soil. The C K-edge XANES spectra acquired by Gillespie et al. (2009) were complicated by the presence of residual C in the beamline and second-order O K-edge features that are typically absent from spectra acquired for pure organic compounds or samples with high (>50 mg C g<sup>-1</sup> sample) carbon contents. XANES has also been combined with scanning transmission x-ray microscopy (STXM) to define spatial changes in carbon composition across microaggregates (Kinyangi et al., 2006; Lehmann et al., 2008) and black carbon particles (Lehmann et al., 2005; Liang et al., 2006, 2008). Solomon et al. (2009) concluded that C K-edge XANES may provide a means of fingerprinting complex organic C compounds of ecological importance; however, due to the broad spectral features found for organic carbon in soils (e.g., Lehmann et al., 2008), it is unlikely that XANES can be used on its own to provide an unambiguous chemical characterization of SOC.

Gillespie et al. (2009) performed N K-edge XANES on whole soils (Figure 11.2b) and attributed the following resonances to organic N structures: aromatic N in six-membered rings (398.7 eV), nitrilic and pyrazolic N (400.0 eV), amide (protein) N (401.2 eV), pyrrolic N (402.5 eV), nitroaromatic N (403.5 eV), and alkyl N (406.2 eV). Leinweber et al. (2007) presented a detailed systematic analysis of N K-edge XANES resonances obtained for a range of known organic N structures likely to occur in soils and concluded that N K-edge XANES can be used to reliably distinguish pyridinic and nitrile N (≤400 eV) from amide, nitro, and pyrrolic N (>400 eV). Jokic et al. (2004) used N K-edge XANES to detect the presence of heterocyclic N compounds in chemically unaltered whole soil samples.

Most applications of P XANES spectroscopy have focused on the K-edge; however, the speciation of P forms, particularly organic P, can be difficult or even impossible at the P K-edge. Kruse and Leinweber (2008) determined the nature of the P present in a series of inorganic and organic standard compounds as well as the topsoil (Figure 11.2c) and subsoil of a German peat using P K-edge XANES. The spectra obtained for the inorganic and organic standards showed only slight variations in the energy position of the main resonance and thereby offered little potential to distinguish inorganic from organic P. Additionally, little distinction was noted between the three organic P compounds (asolectin, ATP, and phytic acid). P XANES spectra collected at the L<sub>2,3</sub>-edge instead of the K-edge contain more distinguishable features. Kruse et al. (2009) present a detailed analysis of the P L<sub>2,3</sub>-edge XANES spectra obtained for a range of inorganic and organic forms of P. The P L<sub>2,3</sub>-edge XANES spectra contained more spectral features than P K-edge spectra, particularly for the organic P compounds, leading Kruse et al. (2009) to suggest that quantitative differentiation of different types of P may be possible by applying linear combination fitting to P L<sub>2,3</sub>-edge XANES spectra.

K-edge XANES can also be used to examine S speciation in soils (Prietz et al., 2003; Solomon et al., 2005) (Figure 11.2d). S K-edge XANES resonances have been defined as 2472.6–2473.4 eV (reduced S in organic polysulfide, disulfide, mono-sulfide, and thiol structures), 2475.8–2481.3 eV (intermediate S

in sulfoxide, sulfone, and sulfonate structures), and 2482.5 eV (oxidized S in ester sulfate structures). Prietzel et al. (2007) used S K-edge XANES spectra to characterize the differences between S in whole soils with their corresponding humic extracts. In all soils examined by Prietzel et al. (2007), S was mainly present as organic mono- and disulfide (27%–52%), ester sulfate (14%–39%), and sulfone (15%–27%) with sulfoxide and sulfite having more minor contributes and an absence of sulfonate and inorganic sulfide. However, inorganic  $\text{SO}_4^{2-}$  cannot be differentiated from ester sulfate because both species have an equivalent oxidation state of +6. Prietzel et al. (2007) noted that the contribution of reduced forms of organic S (organic mono- and disulfides) increases and the contribution of ester sulfate and  $\text{SO}_4^{2-}$  decreases with increasing OC content and decreasing  $\text{O}_2$  availability.

### 11.2.3 Physical Composition

The major input of organic carbon into soils results from the deposition of carbon captured by photosynthesis. Deposition within the soil matrix occurs in the form of root residues and the organic materials exuded during root growth. Shoot residues are first deposited onto the soil surface and enter the soil via leaching, in the case of dissolved organic materials (DOM), or through some form of mixing process that can be biotic (bioturbation), abiotic (opening of crack as swelling soils dry), or anthropogenic (cultivation). Approaches used to characterize the physical composition of SOM have been based on solubility, particle size, and density.

#### 11.2.3.1 Dissolved Organic Materials

Dissolved organic materials represents a small proportion of the total organic material present in a soil. However, owing to its mobility and chemical properties, it can contribute significantly to soil processes through the provision of energy to microorganisms, complexation and transport of elements within the soil profile, and dissolution of soil minerals. DOM refers to the organic materials that do not settle out of the soil solution phase under the influence of gravity. It is operationally defined as the organic matter that passes through a 0.45  $\mu\text{m}$  filter. At the upper limit of the DOM size, the distinction between DOM and particulate forms of SOM becomes ambiguous. DOM must be extracted from soils to allow quantitative and qualitative analysis. In the laboratory, DOM has been extracted in leachate collected at the base of undisturbed or disturbed soil columns or by suspension of soil in water or dilute salt solutions and collection of the <0.45  $\mu\text{m}$  fraction (e.g., Dunnivant et al., 1992; Nelson et al., 1993). In the field, DOM can be collected using a variety of in situ devices, such as zero-tension or tension lysimeters using porous cups or plates (e.g., Weihermuller et al., 2007; Sanderman et al., 2008). It is important that the methods used to collect and isolate DOM are clearly specified and to assess the potential impacts that adsorption processes and filtering procedures could have on both the nature and amount of DOM isolated. Reviews pertaining to the collection, analysis, and fate of DOM in soils include Herbert and Bertsch (1995), Kalbitz et al. (2000), Neff and Asner (2001), and Kalbitz and Kaiser (2008).

DOM enters the soil as soluble material in water passing through vegetation, litter layers, or organic-rich soil surface horizons. It can also be generated in situ by adsorption/desorption reactions occurring on mineral surfaces, excretion of organic compounds from plant roots, excretion of metabolic waste products from soil organisms, and excretion and action of extracellular enzymes. DOM is lost through uptake and mineralization by soil organisms, sorption reactions with soil particles, precipitation reactions, and in leachate exiting the soil profile. The concentration of DOM in soil is governed by all these processes, and when expressed in terms of dissolved organic carbon (DOC), values typically range from 5 to 50  $\text{mg L}^{-1}$  in surface and litter horizons, and from 0.5 to 5  $\text{mg L}^{-1}$  or less in B and C horizons. When expressed on as annual fluxes, Michalzik et al. (2001) presented values of 10–40  $\text{g DOC m}^{-2} \text{ year}^{-1}$  for surface organic horizons of temperate forest soils with an attenuation to 1–10  $\text{g DOC m}^{-2} \text{ year}^{-1}$  through soil C horizons. Hope et al. (1994) suggested that DOC fluxes from terrestrial ecosystems should range from 1 to 10  $\text{g DOC m}^{-2} \text{ year}^{-1}$  based on river DOC fluxes.

Reductions in DOC flux on passage through mineral soils are typically attributed to the processes of biologically mediated mineralization and adsorption to soil minerals. In a review of laboratory incubation studies, Kalbitz and Kaiser (2008) indicated that between 5% and 93% of the DOM present in soil solutions can be biologically mineralized. Kalbitz et al. (2003) concluded that the susceptibility to biological mineralization of DOM derived from forest floors, peats, and A horizons decreased with increasing degree of decomposition of the materials from which it was derived. Aromatic compounds potentially derived from lignin appeared to be the most biologically stable form of DOM (Kalbitz et al., 2003). Other important chemical characteristics of DOM that influence its reactivity, sorption behavior, and susceptibility to decomposition include its molecular size ( $10^2$  to  $>10^5 \text{ g mol}^{-1}$  [Homann and Grigal, 1992]), acidity (6–15  $\text{mol C kg}^{-1}$  [Herbert and Bertsch, 1995]), and degree of hydrophobicity.

Differential adsorption of DOC onto soil minerals in two adjacent catchments with similar vegetation but different geological origins was proposed to account for the large differences in DOC concentration in catchment drainage water (Nelson et al., 1993). DOC sorption capacity was shown to vary significantly with soil depth, mineralogy, and organic C content (Guggenberger and Kaiser, 2003). Guggenberger and Kaiser (2003) found that surface-mineral horizons rich in organic carbon had little capacity to adsorb additional DOC (1–2  $\text{g DOC m}^{-2}$ ) compared to iron- and aluminum-rich B horizons (often  $>150 \text{ g DOC m}^{-2}$ ). Such measurements suggest that attenuation of DOC flux with increasing depth is most likely dominated by mineralization in the organic-rich surface horizons and then by adsorption reactions in iron- and/or aluminum-rich B horizons.

#### 11.2.3.2 Particulate- and Mineral-Associated Organic Materials

Other than the organic matter that enters as individual molecules (DOM and root exudates), organic matter enters soil as particles that can vary significantly in size and chemical composition.

Particulate organic matter (POM) is composed of a variety of molecular components (e.g., cellulose, lignin, lipids, proteins) that have different availabilities to processes of decomposition. As POM is decomposed and mixed into the mineral soil, particle size is reduced and the potential for interacting with soil minerals and entering the mineral-associated organic matter fraction increases. A variety of names have been applied to the mineral-associated organic matter. In this work, we will use the abbreviation of mSOM to denote mineral-associated SOM. Interactions between minerals and decomposing SOM will result in SOM/mineral particle associations that increase in density as the extent of association increases. The density will be greatest for individual organic molecules adsorbed onto the surfaces of soil minerals (mSOM). Density will be lowest for large POM particles with only a small mass of mineral particles bound to their surfaces. As a result, methods for extracting, quantifying, and characterizing the POM in soils are based on selective collection of materials with different particle sizes, densities, or a combination of both (Christensen, 1996a, 2001).

A prerequisite to quantifying the allocation of SOM to different particle-size or density fractions is the use of disruptive techniques that separate the soil into primary particles or aggregations of particles. It is essential that any chemically or biologically induced alteration of the SOM or redistribution of SOM in response to soil structural degradation and exposure of mineral surfaces previously inaccessible mineral surfaces be minimized. Thus, the use of strong acids, alkalis, or chemical oxidation pretreatments and the exposure of disrupted suspensions to high temperatures for prolonged periods should be avoided.

Early approaches to SOM fractionation used a strong initial ultrasonic disruption to disperse soil in an attempt to destroy all aggregation and obtain a suspension of primary particles after which particle-size and density fractionation procedures were initiated (e.g., Baldock et al., 1992). However, Golchin et al. (1994a) and Amelung and Zech (1999) showed that recovery of coarse POM decreased with increasing sonification time or energy resulting in a decrease in the physical size of POM and a redistribution of carbon into finer particle-size classes. Development of a two-step disruption process was demonstrated to minimize these problems (Amelung and Zech, 1999). Free POM not associated with mineral materials was removed subsequent to an initial minimal disruption process in which the integrity of soil aggregates was maintained. A more vigorous second step achieving complete aggregate disruption and dispersion was then applied to release pieces of SOM that were occluded within soil aggregates and allow the separation of this material from mSOM. In its simplest form, this approach results in the isolation of three SOM fractions:

- fPOM—free pieces of organic residue found between soil particles
- oPOM—occluded pieces of organic residue found within aggregations of soil particles
- mSOM—organic matter strongly bound to mineral particle surfaces

Additional approaches to disrupt soils and perform particle-size and density fractionations have used a combination of sodium saturation and physical dispersion methods (e.g., Skjemstad et al., 2004) or have applied a more complex combination of particle-size and density fractionation steps with increasing amounts of disruption and/or increasing density fractionation steps. These latter approaches have been designed to progressively isolate SOM materials from free through occluded to various fractions associated to different extents with mineral components (e.g., Six et al., 2001; John et al., 2005; Sohi et al., 2005; Swanston et al., 2005).

Once isolated from bulk soil, a variety of methodologies can be applied to particle-size and density fractions to quantify rates of turnover and chemical composition. Acquiring  $\Delta^{14}\text{C}$  measurements for the organic carbon found in 2000–63, 63–2, and  $<2\ \mu\text{m}$  fractions of soils allowed Trumbore and Zheng (1996) to estimate turnover rates. After normalization of the  $\Delta^{14}\text{C}$  values to those measured for the 2000–63  $\mu\text{m}$  fraction, both depletions and enrichment of  $^{14}\text{C}$  were found with decreases in particle size, indicating a respective increase or decrease in age of the carbon with decreasing particle size. Schöning et al. (2005) measured the percentage of modern carbon in the Ah horizons of luvisols, leptosols, and phaeozems under a European beech (*Fagus sylvatica* L.) forest and found a consistent trend of decreasing amounts of modern SOC with decreasing particle size.

The extent of decomposition and turnover times of organic carbon found in fine ( $<0.2\ \mu\text{m}$ ) and coarse ( $0.2\text{--}2.0\ \mu\text{m}$ ) mSOM fractions was assessed by Kahle et al. (2003) using  $\delta^{13}\text{C}$  and  $\Delta^{14}\text{C}$  measurements. Organic carbon found in the fine-clay fraction was more enriched with  $^{13}\text{C}$  and  $^{14}\text{C}$ , suggesting a greater extent of microbial processing but a shorter turnover time than coarse-clay organic carbon. Enrichments in  $^{13}\text{C}$  and a decrease in C/N ratio with decreasing particle size were also observed by Amelung et al. (1999). The general lack of consistency with respect to changes in  $^{13}\text{C}$  and  $^{14}\text{C}$  enrichment with decreasing particle size suggests that different processes of SOC stabilization operate in different soils and that relatively young and potentially labile SOC may be stabilized against mineralization, particularly through the formation of mSOM via interactions with mineral surfaces.

The application of density fractionation, either independently or combined with particle-size fractionation methods, has also been used to isolate and characterize SOC fractions with different liabilities. Trumbore and Zheng (1996) found that SOC in dense soil fractions ( $>2.0\ \text{g cm}^{-3}$ ) was more depleted in  $^{14}\text{C}$  than that found in less-dense fractions ( $<2.0\ \text{g cm}^{-3}$ ). John et al. (2005) determined the  $\delta^{13}\text{C}$  of the following four density fractions isolated from a silty soil that had undergone a C3/C4 plant species transition:

- Free-POM  $<1.6\ \text{g cm}^{-3}$  (fPOM $_{<1.6}$ )
- Light-occluded POM  $<1.6\ \text{g cm}^{-3}$  (oPOM $_{<1.6}$ )
- Dense-occluded POM  $1.6\text{--}2.0\ \text{g cm}^{-3}$  (mSOM $_{1.6\text{--}2.0}$ )
- Mineral-associated SOM  $>2\ \text{g cm}^{-3}$  (mSOM $_{>2.0}$ )

The  $\delta^{13}\text{C}$  data were used to calculate a mean age of the C in each pool. Elemental analyses showed a decreasing trend in C:N ratio in progressing from the fSOM $_{<1.6}$  through to the mSOM $_{>2.0}$  fractions

that were suggested to indicate an increase in the degree of degradation and humification. The mean age of SOC in these fractions and the values obtained for percent modern carbon (Rethemeyer et al., 2005) did not follow the same trend, suggesting that the oldest carbon in a soil may not be the most decomposed. Such a situation can only arise when organic materials having a chemical composition that renders them biologically labile are stabilized against biological attack within the soil matrix.

A simpler density fractionation scheme using a density solution of  $1.7 \text{ g cm}^{-3}$  was used by Swanston et al. (2005) to isolate three fractions (fSOM $_{<1.7}$ , oSOM $_{<1.7}$  and mSOM $_{>1.7}$ ) from  $^{14}\text{C}$ -labeled and unlabeled forest soils. The fSOM $_{<1.7}$  was found to be the most active fraction based on the measurement of SOC content, C/N ratio, and  $\Delta^{14}\text{C}$ . The oSOM $_{<1.7}$  fraction appeared to be less dynamic with a minimal entry of  $^{14}\text{C}$  since the labeling event. Based on  $^{13}\text{C}$  NMR analyses (Golchin et al., 1994a; Sohi et al., 2001, 2005; Poirier et al., 2005), oPOM is more degraded compared to fPOM; however, this is not consistent with the higher C/N ratios measured by Swanston et al. (2005). Such high C/N ratios would be consistent with the presence of a significant amount of charcoal C, which could mask the entry of new labeled  $^{14}\text{C}$  into this pool based on  $\Delta^{14}\text{C}$  measurements alone.  $^{13}\text{C}$  NMR analyses of oPOM fractions shown in Figure 11.3 (Sohi et al., 2001; Poirier et al., 2005) do indeed suggest the presence of charcoal-like carbon given the significant resonances in the vicinity of  $130 \text{ mg kg}^{-1}$ . A significant movement of new labeled  $^{14}\text{C}$  into the dense mineral-associated SOC fraction was also measured by Swanston et al. (2005). The depleted  $^{14}\text{C}$  signature of this dense fraction at the near-background control site suggested that at the  $^{14}\text{C}$ -labeled site, the dense fraction consisted of at least two different pools of SOM: a fast-cycling pool and an older more stable pool. The presence of a labile pool of carbon within the dense mineral-associated SOM fraction was

supported by the lack of a difference in rate of carbon respiration from free particulate and dense mineral-associated SOM over the first 120 days of an incubation study (Swanston et al., 2002).

Although it is challenging to apply all the methods of analysis described to a soil sample (i.e., elemental contents and ratios, isotopic measurements for establishing turnover rates, and NMR to define chemical composition), doing so allows a more complete picture of the nature and dynamics of SOM fractions.

#### 11.2.4 Biological Composition

Research aimed at examining SOM in a biological context have attempted to differentiate organic matter on the basis of its susceptibility to decomposition and mineralization. Schemes developed to quantify the amount of biologically labile carbon have taken two general approaches: (1) quantification of the amount of carbon or nitrogen associated with the living soil microbial biomass or (2) quantification of a product of a biological process (e.g.,  $\text{CO}_2\text{-C}$  mineralized over a defined time interval).

Measurements of soil microbial biomass are assumed to be representative of the total mass of living microorganisms present in a soil. The importance of microorganisms to soil functioning is well recognized (Dalal, 1998; Stockdale and Brookes, 2006). The soil microbial biomass regulates most transformations of SOM, responds rapidly to variations in climate or management, and has been defined as the eye of the needle through which all soil carbon passes (Jenkinson, 1977; Smith and Paul, 1990). Soil microbial biomass is routinely measured using a variety of direct and indirect techniques based on either carbon or nitrogen dynamics. Direct techniques attempt to quantify the amount of carbon released to the soil after a fumigation event designed to lyse living microbial cells. The carbon released is measured by an extraction or incubation technique (Jenkinson, 1976;

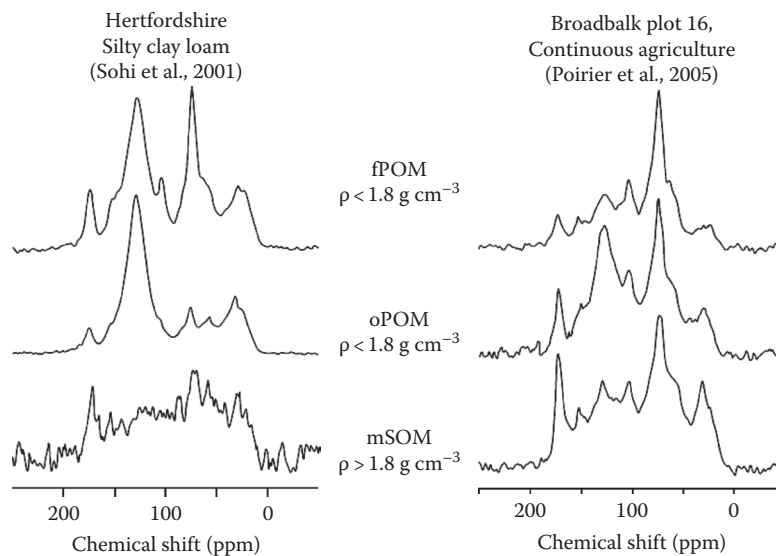


**FIGURE 11.3** Solid-state  $^{13}\text{C}$  NMR spectra obtained for fPOM, oPOM, and mSOM collected by Sohi et al. (2001) and Poirier et al. (2005) showing strong unsaturated carbon resonances, particularly in the oPOM fraction, consistent with the presence of charcoal and other forms of thermally altered organic matter.

Vance et al., 1987a, 1987b). Indirect techniques involve quantification of the respiration response on addition of a degradable substrate (Anderson and Domsch, 1978). Although the preceding comments have focused on the use of carbon to quantify soil microbial biomass, equivalent approaches exist based on the measurements of nitrogen (Brookes et al., 1985), sulfur (Saggar et al., 1981), and phosphorus (Brookes et al., 1982).

Once the measurements of extracted or mineralized carbon, nitrogen, phosphorus, or sulfur are obtained, conversion factors are applied to account for a lack of complete cell lysis and non-quantitative detection. For example, conversion factors of 0.45, 0.45, and 0.40 have been suggested to convert measurements of extracted carbon, nitrogen, and phosphorus, respectively, into their equivalent values within soil microbial biomass (Brookes et al., 1982, 1984, 1985; Jenkinson et al., 2004). Although these conversion factors have been shown to be adequate for microorganisms in cultures, they may vary across the diverse community of microorganisms found in soils and between different soils. Furthermore, the calculation of the size of the microbial biomass from CO<sub>2</sub> production requires a reliable estimate of the proportion of C that is assimilated and retained by the cell, that is, the microbial efficiency. This microbial efficiency, is not easily quantified, differs for different species within the soil microbial community (Anderson and Domsch, 1973) and varies on the basis of soil properties (Schimel, 1988) and the quality of the decomposing residue (Hart et al., 1994).

Carbon associated with the soil microbial biomass can account for 0.3%–7% of the total SOC (Wardle, 1992). Due to its short turnover time of <1 year (Jenkinson and Rayner, 1977; Jenkinson and Ladd, 1981; Ladd et al., 1981; Jenkinson and Parry, 1989; Wardle, 1992), the carbon associated with soil microbial biomass is considered to be a component of the active or labile pool of SOM. Measurements of soil microbial biomass are considered to provide a sensitive indicator of potential direction and relative magnitude of management-induced changes in SOM (Powlson and Jenkinson, 1976). However, the high spatial and temporal variability in the measurements of the soil microbial biomass and its dependence on soil water content, temperature, and substrate availability in the field will limit the usefulness of single point in time measures as a robust indicator of changes in SOC status. This was shown in an assessment of several Australian field trials, which indicated that very high numbers of field replicates (up to 93) were needed to significantly detect a 20% difference in soil microbial biomass carbon from control treatments (Broos et al., 2007).

There is no doubt that measures of soil microbial biomass provide an assessment of the potential rate of soil biological processes. However, such measures may or may not be related to actual biological process rates. Strong relationships will not exist where only a certain component of the entire microbial community involved in the process being quantified or where all individuals capable of contributing are doing so at different rates.

Quantification of process rates provides an alternative to define the functional capability a soil microbial population. An example of quantifying a process rate is the measurement of the

amount of organic carbon mineralized to carbon dioxide over a given time period. Haynes (2005) has reviewed the use of potentially mineralizable carbon and nitrogen to assess the biological lability of SOM. In this approach, the amount of organic carbon or nutrient (typically nitrogen) that can be converted into an inorganic form over a defined time interval is quantified (e.g., Campbell et al., 1991; Franzluebbers et al., 1994). It is important to note that the mineralization of carbon and nitrogen are not analogous. Mineralization of organic carbon results in a gaseous product that, for the most part, cannot be used by soil microorganisms and can be quantitatively recovered in an adequate experimental apparatus. Alternatively, organic nitrogen that has been mineralized to ammonium can be reused (immobilized) by soil organisms, volatilized as ammonia under certain soil pH conditions, nitrified to nitrate, and subsequently denitrified or leached if open incubation systems are used. Estimates of gross nitrogen mineralization are required to obtain data analogous to carbon mineralization (Bengtsson et al., 2003; Murphy et al., 2003; Flavel and Murphy, 2006).

Mineralization of carbon and nutrients results from a complex set of biochemical processes conducted by a wide range of organisms and thus provides a measure of soil functional capacity. Organic C mineralization is often called “soil respiration,” “basal respiration,” or “microbial respiration.” The amount or rate of C mineralization measured over periods from a few days to a few weeks is commonly used as an indicator of biological activity, whereas the total amount of CO<sub>2</sub>-C released on a longer time frame (>3 months) is considered to provide information about the fraction of SOC that is readily available to decomposer organisms. Mineralized C can be expressed either per unit mass of soil (mg CO<sub>2</sub>-C g<sup>-1</sup> soil) or as a proportion of the original SOC present (mg CO<sub>2</sub>-C g<sup>-1</sup> SOC). When expressed per unit mass of soil, information regarding the size of the mineralizable C fraction is obtained; whereas, when expressed per unit mass of SOC, an indication of the degradability of the organic carbon present in a soil is obtained.

Although measurements of mineralizable nitrogen require careful interpretation, the measure of net nitrogen mineralization (change in inorganic nitrogen status through time) can provide a measure of the contribution that decomposition processes can make to the supply of plant-available N. Mineralizable soil organic N (SON) is composed of various organic substrates, including microbial biomass, residues of recent crops (mainly POM), and humus (HUM). The mineralizable SON can be measured as potentially mineralizable N using an aerobic incubation under optimum moisture and temperature conditions (Franzluebbers et al., 1994; Chan et al., 2002) or under field conditions (Dalal et al., 2005) using the method developed by Raison et al. (1987). Attempts to correlate mineralizable SON with measures of total SON or SOC have not been very successful. It is suspected that one of the major reasons for this lack of success is related to differences in the allocation of SON and SOC to different forms of SOM, the variability of C:N ratio of these materials and the impact this would have on the mineralization/immobilization balance.

### 11.2.5 Defining Biologically Relevant Soil Organic Matter Fractions

Variability in elemental, chemical, physical, and biological composition provides the different components of SOM with an ability to contribute to a range of soil properties and processes (see Section 11.4). This variability also leads to differences in rates of turnover as demonstrated using  $^{14}\text{C}$  measurements (e.g., Ladd et al., 1981; Anderson and Paul, 1984; Swanston et al., 2005). In the context of SOM turnover studies, one objective of fractionating SOM is to quantify the allocation of SOM to materials that are differentially available to decomposition. In this section, a conceptual model of SOM decomposition will be presented and used to identify biologically relevant SOM fractions that can be quantified through measurement.

Prior to the presentation of the model, decomposition and its component processes will be defined to ensure no ambiguity exists pertaining to the processes being referred to. Decomposition is used to define the alteration of the original form of an organic material. Mineralization is used to define the conversion of an organic form of an element into an inorganic form (e.g., organic carbon to  $\text{CO}_2$  or organic N to  $\text{NH}_3$ ). Mineralization of carbon and nutrients is thought to dominantly occur within cells in response to respiration and other metabolic processes. The extent to which mineralization, particularly nutrient mineralization, can occur external to cells remains unquantified. However, if mineralization external to the cell is a dominant process, then the concept of ecological stoichiometry would be flawed and constraining carbon and nutrient cycling simulation models with carbon to nutrient ratios would be unsuccessful. Assimilation is defined as the use of carbon and

other elements in an organic material to create new biochemicals required for maintenance and growth of the decomposer community. As some of the assimilated carbon and nutrients may be excreted in an organic form as metabolic waste products, net assimilation should be used to refer to the amount of carbon and nutrients taken up and retained within the decomposer community. Additionally, since organic materials in soils are acted on by extracellular enzymes, it is possible that substrate alteration can occur without subsequent assimilation or mineralization. Possible examples of this include the adsorption of products of extracellular enzyme activity on soil mineral surfaces or the leaching of these products through the soil profile before they can be used. In both instances, the original organic material is altered but not accompanied by either a mineralization or assimilation. In the context of these definitions, decomposition is taken to represent the total of the individual processes of mineralization, assimilation, and alteration.

In the decomposition model (Figure 11.4), all processes occur in the aqueous phase of the soil and the behavior of simple and complex substrates is differentiated. Simple substrates are defined as soluble molecules that can cross cell membranes without further alteration. Once inside a cell, simple substrates can be mineralized, assimilated, or transformed into products of metabolic activity that are excreted back into the soil solution. Excreted metabolic products may be further transformed in the soil solution and/or reused by individuals within the decomposer community. Complex substrates consist of polymeric or multicomponent mixtures that are not soluble and cannot pass through a cell membrane in their original state.

Additional processes are required for decomposer organisms to use complex substrates including excretion of extracellular

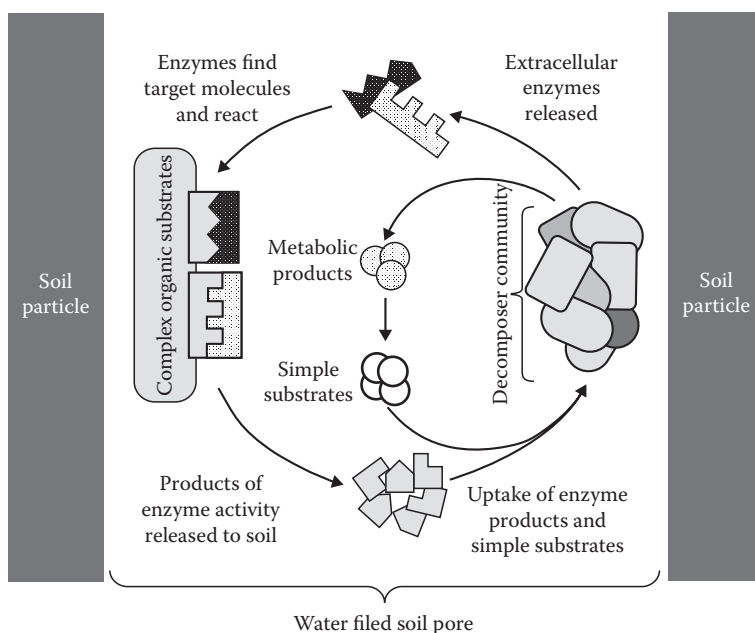


**FIGURE 11.4** Schematic model of the decomposition of organic materials in soil. Substrates may exist as simple soluble molecules or in particulate form requiring enzymes to liberate molecules capable of passing cell membranes. Products of metabolic activity may or may not serve as subsequent sources of either energy or nutrients.



enzymes, diffusion of the enzymes to their target sites, release of the products of enzyme activity, diffusion of the products back to the decomposers, and uptake of the products. For both simple and complex substrates, diffusion of soluble materials is required, and thus, the relative position of the substrate and the organism is important. Minimizing the path lengths of diffusion of both enzymes and products will enhance the rates of substrate decomposition and assimilation. Although each of the various organic components identified in Figure 11.4 (extracellular enzymes, products of enzyme activity, simple substrates, and metabolic products) is grouped together in the figure, this is only to illustrate the components involved in the process of decomposition. In reality, all these components will diffuse throughout the soil solution.

Baldock (2007) indicated that two types of controls operate to determine the biological stability of organic materials in soils (Figure 11.5). Biological capability controls whether or not a particular form of organic matter can decompose, while biological capacity controls the rate at which decomposition will proceed. Controls over the biological capability were suggested to include three factors: chemical recalcitrance, decomposer capability, and protection by the soil matrix. Chemical recalcitrance describes the type and arrangement of atoms and bonds within an organic substrate. Some organic material in soil offers little chemical recalcitrance to decomposition (e.g., cellulose and proteins) while others contain components that are highly resistant at least on a timescale of decades (e.g., charcoal). Decomposer capability refers to the presence of the appropriate DNA sequences required to construct the enzymes needed to attack and decompose the molecular components within the organic materials present. The third factor is protection by the soil matrix, which describes whether a molecule is in a position in the soil where it is accessible to enzymes. Biological capacity

refers to processes that affect the rate of decomposition but not whether a given molecule is decomposable. Biological capacity is defined by a series of factors governing the rate of biological processes (e.g., soil temperature and water content) and the duration of exposure to favorable conditions.

Combining the model of decomposition processes (Figure 11.4) with the concepts of biological stability (Figure 11.5) provides a means to identify biologically relevant fractions of SOM that decompose at different rates. DOM contains a variety of molecular structures with different chemical recalcitrance that are free to diffuse throughout the soil solution. Given the requirement for all substrates to pass through an aqueous phase prior to uptake and utilization by the soil decomposer community, DOM is likely to be the best indicator of the instantaneous availability of organic material at any given point in time. However, quantitative estimates of DOM content are unlikely to provide a good indication of the longer-term biological availability of SOM.

One of the most important forms of SOM, from the point of view of provision of a longer-term supply of energy to soil organisms, is the POM fraction with its high content of more easily degradable material (e.g., cellulose). POM may or may not provide nutrients depending on its elemental ratios. POM with high C:nutrient ratios (e.g., C/N ratio >40) will tend to immobilize nutrients as its carbon is mineralized. This may reduce the availability of nutrients to plants, but also enhance nutrient retention within surface soil layers by limiting losses due to leaching. The mSOM fraction tends to have a chemical composition more indicative of decomposed materials [lower C:nutrient ratios and higher ratio of alkyl:O-alkyl carbon (Baldock et al., 1997a)]. When considered in conjunction with its high level of interaction with mineral surfaces, the mSOM fraction is more resistant to decomposition than the POM fraction. The low C:nutrient ratios of mSOM suggest that it can contribute significantly to the provision of nutrients to plants and decomposer organisms. An additional fraction of SOM that is important to consider and monitor is charcoal or black carbon. This material has been found to account for up to 60% of the carbon in a soil (Skjemstad et al., 1996, 1998, 1999, 2002; Schmidt et al., 1999; Skjemstad and Taylor, 1999). Although a fraction of newly created charcoal may be decomposable (Hamer et al., 2004; Marschner et al., 2008), a high recalcitrance of charcoal C to biological mineralization in laboratory-based incubation has also been demonstrated (Baldock and Smernik, 2002). Long-residence times measured for charcoal in soil also suggest that a significant proportion is resistant to decomposition (Pressenda et al., 1996; Skjemstad et al., 1998; Swift, 2001; Krull et al., 2003, 2006).

Given the more recalcitrant behavior of charcoal carbon than the other forms of soil carbon, it is important to be able to selectively quantify the amount of charcoal carbon. In Figure 11.6, the impact that the presence of increasing proportions of charcoal carbon can have on SOC dynamics is shown using a modeling exercise completed with a modified RothC soil carbon model. In this modified model, the original resistant plant material (RPM)

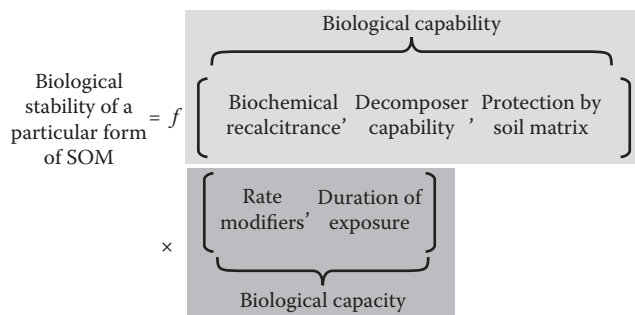


**FIGURE 11.5** Factors important to defining the biological stability of organic materials in soil. Factors describing biological capability define whether a particular form of SOM can be decomposed or not. Factors describing biological capacity define the rate at which decomposition occurs rather than whether it will or will not occur. Rate modifiers include properties such as temperature and water content, which need to be combined with the duration of exposure to favorable conditions to define the biological capacity. (Modified from Baldock, J.A. 2007. Composition and cycling of organic carbon in soil, p. 1–35. In P. Marschner and Z. Rengel (eds.) Soil biology. Vol. 10. Nutrient cycling in terrestrial ecosystems. Springer-Verlag, Berlin, Germany.)

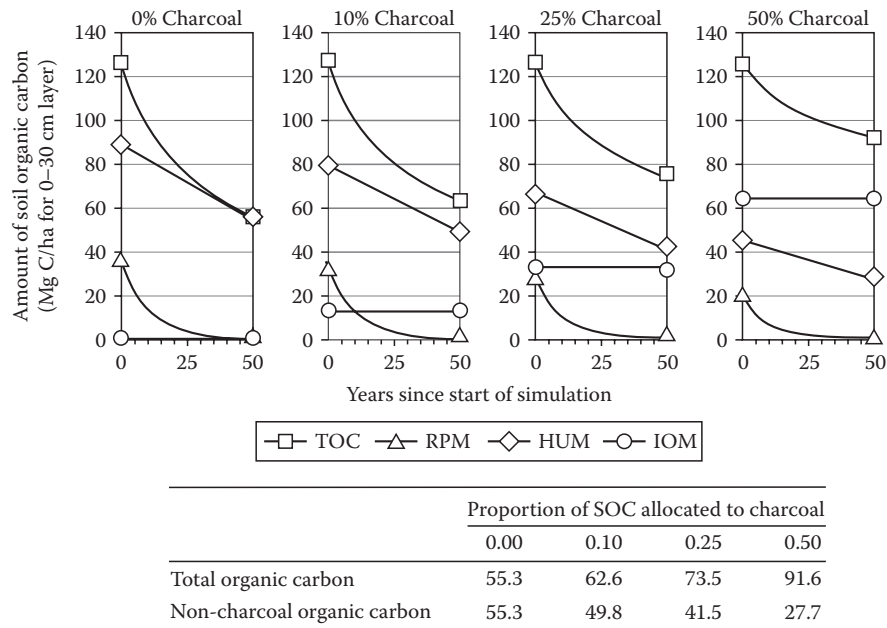


**FIGURE 11.6** Changes in total organic carbon (TOC), 2.0–0.053 mm POC, carbon associated with the <0.053 mm fraction (HUM), and charcoal carbon (Char-C) estimated from the RothC soil carbon model with different initial contents of charcoal carbon. For this modeling exercise, the total organic carbon at the start of the simulation was kept constant, the fraction of noncharcoal carbon allocated to the POC and HUM fractions was kept constant, and carbon inputs over the simulation period were set to zero. The DPM and two biomass pools in the RothC model were included in the modeling exercise but are omitted from the figure. The 1970–2005 average climate data for Beverly, WA, Australia were used. The table at the bottom of the figure gives the final values obtained after 50 years of simulation for total organic carbon and the noncharcoal organic carbon (POC + HUM) in units of  $\text{Mg C ha}^{-1}$  for the 0–30 cm soil layer.

and HUM fractions are equated to the POM and mSOM fractions described above. For all four modeling scenarios, the same starting level of SOC was used ( $127 \text{ Mg C ha}^{-1}$ ), and the allocation of carbon to each of the noncharcoal fractions was fixed at a given percentage of the total noncharcoal C components (27% for POC and 69% for mSOM). Over the 50-year period, inputs of carbon were set to 0. With increasing initial allocation of SOC to the charcoal fraction, the decline in TOC over the simulation period was reduced. However, when the dynamics of the POC and mSOM fractions are examined, despite there being more total carbon where charcoal accounted for 50% of the initial SOC, the amount of noncharcoal C remaining after 50 years was largest in the soil with no charcoal. If soil productivity was related more to the amount of mSOM carbon than charcoal carbon present, despite the greater loss of carbon from the soil with no charcoal, a higher level of productivity would be retained in this soil due to the higher amounts of mSOM maintained.

As a result of the preceding discussion, selective quantification of biologically relevant fractions of SOM requires an allocation of SOM across POM, mSOM, and charcoal fractions for longer-term studies (weeks to years) and an additional inclusion of DOM for short-term studies (hours to days). Although many approaches varying in number of fractions isolated and complexity of the fractionation process exist, it is suggested that the most simple fractionation system capable of allocating SOM to the POM, mSOM, charcoal fractions, and possibly DOM, depending on the application, would be most practical for the

potential broadscale application of quantifying the implications of land use and land-use change on SOM cycling. Baldock and Skjemstad (1999) proposed a three-component fractionation scheme to identify measurable SOM fractions for soil samples sieved to <2 mm: POC (organic carbon associated with 2000–53  $\mu\text{m}$  particles), HUM (organic carbon associated with <53  $\mu\text{m}$  particles), and ROC (resistant organic carbon associated with <53  $\mu\text{m}$  particles after removal of nonresistant materials with UV photo-oxidation and correction with  $^{13}\text{C}$  NMR analyses). Recently, modifications have been made to the Baldock and Skjemstad (1999) fractionation scheme to cover all forms of SOM at a given location and to account for recent analyses that have indicated the presence of significant quantities of charcoal in the POM fraction (Figure 11.7).

### 11.2.6 Consistency between Biologically Relevant Soil Organic Matter Fractions and Pools of Carbon in Simulation Models

Simulation models of SOC cycling (e.g., Rothamsted [Jenkinson et al., 1987], Century [Parton et al., 1987], and APSIM [McCown et al., 1996]) are often based on conceptual pools of carbon that are not measured directly. The construct of most SOC models is similar and includes fractions of SOC with a rapid turnover (annual), moderate turnover (decadal), and slow turnover (millennial) as well as a passive or inert component. It has been

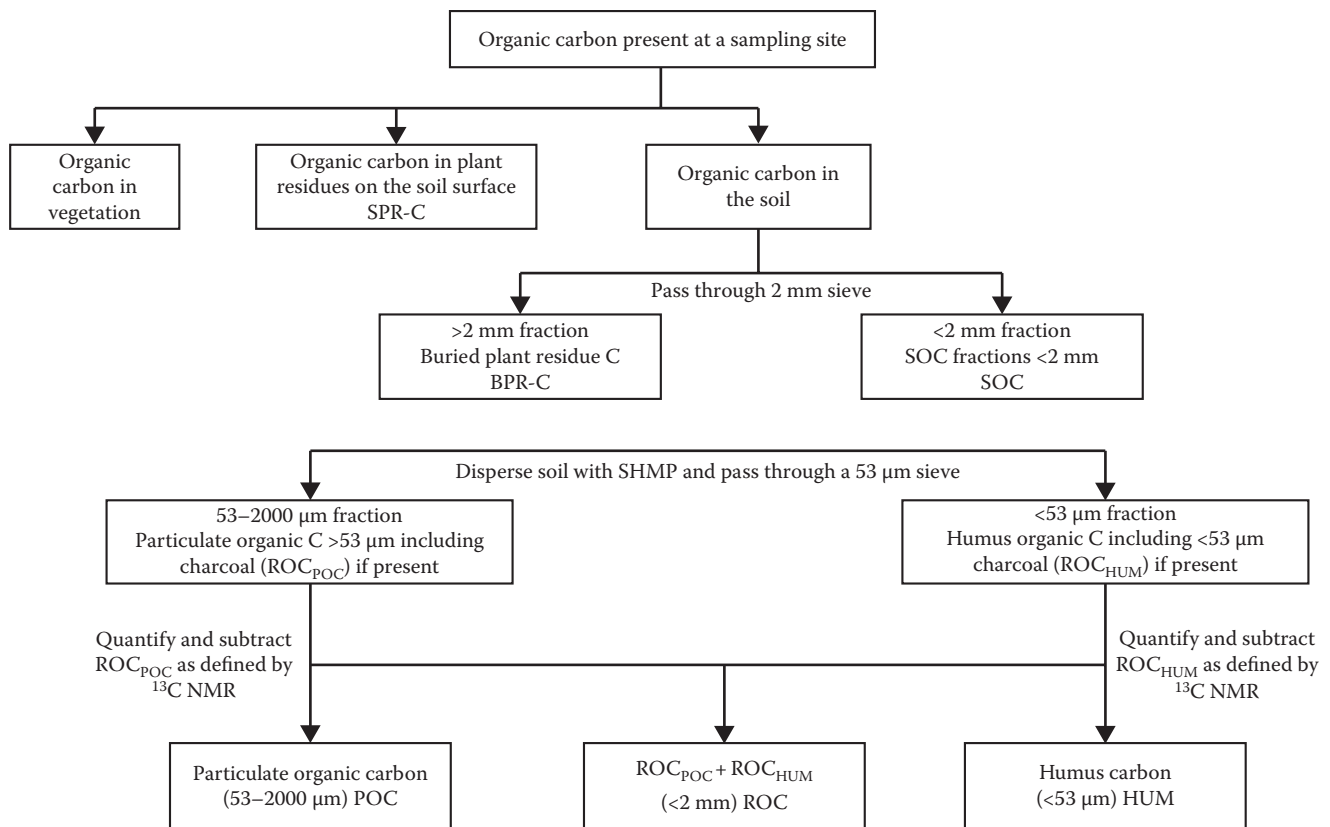


**FIGURE 11.7** Schematic presentation of the proposed methodology for defining the allocation of total SOC to its ecologically significant component fractions. SPR-C is the organic carbon associated with plant residues on the soil surface collected on an area basis. BPR-C is the organic carbon in buried plant residues having a size >2 mm. SOC is the total amount of organic carbon found in the <2 mm fraction of the soil. POC is the organic carbon found in the noncharcoal component of particles 53–2000 μm in size. HUM is the organic carbon found in the noncharcoal component of particles <53 μm. ROC is the resistant organic carbon obtained by adding together the charcoal C found in particles <2 mm (the sum of charcoal C found in the 53–2000 μm and the <53 μm fractions). SHMP is sodium hexametaphosphate.

recognized that developing a capability to replace these conceptual pools of SOC with measurable pools would offer several advantages: (1) internal verification of appropriate allocations of SOC to pools, (2) greater mechanistic understanding of the implication of management and environment on the components of SOC most affected, and (3) improved confidence in simulation outcomes. A suitable fractionation procedure should be capable of isolating and quantifying the allocation of SOC to pools that differ significantly in their biological availability (Baldock, 2007).

Several methods have been proposed to link measurable fractions of SOC to the conceptual pools contained within models using density fractionation techniques (Christensen, 1996b; Poirier et al., 2005; Sohi et al., 2005). However, the biological availability of the carbon in each fraction of these studies was never measured, and no attempt was made to substitute the measurable pools of SOC into a working carbon simulation model to demonstrate the utility of this proposal. Skjemstad et al. (2004) showed that the pool structure of the RothC model could be approximated using a three-component fractionation scheme as described by Baldock and Skjemstad (1999). Skjemstad et al. (2004) demonstrated that the POC, HUM, and ROC fractions

could be used to replace the RPM, HUM, and inert organic matter (IOM) pools of the RothC model, respectively. This was an important step forward in simulating SOC dynamics and demonstrated the potential for “modeling the measurable” (Christensen, 1996b; Magid et al., 1996; Baldock, 2007).

It must be noted that the soil microbial biomass (BIO<sub>f</sub> and BIO<sub>s</sub> in the RothC model) and decomposable plant materials (DPM in the RothC model) were not included in the fractionation scheme described by Baldock and Skjemstad (1999) or used in the RothC calibration by Skjemstad et al. (2004). The main reasons for this were as follows:

1. Difficulties associated with quantitatively separating the microbial biomass from the other forms of SOC
2. The questionable link between measures of microbial biomass carbon and rates of mineralization of SOC
3. The contributions made by the DPM, BIO<sub>f</sub>, and BIO<sub>s</sub> fractions to the total SOC are small and within the errors associated with measurement of the other larger fractions
4. These fractions equilibrate quickly in SOC simulation models

## 11.3 Quantifying Soil Organic Matter Content and Allocation to Fractions

Soil organic matter content, as indicated in Section 11.2, is typically quantified by measuring the content of organic carbon. Initially, measurements of SOM or SOC were completed to investigate pedogenic processes and, given its diverse and important functions in soils (Section 11.1), to provide a measure of soil productivity. However, being able to accurately define the content of organic carbon in soil has become important because of the potential for soils to sequester atmospheric CO<sub>2</sub>-C (Section 11.1). An additional requirement to move beyond the measurements of total organic carbon content and define the allocation of organic carbon to its ecologically significant fractions has emerged to support and improve predictions related to the influence of land use and management on soil carbon dynamics.

### 11.3.1 Direct Measurement of Soil Organic Content and Component Fractions

Methods to measure the content of SOC have been assembled recently by Skjemstad and Baldock (2008) and previously by Nelson and Sommers (1996) and include dry and wet combustion methods. Total C analyses involve the complete conversion of all C (organic and inorganic) in a soil to CO<sub>2</sub> and quantification of the evolved CO<sub>2</sub> by various means (e.g., infrared detection, increased mass of an ascarite trap, or others). Corrections for the presence of inorganic C must be performed when using total C methods to quantify SOC contents. Of the methodologies currently available, a dry combustion-automated analyzer that measures CO<sub>2</sub> evolution with an infrared detector is the preferred methodology for determining SOC, provided accurate estimates of inorganic C contents can be obtained where required or samples can be pretreated to remove all inorganic C (Baldock and Skjemstad, 1999).

The successful calibration of the RothC model using measurable fractions of SOC has led to the development of the protocol described in Figure 11.7. This methodology differs slightly from that presented by Baldock and Skjemstad (1999) in that the resistant fraction (charcoal) is quantified in both the 2000–53 μm particulate and <53 μm HUM fractions rather than just the HUM fraction. Once isolated and dried, the carbon content of the various fractions (SPR-C, BPR-C, SOC, 53–2000, and <53 μm) is quantified using the dry combustion technique. The amounts of carbon associated with the POC, ROC, and HUM fractions are then defined after using <sup>13</sup>C NMR to quantify the allocation of carbon to the ROC fractions in the 53–2000 and <53 μm materials (ROC<sub>POC</sub> and ROC<sub>HUM</sub>, respectively).

### 11.3.2 Proximate Analyses

The SOM fractionation process described in Section 11.1 is time-consuming to complete (3–6 weeks to progress a sample from start to finish depending on the contents of carbon present in the

soil and its fractions), requires the use of expensive analytical instrumentation (e.g., a <sup>13</sup>C NMR spectrometer and a UV photo-oxidizer system), and involves the use of hazardous chemicals (e.g., HF). It would therefore be unlikely that this SOM fractionation process would move beyond a research implementation and become a routine measure available to land managers interested in understanding the impact of management practices. Provision of a more cost-effective and rapid means of quantifying SOC content and its allocation to component fractions is required. The development of such a capability would also be very useful to support the carbon cycling work and scenario predictions by providing appropriate data for initializing soil carbon models.

Diffuse reflectance mid-infrared spectroscopy (MIR) offers a simple, rapid, and low-cost methodology that is sensitive to both mineral and organic materials present in soils. In MIR, the chemical bonds associated with a variety of organic functional groups (alkyl, carbohydrate, carboxyl, amide, amine, aryl) can be identified (Janik et al., 2007). The problem is that signals from these components are often hidden within soil MIR spectra by signals derived from soil mineral components. The development of partial least squares (PLS) regression approaches and their application to spectroscopic data has allowed the signals obtained throughout the entire MIR spectrum to be examined for correlation to a set of analytical values derived from traditional laboratory procedures. The ability of MIR/PLS to predict total organic carbon was demonstrated by Janik and Skjemstad (1995) and Janik et al. (1998). Using the PLS process detailed by Haaland and Thomas (1988), Janik et al. (2007) applied the MIR/PLS approach to the data collected for total organic carbon content and its allocation to the POC and ROC (charcoal C) fractions. Successful calibration was achieved and used to compare laboratory-derived analytical data with corresponding data derived from the MIR/PLS predictions (Figure 11.8). The predictive capability for total organic carbon was excellent and that for ROC (charcoal C) was good. Agreement between predicted and measured values for POC was not as good but remained acceptable. Given the stronger dependence of POC on the nature of the vegetation from which it was derived, it is perhaps not surprising that predictability of this fraction was lower. With time and the development of additional calibration data, it may be possible to define more specific calibrations for POC derived from soils under different vegetation types. The current approach defined by Janik et al. (2007) calculates the allocation of carbon to the HUM fraction by difference (HUM = total – particulate – resistant).

It should be recognized that the MIR/PLS process is completely empirical and may be based as much on positive correlation with MIR signals from organic materials as positive or negative signals derived from particular soil minerals. Subsequent unpublished MIR/PLS work completed in the same laboratory has indicated that although the calibrations presented by Janik et al. (2007) provided adequate estimates of soil carbon fractions, improved predictions could be obtained by performing sample set-specific calibrations. To perform these sample set-specific

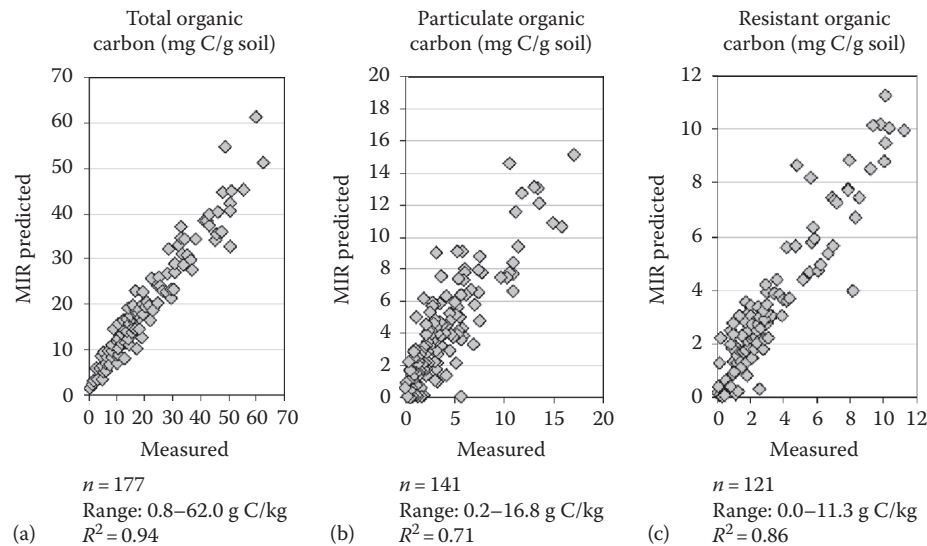


**FIGURE 11.8** Relationship between measured and MIR/PLS predicted contents of (a) total organic carbon, (b) POC (53–2000  $\mu\text{m}$ ), and (c) ROC (dominated by charcoal). (Adapted from Janik, L.J., J.O. Skjemstad, K.D. Shepherd, and L.R. Spouncer. 2007. The prediction of soil carbon fractions using mid-infrared-partial least square analysis. *Aust. J. Soil Res.* 45:73–81.)

calibrations, a subset of 10%–20% of the samples were selected to span the range of predicted values, analyzed using the laboratory procedure and used to recalibrate the MIR/PLS estimation procedure.

The MIR/PLS procedure appears to offer a robust, rapid, and cost-effective way to predict the total amount of organic carbon in soils as well as its allocation to fractions. With further testing and development of calibration data sets, this methodology may be able to underpin soil carbon modeling activities and provide useful data to land managers.

## 11.4 Functions of Organic Matter in Soil

Despite its often minor contribution to the total mass of mineral soils, SOM can influence a variety of soil properties, ecosystem functioning, and the magnitude of various obligatory ecosystem processes (Table 11.3). The properties influenced by SOM have been classified into three groups: biological, chemical, and physical. It should be noted that strong interactions and interdependencies exist between these groups. For example, the ability of SOM to chelate multivalent cations can affect its potential to

**TABLE 11.3** Properties and Functions of Organic Matter in Soil

Property	Function
<i>Biological properties</i>	
Reservoir of metabolic energy	Organic matter provides the metabolic energy, which drives soil biological processes
Source of macronutrients	The mineralization of SOM can significantly influence (positively or negatively) the size of the plant-available macronutrient (N, P, and S) pools
Ecosystem resilience	The buildup of significant pools of organic matter and associated nutrients can enhance the ability of an ecosystem to recover after imposed natural or anthropogenic perturbations
<i>Physical properties</i>	
Stabilization of soil structure	Through the formation of bonds with the reactive surfaces of soil mineral particles, organic matter is capable of binding individual particles and aggregations of soil particles into water-stable aggregates at scales ranging from $<2\ \mu\text{m}$ for organic molecules through to mm for plant roots and fungal hyphae
Water retention	Organic matter can directly affect water retention because of its ability to absorb up to 20 times its mass of water and indirectly through its impact on soil structure and pore geometry
Thermal properties	The dark color that SOM imparts on a soil may alter soil thermal properties
<i>Chemical properties</i>	
CEC	The high-charge characteristics of SOM enhance retention of cations (e.g., $\text{Al}^{3+}$ , $\text{Fe}^{3+}$ , $\text{Ca}^{2+}$ , $\text{Mg}^{2+}$ , $\text{NH}_4^+$ , and transition metal micronutrients)
Buffering capacity and pH effects	In slightly acidic to alkaline soils, organic matter can act as a buffer and aids in the maintenance of acceptable soil pH conditions
Chelation of metals	Stable complexes formed with metals and trace elements enhance the dissolution of soil minerals, reduce losses of soil micronutrients, reduce the potential toxicity of metals, and enhance the availability of phosphorus
Interactions with xenobiotics	Organic matter can alter the biodegradability, activity, and persistence of pesticides in soils

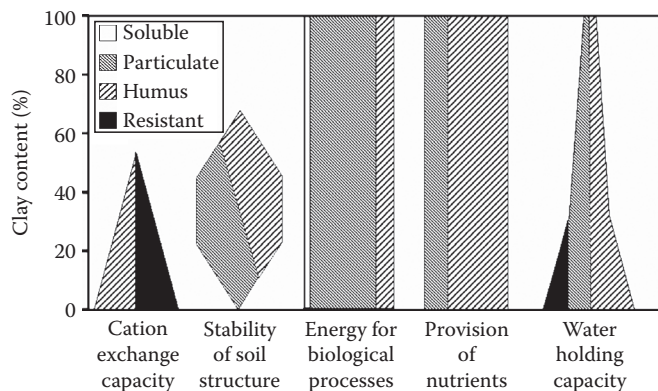


**FIGURE 11.9** Conceptual representation of the contribution that SOM and its component fractions make to some of the soil properties to which organic matter makes a positive contribution. Changes in the width of the overall shape with changing clay content define the relative contribution made by organic matter to the function defined. Within each shape, the width of the various shadings defines the importance of each type of organic matter to the function defined. (Adapted from Krull, E.S., J.O. Skjemstad, and J.A. Baldock. 2005. Functions of soil organic matter and effects on soil properties, p. 107. Cooperative Research Centre for Greenhouse Accounting, Canberra, Australia.)

stabilize soil structure and also its biodegradability. In addition, the effects of SOM on soil properties often involve interactions with the soil mineral fraction. Thus, variations in SOM function across different soils may not be solely a consequence of qualitative or quantitative variations in the soil organic component but may also arise in response to changes in soil clay content. In Figure 11.9, an attempt has been made to conceptualize this idea using a series of shapes to illustrate the selective importance of SOM fractions in performing specific functions. In Figure 11.9, the width of the overall shape and that of the SOM components are meant to provide an indication of the relative importance to the function identified at the base of the figure. As the shapes widen, the relative importance increases and vice versa. Shapes have been used in this conceptual framework due to the absence of strong quantitative relationships linking SOM content and composition to the functions identified. The generation of quantitative relationships linking SOM content and composition to functions performed in soil should form the basis for future research projects.

## 11.4.1 Biochemical Functions

### 11.4.1.1 Reservoir of Metabolic Energy

The most fundamental function of SOM is the provision of metabolic energy, which drives soil biological processes and the direct and indirect effects, which this has on other soil properties and processes. Photosynthesis fixes  $\text{CO}_2$  into glucose, which is then converted into a wide range of organic compounds (e.g., cellulose, hemicellulose, lignin, lipids, and proteins) by various enzymatic processes. The C fixed into such compounds is deposited in or on the soil during plant growth and as the plant or a portion of its tissues senesce, thereby providing C substrates for soil decomposer organisms. Oades (1989) presented an estimate of the C flow

through fertile grassland where primary production via photosynthesis was  $10 \text{ Mg C ha}^{-1} \text{ year}^{-1}$ . Of the  $3 \text{ Mg C ha}^{-1} \text{ year}^{-1}$  that was added to the SOC fraction, the soil fauna were estimated to utilize  $0.3\text{--}0.45 \text{ Mg C ha}^{-1} \text{ year}^{-1}$ , while the soil microbial biomass was estimated to utilize  $2.4 \text{ Mg C ha}^{-1} \text{ year}^{-1}$ . The majority of SOM processing is thought to be completed by the soil microbial biomass. However, other activities of the soil fauna enhance the ability of soil microbial decomposers to utilize organic residues added to soil. These include (1) fragmentation of plant debris, which enhances the surface area per unit weight of plant residue available to microbial attack and (2) distributing organic materials throughout the soil matrix, which provides an avenue for greater contact between decomposer microorganisms and substrates. Of the various SOM fractions, the POC fraction is suspected to play the biggest role in the provision of metabolic energy to decomposer populations.

### 11.4.1.2 Source of Macronutrients

A result of SOM decomposition is the conversion of macronutrients (N, P, and S) locked within organic chemical structures into inorganic forms, which are either immobilized and used in the synthesis of new tissues within soil organisms or mineralized and released into the soil mineral nutrient pool. With the exception of intensively managed soil receiving significant fertilizer inputs, organic matter provides the largest pool of macronutrients in the soil, with HUM being clearly the dominant fraction holding most macronutrients. McGill and Cole (1981) proposed that the mineralization of C, N, P, and S followed a dichotomous system involving both biological and biochemical mineralization. Biological mineralization is driven by the need of decomposer organisms for C as an energy source and accounts for the mineralization of N- and C-bonded S. Biochemical mineralization refers to the release of phosphate and sulfate from the P and S ester pool via enzymatic hydrolysis outside of the cell membrane. As a result and in contrast to organic N, organic P and S accumulation and mineralization in soils can occur independently of C and N dynamics.

#### 11.4.1.2.1 Nitrogen

The soil N pool is dominated by N found in organic structures. In soils with significant contents of  $\text{K}^+$ -containing clay minerals (e.g., illite) capable of fixing  $\text{NH}_4^+$ , approximately 90% of the soil N is contained in organic structures, 8% exists as fixed  $\text{NH}_4^+$ , and 1%–3% can be found in the inorganic plant-available pool ( $\text{NO}_3^-$  and  $\text{NH}_4^+$ ). In soils with little capacity to fix  $\text{NH}_4^+$  in clay minerals, the proportion of organic N is >97% and the inorganic fraction is 1%–3%. On a global scale, Söderlund and Svensson (1976) estimated that the organic N fraction of soils accounted for 95% of the total soil N pool, which is equivalent to the average value presented by Bremner (1968).

SON has been traditionally divided into the following five fractions based on a variety of acid hydrolysis procedures: (1) acid-insoluble N, (2) ammonia N recovered after hydrolysis, (3) amino acid N, (4) amino sugar N, and (5) hydrolyzable unidentified N. Data summarized by Stevenson (1994) for 11 studies where acid hydrolysis procedures were applied to different soil types showed that there was as much variation in the contents

of each form of N within similar soils as between different soil types. The proportions of each form of organic N were 7%–44% acid-insoluble N, 9%–37% ammonia N, 13%–50% amino acid N, 1%–14% amino sugar N, and 4%–40% hydrolyzable unidentified N. Although methodological differences may account for a portion of the large variations noted in the composition of SON, it is evident that approximately 50% of the total soil N cannot be identified by acid hydrolysis procedures (acid-insoluble N + hydrolyzable unidentified N).

Initial attempts to identify the chemical composition of unidentifiable organic N utilized gel filtration followed by acetylation and GC/MS (Schnitzer, 1985; Schnitzer and Spittler, 1986). Schulten et al. (1995, 1997) used Curie-point—Py-GC/MS with N-selective detection of the pyrolysis products. These studies suggested that heterocyclic N compounds represented an important component of unidentified SON (see Schulten et al., 1997, for examples of the chemical structure of the heterocyclic N compounds). The formation of heterocyclic N compounds via non-biological fixation of  $^{15}\text{NH}_3$  by humic substances (IHSS Suwannee River fulvic acid and peat and Leonardite humic acids) and by reacting  $^{15}\text{N}$ -labeled aniline with humic materials was noted by Thorn and Mikita (1992) and by Thorn et al. (1996), respectively. In contrast to these results, studies utilizing solid-state  $^{15}\text{N}$  NMR spectroscopy have failed to observe substantial contributions from heterocyclic N, and spectra tend to be dominated by signals arising from amides and terminal amino groups (Clinton et al., 1995; Knicker and Lüdemann, 1995; Knicker et al., 1995). Further effort is required to address these inconsistencies and to quantitatively characterize the composition of the fraction of N, which cannot be identified by conventional acid hydrolysis procedures.

#### 11.4.1.2.2 Phosphorus

The composition and cycling of soil organic P have been reviewed by Stevenson (1986, 1994) and Sanyal and Datta (1991). As a result of potential adsorption and inorganic precipitation reactions capable of reducing the availability of P in soils, mineralization of organic P is important to soil fertility (Tiessen et al., 1984; Beck and Sanchez, 1994). The relative importance of organic P as a nutrient source tends to be greater on highly weathered soils (Duxbury et al., 1989). The principal organic P-containing compounds in soils and their approximate proportions include inositol phosphates (2%–50%), phospholipids (1%–5%), nucleic acids (0.2%–2.5%), trace amounts of phosphoproteins, and metabolic phosphates (Stevenson, 1994). Soil organic P accounts for a variable proportion of the total soil P. Halstead and Mc Kercher (1975) and Uriyo and Kesseba (1975) presented soil organic P values ranging from 4 to 1400  $\mu\text{g g}^{-1}$  soil, which accounted for 3%–90% of the total soil P. Uriyo and Kesseba (1975) derived the relationship between organic P and organic C given in Equation 11.8, which produces an organic C:P ratio of 115 and is consistent with the average value of 117 proposed by Stevenson (1994):

$$\begin{aligned} \text{Organic C (mg g}^{-1}\text{ soil)} \\ = 4.9 + 0.059 \text{ organic P (mg g}^{-1}\text{ soil)} (R^2 = 0.49). \end{aligned} \quad (11.8)$$

#### 11.4.1.2.3 Sulfur

Reviews of the cycling and chemical composition of soil organic S include Stevenson (1986, 1994) and Nguyen and Goh (1994). Sulfur-containing organic compounds found in soils are generally grouped into two pools: compounds in which the S can be reduced to  $\text{H}_2\text{S}$  by hydroiodic acid (HI) and compounds in which the S is directly bound to C. The HI-reducible fraction consists mainly of ester sulfates (C–O–S bonds) and some ester sulfamates (C–N–S bonds). The C-bonded S fraction contains amino acid S (C–S bonds) or sulfonates (C– $\text{SO}_3$  bonds). The ester sulfates and sulfamates are typically associated with aliphatic side chains of soil organic compounds (Bettany et al., 1979), while the C-bonded S is incorporated along with C and N into the core of soil organic compounds and is generally less biologically accessible (McGill and Cole, 1981; Stewart and Cole, 1989). Organic S typically accounts for >90% of the total S found in nonsaline and nontidal soils (Nguyen and Goh, 1994; Stevenson, 1994).

#### 11.4.1.3 Ecosystem Resilience

The resilience of an ecosystem can be defined as its capacity to return to its initial state after being subjected to some form of disturbance or stress (e.g., Webster et al., 1975; DeAngelis, 1980). The important role played by SOM in determining the resilience of an ecosystem can be exemplified by a comparison of the contents of chemical energy and nutrients stored within the soil organic fractions in several ecosystems. In temperate grasslands, high SOM contents result from large belowground additions of photosynthate, limited leaching, and slow decomposition rates. Storage of C in such ecosystems is greater in the soil than in vegetation (Szabolcs, 1994). The large store of chemical energy and nutrients contained in SOM offers resistance to the loss of soil fertility induced by natural or agricultural disturbance. Temperate grassland soils (e.g., mollisols) will remain agriculturally productive with limited inputs for many years, despite the mining of energy and nutrient reserves contained within SOM (Janzen, 1987; Tiessen et al., 1994). Such systems can be considered resilient, at least initially, but one must question how long such systems can be sustained. Tiessen et al. (1983) showed that rates of organic P mineralization in a grassland soil were in excess of crop requirements over the first 60 years of agricultural production. Subsequent to the first 60 years, only the less labile, low-energy-providing forms of organic matter remained, and organic P mineralization rates decreased below crop demand.

In temperate forests, SOM contents are less than that of temperate grasslands and more C and nutrients are stored in aboveground vegetation than in the readily available soil organic materials (Szabolcs, 1994). As a result, the impact of a natural disturbance such as fire can significantly deplete ecosystem stores of energy and nutrients, and ecosystem recoveries (resilience) are slow due to low residual contents of SOC and associated nutrients. Where temperate forests are cleared and agricultural production is initiated, SOM losses must be minimized; however, production systems that increase SOM and nutrient reserves (e.g., crop rotations including legume pastures) can lead to highly productive and sustainable agriculture.

In tropical forest ecosystems, the storage of energy and nutrients in vegetation dominates, and the rapid utilization of plant residues by decomposer organisms and cycling of nutrients maintain ecosystem stability. This, when coupled with the low stores of energy and nutrients in organic matter of tropical soils, indicates a reduced importance of SOM in ecosystem resilience (Anderson, 1995). A comparison of a temperate grassland mollisol with a tropical oxisol (Tiessen et al., 1994) demonstrated the important contribution of SOM to the resilience of the grassland soil and its reduced significance in the tropical soil.

#### 11.4.1.4 Stimulation and Inhibition of Enzyme Activities and Plant and Microbial Growth

Research pertaining to the impacts of SOM on plants, microorganisms, and enzyme activities has typically used humic substances (e.g., humic and fulvic acids) as surrogates for SOM. The influence of humic and fulvic acids, tannins, and melanins on the activity of various enzymes was summarized by Ladd and Butler (1975), Müller-Wegener (1988), and Gianfreda and Bollag (1996). Based on earlier studies, Ladd and Butler (1975) concluded that the effect of humic acids on the activity of proteolytic enzymes varied and that the mechanism of humic acid–enzyme interaction involved primarily the carboxyl groups of humic acids. Inhibition of nonproteolytic enzyme activities by humic acids has also been demonstrated (Sarkar and Bollag, 1987). Müller-Wegener (1988) indicated that possible humic acid–enzyme interactions, which could impact on enzyme activity, included the following: (1) a direct interaction of the humic acid with the enzyme resulting in a modification of enzyme structure or changes in the functioning of active sites, (2) interference in the equilibrium of the enzyme reaction via the humic substances acting as analogue substrates, and/or (3) a reduction in the availability of cations, which often act as cofactors required for enzyme catalysis or structural stabilization of the protein molecule, by fixation on the humic acid molecule.

The influence of soil humic substances on plant growth and cellular activity have been reviewed (Chen and Aviad, 1990; Clapp et al., 2001; Varanini and Pinton, 2001; Nardi et al., 2002) and are generally attributed to direct (e.g., enhanced biochemical activity of plants) and indirect (e.g., increased efficiency of nutrient uptake) effects typically involve the absorption or adsorption of humic substances and the impact of these processes on biochemical properties at cell walls, cell membranes, and/or in the cytoplasm. Information on the impacts of humic materials in field studies is scarce and often confounded with other impacts of humic materials on soil properties (e.g., cation exchange capacity [CEC], nutrient status). Favorable effects on plants grown in defined media have included the following: (1) increased uptake of water and germination rate of seeds, (2) enhanced growth of shoots and roots as assessed by measurements of length and fresh and/or dry mass, and (3) increased root elongation, number of lateral roots, and root initiation (Nardi et al., 1996, 2002). Canellas et al. (2009) found that exposure of maize seedlings to solutions with 20 mg of humic acid carbon per liter for 7 days significantly altered metabolic activity and

enhanced root growth (length or density). Da Rosa et al. (2009) observed enhanced growth and K uptake by common beans when exposed to humic substances extracted from charcoal. Vaccaro et al. (2009) noted positive effects on growth and enzymatic activity of maize seedlings when exposed to the hydrophilic component or the entire soluble component extracted from a compost. Verlinden et al. (2009) noted an overall positive effect on dry matter yield and N uptake for a variety of plants (permanent grassland, maize, potato, and spinach) due to the application of humic substances originating from Leonardite formations. Such positive effects on plant growth have been postulated to result from increased permeability of cell membranes, increased chlorophyll content, increased rates of photosynthesis and respiration, enhanced protein synthesis resulting from a stimulation of ribonucleic acid synthesis, and enhanced enzyme activity (Vaughan and Malcolm, 1985).

Addition of humic substances to soil can also influence the activity of soil microorganisms through the provision of a metabolizable source of carbon, increased nutrient supply, and enhanced permeability of cell membranes toward required solutes (Valdrighi et al., 1996). Addition of humic substances at concentrations  $\leq 30 \text{ mg L}^{-1}$  to a nutrient solution increased growth rates in microbial cultures (Visser, 1985). Humic acid addition was also found to stimulate *in vitro* growth and activity of aerobic nitrifying bacteria, but not actinomycetes or filamentous fungi (Vallini et al., 1993, 1997; Valdrighi et al., 1995, 1996). A greater promotion of microbial growth has been noted as the molecular weight of the added humic substances decreased (Garcia et al., 1991; Valdrighi et al., 1995). It has been suggested that interactions between added humic materials and microbial cell surfaces (Stehlickova et al., 2009) or humic materials and hydrophobic pollutants (Vacca et al., 2005) may be responsible for enhanced rates of decomposition and mineralization. Enhanced microbial activity due to the addition of humic substances is not always noted, particularly where the added humic substances form the sole source of available carbon (Filip and Tesarova, 2004). Whiteley and Pettit (1994) noted a decreased ability to decompose wheat straw in the presence of humic acid derived from lignite, and Yasmeen et al. (2009) observed that humic acids isolated from oil palm compost inhibited the mycelial growth indicating the presence of a fungicidal activity.

### 11.4.2 Physical Functions

#### 11.4.2.1 Stabilization of Soil Aggregates

Organic matter is considered important to the maintenance of the structural stability of a wide range of soil types including mollisols, alfisols, ultisols, and inceptisols. Its importance tends to be less in oxisols and andisols, where hydrous oxides play an important stabilizing role, and in self-mulching soils (e.g., some vertisols), which contain clays with a high shrink/swell potential. In soils where organic matter is an important agent binding mineral particles together, a hierarchical arrangement of soil aggregates exists in which aggregates break down in a stepwise



manner as the magnitude of an applied disruptive force increases (Tisdall and Oades, 1982; Oades and Waters, 1991; Oades, 1993). Golchin et al. (1997a) and others have proposed the existence of three levels of aggregation: (1) the binding together of clay plates into packets  $<20\ \mu\text{m}$ , (2) the binding of clay packets into stable microaggregates ( $20\text{--}250\ \mu\text{m}$ ), and (3) the binding of stable microaggregates into macroaggregates ( $>250\ \mu\text{m}$ ).

The importance and nature of the organic materials associated with each level of aggregation varies. At the scale of packets of clays, aggregation is primarily dictated by soil mineralogical and chemical properties important in controlling the extent of dispersion and is often a function of pedological processes. The binding together of clay packets to form microaggregates occurs via a range of mechanisms. The dominant mechanism is proposed to involve polysaccharide-based glues (mucilages or mucigels) produced by plant roots and soil microorganisms (Ladd et al., 1996). Emerson et al. (1986) presented transmission electron micrographs showing mucilage located between packets of clay plates. Small microaggregates ( $<53\ \mu\text{m}$ ) held together by humified organic matter and biologically processed materials are bound together around a particulate organic core (Oades, 1984; Elliott, 1986; Beare et al., 1994a; Golchin et al., 1994b) to produce larger microaggregates and small macroaggregates  $<2000\ \mu\text{m}$ . Macroaggregates  $>2000\ \mu\text{m}$  are stabilized by the presence of roots, fungal hyphae, and larger fragments of plant residues, which interconnect soil aggregates via bonding to aggregate surfaces, penetration into or through aggregates, and/or physical enmeshment (Tisdall and Oades, 1982; Churchman and Foster, 1994; Foster, 1994).

#### 11.4.2.2 Water Retention

Organic materials can influence soil water retention directly and indirectly. SOM can absorb and hold substantial quantities of water, up to 20 times its mass (Stevenson, 1994). This direct effect, however, depends on the morphological structure of the organic materials and will not impart any beneficial effect to the soil unless it serves to enhance the ability of soil to hold water at potentials within the plant-available range. Organic matter in the form of surface residues can also influence water retention directly by reducing evaporation and increasing the infiltration of water.

The indirect effect of SOM on water retention arises from its impact on soil aggregation and pore-size distribution, and thus on plant-available water-holding capacity, AWHC, of the soil (the difference between volumetric water content at field capacity and permanent wilting point). This effect is best exemplified by the inclusion of SOC content as a significant parameter in pedotransfer functions, which predict pore-size distribution (e.g., Vereecken et al., 1989; da Silva and Kay, 1997; Kay et al., 1997). Equation 11.9 presents the pedotransfer function derived by da Silva and Kay (1997) to describe the relationship between volumetric water content,  $\theta_v$  ( $\text{m}^3\ \text{m}^{-3}$ ), and matric potential,  $\psi$  (MPa), clay content, CL (%), organic C content, OC (%), and bulk density, BD ( $\text{Mg}\ \text{m}^{-3}$ ). Using this equation, Kay et al. (1997) calculated predicted changes in AWHC for soils ranging in clay content from 7% to 35% when organic C content was increased

by  $0.01\ \text{kg}\ \text{kg}^{-1}$ . Increases in AWHC of 0.039 and 0.020 ( $\text{m}^3\ \text{m}^{-3}$ ) were obtained for the soils with 7% and 35% clay, respectively, at a relative bulk density of 0.75. Application of the same equations to a data set acquired by Wegner et al. (1989) for 80 South Australian red brown earths (alfisols) showed that the increase in AWHC induced by increasing organic C content by  $0.01\ \text{kg}\ \text{kg}^{-1}$  soil could be expressed by Equation 11.10. These results indicate that the presence of additional organic matter enhances AWHC of soils. Although the magnitude of the increase decreases with increasing clay content, building SOC content would be expected to be more difficult on a sand than on a clay soil:

$$\theta_v = a\psi_m^b, \quad (11.9)$$

where

$$a = \exp(-4.15 + 0.68 \ln \text{CL} + 0.42 \ln \text{OC} + 0.27 \ln \text{BD}),$$

$$b = -0.54 + 0.11 \ln \text{CL} + 0.02 \ln \text{OC} + 0.10 \ln \text{BD},$$

$$\text{Change in AWHC} = -0.0012(\% \text{clay}) + 0.055(R^2 = 0.82). \quad (11.10)$$

#### 11.4.2.3 Soil Thermal Properties

The typical dark color of SOM contributes to the dark color of surface-mineral soils and can enhance soil warming and promote biological processes related to temperature in cooler climates (e.g., plant growth and mineralization of C and nutrients contained in SOM). However, the presence of litter layers or organic horizons can insulate a soil against fluctuations in air temperature and solar heating. On several Canadian forest soils subject to cold winters and cool springs, average soil temperatures and the growth of fertilized seedlings were greater where the litter layers were removed compared to where they were left intact (Burgess et al., 1995). Similar effects have been observed in a comparison of cropping systems, which leave different amounts of crop residue on the surface of the mineral soil (Fortin, 1993).

### 11.4.3 Chemical Functions

#### 11.4.3.1 Cation Exchange Capacity

Organic matter contributes 25%–90% of CEC of the surface layers of mineral soils and practically all of the CEC of peats and forest litter and humus layers (Stevenson, 1994). The percent contribution is greatest for soils with low clay content or where the clay fraction is dominated by minerals with a low-charge density, such as kaolinite, and is lowest for soils with high contents of highly charged minerals, such as vermiculite or smectite. Organic matter will contribute most significantly to soil CEC in sandy soils.

The contribution of organic matter to soil CEC is pH dependent. At typical soil pH values ( $>5$ ), the CEC of organic matter is derived principally from carboxyl functional groups, but phenol, enol, and imide groups may also contribute at higher pH values. Given that an increase in degree of oxidation is typically associated with decomposition of organic materials in soil, more

highly degraded organic materials would be expected to have a higher CEC than their less decomposed analogues. An increase in CEC was noted by Roig et al. (1988) during the degradation of manure over time. Beldin et al. (2007) measured the CEC of light and heavy soil fractions and found a positive correlation between CEC and %C for the light fractions but not for the heavy fractions, presumably due to the high content of mineral soil constituents that contribute to CEC in the heavy fractions (e.g., clay). The result from Beldin et al. (2007) and results obtained for black carbon by Liang et al. (2006) indicate that the different forms of SOM found in soil will contribute differently to CEC and that significant contributions can be made by the nonhumified components of SOM.

Beldin et al. (2007) also noted that predicted whole soil CEC values obtained by mathematically combining the CEC values measured for the light and heavy fractions on a mass basis were much greater than those measured for the whole unfractionated soils. The potential for carboxylic acid groups to be involved in organomineral interactions and the complexation of cations may reduce their ability to contribute to soil CEC. CEC measurements made on organic matter fractions isolated from soils must therefore be treated with caution, particularly where the potential exists to break organomineral associations and displace complexed cations during the fractionation process.

One approach used to assess the impact of SOM on soil CEC has involved performing CEC measurements before and after organic matter removal (Tan and Dowling, 1984; Thompson et al., 1989; Turnpaul et al., 1996). However, this approach may result in an underestimation of the CEC of SOM since organic matter removal may expose inorganic CEC sites that were previously involved in organomineral interactions and not capable of contributing to whole soil CEC. Derivation of regression relationships between CEC and SOM/carbon has also been used to define the contribution of organic materials to soil CEC (Asadu et al., 1997; Oorts et al., 2003; Liang et al., 2006; Rashidi and Seilsepour, 2008; Seilsepour and Rashidi, 2008; Yimer et al., 2008). CEC values generated for SOM have ranged from 15 to >600 cmol<sub>c</sub> kg<sup>-1</sup> C. As a general rule, each weight percentage of SOC contributes approximately 3 cmol<sub>c</sub> kg<sup>-1</sup> soil (300 cmol<sub>c</sub> kg<sup>-1</sup> SOC) to the CEC of neutral permanent charge soils (McBride, 1994) and approximately 1 cmol<sub>c</sub> kg<sup>-1</sup> soil (100 cmol<sub>c</sub> kg<sup>-1</sup> SOC) to the CEC of variable charge soils (Oades, 1989).

#### 11.4.3.2 Buffering Capacity and Soil pH

The presence of weakly acidic chemical functional groups on soil organic molecules that can act as conjugate acid/base pairs makes SOM an effective buffer. The diversity in chemical composition of the functional groups (e.g., carboxylic, phenolic, acidic alcoholic, amine, amide, and others) provides organic matter with the ability to act as a buffer over a wide range of soil pH. James and Riha (1986) reported buffer capacities of 18–36 and 1.5–3.5 cmol<sub>c</sub> kg<sup>-1</sup> (pH unit)<sup>-1</sup> for the organic and mineral horizons, respectively, of forest soils. Starr et al. (1996) obtained a good correlation between acid buffer capacity and organic matter content for 29 organic and 87 mineral soil horizons (E, B, and C horizons)

exhibiting buffering capacities of 9.8–40.8 and 0.1–5.2 cmol<sub>c</sub> kg<sup>-1</sup> (pH unit)<sup>-1</sup>, respectively. For 59 agricultural soil samples taken from the 0–15 cm layer of cultivated fields, Curtin et al. (1996) noted that titratable acidity could be described by Equation 11.11 in which the terms OC and clay represent the soil organic C and clay contents expressed in units of kg kg<sup>-1</sup> soil and ΔpH is the reference pH (e.g., 8) minus the initial pH. Assuming the organic C content of SOM is 58%, Equation 11.11 indicates that the buffering capacity offered by organic matter was approximately 34 cmol<sub>c</sub> kg<sup>-1</sup> (pH unit)<sup>-1</sup> and was an order of magnitude greater than that offered by clay (34 versus 3 cmol<sub>c</sub> kg<sup>-1</sup> [pH unit]<sup>-1</sup>). The average clay/organic C ratio for the soils studied by Curtin et al. (1996) was 7.9/1, indicating that even though most soils contained much more clay than organic C, organic C accounted for about two-thirds of the soil buffering capacity.

#### Titrateable acidity to pH 8

$$= 0.02 + 59\text{OC}\Delta\text{pH} + 3.0 \text{ clay } \Delta\text{pH} \quad (R^2 = 0.95). \quad (11.11)$$

Addition of organic matter to soil may result in increases or decreases in soil pH, depending on the influence that the addition has on the balance of the various processes that consume and release protons. A detailed presentation of these soil processes and their ability to release or consume protons is given by van Breemen et al. (1983). Factors that need to be considered include the chemical nature of the soil and that of the organic materials added as well as environmental properties including water content and extent of leaching. The net effect of adding organic matter to acidic soils is generally an increase in pH values (e.g., Yan et al., 1996; Pocknee and Sumner, 1997) with the main processes leading to the increase being (1) a decomplexation of metal cations, (2) mineralization of organic N, and (3) denitrification. Pocknee and Sumner (1997) found that on the acid Cecil soil, the extent of the increase in pH was controlled by the N content to basic cation content ratio. The decarboxylation of organic acids has also been shown to increase the pH of acid soils (Yan et al., 1996). Under alkaline soil conditions, however, these processes would be ineffective and would contribute to a reduction in soil pH as a result of their influence on soil CO<sub>2</sub> concentrations. The addition of organic matter to alkaline soils tends to acidify them especially under waterlogged and leaching conditions (Nelson and Oades, 1997). The main processes involved in the acidification of alkaline soils on addition of organic materials include (1) mineralization of organic S and P, (2) mineralization followed by nitrification of N, (3) leaching of the mineralized and nitrified organic N, (4) dissociation of organic ligands, and (5) dissociation of CO<sub>2</sub> during decomposition.

#### 11.4.4 Complexation of Inorganic Cations

The presence of various functional groups on SOM provides the capacity for interaction with inorganic cations. Possible interactions can take the form of simple cation exchange reactions, such as that between negatively charged carboxyl groups

and monovalent cations, or more complex interactions where coordinate linkages with organic ligands are formed, such as occurs between amino acids and  $\text{Cu}^{2+}$  (Harter and Naidu, 1995; Baldock and Skjemstad, 2000). The influence that the complexation of inorganic cations by SOM has on soil properties and processes includes the following:

1. Altered solubility and degradability of associated organic materials (Skjellberg and Magnusson, 1995; Christl and Kretschmar, 2007; Scheel et al., 2007)
2. Increased availability of insoluble mineral P through complexation of  $\text{Fe}^{3+}$  and  $\text{Al}^{3+}$  in acid soil and  $\text{Ca}^{2+}$  in calcareous soil, competition for P adsorption sites, and displacement of adsorbed P (Stevenson, 1994; Cajuste et al., 1996)
3. The release of plant nutrients through the weathering of rocks and soil parent materials by the removal of structural cations from silicate minerals (Robert and Berthelin, 1986; Tan, 1986)
4. Enhanced availability of trace elements in the upper portion of the soil profile as a result of upward translocation by plant roots and subsequent deposition on the soil surface and complexation during residue decomposition (Stevenson, 1994)
5. Facilitated adsorption of organic materials to soil minerals, which aids in the generation and/or stabilization of soil structure (Oades, 1984; Emerson et al., 1986)
6. Buffering of excessive concentrations of otherwise toxic levels of metal cations (e.g.,  $\text{Al}^{3+}$ ,  $\text{Cd}^{2+}$ , and  $\text{Pb}^{2+}$ ; Anderson, 1995)
7. Pedogenic translocation of metal cations to deeper soil horizons (McKeague et al., 1986) and the formation of minerals (Huang and Violante, 1986)

## 11.5 Factors Determining the Content of Organic Matter in Soil

The amount of organic matter present in a soil is defined by the balance between the competing rates of input and loss of organic matter. Rates of input are typically defined by the amount of plant residue added to the soil. Any practice that enhances the amount of carbon captured by plants and the return of organic residues to the soil (above- and belowground) will increase inputs. For example, appropriate use of fertilizers to maximize productivity will also maximize returns of organic residues to the soil under any given management regime. Other factors such as the availability of water may place an upper limit on input rates by constraining potential plant productivity and thereby placing an upper limit on input rates. Where organic wastes are available (e.g., municipal green waste, residual materials derived from animal production, and biosolids), their application to soil can increase rates of input beyond that defined by environmental, soil, and management factors that normally limit plant production.

Losses of organic matter from soil result from decomposition and subsequent mineralization of organic carbon and its

associated elements. Processes that accelerate decomposition increase the rate of loss. Additionally, losses of organic matter can occur through erosion or leaching. Erosion losses are rapid and event driven and may be catastrophic in localized areas. Losses by leaching are typically small compared to mineralization losses, but over time can lead to a significant removal or redistribution of organic matter within the soil profile.

During pedogenesis, organic matter accumulation in soil goes through a series of development phases. In the initial phase, a slow colonization by photosynthetic organisms occurs. A lack of available nutrients places a ceiling on the amount of  $\text{CO}_2\text{-C}$  that can be fixed. Low rates of carbon capture and low nutrient status limit both production and decomposition of SOM. Accumulation of SOM in this phase, expressed in units of  $\text{g m}^{-2}$ , proceeds slowly and can be aided by interactions with soil mineral components that are capable of biologically protecting SOM against decomposition. With continued soil development, SOM content and the activity of decomposer organisms increase to a point where a continued supply of nutrients in a plant-available form is reached. At this point, the rate of  $\text{CO}_2\text{-C}$  capture and organic matter deposition is greater than mineralization, and SOM accumulates at an exponential rate. With increasing SOM content, the ability of the soil to protect additional organic matter declines and an increasing proportion of added organic matter remains accessible to decomposition. As a result, the increase in organic matter content through time proceeds through an inflection point and then begins to decrease. Once the capacity for biological protection offered by soil mineral components is approached, the rate of mineralization of SOM tends toward the rate of deposition of fresh organic residues and SOM levels approach an equilibrium value. It is important to note that this biological protection rarely equates to a permanent and complete removal of organic C from the decomposing pool, but rather to a reduction in its rate of decomposition, when compared to similar materials existing in an unprotected state (Baldock and Skjemstad, 2000). As the older protected C is slowly mineralized, its position in the biologically protected pool is replaced with younger modern organic C.

The progression of SOM content with soil development and the magnitude of the equilibrium level of SOM will also depend on interactions, which occur between the factors of soil formation. Where cold and water-saturated soil conditions persist, decomposition is confined to slow anaerobic processes and organic matter contents expressed in units of gram per square meter may continue to increase leading to the formation of organic soils. In sandy soils, the extent of biological protection offered by the soil mineral component will be lower than that offered by clay-rich soils and large differences in SOM content can develop. Therefore, with the exceptions of peatland and wetland soils, which have been estimated to accumulate  $0.1\text{--}0.3\text{ Pg C year}^{-1}$  globally (Post et al., 1990), organic matter levels in soil do not increase indefinitely but rather tend to equilibrium values dictated by the soil-forming factors of climate, biota (vegetation and soil organisms), parent material, and topography (Baldock and Skjemstad, 1999; Six et al., 2002).

An additional factor that must be considered in an examination of factors influencing organic matter contents in soils used for agriculture and forestry is land management practice. Land management can induce rapid and drastic changes to equilibrium contents of SOM attained under natural undisturbed conditions and completely override the influence of soil-forming factors. For example, the conversion of native ecosystems to agriculture often, but not always (Skjemstad and Spouncer, 2003), results in a net loss of SOM (Mann, 1986; Davidson and Ackerman, 1993; Paustian et al., 1997b).

When measurements of SOM are conducted on perturbed systems, it must be acknowledged that they may still be in the process of attaining a new equilibrium content. When combined with the potential impacts that variations in climatic conditions can have, it can be difficult to detect the true direction of SOM change induced by alterations to land use at timescales <10 years. In fact, more than 50 years may be required to reestablish equilibrium conditions representative of a new land use (Baldock and Skjemstad, 1999). Combining this observation with early results presented by Jenny (1930) suggests that the relative importance of the soil-forming factors on SOM content can be viewed as management > climate > biota (vegetation and soil organisms) > topography = parent material (Baldock and Skjemstad, 1999).

An independent evaluation of the influence of any single factor on SOM contents is difficult because of the requirement that all other factors remain constant. Variations in the soil-forming factors experienced on a landscape scale and the interdependence of these factors contribute to the large variability noted for SOM contents, even within localized areas. When trying to assess changes of SOM content in a soil, it must be noted that rates of change in SOM (typically less than  $0.5 \text{ Mg C ha}^{-1} \text{ year}^{-1}$ ) are quite small compared to the large amounts of SOM often present (as high as  $100 \text{ Mg C ha}^{-1}$ , or more, in the top 60 cm soil layer; Ellert et al., 2008). Thus, changes in SOM can only be reliably measured over a period of years or even decades (Post et al., 2001). Since the distribution of SOM in space is inherently variable, temporal changes (e.g., attributable to management practices, environmental shifts, successional change) must be distinguishable from spatial ones (e.g., attributable to landform, long-term geomorphic processes, nonuniform management) to assess whether SOM is either increasing or decreasing (Ellert et al., 2008).

Computer simulation models of SOM dynamics, as defined through changes in SOC (Jenkinson et al., 1987; Parton et al., 1987; McCown et al., 1996), can be used to provide valuable information pertaining to the interaction of soil-forming factors on SOC levels and thus, ecosystem functioning, provided the models are structured appropriately. However, it is essential that field data are available to validate predictions (Burke et al., 1989).

### 11.5.1 Climate

Climate impacts SOM content primarily through the effects of temperature, moisture, and solar radiation on the array and growth rate of plant species and the rate of SOC mineralization. Post et al. (1982) found that the amount of SOC was positively

correlated with precipitation and, at a given level of precipitation, negatively correlated with temperature. Similar results were observed by Guo et al. (2006) in an analysis of factors controlling SOC in the United States using maps generated from the State Soil Geographical database (STATSGO). Guo et al. (2006) found that SOC content increased as the mean annual precipitation (MAP) increased up to 700–850 mm and then fluctuated as the MAP increased further. When other variables were highly restricted, there was a clear decline in SOC with increasing temperature. In the Great Plains of North America, precipitation controls NPP and temperature is considered to exert its strongest control over rates of SOC mineralization (Parton et al., 1987; Sala et al., 1988; Burke et al., 1989). Ladd et al. (1985) compared the mean loss of  $^{14}\text{C}$ -labeled plant residues from four soils in South Australia with that obtained by Jenkinson and Ayanaba (1977) for soils in England and Nigeria and observed a doubling of the rate of substrate C mineralization for an  $8^\circ\text{C}$ – $9^\circ\text{C}$  increase in mean annual temperature. An influence of temperature on decomposition can also be inferred from  $^{14}\text{C}$  content of SOC, which showed a latitudinal gradient in the mean residence time of SOC (Bird et al., 1996).

The observed trend of decreasing SOC content with increasing temperature implies that the relative temperature sensitivity of decomposition is greater than that of NPP. Because of the strong interactions between temperature, water availability, and substrate quantity, it is difficult to assess the temperature dependence of decomposition without confounding effects. In a compilation of data extracted from controlled incubation studies where water limitations were avoided and a common substrate was used at all temperatures, Kirschbaum (1995) showed that the  $Q_{10}$  value (rate of change of a process with a  $10^\circ\text{C}$  temperature increase) of C mineralization from soil was greater than that for NPP developed by Lieth (1973), especially at temperatures  $<15^\circ\text{C}$ . Increases in temperature, particularly when starting from temperatures  $<15^\circ\text{C}$ , will enhance decomposition more than NPP. The greater sensitivity of carbon mineralization to climatic variation was also observed at a regional (Goulden et al., 1998; Saleska et al., 2003) and global scale (Hicke et al., 2002). Hicke et al. (2002) showed that the variability in NPP was considerably less than the variability in growth rate of atmospheric  $\text{CO}_2$  using inverse modeling, suggesting that the cause of the year-to-year variability in carbon fluxes is largely from varying rates of respiration rather than photosynthesis.

Climate has also been shown to affect the chemical structure of SOC. Using Py-GC to characterize the chemical structure of SOC in a climosequence of nine New Zealand soils, Bracewell et al. (1976) observed significant correlations between changes in the intensity of peaks in the chromatograms and MAP and temperature. By including both temperature and precipitation in a regression analysis, the resultant regression line explained 90% of the variation in chromatogram peak intensities. Amelung et al. (1997) used 10 grassland samples originating from different climatic zones of the North American Great Plains to investigate the impacts of mean annual temperature and precipitation on the chemical structure of SOC using a combination of chemical

methods and  $^{13}\text{C}$  NMR. MAP was capable of accounting for only 10% of the variation in alkaline CuO oxidizable lignin. Higher precipitation tended to favor an accumulation of polysaccharide carbon; however, at a given MAP, polysaccharide carbon tended to decrease with increasing temperature. Amelung et al. (1997) suggested that the increased content of polysaccharide carbon in more humid conditions may have resulted from (1) a positive feedback mechanism in which increased plant production enhanced microbial activity and soil structural conditions, thereby offering the potential for protecting microbial polysaccharides within aggregates, and/or (2) an enhanced activity of earthworms that elevated polysaccharide content relative to the surrounding soils (Guggenberger et al., 1995) and offered organic carbon some physical protection against mineralization (Lavelle and Martin, 1992). Accompanying the decrease in polysaccharide carbon noted with increasing temperature, Amelung et al. (1997) further noted an increase in aliphatic carbon content. This accumulation of alkyl carbon at high temperature may be explained by (1) enhanced mineralization of carbohydrates and selective preservation of plant or microbially derived alkyl structures by adsorption onto clay particles (Baldock et al., 1989, 1992) and/or (2) higher inputs of plant-derived alkyl carbon in plant residues due to the presence of thicker cuticles on plants growing in warmer climates.

In a study using a soil sequence along an elevational gradient ranging from subtropical to subalpine climate zones in the Etna region (Sicily, southern Italy), Egli et al. (2007) examined changes in SOC and C:N ratios. Egli et al. (2007) showed that the concentration of SOC in the topsoil, the stocks of SOC in soil profile and the nature of the SOC were strongly related to elevation and, thus climate and vegetation. However, the C:N ratio in the topsoil was more defined by the vegetation type. A better protection of SOC at lower altitude was found and suggested to be an effect of the specific climate conditions with more pronounced change in periods of humidity alternating with periods of drought and resultant fire activity. Repeated bushfires had played a significant role in the soil formation as indicated by the presence of aromatic compounds and charcoal (Egli et al., 2007).

### 11.5.2 Soil Mineral Parent Materials and Products of Pedogenesis

The mineral phase of soils can exert a strong influence on SOM contents as a result of mechanisms capable of protecting organic materials against biological attack (Baldock and Skjemstad, 2000). Each soil has a given capacity to protect SOC dictated by the following:

1. The chemical nature of soil minerals
2. The presence of multivalent cations and their ability to form complexes with organic molecules in soils
3. The adsorptive capacity of soil minerals for organic materials as governed by particle size and surface area
4. Physical protection mechanisms, which restrict access of organic materials to biological attack, that is, the architecture of the soil matrix

The degree and amount of protection offered by each mechanism depends on the chemical and physical properties of the mineral matrix and the morphology and chemical structure of the organic matter. Furthermore, as with other aspects of SOC dynamics, strong interactions can exist between these characteristics (e.g., the presence and type of multivalent cations will undoubtedly be related to the chemical nature of the minerals present). Finally, each mineral matrix will have its unique and finite capacity to protect organic matter. In the extreme case where mineral protection mechanisms are not present, such as in well-aerated peat or forest litter layers, decomposability will be controlled by the recalcitrance offered by the chemical structure of the SOM itself.

#### 11.5.2.1 Chemical Nature of the Soil Mineral Fraction

An analysis of different soil types indicates that soils with high contents of calcium carbonate ( $\text{CaCO}_3$ ) and amorphous Al and Fe tend to have higher organic C contents compared to other soil types (Spain et al., 1983; Oades, 1988; Sombroek et al., 1993). In a study of the influence of soil properties on SOC genesis, Duchaufour (1976) suggested that the presence of calcium carbonate in a rendzina could protect both particulate organic and HUM carbon. Thin carbonate coatings visible under magnification and a precipitation of organic molecules induced by  $\text{Ca}^{2+}$  complexation were implicated in the protection of POM and HUM, respectively, and helped to explain the observed impedance of mineralization. Protection of SOC in high-base-status soils with less reactive or low contents of calcium carbonate results predominantly from the formation of Ca-organic linkages. In such soils, the initial decomposition of plant residues is rapid, but the subsequent utilization of initial decomposition products is slow leading to higher SOC contents, lower C:N ratios, and longer retention times. Soils with high base status typically have higher clay contents, are more fertile, and have greater annual vegetative inputs than similar low-base-status soils. Establishment of causative relationships between base status and SOC contents must therefore be examined carefully because of the potential confounding effects of increased vegetative inputs and protection mechanisms involving clay minerals.

Soils derived from volcanic ash (andisols) are typically characterized by large accumulations of SOC, high C:N ratios, and high allophane contents. The formation of Al-organic complexes is considered to be important to the biological protection of organic C in andisols. Boudot et al. (1986, 1988) obtained a significant correlation between the amount of native C mineralized from 10 French highland soils and the contents of amorphous Al and allophane, without observing significant correlations with clay content, exchangeable  $\text{Al}^{3+}$ , or crystalline iron oxides. Decreased organic C mineralization rates from  $^{14}\text{C}$ -labeled organic substrates in allophanic soils and nonallophanic soils amended with allophane, relative to that noted in unamended nonallophanic soils, also demonstrated a protective effect of allophanic material on SOC (Zunino et al., 1982; Boudot et al., 1988, 1989). Zunino et al. (1982) demonstrated that the influence of allophane on mineralization of C from an organic substrate

varied with the chemical structure of the substrate. The presence of amorphous Fe compounds and  $\text{Fe}^{3+}$  cations has been shown to have a similar effect to that of allophane and  $\text{Al}^{3+}$  cations on the mineralization of C from organic materials; however, the magnitude of the protective effect was reduced (Boudot et al., 1989).

### 11.5.2.2 Impacts of Multivalent Cations

The presence of multivalent cations in soil has important implications on the behavior of clays and organic materials and the biological availability of organic C. When saturated with multivalent cations, clays remain flocculated, which reduces exposure of organic materials adsorbed onto their surfaces (Section 11.5.2.3) and macromolecular organic materials bearing functional groups become more condensed (altering their 3D structure) and thus less susceptible to the enzymatic attack.

The dominant multivalent cations present in soils include  $\text{Ca}^{2+}$  and  $\text{Mg}^{2+}$  in neutral and alkaline soils and hydroxypolycations of  $\text{Fe}^{3+}$  and  $\text{Al}^{3+}$  in acidic, ferrallitic, and andic soils. A protecting effect of  $\text{Ca}^{2+}$ , relative to  $\text{Na}^+$ , on organic C mineralization was effectively demonstrated by Sokoloff (1938), where the extent of mineralization and solubility of organic C in two soils was reduced by the addition of  $\text{Ca}^{2+}$  salts and enhanced by the addition of  $\text{Na}^+$  salts. Other studies have also shown a decreased solubility of SOC in the presence of  $\text{Ca}^{2+}$  (Muneer and Oades, 1989c) and reduced mineralization of native organic materials and organic substrates on the addition of  $\text{Ca}^{2+}$  in incubation studies (Linhares, 1977; Muneer and Oades, 1989a, 1989b). In such studies, the question remained as to whether the effect of  $\text{Ca}^{2+}$  addition on mineralizable C resulted from an indirect effect on colloidal dispersibility or from a direct effect of  $\text{Ca}^{2+}$  complexation on the biodegradability of the organic molecule.

A direct effect of multivalent cation complexation on biodegradability in soil has been demonstrated by the following results:

1. A reduced oxygen absorption on incubation of humic acids saturated with  $\text{Ca}^{2+}$ ,  $\text{Al}^{3+}$ , or  $\text{Fe}^{3+}$  in the same soil, relative to that noted for  $\text{Na}^+$ -saturated humic acids (Juste and Delas, 1970; Juste et al., 1975)
2. An increased protection of  $\text{Al}^{3+}$  and  $\text{Fe}^{3+}$  forms of plant and microbial polysaccharides (Martin et al., 1966, 1972)
3. A threefold increase in the amount of C mineralized from an organic soil after replacing  $\text{Ca}^{2+}$  cations with  $\text{K}^+$  during a 25 week incubation (Gaiffe et al., 1984)

Indirect evidence for the involvement of cations in the accumulation of SOC can also be obtained through a comparison of the organic C contents of a variety of soil types. Using data derived from Spain et al. (1983) for the organic C contents of 29 Australian great soil groups, Oades (1988) showed that, excluding soils subject to waterlogging, there was a positive correlation between SOC contents and either high base status or the presence of substantial contents of Al and Fe oxides. Of interest was the comparison of siliceous and calcareous sands, which have little or no clay, but indicate an increased SOC content in the presence of  $\text{Ca}^{2+}$ -containing mineral fractions (<0.5% to 1.5% versus 1.5% to >4% organic C, respectively.)

### 11.5.2.3 Adsorption of Organic Materials onto Mineral Surfaces

Clay particles provide a reactive surface onto which organic materials can be adsorbed, and it is generally accepted that such adsorption reactions provide a mechanism of protecting SOC against microbial attack. The mineralogy, surface charge characteristics, and precipitation of amorphous Fe and Al oxides on clay mineral surfaces give clay minerals the capacity to adsorb organic matter and protect it from biological degradation. Correlations between SOC and clay contents have been observed (Schimel et al., 1985a, 1985b; Spain, 1990; Feller et al., 1991), and the various interactions between soil clays and organic materials have been summarized by Oades (1989). Such interactions are principally defined by the chemical nature of organic materials (functional group content, molecular size, etc.) and the type of clay mineral (kaolinite, illite, smectite, etc.). Numerous studies utilizing isotopically labeled organic substrates have shown a positive relationship between the contents of residual substrate C and soil clay content (Amato and Ladd, 1992). Clay particles have also been observed to encapsulate particles or patches of SOM (Baldock, 2002).

Not only the amount of clay, but also the specific surface area (SSA) of the clay and more generally the soil mineral particles is of importance. For example, Ransom et al. (1998) showed that adding even small amounts of high-SSA ( $100\text{ m}^2\text{ g}^{-1}$ ) clay-size (<2  $\mu\text{m}$ ) material can have a significant effect on the total SSA of mineral particle mixtures. It must be noted that the relative magnitude of the effect of adding high-SSA clays to nonclay mineral particles decreases as the size of the nonclay mineral particles decreases (Baldock and Skjemstad, 2000).

In a field experiment where  $^{14}\text{C}$ -labeled plant residues were added to four cultivated soils varying in clay content (5%–42%) but having similar clay mineralogy, climatic conditions, and no other organic inputs, the amounts of residual  $^{14}\text{C}$  and total organic C in the topsoil (0–10 cm) remaining after 8 years of decomposition were nearly proportional to soil clay content (Ladd et al., 1985). Saggar et al. (1996) completed a similar study in which the decomposition of  $^{14}\text{C}$ -labeled ryegrass was monitored over 6 years in four soils having variable clay content (16%–60%) and clay mineralogy. The mean residence time of the  $^{14}\text{C}$ -labeled ryegrass was not related to clay content but rather to the SSA as measured by adsorption of *p*-nitrophenol. The increase in mean residence time with increasing SSA, suggested that the protective capacity of the soils toward transformed metabolites derived from plant residues was principally controlled by adsorption onto soil surfaces. Since the data presented by Ladd et al. (1985) were derived from soils with a similar clay mineralogy, SSAs would have been well correlated with clay content. The importance of available surface area was also suggested by the results of Sørensen (1972, 1975) where the addition of high-SSA montmorillonite to a soil/sand mixture protected microbial metabolites, but the addition of low-SSA kaolinite had little influence.

Hassink (1997) found a relationship between the silt- and clay-associated C and soil texture, whereas this relationship

did not exist for the C in the sand-sized fraction (i.e., POM C) suggesting that the capacity of soil to preserve C was linked to silt and clay particles. Using data from Hassink (1997), Six et al. (2002) were able to define significantly different relationships for 1:1 clays versus 2:1 clays, demonstrating the effect of clay type in C protection. Clearly, 1:1 and 2:1 clays have significant differences in CEC and SSA that may lead to a different capacity to adsorb organic materials.

SSA and mineralogy have been identified as key components in the preservation of organic matter in marine sediments (Keil et al., 1994; Mayer, 1994a, 1994b). Based on data generated in these studies, Ransom et al. (1998) showed that total organic carbon in the marine sediments was linearly related to SSA as well as to the content of high surface area minerals present. All these results suggest that the potential protective capacity of soil mineral particles, and more specifically that of the clay minerals, is more a function of the SSA available for adsorption of SOC than the absolute amount of clay.

The protective effect of mineral surfaces can also be shown experimentally by removing the minerals associated with the various fractions as defined by Skjemstad et al. (1999) with HF, since HF is known to dissolve soil minerals with little alteration to the composition of organic matter. In a recent experiment conducted by the authors, incubation studies were used to compare the mineralizability of HF- and non-HF-treated fractions of SOM (unpublished data, Figure 11.10). Mineralizability was defined as the cumulative amount of  $\text{CO}_2\text{-C}$  emitted per gram of organic C present in the sample being incubated.  $\text{CO}_2\text{-C}$  emissions were quantified by repeatedly sampling and then refreshing the headspace of an incubator system for up to 70 days using infrared detection of  $\text{CO}_2\text{-C}$ . Comparison of the mineralizability of SOC with and without HF treatment revealed an increased mineralizability with destruction of soil minerals consistent with the ability of minerals to stabilize a portion of the SOC against biological attack. The magnitude of the difference between the

non-HF- and HF-treated soils provides an assessment of the relative importance of mechanisms of mineral protection in defining the biological stability of the SOC present.

#### 11.5.2.4 Physical Protection within Soil Matrix Offered by Soil Architecture

The architecture or structural condition of a soil can exert significant control over processes of biological decomposition through its effects on water and oxygen availability, dynamics of soil aggregation, and by limiting the accessibility of SOC to decomposer microorganisms and of microorganisms to their faunal predators. This limitation results from the ability of clays to encapsulate organic materials (Tisdall and Oades, 1982), the burial of SOC within aggregates (Golchin et al., 1997a, 1997b), and the entrapment of SOC within small pores (Elliott and Coleman, 1988; Strong et al., 2004). As outlined by van Veen and Kuikman (1990) and Hassink (1992), evidence of the importance of these processes in the protection of SOC in soils can be inferred from the following observations:

1. A faster turnover rate of organic substrates in liquid microbial cultures relative to that of similar substrates in mineral soils
2. An enhanced mineralization of C and N when soils are disrupted prior to incubation
3. A more rapid mineralization of organic C and plant residues in sandy soils than clay soils

A continuum of pore sizes exists in soils, starting with large macropores ( $>20\mu\text{m}$ ) and decreasing to micropores ( $<0.1\mu\text{m}$ ). Kilbertus (1980) suggested that bacteria can only enter pores  $>3\mu\text{m}$ , which suggests that a significant proportion of the soil pore space may not be accessible to microbial decomposers. Organic materials adsorbed onto clay particles contained in pores  $<3\mu\text{m}$  would only be decomposed as a result of diffusion of extracellular enzymes released by microorganisms followed

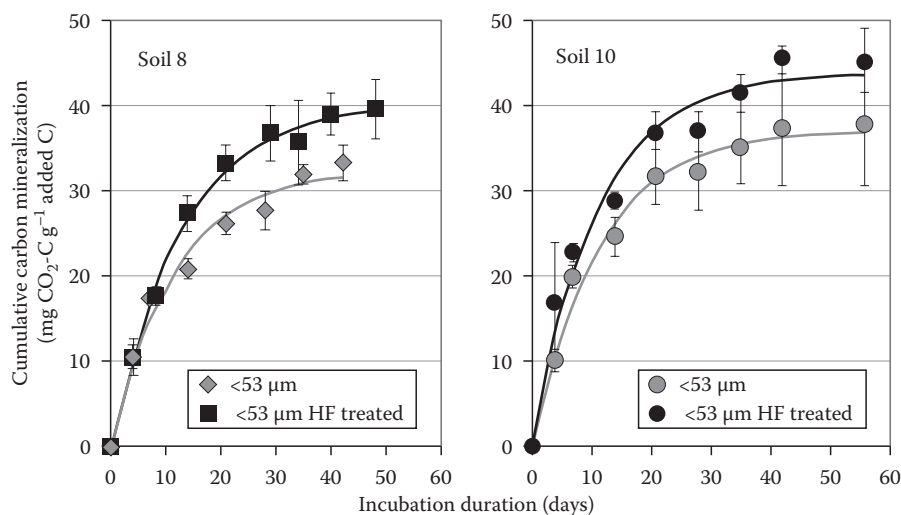


**FIGURE 11.10** Change in mineralizability of  $<53\mu\text{m}$  SOC fractionated from two different Australian soils induced by pretreatment with 2% HF according to Skjemstad (1994).

by a diffusion of the products of enzyme reactions back to the microorganisms (see Section 11.1). With increasing soil clay content, the proportion of the total soil pore space contained in micropores increases, and the potential for protection due to the exclusion of soil microorganisms increases. This concept of exclusion can be extended to the predation of microorganisms by soil fauna. van der Linden et al. (1989) suggested that protozoa and nematodes are excluded from pores  $<5$  and  $<30\mu\text{m}$ , respectively. Killham et al. (1993) showed that although placing glucose into pores  $<6$  or  $<30\mu\text{m}$  did not impact the rate of glucose decomposition, the turnover of glucose C incorporated into the microbial biomass was slower where glucose was only added to pores  $<6\mu\text{m}$ . Strong et al. (2004) showed that decomposition occurs faster in soils with a large volume of pores with neck diameters of  $15\text{--}60\mu\text{m}$ . Their observations pointed to particularly rapid rates of decomposition near the air–water interface, most likely because of the ideal conditions for the organisms' mobility, nutrient or toxin diffusion, and oxygen supply. Furthermore, they suggested that on the one hand, SOC in large air-filled pores decomposes more slowly than in intermediate-sized pores (most likely due to decreased organism mobility, diffusion of solutes, and intimacy of contact between SOC and soil minerals) whereas on the other hand, the carbon trapped in the smallest pores was physically protected against decomposition.

The ability of clay particles to adsorb organic materials can also contribute to a biological protection of SOC through encapsulation and the formation of stable aggregates. Encapsulation of particulate organic residues in soils not only places a physical barrier between decomposer organisms indigenous to soils and potential substrates, but can also limit the movement of water and oxygen to sites of potentially active decomposition. A similar situation develops within soil aggregates. Relative to the larger pores between aggregates, the smaller pores within aggregates are more likely to remain filled with water during drying events, and therefore restrict oxygen movement into the aggregate. The presence of organic cores in aggregates (Beare et al., 1994a, 1994b; Golchin et al., 1994a, 1997a) will serve to increase this effect by enhancing oxygen consumption within the aggregate. It has been found that anaerobic conditions can exist in the core of moist aggregates even under well-aerated conditions (Sexstone et al., 1985). Smaller decomposition rates of SOC enclosed within soil aggregates compared to SOC located outside of soil aggregates have also been shown (Sollins et al., 1996; Angers et al., 1997). In native grasslands, Amelung and Zech (1996) demonstrated that the exterior  $0.5\text{ mm}$  of  $>2\text{ mm}$  diameter peds contained less SOC and had a higher C:N ratio, less lignin, and more microbial-derived saccharides than ped interiors. The SOC associated with ped surfaces, therefore, appeared to turn over more rapidly and exhibited a greater degree of decomposition than that contained within peds.

Soil aggregation is a transient property and aggregates are constantly being formed and destroyed. Quantitative data on soil structural dynamics are, however, lacking. Recently, De Gryze et al. (2005) were able to define a macroaggregate turnover time of  $40\text{--}60$  days using data from a 3 week incubation experiment

and a model assuming an aggregate formation rate proportional to the respiration rate. There was no evidence that aggregate formation differed amongst the three soils examined, which all had a different structure. A subsequent study (De Gryze et al., 2006) confirmed this finding and showed that soil texture affected aggregate stabilization rather than aggregate formation.

### 11.5.3 Biota: Vegetation and Soil Organisms

#### 11.5.3.1 Vegetative Inputs: Variations across and within Ecosystems

Vegetation influences SOC content as a result of the amount, placement, and biodegradability (chemical recalcitrance) of plant residues returned to the soil. Plant residues can be considered the dominant input and thus the primary source of organic carbon into or onto soils (Kögel-Knabner, 2002). Organic molecules created by the soil fauna and microorganisms are the secondary source of decomposable organic carbon in a soil. The greatest effects of vegetation on SOC contents are confined to the A horizon. Concentrations of organic C detected below the A horizon result from a combination of plant input through roots as well as pedogenic processes, which occur over longer timescales. Volkoff and Cerri (1988) showed that for Brazilian soil profiles, current vegetative cover was only in direct equilibrium with topsoil (A horizon) organic C, while that in subsoils was largely unaffected by the nature of vegetative cover. Once the SOC moves to depth (e.g., argillic or spodic horizons), it becomes less accessible to decomposer organisms, as exemplified by the increased depletion of  $^{14}\text{C}$  with soil depth (Pressenda et al., 1996).

Scharpenseel et al. (1992) provided estimates of the amount of organic C contained in the vegetation, soil, and annual litterfall associated with various ecosystems (Figure 11.11). Across the tropical, temperate, and boreal forests, a continuous decrease in the amount of plant biomass and litter C is noted, with little change in the amount of organic C stored in soils. The decrease in the ratio of plant biomass C:SOC was associated with an increase in turnover time from 18 to 60 years. Presumably, most of this variation was related to the effect of temperature on litterfall decomposition; however, significant changes in litterfall quality and morphology are also evident. The amount of residue returned to the soil under similar types of vegetation appears to be a function of climatic factors, principally the amount of precipitation; however, this will depend on the nature of the factor most limiting plant growth. Where ample water is available, the amount of residues returned to the soil may be a function of some other factor such as nutrient supply. For example, it has been shown that P fertilization of Australian pasture soils can increase SOC by 150% or more relative to the native condition (Russel, 1960; Barrow, 1969; Ridley et al., 1990).

Where climatic and soil factors are constant, residue placement may become important. A comparison of the amounts of organic C contained in the plant biomass and soils of temperate grassland and forest ecosystems reveals that despite a much smaller amount of plant biomass in the grassland, annual litter C inputs, and SOC contents were approximately twice that of the



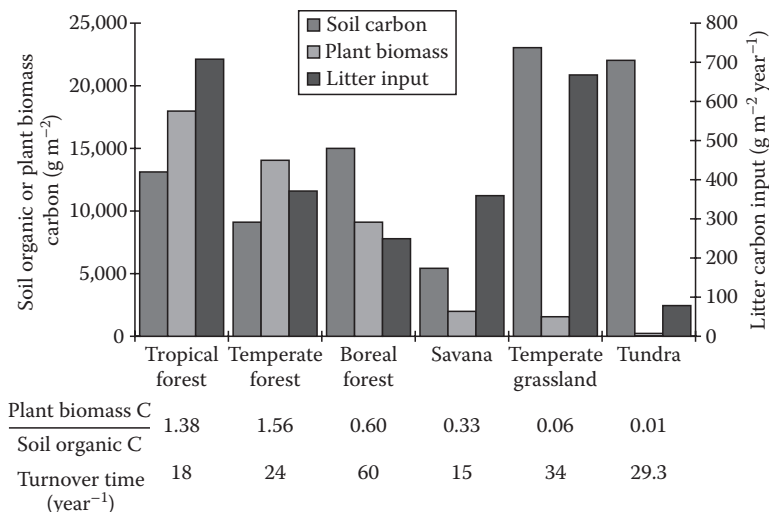


**FIGURE 11.11** Variations in mean soil organic C contents, plant biomass C contents, and rate of litter deposition in various ecosystems. (From Scharpenseel, H.W., H.U. Neue, and S. Singer. 1992. Biotransformations in different climatic belts: Source sink relationships, p. 91–105. *In* J. Kubat (ed.) *Humus, its structure and role in agriculture and environment*. Elsevier Science Publishers, Amsterdam, the Netherlands.)

forests. The occurrence of deep organic-rich mineral horizons in temperate grassland soils (e.g., mollisols), in comparison with the concentration of organic materials in litter layers in boreal forest soil (e.g., spodosols), is an example of the influence that vegetation can have on SOC content and distribution within the soil profile. The apparent larger input of belowground residues in grassland soils compared to forest soils places organic C in close vicinity to the soil mineral components, thereby enhancing the potential for biological protection via the mechanisms discussed in Section 11.1.

The fate of surface-deposited residues depends on the activity of soil microorganisms and fauna and their ability to mix these residues into the surface-mineral horizons. In well-drained soils with high calcium status, the activity of earthworms and other soil fauna is high, leading to a mixing of organic residues through processes of particle-size diminution, ingestion and casting, and bioturbation. Under such conditions, a mull-type HUM layer is formed and litter layers do not develop. Plant residues and their decomposition products are intimately mixed with soil mineral particles, which facilitates potential biological protection through the various organomineral interactions, as discussed in Section 11.5.2. Soils low in calcium do not support as active soil faunal populations and plant residues tend to accumulate on the soil surface forming organic-rich, mor-type HUM layers. Within mor-type HUM, little potential exists for biological protection other than that due to the chemical recalcitrance of highly decomposed residues. The intermediate form of HUM is referred to as a moder.

### 11.5.3.2 Composition of Plant Materials: The Parent Material for Soil Organic C

Plant materials can be viewed as the parent material for SOC in much the same manner as we view primary minerals as the parent materials of soil mineral components. Plant materials are

altered by soil fauna and microorganisms, predominantly after deposition in or on the soil, resulting in changes in the original chemical structure and in the synthesis of new compounds; just as some soil minerals dissolve and others precipitate during pedogenesis. An understanding of the chemical nature of plant materials is therefore important to studies of SOC genesis and composition. Kögel-Knabner (2002) provides a comprehensive review of the molecular composition of plant matter.

Plant materials consist of a range of different compounds varying in concentration across plant species, plant components (e.g., conducting, supporting, or photosynthetic tissues), growth stages, and space (distribution in the landscape). Plant cells can be divided up into three components, the cytoplasm, cell membranes, and cell walls. The cytoplasm contains the simple sugars, organic acids, amino acids, and enzymes essential to maintain metabolic activity. Cell membranes consist of globular proteins embedded within a lipid bilayer. Plant cell-wall components include hemicelluloses, celluloses, lignins, proteins, cuticular, and root waxes. Oades (1989) presented the following average contents for the major types of organic C in plant residues:

1. Extractable materials including water extractables (simple sugars, amino acids, and organic acids) and organic solvent extractables (free and bound alkyl molecules including fats, oils, and waxes)—200 g kg<sup>-1</sup>
2. Hemicelluloses—200 g kg<sup>-1</sup>
3. Celluloses—300 g kg<sup>-1</sup>
4. Lignins—200 g kg<sup>-1</sup>
5. Proteins—60 g kg<sup>-1</sup>

The organic components of plant cell walls account for the majority of the mass of plant residues deposited in soils. Carbohydrate structures consist mainly of the polysaccharides cellulose and hemicellulose. Cellulose is the primary component of cell walls with a dominant structure of D-glucopyranose

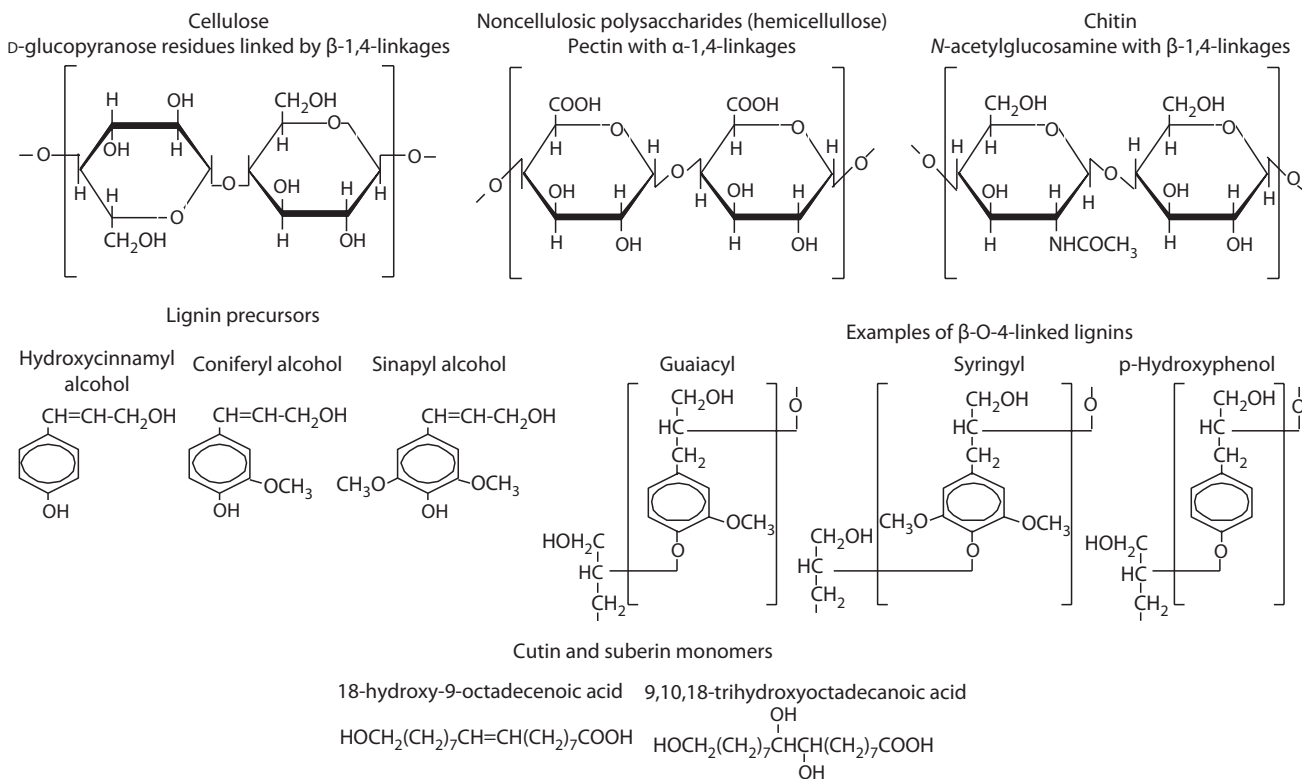


FIGURE 11.12 Representative chemical structures of the organic macromolecules found in plant and microbial residues entering the soil.

residues linked into a polymer via  $\beta$ -1,4-linkages (Figure 11.12). Cellulose can exist in either a crystalline or amorphous state as indicated by x-ray diffraction (Atalla and Vanderhart, 1984) and solid-state  $^{13}\text{C}$  NMR (Vanderhart and Atalla, 1984). The crystalline state is more highly resistant to microbial and enzymatic degradation than the amorphous form (Ljungdahl and Eriksson, 1985). Hemicellulose is defined as the polysaccharide extractable in alkali solution. The hemicelluloses exist as linear and branched polymers of D-xylose, L-arabinose, D-mannose, D-glucose, D-galactose, and D-glucuronic acid monomers, which may be acetylated or methylated. Most hemicelluloses are composed of 2–6 of these monomers linked together primarily via a 1,4- $\beta$ -linkage backbone as shown in Figure 11.12 for pectin, a glucuronic acid polymer.

Lignin represents the second most abundant organic compound in plant residues and accounts for approximately 5% of the mass of grasses and up to 30% of the mass of hardwood forest species (Haider, 1992). The basic building block of lignin, coumaryl alcohol, can be substituted with none, one, or two methoxyl groups at the C-3 and C-5 positions on the benzene ring to produce the p-hydroxyphenol, guaiacyl, and syringyl lignin monomeric units, respectively (Figure 11.12). The units are then linked together by more than 12 possible interunit linkages based on C–O or C–C bonds (McDougall et al., 1993). The major interunit linkage, accounting for about 60% of the linkages, is the  $\beta$ -O-4-linkage depicted in Figure 11.12 for the three lignin monomeric units. The nature of the lignin molecule changes with plant type: softwoods (gymnosperms) are dominated by

guaiacyl-based lignin, hardwoods (angiosperms) contain a mixture of guaiacyl- and syringyl-based lignin, and grasses are dominated by syringyl lignin. Results presented by Hedges et al. (1985) suggested that such changes in lignin composition can affect its biodegradability, with syringyl lignin being more susceptible to decomposition than guaiacyl lignin.

The protein and water-soluble components of plant residues, unless protected against biological attack, provide a readily decomposable substrate capable of supplying the chemical energy and nutrients required to drive soil biological processes. Enzymatic cleavage of the peptide linkages to form amino acids and mineralization of amino acid N to form  $\text{NH}_4^+$  provide sources of N for soil biological processes, and the abiotic chemical processes, to be discussed subsequently.

Alkyl components of plant materials include free and bound lipids, polyesters, and nonsaponifiable alkyl C dominated biopolymers. Free and bound lipids represent a heterogeneous group of neutral and polar molecules, which are classified together based on their solubility in organic solvents (Tegelaar et al., 1989). The neutral component consists of triacylglycerols and waxes, which serve to protect external plant surfaces and to store energy. The polar component is dominated by the esterified fatty acids found in cell membranes. Insoluble polyesters, derived from hydroxy fatty acids, are found in cutin in plant cuticles and in suberin in roots. Cutin and suberin are composed of various long-chain ( $\text{C}_{16}$  and  $\text{C}_{18}$ ), substituted fatty acids. The main substituent group is hydroxyl with lesser amounts of epoxy, ketone, and carboxyl groups also present (Holloway, 1982).

Two examples of cutin and suberin monomers are presented in Figure 11.12, and Tegelaar et al. (1989) have presented figures showing additional monomeric chemical structures and a proposed model of the structure of intact cutin and suberin. Plant cuticles and roots have also been shown to contain nonsaponifiable aliphatic biopolymers, which have been labeled cutan and suberan (Nip et al., 1986a, 1986b, 1987). Cutan and suberan are considered similar to cutin and suberin with the exception that they are highly cross-linked by nonester bonds.

In order to assess the influence of plant-residue composition on decomposition and mineralization, it is essential to remove other confounding effects such as climatic, soil, and biological parameters. In field studies, this can be accomplished by examining decomposition of all residues of interest at a single site. Vedrova (1997) assessed the impact of forest species on litter decomposition rates by placing litter collected from each species on small plots located within a single unforested site. Mean rates of mineralization measured for cedar, pine, larch, spruce, aspen, and birch litter over  $\approx 2$  years were 1.93, 1.57, 1.85, 2.20, 2.56, and 2.57 mg C g<sup>-1</sup> litter C day<sup>-1</sup>, respectively. A limitation of such studies is demonstrated, however, by the work of Elliott et al. (1993), in which the decomposition of four different forest litters (mixed hardwood, red pine, beech, and hemlock) was examined in each of the original four forest types. The rates of decomposition were principally a function of litter type, with mixed hardwood litter decomposing the fastest and hemlock litter the slowest. However, with the exception of the mixed hardwood litter, decomposition rates of the individual litter types were highest when they were placed in the forest type from which they were derived (i.e., decomposition of the hemlock litter was greatest in the hemlock forest). This interaction between litter type and forest type suggests that decomposition pathways in any given ecosystem may be tailored to the type of litter deposited. Thus, the results of decomposition studies where litters are removed from their ecosystem of origin, or where the community structure of the decomposer organisms is altered, may not accurately reflect the relative effects of residue composition on decomposability.

### 11.5.3.3 Relative Impacts of Soil Fauna and Microorganisms

The requirement of soil organisms for chemical energy and nutrients drives processes of heterotrophic decomposition in soils, which account for the major pathways through which SOC is mineralized. Abiotic chemical oxidation is unlikely to account for >20% of total C mineralization (Moorhead and Reynolds, 1989) and more often accounts for <5% (Lavelle et al., 1993). Microorganisms are the major contributors to soil respiration and are responsible for 80%–95% of the mineralization of C (Brady, 1990; Hassink et al., 1994). Hassink et al. (1994) calculated that the contribution of the fauna to C mineralization in two sandy and two loamy grassland soils to range from 5% to 13% of the total C mineralization. The pattern of C mineralization by the soil fauna through time differed from that of total C mineralization, suggesting that the activity of the soil fauna did not contribute substantially to the differences in total C

mineralization observed between the soils. Hassink et al. (1993) concluded that soil protozoa and nematodes did not significantly influence soil C mineralization despite a positive response of bacterivorous nematodes on the amount of N mineralized. Several other studies have shown that soil fauna enhanced nutrient mineralization had both positive and negative effects on SOC mineralization (Griffiths, 1994; Kajak, 1995; Alpehi et al., 1996). In a study including protozoa, nematodes, and earthworms, Alpehi et al. (1996) noted that none of the fauna studied significantly affected basal respiration. However, other studies showed that earthworm invasion can have a marked potential to alter (usually reduce) soil C storage on local and regional scales (Alban and Berry, 1994; Bohlen et al., 2004).

The role of soil fauna in decomposition processes should not be based only on their direct contribution to C mineralization. Soil fauna also act to reduce the particle size of litter, distribute it within the soil, transport otherwise immobile microorganisms to new sites within the soil matrix, and prime microorganism activities by the production of readily available substrates (e.g., earthworm intestinal mucus). In so doing, soil fauna generally enhance microbial activity and rates of decomposition. Soil conditions, which limit (e.g., water saturation and the development of anaerobic conditions) or enhance (e.g., tillage or installation of drains in imperfectly drained soils) the activity of soil microorganisms or fauna, will also impact significantly SOC mineralization rates and thus alter SOC levels.

### 11.5.3.4 Composition of the Microbial Community

The population of decomposer microorganisms in soil is extensive; densities up to 10<sup>10</sup> bacteria and several kilometers of fungal hyphae per gram of soil have been measured in a wide range of soils (Lavelle et al., 1993). As a result of the diversity of decomposer organisms, the existence of interactions between specific types of organic residue and species of decomposer organisms can have pronounced effects on the chemical structure and biological availability of residual organic materials. The decomposition of woody materials provides an excellent example of how the species composition of the decomposer population can influence the chemical nature of decomposition products. Laboratory incubations of *Eucryphia cordifolia* wood with a brown-rot fungus (unidentified species) and a white-rot fungus (*Ganoderma australe*) showed a more selective utilization of carbohydrate C by the brown-rot fungus and a delignification by the white-rot fungus (Martínez et al., 1991). Using the same white-rot fungus in a solid-state fermentation procedure with beech wood, Martínez et al. (1991) noted little change in the chemical composition of the wood, despite a 36% mass loss. Barrasa et al. (1992) obtained similar results in an ultrastructural study. Selective delignification of *Laurelia philippiana* wood by the white-rot fungus *Phlebia chrysocrea* was noted, but decomposition of the same wood by *G. australe* resulted in increased lignin contents. The selective degradation of carbohydrates by brown-rot fungi appears to occur independently of the fungal or wood species involved. However, the presence of a selective or nonselective degradation process for white-rot fungi

appears to depend on interactions between the species of fungus and wood. Under anaerobic conditions, the activity of obligate aerobes such as wood-degrading fungi is limited and bacterial decomposition processes dominate. In examinations of buried woods, it has been found that decomposition processes invariably result in a preferential utilization of carbohydrates and a concentration of lignin (e.g., Bates and Hatcher, 1989; Bates et al., 1991). Such data indicate that changes in species composition of the decomposer community can significantly alter the decomposition processes and thus, rates of accumulation or loss of organic C from soils.

Earlier in this chapter, a conceptual framework to describe the controls over the decomposition process was presented (Figure 11.5) that was built around the concepts of biological capability and capacity. Various methods can provide information regarding the biological capability and capacity of decomposer communities and the way these properties can be affected by environmental parameters and management practices. For example, the potential degradative capabilities of decomposer communities can be measured using substrate utilization profiles based on Biolog plates (e.g., Bochner, 1989; Bucher and Lanyon, 2005) or microrespirometry like the MicroResp™ method (e.g., Campbell et al., 2003; Wakelin et al., 2008), which is a relatively recent method of community level physiological profiling (CLPP) and uses whole soil samples rather than soil extracts thereby eliminating extraction bias. Furthermore, the extraction and analysis of DNA and RNA (e.g., PCR-DGGE) from soils as well as phospholipid fatty acids (PLFA) can provide an indication of the genetic diversity and structure of soil microbial communities (Muyzer et al., 1993; Widmer et al., 2001; Crecchio et al., 2004; Wakelin et al., 2008). Several indices and multivariate statistical analyses can be used with these techniques to determine the influence of soil and environmental properties on the capability and capacity of the microbial community. Several factors have already been investigated like the influence of soil type (Schutter and Dick, 2000; Banu et al., 2004; Wakelin et al., 2008), crop rotation (Bending et al., 2004; Crecchio et al., 2004), application of various fertilizers (Bucher and Lanyon, 2005), vegetation (De Fede et al., 2001), and agricultural management practice (Wakelin et al., 2008). Although the methods have proven to be reproducible, different results between the different methods have been identified (Widmer et al., 2001). Therefore, it is recommended not to use these methods in isolation if a representative assessment of the composition of the microbial community is desired.

### 11.5.3.5 Relationship between Organic Residue Composition and Biochemical Recalcitrance

All organic C in soils can serve as a substrate. In addition to the potential mechanisms of biological protection of organic materials offered by the soil mineral fraction, the chemical structure of the organic residue itself can also impart a degree of biochemical recalcitrance. This biochemical recalcitrance of the potential substrate is defined by the strength of intra- and intermolecular bonds, the degree of polymerization and regularity of structural

units in polymers, and the content of aromatic and aliphatic functional groups (Baldock et al., 1997a; Gleixner et al., 2001). Rates of decomposition of known organic substances in soils were reviewed by Paul and van Veen (1978). Although variations in decomposition rates for any single substrate were evident as a result of differences in soils and incubation conditions, simple organic molecules and monomeric compounds decomposed most rapidly. Oades (1989) showed that the extent and rate of mineralization of C for a series of polysaccharides (glucose, dextran, cellulose, and a fungal polysaccharide) decreased with increasing molecular complexity and branching. Similar results were obtained by Martin and Haider (1975) for the mineralization of C from specifically <sup>14</sup>C-labeled benzoic and caffeic acid monomers and polymers. C mineralization was most extensive from carboxylic acid groups, less extensive from the aromatic ring C of the monomers, and least extensive from the polymeric aromatic ring C. Of the polymeric materials contained in plant residues, lignin and other polyphenolic C and aliphatic C appear to be the most recalcitrant, but, as discussed in the previous section, the stability of lignin C will be also related to the species composition of the decomposer community.

Many studies have demonstrated a relationship between decomposition and plant-residue characteristics thought to be indicative of residue quality (e.g., Edmonds and Thomas, 1995; Ågren and Bosatta, 1996; Cortez et al., 1996; Hobbie, 1996). Included in these residue characteristics are N concentration, C:N ratios, lignin and/or polyphenol concentration, lignin:nitrogen ratios, and acid-soluble carbohydrates (Heal et al., 1997). Ågren and Bosatta (1996) found that the proportions of extractable, acid-soluble, and acid-insoluble C obtained from a conventional chemical fractionation could be used to assess the quality of forest litter, particularly when the acid-insoluble fraction did not dominate.

During the decomposition of plant residues, significant changes in chemical composition of residual C are evident (Baldock et al., 1997a). In response to such changes, Berg and Staaf (1980) proposed a model of litter decay in which decomposition was controlled initially by N content but subsequently by lignin concentration. This was supported by the results of Edmonds and Thomas (1995), which showed that organic C mineralization rates from green needles of western hemlock and pacific silver fir were initially similar, but became more a function of litter chemistry (e.g., lignin:N ratio) as decomposition progressed.

### 11.5.4 Topography

Topography exerts its major control over SOC contents through a modification of climate and soil textural factors and through its impacts on the redistribution of water within a landscape. Soils in downslope positions are often wetter and have finer textures than soils in upslope positions or at the top of knolls. Topographic-induced changes in the soil microenvironment often lead to changes in plant communities (Sebastian, 2004), which in turn can influence the magnitude and quality of residue returns. Burke et al. (1995) examined the extent to which

SOC content varied at a landscape scale at two sites differing in soil texture but having similar climatic characteristics. Burke et al. (1995) noted increased organic C contents (and clay and silt contents) in downslope positions relative to the summits at both sites. Such a finding has been attributed to the downslope movement of organic C and organic-rich clay (Reiners, 1983). However, additional gradients in available water along slopes, especially in water-limited systems, influence plant production (Peterson et al., 1988), with greater biomass inputs and greater potential biological protection of organic C via higher clay contents at the base of slopes. Where excessive water exists, drainage of depressions in the landscape can be restricted, leading to the development of anaerobic conditions and a preservation of organic C relative to the better-drained higher landscape elements during wetter times of the year.

Guo et al. (2006) showed that the SOC decreases as elevation increases and that level topography had twice the SOC content of other slope classes. Particularly, in mountain areas that are by nature highly heterogeneous, taking topography into account is required to predict SOC stocks across the landscape. In a study investigating the SOC storage in mountain grasslands of the Pyrenees, Garcia-Pausas et al. (2007) found that the SOC stocks were particularly low at high altitudes probably as a result of an overall temperature limitation of NPP. Climatic and topographic variables were able to predict a significant part of the C storage variability in the mountain grasslands examined by Garcia-Pausas et al. (2007). The microclimate conditions related to topographic position (aspect and slope) were identified as important factors for predicting C storage in soils of the high-altitude grasslands and should be taken into account to achieve accurate estimations of C stocks in mountain ecosystems.

As a consequence of all the possible confounding factors, it is difficult to study the sole effects of topography. For example, the interactive effects of topography (depositional and erodible zones) and tillage (conventional versus minimum tillage [MT]) on the redistribution of C, N, and P within an agricultural landscape were examined by De Gryze et al. (2008). In general, organic matter content and moisture content were greater in lower, depositional areas compared to erodible areas, and the impact of topography on the stabilization and redistribution processes of nutrients was more pronounced in conventional tillage (CT) than MT. This last finding clearly demonstrates that interactions between topographic characteristics and land management practices should be considered in regional inventory assessments of SOC (De Gryze et al., 2008).

### 11.5.5 Land Management Practices

Paustian et al. (1997b) reviewed the influence of agricultural management practices on SOC levels. Hutchinson et al. (2007) summarized the relative rates of SOC change for a range of “carbon friendly” agricultural management treatments and found that most changes were  $<0.6 \text{ Mg C ha}^{-1} \text{ year}^{-1}$ . The influence of forestry management practices has also been reviewed (Johnson, 1992; Johnson and Curtis, 2001; Johnson et al., 2002).

The most dramatic influence of agricultural practices occurs when soils are first brought into production. Typically, SOC levels decrease for the first few decades after cultivation and then stabilize at a new equilibrium level, which is dictated principally by the ability of the soil to protect organic C and the amount, quality, and distribution of plant-residue inputs. For example, Haas et al. (1957) observed a loss of 28%–59% of the SOC following 30–43 years of cropping at 11 sites within the North American prairies. David et al. (2009) also measured reductions SOC (30%–50%) due to the conversion of prairies to annual cultivation and artificial drainage using archived samples and long-term resampling of soils.

The following characteristics of crop production systems, in comparison with those of native grasslands, help to explain the observed losses of SOC induced by cultivation:

1. 80% lower allocation of organic C to soils (Buyanovsky et al., 1987)
2. Reduced belowground allocation of photosynthate (Anderson and Coleman, 1985)
3. Enhanced aggregate disruption and exposure of physically protected organic C due to cultivation
4. Enhanced rates of decomposition of available organic C substrates due to more favorable abiotic conditions (e.g., aeration, temperature, and water content)

In practice, continuous alteration of land management and cropping practices (e.g., adoption of reduced tillage, the inclusion, or removal of pasture) will lead to a system where SOC levels are always in a state of flux, increasing with some practices and decreasing with others (Baldock and Skjemstad, 1999). Only if management practices are left in place long enough, it is possible to gain an indication of what the new equilibrium SOC value would be for any given land management system.

Field trials set up to examine the impact of fertilizer additions on SOC content, have revealed that the addition of N fertilizers typically enhances SOC contents. This is particularly true in temperate-zone ecosystems where N availability is thought to limit NPP (Peterson and Melillo, 1985; Schimel et al., 1996; Holland et al., 1997). Explanatory mechanisms suggest that N-fertilizer additions result in a greater return of plant residues to soils due to enhanced production, a reduction in decomposition rates due to enhanced soil drying (Andr n, 1987), a promotion of soil acidification (Thurston et al., 1976), a repression of lignolytic enzymes, and a formation of recalcitrant humic materials through the reaction of amino acids with humic precursors (Fog, 1988).

In tropical systems, the establishment of pastures after clearing of forests is widespread (Sombroek et al., 1993). Pasture establishment immediately after deforestation, using species with high proportions of belowground biomass, may increase SOC contents as demonstrated in the Brazilian Amazon (Serr o et al., 1979), Latin America (Ligel, 1992), and East Africa (Boonman, 1993).

The intensity with which a soil is cultivated can impact both the total amount of SOC and its distribution with soil depth. No-till systems tend to concentrate residue inputs at the soil

surface and generally enhance soil organic C and N contents in soil surface layers (Angers and Eriksen-Hamel, 2008). To accurately evaluate the influence of tillage practices on SOC stocks, it is important to collect soil samples beyond the depth of tillage and to account for variations in soil bulk density. Paustian et al. (1997b) presented data from a number of long-term field trials indicating that SOC retention is typically enhanced under no-till relative to more intensive CT systems. However, in a review of Australian publications, Valzano et al. (2005) found that a positive effect of no-till or reduced till on SOC in the 0–30-cm soil layer could only be demonstrated at high annual rainfalls (>660 mm). Valzano et al. (2005) also noted that the separation of residue handling from the physical effect of passing an implement through the soil was difficult to separate given the wide range of residue handling practices associated with the different tillage systems.

## 11.6 Contribution of Soil Organic Matter to the Global Carbon Cycle

The organic carbon contained within SOM represents a significant reservoir of carbon within this global carbon cycle (Figure 11.13). SOC has been estimated to account for 1200–1550 Pg of C (1 Pg =  $10^{15}$  g) to a depth of 1 m and for 2300–2450 Pg of C to a depth of 2 or 3 m (Eswaran et al., 1995; Jobbagy and Jackson, 2000; Lal, 2004a; Houghton, 2005). Comparative estimates of organic C contained in living biomass (550–560 Pg) and the atmosphere  $\text{CO}_2\text{-C}$  (760–780 Pg; Lal, 2004a; Houghton, 2005) indicate that variations in the size of the SOC store could significantly alter atmospheric  $\text{CO}_2\text{-C}$  concentrations. For example, a 5% shift in the amount of SOC stored in the 0–2 m soil profile has the potential to alter atmospheric  $\text{CO}_2\text{-C}$  by up to 16%.

Land-use changes can induce either a net emission or a net sequestration of organic carbon in soil depending on the

resultant balance between losses and inputs. The net change in inputs and losses will be defined by the soil and environmental properties and land management practices discussed previously. Sequestration of organic carbon in soil is a slow process typically requiring decades, but is suggested to offer the most efficient natural strategy for offsetting increased atmospheric  $\text{CO}_2\text{-C}$  concentrations (Metting et al., 1999; Post et al., 1999; Lal, 2004b). Over the next century, improved land management strategies may have the capacity to sequester up to 150 Pg of  $\text{CO}_2\text{-C}$  (Lal et al., 1998; Lal, 2004a). Considerable uncertainty exists in such estimates because of an inability to accurately predict the potential sequestration of carbon that is possible in soil. Improving our understanding of SOC cycling processes and how these are affected by environment and land management practices will be vital to identify opportunities for building SOM and sequestering carbon in soils.

Estimates of the potential to sequester carbon in agricultural soils have been made for the United States (Lal et al., 1998), Canada (Bolinder et al., 2008), China (Han et al., 2005, 2006), the European Union (Freibauer et al., 2004; Janssens et al., 2005; Romanenkov et al., 2007), and South America (Cerri et al., 2004, 2006). Such estimates are typically based on the use of long-term field experiments or simulation modeling. Where estimates are based on field experiments, it is important to ensure that the potential for saturation of the soils capacity to protect carbon from decomposition is acknowledged and that measured carbon sequestration rates are not projected unimpeded into the future. A similar consideration must be applied to soil carbon simulation modeling activities. Most soil carbon models apply first-order kinetics to the decomposition of component carbon pools (Paustian, 1994). Therefore, predicted equilibrium carbon stocks are linearly proportional to carbon inputs (Paustian et al., 1997a, 1997b; Six et al., 2002), and modeling activities predict that unlimited increases in soil carbon stocks can occur provided inputs of carbon to the soil can continue to increase.

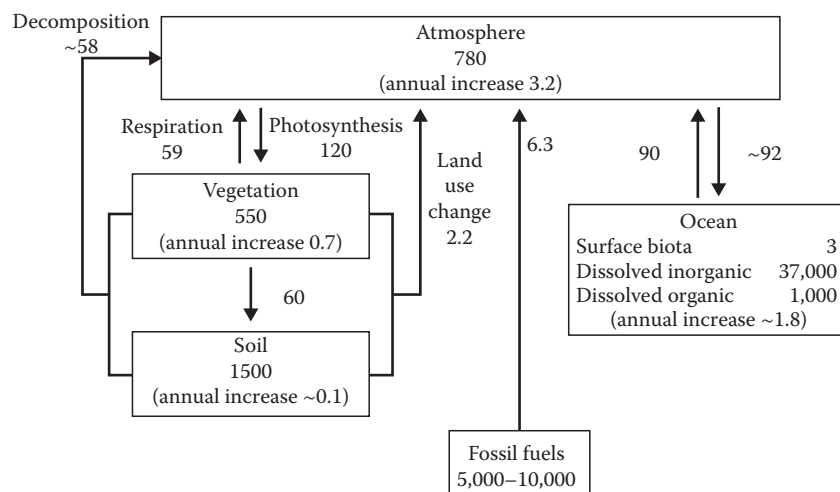


**FIGURE 11.13** The global carbon cycle. All pool sizes are in units of Pg C and all fluxes are given in units of Pg C year<sup>-1</sup>. (Adapted from Houghton, R.A. 2005. The contemporary carbon cycle, p. 473–513. In W.H. Schlesinger (ed.) Biogeochemistry. Elsevier Science, Amsterdam, the Netherlands.)

Since carbon inputs to soil will be limited by constraints placed on photosynthesis (e.g., availability of water, nutrients, heat, and ultimately light) and current soil carbon simulation models do not define a maximum soil carbon protective capacity, modeled estimates of potential carbon sequestration in soils need to be carefully scrutinized.

The concept of soil carbon saturation suggests that each soil has a unique carbon saturation level dictated by soil properties including texture, mineralogy, bulk density, and depth (Ingram and Fernandes, 2001; Six et al., 2002; Stewart et al., 2008a, 2008b). Soil carbon sequestration potential should therefore be estimated as the difference between the current and saturated soil carbon content. Defining soil carbon saturation values has proven difficult, although Hassink (1992) suggested that the amount of carbon obtained under long-term pastures may provide an indication. Furthermore, true soil carbon saturation values may be of limited importance if the inputs of organic carbon required to attain and maintain such levels are beyond the capture of carbon by photosynthesis and deposition within soil. Of more practical interest would be the behavior of soils as they approach their carbon saturation capacity as well as the influence of soil carbon saturation deficit on the efficiency of the SOC accumulation in saturated soils.

Although soil carbon does offer the possibility for sequestering atmospheric CO<sub>2</sub>-C, the potential for soil carbon sequestration in soil is small compared to projected emission of CO<sub>2</sub> from current energy practices (about 150 Pg versus 600 Pg over the next 100 years). Soil carbon sequestration is also finite, an upper limit exists, and as soils move toward the upper limit, the rate of soil carbon sequestration will diminish. Enhancing soil carbon from atmospheric CO<sub>2</sub>-C sequestration should therefore be viewed as a mechanism for “buying time” for the development and implementation of longer-lasting measures for reducing fossil fuel emissions (Watson et al., 2000; Houghton, 2005). However, it is also important to recognize that increasing sequestration of carbon in soils by building SOM may offer the added benefit of increased productivity through mechanisms discussed previously.

## 11.7 Summary

Soil organic matter is a complex mixture of a variety of materials derived initially from photosynthesis by plants but then altered through decomposition processes that enhance its diversity in composition. Such compositional diversity provides the SOM with the capability to contribute beneficially to the many functions that it serves in a soil. Key goals for future work on SOM should include the following:

1. An acknowledgment of the diversity in SOM composition and a development of fractionation systems capable of quantitatively dividing SOM up into biologically relevant components
2. Development of predictive relationships that quantify the role of each component to the various functions to which

SOM contributes and an assessment of any soil type specificity that may exist

3. Parameterization of carbon cycling models build on measurable components and inclusion of the quantitative relationships between SOM composition and soil properties (functions) to allow the prediction of both SOM dynamics and the subsequent impacts on soil properties

With the potential for large-scale introduction of carbon trading schemes and a requirement to reduce the emission of greenhouse gases, a more complete understanding of SOM dynamics and how altering SOM will alter soil properties will be essential. Such understanding is required to develop viable land management practices that accommodate the potentially conflicting issues of maintaining food security for an increasing global population, ensuring profitability of individual farming enterprises, and enhancing the capture of atmospheric CO<sub>2</sub> as organic matter in soils while reducing emissions of other greenhouse gases (nitrous oxide and methane).

## Acknowledgments

Contributions from the Australian Department of Climate Change and the Grains Research and Development Corporation of Australia to research projects of the Carbon and Nutrient Cycling Group within CSIRO Land and Water as well as the many interactions that the authors have had with research scientists globally are gratefully acknowledged.

## References

- Achard, F.K. 1786. Chemische untersuchungen des torts. *Crell's Chem. Ann.* 2:391–403.
- Ågren, G.I., and E. Bosatta. 1996. Quality: A bridge between theory and experiment in soil organic matter studies. *Oikos* 76:522–528.
- Alban, D.H., and E.C. Berry. 1994. Effects of earthworm invasion on morphology, carbon, and nitrogen of a forest soil. *Appl. Soil Ecol.* 1:243–249.
- Alphei, J., M. Bonkowski, and S. Scheu. 1996. Protozoa, nematoda and lumbricidae in the rhizosphere of *Hordelymus europaeus* (Poaceae): Faunal interactions, response of microorganisms and effects on plant growth. *Oecologia* 106:111–126.
- Amato, M.A., and J.N. Ladd. 1992. Decomposition of <sup>14</sup>C-labelled glucose and legume material in soils: Properties influencing the accumulation of organic residue C and microbial biomass C. *Soil Biol. Biochem.* 24:455–464.
- Amelung, W., R. Bol, and C. Friedrich. 1999. Natural <sup>13</sup>C abundance: A tool to trace the incorporation of dung-derived carbon into soil particle-size fractions. *Rapid Commun. Mass Spectrom.* 13:1291–1294.
- Amelung, W., K.W. Flach, and W. Zech. 1997. Climatic effects on soil organic matter composition in the great plains. *Soil Sci. Soc. Am. J.* 61:115–123.

- Amelung, W., and W. Zech. 1996. Organic species in ped surface and core fractions along a climosequence in the prairie, North America. *Geoderma* 74:193–206.
- Amelung, W., and W. Zech. 1999. Minimisation of organic matter disruption during particle-size fractionation of grassland epipedons. *Geoderma* 92:73–85.
- Anderson, D.W. 1995. The role of nonliving organic matter in soils, p. 81–92. *In* R.G. Zepp and C. Sonntag (eds.) Role of nonliving organic matter in the earth's carbon cycle. Vol. 16. John Wiley & Sons Ltd., Chichester, West Sussex, England.
- Anderson, D.W., and D.C. Coleman. 1985. The dynamics of organic matter in grassland soils. *J. Soil Water Conserv.* 40:211–216.
- Anderson, J.P., and K.H. Domsch. 1973. Quantification of bacterial and fungal contributions to soil respiration. *Arch. Mikrobiol.* 93:113–127.
- Anderson, J.P.E., and K.H. Domsch. 1978. Physiological method for quantitative measurement of microbial biomass in soils. *Soil Biol. Biochem.* 10:215–221.
- Anderson, D.W., and E.A. Paul. 1984. Organo-mineral complexes and their study by radiocarbon dating. *Soil Sci. Soc. Am. J.* 48:298–301.
- Andrén, O. 1987. Decomposition of shoot and root litter of barley, lucerne and meadow fescue under field conditions. *Swed. J. Agric. Res.* 17:113–122.
- Angers, D.A., and N.S. Eriksen-Hamel. 2008. Full-inversion tillage and organic carbon distribution in soil profiles: A meta-analysis. *Soil Sci. Soc. Am. J.* 72:1370–1374.
- Angers, D.A., S. Recous, and C. Aita. 1997. Fate of carbon and nitrogen in water-stable aggregates during decomposition of  $^{13}\text{C}$   $^{15}\text{N}$  labelled wheat straw. *Eur. J. Soil Sci.* 48:295–300.
- Appuhn, A., R.G. Joergensen, M. Raubuch, E. Scheller, and B. Wilke. 2004. The automated determination of glucosamine, galactosamine, muramic acid, and mannosamine in soil and root hydrolysates by HPLC. *J. Plant Nutr. Soil Sci.* 167:17–21.
- Asadu, C.L.A., J. Diels, and B. Vanlauwe. 1997. A comparison of the contributions of clay, silt, and organic matter to the effective CEC of soils of subSaharan Africa. *Soil Sci.* 162:785–794.
- Atalla, R.H., and D.L. Vanderhart. 1984. Native cellulose: A composite of two distinct crystalline forms. *Science* 223:283–285.
- Bachmann, J., G. Guggenberger, T. Baumgartl, R.H. Ellerbrock, E. Urbanek, M.O. Goebel, K. Kaiser, R. Horn, and W.R. Fischer. 2008. Physical carbon-sequestration mechanisms under special consideration of soil wettability. *J. Plant Nutr. Soil Sci.* 171:14–26.
- Baldock, J.A. 2002. Interactions of organic materials and microorganisms with minerals in the stabilization of soil structure, p. 85–131. *In* P.M. Huang et al. (eds.) Interactions between soil particles and microorganisms and the impact on the terrestrial ecosystem. John Wiley & Sons, New York.
- Baldock, J.A. 2007. Composition and cycling of organic carbon in soil, p. 1–35. *In* P. Marschner and Z. Rengel (eds.) Soil biology. Vol. 10. Nutrient cycling in terrestrial ecosystems. Springer-Verlag, Berlin, Germany.
- Baldock, J.A., C.A. Masiello, Y. Gélinas, and J.I. Hedges. 2004. Cycling and composition of organic matter in terrestrial and marine ecosystems. *Mar. Chem.* 92:39–64.
- Baldock, J.A., and P.N. Nelson. 2000. Soil organic matter, p. B25–B84. *In* M. Sumner (ed.) Handbook of soil science. CRC Press, Boca Raton, FL.
- Baldock, J.A., J.M. Oades, P.N. Nelson, T.M. Skene, A. Golchin, and P. Clarke. 1997a. Assessing the extent of decomposition of natural organic materials using solid-state  $^{13}\text{C}$  NMR spectroscopy. *Aust. J. Soil Res.* 35:1061–1084.
- Baldock, J.A., J.M. Oades, A.M. Vassallo, and M.A. Wilson. 1989. Incorporation of uniformly labeled C-13 glucose carbon into the organic fraction of a soil. Carbon balance and CP MAS C-13 NMR measurements. *Aust. J. Soil Res.* 27:725–746.
- Baldock, J.A., J.M. Oades, A.G. Waters, X. Peng, A.M. Vassallo, and M.A. Wilson. 1992. Aspects of the chemical structure of soil organic materials as revealed by solid-state  $^{13}\text{C}$  NMR spectroscopy. *Biogeochemistry* 16:1–42.
- Baldock, J.A., T. Sewell, and P.G. Hatcher. 1997b. Decomposition induced changes in the chemical structure of fallen red pine, white spruce and tamarack logs, p. 75–83. *In* G. Cadisch and K.E. Giller (eds.) Driven by nature: Plant litter quality and decomposition. CAB International, Wallingford, U.K.
- Baldock, J.A., and J.O. Skjemstad. 1999. Soil organic carbon/soil organic matter, p. 159–170. *In* K.I. Peverill et al. (eds.) Soil analysis: An interpretation manual. CSIRO Publishing, Collingswood, Victoria, Australia.
- Baldock, J.A., and J.O. Skjemstad. 2000. Role of the soil matrix and minerals in protecting natural organic materials against biological attack. *Org. Geochem.* 31:697–710.
- Baldock, J.A., and R.J. Smernik. 2002. Chemical composition and bioavailability of thermally altered *Pinus resinosa* (Red pine) wood. *Org. Geochem.* 33:1093–1109.
- Banu, N.A., B. Singh, and L. Copeland. 2004. Microbial biomass and microbial biodiversity in some soils from New South Wales, Australia. *Aust. J. Soil Res.* 42:777–782.
- Barrasa, J.M., A.E. Gonzalez, and A.T. Martinez. 1992. Ultrastructural aspects of fungal delignification of Chilean woods by *Ganoderma australe* and *Phlebia chrysocrea*. A study of natural and *in vitro* degradation. *Holzforschung* 46:1–8.
- Barrow, N.J. 1969. The accumulation of soil organic matter under pasture and its effect on soil properties. *Aust. J. Exp. Agric. Anim. Husb.* 9:437–444.
- Bates, A.L., and P.G. Hatcher. 1989. Solid-state C-13 NMR studies of a large fossil gymnosperm from the Yallourn open cut, Latrobe Valley, Australia. *Org. Geochem.* 14:609–617.
- Bates, A.L., P.G. Hatcher, H.E. Lerch, C.B. Cecil, S.G. Neuzil, and Supardi. 1991. Studies of a peatified angiosperm log cross section from Indonesia by nuclear magnetic resonance spectroscopy and analytical pyrolysis. *Org. Geochem.* 17:37–45.
- Beare, M.H., M.L. Caberra, P.F. Hendrix, and D.C. Coleman. 1994a. Aggregate-protected and unprotected organic matter pools in conventional- and no-tillage soils. *Soil Sci. Soc. Am. J.* 58:787–795.



- Beare, M.H., P.F. Hendrix, and D.C. Coleman. 1994b. Water-stable aggregates and organic matter fractions in conventional and no-tillage soils. *Soil Sci. Soc. Am. J.* 58:777–786.
- Beck, M.A., and P.A. Sanchez. 1994. Soil phosphorus fraction dynamics during 18 years of cultivation on a Typic Paleudult. *Soil Sci. Soc. Am. J.* 58:1424–1431.
- Beldin, S.I., B.A. Caldwell, P. Sollins, E.W. Sulzman, K. Lajtha, and S.E. Crow. 2007. Cation exchange capacity of density fractions from paired conifer/grassland soils. *Biol. Fertil. Soils* 43:837–841.
- Bending, G.D., M.K. Turner, F. Rayns, M.-C. Marx, and M. Wood. 2004. Microbial and biochemical soil quality indicators and their potential for differentiating areas under contrasting agricultural management regimes. *Soil Biol. Biochem.* 36:1785–1792.
- Bengtsson, G., P. Bengtson, and K.F. Månsson. 2003. Gross nitrogen mineralization-, immobilization-, and nitrification rates as a function of soil C/N ratio and microbial activity. *Soil Biol. Biochem.* 35:143–154.
- Berg, B., and H. Staaf. 1980. Decomposition rate and chemical changes of Scots pine needle litter. II. Influence of chemical composition. *Ecol. Bull.* 32:373–390.
- Bettany, J.R., J.W.B. Stewart, and S. Saggart. 1979. Nature and forms of sulfur in organic matter fractions of soils selected along an environmental gradient. *Soil Sci. Soc. Am. J.* 43:981–985.
- Beyer, L. 1996. The chemical composition of soil organic matter in classical humic compound fractions and in bulk samples—A review. *J. Plant Nutr. Soil Sci.* 159:527–539.
- Bird, M.I., A.R. Chivas, and J. Head. 1996. A latitudinal gradient in carbon turnover times in forest soils. *Nature* 381:143–146.
- Blair, G.J., R.D.B. Lefroy, and L. Lisle. 1995. Soil carbon fractions based on their degree of oxidation, and the development of a carbon management index for agricultural systems. *Aust. J. Agric. Res.* 46:1459–1466.
- Bochner, B.R. 1989. Sleuthing out bacterial identities. *Nature* 339:157–158.
- Bohlen, P.J., P.M. Groffman, T.J. Fahey, M.C. Fisk, E. Suarez, D.M. Pelletier, and R.T. Fahey. 2004. Ecosystem consequences of exotic earthworm invasion of north temperate forests. *Ecosystems* 7:1–12.
- Bolinder, M.A., O. Andren, T. Katterer, and L.E. Parent. 2008. Soil organic carbon sequestration potential for Canadian agricultural ecoregions calculated using the introductory carbon balance model. *Can. J. Soil Sci.* 88:451–460.
- Boonman, J.G. 1993. East Africa's grasses and fodders: Their ecology and husbandry. Kluwer Academic Publishers, Dordrecht, the Netherlands.
- Boudot, J.P., A. Bel Hadi Brahim, and T. Chone. 1986. Carbon mineralisation in andisols and aluminium-rich highland soils. *Soil Biol. Biochem.* 18:457–461.
- Boudot, J.P., A. Bel Hadi Brahim, and T. Chone. 1988. Dependence of carbon and nitrogen mineralisation rates upon amorphous metallic constituents and allophanes in highland soils. *Geoderma* 42:245–260.
- Boudot, J.P., A. Bel Hadi Brahim, R. Steiman, and F. Seigle-Murandi. 1989. Biodegradation of synthetic organo-metallic complexes of iron and aluminium with selected metal to carbon ratios. *Soil Biol. Biochem.* 21:961–966.
- Bracewell, J.M., G.W. Robertson, and K.R. Tate. 1976. Pyrolysis-gas chromatography studies on a climosequence of soils in tussock grasslands, New Zealand. *Geoderma* 15:209–215.
- Brady, N.C. 1990. The nature and properties of soils. Macmillan Publishing Company, New York.
- Bremner, J.M. 1968. The nitrogenous constituents of soil organic matter and their role in soil fertility. "Organic matter and soil fertility." *Pontif. Acad. Sci. Scripta Varia.* 32:143–180.
- Brookes, P.C., A. Landman, G. Pruden, and D.S. Jenkinson. 1985. Chloroform fumigation and the release of soil nitrogen. A rapid extraction method to measure microbial biomass nitrogen in soil. *Soil Biol. Biochem.* 17:837–842.
- Brookes, P.C., D.S. Powlson, and D.S. Jenkinson. 1982. Measurement of microbial biomass phosphorus in soil. *Soil Biol. Biochem.* 14:319–329.
- Brookes, P.C., D.S. Powlson, and D.S. Jenkinson. 1984. Phosphorus in the soil microbial biomass. *Soil Biol. Biochem.* 16:169–175.
- Broos, K., L.M. Macdonald, M.S.J. Warne, D.A. Heemsbergen, M.B. Barnes, M. Bell, and M.J. McLaughlin. 2007. Limitations of soil microbial biomass carbon as an indicator of soil pollution in the field. *Soil Biol. Biochem.* 39:2693–2695.
- Bucher, A.E., and L.E. Lanyon. 2005. Evaluating soil management with microbial community-level physiological profiles. *Appl. Soil Ecol.* 29:59–71.
- Burgess, D., J.A. Baldock, S. Wetzell, and D.G. Brand. 1995. Scarification, fertilization and herbicide treatment effects on planted conifers and soil fertility. *Plant Soil* 168:513–522.
- Burke, I.C., E.T. Elliott, and C.V. Cole. 1995. Influence of macroclimate, landscape position, and management on soil organic matter in agroecosystems. *Ecol. Appl.* 5:124–131.
- Burke, I.C., C.M. Yonker, W.J. Parton, C.V. Cole, K. Flach, and D.S. Schimel. 1989. Texture, climate and cultivation effects on soil organic matter in U.S. grassland soils. *Soil Sci. Soc. Am. J.* 53:800–805.
- Buyanovsky, G.A., C.L. Kucera, and G.H. Wagner. 1987. Comparative analysis of carbon dynamics in native and cultivated ecosystems. *Ecology* 68:2023–2031.
- Cadisch, G., and K.E. Giller. 1997. Driven by nature: Plant litter quality and decomposition. CAB International, Wallingford, U.K.
- Cajuste, L.J., R.J. Laird, L. Cajuste, and B.G. Cuevas. 1996. Citrate and oxalate influence on phosphate, aluminum, and iron in tropical soils. *Commun. Soil Sci. Plant Anal.* 27:1377–1386.
- Campbell, C.A., V.O. Biederbeck, R.P. Zentner, and G.P. Lafond. 1991. Effect of crop rotations and cultural practices on soil organic matter, microbial biomass and respiration in a thin black Chernozem. *Can. J. Soil Sci.* 71:363–376.
- Campbell, C.D., S.J. Chapman, C.M. Cameron, M.S. Davidson, and J.M. Potts. 2003. A rapid microtiter plate method to measure carbon dioxide evolved from carbon substrate

- amendments so as to determine the physiological profiles of soil microbial communities by using whole soil. *Appl. Environ. Microbiol.* 69:3593–3599.
- Canellas, L.P., R. Spaccini, A. Piccolo, L.B. Dobbss, A.L. Okorokova-Facanha, G.D. Santos, F.L. Olivares, and A.R. Facanha. 2009. Relationships between chemical characteristics and root growth promotion of humic acids isolated from Brazilian oxisols. *Soil Sci.* 174:611–620.
- Cerri, C.C., M. Bernoux, C.E.P. Cerri, and C. Feller. 2004. Carbon cycling and sequestration opportunities in South America: The case of Brazil. *Soil Use Manage.* 20:248–254.
- Cerri, C.E.P., C.C. Cerri, M. Bernoux, B. Volkoff, and M.A. Rondon. 2006. Potential of soil carbon sequestration in the Amazonian tropical rainforests, p. 245–266. *In* R. Lal et al. (eds.) *Carbon sequestration in soils of Latin America*. Food products press/Harworthpress, Inc., New York.
- Chan, K.Y., D.P. Heenan, and A. Oates. 2002. Soil carbon fractions and relationship to soil quality under different tillage and stubble management. *Soil Tillage. Res.* 63:133–139.
- Chefetz, B., M.J. Salloum, A.P. Deshmukh, and P.G. Hatcher. 2002. Structural components of humic acids as determined by chemical modifications and carbon-13 NMR, pyrolysis, and thermochemolysis-gas chromatography/mass spectrometry. *Soil Sci. Soc. Am. J.* 66:1159–1171.
- Chen, Y., and T. Aviad. 1990. Effects of humic substances on plant growth, p. 161–186. *In* P. MacCarthy et al. (eds.) *Humic substances in soil and crop sciences: Selected readings*. American Society of Agronomy, Inc., Soil Science Society of America, Inc., Madison, WI.
- Cheng, W.X., and Y. Kuzyakov. 2005. Root effects on soil organic matter decomposition, p. 119–143. *In* Lobel, W., and S.F. Wright (eds.) *Roots and soil management: Interactions between roots and the soil*. American Society of Agronomy, Madison, WI.
- Christensen, B.T. 1996a. Carbon in primary and secondary organomineral complexes, p. 97–165. *In* M.R. Carter and B.A. Stewart (eds.) *Advances in soil science: Structure and organic matter storage in agricultural soils*. CRC Lewis Publishers, Boca Raton, FL.
- Christensen, B.T. 1996b. Matching measurable soil organic matter fractions with conceptual pools in simulation models of carbon turnover: Revision of model structure, p. 143–159. *In* D.S. Powlson et al. (eds.) *Evaluation of soil organic matter models using existing long-term datasets*. NATO ASI Series I: Global Environmental Change. Vol. 38. Springer-Verlag, Berlin, Germany.
- Christensen, B.T. 2001. Physical fractionation of soil and structural and functional complexity in organic matter turnover. *Eur. J. Soil Sci.* 52:345–353.
- Christl, I., and R. Kretzschmar. 2007. C-1s NEXAFS spectroscopy reveals chemical fractionation of humic acid by cation-induced coagulation. *Environ. Sci. Technol.* 41:1915–1920.
- Churchman, G.J., and R.C. Foster. 1994. The role of clay minerals in the maintenance of soil structure, p. 17–34. 15th World Congr. Soil Sci., Acapulco, Mexico, July 10–16, 1994. *Transactions*, Vol. 8a: Commission VII Symposia, International Society of Soil Science, Acapulco, Mexico.
- Clapp, C.E., Y. Chen, M.H.B. Hayes, and H.H. Cheng. 2001. Plant growth promoting activity of humic substances, p. 243–255. *In* R.S. Swift and K.M. Sparks (eds.) *Understanding and managing organic matter in soils, sediments, and waters*. International Humic Science Society, Madison, WI.
- Cleveland, C.C., and D. Liptzin. 2007. C:N:P stoichiometry in soil: Is there a “redfield ratio” for the microbial biomass? *Biogeochemistry* 85:235–252.
- Clinton, P.W., R.H. Newman, and R.B. Allen. 1995. Immobilization of <sup>15</sup>N in forest litter studies by <sup>15</sup>N CPMAS NMR spectroscopy. *Eur. J. Soil Sci.* 46:551–556.
- Cortez, J., J.M. Demard, P. Bottner, and L.J. Monrozier. 1996. Decomposition of Mediterranean leaf litters: A microcosm experiment investigating relationships between decomposition rates and litter quality. *Soil Biol. Biochem.* 28:443–452.
- Crecchio, C., A. Gelsomino, R. Ambrosoli, J.L. Minati, and P. Ruggiero. 2004. Functional and molecular responses of soil microbial communities under differing soil management practices. *Soil Biol. Biochem.* 36:1873–1883.
- Curtin, D., C.A. Campbell, and D. Messer. 1996. Prediction of titratable acidity and soil sensitivity to pH change. *J. Environ. Qual.* 25:1280–1284.
- Dalal, R.C. 1998. Soil microbial biomass—What do the numbers really mean? *Aust. J. Exp. Agric.* 38:649–695.
- Dalal, R.C., B.P. Harms, E. Krull, and W.J. Wang. 2005. Total soil organic matter and its labile pools following mulga (*Acacia aneura*) clearing for pasture development and cropping 1. Total and labile carbon. *Aust. J. Soil Res.* 43:13–20.
- da Rosa, C.M., R.M.V. Castilhos, L.C. Vahl, D.D. Castilhos, L.F.S. Pinto, E.S. Oliveira, and O.D. Leal. 2009. Effect of humic-like substances on potassium uptake kinetics, plant growth and nutrient concentration in *Phaseolus vulgaris* L. *Rev. Bras. Cienc. Do Solo* 33:959–967.
- da Silva, A.P., and B.D. Kay. 1997. Estimating the least limiting water range of soils from properties and management. *Soil Sci. Soc. Am. J.* 61:877–883.
- David, M.B., G.F. McIsaac, R.G. Darmody, and R.A. Omonode. 2009. Long-term changes in mollisol organic carbon and nitrogen. *J. Environ. Qual.* 38:200–211.
- Davidson, E.A., and I.L. Ackerman. 1993. Changes in soil carbon inventories following cultivation of previously untilled soils. *Biogeochemistry* 20:161–193.
- DeAngelis, D.L. 1980. Energy flow, nutrient cycling, and ecosystem resilience. *Ecology* 61:764–771.
- De Fede, K.L., D.G. Panaccione, and A.J. Sexstone. 2001. Characterization of dilution enrichment cultures obtained from size-fractionated soil bacteria by BIOLOG® community-level physiological profiles and restriction analysis of 16S rRNA genes. *Soil Biol. Biochem.* 33:1555–1562.

- De Gryze, S., J. Six, H. Bossuyt, K. Van Oost, and R. Merckx. 2008. The relationship between landform and the distribution of soil C, N and P under conventional and minimum tillage. *Geoderma* 144:180–188.
- De Gryze, S., J. Six, C. Brits, and R. Merckx. 2005. A quantification of short-term macroaggregate dynamics: Influences of wheat residue input and texture. *Soil Biol. Biochem.* 37:55–66.
- De Gryze, S., J. Six, and R. Merckx. 2006. Quantifying water-stable soil aggregate turnover and its implication for soil organic matter dynamics in a model study. *Eur. J. Soil Sci.* 57:693–707.
- Duchaufour, P. 1976. Dynamics of organic matter in soils of temperate regions: Its action on pedogenesis. *Geoderma* 15:31–40.
- Duncan, T.M., 1987. C-13 chemical shielding in solids. *J. Chem. Phys. Ref. Data.* 16:125–151.
- Dunnivant, F.M., P.M. Jardine, D.L. Taylor, and J.F. McCarthy. 1992. Transport of naturally-occurring dissolved organic-carbon in laboratory columns containing aquifer material. *Soil Sci. Soc. Am. J.* 56:437–444.
- Duxbury, J.M., M.S. Smith, and J.W. Doran. 1989. Soil organic matter as a source and sink of plant nutrients, p. 33–67. *In* D.C. Coleman et al. (eds.) *Dynamics of soil organic matter in tropical ecosystems*. NifTAL Project, University of Hawaii Press, Honolulu, HI.
- Edmonds, R.L., and T.B. Thomas. 1995. Decomposition and nutrient release from green needles of western hemlock and Pacific silver fir in an old-growth temperate rain-forest, Olympic National Park, Washington. *Can. J. For. Res.* 25:1049–1057.
- Egli, M., L. Alioth, A. Mirabella, S. Raimondi, M. Nater, and R. Verel. 2007. Effect of climate and vegetation on soil organic carbon, humus fractions, allophanes, imogolite, kaolinite, and oxyhydroxides in volcanic soils of Etna (Sicily). *Soil Sci.* 172:673–691.
- Ekschmitt, K., E. Kandeler, C. Poll, A. Brune, F. Buscot, M. Friedrich, G. Gleixner et al. 2008. Soil-carbon preservation through habitat constraints and biological limitations on decomposer activity. *J. Plant Nutr. Soil Sci.* 171:27–35.
- Ellert, B.H., H.H. Janzen, A.J. VandenBygaart, and E. Bremer. 2008. Measuring change in soil organic carbon storage, p. 25–38. *In* M.R. Carter and E.G. Gregorich (eds.) *Soil sampling and methods of analysis*. 2nd edn. CRC Press, Taylor & Francis, Boca Raton, FL.
- Elliott, E.T. 1986. Aggregate structure and carbon, nitrogen and phosphorus in native and cultivated soils. *Soil Sci. Soc. Am. J.* 50:627–633.
- Elliott, E.T., and D.C. Coleman. 1988. Let the soil work for us. *Ecol. Bull.* 39:23–32.
- Elliott, W.M., N.B. Elliott, and R.L. Wyman. 1993. Relative effect of litter and forest type on rate of decomposition. *Am. Midl. Nat.* 129:87–95.
- Emerson, W.W., R.C. Foster, and J.M. Oades. 1986. Organo mineral complexes in relation to soil aggregation and structure, p. 521–548. *In* P.M. Huang and M. Schnitzer (eds.) *Interactions of soil minerals with natural organics and microbes*. Soil Science Society of America, Madison, WI.
- Eswaran, H., E. Van den Berg, P. Reich, and J.M. Kimble. 1995. Global soil carbon resources, p. 27–43. *In* R. Lal et al. (eds.) *Soils and global change*. Lewis Publishers, Boca Raton, FL.
- Feller, C., E. Fritsch, R. Poss, and C. Valentin. 1991. Effect of the texture on the storage and dynamics of organic matter in some low activity clay soils (West Africa, particularly). *Cahiers ORSTOM Pedologie XXVI*:25–36.
- Filip, Z., and M. Tesarova. 2004. Microbial degradation and transformation of humic acids from permanent meadow and forest soils. *Int. Biodeterior. Biodegrad.* 54:225–231.
- Flaig, W., H. Beutelspacher, and E. Rietz. 1975. Chemical composition and physical properties of humic substances, p. 1–211. *In* J.E. Gieseking (ed.) *Soil components, Vol. I, Organic components*. Springer-Verlag, New York.
- Flavel, T.C., and D.V. Murphy. 2006. Carbon and nitrogen mineralization rates after application of organic amendments to soil. *J. Environ. Qual.* 35:183–193.
- Flessa, H., W. Amelung, M. Helfrich, G.L.B. Wiesenberg, G. Gleixner, S. Brodowski, J. Rethemeyer, C. Kramer, and P.M. Grootes. 2008. Storage and stability of organic matter and fossil carbon in a luvisol and phaeozem with continuous maize cropping: A synthesis. *J. Plant Nutr. Soil Sci.* 171:36–51.
- Fog, K. 1988. The effect of added nitrogen on the rate of decomposition of organic matter. *Biol. Rev. Camb. Philos. Soc.* 63:432–462.
- Fortin, M.C. 1993. Soil temperature, soil water and no-till corn development following in-row residue removal. *Agron. J.* 85:571–576.
- Foster, R.C. 1994. Microorganisms and soil aggregates, p. 144–155. *In* C.E. Pankhurst et al. (eds.) *Soil biota: Management in sustainable farming systems*. CSIRO Publishing, East Melbourne, Victoria, Australia.
- Franzluebbers, A.J., F.M. Hons, and D.A. Zuberer. 1994. Seasonal changes in soil microbial biomass and mineralizable C and N in wheat management systems. *Soil Biol. Biochem.* 26:1469–1475.
- Freibauer, A., M.D.A. Rounsevell, P. Smith, and J. Verhagen. 2004. Carbon sequestration in the agricultural soils of Europe. *Geoderma* 122:1–23.
- Friedel, J.K., and E. Scheller. 2002. Composition of hydrolysable amino acids in soil organic matter and soil microbial biomass. *Soil Biol. Biochem.* 34:315–325.
- Gaiffe, M., G. Duquet, H. Tavant, Y. Tavant, and S. Bruckert. 1984. Stabilité biologique et comportement physique d'un complet argilo-humic placé dans différentes condition de saturation en calcium ou en potassium. *Plant Soil* 77:271–284.
- Garcia, C., T. Hernandez, F. Costa, and A. Polo. 1991. Humic substances in composted sewage sludge. *Waste Manage. Res.* 9:189–194.

- Garcia-Pausas, J., P. Casals, L. Camarero, C. Huguet, M.T. Sebastià, R. Thompson, and J. Romanyà. 2007. Soil organic carbon storage in mountain grasslands of the Pyrenees: Effects of climate and topography. *Biogeochemistry* 82:279–289.
- Gianfreda, L., and J.-M. Bollag. 1996. Influence of natural and anthropogenic factors on enzyme activity in soil, p. 123–193. *In* Stotzky, G., and J.-M. Bollag (eds.). *Soil Biochemistry*. Vol. 9 Marcel Dekker, New York.
- Gillespie, A.W., F.L. Walley, R.E. Farrell, P. Leinweber, A. Schlichting, K.U. Eckhardt, T.Z. Regier, and R.I.R. Blyth. 2009. Profiling rhizosphere chemistry: Evidence from carbon and nitrogen K-edge XANES and pyrolysis-FIMS. *Soil Sci. Soc. Am. J.* 73:2002–2012.
- Gleixner, G., C.J. Czimczik, C. Kramer, B. Luehker, and M.W.I. Schmidt. 2001. Plant compounds and their turnover and stabilization as soil organic matter, p. 201–215. *In* E.D. Schulze et al. (eds.) *Global biogeochemical cycles in the climate system*. Academic Press, San Diego, CA.
- Golchin, A., J.A. Baldock, and J.M. Oades. 1997a. A model linking organic matter decomposition, chemistry and aggregate dynamics, p. 245–266. *In* R. Lal et al. (eds.) *Soil processes and the carbon cycle*. CRC Press, Boca Raton, FL.
- Golchin, A., P. Clarke, J.A. Baldock, T. Higashi, J.O. Skjemstad, and J.M. Oades. 1997b. The effects of vegetation burning on the chemical composition of soil organic matter in a volcanic ash soil as shown by <sup>13</sup>C NMR spectroscopy. I. Whole soil and humic acid fraction. *Geoderma* 76:155–174.
- Golchin, A., J.M. Oades, J.O. Skjemstad, and P. Clarke. 1994a. Study of free and occluded particulate organic matter in soils by solid state <sup>13</sup>C Cp/MAS NMR spectroscopy and scanning electron microscopy. *Aust. J. Soil Res.* 32:285–309.
- Golchin, A., J.M. Oades, J.O. Skjemstad, and P. Clarke. 1994b. Soil structure and carbon cycling. *Aust. J. Soil Res.* 32:1043–1068.
- Goulden, M.L., S.C. Wofsy, J.W. Harden, S.E. Trumbore, P.M. Crill, S.T. Gower, T. Fries et al. 1998. Sensitivity of boreal forest carbon balance to soil thaw. *Science* 279:214–217.
- Griffiths, B.S. 1994. Microbial feeding nematodes and protozoa in soil: Their effects on microbial activity and nitrogen mineralization in decomposition hotspots and the rhizosphere. *Plant Soil* 164:25–33.
- Guggenberger, G., and K. Kaiser. 2003. Dissolved organic matter in soil: Challenging the paradigm of sorptive preservation. *Geoderma* 113:293–310.
- Guggenberger, G., W. Zech, and R.J. Thomas. 1995. Lignin and carbohydrate alteration in particle-size separates of an oxisol under tropical pastures following native savanna. *Soil Biol. Biochem.* 27:1629–1638.
- Guo, Y.Y., P. Gong, R. Amundson, and Q. Yu. 2006. Analysis of factors controlling soil carbon in the conterminous United States. *Soil Sci. Soc. Am. J.* 70:601–612.
- Haaland, D.M., and E.V. Thomas. 1988. Partial least squares methods for spectral analyses 1: Relation to other quantitative calibration methods and the extraction of qualitative information. *Anal. Chem.* 60:1193–1202.
- Haas, H.J., C.E. Evans, and E.F. Miles. 1957. Nitrogen and carbon changes in Great Plains soils as influenced by cropping and soil treatments. Technical Bulletin No. 1164. United States Department of Agriculture, Government Printing Office, Washington, DC. 111 pp.
- Haider, K. 1992. Problems related to the humification processes in soils of temperate climates, p. 55–94. *In* G. Stotzky and J.M. Bollag (eds.) *Soil biochemistry*. Vol. 7. Marcel Dekker, New York.
- Haider, K., and G. Guggenberger. 2005. Soil minerals and organic components: Impact on biological processes, human welfare, and nutrition, p. 3–16. Science Publishers, Inc., Enfield, NH.
- Halstead, R.L., and R.B. Mc Kercher. 1975. Biochemistry and cycling of phosphorus, p. 31–64. *In* E.A. Paul and A.D. McLaren (eds.) *Soil biochemistry*. Vol. 4. Marcel Dekker, New York.
- Hamer, U., B. Marschner, S. Brodowski, and W. Amelung. 2004. Interactive priming of black carbon and glucose mineralisation. *Org. Geochem.* 35:823–830.
- Han, B., X. Wang, and Z. Ouyang. 2005. Saturation levels and carbon sequestration potentials of soil carbon pools in farmland ecosystems of China. *Rural Eco-Environ.* 21:6–11.
- Han, B., X.K. Wang, Z.Y. Ouyang, and F. Lu. 2006. Estimation of soil carbon saturation and carbon sequestration potential of an agro-ecosystem in China. *Int. J. Sust. Dev. World Ecol.* 13:459–468.
- Hart, S.C., G.E. Nason, D.D. Myrold, and D.A. Perry. 1994. Dynamics of gross nitrogen transformations in an old-growth forest: The carbon connection. *Ecology* 75:880–891.
- Harter, R.D., and R. Naidu. 1995. Role of metal-organic complexation in metal sorption by soils. *Adv. Agron.* 55:219–263.
- Hassink, J. 1992. Effects of soil texture and structure on carbon and nitrogen mineralization in grassland soils. *Biol. Fertil. Soils* 14:126–134.
- Hassink, J. 1997. The capacity of soils to preserve organic C and N by their association with clay and silt particles. *Plant Soil* 191:77–87.
- Hassink, J., L.A. Bouwman, K.B. Zwart, and L. Brussard. 1993. Relationship between habitable pore space, soil biota and mineralization rates in grassland soils. *Soil Biol. Biochem.* 25:47–55.
- Hassink, J., C. Chenu, J.W. Dalenberg, J. Bole, and L.A. Bouwman. 1994. Interactions between soil biota, soil organic matter and soil structure, p. 57–58. 15th world congress of soil science, vol. 49, Acapulco, Mexico.
- Haynes, R.J. 2005. Labile organic matter fractions as central components of the quality of agricultural soils: An overview, p. 221–268. *In* D.L. Sparks (ed.) *Advances in agronomy*. Vol. 85. Academic Press, San Diego, CA.
- Heal, O.W., J.M. Anderson, and M.J. Swift. 1997. Plant litter quality and decomposition: An historical overview, p. 3–30. *In* G. Cadisch and K.E. Giller (eds.) *Driven by nature: Plant litter quality and decomposition*. CAB International, Wallingford, U.K.

- Hecky, R.E., and P. Kilham. 1988. Nutrient limitation of phytoplankton in fresh-water and marine environments: A review of recent evidence on the effects of enrichment. *Limnol. Oceanogr.* 33:796–822.
- Hedges, J.I., J.A. Baldock, Y. Gélinas, C. Lee, M.L. Peterson, and S.G. Wakeham. 2002. The biochemical and elemental compositions of marine plankton: A NMR perspective. *Mar. Chem.* 78:47–63.
- Hedges, J.I., G.L. Cowie, J.R. Ertel, R.J. Barbour, and P.G. Hatcher. 1985. Degradation of carbohydrates and lignins in buried woods. *Geochim. Cosmochim. Acta* 49:701–711.
- Hedges, J.I., and J.M. Oades. 1997. Comparative organic geochemistries of soils and marine sediments. *Org. Geochem.* 27:319–361.
- Herbert, B.E., and P.M. Bertsch. 1995. Characterization of dissolved and colloidal organic matter in solutions: A review, p. 62–88. *In* W.W. McFee and J.M. Kelly (eds.) *Carbon forms and functions in forest soils*. Soil Science Society of America, Madison, WI.
- Hicke, J.A., G.P. Asner, J.T. Randerson, C. Tucker, S. Los, R. Birdsey, J.C. Jenkins, C. Field, and E. Holland. 2002. Satellite-derived increases in net primary productivity across North America, 1982–1998. *Geophys. Res. Lett.* 29:69/1–69/4.
- Hobbie, S.E. 1996. Temperature and plant species control over litter decomposition in Alaskan tundra. *Ecol. Monogr.* 66:503–522.
- Holland, E.A., B.H. Braswell, J.F. Lamarque, A. Townsend, J. Sulzman, J.F. Muller, F. Dentener, G. Brasseur, H. Levy, J.E. Penner, and G.J. Roelofs. 1997. Variations in the predicted spatial distribution of atmospheric nitrogen deposition and their impact on carbon uptake by terrestrial ecosystems. *J. Geophys. Res. Atmos.* 102:15849–15866.
- Holloway, P.J. 1982. The chemical constitution of plant cutin, p. 45–85. *In* D.F. Cutler et al. (eds.) *The plant cuticle*. Academic Press, London, U.K.
- Homann, P.S., and D.F. Grigal. 1992. Molecular-weight distribution of soluble organics from laboratory-manipulated surface soils. *Soil Sci. Soc. Am. J.* 56:1305–1310.
- Hope, D., M.F. Billett, and M.S. Cresser. 1994. A review of the export of carbon in river water: Fluxes and processes. *Environ. Pollut.* 84:301–324.
- Houghton, R.A. 2005. The contemporary carbon cycle, p. 473–513. *In* W.H. Schlesinger (ed.) *Biogeochemistry*. Elsevier Science, Amsterdam, the Netherlands.
- Huang, P.M. 2004. Soil mineral-organic matter-microorganism interactions: Fundamentals and impacts, p. 391–472. *In* D.L. Sparks (ed.) *Advances in agronomy*. Vol. 82. Academic Press, San Diego, CA.
- Huang, P.M., and A. Violante. 1986. Influence of organic acids on crystallization and surface properties of precipitation products of aluminum, p. 160–221. *In* P.M. Huang and M. Schnitzer (eds.) *Interactions of soil minerals with natural organics and microbes*. Soil Science Society of America, Madison, WI.
- Hutchinson, J.J., C.A. Campbell, and R.L. Desjardins. 2007. Some perspectives on carbon sequestration in agriculture. *Agric. For. Meteorol.* 142:288–302.
- Ingram, J.S.I., and E.C.M. Fernandes. 2001. Managing carbon sequestration in soils: Concepts and terminology. *Agric. Ecosyst. Environ.* 87:111–117.
- James, B.R., and S.J. Riha. 1986. pH buffering in forest soil organic horizons: Relevance to acid precipitation. *J. Environ. Qual.* 15:229–234.
- Janik, L.J., R.H. Merry, and J.O. Skjemstad. 1998. Can mid infrared diffuse reflectance analysis replace soil extractions? *Aust. J. Exp. Agric.* 38:681–696.
- Janik, L.J., and J.O. Skjemstad. 1995. Characterization and analysis of soils using mid-infrared partial least-squares. 2. Correlations with some laboratory data. *Aust. J. Soil Res.* 33:637–650.
- Janik, L.J., J.O. Skjemstad, K.D. Shepherd, and L.R. Spouncer. 2007. The prediction of soil carbon fractions using mid-infrared-partial least square analysis. *Aust. J. Soil Res.* 45:73–81.
- Janssens, I.A., A. Freibauer, B. Schlamadinger, R. Ceulemans, P. Ciais, A.J. Dolman, M. Heimann, G.J. Nabuurs, P. Smith, R. Valentini, and E.D. Schulze. 2005. The carbon budget of terrestrial ecosystems at country-scale: A European case study. *Biogeosciences* 2:15–26.
- Janzen, H.H. 1987. Soil organic matter characteristics after long term cropping to various spring wheat rotations. *Can. J. Soil Sci.* 67:845–856.
- Jenkinson, D.S. 1976. Effects of biocidal treatments on metabolism in soil. 4. Decomposition of fumigated organisms in soil. *Soil Biol. Biochem.* 8:203–208.
- Jenkinson, D.S. 1977. The soil microbial biomass. *N. Z. Soil News* 25:213–218.
- Jenkinson, D.S., and A. Ayanaba. 1977. Decomposition of C-14 labeled plant material under tropical conditions. *Soil Sci. Soc. Am. J.* 41:912–915.
- Jenkinson, D.S., P.C. Brookes, and D.S. Powlson. 2004. Measuring soil microbial biomass. *Soil Biol. Biochem.* 36:5–7.
- Jenkinson, D.S., P.B.S. Hart, J.H. Rayner, and L.C. Parry. 1987. Modelling the turnover of organic matter in long-term experiments at Rothamsted. *INTECOL Bull.* 15:1–8.
- Jenkinson, D.S., and J.N. Ladd. 1981. Microbial biomass in soil: Measurement and turnover. *Soil Biochem.* 5:415–471.
- Jenkinson, D.S., and L.C. Parry. 1989. The nitrogen cycle in the Broadbalk wheat experiment: A model for the turnover of nitrogen through the soil microbial biomass. *Soil Biol. Biochem.* 21:535–541.
- Jenkinson, D.S., and J.H. Rayner. 1977. Turnover of soil organic matter in some Rothamsted classical experiments. *Soil Sci.* 123:298–305.
- Jenny, H. 1930. A study on the influence of climate upon the nitrogen and organic matter content of the soil. *Missouri Agricultural Experimental station Bulletin* 15, 66pp.
- Jobbagy, E.G., and R.B. Jackson. 2000. The vertical distribution of soil organic carbon and its relation to climate and vegetation. *Ecol. Appl.* 10:423–436.
- John, B., T. Yamashita, B. Ludwig, and H. Flessa. 2005. Storage of organic carbon in aggregate and density fractions of silty soils under different types of land use. *Geoderma* 128:63–79.

- Johnson, D.W. 1992. Effects of forest management on soil carbon storage. *Water Air Soil Pollut.* 64:83–120.
- Johnson, D.W., and P.S. Curtis. 2001. Effects of forest management on soil C and N storage: Meta analysis. *Forest Ecol. Manage.* 140:227–238.
- Johnson, D.W., J.D. Knoepp, W.T. Swank, J. Shan, L.A. Morris, D.H. Van Lear, and P.R. Kapeluck. 2002. Effects of forest management on soil carbon: Results of some long-term resampling studies. *Environ. Pollut.* 116:S201–S208.
- Jokic, A., J.N. Cutler, D.W. Anderson, and F.L. Walley. 2004. Detection of heterocyclic N compounds in whole soils using N-XANES spectroscopy. *Can. J. Soil Sci.* 84:291–293.
- Juste, C., and J. Delas. 1970. Comparaison par une méthode repiro-métrique, des solubilités biochimiques d'un humate de calcium et d'un humate de sodium. *C. R. Hebd. Seances Acad. Sci. D* 270:1127–1129.
- Juste, C., J. Delas, and M. Langon. 1975. Comparaison de la stabilité biologique de différents humates métalliques. *C. R. Hebd. Seances Acad. Sci. D* 281:1685–1688.
- Kahle, M., M. Kleber, M.S. Torn, and R. Jahn. 2003. Carbon storage in coarse and fine clay fractions of illitic soils. *Soil Sci. Soc. Am. J.* 67:1732–1739.
- Kajak, A. 1995. The role of soil predators in decomposition processes. *Eur. J. Entomol.* 92:573–580.
- Kalbitz, K., and K. Kaiser. 2008. Contribution of dissolved organic matter to carbon storage in forest mineral soils. *J. Plant Nutr. Soil Sci.* 171:52–60.
- Kalbitz, K., J. Schmerwitz, D. Schwesig, and E. Matzner. 2003. Biodegradation of soil-derived dissolved organic matter as related to its properties. *Geoderma* 113:273–291.
- Kalbitz, K., S. Solinger, J.H. Park, B. Michalzik, and E. Matzner. 2000. Controls on the dynamics of dissolved organic matter in soils: A review. *Soil Sci.* 165:277–304.
- Kay, B.D., A.P. da Silva, and J.A. Baldock. 1997. Sensitivity of soil structure to changes in organic carbon content: Predictions using pedotransfer functions. *Can. J. Soil Sci.* 77:655–667.
- Keil, R.G., E. Tsamakis, C.B. Fuh, C. Giddings, and J.I. Hedges. 1994. Mineralogical and textural controls on the organic composition of coastal marine sediments: Hydrodynamic separation using SPLITT-fractionation. *Geochim. Cosmochim. Acta* 58:879–893.
- Keleman, S.R., M. Afeworki, M.L. Gorbaty, P.J. Kwiatek, M.S. Solum, J.Z. Hu, and R.J. Pugmire. 2002. XPS and <sup>15</sup>N NMR study of nitrogen forms in carbonaceous solids. *Energy Fuels* 16:1507–1515.
- Kilbertus, G. 1980. Study of microhabitats in soil aggregates. Relation to bacterial biomass and size of procaryotes. *Revue D Ecologie Et De Biologie Du Sol* 17:543–557.
- Killham, K., M. Amato, and J.N. Ladd. 1993. Effects of substrate location in soil and soil pore-water regime on carbon turnover. *Soil Biol. Biochem.* 25:57–62.
- Kimble, J.M., C.W. Rice, D. Reed, S. Mooney, R.F. Follett, and R. Lal. 2007. *Soil carbon management: Economic, environmental and societal benefits*, CRC Press, Taylor & Francis Group, Boca Raton, FL, 280pp.
- Kinyangi, J., D. Solomon, B.I. Liang, M. Lerotic, S. Wirick, and J. Lehmann. 2006. Nanoscale biogeocomplexity of the organomineral assemblage in soil: Application of STXM microscopy and C 1s-NEXAFS spectroscopy. *Soil Sci. Soc. Am. J.* 70:1708–1718.
- Kirschbaum, M.U.F. 1995. The temperature dependence of soil organic matter decomposition and the effect of global warming on soil organic C storage. *Soil Biol. Biochem.* 27:753–760.
- Knicker, H., G. Almendros, F.J. González-vila, H.-D. Lüdemann, and F. Martin. 1995. <sup>13</sup>C and <sup>15</sup>N NMR analysis of some fungal melanins in comparison with soil organic matter. *Org. Geochem.* 23:1023–1028.
- Knicker, H., R. Fründ, and H.-D. Lüdeman. 1993. The chemical nature of nitrogen in native soil organic matter. *Naturwissenschaften* 80:219–221.
- Knicker, H., and H.-D. Lüdemann. 1995. N-15 and C-13 CPMAS and solution NMR studies of N-15 enriched plant material during 600 days of microbial degradation. *Org. Geochem.* 23:329–341.
- Knicker, H., and J.O. Skjemstad. 2000. Nature of organic carbon and nitrogen in physically protected organic matter of some Australian soils as revealed by solid-state <sup>13</sup>C and <sup>15</sup>N NMR spectroscopy. *Aust. J. Soil Res.* 38:113–127.
- Kögel-Knabner, I. 2002. The macromolecular organic composition of plant and microbial residues as inputs to soil organic matter. *Soil Biol. Biochem.* 34:139–162.
- Kögel-Knabner, I., K. Ekschmitt, H. Flessa, G. Guggenberger, E. Matzner, B. Marschner, and M. von Luetzow. 2008a. An integrative approach of organic matter stabilization in temperate soils: Linking chemistry, physics, and biology. *J. Plant Nutr. Soil Sci.* 171:5–13.
- Kögel-Knabner, I., G. Guggenberger, M. Kleber, E. Kandeler, K. Kalbitz, S. Scheu, K. Eusterhues, and P. Leinweber. 2008b. Organo-mineral associations in temperate soils: Integrating biology, mineralogy, and organic matter chemistry. *J. Plant Nutr. Soil Sci.* 171:61–82.
- Kögel-Knabner, I., M.V. Lützw, G. Guggenberger, H. Flessa, B. Marschner, E. Matzner, and K. Ekschmitt. 2005. Mechanisms and regulation of organic matter stabilisation in soils. *Geoderma* 128:1–2.
- Krull, E.S., J.A. Baldock, and J.O. Skjemstad. 2003. Importance of mechanisms and processes of the stabilisation of soil organic matter for modelling carbon turnover. *Funct. Plant Biol.* 30:207–222.
- Krull, E.S., J.O. Skjemstad, and J.A. Baldock. 2005. Functions of soil organic matter and effects on soil properties, p. 107. Cooperative Research Centre for Greenhouse Accounting, Canberra, Australia.
- Krull, E.S., C.W. Swanston, J.O. Skjemstad, and J.A. McGowan. 2006. Importance of charcoal in determining the age and chemistry of organic carbon in surface soils. *J. Geophys. Res. Biogeosci.* 111, 6.04001, doi: 10.1029/2006J6.0001
- Kruse, J., and P. Leinweber. 2008. Phosphorus in sequentially extracted fen peat soils: A K-edge X-ray absorption near-edge structure (XANES) spectroscopy study. *J. Plant Nutr. Soil Sci.* 171:613–620.

- Kruse, J., P. Leinweber, K.U. Eckhardt, F. Godlinski, Y.F. Hu, and L. Zuin. 2009. Phosphorus L-2,L-3-edge XANES: Overview of reference compounds. *J. Synchrotron Radiat.* 16:247–259.
- Ladd, J.N., M. Amato, and J.M. Oades. 1985. Decomposition of plant materials in Australian soils. III Residual organic and microbial biomass C and N from isotope-labelled legume materials and soil organic matter decomposing under field conditions. *Aust. J. Soil Res.* 23:603–611.
- Ladd, J.N., and J.H.A. Butler. 1975. Humus-enzyme systems and synthetic, organic polymer-enzyme analogs, p. 143–194. *In* E.A. Paul and A.D. McLaren (eds.) *Soil biochemistry*. Vol. 4. Marcel Dekker, Inc., New York.
- Ladd, J.N., R.C. Foster, P. Nannipieri, and J.M. Oades. 1996. Soil structure and biological activity, p. 23–78. *In* G. Stotzky and J.M. Bollag (eds.) *Soil biochemistry*. Vol. 9. Marcel Dekker, Inc., New York.
- Ladd, J.N., J.M. Oades, and M. Amato. 1981. Microbial biomass formed from  $^{14}\text{C}$ ,  $^{15}\text{N}$ -labelled plant material decomposing in soils in the field. *Soil Biol. Biochem.* 13:119–126.
- Lal, R. 2004a. Soil carbon sequestration to mitigate climate change. *Geoderma* 123:1–22.
- Lal, R. 2004b. Agricultural activities and the global carbon cycle. *Nutr. Cycl. Agroecosyst.* 70:103–116.
- Lal, R., K. Kimble, R. Follet, and C. Cole (eds.). 1998. The potential of US cropland to sequester carbon and mitigate the greenhouse effect. Ann Arbor Press, Chelsea, MI.
- Lavelle, P., E. Blanchart, A. Martin, S. Martin, A. Spain, F. Toutain, I. Barois, and R. Schaefer. 1993. A hierarchical model for decomposition in terrestrial ecosystems: Application to soils of the humid tropics. *Biotropica* 25:130–150.
- Lavelle, P., and A. Martin. 1992. Small-scale and large-scale effects of endogenic earthworms on soil organic matter dynamics in soils of the humid tropics. *Soil Biol. Biochem.* 24:1491–1498.
- Lawes, J. 1861. On the application of different manures to different crops and their proper distribution on the farm. Private publication cited Dyke (1993) (as cited by Heal et al. 1997).
- Leavitt, S.W., R.F. Follett, and E.A. Paul. 1996. Estimation of slow- and fast-cycling soil organic carbon pools from 6 N HCl hydrolysis. *Radiocarbon* 38:231–239.
- Lefroy, R.D.B., G.J. Blair, and E.T. Craswell. 1995. Soil organic matter management for sustainable agriculture: A workshop held in Ubon, Thailand, August 24–26, 1994.
- Lefroy, R.D.B., G.J. Blair, and W.M. Strong. 1993. Changes in soil organic matter with cropping as measured by organic carbon fractions and  $^{13}\text{C}$  natural isotope abundance. *Plant Soil* 155–156:399–402.
- Lehmann, J., B.Q. Liang, D. Solomon, M. Lerotic, F. Luizao, J. Kinyangi, T. Schafer, S. Wirick, and C. Jacobsen. 2005. Near-edge X-ray absorption fine structure (NEXAFS) spectroscopy for mapping nano-scale distribution of organic carbon forms in soil: Application to black carbon particles. *Global Biogeochem. Cy.* 19:GB1013.
- Lehmann, J., D. Solomon, J. Kinyangi, L. Dathe, S. Wirick, and C. Jacobsen. 2008. Spatial complexity of soil organic matter forms at nanometre scales. *Nat. Geosci.* 1:238–242.
- Leifeld, J., and I. Kögel-Knabner. 2005. Soil organic matter fractions as early indicators for carbon stock changes under different land-use? *Geoderma* 124:143–155.
- Leinweber, P., J. Kruse, F.L. Walley, A. Gillespie, K.U. Eckhardt, R.I.R. Blyth, and T. Regier. 2007. Nitrogen K-edge XANES—An overview of reference compounds used to identify ‘unknown’ organic nitrogen in environmental samples. *J. Synchrotron Radiat.* 14:500–511.
- Liang, B., J. Lehmann, D. Solomon, J. Kinyangi, J. Grossman, B. O’Neill, J.O. Skjemstad, J. Thies, F.J. Luizao, J. Petersen, and E.G. Neves. 2006. Black carbon increases cation exchange capacity in soils. *Soil Sci. Soc. Am. J.* 70:1719–1730.
- Liang, B., J. Lehmann, D. Solomon, S. Sohi, J.E. Thies, J.O. Skjemstad, F.J. Luizao, M.H. Engelhard, E.G. Neves, and S. Wirick. 2008. Stability of biomass-derived black carbon in soils. *Geochim. Cosmochim. Acta* 72:6069–6078.
- Lieth, H. 1973. Primary production: Terrestrial ecosystems. *Hum. Ecol.* 1:303–332.
- Ligel, L.H. 1992. An overview of carbon sequestration in soils of Latin America. *In* F.H. Beinroth (ed.) *Organic carbon sequestration in the soils of Puerto Rico*. Agronomy and Soils. University of Puerto Rico, Mayaguez, Puerto Rico.
- Linhares, M. 1977. Contribution de l’ion calcium à la stabilisation biologique de la matière organique des sols. Thèse Doc. Spéc., Université de Bordeaux III.
- Ljungdahl, L.G., and K.-E. Eriksson. 1985. Ecology of microbial cellulose degradation, p. 237–299. *In* K.C. Marshall (ed.) *Advances in microbial ecology*. Vol. 8. Plenum press, New York.
- Lorenz, K., and R. Lal. 2005. The depth distribution of soil organic carbon in relation to land use and management and the potential of carbon sequestration in subsoil horizons, p. 35–66. *In* D.L. Sparks (ed.) *Advances in agronomy*. Vol. 88. Academic Press, San Diego, CA.
- Ludwig, B., K. Kuka, U. Franko, and M. von Luetzow. 2008. Comparison of two quantitative soil organic carbon models with a conceptual model using data from an agricultural long-term experiment. *J. Plant Nutr. Soil Sci.* 171:83–90.
- MacCarthy, P., R.L. Malcolm, C.E. Clapp, and P.R. Bloom. 1990. An introduction to soil humic substances, p. 1–12. *In* P. MacCarthy et al. (eds.) *Humic substances in crop and soil sciences: Selected readings*. Soil Science Society of America, Madison, WI.
- Magid, J., T. Mueller, L.S. Jansen, and N.E. Nielsen. 1996. Modelling the measurable: Interpretation of field-scale  $\text{CO}_2$  and N-mineralisation, soil microbial biomass and light fractions as indicators of oilseed rape, maize and barley straw decomposition, p. 349–362. *In* G. Cadisch and K.E. Giller (eds.) *Driven by nature: Plant litter quality and decomposition*. CAB International, Wallingford, U.K.
- Mahieu, N., D.C. Olk, and E.W. Randall. 2000. Accumulation of heterocyclic nitrogen in humified organic matter: A  $^{15}\text{N}$ -NMR study of lowland rice soils. *Eur. J. Soil Sci.* 51:379–389.
- Mainari, S., and F. Caporali. 2008. Soil carbon sequestration under organic farming in the Mediterranean environment. *Transworld. Research Network, Kerala, India.* 178 pp.

- Mann, L.K. 1986. Changes in soil carbon storage after cultivation. *Soil Sci.* 142:289–288.
- Marschner, B., S. Brodowski, A. Dreves, G. Gleixner, A. Gude, P.M. Grootes, U. Hamer et al. 2008. How relevant is recalcitrance for the stabilization of organic matter in soils? *J. Plant Nutr. Soil Sci.* 171:91–110.
- Martens, D.A., and K.L. Loeffelmann. 2002. Improved accounting of carbohydrate carbon from plants and soils. *Soil Biol. Biochem.* 34:1393–1399.
- Martens, D.A., and K.L. Loeffelmann. 2003. Soil amino acid composition quantified by acid hydrolysis and anion chromatography-pulsed amperometry. *J. Agric. Food Chem.* 51:6521–6529.
- Martin, J.P., J.O. Ervin, and R.A. Shepherd. 1966. Decomposition of the iron, aluminium, zinc, and copper salts or complexes of some microbial and plant polysaccharides in soil. *Proc. Soil Sci. Soc. Am.* 30:196–200.
- Martin, J.P., and K. Haider. 1975. Decomposition of specifically labelled benzoic acid and cinnamic acid derivatives in soil. *Proc. Soil Sci. Soc. Am.* 39:657–662.
- Martin, J.P., S.J. Richards, and J.O. Ervin. 1972. Decomposition and binding action in soil of some mannose containing microbial polysaccharides and their Fe, Al, Zn and Cu complexes. *Soil Sci.* 113:322–327.
- Martínez, A.T., A.E. González-Vila, M. Valmaseda, B.E. Dale, M.J. Lambregts, and J.F. Haw. 1991. Solid-state NMR studies of lignin and plant polysaccharide degradation by fungi. *Holzforschung* 45:49–54.
- Masiello, C.A., M.E. Gallagher, J.T. Randerson, R.M. Deco, and O.A. Chadwick. 2008. Evaluating two experimental approaches for measuring ecosystem carbon oxidation state and oxidative ratio. *J. Geophys. Res. Biogeosci.* 113:9.
- Mayer, L.M. 1994a. Surface area control of organic carbon accumulation in continental shelf sediments. *Geochim. Cosmochim. Acta* 58:1271–1284.
- Mayer, L.M. 1994b. Relationships between mineral surfaces and organic carbon concentrations in soils and sediments. *Chem. Geol.* 114:347–363.
- McBride, M.B. 1994. *Environmental chemistry of soils.* Oxford University Press, New York.
- McCown, R.L., G.L. Hammer, J.N.G. Hargreaves, D.P. Holzworth, and D.M. Freebairn. 1996. APSIM: A novel software system for model development, model testing and simulation in agricultural systems research. *Agric. Syst.* 50:255–271.
- McDougall, G.J., I.M. Morrison, D. Stewart, J.D.B. Weyers, and J.R. Hillman. 1993. Plant fibers: Botany, chemistry and processing for industrial use. *J. Sci. Food Agric.* 62:1–20.
- McFee, W.W., and J.M. Kelly. 1995. Carbon forms and functions in forest soils. *Soil Science Society of America, Madison, WI.* 594 pp.
- McGill, W.B., and C.V. Cole. 1981. Comparative aspects of cycling of organic C, N, S and P through soil organic matter. *Geoderma* 26:267–286.
- McKeague, J.A., M.V. Cheshire, F. Andreux, and J. Berthelin. 1986. Organo-mineral complexes in relation to pedogenesis, p. 549–592. *In* P.M. Huang and M. Schnitzer (eds.) *Interactions of soil minerals with natural organics and microbes.* Soil Science Society of America, Madison, WI.
- Mendham, D.S., A.M. O'Connell, and T.S. Grove. 2002. Organic matter characteristics under native forest, long-term pasture, and recent conversion to eucalyptus plantations in Western Australia: Microbial biomass, soil respiration, and permanganate oxidation. *Aust. J. Soil Res.* 40:859–872.
- Metting, F., J. Smith, and J. Amthor. 1999. Science needs and new technology for carbon sequestration, p. 1–34. *In* N. Rosenberg et al. (eds.) *Carbon sequestration in soils: Science, monitoring and beyond.* Battelle Press, Columbus, OH.
- Michalzik, B., K. Kalbitz, J.-H. Park, S. Solinger, and E. Matzner. 2001. Fluxes and concentrations of dissolved organic carbon and nitrogen: A synthesis for temperate forests. *Biogeochemistry* 52:173–205.
- Moorhead, D.L., and J.F. Reynolds. 1989. The contribution of abiotic processes to buried litter decomposition in the northern Chihuahuan desert. *Oecologia* 79:133–135.
- Muller, P.E. (ed.) 1887. *Studien über die natürlichen Humusformen und deren Einwirkung auf Vegetation und Boden.* Springer, Berlin, Germany.
- Müller-Wegener, U. 1988. Interactions of humic substances with biota, p. 179–192. *In* F.H. Frimmel and R.F. Christman (eds.) *Humic substances and their role in the environment.* John Wiley & Sons, New York.
- Muneer, M., and J.M. Oades. 1989a. The role of Ca-organic interactions in soil aggregate stability. I. Laboratory studies with <sup>14</sup>C-glucose, CaCO<sub>3</sub> and CaSO<sub>4</sub>·2H<sub>2</sub>O. *Aust. J. Soil Res.* 27:389–399.
- Muneer, M., and J.M. Oades. 1989b. The role of Ca-organic interactions in soil aggregate stability. II. Field studies with <sup>14</sup>C-labelled straw, CaCO<sub>3</sub> and CaSO<sub>4</sub>·2H<sub>2</sub>O. *Aust. J. Soil Res.* 27:401–409.
- Muneer, M., and J.M. Oades. 1989c. The role of Ca-organic interactions in soil aggregate stability. III. Mechanisms and models. *Aust. J. Soil Res.* 27:411–423.
- Murphy, D.V., S. Recous, E.A. Stockdale, I.R.P. Fillery, L.S. Jensen, D.J. Hatch, and K.W.T. Goulding. 2003. Gross nitrogen fluxes in soil: Theory, measurement and application of <sup>15</sup>N pool dilution techniques, p. 69–118. *In* D.L. Sparks (ed.) *Advances in agronomy.* Vol. 79. Academic Press, San Diego, CA.
- Muyzer, G., E.C. Dewaal, and A.G. Uitterlinden. 1993. Profiling of complex microbial populations by denaturing gradient gel-electrophoresis analysis of polymerase chain reaction amplified genes coding for 16s ribosomal RNA. *Appl. Environ. Microbiol.* 59:695–700.
- Nardi, S., G. Concheri, and G. Dell'Agnola. 1996. Biological activity of humic substances, p. 361–406. *In* A. Piccolo (ed.) *Humic substances in terrestrial ecosystems.* Elsevier, Amsterdam, the Netherlands.



- Nardi, S., D. Pizzeghello, A. Muscolo, and A. Vianello. 2002. Physiological effects of humic substances on higher plants. *Soil Biol. Biochem.* 34:1527–1536.
- Neff, J.C., and G.P. Asner. 2001. Dissolved organic carbon in terrestrial ecosystems: Synthesis and a model. *Ecosystems* 4:0029–0048.
- Nelson, P.N., and J.A. Baldock. 2005. Estimating the molecular composition of a diverse range of natural organic materials from solid-state C-13 NMR and elemental analyses. *Biogeochemistry* 72:1–34.
- Nelson, P.N., J.A. Baldock, and J.M. Oades. 1993. Concentration and composition of dissolved organic carbon in streams in relation to catchment soil properties. *Biogeochemistry* 19:27–50.
- Nelson, P.N., and J.M. Oades. 1997. Organic matter, sodicity and soil structure, p. 67. *In* M.E. Sumner and R. Naidu (eds.) *Sodic soils: Distribution, processes, management and environmental consequences*. Oxford University Press, New York.
- Nelson, D.W., and L.E. Sommers. 1996. Total carbon, organic carbon, and organic matter, p. 961–1010. *In* D.L. Sparks et al. (eds.) *Methods of soil analysis. Part 3. Chemical methods*. ASA-CSSA-SSSA, Madison, WI.
- Nguyen, M.L., and K.M. Goh. 1994. Sulfur cycling and its implications on sulfur fertiliser requirements of grazed grassland ecosystems. *Agric. Ecosyst. Environ.* 49:173–206.
- Nip, M., J.W. Deleeuw, P.J. Holloway, J.P.T. Jensen, J.C.M. Sprenkels, M. Depooter, and J.J.M. Sleekx. 1987. Comparison of flash pyrolysis, differential scanning calorimetry, C-13 NMR and IR spectroscopy in the analysis of a highly aliphatic biopolymer from plant cuticles. *J. Anal. Appl. Pyrol.* 11:287–295.
- Nip, M., E.W. Tegelaar, H. Brinkhuis, J.W. Deleeuw, P.A. Schenck, and P.J. Holloway. 1986a. Analysis of modern and fossil plant cuticles by curie-point PY-GC and curie-point PY-GC-MS. Recognition of a new, highly aliphatic and resistant biopolymer. *Org. Geochem.* 10:769–778.
- Nip, M., E.W. Tegelaar, J.W. Deleeuw, P.A. Schenck, and P.J. Holloway. 1986b. A new non-saponifiable highly aliphatic and resistant biopolymer in plant cuticles: Evidence from pyrolysis and C-13-NMR analysis of present day and fossil plants. *Naturwissenschaften* 73:579–585.
- Oades, J.M. 1984. Soil organic matter and structural stability: Mechanisms and implications for management. *Plant Soil* 76:319–337.
- Oades, J.M. 1988. The retention of organic matter in soil. *Biogeochemistry* 5:35–70.
- Oades, J.M. 1989. An introduction to organic matter in mineral soils, p. 89–159. *In* J.B. Dixon and S.B. Weed (eds.) *Minerals in soil environments*. 2nd edn. Soil Science Society of America, Madison, WI.
- Oades, J.M. 1993. The role of biology in the formation, stabilization and degradation of soil structure. *Geoderma* 56:377–400.
- Oades, J.M. 1995. Krasnozems: Organic matter. *Aust. J. Soil Res.* 33:43–57.
- Oades, J.M., and A.G. Waters. 1991. Aggregate hierarchy in soils. *Aust. J. Soil Res.* 29:815–828.
- Oorts, K., B. Vanlauwe, and R. Merckx. 2003. Cation exchange capacities of soil organic matter fractions in a ferric lixisol with different organic matter inputs. *Agric. Ecosyst. Environ.* 100:161–171.
- Orlov, D.S. 1995. *Humic substances of soils and general theory of humification*. Brookfield, Rotterdam, the Netherlands. 323 pp.
- Parton, W.J., D.C. Schimel, C.V. Cole, and D.S. Ojima. 1987. Analysis of factors controlling soil organic matter levels in Great Plains grasslands. *Soil Sci. Soc. Am. J.* 51:1173–1179.
- Parton, W.J., J.W.B. Stewart, and C.V. Cole. 1988. Dynamics of C, N, P and S in grassland soils: A model. *Biogeochemistry* 5:109–131.
- Paul, E.A., H.P. Collins, and S.W. Leavitt. 2001. Dynamics of resistant soil carbon of midwestern agricultural soils measured by naturally occurring <sup>14</sup>C abundance. *Geoderma* 104:239–256.
- Paul, E.A., and H. van Veen. 1978. The use of tracers to determine the dynamic nature of organic matter, p. 61–102. *Trans. 11th Int. Congr. Soil Sci. Vol. 3. International Society of Soil Science*, Edmonton, Alberta, Canada.
- Paustian, K. 1994. Modelling soil biology and biochemical processes for sustainable agriculture research, p. 182–193. *In* C.E. Pankhurst et al. (eds.) *Soil biota: Management in sustainable farming systems*. CSIRO Publishing, Melbourne, Australia.
- Paustian, K., O. Andren, H.H. Janzen, R. Lal, P. Smith, G. Tian, H. Tiessen, M. Van Noordwijk, and P.L. Woomer. 1997a. Agricultural soils as a sink to mitigate CO<sub>2</sub> emissions. *Soil Use Manage.* 13:230–244.
- Paustian, K., H.P. Collins, and E.A. Paul. 1997b. Management controls on soil carbon, p. 1549. *In* E.A. Paul et al. (eds.) *Soil organic matter in temperate agroecosystems: Longterm experiments in North America*. CRC Press, Boca Raton, FL.
- Peterson, B.J., and J.M. Melillo. 1985. The potential storage of carbon caused by eutrophication of the biosphere. *Tellus Ser.B Chem. Phys. Meteorol.* 37:117–127.
- Peterson, G.A., D.G. Westfall, C.W. Wood, and S. Ross. 1988. Crop and soil management in dryland agroecosystems. *Colorado State University Technical Bulletin LTB886*.
- Piccolo, A. 2002. The supramolecular structure of humic substances: A novel understanding of humus chemistry and implications in soil science, p. 57–134. *In* D.L. Sparks (ed.) *Advances in agronomy*. Vol. 75. Academic Press, San Diego, CA.
- Pocknee, S., and M.E. Sumner. 1997. Cation and nitrogen contents of organic matter determine its soil liming potential. *Soil Sci. Soc. Am. J.* 61:86–92.
- Poirier, N., S.P. Sohi, J.L. Gaunt, N. Mahieu, E.W. Randall, D.S. Powlson, and R.P. Evershed. 2005. The chemical composition of measurable soil organic matter pools. *Org. Geochem.* 36:1174–1189.

- Post, W.M., W.R. Emmanuel, P.J. Zinke, and A.G. Stangenberger. 1982. Soil carbon pools and world life zones. *Nature* 298:156–159.
- Post, W., R. Izaurralde, L. Mann, and N. Bliss. 1999. Monitoring and verifying soil organic carbon sequestration, p. 41–66. *In* N. Rosenberg et al. (eds.) *Carbon sequestration in soils: Science, monitoring and beyond*. Battelle Press, Columbus, OH.
- Post, W.M., R.C. Izaurralde, L.K. Mann, and N. Bliss. 2001. Monitoring and verifying changes of organic carbon in soil. *Clim. Change* 51:73–99.
- Post, W.M., T.-H. Peng, W.R. Emanuel, A.W. King, V.H. Dale, and D.L. DeAngelis. 1990. The global carbon cycle. *Am. Sci.* 78:310–326.
- Poulenard, J., J.C. Michel, F. Bartoli, J.M. Portal, and P. Podwojewski. 2004. Water repellency of volcanic ash soils from Ecuadorian páramo: Effect of water content and characteristics of hydrophobic organic matter. *Eur. J. Soil Sci.* 55:487–496.
- Powlson, D.S., and D.S. Jenkinson. 1976. Effects of biocidal treatments on metabolism in soil. 2. Gamma-irradiation, autoclaving, air-drying and fumigation. *Soil Biol. Biochem.* 8:179–188.
- Pressenda, L.C.R., R. Aravena, A.J. Melfi, E.C.C. Telles, R. Boulet, E.P.E. Vanencia, and M. Tomazello. 1996. The use of carbon isotopes (C13, C14) in soil to evaluate vegetation changes during the Holocene in central Brazil. *Radiocarbon* 38:191–201.
- Preston, C.M. 1996. Applications of NMR to soil organic matter analysis: History and prospects. *Soil Sci.* 161:144–166.
- Preston, C.M., J.A. Trofymow, B.G. Sayer, and J. Niu. 1997. <sup>13</sup>C nuclear magnetic resonance spectroscopy with cross-polarization and magic-angle spinning investigation of the proximate-analysis fractions used to assess litter quality in decomposition studies. *Can. J. Bot.* 75:1601–1613.
- Prietzl, J., J. Thieme, U. Neuhäusler, J. Susini, and I. Kögel-Knabner. 2003. Speciation of sulphur in soils and soil particles by X-ray spectromicroscopy. *Eur. J. Soil Sci.* 54:423–433.
- Prietzl, J., J. Thieme, M. Salome, and H. Knicker. 2007. Sulfur K-edge XANES spectroscopy reveals differences in sulfur speciation of bulk soils, humic acid, fulvic acid, and particle size separates. *Soil Biol. Biochem.* 39:877–890.
- Raison, R.J., M.J. Connell, and P.K. Khanna. 1987. Methodology for studying fluxes of soil mineral N *in situ*. *Soil Biol. Biochem.* 19:521–530.
- Randerson, J.T., C.A. Masiello, C.J. Still, T. Rahn, H. Poorter, and C.B. Field. 2006. Is carbon within the global terrestrial biosphere becoming more oxidized? Implications for trends in atmospheric O<sub>2</sub>. *Global Change Biol.* 12:260–271.
- Ransom, B., D. Kim, M. Kastner, and S. Wainwright. 1998. Organic matter preservation on continental slopes: Importance of mineralogy and surface area. *Geochim. Cosmochim. Acta* 62:1329–1345.
- Rashidi, M., and M. Seilsepour. 2008. Modeling of soil cation exchange capacity based on some soil physical and chemical properties. *J. Agric. Biol. Sci.* 3:6–13.
- Redfield, A. 1958. The biological control of chemical factors in the environment. *Am. Sci.* 46:205–221.
- Reichstein, M. 2007. Impacts of climate change on forest soil carbon: Principles, factors, models, uncertainties, p. 127–135. Tree-Smith, P.H. et al. (eds.) CAB International, Wallingford, U.K.
- Reiners, W.A. 1983. Transport processes in the biogeochemical cycles of carbon, nitrogen, phosphorus, and sulfur, p. 143–176. *In* B. Bolin and R.B. Cook (eds.) *The major biogeochemical cycles and their interactions*. Scope 21. John Wiley & Sons, New York.
- Rethemeyer, J., C. Kramer, G. Gleixner, B. John, T. Yamashita, H. Flessa, N. Andersen, M.-J. Nadeau, and P.M. Grootes. 2005. Transformation of organic matter in agricultural soils: Radiocarbon concentration versus soil depth. *Geoderma* 128:94–105.
- Ridley, A.M., W.J. Slattery, K.R. Helyar, and A. Cowling. 1990. The importance of the carbon cycle to acidification of a grazed annual pasture. *Aust. J. Exp. Agric.* 30:529–537.
- Robert, M., and J. Berthelin. 1986. Role of biological and biochemical factors in soil mineral weathering, p. 455–495. *In* P.M. Huang and M. Schnitzer (eds.) *Interactions of soil minerals with natural organics and microbes*. Soil Science Society of America, Madison, WI.
- Roig, A., A. Lax, J. Cegarra, F. Costa, and M.T. Hernandez. 1988. Cation exchange capacity as a parameter for measuring the humification degree of manures. *Soil Sci.* 146:311–316.
- Romanenkov, V.A., J.U. Smith, P. Smith, O.D. Sirotenko, D.I. Rukhovitch, and I.A. Romanenko. 2007. Soil organic carbon dynamics of croplands in European Russia: Estimates from the “model of humus balance”. *Reg. Environ. Change* 7:93–104.
- Rovira, P., and V.R. Vallejo. 2000. Examination of thermal and acid hydrolysis procedures in characterization of soil organic matter. *Commun. Soil Sci. Plant Anal.* 31:81–100.
- Rumpel, C., A. Seraphin, M.-O. Goebel, G. Wiesenberg, F. Gonzales-Vila, J. Bachmann, L. Schwark, W. Michaelis, A. Mariotti, and I. Kögel-Knabner. 2004. Alkyl C and hydrophobicity in B and C horizons of an acid forest soil. *J. Plant Nutr. Soil Sci.* 167:685–692.
- Russel, J.S. 1960. Soil fertility changes in the long-term experimental plots at Kybybolite, South Australia. I. Changes in pH, total nitrogen, organic carbon and bulk density. *Aust. J. Agric. Sci.* 11:902–926.
- Saggar, S., J.R. Bettany, and J.W.B. Stewart. 1981. Measurement of microbial sulfur in soil. *Soil Biol. Biochem.* 13:493–498.
- Saggar, S., A. Parshotam, G.P. Sparling, C.W. Feltham, and P.B.S. Hart. 1996. <sup>14</sup>C-labelled ryegrass turnover and residence times in soils varying in clay content and mineralogy. *Soil Biol. Biochem.* 28:1677–1686.
- Sala, O.E., W.J. Parton, L.A. Joyce, and W.K. Lauenroth. 1988. Primary production of the central grassland region of the United States. *Ecology* 69:40–45.
- Saleska, S.R., S.D. Miller, D.M. Matross, M.L. Goulden, S.C. Wofsy, H.R. da Rocha, P.B. de Camargo et al. 2003. Carbon in Amazon forests: Unexpected seasonal fluxes and disturbance-induced losses. *Science* 302:1554–1557.

- Sanderman, J., J.A. Baldock, and R. Amundson. 2008. Dissolved organic carbon chemistry and dynamics in contrasting forest and grassland soils. *Biogeochemistry* 89:181–198.
- Sanyal, S.K., and S.K.D. Datta. 1991. Chemistry of phosphorus transformations in soil. *Adv. Soil Sci.* 16:1–20.
- Sarkar, J.M., and J.M. Bollag. 1987. Inhibitory effect of humic and fulvic acids on oxidoreductases as measured by the coupling of 2,4-dichlorophenol to humic substances. *Sci. Total Environ.* 62:367–377.
- Scharpenseel, H.W., H.U. Neue, and S. Singer. 1992. Biotransformations in different climatic belts: Source sink relationships, p. 91–105. *In* J. Kubat (ed.) *Humus, its structure and role in agriculture and environment*. Elsevier Science Publishers, Amsterdam, the Netherlands.
- Scheel, T., C. Dörfler, and K. Kalbitz. 2007. Precipitation of dissolved organic matter by aluminum stabilizes carbon in acidic forest soils. *Soil Sci. Soc. Am. J.* 71:64–74.
- Schimmel, D.S. 1988. Calculation of microbial-growth efficiency from N-15 immobilization. *Biogeochemistry* 6:239–243.
- Schimmel, D.S., D. Alves, I. Enting, M. Heimann, F. Joos, D. Raynaud, and T. Wigley. 1996. CO<sub>2</sub> and the carbon cycle, p. 76–86. *In* J.T. Houghton, L.G. Meira Filho, B.A. Callendar, N. Harris, A. Kattenberg, and K. Maskell (eds.) *Climate change 1995*. Cambridge University Press, Cambridge, U.K.
- Schimmel, D.S., D.C. Coleman, and K.A. Horton. 1985a. Soil organic matter dynamics in paired rangeland and cropland topequences in North Dakota. *Geoderma* 36:201–214.
- Schimmel, D.S., M.A. Stillwell, and R.G. Woodmansee. 1985b. Biogeochemistry of C, N, and P in a soil catena of the short grass steppe. *Ecology* 66:276–282.
- Schmidt, M.W.I., and G. Gleixner. 2005. Carbon and nitrogen isotope composition of bulk soils, particle-size fractions and organic material after treatment with hydrofluoric acid. *Eur. J. Soil Sci.* 56:407–416.
- Schmidt, M.W.I., J.O. Skjemstad, E. Gehrt, and I. Kögel-Knaber. 1999. Charred organic carbon in German chernozemic soils. *Eur. J. Soil Sci.* 50:351–365.
- Schnitzer, M. 1985. Nature of nitrogen in humic substances, p. 303–325. *In* G.R. Aiken et al. (eds.) *Humic substances in soil, sediment and water: Geochemistry, isolation and characterization*. John Wiley & Sons, New York.
- Schnitzer, M. 2000. A lifetime perspective on the chemistry of soil organic matter. *Adv. Agron.* 68:1–58.
- Schnitzer, M., and H.R. Schulten. 1995. Analysis of organic matter in soil extracts and whole soils by pyrolysis-mass spectrometry. *Adv. Agron.* 55:167–198, C1–C2, 199–217.
- Schnitzer, M., and M. Spiteller. 1986. The chemistry of the “unknown” soil nitrogen. *Trans. 13th Int. Congr. Soil Sci.* 3:473–474.
- Schöning, I., G. Morgenroth, and I. Kögel-Knabner. 2005. O/N-alkyl and alkyl C are stabilised in fine particle size fractions of forest soils. *Biogeochemistry* 73:475–497.
- Schulten, H.R. 1987. Pyrolysis and soft ionization mass-spectroscopy of aquatic-terrestrial humic substances and soils. *J. Anal. Pyrol.* 12:149–186.
- Schulten, H.-R., and P. Leinweber. 1996. Characterization of humic and soil particles by analytical pyrolysis and computer modeling. *J. Anal. Appl. Pyrol.* 38:1–53.
- Schulten, H.R., P. Leinweber, and M. Schnitzer. 1998. Analytical pyrolysis and computer modelling of humic and soil particles, p. 281–324. *In* P.M. Huang, N. Senesi, and J. Buffle (eds.) *Structure and surface reactions of soil particles*. Wiley, New York.
- Schulten, H.R., C. Sorge, and M. Schnitzer. 1995. Structural studies on soil nitrogen by curie-point pyrolysis gas chromatography mass spectrometry with nitrogen selective detection. *Biol. Fertil. Soils* 20:174–184.
- Schulten, H.R., C. SorgeLewin, and M. Schnitzer. 1997. Structure of “unknown” soil nitrogen investigated by analytical pyrolysis. *Biol. Fertil. Soils* 24:249–254.
- Schulze, D.G., and P.M. Bertsch. 1995. Synchrotron X-ray techniques in soil, plant, and environmental research. *Adv. Agron.* 55:1–66.
- Schutter, M.E., and R.P. Dick. 2000. Comparison of fatty acid methyl ester (FAME) methods for characterizing microbial communities. *Soil Sci. Soc. Am. J.* 64:1659–1668.
- Sebastia, M.T. 2004. Role of topography and soils in grassland structuring at the landscape and community scales. *Basic Appl. Ecol.* 5:331–346.
- Seilsepour, M., and M. Rashidi. 2008. Modeling of soil cation exchange capacity based on soil colloidal matrix. *American-Eurasian J. Agric. Environ. Sci.* 3:365–369.
- Serrão, E.A.S., I.C. Falesi, J.B. da Vega, and J.R. Teizeira Neto. 1979. Productivity of cultivated pastures on low fertility soils of the Amazon region of Brazil, p. 195–225. *In* P.A. Sanchez and L.W. Tergas (eds.) *Pasture production on acid soils of the tropics*. CIAT, Cali, Columbia.
- Sexstone, A.J., N.P. Revsbech, T.B. Parkin, and J.M. Tiedje. 1985. Direct measurement of oxygen profiles and denitrification rates in soil aggregates. *Soil Sci. Soc. Am. J.* 49:645–651.
- Shevchenko, S.M., and G.W. Bailey. 1996. Life after death: Lignin-humic relationships reexamined. *Crit. Rev. Environ. Sci. Technol.* 26:95–153.
- Six, J., R.T. Conant, E.A. Paul, and K. Paustian. 2002. Stabilization mechanisms of soil organic matter: Implications for C-saturation of soils. *Plant Soil* 241:155–176.
- Six, J., G. Guggenberger, K. Paustian, L. Haumaier, E.T. Elliott, and W. Zech. 2001. Sources and composition of soil organic matter fractions between and within soil aggregates. *Eur. J. Soil Sci.* 52:607–618.
- Skjemstad, J., and J.A. Baldock. 2008. Total and organic carbon, p. 225–238. *In* M.R. Carter and E.G. Gregorich (eds.) *Soil sampling and methods of analysis*. 2nd edn. CRC Press, Taylor & Francis Group, Boca Raton, FL.
- Skjemstad, J.O., P. Clarke, J.A. Taylor, J.M. Oades, and S.G. McClure. 1996. The chemistry and nature of protected carbon in soil. *Aust. J. Soil Res.* 34:251–271.
- Skjemstad, J.O., P. Clarke, J.A. Taylor, J.M. Oades, and R.H. Newman. 1994. The removal of magnetic materials from surface soils: A solid state <sup>13</sup>C CP/MAS NMR study. *Aust. J. Soil Res.* 32:1215–1229.

- Skjemstad, J.O., L.J. Janik, and J.A. Taylor. 1998. Non-living soil organic matter: What do we know about it? *Aust. J. Exp. Agric.* 38:667–680.
- Skjemstad, J.O., D.C. Reicosky, A.R. Wilts, and J.A. McGowan. 2002. Charcoal carbon in US agricultural soils. *Soil Sci. Soc. Am. J.* 66:1249–1255.
- Skjemstad, J.O., and L. Spouncer. 2003. Integrated soils modelling for the national carbon accounting system. Estimating changes in soil carbon resulting from changes in land use. National Carbon Accounting System Technical Report No. 36.
- Skjemstad, J.O., L.R. Spouncer, B. Cowie, and R.S. Swift. 2004. Calibration of the Rothamsted organic carbon turnover model (RothC ver. 26.3), using measurable soil organic carbon pools. *Aust. J. Soil Res.* 42:79–88.
- Skjemstad, J.O., and J.A. Taylor. 1999. Does the Walkley-Black method determine soil charcoal? *Commun. Soil Sci. Plant Anal.* 30:2299–2310.
- Skjemstad, J.O., J.A. Taylor, and R.J. Smernik. 1999. Estimation of charcoal (char) in soils. *Commun. Soil Sci. Plant Anal.* 30:2283–2298.
- Skyllberg, U., and T. Magnusson. 1995. Cations adsorbed to soil organic matter—A regulatory factor for the release of organic carbon and hydrogen ions from soils to waters. *Water Air Soil Pollut.* 85:1095–1100.
- Smernik, R.J., and J.A. Baldock. 2005. Does solid-state  $^{15}\text{N}$  NMR spectroscopy detect all soil organic nitrogen? *Biogeochemistry* 75:507–528.
- Smernik, R.J., and J.M. Oades. 2000a. The use of spin counting for determining quantitation in solid state  $^{13}\text{C}$  NMR spectra of natural organic matter. 1. Model systems and the effects of paramagnetic impurities. *Geoderma* 96:101–129.
- Smernik, R.J., and J.M. Oades. 2000b. The use of spin counting for determining quantitation in solid state  $^{13}\text{C}$  NMR spectra of natural organic matter. 2. HF-treated soil fractions. *Geoderma* 96:159–171.
- Smith, P., and P. Ineson. 2007. The soil carbon dioxide sink, p. 50–57. *In* D. Reay, C.N. Hewitt, K.A. Smith, and J. Grace (eds.) *Greenhouse gas sinks*. CAB International, Oxfordshire, U.K.
- Smith, J.L., and E.A. Paul. 1990. The significance of soil microbial biomass estimations. *Soil Biochem.* 6:357–396.
- Snowdon, P., P. Ryan, and J. Raison. 2005. Review of C:N ratios in vegetation, litter and soil under Australian native forests and plantations. National Carbon Accounting System—Technical Report 45:72 pp.
- Söderlund, R., and B.H. Svensson. 1976. The global nitrogen cycle. *In* B.H. Svensson and R. Söderlund (eds.) *Nitrogen, phosphorous and sulphur-global cycles*, SCOPE Report 7, Ecol. Bull. (Stockholm), 22:23–73.
- Sørensen, L.H. 1972. Stabilization of newly formed amino acid metabolites in soil by clay minerals. *Soil Sci.* 114:5–11.
- Sørensen, L.H. 1975. Influence of clay on rate of decay of amino acid metabolites synthesized in soils during decomposition of cellulose. *Soil Biol. Biochem.* 7:171–177.
- Sohi, S.P., N. Mahieu, J.R.M. Arah, D.S. Powlson, B. Madari, and J.L. Gaunt. 2001. A procedure for isolating soil organic matter fractions suitable for modeling. *Soil Sci. Soc. Am. J.* 65:1121–1128.
- Sohi, S.P., N. Mahieu, D.S. Powlson, B. Madari, R.H. Smittenberg, and J.L. Gaunt. 2005. Investigating the chemical characteristics of soil organic matter fractions suitable for modeling. *Soil Sci. Soc. Am. J.* 69:1248–1255.
- Sokoloff, V.P. 1938. Effect of neutral salts of sodium and calcium on carbon and nitrogen in soils. *J. Agric. Res.* 57:201–216.
- Sollins, P., P. Homann, and B.A. Caldwell. 1996. Stabilization and destabilization of soil organic matter: Mechanisms and controls. *Geoderma* 74:65–105.
- Solomon, D., J. Lehmann, J. Kinyangi, B.Q. Liang, K. Heymann, L. Dathe, K. Hanley, S. Wirick, and C. Jacobsen. 2009. Carbon (1s) NEXAFS spectroscopy of biogeochemically relevant reference organic compounds. *Soil Sci. Soc. Am. J.* 73:1817–1830.
- Solomon, D., J. Lehmann, I. Lobe, C.E. Martinez, S. Tveitnes, C.C. Du Preez, and W. Amelung. 2005. Sulphur speciation and biogeochemical cycling in long-term arable cropping of subtropical soils: Evidence from wet-chemical reduction and S K-edge XANES spectroscopy. *Eur. J. Soil Sci.* 56:621–634.
- Sombroek, W.G., F.O. Nachtergaele, and A. Hebel. 1993. Amounts, dynamics and sequestering of carbon in tropical and subtropical soils. *Ambio* 22:417–426.
- Spain, A.V. 1990. Influence of environmental conditions and some soil chemical properties on the carbon and nitrogen contents of some Australian rainforest soils. *Aust. J. Soil Res.* 28:825–839.
- Spain, A.V., R.F. Isbell, and M.E. Probert. 1983. Soil organic matter, p. 551–563. *Soils: An Australian viewpoint*. CSIRO, Melbourne, Australia.
- Starr, M., C.J. Westman, and J. AlaReini. 1996. The acid buffer capacity of some Finnish forest soils: Results of acid addition laboratory experiments. *Water Air Soil Pollut.* 89:147–157.
- Stehlickova, L., M. Svab, L. Wimmerova, and J. Kozler. 2009. Intensification of phenol biodegradation by humic substances. *Int. Biodeterior. Biodegrad.* 63:923–927.
- Stevenson, F.J. 1986. *Cycles of soil: Carbon, nitrogen, phosphorus, sulfur, micronutrients*. John Wiley & Sons, New York.
- Stevenson, F.J. (ed.). 1994. *Humus chemistry: Genesis, composition and reactions*. John Wiley & Sons, New York.
- Stewart, J.W.B., and C.V. Cole. 1989. Influences of elemental interactions and pedogenic processes in organic matter dynamics. *Plant Soil* 115:199–209.
- Stewart, C.E., K. Paustian, R.T. Conant, A.F. Plante, and J. Six. 2008a. Soil carbon saturation: Evaluation and corroboration by long-term incubations. *Soil Biol. Biochem.* 40:1741–1750.
- Stewart, C.E., A.F. Plante, K. Paustian, R.T. Conant, and J. Six. 2008b. Soil carbon saturation: Linking concept and measurable carbon pools. *Soil Sci. Soc. Am. J.* 72:379–392.
- Stockdale, E.A., and P.C. Brookes. 2006. Detection and quantification of the soil microbial biomass—Impacts on the management of agricultural soils. *J. Agric. Sci.* 144:285–302.

- Strong, D.T., H. De Wever, R. Merckx, and S. Recous. 2004. Spatial location of carbon decomposition in the soil pore system. *Eur. J. Soil Sci.* 55:739–750.
- Swanston, C.W., B.A. Caldwell, P.S. Homann, L. Ganio, and P. Sollins. 2002. Carbon dynamics during a long-term incubation of separate and recombined density fractions from seven forest soils. *Soil Biol. Biochem.* 34:1121–1130.
- Swanston, C.W., M.S. Torn, P.J. Hanson, J.R. Southon, C.T. Garten, E.M. Hanlon, and L. Ganio. 2005. Initial characterization of processes of soil carbon stabilization using forest stand-level radiocarbon enrichment. *Geoderma* 128:52–62.
- Swift, R.S. 2001. Sequestration of carbon by soil. *Soil Sci.* 166:858–871.
- Szabolcs, I. 1994. The concept of soil resilience, p. 33–39. *In* D. Greenland and I. Szabolcs (eds.) *Soil resilience and sustainable land use*. CAB International, Wallingford, Oxon, England.
- Tan, K.H. 1986. Degradation of soil minerals by organic acids, p. 1–27. *In* P.M. Huang and M. Schnitzer (eds.) *Interactions of soil minerals with natural organics and microbes*. Soil Science Society of America, Inc., Madison, WI.
- Tan, K.H., and P.S. Dowling. 1984. Effect of organic-matter on CEC due to permanent and variable changes in selected temperate region soils. *Geoderma* 32:89–101.
- Tegelaar, E.W., J.W. Deleeuw, and C. Saizjimenez. 1989. Possible origin of aliphatic moieties in humic substances. *Sci. Total Environ.* 81–82:1–17.
- Thompson, M.L., H. Zhang, M. Kazemi, and J.A. Sandor. 1989. Contribution of organic matter to cation exchange capacity and specific surface area of fractionated soil materials. *Soil Sci.* 148:250–257.
- Thorn, K.A., and M.A. Mikita. 1992. Ammonia fixation by humic substances: A N-15 and C-13 NMR study. *Sci. Total Environ.* 113:67–87.
- Thorn, K.A., P.J. Pettigrew, and W.S. Goldenberg. 1996. Covalent binding of aniline to humic substances. 2. N-15 NMR studies of nucleophilic addition reactions. *Environ. Sci. Technol.* 30:2764–2775.
- Thurston, J.M., E.D. Williams, and A.E. Johnston. 1976. Modern developments in an experiment on permanent grassland started in 1856: Effects of fertilizers and lime on botanical composition and crop and soil analyses. *Ann. Agron.* 27:1043–1082.
- Tiessen, H., J.W.B. Stewart, and D.W. Anderson. 1994. Determinants of resilience in soil nutrient dynamics, p. 157–170. *In* D. Greenland and I. Szabolcs (eds.) *Soil resilience and sustainable land use*. CAB International, Wallingford, Oxon, England.
- Tiessen, H., J.W.B. Stewart, and C.V. Cole. 1984. Pathways of phosphorus transformations in soils of differing pedogenesis. *Soil Sci. Soc. Am. J.* 48:853–858.
- Tiessen, H., J.W.B. Stewart, and J.O. Moir. 1983. Changes in organic and inorganic phosphorus composition of two grassland soils and their particle size fractions during 60–90 years of cultivation. *J. Soil Sci.* 34:815–823.
- Tisdall, J.M., and J.M. Oades. 1982. Organic matter and water-stable aggregates in soils. *J. Soil Sci.* 33:141–163.
- Toor, G.S., S. Hunger, J.D. Peak, J.T. Sims, and D.L. Sparks. 2006. Advances in the characterization of phosphorus in organic wastes: Environmental and agronomic applications, p. 1–72. *In* D.L. Sparks (ed.) *Advances in agronomy*. Vol. 89. Academic Press, San Diego, CA.
- Trumbore, S.E., and S.H. Zheng. 1996. Comparison of fractionation methods for soil organic matter <sup>14</sup>C analysis. *Radiocarbon* 38:219–229.
- Tuomela, M., M. Vikman, A. Hatakka, and M. Itävaara. 2000. Biodegradation of lignin in a compost environment: A review. *Bioresour. Technol.* 72:169–183.
- Turner, R.E., N.N. Nancy, D. Justic, and Q. Dortch. 2003. Future aquatic nutrient limitations. *Mar. Pollut. Bull.* 46:1032–1034.
- Turnpault, M.P., P. Bonnaud, J. Fichter, J. Ranger, and E. Dambrine. 1996. Distribution of cation exchange capacity between organic matter and mineral fractions in acid forest soils (Vosges mountains, France). *Eur. J. Soil Sci.* 47:545–556.
- Uriyo, A.P., and A. Kesseba. 1975. Amounts and distribution of organic phosphorus in some profiles in Tanzania. *Geoderma* 13:201–210.
- Vacca, D.J., W.F. Bleam, and W.J. Hickey. 2005. Isolation of soil bacteria adapted to degrade humic acid-sorbed phenanthrene. *Appl. Environ. Microbiol.* 71:3797–3805.
- Vaccaro, S., A. Muscolo, D. Pizzeghello, R. Spaccini, A. Piccolo, and S. Nardi. 2009. Effect of a compost and its water-soluble fractions on key enzymes of nitrogen metabolism in maize seedlings. *J. Agric. Food Chem.* 57: 11267–11276.
- Valdrighi, M.M., A. Pera, M. Agnolucci, S. Frassinetti, D. Lunardi, and G. Vallini. 1996. Effects of compost-derived humic acids on vegetable biomass production and microbial growth within a plant (*Cichorium intybus*)-soil system: A comparative study. *Agric. Ecosyst. Environ.* 58:133–144.
- Valdrighi, M.M., A. Pera, S. Scatena, M. Agnolucci, and G. Vallini. 1995. Effects of humic acids extracted from mined lignite or composted vegetable residues on plant growth and soil microbial population. *Compost. Sci. Util.* 3:30–38.
- Vallini, G., A. Pera, M. Agnolucci, and M.M. Valdrighi. 1997. Humic acids stimulate growth and activity of in vitro tested axenic cultures of soil autotrophic nitrifying bacteria. *Biol. Fertil. Soils* 24:243–248.
- Vallini, G., A. Pera, L. Avio, M.M. Valdrighi, and M. Giovannetti. 1993. Influence of humic acids on laurel growth, associated rhizospheric microorganisms, and mycorrhizal fungi. *Biol. Fertil. Soils* 16:1–4.
- Valzano, F., B. Murphy, and T. Loen. 2005. The impact of tillage on changes in soil carbon with special emphasis on Australian conditions. *National Carbon Accounting System-Technical Report* 43:164 pp.
- van Breemen, N., J. Mulder, and C.T. Driscoll. 1983. Acidification and alkalization of soils. *Plant Soil* 75:283–308.

- Vance, E.D., P.C. Brookes, and D.S. Jenkinson. 1987a. Microbial biomass measurements in forest soils: The use of the chloroform fumigation incubation method in strongly acid soils. *Soil Biol. Biochem.* 19:697–702.
- Vance, E.D., P.C. Brookes, and D.S. Jenkinson. 1987b. An extraction method for measuring soil microbial biomass-C. *Soil Biol. Biochem.* 19:703–707.
- van der Linden, A.M.A., L.J.J. Jeurisson, J.A. Van Veen, and B. Schippers. 1989. Turnover of soil microbial biomass as influenced by soil compaction, p. 25–36. *In* J. Attansen and K. Henriksen (eds.) *Nitrogen in organic wastes applied to soil*. Academic Press, London, U.K.
- van Krevelen, D.W. 1950. Graphical-statistical method for the study of structure and reaction processes of coal. *Fuel* 29:269–284.
- van Veen, J.A., and P.J. Kuikman. 1990. Soil structural aspects of decomposition of organic matter by microorganisms. *Biogeochemistry* 11:213–233.
- Vanderhart, D.L., and R.H. Atalla. 1984. Studies of microstructure in native celluloses using solid-state C-13 NMR. *Macromolecules* 17:1465–1472.
- Varanini, Z., and R. Pinton. 2001. Direct versus indirect effects of soil humic substances on plant growth and nutrition, p. 141–158. *In* R. Pinton et al. (eds.) *The rhizosphere*. Marcel Dekker, Basel, Switzerland.
- Vaughan, D., and R.E. Malcolm. 1985. Soil organic matter and biological activity. Martinus Nijhoff/Dr. W. Junk Publishers, Dordrecht, the Netherlands.
- Vedrova, E.F. 1997. Organic matter decomposition in forest litter. *Eurasian Soil Sci.* 30:181–188.
- Vereecken, H., J. Maes, J. Feyen, and P. Darius. 1989. Estimating the soil moisture retention characteristic from texture, bulk density and carbon content. *Soil Sci.* 148:389–403.
- Verlinden, G., B. Pycke, J. Mertens, F. Debersaques, K. Verheyen, G. Baert, J. Bries, and G. Haesaert. 2009. Application of humic substances results in consistent increases in crop yield and nutrient uptake. *J. Plant Nutr.* 32:1407–1426.
- Visser, S.A. 1985. Physiological action of humic substances on microbial cells. *Soil Biol. Biochem.* 17:457–462.
- Volkoff, B., and C.C. Cerri. 1988. Humus of Brazilian soils. Nature and relationship with the environment. *Cahiers ORSTOM* 24:83–95.
- von Liebig, J. 1840. *Die Chemie in ihrer Anwendung auf Agrikultur und Physiologie* Braunschweig. Vieweg. As cited by Hedges and Oades (1997).
- von Lützw, M., I. Kogel-Knabner, B. Ludwig, E. Matzner, H. Flessa, K. Ekschmitt, G. Guggenberger, B. Marschner, and K. Kalbitz. 2008. Stabilization mechanisms of organic matter in four temperate soils: Development and application of a conceptual model. *J. Plant Nutr. Soil Sci.* 171:111–124.
- von Lützw, M., J. Leifeld, M. Kainz, I. Kögel-Knabner, and J.C. Munch. 2002. Indications for soil organic matter quality in soils under different management. *Geoderma* 105:243–258.
- Wakelin, S.A., L.M. Macdonald, S.L. Rogers, A.L. Gregg, T.P. Bolger, and J.A. Baldock. 2008. Habitat selective factors influencing the structural composition and functional capacity of microbial communities in agricultural soils. *Soil Biol. Biochem.* 40:803–813.
- Wardle, D.A. 1992. A comparative assessment of factors which influence microbial biomass carbon and nitrogen levels in soil. *Biol. Rev. Camb. Philos. Soc.* 67:321–358.
- Watson, C.J., G. Travers, D.J. Kilpatrick, A.S. Laidlaw, and E. O’Riordan. 2000. Overestimation of gross N transformation rates in grassland soils due to non-uniform exploitation of applied and native pools. *Soil Biol. Biochem.* 32:2019–2030.
- Webster, J.R., J.B. Waide, and B.C. Patten. 1975. Nutrient recycling and stability of ecosystems, p. 1–27. *In* F.G. Howell et al. (eds.) *Mineral cycling in Southeastern ecosystems*. National Technical Information Service, Springfield, VA.
- Wegner, P.F., C.J. McDowall, and A.B. Frensham. 1989. Monitoring farming systems. Effects of cropping practices. Limitations to wheat yields. Technical Paper 23. Department of Agriculture of South Australia.
- Weihermuller, L., J. Siemens, M. Deurer, S. Knoblauch, H. Rupp, A. Gottlein, and I. Putz. 2007. In situ soil water extraction: A review. *J. Environ. Qual.* 36:1735–1748.
- Whiteley, G.M., and C. Pettit. 1994. Effect of lignite humic acid treatment on the rate of decomposition of wheat straw. *Biol. Fertil. Soils* 17:18–20.
- Widmer, F., A. Fließbach, E. Laczkó, J. Schulze-Aurich, and J. Zeyer. 2001. Assessing soil biological characteristics: A comparison of bulk soil community DNA-, PLFA-, and Biolog-analyses. *Soil Biol. Biochem.* 33:1029–1036.
- Yan, F., S. Schubert, and K. Mengel. 1996. Soil pH increase due to biological decarboxylation of organic anions. *Soil Biol. Biochem.* 28:617–624.
- Yasmeen, S., M. Sariah, I. Razi, R. Mawardi, and A. Asgar. 2009. In vitro fungicidal activity of humic acid fraction from oil palm compost. *Int. J. Agric. Biol.* 11:448–452.
- Yimer, F., S. Ledin, and A. Abdelkadir. 2008. Concentrations of exchangeable bases and cation exchange capacity in soils of cropland, grazing and forest in the Bale Mountains, Ethiopia. *For. Ecol. Manage.* 256:1298–1302.
- Zepp, R.G., and C. Sonntag. 1995. The role of nonliving organic matter in the earth’s carbon cycle. Wiley, New York, 342 pp.
- Zunino, H., F. Borie, S. Aguilera, J.P. Martin, and K. Haider. 1982. Decomposition of <sup>14</sup>C-labeled glucose, plant and microbial products and phenols in volcanic ash-derived soils of Chile. *Soil Biol. Biochem.* 14:37–43.

# 12

## Soil Solution

---

12.1	Basic Concepts.....	12-1
	Definitions • Composition	
12.2	Sampling the Soil Solution .....	12-3
	Laboratory Methods • Field Methods	
12.3	Thermodynamics of the Soil Solution .....	12-5
	Fundamentals, Units, and Variables • First and Second Laws of Thermodynamics • Associated Thermodynamic Relationships • Chemical Potential and Free Energy • Chemical Potential and Activities in Ideal Solutions • Activities and Activity Coefficients: Nonideal Solutions • Equilibrium Constants • Effects of Temperature and Pressure • Single-Ion Activity Coefficients • Electrochemical Potential • Heat of Hydration of Ions	
12.4	Interactions of Gases with the Soil Solution.....	12-10
	Henry's Law • Volatile Organic Compounds • Rates of Dissolution of Gases in Water	
12.5	Acid–Base Reactions in the Soil Solution .....	12-12
	Fundamentals of Acid–Base Chemistry in Soil Solution • Calculations for Acid–Base Equilibria • Buffering Capacity of Soil Solutions • Soluble Organic Acids	
12.6	Formation of Soluble Complexes .....	12-14
	Types of Complexes • Hard and Soft Acid–Base Rules • Rates of Formation of Solution Complexes	
12.7	Application of Thermodynamic and Equilibrium Concepts to Soil Solutions.....	12-16
	Speciation and Single-Ion Activity Determinations • Geochemical Models • Oxidation/Reduction Reactions • Successful Applications of Geochemical Modeling to Soil Solutions • Limitations to Applying Geochemical Models to Soil Solutions	
12.8	Current Status and Future Research Directions.....	12-21
	References.....	12-21

Paul Schwab  
*Purdue University*

The soil solution is the hub of chemical and biological activity in the soil. Most reactions are slow in the absence of water: Soil organisms become dormant or die, mineral transformations become imperceptibly slow, and soil chemical weathering and formation processes become greatly impeded. Addition of moisture to previously dry systems reinitiates these reactions.

### 12.1 Basic Concepts

#### 12.1.1 Definitions

The simplest definition of the soil solution is “aqueous liquid phase of the soil and its solutes” (SSSA, 2009). A broader definition describes the soil solution as a natural system that is both open and dynamic. Its composition is the result of the concurrent reactions of the labile soil minerals, organic materials, and biological metabolism. Any discussion of the soil solution, however, must take into account that from physical, chemical, and biological perspectives, a significant fraction of the soil solution

seemingly does not participate in some important phenomena. Many examples exist in different disciplines of soil science that illustrate this point. In soil physics, the concepts of “mobile” and “immobile” water have been introduced to explain why water is often observed to move more rapidly through soil than would be predicted assuming that water participates in the transport process. Higher plants and microorganisms undergo serious moisture deficit even when measurable water still exists in the soil. The composition and kinetics of reaction of water very near solid surfaces in the soil are significantly different than in the bulk solution. Therefore, a more functional definition of soil solution goes beyond simply the “aqueous liquid phase” and reflects that the soil solution may be dependent upon the application and, in some instances, the methodology used to obtain this solution from the soil.

From the viewpoint of a soil chemist, the soil solution may be defined as “the aqueous liquid phase in soil with a composition that is influenced by exchanges of matter and energy with soil air, soil solid phases, the biota, and the gravitational field of the

earth” (Sposito, 2008). By defining it as a phase, Sposito implicitly requires that the soil solution has uniform bulk properties (such as composition and temperature) and can be isolated from the soil. The requirement of uniformity can be met only on small scales of time and space because of the dynamic and spatially variable nature of soils.

The soil solution viewed on a molecular level would reveal that it is not a distinct entity but a part of the

continuum of phases exhibiting indistinct interfaces at the molecular level. Solutes in the aqueous phase may be associated with bound water at the surfaces of soil colloids, free water percolating through soil macropores, water in the free space of plant roots, or immobile water in soil micropores.

(Wolt, 1994)

## 12.1.2 Composition

Because soil solutions are highly variable over space and time, their composition can be discussed only in general terms. Trends in relative concentrations of soluble inorganic and organic constituents (see Chapter 11) are similar for most soils, but natural and anthropogenic factors influence some or all components.

### 12.1.2.1 Inorganic Constituents

The most common inorganic cations in the soil solution (Table 12.1) usually are  $\text{Ca}^{2+}$ ,  $\text{Mg}^{2+}$ , and  $\text{K}^+$  (in that order) with a large number of minor cations, including various forms of  $\text{Na}^+$ ,  $\text{Fe}^{2+}$ ,  $\text{Cu}^{2+}$ , and  $\text{Zn}^{2+}$ . The most prevalent anions are  $\text{HCO}_3^-$ ,  $\text{Cl}^-$ , and  $\text{SO}_4^{2-}$ . Soils that become flooded are strongly influenced by reducing conditions and microbial activities, and  $\text{Fe}^{2+}$ ,  $\text{HS}^-$ , and  $\text{SO}_4^{2-}$  can take on greater importance. In contaminated environments, the entire composition of the soil solution will change to reflect the most soluble components of the contaminants.

The sum of soluble cations and anions usually is less than  $10^{-2}$  mol  $\text{L}^{-1}$ . Among the cations,  $\text{Ca}^{2+}$  will comprise at least half of this total; for the anions, the division among  $\text{HCO}_3^-$ ,  $\text{Cl}^-$ , and  $\text{SO}_4^{2-}$  will be dependent upon soil pH and composition of the soil solids. Naturally, saline soils (see Chapter 17 of *Handbook of Soil Sciences: Resource Management and Environmental Impacts*) will

**TABLE 12.1** Inorganic Components Found in Soil Solutions

Category	Major Components ( $10^{-4}$ – $10^{-2}$ mol $\text{L}^{-1}$ )	Minor Components ( $10^{-6}$ – $10^{-4}$ mol $\text{L}^{-1}$ )	Others <sup>a</sup>
Cations	$\text{Ca}^{2+}$ , $\text{Mg}^{2+}$ , $\text{Na}^+$ , $\text{K}^+$	$\text{Fe}^{2+}$ , $\text{Mn}^{2+}$ , $\text{Zn}^{2+}$ , $\text{Cu}^{2+}$ , $\text{NH}_4^+$ , $\text{Al}^{3+}$	$\text{Cr}^{3+}$ , $\text{Ni}^{2+}$ , $\text{Cd}^{2+}$ , $\text{Pb}^{2+}$
Anions	$\text{HCO}_3^-$ , $\text{Cl}^-$ , $\text{SO}_4^{2-}$	$\text{H}_2\text{PO}_4^-$ , $\text{F}^-$ , $\text{HS}^-$	$\text{CrO}_4^{2-}$ , $\text{HMoO}_4^-$
Neutral	$\text{Si}(\text{OH})_4$	$\text{B}(\text{OH})_3$	

Concentration ranges are estimates and could change depending upon specific environments. The components listed are not necessarily the dominant solution species.

<sup>a</sup> Components normally found in concentrations  $<10^{-6}$  mol  $\text{L}^{-1}$  unless in a contaminated environment.

contain elevated concentrations of  $\text{Ca}^{2+}$ ,  $\text{Mg}^{2+}$ ,  $\text{Cl}^-$ ,  $\text{SO}_4^{2-}$ , and sometimes  $\text{Na}^+$ , depending upon pH and the source of the salts.

Concentrations of inorganic constituents in the soil solution are controlled by many factors, including pH, redox potential, and solid-phase composition. These considerations will be addressed later in this chapter and elsewhere in Chapters 15 through 18.

### 12.1.2.2 Organic Constituents

The composition of the soluble organic compounds in the soil solution is not as complex as that in the organic solid phase (see Chapter 11) but is a reflection of the organic components of the solid phase. Soluble organics also originate from the organisms in the soil including exudates from plant roots and soil microbes. Because these compounds are generated and degraded by microbial activity, the concentrations of these compounds in the soil solution can be more transient and more variable than soluble inorganic constituents.

As with soluble inorganic species, the organic constituents can be positively charged, negatively charged, or neutral. The chemical reactions of these compounds will be influenced by their electronic charge, but hydrophobic and hydrophilic tendencies are critical as well. For example, positively charged compounds that are water soluble can be adsorbed by cation exchange sites, negatively charged organics may form strong complexes with iron or aluminum oxides, and uncharged compounds may adsorb onto hydrophobic sites of soil minerals and organic matter.

The low-molecular-weight carboxylic acids typify soluble organics (Table 12.2). They are continually exuded by plant roots and soil microorganisms and are readily degraded with a half-life of hours. Carboxylic acids have the  $\text{COOH}$  functional group. The proton usually is dissociated in soil solutions, and the resulting negatively charged ligand often can act as a complexing agent for metals. Formic and tartaric acids are exuded by grass roots, acetic acid is generated under anaerobic conditions, oxalic acid is often associated with ectomycorrhizae, and citric acid is excreted by fungi and plant roots (Sposito, 2008). Typical concentrations for these acids range from  $10^{-5}$  to  $10^{-3}$  mol  $\text{L}^{-1}$ . Stevenson (1967) published an extensive review of these and other organic constituents in the soil solution.

**TABLE 12.2** Organic Components Found in Typical Soil Solutions

Category	Major Components ( $10^{-4}$ – $10^{-2}$ mol $\text{L}^{-1}$ )	Minor Components ( $10^{-6}$ – $10^{-4}$ mol $\text{L}^{-1}$ )
Naturally occurring	Formate, acetate, oxalate, amino acids, simple sugars	Citrate, phenolics, siderophores, proteins, alcohols, sulfhydryls
Anthropogenic	<sup>a</sup>	Herbicides, fungicides, insecticides, PCBs, petroleum hydrocarbons, surfactants, solvents, antibiotics, hormones

Concentration ranges are estimates and are subject to variability depending upon specific environmental conditions.

<sup>a</sup> Organic contaminants are present in low concentrations except in the case of spills, leaks, and accidental releases.



Organic pollutants include those compounds that have been introduced artificially into the soil, whether by design or accident. Most organic pesticides are applied at very low concentrations ( $0.1\text{--}10\text{ kg ha}^{-1}$ ). Organics that have been spilled or accidentally leaked onto the soil can be present at many orders of magnitude higher. The resulting concentration in the soil solution will be dependent upon the total concentration in the soil, water solubility, strength of adsorption, volatility, and degradability of the compound in question. For example, the triazine herbicide, atrazine, normally is applied at a rate of approximately  $2\text{ kg ha}^{-1}$ , has a water solubility of  $35\text{ mg L}^{-1}$ , is weakly adsorbed by the soil, has a half-life of approximately 30 days, and has limited volatility. In contrast, glyphosate is applied at about the same rate as atrazine but is 1000 times more soluble, very strongly adsorbed, and not volatile. Immediately after application, atrazine concentrations in the soil solution can exceed  $5\text{ mg L}^{-1}$  and represent an environmental threat to surface and groundwater. In contrast, aqueous glyphosate concentrations are nearly always  $<1\text{ }\mu\text{g L}^{-1}$ , and glyphosate is seldom detected in drinking water. (McBride, 1994, provides an excellent overview of the chemical behavior of pesticides in soil.) Organic solvents and petroleum hydrocarbons tend to have very low water solubilities ( $<1\text{ }\mu\text{g L}^{-1}$ ), but their potential toxicity is high, and even trace concentrations in the soil solution may be environmentally significant.

## 12.2 Sampling the Soil Solution

The definition of the soil solution given in Section 12.1.1 is idealized and serves as a point from which the soil solution may be conceptualized. At the experimental level, the "soil solution" is defined by the method used to separate the aqueous phase from the rest of the soil. As discussed later, sampling methodology has a profound influence on the composition of the soluble constituents. Thus, consistent with the Heisenberg uncertainty principle for the study of subatomic particles, one cannot sample and examine the soil solution without altering it.

For both laboratory and field studies of the soil solution, one of the major problems associated with obtaining an unaltered soil solution is that the moisture content of field soils can rapidly change from air dry to saturated, and the moisture content influences the chemical and microbiological dynamics in the aqueous phase. Most techniques for obtaining samples of the soil solution function poorly when the moisture content is below saturation, and very few function at all moisture tensions of  $\leq 33\text{ kPa}$  ( $1/3\text{ bar}$ ). The choice of method and moisture content for obtaining a sample of the soil solution must be made to minimize the impact on solution composition while realizing that the act of sampling necessarily changes it.

An example of the influence of moisture content on soil chemical properties is the often-observed change in pH at different soil:solution ratios (Figure 12.1). Soil pH was measured for four soils with moisture contents ranging from 1:1 to a ratio of 10:1 water:soil (on a volume/mass basis). As the amount of

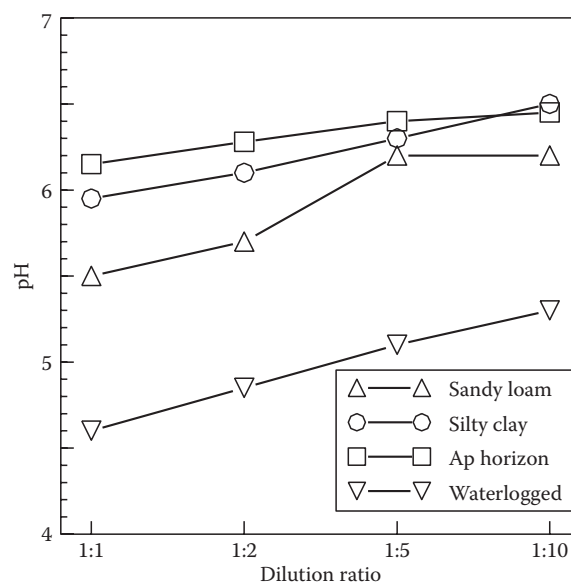


**FIGURE 12.1** The impact of soil:solution ratio on the measured pH of two soils. Data for sandy loam and silty clay soils from Schwab (1992); surface horizon and waterlogged soil from Elberling and Matthiesen (2007). (Data from Schwab, A.P. 1992. Chemical and physical characterization of soils. In L.E. Erickson, S.C. Grant, and J.P. McDonald (eds.) Conf. Proc. Hazard. Subst. Res. University of Colorado, Boulder, Co., p. 326–344; Elberling, B., and H. Matthiesen. 2007. Methodologically controlled variations in laboratory and field pH measurements in waterlogged soils. Eur. J. Soil Sci. 58:207–214.)

water increased, the pH increased significantly. These observations lead to the following inescapable conclusion:

Consideration of soil at field moisture contents is necessitated by the inability to predict consistently the effects of variation in soil to water ratios across broad ranges of soil solution composition; neither variation in total electrolyte concentrations or the activity ratios of specific ion components of the soil solution can be adequately resolved when water to soil ratios vary from field moisture contents to ratios  $>1$ . This is the main limitation to the use of water extracts as models of soil solution.

(Wolt, 1994)

### 12.2.1 Laboratory Methods

Many laboratory methods have been developed for sampling the soil solution; only a few will be summarized here. The methods may be broadly categorized as aqueous extracts, column displacement, and pressure extraction. Each technique has advantages and limitations. (One must also consider proper sampling and handling techniques for the samples. For example, the simple act of air-drying the soil can have a profound effect on the soil chemical and microbiological properties [Bartlett and James, 1980; West et al., 1992].)

The steps to obtaining aqueous extracts include adding water to the soil to the point of saturation or beyond, equilibrating, and

removing solution. Equilibration times and separation techniques will depend upon the method used and desired application. If a saturated paste is prepared (United States Salinity Laboratory Staff, 1954) for the assessment of soil salinity, the paste is equilibrated for 16 h followed by vacuum removal of the soil solution. If equilibrium with soil solid phases is desired, equilibrations of hundreds to thousands of hours may be required (Kittrick, 1977; Schwab, 1989; Evans and Banwart, 2006; Sposito, 2008). The advantages of these techniques include ease of preparation, simple separation of soil and solution, and the ability to control many experimental parameters such as aeration and shaking. Limitations are unrealistic moisture contents, abrasion of soil surfaces during shaking, and uncertain impacts of wide soil:solution ratios on solution composition. This method has been applied with success in many instances (Lindsay, 1979; Berggren and Mulder, 1995).

Column displacement consists of forcing a fraction of the soil solution from the soil by leaching the soil with an aqueous solution (miscible displacement) or a water-insoluble organic solvent (immiscible displacement). These techniques have a long history, perhaps beginning with Thompson (1850) and Way (1850) leaching ammonium sulfate solutions through columns of soil and finding that the ammonium had been replaced by calcium. Schloesing (1866) used miscible displacement to obtain a sample of the soil solution; this method is quite similar to modern miscible displacement techniques (Adams, 1974). In all column displacement procedures, moist soil is packed into columns to a desired bulk density, sealing the surface by mechanically dispersing the clays, and leaching with the displacing liquid. The soil solution is collected in fractions until the displacing liquid appears in the leachate. This system may be modified to include pressure from the top (Ross and Bartlett, 1990) or vacuum applied to the bottom of the column (Wolt and Graveel, 1986).

The advantages of column displacement methods are obtaining soil solution from a soil at field moisture conditions, no requirement for grinding or shaking, and maintaining the dissolved gas content (except in the vacuum modification). Disadvantages include (1) generally short incubation times to prevent unusual microbial growth or changes in moisture content; (2) lack of knowledge of the fraction of the “true” soil solution that is obtained because of chemical and physical heterogeneity of the columns and because a large fraction of the water-filled pore space being occupied by the diffuse double layer; and (3) (in the case of immiscible displacement) an unknown influence of organic solvents on the displacement of ions.

Pressure extraction is the use of positive pressure, vacuum (negative pressure), or force applied by a centrifuge to remove the soil solution. For soils with moisture contents below saturation, the centrifuge method is more efficient than the positive pressure or vacuum methods. The efficiency of the latter two methods can be increased by employing a displacing solution, similar to some of the techniques described immediately above. Positive pressure methods generally refer to the use of a pressure membrane (Richards, 1941). A cylinder, equipped with small-pore filters on the inlet and outlet, is packed with the moist soil. Pressure of approximately 2 MPa (20 bar) is applied to the inlet, and the solution is collected

from the outlet. The centrifugation method, similarly, requires specialized equipment. The apparatus usually consists of a centrifuge tube to contain the moist soil; a permeable frit, filter, or ceramic beneath the soil; and a small volume at the bottom of the apparatus for collection of the extruded solution (Elkhatib et al., 1986). Large samples (up to 1 kg) usually are centrifuged at low speed, but smaller samples can be subjected to much greater speed and result in a greater fraction of the soil water being collected. An immiscible liquid also may be placed on the top of a small sample prior to centrifugation, a modification of immiscible displacement.

The pressure-membrane approach has not been used as widely as the centrifuge method because of lower yields, requirement for large samples, and specialty apparatus. The high-speed centrifuge method is an excellent choice because it uses equipment that is normally available in a soil chemistry laboratory, yields a sample very quickly (<1 h), and is amenable to a large number of samples. The disadvantages are similar to other displacement-type methods: short incubation times, an unknown fraction of the “true” soil solution that is sampled, uncertain impact of organic solvents (if used), and potential changes in the dissolved gas composition. The centrifugation method was used by van Hees et al. (2001) to infer the importance of organic matter and exchange reactions in the chemistry of Al in soils.

## 12.2.2 Field Methods

As is often the case in soil science, field methods of sampling the soil solution are more challenging than laboratory methods, particularly when one is interested in obtaining samples that are truly representative. Field methods cover a wide range of configurations: block or monolithic lysimeters; zero-tension or pan lysimeters; and porous-cup vacuum samplers.

Monolithic lysimeters are large blocks of soil (undisturbed or refilled) contained in a structure that has some means of collecting leachates. The apparatus are labor intensive and expensive to construct but are generally placed in a typical field setting to allow growth of vegetation while measuring a variety of soil parameters. The leachate collection system may be free drainage (i.e., zero-tension or air-entry potential) or use a vacuum system to impose a moderate moisture tension. Soil in contact with a free-drainage collection system must be very near saturation to allow water to move from the column to the collection area. The thickness of the near-saturated zone above the collection area will be dependent upon the texture of the soil, and the saturated condition will impact the chemistry, microbiology, and physics of the soil. Addition of a vacuum system, while adding to the complexity and cost of construction, will overcome the saturation problem. Unfortunately, the vacuum will at least partially “degas” the collected leachates.

Water flow through large lysimeters will affect directly the chemical composition of the leachates. In refilled versions, the original structure is destroyed, and, in the absence of plants, preferential flow within the soil is eliminated. However, this is unrepresentative of natural conditions. Block-type “undisturbed” lysimeters preserve much of the original soil structure, and water movement will be similar to the original field condition. In both block and refilled

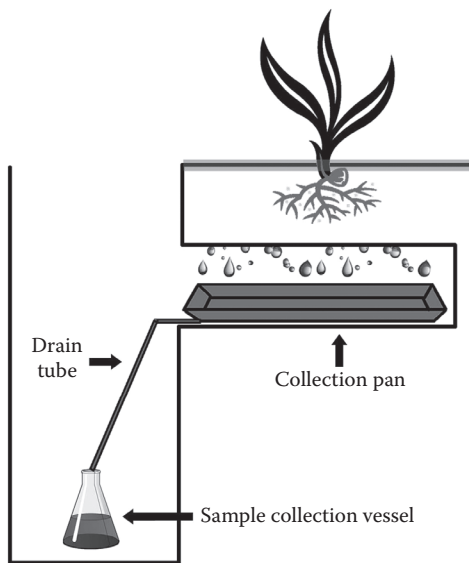


**FIGURE 12.2** A zero-tension, pan lysimeter in a typical field context. The collection vessel and drain tube are located in an excavated trench cut into the soil along the side of the sample area.

lysimeters, wall flow (movement of water in the spaces between the lysimeter walls and the soil) can be an important form of preferential transport of water and solutes (Till and McCabe, 1976). Wall flow can be minimized through careful design and construction, and its relative impact is lessened as the ratio of surface area of the side walls to the total volume of soil increases.

Zero-tension lysimeters include any device installed in the soil that collects water by free drainage of the soil above including pans, troughs, funnels, and plates. These lysimeters usually are installed from a trench. A slot is excavated from the trench into the soil that allows installation of the lysimeters (Figure 12.2). Leachate collects in the lysimeter, and the sample is removed by means of a hose or tube leading to the trench or to the soil surface. This lysimeter design is useful for monitoring the solutes that move with water. The assumption is made that the soil disturbance from digging the trench and installing the pan will have little impact on water flow and solute composition. However, water will not flow into the pan until the soil is nearly saturated. Water can accumulate above the interface between the soil and lysimeter and cause incoming water to move laterally away from the lysimeter. Modifications to this procedure such as putting the lysimeter under tension (Cole et al., 1961) can overcome this problem in part.

Porous-cup vacuum lysimeters (Figure 12.3) are widely used in sampling the soil solution. Their design is simple, and they are easily installed using standard soil sampling equipment. Entire assemblies are readily built or available commercially. A length of PVC pipe is fitted with and glued to a ceramic cup. A rubber stopper with two air lines is placed in the opposite end of the pipe. The lysimeter is buried in the soil with the ceramic cup facing down and the air lines extending to the soil surface. One air line is used for drawing a vacuum, either with a hand pump or with a portable electric pump. The lines are sealed, and the lysimeter is allowed to draw the soil solution into the ceramic

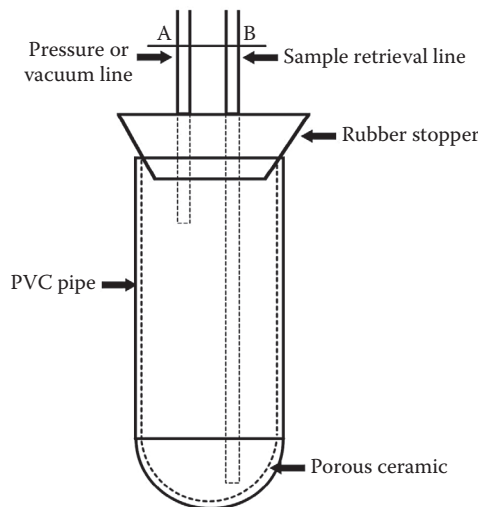


**FIGURE 12.3** Design of a typical porous-cup vacuum lysimeter.

cup. (A continuous vacuum may be applied, or the vacuum may be applied intermittently.) The second air line extends to the bottom of the cup and is used for retrieving the collected sample either by drawing a vacuum on the retrieval line (marked B in Figure 12.3) or by applying pressure on the other line (A).

Porous-cup lysimeters have been criticized as field samplers of the soil solution (Caron et al., 1999). The ceramic cup has the potential to retain analytes or to contaminate the sample (Wood, 1973), particularly for inorganic species. Likewise, the PVC tube can retain organic compounds of interest. The area of soil that is sampled is not known (Warrick and Amoozegar, 1977), but will be influenced by the vacuum applied (Morrison and Lowry, 1990), the texture of the soil, the method of installation, and soil moisture content. Unlike the other field methods described above, vacuum pore water samplers will operate only when the operator engages them. Unless the porous cup is in saturated soil, the soil solution will not flow into it until vacuum is applied.

Each field method has positive and negative aspects. The monolithic lysimeters are, in essence, a field laboratory with all parameters either controllable or measurable. However, they are difficult and expensive to construct and maintain, and wall effects can be dominant. Zero-tension lysimeters are less expensive but require significant disturbance to the soil adjacent to the site, and water flow patterns may be altered immediately above the interface between soil and lysimeter. Vacuum pore water samplers are the least expensive of all field methods but collect the smallest fraction of the soil solution. In all cases, the soil solution will be defined by the specifics of the method used.

## 12.3 Thermodynamics of the Soil Solution

In discussing the thermodynamics of aqueous systems, strong distinctions are made between chemical equilibrium and nonequilibrium (kinetic) systems. Overlap exists between the statics and dynamics of solutions both on theoretical and

practical basis. In this section, only equilibrium thermodynamics will be addressed. Kinetics are addressed in Chapter 13. The assumption of equilibrium may be applied safely to only a fraction of the reactions occurring in soils; many reactions do not achieve equilibrium before new perturbations are imposed. Despite serious practical limitations, equilibrium models are important because “they are simpler in that they require less information, but they are nevertheless powerful when applied within their proper limits” (Stumm and Morgan, 1996).

Soil solutions are open systems in which energy and matter are exchanged readily with the surrounding environment. Experimentalists often are more familiar with closed systems in which such exchanges do not occur and rigorous mass and energy balances can be applied. Thus, the study of soils in natural settings can require some adjustments in design, execution, and interpretation. Open systems will be assumed in all derivations discussed later unless otherwise noted.

Chemical thermodynamics of aqueous solutions have been developed to various degrees of depth and detail, depending upon the application. Stumm and Morgan (1996) provide an excellent, in-depth discussion of equilibrium thermodynamics for aqueous systems. Wolt (1994) provided a discussion of similar depth but with the ultimate application to soil solutions. Sposito (1981) dedicated an entire textbook to the subject of the thermodynamics of soil solutions. The reader is referred to these references for a thorough discussion of chemical thermodynamics applied to aqueous solutions. In this chapter, important thermodynamic laws and equations will be stated and discussed; they will not be derived.

### 12.3.1 Fundamentals, Units, and Variables

As mentioned previously, true equilibrium is achieved in only a fraction of the reactions that occur in soil solutions but is a powerful tool when properly applied. Some of the reasons for investigating the application of equilibrium thermodynamics to systems that are frequently not in equilibrium include determining whether some or all of the components of the solution are in equilibrium; comparing the measured system with systems in equilibrium; quantifying the energy of disequilibrium (i.e., the energy input necessary to achieve equilibrium); and calculating the effects of temperature on equilibria. The equations necessary to obtain these goals are presented in the following sections.

**TABLE 12.3** Variables, Thermodynamic Functions, and Equations of State

Variable	Units	Function	Equation of State
Temperature ( $T$ )	K	Enthalpy ( $H$ )	$dH = T dS + V dP$
Entropy ( $S$ )	J deg <sup>-1</sup>	Helmholtz free energy ( $A$ )	$dA = -S dT - P dV$
Pressure ( $P$ )	kPa	Gibbs free energy ( $G$ )	$dG = -S dT + V dP$
Volume ( $V$ )	L	Internal energy ( $E$ )	$dE = T dS - P dV$
Chemical potential	J mol <sup>-1</sup>		
Quantity	mol		

Important variables and functions and associated units are given in Table 12.3. Nearly all thermodynamic equations relative to soil solutions are derived from the four principles of thermodynamics and the first and second laws of thermodynamics (Stumm and Morgan, 1996). The four principles of thermodynamics establish an absolute temperature scale, define the internal energy of a system, and describe the relationship between entropy and temperature.

### 12.3.2 First and Second Laws of Thermodynamics

The first law of thermodynamics for equilibrium systems of fixed compositions,

$$dE = dq - dw, \quad (12.1)$$

represents the changes in internal energy ( $E$ ) as affected by heat transferred to the system ( $q$ ) and work done by the system ( $w$ ). For a reversible process, the second law is given by

$$dS_{\text{sys}} = \frac{dq}{T} \quad (12.2)$$

and relates the temperature and heat transferred to a system with entropy ( $S$ ). Other forms of this equation exist for the system plus its surroundings as well as irreversible changes in a system.

From the basic (not differentiated) equations  $H = E + PV$  and  $G = E + PV - TS$ , one can obtain the important relationship,  $G = H - TS$ , where  $G$  is the Gibbs free energy,  $H$  is enthalpy,  $P$  is pressure, and  $V$  is volume. For a finite state change at constant pressure and temperature,

$$\Delta G = \Delta H - T\Delta S. \quad (12.3)$$

This equation, a restatement of the second law of thermodynamics in terms of state functions of the system, is used in the application of thermodynamics to numerical solutions of chemical problems.

### 12.3.3 Associated Thermodynamic Relationships

The development of theoretical thermodynamics can be quite detailed, but its utility can be realized only if expressed in measurable variables. For example, enthalpy change ( $dH$ ) in Table 12.3 can be described as  $dH = dq + V dP$ ; if  $dP = 0$  (constant pressure process), then  $dH = dq_p$ . This expression is particularly useful in determining temperature effects because constant pressure heat capacity ( $C_p$ ) is measurable and is given by

$$C_p = \left( \frac{dq}{dT} \right)_p. \quad (12.4)$$

In the absence of external work,  $q_p = \Delta H$ .

Under conditions of constant pressure and constant temperature the state of a system is characterized by  $dG$ . For irreversible changes in a system,

$$dG - V dP + S dT < 0, \quad (12.5)$$

and for reversible changes,

$$dG - V dP + S dT = 0. \quad (12.6)$$

The above equations are applicable only for systems of constant chemical composition,  $dn_i = 0$ . When the composition of only species  $i$  is allowed to change,

$$dG = \left(\frac{\partial G}{\partial T}\right)_{P,n_j} dT + \left(\frac{\partial G}{\partial P}\right)_{T,n_j} dP + \sum_i \left(\frac{\partial G}{\partial n_i}\right)_{P,T,n_j} dn_i. \quad (12.7)$$

### 12.3.4 Chemical Potential and Free Energy

The chemical potential,  $\mu$ , of a species  $i$  is defined as

$$\mu_i = \left(\frac{\partial G}{\partial n_i}\right)_{P,T,n_j}. \quad (12.8)$$

Employing the relationships  $(\partial G/\partial T)_{P,n_j} = -S$  and  $(\partial G/\partial P)_{T,n_j} = V$  yields the equation

$$dG = -S dT + V dP + \sum \mu_i dn_i, \quad (12.9)$$

and for a single-phase system at constant temperature and pressure,

$$dG = \sum \mu_i dn_i. \quad (12.10)$$

For a multiphase system,  $dG$  for the entire system is obtained by summing  $\mu_i dn_i$  over all phases. When equilibrium is established for all reactions and phases,  $dG = 0$ .

These basic equations can be manipulated further to yield equations for chemical potentials of components in various phases.

The resulting relationships depend upon assumptions made during the derivation. Equations for gases and electrolytes are summarized in Table 12.4. As an example derivation for an ideal gas, consider the partial free energy of this gas with respect to  $P$  at constant  $T$  and  $n$ :

$$\left(\frac{\partial G}{\partial P}\right)_{T,n} = V \quad (12.11)$$

and, thus,

$$\left(\frac{\partial G}{\partial P}\right)_{T,n} = \frac{nRT}{P}. \quad (12.12)$$

If the second equation is rearranged and integrated from  $G^o$  (standard free energy) to  $G$  and from  $P^o$  (standard pressure) to  $P$ , the result is

$$G - G^o = nRT \ln\left(\frac{P}{P^o}\right). \quad (12.13)$$

Differentiation with respect to  $n$  and recalling the definition for chemical potential gives

$$\mu_i = \mu_i^o + RT \ln\left(\frac{P_i}{P^o}\right), \quad (12.14)$$

where  $\mu_i^o$  is the chemical potential for the ideal gas in its standard state (e.g., as defined by the conditions given in Table 12.4) at  $T = 298.15$  K and  $P = 101.33$  kPa (1 atm). Similar derivations for real gases, condensed phases that obey Raoult's law and condensed phases that obey Henry's law, are summarized by Wolt (1994).

Sposito (1994) discussed the standard states for phases and elements relevant to the study of soil solutions.

**TABLE 12.4** Expressions for the Chemical Potential of Components in Gas and Condensed Phases as Influenced by the Assumptions of the Behavior of the Component

Phase	Chemical Potential	Coefficients	Standard State
Ideal gas	$\mu_i = \mu_i^o + RT \ln(P_i/P^o)$		298.15 K, 101.33 kPa; pure ideal gas at 101.33 kPa
Nonideal gas	$\mu_i = \mu_i^o + RT \ln(P_i \lambda_i)$	$\lambda_i \equiv$ fugacity coefficient	298.15 K, 101.33 kPa; pure nonideal gas at 101.33 kPa, $\lambda_i = 1$
Condensed phase: follows Henry's law	$\mu_i = \mu_i^o + RT \ln(C_i)$	$C_i \equiv P_i/K_{Hi}$	Pure condensed phase component, $C_i^o = 1$
Condensed phase: does not follow Henry's law	$\mu_i = \mu_i^o + RT \ln(C_i \lambda_i)$	$\lambda_i \equiv$ Henry's law coefficient	Pure condensed phase component, $C_i^o = 1$ and $\lambda_i = 1$
Condensed phase: follows Raoult's law	$\mu_i = \mu_i^o + RT \ln(\chi_i)$	$\chi_i = P_i/P^o$	Pure condensed phase component, $\chi_i^o = 1$
Condensed phase: does not follow Raoult's law	$\mu_i = \mu_i^o + RT \ln(\chi_i \lambda_i)$	$\lambda_i \equiv$ Raoult's law coefficient	Pure condensed phase component, $\chi_i^o = 1$ and $\lambda_i = 1$
Solute in ideal, dilute solution	$\mu_i = \mu_i^o + RT \ln(C_i)$		Pure condensed phase component, $C_i^o = 1$
Solute in nonideal solution	$\mu_i = \mu_i^o + \mu RT \ln(C_i \gamma_i)$	$\gamma_i \equiv$ single ion activity coefficient	Pure condensed phase component, $C_i^o = 1$ and $\gamma_i = 1$
Solute in nonideal solution	$\mu_i = \mu_{\pm}^o + \nu RT \ln(C_{\pm} \gamma_{\pm})$	$\gamma_{\pm} \equiv$ mean activity coefficient $\nu =$ stoichiometric coefficient	Pure condensed phase component, $C_{\pm}^o = 1$ and $\gamma_{\pm} = 1$

Sources: Wolt, J.D. 1994. Soil solution chemistry. Applications to environmental science and agriculture. John Wiley & Sons, New York; Stumm, W., and J.J. Morgan. 1996. Aquatic chemistry. Chemical equilibria and rates in natural waters. Wiley Interscience, New York.

### 12.3.5 Chemical Potential and Activities in Ideal Solutions

Perhaps the most important expressions for chemical potential in dealing with soil solutions are those for solutions of electrolytes. A classical case is that of NaCl dissolved in water. Sodium chloride is a strong electrolyte, indicating that it is dissociated fully with no NaCl complexes in the aqueous solution. The chemical potential of this solution is the sum of the chemical potentials for the  $\text{Cl}^-$  and  $\text{Na}^+$  species:

$$\mu_{\text{NaCl}} = \mu_{\text{Na}^+} + \mu_{\text{Cl}^-}. \quad (12.15)$$

In an ideal, dilute solution, the equations for the chemical potentials of the individual ions with concentrations  $C_{\text{Na}^+}$  and  $C_{\text{Cl}^-}$  would be

$$\mu_{\text{Na}^+} = \mu_{\text{Na}^+}^{\circ} + RT \ln(C_{\text{Na}^+}), \quad (12.16)$$

$$\mu_{\text{Cl}^-} = \mu_{\text{Cl}^-}^{\circ} + RT \ln(C_{\text{Cl}^-}). \quad (12.17)$$

The standard potential for an aqueous solution of NaCl ( $\mu_{\text{NaCl(aq)}}^{\circ}$ ) is defined as

$$\mu_{\text{NaCl(aq)}}^{\circ} \equiv \mu_{\text{Na}^+}^{\circ} + \mu_{\text{Cl}^-}^{\circ}, \quad (12.18)$$

and the total chemical potential is

$$\mu_{\text{NaCl(aq)}} = \mu_{\text{NaCl(aq)}}^{\circ} + RT \ln(C_{\text{Na}^+} C_{\text{Cl}^-}). \quad (12.19)$$

If the concentration of the salt is defined as  $C_{\text{NaCl}}$  and realizing that  $C_{\text{NaCl}} = C_{\text{Na}^+} = C_{\text{Cl}^-}$ , then

$$\mu_{\text{NaCl}} = \mu_{\text{NaCl}}^{\circ} + RT \ln(C_{\text{NaCl}})^2. \quad (12.20)$$

### 12.3.6 Activities and Activity Coefficients: Nonideal Solutions

For nonideal solutions, the concept of activity and activity coefficient is introduced. A nonideal solution of NaCl would have a chemical potential of

$$\mu_{\text{NaCl(eq)}} = \mu_{\text{NaCl(aq)}}^{\circ} + RT \ln(a_{\text{Cl}^-} a_{\text{Na}^+}) \quad (12.21)$$

or

$$\mu_{\text{NaCl(eq)}} = \mu_{\text{NaCl(aq)}}^{\circ} + RT \ln(C_{\text{Cl}^-} \gamma_{\text{Cl}^-} C_{\text{Na}^+} \gamma_{\text{Na}^+}), \quad (12.22)$$

in which  $a_i$  is the activity of component  $i$  and  $\gamma_i$  is the activity coefficient of component  $i$ . The product  $a_{\text{Na}^+} a_{\text{Cl}^-}$  is designated by  $a_{\text{NaCl}}$ , which is the activity of the aqueous solute, and its mean activity is  $a_{\pm} = (a_{\text{Na}^+} a_{\text{Cl}^-})^{1/2}$ , which can be determined experimentally. Similarly, the mean activity coefficient,  $\gamma_{\pm}$ , is equal

to  $(\gamma_{\text{Na}^+} \gamma_{\text{Cl}^-})^{1/2}$ ;  $\gamma_{\text{Na}^+} \gamma_{\text{Cl}^-}$  can be determined experimentally by measuring water vapor pressures over NaCl solutions of varying concentrations.

### 12.3.7 Equilibrium Constants

The Gibbs free energy of a reaction can be related to the system composition through the expressions for chemical potential:

$$\mu_i = \mu_i^{\circ} + RT \ln a_i \quad (12.23)$$

and  $\Delta G$

$$\Delta G = \sum_i \nu_i \mu_i, \quad (12.24)$$

in which  $\nu_i$  is the stoichiometric coefficient of a component  $i$  in the reaction. Combining these equations gives

$$\Delta G = \sum_i \nu_i \mu_i^{\circ} + RT \sum_i \nu_i \ln(a_i) \quad (12.25)$$

or

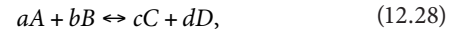
$$\Delta G = \Delta G^{\circ} + RT \ln \prod_i (a_i)^{\nu_i}, \quad (12.26)$$

where

$$\Delta G^{\circ} = \sum_i \nu_i \mu_i^{\circ}, \quad (12.27)$$

$\Delta G^{\circ}$  is the standard Gibbs free energy change of the reaction  
 $\Pi_i$  is the quotient of concentrations of products over reactants

Consider the reaction,



in which

$a$  and  $b$  are the stoichiometric coefficients of reactants  $A$  and  $B$

$c$  and  $d$  are the stoichiometric coefficients of products  $C$  and  $D$

The expression for  $\Pi_i$  would be

$$\left[ \frac{a_C^c a_D^d}{a_A^a a_B^b} \right].$$

The expression often is given the symbol  $Q$ . Thus,

$$\Delta G = \Delta G^{\circ} + RT \ln Q. \quad (12.29)$$

At equilibrium,  $\Delta G = 0$ ,  $Q = K$  (the equilibrium constant), and

$$\Delta G^\circ = -RT \ln K. \quad (12.30)$$

Both  $K$  and  $Q$  are written in terms of activities ( $a_i$ ), but activities of individual species are not measurable. However, both can be written in terms of concentrations using the relationship between activity and concentration,  $a_i = C_i \gamma_i$ :

$$K = \frac{a_C^c a_D^d}{a_A^a a_B^b} = \frac{(C_C \gamma_C)^c (C_D \gamma_D)^d}{(C_A \gamma_A)^a (C_B \gamma_B)^b}. \quad (12.31)$$

### 12.3.8 Effects of Temperature and Pressure

The general expression for the effect of temperature on the free energy of reaction is

$$\left( \frac{\partial \Delta G^\circ / T}{\partial T} \right)_P = -\frac{\Delta H^\circ}{T^2}, \quad (12.32)$$

and the van't Hoff equation for the corresponding equilibrium constant is

$$\frac{d \ln K}{dT} = \frac{\Delta H^\circ}{RT^2}. \quad (12.33)$$

The temperature dependence of enthalpy of reaction is

$$H_2 - H_1 = \int_{T_1}^{T_2} C_p dT. \quad (12.34)$$

If  $\Delta H^\circ$  is independent of temperature,

$$\ln \frac{K_2}{K_1} = \frac{\Delta H^\circ}{R} \left( \frac{1}{T_1} - \frac{1}{T_2} \right) \quad (12.35)$$

or, when the heat capacity ( $\square C_p^\circ$ ) is independent of temperature,

$$\ln \frac{K_2}{K_1} = \frac{\Delta H^\circ}{R} \left( \frac{1}{T_1} - \frac{1}{T_2} \right) + \frac{\Delta C_p^\circ}{R} \left( \frac{T_1}{T_2} - 1 - \ln \frac{T_1}{T_2} \right) \quad (12.36)$$

or

$$\ln K = B - \left( \frac{\Delta H_o}{RT} \right) + \frac{\Delta C_p^\circ}{R} \ln T, \quad (12.37)$$

where  $B$  and  $\Delta H_o$  are constants (Stumm and Morgan, 1996). When  $\square C_p^\circ$  is a function of temperature, the form of the final equation will reflect the temperature-dependent expression for the heat capacity.

The effects of pressure on free energy and equilibrium constants are handled in a fashion similar to temperature (Stumm

and Morgan, 1996). The general expression, when  $\Delta V^\circ$  is independent of pressure,

$$\left( \ln \frac{K_P}{K_1} \right)_P = -\frac{\Delta V^\circ (P-1)}{RT}. \quad (12.38)$$

With specific reference to aqueous solutions,

$$\mu_i = \mu_i^\circ + RT \ln \gamma_i C, \quad (12.39)$$

$$\left( \frac{\partial \ln K}{\partial P} \right)_{T,C} = -\frac{\Delta V^\circ}{RT}, \quad (12.40)$$

$$\left( \frac{\partial \ln \gamma_i}{\partial P} \right)_{T,C} = -\frac{\bar{V}_i - \bar{V}_i^\circ}{RT}, \quad (12.41)$$

where

$\bar{V}_i$  is the partial molar volume

$\bar{V}_i^\circ$  is the standard partial molar volume of species  $i$

### 12.3.9 Single-Ion Activity Coefficients

The mean activity coefficient of a salt in solution,  $\gamma_{\pm}$ , is measurable by experimental methods. However, the activity coefficient of a single ion, such as  $\gamma_{\text{Na}^+}$  or  $\gamma_{\text{Cl}^-}$ , is not measurable and must be estimated by theoretical models. Such a model was provided by the Debye-Huckel theory, which combined thermodynamic and electrostatic expressions to describe the interaction between charged species in solution. In its first configuration, the theory was based upon the assumption that the ions act as point charges. The resulting equation, the Debye-Huckel limiting law, was

$$\log \gamma_i = -AZ_i^2(I^{0.5}), \quad (12.42)$$

where

$Z_i$  is the valence of the ion

$I$  is the ionic strength of the solution ( $I = 0.5 \sum C_i Z_i^2$ )

$A$  is related to the dielectric constant for water and has a value of 0.509 at 298.15 K and 101.33 kPa

Activity coefficients calculated from this equation begin to deviate from measurements when  $I > 0.005 \text{ mol L}^{-1}$ . The Debye-Huckel theory was extended to greater ionic strengths ( $I = 0.1 \text{ mol L}^{-1}$ ) by adding terms that account for the spatial interaction of the ions:

$$\log \gamma_i = \frac{-AZ_i^2 I^{0.5}}{1 + \beta a_i^\circ I^{0.5}}, \quad (12.43)$$

in which  $\beta$  is a constant that depends upon the nature of the solvent and temperature. For water,  $\beta$  is equal to  $0.328 \times 10^8$  at 298.15 K and 101.33 kPa. The ion size parameter,  $a_i^\circ$ , ranges from

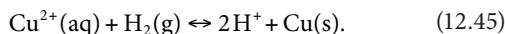
$(2.5 \text{ to } 9) \times 10^{-8}$  and must be obtained from a compilation of values (Kielland, 1937). The Davies equation is a further modification of the Debye-Huckel and is applicable when  $I < 0.5 \text{ mol L}^{-1}$ :

$$\log \gamma_i = -AZ_i^2 \left( \frac{I^{0.5}}{1 + I^{0.5}} - 0.3I \right). \quad (12.44)$$

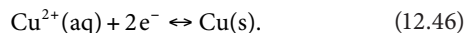
The advantages of the Davies over other equations are the applicability to higher ionic strengths and the elimination of the necessity of using  $\beta$  values.

### 12.3.10 Electrochemical Potential

The standard electrochemical potential of a oxidation/reduction reaction,  $E^\circ$ , is the potential of the reaction relative to the oxidation of  $\text{H}_2(\text{g})$  to  $\text{H}^+$  in aqueous solution. The balanced chemical reaction of such a cell involving the reduction of  $\text{Cu}^{2+}$  to the metal would be



The half-cell reactions are conveniently written as follows, with the implicit understanding that the hydrogen half-cell is always present:



For any given reaction, the Nernst equation may be derived:

$$E_H = E_H^\circ + \frac{2.303RT}{nF} \log \frac{\prod_i \{\text{ox}\}^{n_i}}{\prod_j \{\text{red}\}^{n_j}}, \quad (12.47)$$

where

$E_H$  is the measured potential

$E_H^\circ$  is the standard potential of the cell

$R$  is the gas constant

$T$  is temperature in degrees K

$n$  is the number of electrons involved in the reaction

$F$  is the Faraday constant

$\Pi$  designates the product of either the reactants or products in the equation

For any oxidation/reduction reaction, the relationship between the electrode potential and  $pe$ , negative logarithm of the electron activity,  $-\log(e^-)$ , may be derived as

$$pe = \frac{F}{2.303RT} E_H, \quad (12.48)$$

or  $pe = E_H/59.2$  when  $E_H$  is in mV and determined at 298.15 K. As with  $\text{H}^+$ , aqueous solutions do not contain free electrons, and the concentration of solvated electrons is vanishingly small. Nevertheless,  $pe$  is a very convenient parameter in manipulating equilibrium equations and plotting data.

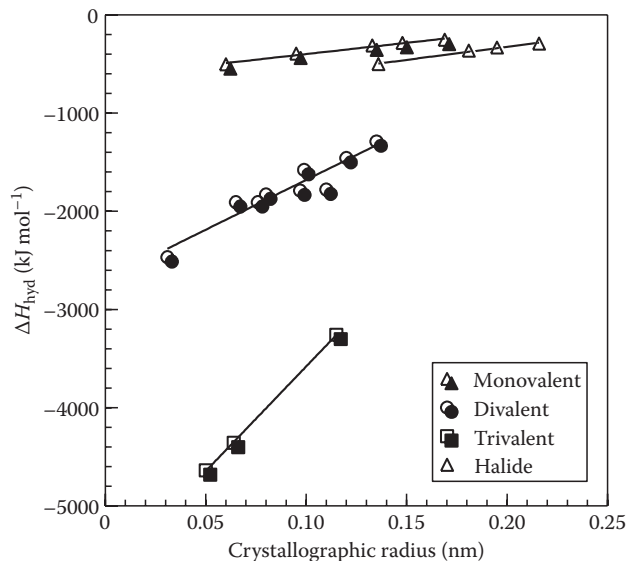


**FIGURE 12.4** Relationship between crystallographic radius and enthalpy of hydration of monovalent, divalent, and trivalent cations and monovalent halide anions. The drawn lines represent linear regressions:  $R^2 = 0.98$  for monovalent cations;  $R^2 = 0.90$  for divalent cations;  $R^2 = 0.99$  for trivalent cations; and  $R^2 = 0.98$  for monovalent anions. (Data from Bohn, H., B. McNeal, and G. O'Connor. 1985. Soil chemistry. Wiley Interscience, New York; Morris, D.F.C. 1969. Ionic radii and enthalpy of hydration of ions. Struct. Bond. 63:157-159.)

### 12.3.11 Heat of Hydration of Ions

One of the most important reactions for ions in solution is hydration, the electrostatic interaction between the polar water molecules and the charged ion. When an ion is released into aqueous solution, heat is released as water molecules form a somewhat ordered structure around the ion. The water that surrounds the ion tends to insulate the charged species from other ions in solution. In infinitely dilute solutions, this solvation effect completely isolates the ions from interacting with each other.

The heat released during solvation of an ion by water is the heat of hydration,  $\Delta H_{\text{hydration}}$ . The strength of the water-ion interaction increases with increasing valence because higher charged ions have the capacity to react with more water molecules. Within a group of ions of the same valence,  $\Delta H_{\text{hydration}}$  decreases (becomes more negative) linearly with decreasing crystallographic radius (Figure 12.4). Thus, a small monovalent ion such as  $\text{Li}^+$  releases more heat upon hydration than the much larger  $\text{Cs}^+$  ion. A direct result of this is that  $\text{Li}^+$  also has a greater hydrated radius than  $\text{Cs}^+$ , which is partly responsible for some of the differences in strength of retention of these ions by cation exchange sites in soil (see Chapter 17).

## 12.4 Interactions of Gases with the Soil Solution

Chemical reactions between gases and the liquid aqueous phase are important not only in the soil solution but also in biological systems, surface water, groundwater, and the atmosphere.



For example, acid rain is a long-recognized problem that results from the combustion of fossil fuels. The oxidation of C, S, and N in the fuels generates several gaseous oxides including CO<sub>2</sub>, NO<sub>2</sub>, NO, SO<sub>2</sub>, and SO<sub>3</sub>. When these oxides dissolve in water, they generate acids: H<sub>2</sub>CO<sub>3</sub>, HNO<sub>3</sub>, HNO<sub>2</sub>, H<sub>2</sub>SO<sub>3</sub>, and H<sub>2</sub>SO<sub>4</sub>. The extent to which the gaseous oxides dissolve in the water can be described by Henry's law referenced in Section 12.3.4 and given in Table 12.4.

### 12.4.1 Henry's Law

The equilibrium distribution of a species between the gas phase and the aqueous is given by Henry's law. The expression is based upon the thermodynamic parameter, chemical potential, and requires the determination of a partitioning coefficient for each gas. The thermodynamic expression is

$$f_A = Ka_A, \quad (12.49)$$

where

$K$  is a constant

$f_A$  is the fugacity of the gas

$a_A$  is the activity of the species in the aqueous phase

The transition between the above thermodynamic equation and a usable expression with measurable terms is made simpler if one first assumes the condition of dilute solutions and low concentrations in the gas phase. Under these circumstances, Henry's law may be written in one of two ways, either of which is correct. In the first expression, the partitioning coefficient ( $H$ ) is dimensionless:

$$\frac{[A(\text{aq})]}{[A(\text{g})]} = H. \quad (12.50)$$

The units of concentration for the gaseous and aqueous species must be the same (e.g., mol L<sup>-1</sup>). In the second form of Henry's law, the partitioning coefficient is not dimensionless:

$$\frac{[A(\text{aq})]}{P_A} = K_H. \quad (12.51)$$

If the units of concentration for the aqueous component are mol L<sup>-1</sup> and the partial pressure is in atmospheres, then  $K_H$  must have units of mol L<sup>-1</sup> atm<sup>-1</sup>. The conversion between  $H$  and  $K_H$  is

$$K_H = \frac{H}{RT}. \quad (12.52)$$

Table 12.5 contains a compilation of  $K_H$  values for important gases in soils and other settings.

Although Henry's law dictates that the solubility of gases in water is a linear function only of their partial pressures, many of the dissolved species react further with water to form acids that are subject to deprotonation. Thus, pH is an important

**TABLE 12.5** Henry's Law Constants ( $K_H$ ) for Important Gas–Water Reactions

Gas	$K_{H,298.15\text{K}}$ (mol L <sup>-1</sup> atm <sup>-1</sup> )	Gas	$K_{H,298.15\text{K}}$ (mol L <sup>-1</sup> atm <sup>-1</sup> )
H <sub>2</sub>	$7.78 \times 10^{-4}$	O <sub>2</sub>	$1.27 \times 10^{-3}$
N <sub>2</sub>	$6.53 \times 10^{-4}$	N <sub>2</sub> O	$2.42 \times 10^{-2}$
NO	$1.92 \times 10^{-3}$	CO	$9.77 \times 10^{-4}$
CO <sub>2</sub>	$3.39 \times 10^{-2}$	H <sub>2</sub> S	$1.02 \times 10^{-1}$
SO <sub>2</sub>	1.36	Cl <sub>2</sub>	$9.31 \times 10^{-2}$
CH <sub>4</sub>	$1.41 \times 10^{-3}$	NH <sub>3</sub>	$5.71 \times 10^1$
O <sub>3</sub>	$1.04 \times 10^{-4}$		

Constants were calculated from the data of Gevantman (2001) with the exception of NH<sub>3</sub> (Sposito, 2008).

controlling variable for the total dissolved component in aqueous solution. Calculations also can be complicated by whether the system contains an infinite sink of the gas (open system) or if the gas is limited (closed system). These calculations are handled in detail by Stumm and Morgan (1996).

### 12.4.2 Volatile Organic Compounds

Many organic compounds are subject to loss from solid, liquid, or aqueous phases through volatilization. As with inorganic gases, the tendency for volatile organic compounds to partition between the aqueous phase and the atmosphere can be described by Henry's law. Henry's law constants can be calculated by measuring aqueous and gaseous phase concentrations in systems at equilibrium (Table 12.6).

### 12.4.3 Rates of Dissolution of Gases in Water

Quantification of equilibrium distributions of volatile compounds between the atmosphere and aqueous phase is more powerful when accompanied by an understanding of the rates of reactions. Transfer of a gas across the liquid/gas interface can be approximated by a diffusion model with two diffusion films

**TABLE 12.6** Water Solubilities, Vapor Pressures, and Henry's Law Constants for Selected Organic Compounds

Compound	Water Solubility (mol L <sup>-1</sup> )	Vapor Pressure, $P_A$ (atm)	$K_H$ (mol L <sup>-1</sup> atm <sup>-1</sup> )
Hexane	$7.0 \times 10^{-4}$	0.25	$2.8 \times 10^{-3}$
<i>n</i> -Octane	$5.8 \times 10^{-6}$	$1.8 \times 10^{-2}$	$3.1 \times 10^{-4}$
Dieldrin	$5.8 \times 10^{-7}$	$6.6 \times 10^{-9}$	88
Lindane	$2.6 \times 10^{-5}$	$8.3 \times 10^{-8}$	313
Naphthalene	$2.6 \times 10^{-4}$	$1.0 \times 10^{-4}$	2.6
Benzene	$2.3 \times 10^{-2}$	0.12	0.19
Toluene	$5.6 \times 10^{-3}$	$3.7 \times 10^{-2}$	0.15
Biphenyl	$4.9 \times 10^{-5}$	$7.5 \times 10^{-5}$	0.65
Dimethyl sulfide	0.35	0.63	0.56

Source: Stumm, W., and J.J. Morgan. 1996. Aquatic chemistry. Chemical equilibria and rates in natural waters. Wiley Interscience, New York.

A more comprehensive compilation is available in Staudinger and Roberts (1996).

(liquid phase and gas phase) assuming that the bulk phases are well mixed (Stumm and Morgan, 1996). The diffusion films are assumed to be within a very small distance of the interface.

The flux across the films of thickness  $z$  is expressed by Fick's law:

$$F = -D \frac{dc}{dz}. \quad (12.53)$$

The units for flux,  $F$ , will depend upon the units of concentration ( $c$ ), diffusion coefficient ( $D$ ), and thickness; assuming concentrations in  $\text{mol m}^{-3}$ ,  $D$  in  $\text{m}^2 \text{s}^{-1}$ , and distance in  $m$ , then  $F$  will have units of  $\text{mol m}^{-2} \text{s}^{-1}$ . A steady state will have been achieved when the flux across the two films is equal. The thickness of the air diffusion film is assumed to be  $z_{\text{air}}$ ; the thickness of water diffusion film is  $z_{\text{water}}$ ; the concentrations in the air and water are  $c_{\text{air}}$  and  $c_{\text{water}}$ ; the concentrations in the air–water interface is  $c_{a-w}$ ; and the concentration in the water–air interface is  $c_{w-a}$ . Therefore, at steady state,

$$F = -\frac{D_w}{z_w}(c_{w-a} - c_w) = -\frac{D_a}{z_a}(c_a - c_{a-w}). \quad (12.54)$$

Assuming that the transfer across the interfaces is much faster than any ensuing chemical reactions that may occur, Henry's law may be applied to the concentrations in the interface regions (using the dimensionless constant from Section 12.4.1):

$$H = \frac{c_{w-a}}{c_{a-w}} = K_H RT. \quad (12.55)$$

Substituting into the steady-state equation,

$$F = \frac{D_a}{z_a} \left( \frac{c_{w-a}}{H} - c_a \right) = \frac{D_w}{z_w} (c_w - c_{w-a}). \quad (12.56)$$

Using data from Lovelock et al. (1993 in Stumm and Morgan, 1996), one can calculate that the flux of freon across the water–gas interface in marine environments is  $1.5 \times 10^{-9} \text{ g cm}^{-2} \text{ year}^{-1}$ . Extended derivations and similar calculations can be made for other chemical systems after making allowances for chemical reactions. For example, the steady-state flux of  $\text{CO}_2(\text{g})$  from a lake into the atmosphere is  $6 \times 10^{-9} \text{ mol cm}^{-2} \text{ s}^{-1}$  at pH 6.7, total alkalinity of  $3 \times 10^{-3} \text{ mol L}^{-1}$ , and 298.15 K.

## 12.5 Acid–Base Reactions in the Soil Solution

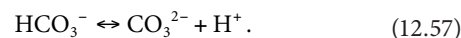
Acid and base reactions are the most fundamental and often the most important in soil solutions. The weathering of primary minerals often generates alkaline conditions, and natural and anthropogenic activities can generate acidic conditions. The rates and extents of many chemical reactions are dependent upon soil solution pH including biological activity, mineral

dissolution, partitioning of some gases, and bioavailability of critical nutrient elements. This section will address some of the important acid–base concepts and discuss the numerical handling of related equilibria.

### 12.5.1 Fundamentals of Acid–Base Chemistry in Soil Solution

The central component of acid–base reactions is the proton or hydrogen ion,  $\text{H}^+$ . This ion does not actually exist as  $\text{H}^+$  in aqueous solutions but is hydrated to form  $\text{H}_3\text{O}^+$ ,  $\text{H}_7\text{O}_3^+$ ,  $\text{H}_9\text{O}_4^+$ , etc. For the sake of simplicity in representing the equilibria involving the proton, the symbol  $\text{H}^+$  will be used.

According to the Bronsted–Lowry concept, an acid is any substance that donates a proton to another substance. Similarly, a Bronsted–Lowry base is any substance that accepts a proton from another substance. Using this definition, hundreds of reactions in soil solutions are examples of acids and bases. For example, bicarbonate ion dissociates readily to form carbonate and  $\text{H}^+$ :

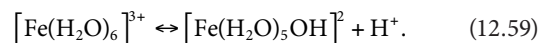


In this case, bicarbonate is acting as an acid. Bicarbonate may also act as a base, accepting a proton to form carbonic acid:



Although the discussions of Bronsted–Lowry theory for acids and bases presented here will be limited to aqueous systems, the theory is applicable to all solvents in which protons may be exchanged, including ammonia, sulfuric acid, and ethanol.

Metal ions in aqueous solutions are readily solvated and, as such, exist as hydrates rather than bare ions. The number of water molecules surrounding a cation in the first hydration layer will be dependent upon the ionic radius of the cation and its charge. The water in the hydration sphere tends to act as a weak acid, donating a proton to the solution and (in essence) contributing a hydroxyl ion to the metal:



The acidity of the water associated with the hydrolysis reaction increases with increasing valence and decreasing ionic radius of the central cation.

Another acid–base concept was formulated by G.N. Lewis (Lewis and Randall, 1923). A Lewis acid accepts a pair of electrons from a Lewis base. All Bronsted–Lowry acids and bases are also Lewis acids and bases, but the Lewis definition encompasses more reactions. In the neutralization reaction of  $\text{H}^+$  with  $\text{OH}^-$  to give water, a lone pair of electrons on the hydroxyl is donated to hydrogen; thus, this reaction fits both acid and base definitions. When an orthophosphate ion reacts with  $\text{Fe}(\text{III})$  in the structure of goethite, the  $\text{Fe}(\text{III})$  accepts an electron pair from the oxygen

on the phosphate group to form the bond. This fits the Lewis definition of an acid–base reaction but is clearly not a Bronsted–Lowry acid–base pair.

### 12.5.2 Calculations for Acid–Base Equilibria

Graphical representations of acid–base equilibria can take several forms, but the underlying calculations are built on the same theoretical foundation. Whether the system is simple or complex, the approach is the same, although organizing and executing the computations can be challenging for large systems. The first step is to identify the participating components, assemble the pertinent equations, identify the master variables, and solve the equations in terms of the master variables. A simple system, aqueous solution of carbonate, will be used as an example with more complex systems developed later in this chapter.

In this system, the species in solution would be  $\text{OH}^-$ ,  $\text{H}^+$ ,  $\text{H}_2\text{CO}_3^*$ ,  $\text{HCO}_3^-$ , and  $\text{CO}_3^{2-}$  with  $\text{CO}_2(\text{g})$  in the gas phase. The defining reactions and equilibrium constants are given in Table 12.7. The equilibrium constants ( $K^\circ$ ) are given at zero ionic strength, 298.15 K, and 101.33 kPa (1 atm) and are taken from Lindsay (1979). By defining the equilibrium constants at zero ionic strength, it is assumed that all species are given in terms of activities. In Figure 12.5, activities of the three solution species in equilibrium with 0.0003 atm  $\text{CO}_2(\text{g})$  are plotted as a function of pH. The predominant solution species below pH 6.33 is  $\text{H}_2\text{CO}_3^*$  at an activity of  $10^{-4.98}$ . Between pH 6.33

**TABLE 12.7** Controlling Equations for Equilibria Involving  $\text{CO}_2(\text{g})$  and  $\text{H}_2\text{O}(\text{l})$

Equation	$\log K^\circ$
$\text{CO}_2(\text{g}) + \text{H}_2\text{O}(\text{l}) \leftrightarrow \text{H}_2\text{CO}_3^*(\text{aq})$	-1.46
$\text{H}_2\text{CO}_3^* \leftrightarrow \text{HCO}_3^- + \text{H}^+$	-6.36
$\text{H}_2\text{CO}_3^* \leftrightarrow \text{CO}_3^{2-} + 2\text{H}^+$	-16.69

Source: Lindsay, W.L., *Chemical Equilibria in Soils*, Wiley Interscience, New York, 1979.

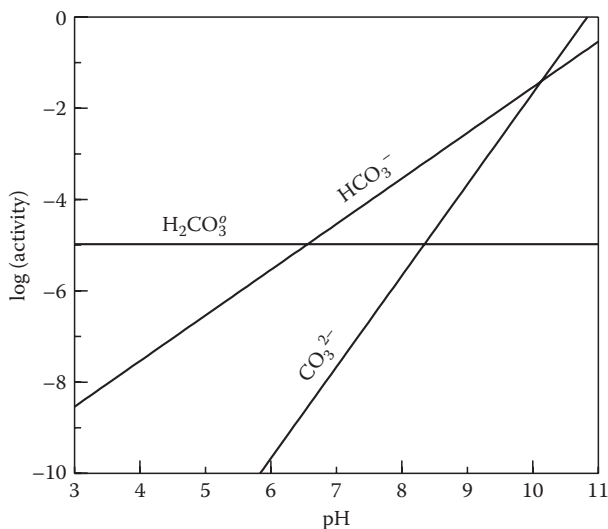


**FIGURE 12.5** Activities of carbonate species as affected by pH assuming equilibrium with  $P_{\text{CO}_2} = 0.0003$  atm.

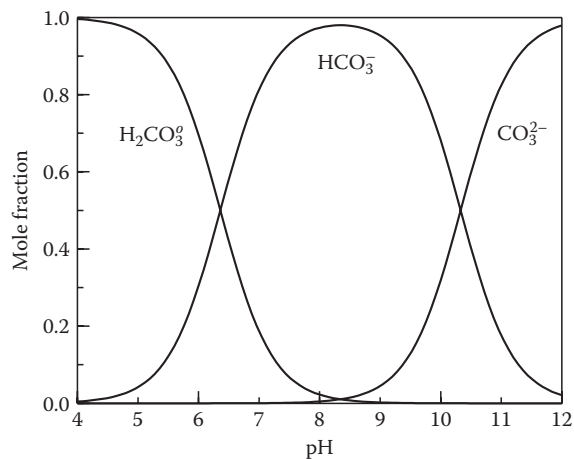


**FIGURE 12.6** Mole fraction distribution of carbonate species as a function of pH. For all calculations, activity coefficients are assumed to be unity ( $\gamma_i = 1.0$ ).

and 10.36, the dominant carbonate species is  $\text{HCO}_3^-$  with  $\text{CO}_3^{2-}$  being present at the greatest activities above pH 10.36. However, the total carbonate in solution approaches molar quantities near pH 10 in equilibrium with carbon dioxide at this pressure, concentrations rarely seen in natural solutions. Thus, the kinetics of  $\text{CO}_2(\text{g})$  dissolution probably predominate over equilibrium predictions at these high pH values in open systems.

Information similar to Figure 12.5 can be provided without the overlying assumption of an open system or predicting equilibrium activities. Figure 12.6 is a mole fraction distribution diagram depicting the relative concentrations of the three carbonate species as a function of pH. The mole fraction is defined as the ratio of the concentrations of a given species to the sum of the concentrations of all the carbonate species. For  $\text{CO}_3^{2-}$ ,

$$\text{Mole fraction (carbonate)} = \frac{[\text{CO}_3^{2-}]}{[\text{H}_2\text{CO}_3^*] + [\text{HCO}_3^-] + [\text{CO}_3^{2-}]} \quad (12.60)$$

The equilibrium expressions for these species in Table 12.4 are substituted appropriately and solved across pH (Lindsay, 1979). The resulting diagram (assuming that  $\gamma_i = 1$ ) is applicable to either open or closed systems and requires equilibrium only among the solution species; equilibrium between the aqueous and gaseous phases is not required. As Figures 12.5 and 12.6 illustrates that bicarbonate ion is dominant between pH 6.36 and 10.33 with carbonic acid dominant below pH 6.36 and carbonate above pH 10.33.

In the examples above, the simple system of carbon dioxide in water was considered. Multiple component systems or other complexities can be handled in the same fashion.

### 12.5.3 Buffering Capacity of Soil Solutions

Because of the many acids and bases present in the soil and dissolved in the soil solution, the acid–base chemistry of soils is

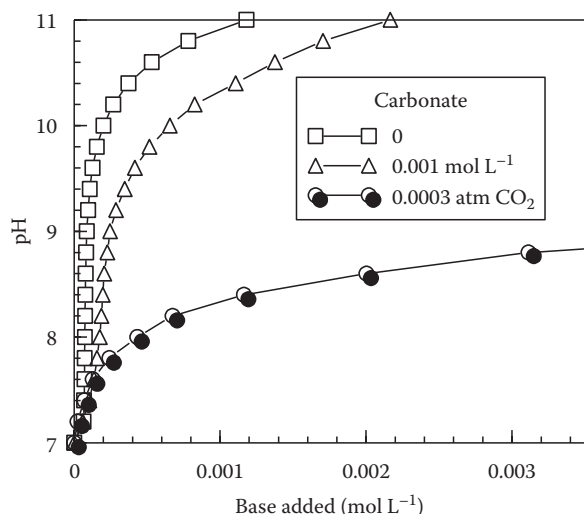


**FIGURE 12.7** Theoretical titration curves of an aqueous solution containing pure water ( $\square$ ) in a closed system (no access to atmospheric  $\text{CO}_2(\text{g})$ ), 0.001 M total carbonate in a closed system ( $\Delta$ ), or an open system in equilibrium with atmospheric  $\text{CO}_2(\text{g})$  at 30 Pa (0.0003 atm) ( $\bullet$ ). In all systems, the assumption is made that  $\gamma_i = 1$  and the volume remains constant.

highly complicated. One of the results of this complex system is that the pH of soils and, to a smaller extent, soil solutions does not change greatly in response to inputs of acid or base. The ability of a system to resist pH changes is called the buffering capacity or buffering intensity and can be determined experimentally by titrating the solution and measuring the pH at each increment of acid or base addition. A simple, qualitative illustration of the buffering power of carbonate in water is illustrated in Figure 12.7 in which aqueous solutions are theoretically titrated with base from pH 7 to 11. In the first case, only pure water is titrated, and the solution shows little capacity to resist pH change; with each increment of base, a large pH change is noted. In the second case, a solution containing 0.001 M total carbonate is initially adjusted to pH 7 and titrated with NaOH to pH 11. In this theoretical titration, activity coefficients are ignored ( $\gamma_i = 1$ ), but the volume is assumed to remain constant. The carbonate solution has a significant resistance to pH change (buffering capacity) compared with the pure solution. The third case in Figure 12.7 is an open system in equilibrium with atmospheric  $\text{CO}_2(\text{g})$  assuming 0.0003 atm (30 Pa). The buffering capacity of this solution is low when  $\text{pH} < 8$ , but at greater pH values, the dissolution of  $\text{CO}_2$  into the solution radically increases the buffering.

Buffering may be quantified mathematically by defining buffering as the change in pH induced by the addition of acid or base to a solution:

$$\text{Buffering} = \frac{\Delta C_{\text{base}}}{\Delta \text{pH}} = -\frac{\Delta C_{\text{acid}}}{\Delta \text{pH}}. \quad (12.61)$$

Thus, the buffering is mathematically defined as the change in pH induced by an increment of acid or base (in  $\text{mol L}^{-1}$ ) added to the system. For a monoprotic acid (HA) dissolved in water,

the buffering can be shown to be represented as (Stumm and Morgan, 1996)

$$\text{Buffering} = 2.3 \left( [\text{H}^+] + [\text{OH}^-] + \frac{[\text{HA}][\text{A}^-]}{[\text{HA}] + [\text{A}^-]} \right). \quad (12.62)$$

This equation defines the buffering of the system at any point in the titration of the monoprotic acid, HA. Similar expressions can be derived for mixtures of acids or for polyprotic acids.

### 12.5.4 Soluble Organic Acids

The chemistry of soluble organic acids in soil solutions has not been studied to the extent of inorganic acids, although detailed reviews exist (e.g., Stevenson, 1967). The relative lack of information is not because of the lack of importance of soluble organic in soils but is a reflection of the difficulty in quantitatively characterizing the organic components in solution and the dynamic nature of soil organic molecules. Many simple organic acids have been identified in solution ranging from formic and acetic acids to more complex aromatic acids such as catechin (McKeague et al., 1986). The aliphatic carboxylic acids are degraded very rapidly, but the aromatic acids tend to be more persistent.

For organic acids that can be identified, the theoretical approach to defining their chemistry is identical to that of inorganic acids. Extensive lists of acidity constants have been compiled (Martell and Smith, 2004), and these constants may be used to generate activity and mole fraction diagrams similar to Figures 12.5 and 12.6. The concepts of buffering intensity and acid neutralizing capacity of organic acids are applied in identical fashion as those of inorganic acids.

Methods also exist for quantifying the acid–base behavior of more complex organic mixtures. A direct approach is to titrate the soil solution or extract, plot the titration curve, and identify the characteristic buffering regions (Dudley and McNeal, 1987; Sposito, 2008). The resulting curves can be modeled based on hypothetical mixtures of organic acid groups, or the acid neutralizing capacity and formation functions may be determined. There is general agreement that complex organic matter in soil and in soil solution is a broad mixture of carboxylic and benzoic acids with a wide range of acidity constants.

## 12.6 Formation of Soluble Complexes

### 12.6.1 Types of Complexes

A solution complex is the close association between a central molecular component (such as a cation) with other atoms or molecules. Very often, metals or other positively charged species act as the central component attracting neutral or negatively charged ligands. In the hydrolysis of  $\text{Fe}^{3+}$  to form  $\text{Fe}(\text{H}_2\text{O})_5\text{OH}^{2+}$ , the  $\text{Fe}^{3+}$  cation is acting as the central unit with water and hydroxyl acting as the ligands. This is a special case of complex formation called a solvation complex. Two other categories of complexes can be formed depending upon the strength of

bonding between the central unit and the ligand. If the interaction between the cation and ligand is strong enough that the ligand displaces the solvation sphere, the resulting association is termed an inner-sphere complex. Typical examples of inner-sphere complexes are  $\text{AlF}_n^{3-n}$  and Fe(III)citrate. If the attraction between the cation and ligands are not strong enough to displace the hydration layer, an outer-sphere complex is formed or, sometimes, an ion pair. An inner-sphere complex can form if the heat evolved during the association exceeds the energy needed to displace the hydration sphere. If the heat evolved is less than the energy necessary to displace the water, then the hydration sheath remains intact and an outer-sphere complex results.

If a ligand occupies more than one coordination site in the complex, the ligand is referred to as multidentate. For example, two of the oxygens in oxalate can bond simultaneously with a central Fe(III) ion. Such a complex is called a chelate, and the process is chelation. The multidentate nature of the interaction can significantly increase the strength of the bond, and the resulting formation constant is much higher than ordinary complexes.

### 12.6.2 Hard and Soft Acid–Base Rules

Other useful concepts in predicting the association between cations and ligands are the hard and soft acid–base rules (Pearson, 1963). Hard acids and bases are those species that tend to have smaller radii and are not readily deformable (Table 12.8). Soft acids and bases are often larger and more polarizable (have a more easily deformed electron sheath). The tendency is that hard acids bond preferentially with hard bases, and soft acids bond preferentially with soft bases. Thus,  $\text{Ca}^{2+}$  would tend to bond with phosphate and carbonate rather than chloride and sulfide.

### 12.6.3 Rates of Formation of Solution Complexes

The rates of formation of solution complexes are often rapid, establishing equilibrium very quickly. Certain reactions, however, proceed very slowly. For example, the reaction



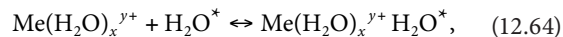
requires nearly 20 min to proceed half way to completion. This is in contrast to the formation of  $\text{MnSO}_4^0$ , which requires  $10^{-5}$  s.

TABLE 12.8 Hard and Soft Acids and Bases

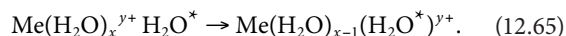
	Hard	Intermediate	Soft
Bases	$\text{F}^-$ , $\text{CO}_3^{2-}$ , $\text{Cl}^-$ , $\text{OH}^-$ , $\text{CH}_3\text{COO}^-$ , $\text{PO}_4^{3-}$ , $\text{SO}_4^{2-}$ , $\text{NH}_3$ , $\text{R-NH}_2$ , $\text{H}_2\text{O}$ , $\text{R-OH}$ , $\text{NO}_3^-$	$\text{SO}_3^{2-}$ , $\text{NO}_2^-$ , $\text{C}_6\text{C}_5\text{NH}_2$ , $\text{Br}^-$	$\text{S}^{2-}$ , $\text{CN}^-$ , $\text{I}^-$ , $\text{R-SH}$ , $\text{SCN}^-$ , $\text{S}_2\text{O}_3^{2-}$
Acids	$\text{H}^+$ , $\text{Li}^+$ , $\text{Na}^+$ , $\text{K}^+$ , $\text{Mg}^{2+}$ , $\text{Ca}^{2+}$ , $\text{Sr}^{2+}$ , $\text{Al}^{3+}$ , $\text{La}^{3+}$ , $\text{Si}^{4+}$ , $\text{Zr}^{4+}$ , $\text{Th}^{4+}$ , $\text{Th}^{4+}$ , $\text{Cr}^{3+}$ , $\text{Mn}^{3+}$ , $\text{Fe}^{3+}$	$\text{Mn}^{2+}$ , $\text{Fe}^{2+}$ , $\text{Cu}^{2+}$ , $\text{Zn}^{2+}$ , $\text{Pb}^{2+}$ , $\text{Bi}^{3+}$ , $\text{Ni}^{2+}$ , $\text{SO}_2$	$\text{Ag}^+$ , $\text{Cu}^+$ , $\text{Cd}^{2+}$ , $\text{Hg}^{2+}$ , $\text{Cs}^+$

Source: Pearson, R.G. 1963. Hard and soft acids and bases. J. Am. Chem. Soc. 85:3533.

Hydrolysis reactions generally are quite rapid for the monovalent and divalent cations but can proceed slowly for the higher charged cations. The rate of these reactions can be approximated by examining the rate of water exchange from a hydrated cation,  $\text{Me}(\text{H}_2\text{O})_x^{y+}$  (Stumm and Morgan, 1996):



where  $\text{H}_2\text{O}^*$  is the water being exchanged into the solvation complex. The forward rate constant in this expression is  $k_1$ , and the rate constant for the reverse reaction is  $k_{-1}$ . The exchange reaction is completed in this equation with a rate constant of  $k_{-w}$ :



The rate of this reaction is

$$\frac{d[\text{Me}(\text{H}_2\text{O})_{x-1}(\text{H}_2\text{O}^*)^{y+}]}{dt} = k_{-w} [\text{Me}(\text{H}_2\text{O})_x^{y+} (\text{H}_2\text{O}^*)] \quad (12.66)$$

At steady state,

$$\begin{aligned} \frac{d[\text{Me}(\text{H}_2\text{O})_x^{y+} (\text{H}_2\text{O}^*)]}{dt} \\ = k_1 [\text{Me}(\text{H}_2\text{O})_x^{y+}] [\text{H}_2\text{O}^*] - (k_{-1} + k_{-w}) [\text{Me}(\text{H}_2\text{O})_x^{y+} \text{H}_2\text{O}^*] = 0. \end{aligned} \quad (12.67)$$

After further manipulation and assuming that  $k_{-1} \gg k_{-w}$ ,

$$\frac{d[\text{Me}(\text{H}_2\text{O})_{x-1}(\text{H}_2\text{O}^*)^{y+}]}{dt} = k_{-w} K_{\text{OS}} [\text{Me}(\text{H}_2\text{O})_x^{y+}] [\text{H}_2\text{O}^*], \quad (12.68)$$

where  $K_{\text{OS}} = k_1/k_{-1}$  is the outer-sphere complex formation equilibrium constant. Thus, the rate constant for the exchange of water in the hydration shell is estimated by  $k_{-w}K_{\text{OS}}$ . The same development can be used to describe the kinetics of complex formation with a ligand,  $L$ , rather than  $\text{H}_2\text{O}^*$ . The resulting equation is

$$\frac{d[\text{Me}(\text{H}_2\text{O})_{x-1}L^{y+}]}{dt} = k_{-w}K_{\text{OS}} [\text{Me}(\text{H}_2\text{O})_x^{y+}] [L]. \quad (12.69)$$

Omitting the waters of hydration results in the standard notation:

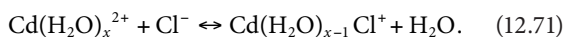
$$\frac{d[\text{Me}L]}{dt} = k[\text{Me}][L], \quad (12.70)$$

where  $k = k_{-w}K_{\text{OS}}$ . This development illustrates the importance of the equilibrium constant for the outer-sphere complex (i.e., the energetics of the reaction) as well as the kinetics of exchange of waters of hydration surrounding the metal.

Stumm and Morgan (1996) compiled the values of  $k_{-w}$  for water exchange reactions for several metals. For  $\text{Pb}^{2+}$ ,  $\text{Hg}^{2+}$ ,  $\text{Cu}^{2+}$ ,  $\text{Ca}^{2+}$ ,  $\text{Cd}^{2+}$ ,  $\text{La}^{3+}$ ,  $\text{Zn}^{2+}$ ,  $\text{Mn}^{2+}$ ,  $\text{Co}^{2+}$ ,  $\text{Fe}(\text{OH})_2^+$ , and  $\text{Fe}(\text{OH})_4^-$ , the values were  $k_{-w} \geq 10^6 \text{ s}^{-1}$ . Values of  $k_{-w}$  for other metals were  $2 \times 10^2$  for  $\text{Fe}^{3+}$ , 1.0 for  $\text{Al}^{3+}$ , and  $5 \times 10^{-7}$  for  $\text{Cr}^{3+}$ .

Sequential reactions can be “coupled” and solved. Exact analytical solutions to these models can be obtained (Sposito, 1994), but it is typical to use experimental observations to help establish simplifying assumptions.

The formation of the solution complex  $\text{CdCl}^+$  in the presence of  $10^{-3} \text{ mol L}^{-1} \text{ Cl}^-$  can be used to illustrate the application of these equations:



The rate of reaction can be given by

$$\begin{aligned} \frac{d[\text{Cd}(\text{H}_2\text{O})_{x-1}\text{Cl}^+]}{dt} &= K_{\text{OS}}k_{-w} [\text{Cd}(\text{H}_2\text{O})_x^{2+}][\text{Cl}^-] \\ &= -\frac{d[\text{Cd}(\text{H}_2\text{O})_x^{2+}]}{dt}, \end{aligned} \quad (12.72)$$

where

$$\begin{aligned} k_{-w} &= 10^{8.48} \text{ (s}^{-1}\text{)} \\ K_{\text{OS}} &= 10^{1.98} \text{ (mol L}^{-1}\text{)}^{-1} \\ (k_{-w})(K_{\text{OS}}) &= 10^{10.46} \text{ (L mol}^{-1} \text{ s}^{-1}\text{)} \end{aligned}$$

Substituting these values into the above equation and simplifying by not expressing the waters of hydration,

$$-\frac{d[\text{Cd}^{2+}]}{dt} = (10^{10.46})(10^{-3})[\text{Cd}^{2+}] = 10^{7.46}[\text{Cd}^{2+}]. \quad (12.73)$$

For a first-order reaction such as this, the half-life of the reaction (i.e., the time required for the reaction to proceed half way to completion) is equal to  $(\ln 2) k^{-1}$ . Thus, the half-life for this reaction is  $0.693/2.88 \times 10^7$  or  $2.40 \times 10^{-8} \text{ s}$ . Sposito (1989) tabulated the half-lives for several solution reactions, and the values ranged from  $10^{-9} \text{ s}$  for the formation of  $\text{MnSO}_4^0$  to  $10^3 \text{ s}$  for the formation of  $\text{AlF}^{2+}$ .

The relationships presented in this section demonstrate that most reactions in the soil solution are rapid enough that equilibrium can be achieved during the course of most experiments. Even the slowest example given above, the formation of  $\text{AlF}^{2+}$  in  $10^3 \text{ s}$ , will be nearly complete in less than 1 h. However, the rate of certain oxidation/reduction reactions can proceed very slowly, particularly reactions that involve oxyanions (such as arsenates or chromate) or that are not microbially catalyzed. These reactions can take days to reach completion, if at all. Therefore, knowledge of equilibrium predictions alone may be of limited utility if the kinetics of reaction are unfavorable.

## 12.7 Application of Thermodynamic and Equilibrium Concepts to Soil Solutions

The chemical composition and dynamics of the soil solution are reflections of all the processes, which depend upon the aqueous phase: biological activity, mineral dissolution/precipitation, adsorption/desorption, physical transport, and anthropogenic inputs. Wolt (1994) described the soil solution as “a window to chemically reacting soil systems where the intensity and distribution of chemicals in the soil aqueous phase represents the integration of multiple physical, chemical, and biological processes occurring concurrently within the soil environment.” The information provided by the chemical composition is further enhanced by the knowledge of time trends and the application of kinetic and thermodynamic theories.

### 12.7.1 Speciation and Single-Ion Activity Determinations

The determination of free ion activities (or concentrations) for soil solution components provides a powerful interpretative tool for chemical reactions in soils. A limited number of ion activities can be determined directly (such as the  $\text{H}^+$  activity using a glass electrode), but the rest must be approximated through rigorous calculations.

The steps in calculating ion activities and the distribution of solution species include obtaining and analyzing the soil solution, identifying the important solution species that can form, assembling relevant equilibrium constants and reactions for the formation of these species, obtaining an analytical or numerical solution for the series of equations, and calculating activity coefficients. All the steps in the calculations can be handled by any of the many geochemical models currently available (discussed later); however, understanding the chemical concepts behind the models and how the activities are determined will be helpful in properly executing the computer models and obtaining the best possible data. The following sections provide a brief review of the important chemical reactions and activity calculations.

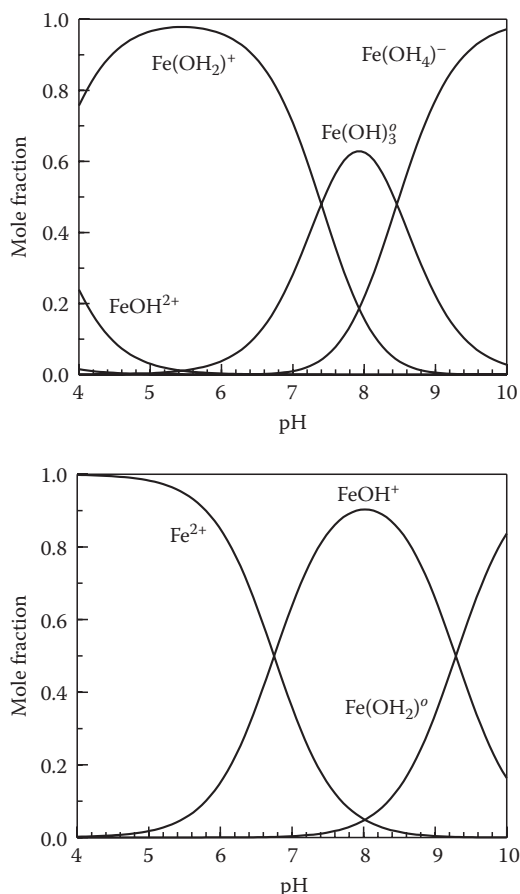
#### 12.7.1.1 Hydrolysis, Complexation, and Oxidation/Reduction Reactions

To help illustrate the steps involved in activity calculations, soluble Fe will be used as an example. The first step is to determine the important reactions in solution, and this can be done with the aid of some of the compilations of thermodynamic data for aqueous systems, such as Garrels and Christ (1965), Lindsay (1979), Sadiq and Lindsay (1979), and Martell and Smith (2004). Many of the metals undergo hydrolysis reactions, and Fe(III) and Fe(II) have many important hydrolysis species as indicated in Table 12.9. The distribution of these Fe(III) and Fe(II) hydrolysis species as a function of pH (Figure 12.8) shows that the predominant species will be strongly dependent upon pH with mole fractions ranging from 0.0 to over 0.9. Examination of Table 12.9 indicates that the complexes listed must be considered if  $(\text{Cl}^-) > 10^{-2}$ ,  $(\text{F}^-) > 10^{-7}$ ,

**TABLE 12.9** Reactions and Equilibrium Constants for Selected Solution Complexes of Iron

Reaction	log $K^\circ$
<i>Fe(III) hydrolysis</i>	
$\text{Fe}^{3+} + \text{H}_2\text{O} \leftrightarrow \text{FeOH}^{2+} + \text{H}^+$	-2.19
$\text{Fe}^{3+} + 2\text{H}_2\text{O} \leftrightarrow \text{Fe}(\text{OH})_2^+ + 2\text{H}^+$	-5.69
$\text{Fe}^{3+} + 3\text{H}_2\text{O} \leftrightarrow \text{Fe}(\text{OH})_3^0 + 3\text{H}^+$	-13.09
$\text{Fe}^{3+} + 4\text{H}_2\text{O} \leftrightarrow \text{Fe}(\text{OH})_4^- + 4\text{H}^+$	-21.59
<i>Fe(II) hydrolysis</i>	
$\text{Fe}^{2+} + \text{H}_2\text{O} \leftrightarrow \text{FeOH}^+ + \text{H}^+$	-6.74
$\text{Fe}^{2+} + 2\text{H}_2\text{O} \leftrightarrow \text{Fe}(\text{OH})_2^0 + 2\text{H}^+$	-16.04
<i>Redox</i>	
$\text{Fe}^{3+} + \text{e}^- \leftrightarrow \text{Fe}^{2+}$	13.04
<i>Complexation</i>	
$\text{Fe}^{3+} + \text{Cl}^- \leftrightarrow \text{FeCl}^{2+}$	1.48
$\text{Fe}^{3+} + \text{F}^- \leftrightarrow \text{FeF}^{2+}$	6.00
$\text{Fe}^{3+} + \text{SO}_4^{2-} \leftrightarrow \text{FeSO}_4^{2-}$	4.15
$\text{Fe}^{3+} + \text{H}_2\text{PO}_4^- \leftrightarrow \text{FeHPO}_4^- + \text{H}^+$	3.71
$\text{Fe}^{2+} + \text{SO}_4^{2-} \leftrightarrow \text{FeSO}_4^0$	2.20

Source: Lindsay, W.L. 1979. Chemical equilibria in soils. Wiley Interscience, New York.

**FIGURE 12.8** Distribution of Fe(III) and Fe(II) hydrolysis species in solution as a function of pH.

$(\text{SO}_4^{2-}) > 10^{-5} \text{ mol L}^{-1}$ . The constants in Table 12.9 and their corresponding equations can be used to solve for ionic activities.

### 12.7.1.2 Solution Composition Example

Consider a soil solution with the following composition:  $0.2 \mu\text{mol L}^{-1}$  total Fe,  $20 \text{ mmol L}^{-1}$  total Cl,  $10 \mu\text{mol L}^{-1}$  total F,  $1 \text{ mmol L}^{-1}$  total sulfate, ionic strength  $0.01 \text{ mol L}^{-1}$ , pH 6.5, and a redox potential of 600 mV. This is enough information to estimate the  $\text{Fe}^{2+}$  and  $\text{Fe}^{3+}$  activities. The solution is fairly complex and requires a few assumptions to make it solvable. The first assumption will be that the ligands will not form complexes with any cations in solution of other  $\text{Fe}^{2+}$  and  $\text{Fe}^{3+}$ . This is a poor assumption because each ligand forms a number of complexes with other cations, particularly  $\text{Al}^{3+}$ ,  $\text{Ca}^{2+}$ , and  $\text{Mg}^{2+}$ . The second assumption is that the only species of Fe to be considered are those given in Table 12.9.

The approach given here is to identify all potential variables, establish the same number of independent equations as the number of variables, and solve the equations simultaneously. The system variables are the activities of  $\text{H}^+$ ,  $\text{OH}^-$ ,  $\text{e}^-$ ,  $\text{Fe}^{3+}$ ,  $\text{Fe}^{2+}$ ,  $\text{Cl}^-$ ,  $\text{SO}_4^{2-}$ ,  $\text{F}^-$ ,  $\text{FeOH}^{2+}$ ,  $\text{Fe}(\text{OH})_2^+$ ,  $\text{Fe}(\text{OH})_3^0$ ,  $\text{Fe}(\text{OH})_4^-$ ,  $\text{FeOH}^+$ ,  $\text{Fe}(\text{OH})_2^0$ ,  $\text{FeCl}^{2+}$ ,  $\text{FeF}^{2+}$ ,  $\text{FeSO}_4^+$ , and  $\text{FeSO}_4^0$ , for a total of 18 variables. The relevant equations include 11 complexation equations from Table 12.9 (all equations except for the formation of  $\text{FeHPO}_4^-$ ),  $K_w$  (water dissociation equation),  $\text{pH} = 6.5$ ,  $Eh = 600 \text{ mV}$  ( $pe = 10.1$ ), and the four mass balance equations for the components:

$$\begin{aligned} \sum \text{Fe} = & [\text{Fe}^{3+}] + [\text{Fe}^{2+}] + [\text{FeOH}^{2+}] + [\text{Fe}(\text{OH})_2^+] + [\text{Fe}(\text{OH})_3^0] \\ & + [\text{FeOH}^+] + [\text{Fe}(\text{OH})_2^0] + [\text{FeCl}^{2+}] \\ & + [\text{FeF}^{2+}] + [\text{FeSO}_4^+] + [\text{FeSO}_4^0], \end{aligned} \quad (12.74)$$

$$\sum \text{SO}_4^{2-} = [\text{SO}_4^{2-}] + [\text{FeSO}_4^+] + [\text{FeSO}_4^0], \quad (12.75)$$

$$\sum \text{Cl} = [\text{Cl}^-] + [\text{FeCl}^{2+}], \quad (12.76)$$

$$\sum \text{F} = [\text{F}^-] + [\text{FeF}^{2+}]. \quad (12.77)$$

In the mass balance expressions, brackets  $[x]$  represent concentrations of species  $x$ . Activity coefficients must be calculated for each species to tie together the mass balance equations with the formation equations. Thus, there are a total of 18 equations for the 18 variables. Many methods exist for solving this system of equations including back substitution and matrix algebra. These systems can be solved by hand, but solutions are reached more rapidly using computers.

## 12.7.2 Geochemical Models

Over the past decades, scientists and research groups have recognized the need for computer programs to solve chemical

equilibrium systems, and several computer models have been established. Models vary widely in their construction and composition as well as their intended use (Baham, 1984; Melchior and Bassett, 1990; van der Lee and de Windt, 2001; Hummel, 2005). Many of the models are based upon single-ion activities, single-ion activity coefficients, and formation constants; Pitzer's equations for applications at high ionic strength; or a free energy minimization approach.

### 12.7.2.1 Formation Constant Approach

In Section 12.7.1.2, an example was given outlining the formation constant approach to determine single-ion activities in soil solutions. Several series of published models take this same approach. The WATEQ series (Truesdall and Jones, 1974; Ball et al., 1979) was developed by the U.S. Geological Survey to compute single-ion activities to predict the fate of critical elements in geochemical environments. Emphasis was placed on obtaining a well-documented thermodynamic database with the best available equilibrium constants; a reaction would be kept out of the database if the constant was estimated or suspected to be of poor quality. The mathematical solution method was back substitution and required recompilation of the programming code if new reactions were added or if constants were changed. The MINEQL series (Westall et al., 1976) was developed using the mathematical approach of REDEQL (Morel and Morgan, 1972) to solve equilibrium problems and provide information about trends in observed data. The mathematical solution method is rapid and efficient, but the thermodynamic database was not rigorously reviewed. The model SOILCHEM (Sposito and Coves, 1988) was an extension of the MINEQL model with emphasis on expanding the database. Some smaller models have been developed, such as SOILSOLN (Wolt, 1989) and CALPHOS (Adams, 1971), for very specific (but limited) applications. SOILSOLN was designed as a teaching tool with an easy-to-use interface and embedded graphics.

### 12.7.2.2 High Ionic Strength Models

The general approach in the models described in Section 12.7.2.1 is the combination of equilibrium constant expressions with mass balances. The impact of ionic strength (and activity coefficients) is disregarded or single-ion activity coefficients are calculated. The single-ion activity coefficient is not rigorously defined in thermodynamic theory, and the equations used to approximate activity coefficients are subject to error, particularly at high ionic strength. A special approach must be taken for aqueous solutions with high-salt concentrations (ionic strength greater than  $0.5 \text{ mol L}^{-1}$ ). One such approach is to use the Pitzer equations (Pitzer, 1979) for calculation of single-ion activity coefficients, and at least two published models currently use this approach. Felmy and Weare (1995) discussed their model and experimental results of simple systems with high ionic strengths. The agreement between theory and experimental determinations is promising. The C-SALT model (Smith et al., 1995) also uses the Pitzer equations. The model has been tested against experimental data.

The Pitzer equations require a relatively large number of parameters that are specific to the ions and systems under consideration. The number of required parameters increases rapidly as the systems become more complex. The Pitzer, Davies, and Debye-Huckel equations calculate single-ion activity coefficients. Unfortunately, these activity coefficients cannot be defined unambiguously because they are dependent upon a clear, thermodynamic definition of single-ion concentrations. As stated by Sposito (1994) when discussing the activity coefficients for a metal ion,  $\gamma_M$ , and a ligand,  $\gamma_L$ , "For  $\gamma_M$  and  $\gamma_L$  to have chemical significance, the species molalities,  $m_M$  and  $m_L$ , must have a well-defined operational meaning. Thus, the single-ion activity coefficient has no meaning apart from the set of operational procedures used to define ionic species and to determine their concentrations in an aqueous solution." Although the determination of single-ion activities can provide useful information, single-ion activity coefficients cannot be experimentally determined and do not have a thermodynamic foundation.

### 12.7.2.3 Solving Example Problem with Visual MINTEQ

The geochemical model, MINTEQ, and later MINTEQA2 (Allison et al., 1990), were developed by merging the mathematics and computer code from MINEQL with the database from the WATEQ series. Although the MINTEQ database is not as extensive as SOILCHEM's, all values were fully documented as to their source and reason for selection. Visual MINTEQ was developed to provide a graphic interface for MINTEQA2 version 4 (Gustafsson, 2009) as well as expanding the database. Visual MINTEQ provides solution speciation, mass transfer through precipitation and dissolution of solid phases, ion adsorption, ion exchange, redox, and humic complexation models, and gas phase calculations.

The hypothetical analytical data for the example problem in Section 12.7.1.2 were entered into a Visual MINTEQ input file, and the program executed. The resulting activities (Table 12.10)

**TABLE 12.10** Activities of Selected Aqueous Species Calculated Using Visual MINTEQ Version 2.61 for the Example Solution Composition Given in Section 12.7.1.2

Species	Log (Activity)	Species	Log (Activity)
Fe <sup>3+</sup>	-14.00	Fe <sup>2+</sup>	-11.11
Fe(OH) <sup>2+</sup>	-9.52	FeOH <sup>+</sup>	-14.00
Fe(OH) <sub>2</sub> <sup>+</sup>	-6.75	Fe(OH) <sub>2</sub> <sup>o</sup>	-18.60
Fe(OH) <sub>3</sub> <sup>o</sup>	-9.50	FeSO <sub>4</sub> <sup>o</sup>	-11.89
Fe(OH) <sub>4</sub> <sup>-</sup>	-10.70	FeF <sup>+</sup>	-14.94
FeF <sup>2+</sup>	-13.00	FeCl <sup>+</sup>	-13.05
FeF <sub>2</sub> <sup>+</sup>	-13.43	F <sup>-</sup>	-5.05
FeF <sub>3</sub> <sup>o</sup>	-15.43	SO <sub>4</sub> <sup>2-</sup>	-3.18
FeSO <sub>4</sub> <sup>+</sup>	-12.92	Cl <sup>-</sup>	-1.74
FeCl <sup>2+</sup>	-14.26		

Source: Gustafsson, J.P. 2009. Visual MINTEQ version 2.61. <http://www.lwr.kth.se/English/OurSoftware/vminteq/>, accessed on May 16, 2011.



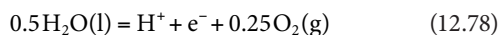
show that the hydrolysis species of Fe(III) and Fe(II) are much more important than the chloro, fluoro, and sulfate species. This is because these ligands react only with the unhydrolyzed cations, and, in the case of Fe(III), the activity of  $\text{Fe}^{3+}$  is very low. In the case of Fe(II), the ligand concentrations simply are not high enough to become the predominant solution species. (It is to be noted that the program was executed with the specification that supersaturated solid phases would not be allowed to precipitate. Many solid phases were supersaturated, and allowing their precipitation would have changed the results.)

The comparison of the Fe(III) and Fe(II) species also is worth noting. In Table 12.9, the constant for the equilibrium between  $\text{Fe}^{3+}$  and  $\text{Fe}^{2+}$  suggests that  $\text{Fe}^{2+}$  will be present at higher activities than  $\text{Fe}^{3+}$  when the  $pe < 13$  (770 mV). In this case,  $\text{Fe}^{2+}$  is nearly 1000 times greater than  $\text{Fe}^{3+}$ , but the Fe(III) hydrolysis species are by far the predominant Fe solution species. At this pH, the oxidation/reduction potential would have to be  $pe < 6.0$  (355 mV) before the predominant Fe(II) species is present at a greater activity than the predominant Fe(III) species.

### 12.7.3 Oxidation/Reduction Reactions

Chemical reactions involving oxidation and reduction are important in all biological systems, and soils are no exception. In all soils, localized areas can be found that are highly oxidized and highly reduced. Areas of reduction generally are associated with small microsites that are saturated with water and have restricted  $\text{O}_2(\text{g})$  diffusion. Microbial activity within these sites rapidly depletes the available oxygen, and the redox potential of the soil solution decreases. The ability to predict the impact of changes in redox on soil solution composition is a useful tool.

The first step in handling oxidation/reduction equilibria in soil solution is defining the limits of stability of aqueous systems. If a solution is subject to a high oxidizing potential, then the water spontaneously can be degraded into oxygen:



with an equilibrium constant expression:

$$K^o = \frac{(\text{H}^+)(\text{e}^-)(\text{O}_2(\text{g}))^{0.25}}{(\text{H}_2\text{O})^{0.5}} = 10^{-20.78} \quad (12.79)$$

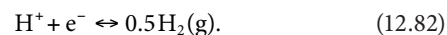
Substituting, rearranging, and solving for  $pe$  in terms of  $p\text{H}$ ,

$$pe = 20.78 + 0.25\log(\text{O}_2) - p\text{H} \quad (12.80)$$

The  $pe$  at which water spontaneously decomposes to oxygen gas would correspond to  $\text{O}_2(\text{g})$  pressure of 1 atm or  $pe = 20.78 - p\text{H}$ . Using the combined parameter,  $pe + p\text{H}$ , the upper oxidizing limit of the stability field of water would be

$$pe + p\text{H} = 20.78 \quad (12.81)$$

A strongly reducing potential can generate hydrogen gas:



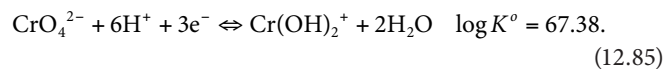
Again solving for  $pe$ ,

$$pe = -0.5\log(\text{H}_2(\text{g})) - p\text{H} \quad (12.83)$$

At 1 atm  $\text{H}_2(\text{g})$ , this reduces to  $pe = -p\text{H}$ . Again converting to the combined parameter,  $pe + p\text{H}$ ,

$$pe + p\text{H} = 0 \quad (12.84)$$

In a plot of  $pe$  versus  $p\text{H}$ , the region between the lines  $pe = -p\text{H}$  and  $pe = 20.78 - p\text{H}$  represents the stability field for water. Water is thermodynamically unstable at potentials outside this region. Another important aspect of these equations is the equilibrium partial pressures of  $\text{H}_2(\text{g})$  and  $\text{O}_2(\text{g})$  at typical redox potentials in soil solutions. For example, highly reduced soils seldom have redox potentials below  $pe + p\text{H} = 4$ , corresponding to  $P_{\text{H}_2} = 10^{-8}$  atm. Measured redox potentials in fully oxidized soils seldom exceed  $pe + p\text{H} = 18$ , and equilibrium at this potential would require  $10^{-11.23}$  atm  $\text{O}_2(\text{g})$ . If equilibrium were rapidly established with these gases, then the partial pressures of hydrogen and oxygen would be expected to be quite small in all situations. An equilibrium approach can be used to investigate many redox reactions in soil solutions. The Fe(III)/Fe(II) system was discussed in a prior section, and many other redox active species exist in soil solutions including  $\text{Cu}^{2+}$ ,  $\text{Mn}^{2+}$ , and  $\text{CrO}_4^{2-}$ . Chromium is an environmentally important metal and has an interesting redox behavior. The Cr(III) species is considered environmentally less hazardous than the Cr(VI), which is closely regulated. Published equilibrium constants can be used to determine the redox potential at pH 7 at which the predominant Cr(III) species,  $\text{Cr}(\text{OH})_2^+$ , converts to the predominant Cr(VI) species,  $\text{CrO}_4^{2-}$ . From the MINTAQ database, the following reaction and constant were obtained:



The expression for the equilibrium constant, converted to logarithms, would be

$$\log \left[ \frac{(\text{Cr}(\text{OH})_2^+)}{(\text{CrO}_4^{2-})} \right] + 6p\text{H} + 3pe = 67.38 \quad (12.86)$$

The redox potential at which Cr(III) converts to Cr(VI) occurs when the predominant species of each oxidation state of Cr have equal activities,  $(\text{Cr}(\text{OH})_2^+) = (\text{CrO}_4^{2-})$ . The ratio of these activities would equal unity, the logarithm of which is 0. Therefore, after dividing by 3,

$$2p\text{H} + pe = 22.46 \quad (12.87)$$

or, solving for  $pe + pH$ ,

$$pe + pH = 22.46 - pH \quad (12.88)$$

and, at  $pH = 7$ ,

$$pe + pH = 15.46. \quad (12.89)$$

This is a moderately reducing condition for soil solutions, roughly the same redox potential at which denitrification occurs (Lindsay, 1979).

### 12.7.4 Successful Applications of Geochemical Modeling to Soil Solutions

The application of equilibrium thermodynamics to soil solutions will have several requirements for success, and the definition of success will depend upon individual interpretations. The kinetics of some reactions in soil solutions were discussed in Section 12.6.3; most reactions were found to proceed quickly, but others are quite slow. Therefore, care must be taken to apply equilibrium thermodynamics only to the systems having enough time to equilibrate, and this is dependent upon the method of sample collection. For example, miscible displacement methods often have equilibration periods of less than 24 h, which is not long enough for some solid-phase equilibria or redox reactions involving oxyanions. However, most of the field methods should be adequate.

The success of applying a model to a chemical system will increase as more information is known. One of the important areas of progress in geochemical modeling in recent years has been the addition of aluminum–phosphate speciation and empirical models for evaluating the impact of soluble organic matter.

A critical aspect of employing a geochemical model is experimental validation. Models have been validated by published laboratory tests followed by extending the model to similar systems in natural settings. Felmy and Weare (1995) incorporated Pitzer's equations into an ion-interaction model, the purpose of which was to allow chemical speciation in high ionic strength solutions. The Davies equation for activity coefficients was found to inadequately predict  $\gamma_{\pm}$  for many salts at ionic strengths as low as  $0.2 \text{ mol L}^{-1}$  for 1:1 electrolytes and  $0.05 \text{ mol L}^{-1}$  for 2:1 electrolytes (Figure 12.9). The parameters for the ion-interaction model were obtained experimentally and applied to several systems, including  $\text{Na}_2\text{B}_4\text{O}_7\text{-Na}_2\text{SO}_4\text{-H}_2\text{O}$ ,  $\text{Na}_2\text{B}_4\text{O}_7\text{-Na}_2\text{CO}_3\text{-H}_2\text{O}$ , and  $\text{NaBO}_2\text{-NaCl-H}_2\text{O}$  systems. Salt concentrations were varied, and other activities measured. The agreement between modeling predictions and experimental results were  $\pm 10\%$ , even in the  $\text{NaBO}_2\text{-NaCl-H}_2\text{O}$  system (Figure 12.10) with very high borate concentrations and ionic strengths as high as  $14 \text{ mol L}^{-1}$ .

The effect of redox on the solubility of Fe in soil and aqueous systems has been a subject of study for decades. The presence of mixed valence state oxides has been observed and implied, and extensive equilibrium studies have been published. One of the

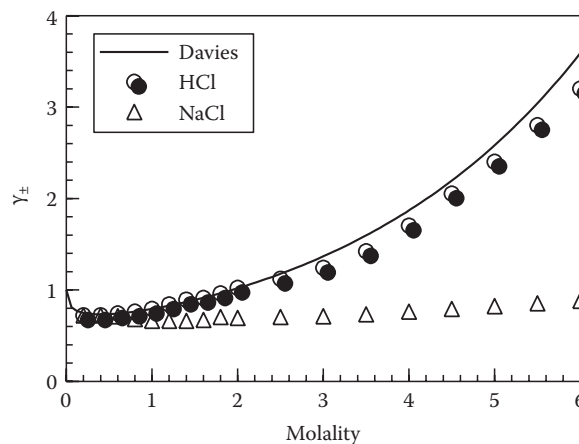


**FIGURE 12.9** Changes in experimentally determined mean activity coefficients ( $\gamma_{\pm}$ ) for various electrolytes compared with those generated by the Davies equation. Measured values are symbols, and predicted values are lines. (From Felmy, A.R., and J.H. Weare. 1995. The development and application of aqueous thermodynamic models: The specific ion-interaction approach. In R. Loeppert et al. (eds.) Chemical equilibrium and reaction models. Soil Science Society of America Special Publications No. 42. ASA, Madison, WI.)

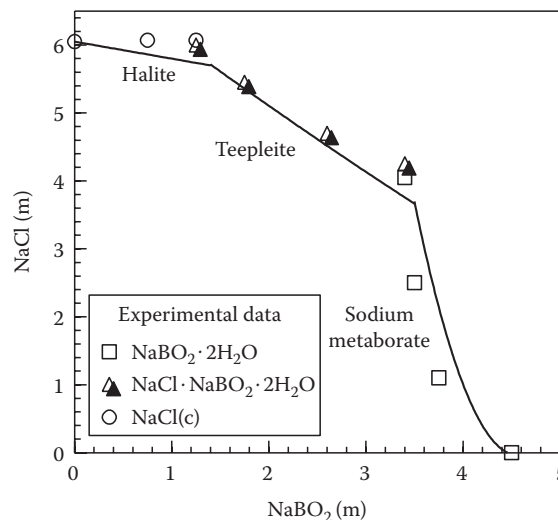


**FIGURE 12.10** The system  $\text{NaBO}_2\text{-NaCl-H}_2\text{O}$  at  $20^\circ\text{C}$ . Experimental data of Skvortsov et al. (1976) are shown as symbols, and the model predictions of Felmy and Weare (1995) are represented as lines.

more thorough studies involved the controlled reduction of ferric oxides (Brennan and Lindsay, 1998). Figure 12.11 is a redrafting of the experimental data in conjunction with the solubility constants of the solid phases from the Visual MINTEQ database. The implications of the original publication are unchanged despite some significant differences between the MINTEQ constants and those used by Brennan and Lindsay (1998). The observed solubilities of  $\text{Fe}^{2+}$  as a function of redox had a slope consistent with a solid phase with a stoichiometry of  $\text{Fe(II)Fe(III)}_2\text{O}_4$ . Although the molecular structure and Fe valence states of the resultant precipitate were not verified, the authors

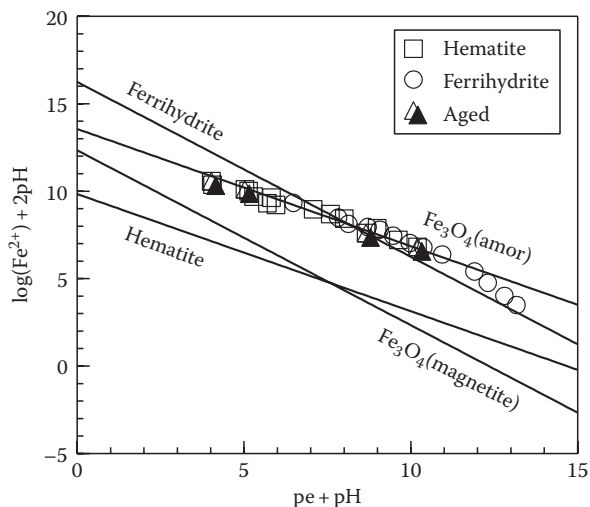


**FIGURE 12.11** Oxidation/reduction experiments under controlled conditions with different starting materials or different incubation periods. The open squares began with hematite, the open circles began with ferrihydrite, and the filled triangles were aged for 15 days. (From Brennan, E.W., and W.L. Lindsay. 1998. Reduction and oxidation effect on the solubility and transformation of iron oxides. *Soil Sci. Soc. Am. J.* 62:930–937.)

suggested that Fe solubility was being controlled by an amorphous form of magnetite,  $\text{Fe}_3\text{O}_4(\text{amorphous})$ .

### 12.7.5 Limitations to Applying Geochemical Models to Soil Solutions

Four major limitations exist in the application of equilibrium geochemical models to soil solutions: the dynamic (nonequilibrium) nature of soils, poorly defined equilibria, limitations in the analytical chemistry, and lack of knowledge of how to accurately handle soluble organic compounds. The ever-changing nature of soils naturally leads to nonequilibrium conditions. Although equilibrium within the soil solution may be attained quickly, solid and gas phases often establish equilibrium at a slow rate, if at all. Unfortunately, these systems have a very strong impact on the composition of the soil solution. Understanding the degree of nonequilibrium and the rate at which a steady state is being approached can be discerned by sampling the soil solution over time and monitoring the progress of the chemical reactions. Suarez (1995) discussed the merits of a nonequilibrium approach to modeling the carbonate system.

The problem of poorly defined equilibria arises when information about the system is lacking or if the database accompanying the geochemical model does not contain all the equilibrium constants to fully characterize important reactions. If data are severely lacking, then a speciation approach may not be possible. However, estimating experimental parameters or equilibrium constants may be an acceptable alternative. Limitations in analytical chemistry (quantification limits, capability to analyze certain species) must be dealt with in the same way.

As discussed in previous sections, soluble organic compounds are among the most important components in the soil solution,

and we have the least thermodynamic information about them. These compounds can be very complex and contain a wide range of functional groups and molecular chemical environments, making it difficult to approximate complexation constants. Thus, a decision must be made either to ignore the effects of soluble organics completely because their impact cannot be quantified exactly or to apply estimates of the constants. The latter approach has been applied with some success, including the addition of an organic component to Visual MINTEQ.

## 12.8 Current Status and Future Research Directions

This review of the chemistry of the soil solution assumed a distinct theoretical approach and did not focus on some of the excellent, recent advances in other aspects of the science. Topics not covered include colloidal chemistry (both inorganic and organic), spectroscopic approaches to identifying important complexes in the soil solution, salinity, xenobiotics in soil solutions, and heavy metals. Most of these topics are covered in other chapters.

The study of the soil solution has its origins in agriculture, and a great portion of soil chemical research remains agriculturally oriented. Many challenges exist in which soil chemists will play a pivotal role including managing soil acidity, growing crops in arid regions with limited or poor quality irrigation water, adapting to the inevitable trend toward lower quality fertilizers, and contributing to the development of truly sustainable agricultural systems.

Although soil chemistry has its history and future firmly rooted in agriculture, soil chemists are increasingly finding a niche in other, less traditional research areas. Geochemists, environmental engineers, hydrologists, and chemical engineers are finding that soil chemists make excellent research partners in solving environmental and production problems. Working knowledge of and the ability to use new technologies have allowed soil chemists to explore new areas: molecular-level spectroscopy to quantify the chemistry of surfaces, complexation reactions in solution, and chemical associations in both the solid and solution phases; analytical instrumentation to quantify ultratrace quantities of contaminants; and molecular genetics of microorganisms to help answer difficult ecological and environmental questions.

## References

- Adams, F. 1971. Ionic concentrations and activities in soil solution. *Soil Sci. Soc. Am. Proc.* 35:420–426.
- Adams, F. 1974. Soil solution, p. 441–481. *In* E.W. Carson (ed.) *The plant root and its environment*. University Press of Virginia, Charlottesville, Virginia.
- Allison, J.D., D.S. Brown, and K.J. Novo-Gradac. 1990. MINTEQA2/PRODEFA2, a geochemical assessment model for environmental systems: Version 3.00 user's manual. EPA-600/3-91-021. U.S. EPA, Athens, GA.

- Baham, J. 1984. Prediction of ion activities in soil solutions: Computer equilibrium modeling. *Soil Sci. Soc. Am. J.* 48:525–531.
- Ball, J.W., E.A. Jenne, and D.K. Nordstrom. 1979. WATEQ—A computerized chemical model for trace and major element speciation and mineral equilibria of natural waters, p. 813–835. *In* E.A. Jenne (ed.) *Chemical modeling in aqueous systems*. ACS Symposium Series No. 93. American Chemical Society, Washington, DC.
- Bartlett, R., and B. James. 1980. Studying dried, stored soil samples—Some pitfalls. *Soil Sci. Soc. Am. J.* 44:721–724.
- Berggren, D., and J. Mulder. 1995. The role of organic matter in controlling aluminum solubility in acidic mineral soil horizons. *Geochim. Cosmochim. Acta* 59:4167–4180.
- Bohn, H., B. McNeal, and G. O'Connor. 1985. *Soil chemistry*. Wiley Interscience, New York.
- Brennan, E.W., and W.L. Lindsay. 1998. Reduction and oxidation effect on the solubility and transformation of iron oxides. *Soil Sci. Soc. Am. J.* 62:930–937.
- Caron, A., S. Ben Jemia, J. Gallichand, and L. Trepanier. 1999. Field bromide transport under transient state: Monitoring with time domain reflectometry and porous cup. *Soil Sci. Soc. Am. J.* 63:1544–1553.
- Cole, D.W., S.P. Gessel, and E.E. Held. 1961. Tension lysimeter studies of ion and moisture movement in glacial till and coral atoll soils. *Soil Sci. Soc. Am. Proc.* 25:321–325.
- Dudley, L.M., and B.L. McNeal. 1987. A model for electrostatic interaction among charged sites of water-soluble organic polyions: I. Description and sensitivity. *Soil Sci.* 143:329–340.
- Elberling, B., and H. Matthiesen. 2007. Methodologically controlled variations in laboratory and field pH measurements in waterlogged soils. *Eur. J. Soil Sci.* 58:207–214.
- Elkhatib, E.A., O.L. Bennett, V.C. Baligar, and R.J. Wright. 1986. A centrifugation method for obtaining soil solution using an immiscible liquid. *Soil Sci. Soc. Am. J.* 50:297–299.
- Evans, K.A., and S.A. Banwart. 2006. Rate controls on the chemical weathering of natural polymineralic material. I. Dissolution behavior of polymineralic assemblages determined using batch and unsaturated column experiments. *Appl. Geochem.* 21:352–376.
- Felmy, A.R., and J.H. Weare. 1995. The development and application of aqueous thermodynamic models: The specific ion-interaction approach. *In* R. Loeppert et al. (eds.) *Chemical equilibrium and reaction models*. Soil Science Society of America Special Publications No. 42. ASA, Madison, WI.
- Garrels, R.M., and C.L. Christ. 1965. *Solutions, minerals, and equilibria*. Freeman, Cooper & Co., San Francisco, CA.
- Geantman, L. 2001. *In* *CRC Handbook of Chemistry and Physics*, 82 Edn., Sec. 8, CRC Press Boca Raton, FL.
- Gustafsson, J.P. 2009. Visual MINTEQ version 2.61. <http://www.lwr.kth.se/English/OurSoftware/vminteq/>, accessed on May 16, 2011.
- Hummel, W. 2005. Solubility equilibria and geochemical modeling in the field of radioactive waste disposal. *Pure Appl. Chem.* 77:631–641.
- Kielland, J. 1937. Individual activity coefficients of ions in aqueous solutions. *J. Am. Chem. Soc.* 59:1675–1678.
- Kittrick, J.A. 1977. Mineral equilibria and the soil system, p. 1–25. *In* J.B. Dixon and S.B. Weed (eds.) *Minerals in soil environments*. SSSA, Madison, WI.
- Lewis, G.N., and M. Randall. 1923. *Thermodynamics and the free energy of chemical substances*. McGraw-Hill, New York.
- Lindsay, W.L. 1979. *Chemical equilibria in soils*. Wiley Interscience, New York.
- Lovelock, J.E. and R.J. Maggs. 1993. Halogenated hydrocarbons in and over the Atlantic. *Nature*. 241:194–196.
- Martell, A.S., and R.M. Smith. 2004. NIST critically selected stability constants of metal complexes database; NIST standard reference database 46, version 8.0. NIST, Gaithersburg, MD.
- McBride, M.B. 1994. *Environmental chemistry of soils*. Oxford University Press, New York.
- McKeague, J.A., M.V. Cheshire, F. Andreux, and J. Berthelin. 1986. Organo-mineral complexes in relation to pedogenesis, p. 549–592. *In* P.M. Huang and M. Schnitzer (eds.) *Interactions of soil minerals with natural organics and microbes*. SSSA, Madison, WI.
- Melchior, D.C., and R.L. Bassett. 1990. *Chemical modeling of aqueous systems II*, ACS Symposium Series 416. American Chemical Society, Washington, DC.
- Morel, F.M.M., and J.J. Morgan. 1972. A numerical method for computing equilibrium in aqueous chemical systems. *Environ. Sci. Technol.* 6:58–67.
- Morris, D.F.C. 1969. Ionic radii and enthalpy of hydration of ions. *Struct. Bond.* 63:157–159.
- Morrison, R.D., and B. Lowry. 1990. Effect of cup properties, sampler geometry and vacuum on the sampling rate of porous cup samplers. *Soil Sci.* 149:308–316.
- Pearson, R.G. 1963. Hard and soft acids and bases. *J. Am. Chem. Soc.* 85:3533.
- Pitzer, K.S. 1979. Theory: Ion interaction approach, p. 157–208. *In* R.M. Pytkowicz (ed.) *Activity coefficients in electrolyte solutions*. CRC Press, Boca Raton, FL.
- Richards, L.A. 1941. A pressure-membrane extraction apparatus for soil solution. *Soil Sci.* 51:377–386.
- Ross, D.S., and R.J. Bartlett. 1990. Effects of extraction methods and sample storage on properties of solutions obtained from forested spodosols. *J. Environ. Qual.* 19:108–113.
- Sadiq, M., and W.L. Lindsay. 1979. Selection of standard free energies of formation for use in soil chemistry. Colorado State University Experiment Station Technical Bulletin No. 134. Colorado State University, Fort Collins, CO.
- Schloesing, T. 1866. Sur l'anlyse des principes solubles de la terre vegetale. *Compt. Rend. Acad. Sci.* 63:1007.
- Schwab, A.P. 1989. Manganese–phosphate solubility relationships in an acid soil. *Soil Sci. Soc. Am. J.* 53:1654–1660.
- Schwab, A.P. 1992. Chemical and physical characterization of soils. *In* L.E. Erickson, S.C. Grant, and J.P. McDonald (eds.) *Conf. Proc. Hazard. Subst. Res.* University of Colorado, Boulder, Co., p. 326–344.

- Skvortsov, V.G., R.S. Tsekhanskii, and A.M. Gavrilov. 1976. System of sodium metaborates–sodium chloride–water at 20 degrees C. *Zh. Neorg. Khim.* 21:583–585.
- Smith, G.R., K.K. Tanji, R.G. Burau, and J.J. Jurinak. 1995. C-salt, a chemical equilibrium model for multicomponent solutions. *In* R. Loeppert et al. (eds.) *Chemical equilibrium and reaction models*. Soil Science Society of America Special Publication No. 42. ASA, Madison, WI.
- Sposito, G. 1981. *The thermodynamics of soil solutions*. Oxford University Press, New York.
- Sposito, G. 1989. *The chemistry of soils*. Oxford University Press, New York.
- Sposito, G. 1994. *Chemical equilibria and kinetics in soils*. Oxford University Press, New York.
- Sposito, G. 2008. *The chemistry of soils*. 2nd edn. Oxford University Press, New York.
- Sposito, G., and J. Coves. 1988. SOILCHEM: A computer program for the calculation of chemical equilibria in soil solutions and other natural water systems. Kearney Foundation of Soil Science, University of California, Riverside, CA.
- SSSA. 2009. Glossary of soil science terms. (Available online with updates at <https://www.soils.org/sssagloss/index.php>, accessed on May 16, 2011.)
- Staudinger, J., and P.V. Roberts. 1996. A critical review of Henry's law constants for environmental applications. *Crit. Rev. Environ. Sci. Technol.* 26:205–297.
- Stevenson, F.J. 1967. Organic acids in soil, p. 119–146. *In* A.D. McLaren and G.H. Peterson (eds.) *Soil biochemistry*. Wiley, New York.
- Stumm, W., and J.J. Morgan. 1996. *Aquatic chemistry. Chemical equilibria and rates in natural waters*. Wiley Interscience, New York.
- Suarez, D.L. 1995. Carbonate chemistry in computer programs and application to soil chemistry. *In* R. Loeppert et al. (eds.) *Chemical equilibrium and reaction models*. Soil Science Society of America Special Publication No. 42. ASA, Madison, WI.
- Thompson, H.S. 1850. On the absorbent power of soils. *R. Agric. Soc. Eng. J.* 11:68–74.
- Till, A.R., and T.P. McCabe. 1976. Sulfur leaching and lysimeter characterization. *Soil Sci.* 121:44–47.
- Truesdall, A.H., and B.F. Jones. 1974. WATEQ, a computer program for calculating chemical equilibria of natural waters. *U.S. Geol. Surv.* 2:223.
- United States Salinity Laboratory Staff. 1954. *Diagnosis and improvement of saline and alkali soils*. USDA handbook no. 60. USDA, Washington, DC.
- van der Lee, J., and L. De Windt. 2001. Present state and future directions of modeling of geochemistry in hydrogeological systems. *J. Contam. Hydrol.* 47:265–282.
- van Hees, P., U. Lundstrom, R. Danielsson, and L. Nyberg. 2001. Controlling mechanisms of aluminum in soil solution—An evaluation of 180 podzolic soils. *Chemosphere* 45:1091–1101.
- Warrick, A.W., and A. Amoozegar-Fard. 1977. Soil water regimes near porous cup water samplers. *Water Resour. Res.* 13:203–207.
- Way, J.T. 1850. On the power of soils to absorb manure. *R. Agric. Soc. Eng. J.* 11:313–379.
- West et al. 1992. Microbial activity and survival in soils dried at different rates. *Aust. J. Soil Res.* 30:209–222.
- Westall, J.C., J.L. Zachary, and F.M.M. Morel. 1976. MINEQL—A computer program for the calculation of chemical equilibrium composition of aqueous systems. Technical Note No. 18. MIT, Cambridge, MA.
- Wolt, J.D. 1989. SOILSOLN: A program for teaching equilibria modeling of soil solution composition. *J. Agron. Educ.* 18:40–42.
- Wolt, J.D. 1994. *Soil solution chemistry. Applications to environmental science and agriculture*. John Wiley & Sons, New York.
- Wolt, J.D., and J.G. Graveel. 1986. A rapid routine method for obtaining soil solution using vacuum displacement. *Soil Sci. Soc. Am. J.* 50:602–605.
- Wood, W.G. 1973. A technique using porous cups for water sampling at any depth in the unsaturated zone. *Water Resour. Res.* 9:468–488.



# Kinetics and Mechanisms of Soil Chemical Reactions

13.1	Introduction .....	13-1
13.2	Timescales of Soil Chemical Processes .....	13-1
13.3	Application of Chemical Kinetics to Heterogeneous Surfaces.....	13-2
	Rate-Limiting Steps • Rate Laws • Determination of Reaction Order and Rate Constants/Coefficients	
13.4	Kinetic Models .....	13-5
	Ordered Models • Elovich Equation • Parabolic Diffusion Equation • Fractional Power or Power Function Equation • $Z(t)$ and Diffusion Models • Implications of Diffusion Models • Multiple Site Models	
13.5	Kinetics of Important Reactions on Soils and Soil Components.....	13-11
	Sorption/Desorption Reaction Rates • Kinetics of Mineral Dissolution • Redox Kinetics	
13.6	Conclusions.....	13-25
	References.....	13-25

Donald L. Sparks  
*University of Delaware*

## 13.1 Introduction

Since its inception in the mid-1850s, soil chemistry has focused on the macroscopic, equilibrium aspects of soil chemical reactions (CRs) and processes. From these studies, much was learned about important soil chemical processes, including sorption, desorption, precipitation, complexation, dissolution, and oxidation/reduction. However, such investigations do not convey information on reaction rates or reaction mechanisms. In the past three decades, as concerns and interests about soil and water quality have increased, soil and environmental chemists, environmental and chemical engineers, and geochemists have increasingly realized that reactions in subsurface environments are time dependent. Thus, to accurately predict the fate, mobility, speciation, and bioavailability of environmentally important plant nutrients, trace elements, radionuclides, and organic chemicals in soils, one must understand the kinetics and mechanisms of the reactions.

While major progress has been made in better understanding the kinetics of soil chemical processes, much uncertainty remains. In part, this is due to the complex, heterogeneous nature of natural materials such as soils. However, with the development of kinetic techniques that can be used to measure a wide range of timescales, time-dependent models that can describe both CR and mass transfer processes, and the employment of state-of-the-art in situ spectroscopic and microscopic surface techniques in combination with rate studies, major advances are being made in understanding the kinetics and mechanisms of

soil CRs. Arguably, this will be a major leitmotif in soil chemistry research for decades to come.

In this review, the application of chemical kinetics to heterogeneous systems, such as soils and soil components (clay minerals, organic matter, metal hydr(oxides), and humic substances), with emphasis on sorption/release processes will be discussed. A critical review of kinetic models that can be used to describe reaction rates on heterogeneous surfaces will be covered. The review will also present discussions on the rates of important soil CRs and processes including inorganic and organic sorption/desorption, dissolution, and redox. For additional details on these topics and other aspects of kinetics of soil chemical and geochemical processes, the reader should consult a number of recent books and monographs (Sparks, 1989, 1995, 2002, 2005; Sparks and Suarez, 1991; Stumm, 1992; Schwarzenbach et al., 1993; Sposito, 1994; Grossl et al., 1997; Matocha et al., 2005; Borda and Sparks, 2008).

## 13.2 Timescales of Soil Chemical Processes

A variety of CRs occur in soils and often in combination with one another. Reaction timescales can vary from microseconds to milliseconds for many ion association and some ion exchange, sorption, and redox reactions to years for many mineral solution and mineral crystallization phenomena and for some sorption/release reactions (Figure 13.1). Ion association reactions include ion pairing, inner- and outer-sphere complexation,

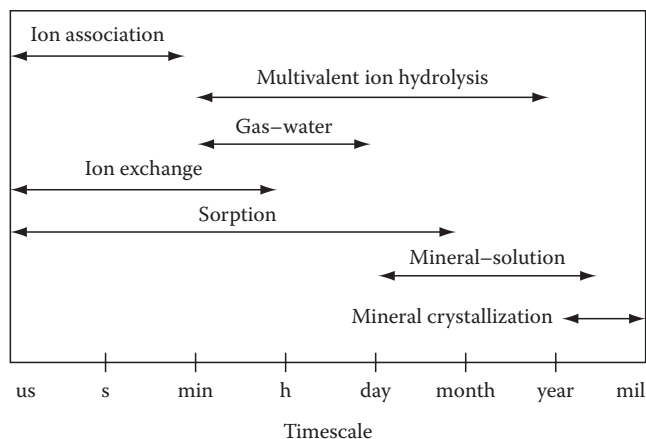


**FIGURE 13.1** Time ranges required to attain equilibrium by different types of reactions in soil environments. (Reprinted with permission from Amacher, M.C. 1991. *Methods of obtaining and analyzing kinetic data*, p. 19–59. In D.L. Sparks and D.L. Suarez (eds.) *Rates of soil chemical processes*. SSSA, Madison, WI.)

and chelation in solution. Gas–water reactions involve gaseous exchange across the air–liquid interface. Ion exchange reactions occur when cations and anions are adsorbed (outer-sphere complexation) and desorbed from soil surfaces by electrostatic attractive forces. Ion exchange reactions are reversible and stoichiometric. Sorption reactions can involve adsorption processes, including partitioning, outer-sphere and inner-sphere complexation, and multinuclear complexation (e.g., surface precipitation). Mineral–solution reactions include precipitation/dissolution of minerals and coprecipitation reactions in which small constituents become a part of mineral structures (Sparks, 1989; Amacher, 1991).

The type of soil component can drastically affect the reaction rate. For example, sorption reactions are often more rapid on clay minerals, such as kaolinite and smectites, than on vermiculitic and micaceous minerals. This is in large part due to the availability of sites for sorption. For example, kaolinite has readily available planar external sites, and smectites have primarily internal sites that are also quite available for retention of sorbates. Thus, sorption reactions on these soil constituents are often quite rapid, even occurring on timescales of seconds and milliseconds (Sparks, 1989, 2005).

On the other hand, vermiculite and micas have multiple sites for retention of metals and organics, including planar, edge, and interlayer sites, with some of the latter sites being partially to totally collapsed. Consequently, sorption and desorption reactions on these sites can be slow, tortuous, and mass transfer controlled. Often, an apparent equilibrium may not be reached even after several days or weeks. Thus, with vermiculite and mica, sorption can involve two to three different reaction rates: high rates on external sites, intermediate rates on edge sites, and low rates on interlayer sites (Jardine and Sparks, 1984; Comans and Hockley, 1992).

Metal sorption reactions on oxides, hydroxides, and humic substances depend on the type of surface and metal being

studied, but the CR rate appears to be rapid. For example, CR rates of metals and oxyanions on goethite occurred on millisecond timescales (Zhang and Sparks, 1989, 1990a, 1990b; Grossl et al., 1994, 1997). Reaction rates of redox processes can also be very rapid. For example, Parikh et al. (2008) found that 50% of the initial reaction process for As(III) oxidation on Mn oxides occurred in 1 min. Half-times for divalent Pb, Cu, and Zn sorption on peat ranged from 5 to 15 s (Bunzl et al., 1976). A number of studies have shown that heavy metal sorption on oxides (Bruemmer et al., 1988; Ainsworth et al., 1994; Scheidegger and Sparks, 1996a; Scheidegger et al., 1998) and clay minerals (Lövgrén et al., 1990) increases with longer residence times. The mechanism for these lower reaction rates is not well understood but has been ascribed to diffusion phenomena, sites of lower reactivity, and surface nucleation/precipitation (Scheidegger and Sparks, 1996b; Sparks, 1998, 1999a, 1999b). Recent findings on slow metal retention rates and mechanisms at the mineral/water interface will be discussed later.

Sorption/desorption of metals and organic chemicals on soils is often very slow, which has been attributed to diffusion into micropores of inorganic minerals and into humic substances, retention on sites of varying reactivity, and surface nucleation/precipitation (Sparks 1989, 1999a, 1999b, 2002, 2005; Scheidegger and Sparks, 1996b; Matocha et al., 2005; Borda and Sparks, 2008). These reactions will be discussed in more detail later.

### 13.3 Application of Chemical Kinetics to Heterogeneous Surfaces

The study of chemical kinetics, even in homogeneous systems, is complex and often arduous. When one attempts to study the kinetics of reactions in heterogeneous systems such as soils, sediments, and even soil components, such as clay minerals, hydrous oxides, and humic substances, the difficulties are greatly magnified. This is largely due to the complexity of soils that are made up of a mixture of inorganic and organic components. These components often interact with each other and display different types of sites with various reactivities for inorganic and organic sorptives. Moreover, the variety of particle sizes and porosities in soils and sediments further adds to their heterogeneity. In most cases, both chemical kinetics and multiple transport processes are occurring simultaneously. Thus, the determination of chemical kinetics, which can be defined as the investigation of rates of CRs and of the molecular processes by which reactions occur where transport is not limiting (Gardiner, 1969), is extremely difficult, if not impossible, in heterogeneous systems. In these systems, one is studying kinetics, which is a generic term referring to time-dependent or nonequilibrium processes. Thus, apparent and nonmechanistic rate laws and rate parameters are determined (Skopp, 1986; Sparks, 1989).

#### 13.3.1 Rate-Limiting Steps

Both transport and CR processes can affect the reaction rates in the subsurface environment. Transport processes include



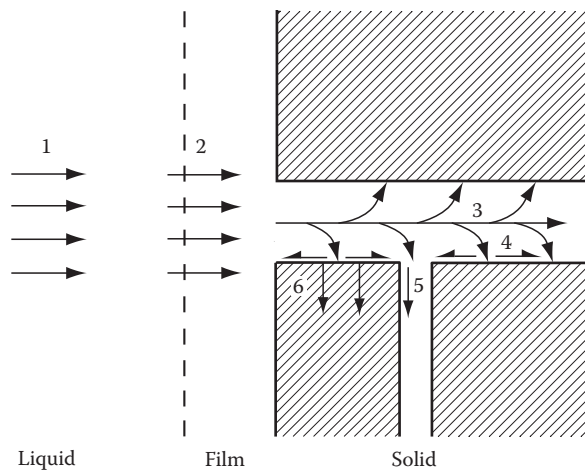
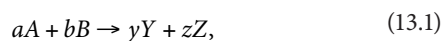


**FIGURE 13.2** Transport processes in solid-liquid soil reactions—nonactivated processes: (1) transport in the soil solution, (2) transport across a liquid film at the solid-liquid interface, (3) transport in a liquid-filled macropore—activated processes, (4) diffusion of a sorbate at the surface of the solid, (5) diffusion of a sorbate occluded in a micropore, (6) diffusion in the bulk of the solid. (Reprinted from Aharoni, C., and D.L. Sparks. 1991. Kinetics of soil chemical reactions: A theoretical treatment, p. 1–18. *In* D.L. Sparks and D.L. Suarez (eds.) Rates of soil chemical processes. SSSA, Madison, WI.)

(Aharoni and Sparks, 1991) the following: (1) transport in the solution phase; (2) transport across a liquid film at the particle/liquid interface (film diffusion [FD]); (3) transport in liquid-filled macropores (>2 nm), all of which are nonactivated diffusion processes and occur in mobile regions; (4) particle diffusion (PD) processes, which include diffusion of sorbate occluded in micropores (<2 nm, pore diffusion) and along pore wall surfaces (surface diffusion); and (5) diffusion processes in the bulk of the solid, all of which are activated diffusion processes (Figure 13.2). Pore and surface diffusion within the immediate region can be referred to as interaggregate (interparticle) diffusion while that in the solid is intraaggregate diffusion. The actual CR at the surface, for example, adsorption, is usually instantaneous. The slowest of the CR and transport processes is rate limiting.

### 13.3.2 Rate Laws

There are two important reasons for investigating the rates of soil chemical processes (Sparks, 1989, 1995, 1998, 1999a, 1999b, 2002) (1) to determine how rapidly reactions attain equilibrium and (2) to infer information on reaction mechanisms. One of the most important aspects of chemical kinetics is the establishment of a rate equation or law. By definition, a rate law is a differential equation. For the following reaction (Bunnett, 1986; Sparks, 1989, 1995, 1998, 1999a, 1999b, 2002),



the rate is proportional to some power of the concentrations of reactants *A* and *B* and/or other species (*C*, *D*, etc.) in the

system, and *a*, *b*, *y*, and *z* are stoichiometric coefficients and are assumed to be equal to 1 in the discussion that follows on rate laws. The power to which the concentration is raised may equal 0 (i.e., the rate is independent of that concentration), even for reactant *A* or *B*. Rates are expressed as a decrease in reactant concentration or an increase in product concentration per unit time. Thus, the rate of conversion of reactant *A* above, which has a concentration [*A*] at any time *t*, is  $(-d[A]/(dt))$  while the rate with regard to product *Y* having a concentration [*Y*] at time *t* is  $(d[Y]/(dt))$ .

The rate expression for Equation 13.1 is therefore as follows:

$$\frac{d[Y]}{dt} = -\frac{d[A]}{dt} = [A]^\alpha [B]^\beta, \quad (13.2)$$

where

*k* is the rate constant

$\alpha$  and  $\beta$  are the orders of the reaction with respect to reactants *A* and *B*, respectively, and can be referred to as a partial orders for the total reaction

These orders are experimentally determined and not necessarily integral numbers. The sum of all the partial orders ( $\alpha$  and  $\beta$ ) is the overall order (*n*) of the total reaction and may be expressed as follows:

$$n = \alpha + \beta + \dots \quad (13.3)$$

Once the values of  $\alpha$ ,  $\beta$ , etc., are determined experimentally, the rate law is defined. Reaction order provides only information about the manner in which rate depends on concentration. Order does not mean the same as molecularity, which concerns the number of reactant particles (atoms, molecules, free radicals, or ions) entering into an elementary reaction. One can define an elementary reaction as one in which no reaction intermediates have been detected or need to be postulated to describe the CR on a molecular scale. An elementary reaction is assumed to occur in a single step and to pass through a single transition state (Bunnett, 1986).

To demonstrate that a reaction is elementary, one can use experimental conditions that are different from those employed in determining the reaction rate law. For example, if one conducted kinetic studies using a flow technique with set steady-state flow rates, one could see if reaction rate and rate constants changed with flow rate. If they did, one would not be determining mechanistic rate laws (see definition below).

Rate laws serve three purposes: (1) they assist one in predicting the reaction rate, (2) mechanisms can be proposed, and (3) reaction orders can be ascertained. There are four types of rate laws that can be determined for soil chemical processes (Skopp, 1986): mechanistic, apparent, transport with apparent, and transport with mechanistic. Mechanistic rate laws assume that only chemical kinetics are operational and transport phenomena are not occurring. Consequently, it is difficult to determine mechanistic rate laws for most soil chemical systems due

to the heterogeneity of the system caused by different particle sizes, porosities, and types of retention sites. There is evidence that with some kinetic studies, using chemical relaxation techniques (Sparks, 1989; Sparks and Zhang, 1991), that mechanistic rate laws are determined or closely approximated since the agreement between equilibrium constants calculated from both kinetic and equilibrium studies are comparable (Hachiya et al., 1984; Tang and Sparks, 1993). Recent studies using molecular scale in situ spectroscopic methods such as attenuated total reflectance Fourier transform infrared (ATR-FTIR) and quick x-ray absorption spectroscopy (QXAS; Parikh et al., 2008; Ginder-Vogel et al., 2009; Landrot et al., 2010) to measure rapid initial reaction rates also show that chemical kinetics are being measured, and, thus, mechanistic rate laws can be proposed.

Since natural materials are heterogeneous and transport processes often affect the reaction rate, apparent rate laws are usually determined for such systems. Apparent rate laws include both chemical kinetics and transport-controlled processes. Thus, soil structure, stirring, mixing, and flow rate all would affect the kinetics. Transport with apparent rate laws emphasizes transport-limited phenomena. One often assumes first-order or zero-order reactions (see the following discussion on reaction order). In determining transport with mechanistic rate laws, one attempts to describe simultaneously transport-controlled and chemical kinetics phenomena. One is thus trying to explain accurately both the chemistry and physics of the system.

### 13.3.3 Determination of Reaction Order and Rate Constants/Coefficients

There are three basic ways to determine rate laws and rate constants/coefficients (Bunnett, 1986; Skopp, 1986; Sparks, 1989, 1995, 1998, 1999a, 1999b, 2002): (1) initial rates, (2) directly using integrated equations and graphing the data, and (3) using nonlinear least-squares analysis.

Let us assume the following elementary reaction between species  $A$ ,  $B$ , and  $Y$ :



A forward reaction rate law can be written as

$$\frac{d[A]}{dt} = -k_1[A][B], \quad (13.5)$$

where

$k_1$  is the forward rate constant

$\alpha$  and  $\beta$  (see Equation 13.2) are each assumed to be 1

The reverse reaction rate law for Equation 13.4 is

$$\frac{d[A]}{dt} = +k_{-1}[Y], \quad (13.6)$$

where  $k_{-1}$  is the reverse rate constant.

Equations 13.5 and 13.6 are only applicable far from equilibrium where back or reverse reactions are insignificant. If both forward and reverse reactions are occurring, Equations 13.5 and 13.6 must be combined such that

$$\frac{d[A]}{dt} = -k_1[A][B] + k_{-1}[Y]. \quad (13.7)$$

Equation 13.7 applies the principle that the net reaction rate is the difference between the sum of all reverse reaction rates and the sum of all forward reaction rates.

One way to ensure that back reactions are not important is to measure initial rates. The initial rate is the limit of the reaction rate as time reaches zero. With an initial rate method, one plots the concentration of a reactant or product over a short reaction time period during which the concentrations of the reactants change so little that the instantaneous rate is hardly affected. Thus, by measuring initial rates, one could assume that only the forward reaction in Equation 13.4 predominates. This would simplify the rate law to that given in Equation 13.5, which, as written, would be a second-order reaction, first order in reactant  $A$  and first order in reactant  $B$ . Equation 13.5, under these conditions, would represent a second-order irreversible elementary reaction. To measure initial rates, one must have available a technique that can measure rapid reactions, such as a chemical relaxation method or a rapid molecular scale spectroscopic technique and an accurate analytical detection system to determine product concentrations. Recently, Parikh et al. (2008) used a novel real-time ATR-FTIR spectroscopic technique to measure the initial rates of As(III) oxidation on Mn oxides. Using a rapid scan technique, IR spectra were collected with a time resolution of up to 2.55 s. Ginder-Vogel et al. (2009) and Landrot et al. (2010) have employed state-of-the-art QXAS to investigate initial rates of As(III) oxidation on hydrous Mn oxide and Cr(III) oxidation on hydrous Mn oxide, respectively. In the study of Ginder-Vogel et al. (2009), QXAS scans were collected every 0.98 s, while scans were collected every 0.75 s in the study of Landrot et al. (2010).

Integrated rate equations can also be used to determine rate constants/coefficients. If one assumes that reactant  $B$  in Equation 13.5 is in large excess of reactant  $A$ , which is an example of the method of isolation to analyze kinetic data, and  $Y_0 = 0$ , where  $Y_0$  is the initial concentration of product  $Y$ , Equation 13.5 can be simplified to

$$\frac{d[A]}{dt} = -k'_1[A], \quad (13.8)$$

where  $k'_1 = k_1[B]$ .

The first-order dependence of  $[A]$  can be evaluated using the integrated form of Equation 13.8 using the initial conditions at  $t = 0$ ,  $A = A_0$ :

$$\log[A]_t = \log[A]_0 - \frac{k'_1 t}{2.303}. \quad (13.9)$$

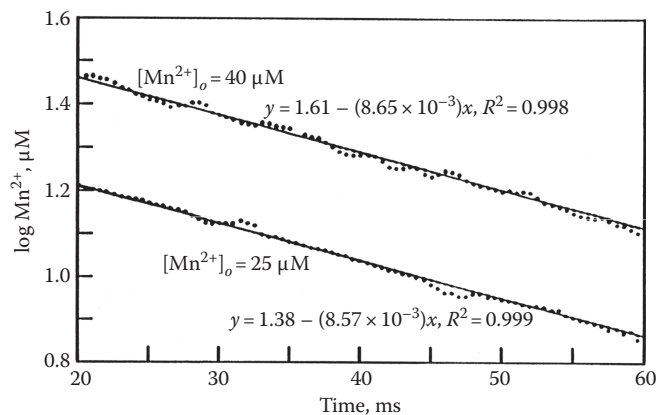


**FIGURE 13.3** Initial reaction rates depicting the first-order dependence of  $\text{Mn}^{2+}$  sorption as a function of time for initial  $\text{Mn}^{2+}$  concentrations ( $[\text{Mn}^{2+}]_o$ ) 25 and  $40\ \mu\text{M}$ . (Reprinted from Fendorf, S.E. et al. 1993. *Soil Sci. Soc. Am. J.*, 57:57–62. With permission of the Soil Science Society of America.)

The half-time ( $t_{1/2}$ ) for the above reaction is equal to  $0.693/k$  and is the time required for half of reactant  $A$  to be consumed.

If a reaction is first order, a plot of  $\log [A]_t$  versus  $t$  should result in a straight line with a slope  $= k_1/2.303$  and an intercept of  $\log [A]_o$ . An example of first-order plots for  $\text{Mn}^{2+}$  sorption on  $\delta\text{-MnO}_2$  at two initial  $\text{Mn}^{2+}$  concentrations,  $[\text{Mn}^{2+}]_o$  (25 and  $40\ \mu\text{M}$ ), is shown in Figure 13.3. One sees that the plots are linear at both concentrations, which would indicate that the sorption process is first order. The  $[\text{Mn}^{2+}]_o$  values obtained from the intercepts in Figure 13.3 were 24 and  $41\ \mu\text{M}$ , which are in good agreement with the two  $[\text{Mn}^{2+}]_o$  values, and the rate constants were  $3.73 \times 10^{-3}$  and  $3.75 \times 10^{-3}\ \text{s}^{-1}$ , respectively. The fact that the rate constants do not significantly change with concentration is a good indication that the reaction in Equation 13.8 is first order under the imposed experimental conditions.

It is dangerous to conclude that a particular reaction order is correct, based simply on the conformity of data to an integrated equation. As illustrated above, multiple initial concentrations that vary considerably should be employed to see if the rate is independent of concentration. One should also test multiple integrated equations. It may also be useful to show that reaction rate is not affected by a species whose concentration does not change considerably during an experiment, such as substances not consumed or present in large excess (Bunnett, 1986; Sparks, 1989, 1991, 1995, 1998, 1999a, 1999b).

Least-squares analysis can also be used to determine rate constants/coefficients. With this method, one fits the best straight line to a set of points that are linearly related as  $y = mx + b$ , where  $y$  is the ordinate and  $x$  is the abscissa datum point, respectively. The slope ( $m$ ) and the intercept ( $b$ ) can be calculated by least-squares analysis.

When kinetic data are plotted, curvature may be observed due to an incorrect assumption of reaction order. If first-order kinetics is assumed and the reaction is really second order, downward curvature results. If second-order kinetics

is assumed but the reaction is first order, upward curvature is observed. Curvature can also be due to fractional, third, higher, or mixed reaction order. Nonattainment of equilibrium often results in downward curvature. Temperature changes during the study can also cause curvature; thus, it is important that temperature be accurately controlled during a kinetic experiment.

## 13.4 Kinetic Models

### 13.4.1 Ordered Models

First-order kinetic models often describe reactions at the soil mineral/water interface. Both single first-order and multiple first-order reactions have been described by many investigators (Sparks, 1989, 1991, 2002; Sparks et al., 1993).

It is not uncommon to observe biphasic kinetics, namely, a rapid reaction rate followed by a much slower reaction rate. Such data can often be described by two first-order reactions. Some investigators have interpreted such biphasic kinetics to suggest reactions on two types of sites, such as external, readily accessible sites (Slope 1) and internal, difficult to access sites (Slope 2) (Jardine and Sparks, 1984; Comans and Hockley, 1992) or molecular sites of differing reactivity such as high-reactivity inner-sphere complex sites and low-reactivity outer-sphere complex sites (Grossl et al., 1994, 1997).

However, it is unsound to conclude anything about mechanisms based solely on multiple rate constants that are calculated from multiple slopes of kinetic plots. There are other ways to definitively ascertain reaction mechanisms, such as calculating energies of activation, elucidating rate-limiting steps through stopped flow and interruption approaches, using independent or direct methods to determine mechanisms such as spectroscopic and microscopic techniques, and employing blocking agents that are specific for certain reaction sites. An example of the latter approach is found in the research of Jardine and Sparks (1984) who studied  $\text{K-Ca}$  exchange on a Delaware soil at three temperatures and observed two apparent simultaneous first-order reactions at 283 and 298 K (Figure 13.4). They hypothesized that the first, more rapid reaction was predominantly due to adsorption on external planar sites of the organic matter and kaolinite in the soil. The slower reaction was ascribed to vermiculitic clay sites that promoted slow pore and surface diffusion. These hypotheses were seemingly validated using a large organic polymer, cetyltrimethylammonium bromide (CTAB), which because of its size is sterically hindered from internal sites. Thus, CTAB should only block external planar sites. When CTAB was applied to the soil, the first slope was eliminated, while the second slope was still present, suggesting multireactive sites.

While first-order models have been used widely to describe the kinetics of CRs on natural materials, a number of other simple kinetic models have also been employed. These include various ordered equations such as zero, second, and fractional order;

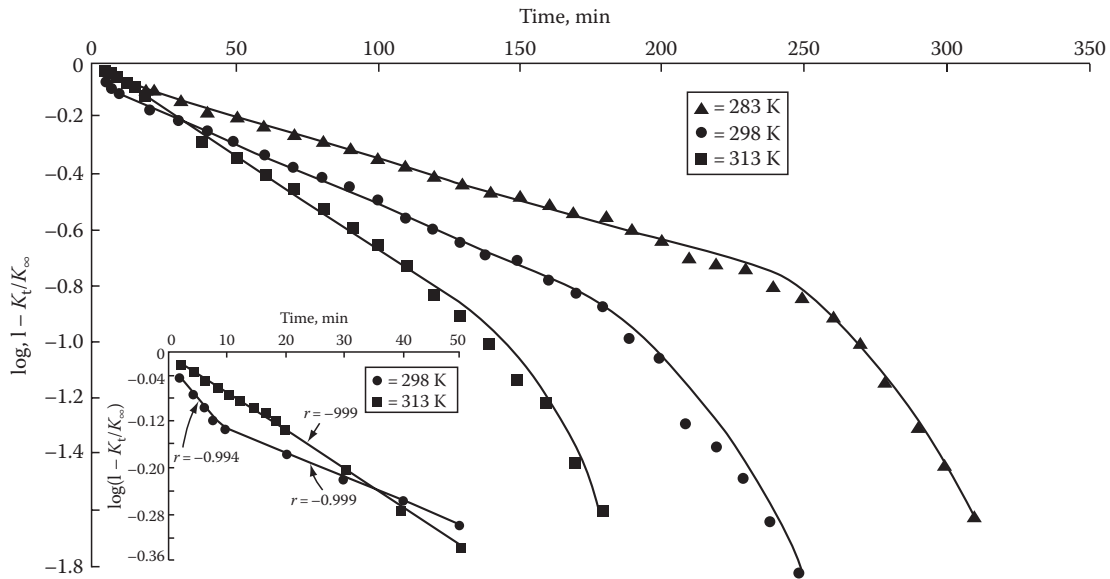


**FIGURE 13.4** First-order kinetics for potassium adsorption at three temperatures on Evesboro soil with inset showing the initial 50 min of the first-order plots at 298 and 313 K. (Reprinted from Jardine, P.M., and D.L. Sparks. 1984. Potassium-calcium exchange in a multireactive soil system. I. Kinetics. Soil Sci. Soc. Am. J. 48:39–45. With permission of the Soil Science Society of America.)

**TABLE 13.1** Linear Forms of Kinetic Equations Commonly Used in Environmental Soil Chemistry

Zero order <sup>a</sup>
$[A]_t = [A]_0 - k'_t t$
First order
$\log[A]_t = \log[A]_0 - \frac{k'_t t}{2.303}$
Second order <sup>b</sup>
$\frac{1}{[A]_t} = \frac{1}{[A]_0} + kt$
Elovich
$q = \left(\frac{1}{\beta}\right) \ln(\alpha\beta) + \left(\frac{1}{\beta}\right) \ln t$
Parabolic diffusion
$\left(\frac{1}{t}\right) \left(\frac{Q_t}{Q_\infty}\right) = \frac{4}{\pi^{1/2}} \left(\frac{D}{r^2}\right)^{1/2} \frac{1}{t^{1/2}} - \frac{D}{r^2}$
Power function
$\ln q_t = \ln k + v \ln t$

Source: Sparks, D.L., *Environmental Soil Chemistry*, Academic Press, San Diego, CA, 1995.

Terms in equations are defined in the text of the chapter.

<sup>a</sup> Describing the reaction  $A \rightarrow Y$ .

<sup>b</sup>  $\ln x = 2.303 \log x$  is the conversion from natural logarithms (ln) to base 10 logarithms (log).

Elovich; power function or fractional power; and parabolic diffusion models. A brief discussion of some of these will be given; the final forms of the equations are given in Table 13.1. For more complete details and applications of these models, one may consult Sparks (1989, 1995, 1998, 1999a, 1999b, 2002).

### 13.4.2 Elovich Equation

The Elovich equation was originally developed to describe the kinetics of heterogeneous chemisorption of gases on solid surfaces (Low, 1960). It seems to describe a number of reaction mechanisms including bulk and surface diffusion and activation and deactivation of catalytic surfaces.

In soil chemistry, the Elovich equation has been used to describe the kinetics of sorption and desorption of various inorganic materials on soils (Sparks, 1989, 1995, 1998, 1999a, 1999b, 2002). It can be expressed as (Chien and Clayton, 1980)

$$q = \left(\frac{1}{\beta}\right) \ln(\alpha\beta) + \left(\frac{1}{\beta}\right) \ln t, \quad (13.10)$$

where

$q$  is the amount of sorbate per unit mass of sorbent at time  $t$   
 $\alpha$  and  $\beta$  are constants during any one experiment

A plot of  $q$  versus  $\ln t$  should give a linear relationship if the Elovich equation is applicable with a slope of  $(1/\beta)$  and an intercept of  $(1/\beta)\ln(\alpha\beta)$ . An application of Equation 13.10 to P sorption on soils is shown in Figure 13.5.

Some investigators have used the  $\alpha$  and  $\beta$  parameters from the Elovich equation to estimate reaction rates. For example, it has been suggested that a decrease in  $\beta$  and/or an increase in  $\alpha$  would increase reaction rate. However, this is questionable. The slope of plots using Equation 13.10 changes with the concentration of the sorptive and with the solution-to-soil ratio (Sharpley, 1983). Therefore, the slopes are not always characteristic of the soil but may depend on various experimental conditions.

Some researchers also have suggested that breaks or multiple linear segments in Elovich plots could indicate a changeover

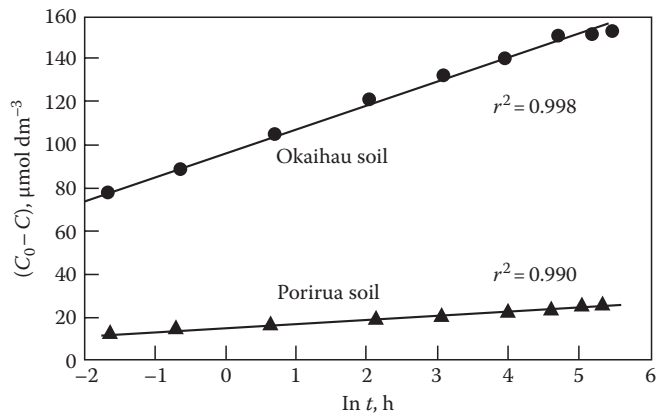


**FIGURE 13.5** Plot of Elovich equation for phosphate sorption on two soils where  $C_0$  is the initial phosphorus concentration in the soil solution at time  $t$ . The quantity  $(C_0 - C)$  can be equated to  $q$ , the amount sorbed at time  $t$ . (Reprinted from Chien, S.H., and W.R. Clayton. 1980. Application of Elovich equation to the kinetics of phosphate release and sorption in soils. *Soil Sci. Soc. Am. J.* 44:265–268. With permission from the Soil Science Society of America.)

from one type of binding site to another (Atkinson et al., 1970). However, such mechanistic suggestions may not be correct (Sparks, 1989, 1995).

### 13.4.3 Parabolic Diffusion Equation

The parabolic diffusion equation is often used to suggest that diffusion-controlled phenomena are rate limiting. It was originally derived from radial diffusion in a cylinder where the ion concentration on the surface is constant, and initially, the ion concentration within the cylinder is uniform. It is also assumed that ion diffusion through the upper and lower faces of the cylinder is negligible. Following Crank (1976), the parabolic diffusion equation as applied to soils can be expressed as

$$\left(\frac{Q_t}{Q_\infty}\right) = \frac{4}{\pi^{1/2}} \frac{Dt^{1/2}}{r^2} - \frac{Dt}{r^2} - \frac{1}{3\pi^{1/2}} \frac{Dt^{3/2}}{r^2}, \quad (13.11)$$

where

$r$  is the radius of the cylinder

$Q_t$  is the quantity of diffusing substance that has left the cylinder at time  $t$

$Q_\infty$  is the corresponding quantity after infinite time

$D$  is an apparent diffusion coefficient

For the relatively short times in most experiments, the third and subsequent terms may be ignored and thus

$$\frac{Q_t}{Q_\infty} = \frac{4}{\pi^{1/2}} \frac{Dt^{1/2}}{r^2} - \frac{Dt}{r^2} \quad (13.12)$$

or

$$\frac{1^c Q_t^m}{t Q_\infty} = \frac{4}{\pi^{1/2}} \frac{Dt^{1/2}}{r^2} \frac{1}{t^{1/2}} - \frac{Dt}{r^2},$$

and thus, a plot of  $Q_t/Q_\infty/t$  versus  $1/t^{1/2}$  should give a straight line with a slope of

$$\frac{4}{\pi^{1/2}} \left(\frac{D}{r^2}\right)^{1/2}$$

and intercept of  $-D/r^2$ . Thus, if  $r$  is known,  $D$  may be calculated from both the slope and intercept.

The parabolic diffusion equation has successfully described metal reactions on soils and soil constituents (Chute and Quirk, 1967; Jardine and Sparks, 1984; Krishnamurti and Huang, 1992; Krishnamurti et al., 1997), feldspar weathering (Wollast, 1967), and pesticide reactions (Weber and Gould, 1966).

### 13.4.4 Fractional Power or Power Function Equation

This equation can be expressed as

$$q = kt^v, \quad (13.13)$$

where

$q$  is amount of sorbate per unit mass of sorbent at time  $t$

$k$  and  $v$  are constants

$v$  is positive and  $<1$

Equation 13.13 is empirical, except for the case where  $v = 0.5$ , when it is similar to the parabolic diffusion equation.

Equation 13.13 and various modified forms have been used by a number of researchers to describe the kinetics of reactions in natural materials (Kuo and Lotse, 1974; Havlin and Westfall, 1985).

### 13.4.5 $Z(t)$ and Diffusion Models

In a number of studies, several simple kinetic models have described rate data well, based on correlation coefficients and standard errors of the estimate (Chien and Clayton, 1980; Onken and Matheson, 1982; Sparks and Jardine, 1984; Allen et al., 1995). Despite this, there is often an inconsistent relation between the equation that gives the best fit and the physico-chemical and mineralogical properties of the sorbent(s) being studied. Another problem with some of the kinetic models is that they are empirical and no meaningful rate parameters can be obtained.

Aharoni and Ungarish (1976) and Aharoni (1984) noted that some simple kinetic models are approximations of more general expressions within certain limited time ranges. They suggested a generalized empirical equation by examining the applicability of power function, Elovich, and first-order equations to experimental data. By writing these as the explicit functions of the reciprocal of the rate ( $Z$ ), which is  $(dq/dt)^{-1}$ , one can show that a plot of  $Z$  versus  $t$  should be convex if the power function equation is operational (1 in Figure 13.6); linear if the Elovich

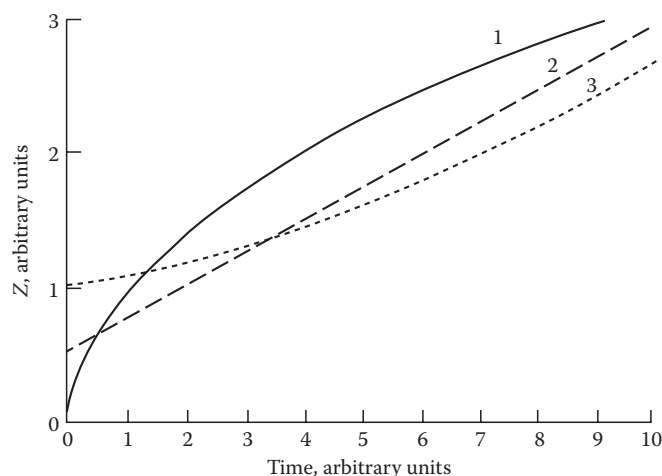


**FIGURE 13.6** Plot of  $Z$  versus time implied by (1) power function model, (2) Elovich model, and (3) first-order model. The equations for the models were differentiated and expressed as explicit functions of the reciprocal of the rate,  $Z$ . (Reprinted with permission from Aharoni, C., and D.L. Sparks. 1991. Kinetics of soil chemical reactions: A theoretical treatment, p. 1–18. In D.L. Sparks and D.L. Suarez (eds.) Rates of soil chemical processes. SSSA, Madison, WI.)

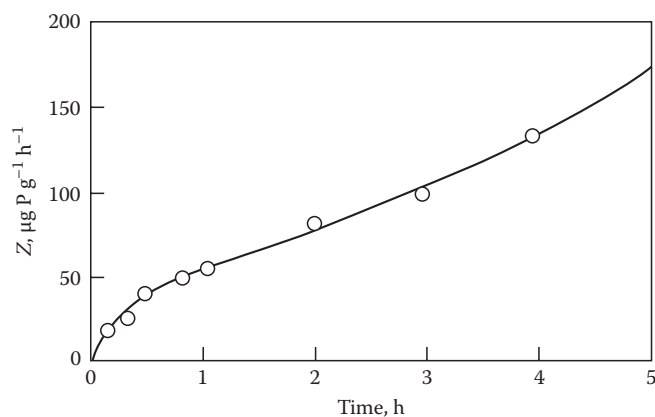


**FIGURE 13.7** Sorption of phosphate by a Typical Dystrachrept soil plotted as  $Z$  versus time. The circles represent the experimental data of Polyzopoulos et al. (1986). The solid line is a curve calculated according to a homogeneous diffusion model. (Reprinted with permission from Aharoni, C., and D.L. Sparks. 1991. Kinetics of soil chemical reactions: A theoretical treatment, p. 1–18. In D.L. Sparks and D.L. Suarez (eds.) Rates of soil chemical processes. SSSA, Madison, WI.)

equation is appropriate (2 in Figure 13.6); and concave if the first-order equation is appropriate (3 in Figure 13.6). However, such plots for soil systems (Figure 13.7) are usually S-shaped, convex at small, concave at large, and linear at some intermediate  $t$  value suggesting that the reaction rate can best be described by the power function, first order and Elovich equations in these ranges of  $t$ , respectively. Thus, the S-shaped curve indicates that the above equations may be applicable, each over some limited time range.

One of the reasons a particular kinetic model appears to be applicable may be that the study is conducted during the time range when the model is most appropriate. While sorption, for example, decreases over many orders of magnitude before equilibrium is approached, with most methods and experiments, only a portion of the entire reaction is measured, and over this time range, the assumptions associated with a simple kinetic model (power function, Elovich, and first order) are valid. Aharoni and Suzin (1982a, 1982b) showed that the S-shaped curves could be well described using homogeneous and heterogeneous diffusion models. In homogeneous diffusion situations, the final and initial portions of the S-shaped curves (conforming to the power function and first-order equations, respectively) predominated, whereas in instances where the heterogeneous diffusion model was operational, the linear portion of the S-shaped curve that conformed to the Elovich equation predominated. Derivations of homogeneous and heterogeneous diffusion models can be found in Aharoni and Sparks (1991).

#### 13.4.6 Implications of Diffusion Models

The finding that slower reactions at the soil mineral/liquid interface can be described by diffusional models indicates that the kinetics of chemical processes cannot be considered separately from physically limited transport phenomena. Thus, such a combination of processes cannot be treated using first- or other-order chemical kinetic equations. When one states that a reaction between the molecular species  $A$  and  $B$  is first order with respect to  $A$ , one assumes that the molecules of  $A$  have equal chances of participating in the reaction, and therefore, the rate is proportional to the concentration ( $C_A$ ). This reasoning can be extended to a reaction between a sorbing surface and a sorptive. In this case,  $C_A$  refers to the number of reactive sites per unit area, which corresponds to the number of unoccupied sites per unit area ( $1 - \theta_A$ ). However, by using first-order kinetics (or other order kinetics), one tacitly assumes that all the surface sites are potential reactants at any time and have an opportunity of participating in the sorption process. If one assumes that there are sites that cannot be reached directly from the fluid phase, but can be reached after the sorbate has undergone sorption and desorption at other sites, one cannot separate chemical kinetics from diffusion-limited kinetics. The overall kinetic process obeys a diffusion equation since diffusion is the rate-limiting process. However, the diffusion coefficient, which reflects the rate at which the sorbate jumps from one site to another, is determined by the rate of the CRs by which the sorbent–sorbate bonds are created and destroyed. Additionally, the activation energy for diffusion is equivalent to the activation energy of the CR.

#### 13.4.7 Multiple Site Models

Based on the previous discussion, it is evident that simple chemical kinetic models such as ordered reaction, power function, and Elovich models may not be appropriate to describe

reactions in heterogeneous systems such as soils, sediments, and soil components. In these systems where there is a range of particle sizes and multiple retention sites, both chemical kinetics and transport phenomena are occurring simultaneously, and a fast reaction is often followed by a slower reaction(s). In such systems, nonequilibrium models that describe both chemical and physical nonequilibrium and that consider multiple components and sites are more appropriate. Physical nonequilibrium is ascribed to some rate-limiting transport mechanism such as FD or PD, while chemical nonequilibrium is due to a rate-limiting mechanism at the particle surface (CR). Nonequilibrium models include two-site, multiple site, radial diffusion (pore diffusion), surface diffusion, and multiprocess models (Table 13.2). Emphasis here will be placed on the use of these models to describe sorption phenomena.

The term sites can have a number of meanings (Brusseau and Rao, 1989): (1) specific, molecular scale reaction sites; (2) sites of differing degrees of accessibility (external and internal);

(3) sites of differing sorbent type (organic matter and inorganic mineral surfaces); and (4) sites with different sorption mechanisms. With chemical nonequilibrium sorption processes, the sorbate may undergo two or more types of sorption reactions, one of which is rate limiting. For example, a metal cation may sorb to organic matter by one mechanism and to mineral surfaces by another mechanism, with one of the mechanisms being time dependent.

### 13.4.7.1 Chemical Nonequilibrium Models

Chemical nonequilibrium models describe time-dependent reactions at sorbent surfaces. The one-site model is a first-order approach that assumes that the reaction rate is limited by only one process or mechanism on a single class of sorbing sites and that all sites are of the time-dependent type. In many cases, this model appears to describe soil CRs quite well. However, often it does not. This model would seem not appropriate for most heterogeneous systems since multiple sorption sites exist.

**TABLE 13.2** Comparison of Sorption Kinetic Models

Conceptual Model	Fitting Parameters	Model Limitations
One-site model $k_d$ $S \rightarrow C$	$k_d$	Cannot describe biphasic sorption/desorption
Two-site model $K_p D_{\text{eff}}$ $S' \rightarrow C'_s \rightarrow C$	$k_d, K_p, X_1$	May not describe the "bleeding" or slow, reversible, nonequilibrium desorption for residual sorbed compounds (Karickhoff, 1980)
Radial diffusion penetration retardation (pore diffusion) model (Wu and Gschwend, 1986) $K_p D_{\text{eff}}$ $S' \leftrightarrow C' \rightarrow C$	$D_{\text{eff}} = f(n,t)D_m n / (1-n)\rho_s K_p$	Cannot describe instantaneous uptake without additional correction factor; did not describe kinetic data for times greater than $10^3$ min (Wu and Gschwend, 1986)
Dual-resistance surface diffusion model (Miller and Pedit, 1992) $D_s k_b$ $S' \rightarrow C'_s \rightarrow C$	$D_s k_b$	Model calibrated with sorption data predicted more desorption than occurred in the desorption experiments (Miller and Pedit, 1992)
Multisite continuum compartment model (Connaughton et al., 1993) $F(t) = 1 - \frac{M(t)}{M} = 1 - \left( \frac{\beta}{\beta + 1} \right)^\alpha$	$\alpha, \beta$	Assumption of homogeneous, spherical particles and diffusion only in aqueous phase
Pore space diffusion model (Fuller et al., 1993) $\left( \epsilon + \frac{S_a}{n} K_s C(r)^{(1-1/n)} \right) \frac{\partial C(r)}{\partial t} = D_e \left( \frac{\partial^2 C(r)}{\partial r^2} + \frac{2\partial C(r)}{r\partial r} \right)$	$D_e, \epsilon, K_s, 1/n, F_{\text{eq}}$	

Source: Partially adapted from Connaughton, D.F., J.R. Stedinger, L.W. Lion, and M.L. Shuler. 1993. Description of time-varying desorption kinetics: Release of naphthalene from contaminated soils. *Environ. Sci. Technol.* 27:2397-2403.

$S$ , concentration of the bulk sorbed contaminant ( $\text{g g}^{-1}$ );  $C$ , concentration of the bulk aqueous-phase contaminant ( $\text{g mL}^{-1}$ );  $k_d$ , first-order desorption rate coefficient ( $\text{min}^{-1}$ );  $S_s$ , concentration of the sorbed contaminant that is rate limited ( $\text{g g}^{-1}$ );  $S_p$ , concentration of the contaminant that is in equilibrium with the bulk aqueous concentration ( $\text{g g}^{-1}$ );  $X_1$ , fraction of the bulk sorbed contaminant that is in equilibrium with the aqueous concentration;  $K_p$ , sorption equilibrium partition coefficient ( $\text{mL g}^{-1}$ );  $D_{\text{eff}}$ , effective diffusivity of sorbate molecules or ions in the particles ( $\text{cm}^2 \text{s}^{-1}$ );  $S'$ , concentration of contaminant in immobile bound state ( $\text{mol g}^{-1}$ );  $C'$ , concentration of contaminant free in the pore fluid ( $\text{mol cm}^{-3}$ );  $n$ , porosity of the sorbent ( $\text{cm}^3$  of fluid  $\text{cm}^{-3}$ );  $D_m$ , pore fluid diffusivity of the sorbate ( $\text{cm}^2 \text{s}^{-1}$ );  $\rho_s$ , specific gravity of the sorbent ( $\text{g cm}^{-3}$ );  $f(n,t)$ , pore geometry factor;  $k_b$ , boundary layer mass transfer coefficient ( $\text{m s}^{-1}$ );  $r$ , radius of the spherical solid particle, assumed constant ( $m$ );  $\rho$ , macroscopic particle density of the solid phase ( $\text{g m}^{-3}$ );  $C_s$ , solution-phase solute concentration corresponding to an equilibrium with the solid-phase solute concentration at the exterior of the particle ( $\text{g L}^{-1}$ );  $D_s$ , surface diffusion coefficient ( $\text{m s}^{-1}$ );  $K_p$ , can be determined independently;  $K_s$ ,  $D_m$ , and  $\rho_s$  can be determined independently;  $F(t)$ , fraction of mass released through time  $t$ ;  $M(t)$ , mass remaining after time  $t$ ;  $M$ , total initial mass;  $\beta$ , scale parameter necessary for determination of mean and standard deviation of  $k_d$ ;  $\alpha$ , shape parameter;  $\epsilon$ , internal porosity of sorbent;  $C(r)$ , concentration of sorptive in the aqueous phase in the pore fluid at radial distance  $r$ ;  $S_a$  is the surface of sorbent per unit volume of solid;  $1/n$ , the adsorption isotherm slope;  $K_s$ , adsorption isotherm intercept;  $D_{\text{eq}}$ , effective diffusion coefficient;  $a$ , radius of the aggregate;  $F_{\text{eq}}$ , equilibrium fraction of absorption sites.

The two-site (two compartment, two box) or bicontinuum model has been widely used to describe chemical nonequilibrium (Leenheer and Ahlrichs, 1971; Hamaker and Thompson, 1972; Karickhoff, 1980; Karickhoff and Morris, 1985; McCall and Agin, 1985; Jardine et al., 1992) and physical nonequilibrium (Nkedi-Kizza et al., 1984; Lee et al., 1988; van Genuchten and Wagenet, 1989; Table 13.2). This model assumes that there are two reactions occurring, one that is fast and reaches equilibrium quickly and a slower reaction that can continue for long time periods. The reactions can occur either in series or in parallel (Brusseau and Rao, 1989).

In describing chemical nonequilibrium with the two-site model, two types of sorbent sites are assumed. One site involves an instantaneous equilibrium reaction and the other, the time-dependent reaction. The former is described by an equilibrium isotherm equation while a first-order equation is usually employed for the latter.

With the two-site model, there are two adjustable or fitting parameters: the fraction of sites at local equilibrium ( $X_1$ ), and the rate constant ( $k$ ). A distribution ( $K_d$ ) or partition coefficient ( $K_p$ ) is determined independently from a sorption/desorption isotherm.

To account for the multiple sites that may exist in heterogeneous systems, Connaughton et al. (1993) developed a multisite compartment (continuum) model ( $\Gamma$ ) that incorporates a continuum of sites or compartments with a distribution of rate coefficients that can be described by a gamma density function. A fraction of the sorbed mass in each compartment is at equilibrium with a desorption rate coefficient or distribution coefficient for each compartment or site (Table 13.2). The multisite model has two fitting parameters  $\alpha$ , a shape parameter, and  $1/\beta$ , which is a scale parameter that determines the mean standard deviation of the rate coefficients. Figure 13.8 shows application of the  $\Gamma$  model to desorption of naphthalene from contaminated soils. The entire desorption process was described well with this model.

### 13.4.7.2 Physical Nonequilibrium Models

A number of models can be used to describe physical nonequilibrium reactions. Since transport processes in the mobile phase are not usually rate limiting, physical nonequilibrium models focus on diffusion in the immobile phase or interaggregate/diffusion processes such as pore and/or surface diffusion. The transport between mobile and immobile regions is accounted for in physical nonequilibrium models in three ways (Brusseau and Rao, 1989): (1) explicitly with Fick's law to describe the physical mechanism of diffusive transfer, (2) explicitly by using an empirical first-order mass transfer expression to approximate solute transfer, and (3) implicitly by using an effective or lumped dispersion coefficient that includes the effects of sink/source differences and hydrodynamic dispersion and axial diffusion.

A pore diffusion model (Table 13.2) has been used by a number of investigators to study sorption processes using batch systems (Wu and Gschwend, 1986; Steinberg et al., 1987; Ball

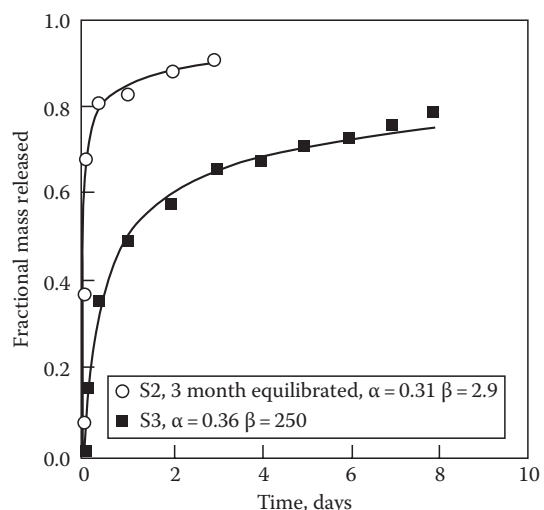


**FIGURE 13.8** Mass fractional release of naphthalene from two soils, S2 and S3 (S2 is a freshly contaminated soil, reacted with naphthalene for 3 months and S3 is a field [aged]-contaminated soil) fitted with a multisite continuum compartment ( $\Gamma$ ) model. (Reprinted from Connaughton, D.F., J.R. Stedinger, L.W. Lion, and M.L. Shuler. 1993. Description of time-varying desorption kinetics: Release of naphthalene from contaminated soils. *Environ. Sci. Technol.* 27:2397–2403. With permission American Chemical Society.)

and Roberts, 1991; Harmon et al., 1992; Pignatello et al., 1993). Wu and Gschwend (1986) successfully used the pore diffusion model to describe chlorobenzene congener sorption/desorption on soils and sediments. Figure 13.9 shows experimental and model fits for tetrachlorobenzene and pentachlorobenzene

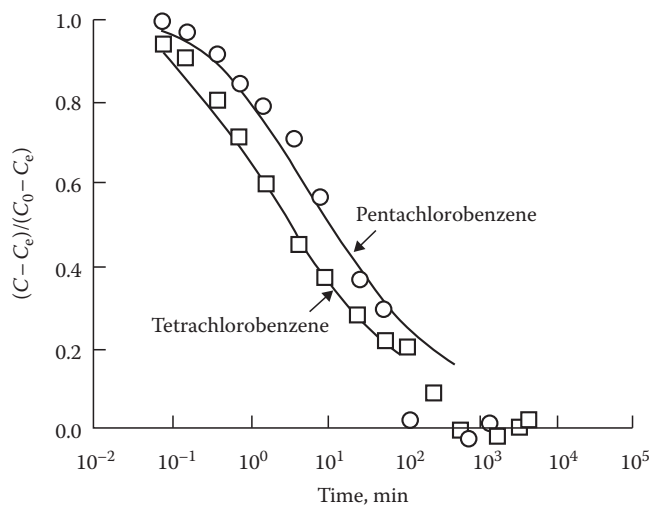


**FIGURE 13.9** Experimental and model fitting results for pentachlorobenzene and tetrachlorobenzene sorption on Iowa soils where  $C$  is the dissolved concentration of organic chemical in the bulk solution,  $C_0$  is the initial concentration, and  $C_e$  is the equilibrium concentration. The points represent experimental data and the solid lines represent fit of the data to the radial diffusion (pore diffusion) model. (Reprinted from Wu, S., and P.M. Gschwend. 1986. Sorption kinetics of hydrophobic organic compounds to natural sediments and soils. *Environ. Sci. Technol.* 20:717–725. With permission from American Chemical Society.)



sorption on soils. The sole fitting parameter in this model is the effective diffusion coefficient ( $D_e$ ), which may be estimated a priori from chemical and colloidal properties. However, this estimation is only valid if the sorbent material has a narrow particle size distribution so that an accurate, average particle size can be defined. Moreover, in the pore diffusion model, an average representative  $D_e$  is assumed, which means there is a continuum in properties across an entire pore size spectrum. This is not a valid assumption for micropores in which there are higher adsorption energies of sorbates causing increased sorption. The increased sorption reduces diffusive transport rates and results in nonlinear isotherms for sorbents with pores less than several sorbate diameters in size. Other factors can cause reduced transport rates in micropores including steric hindrance, which increases as the pore size approaches the solute size and greatly increased surface area to pore volume ratios (which occurs as pore size decreases).

Another problem with the pore diffusion model is that sorption and desorption kinetics may have been measured over a narrow concentration range. This is a problem since a sorption/desorption mechanism in micropores at one concentration may be insignificant at another concentration.

Fuller et al. (1993) used a pore space diffusion model (Table 13.2) to describe arsenate adsorption on ferrihydrite that included a subset of sites whereby sorption was at equilibrium. A Freundlich model was used to describe sorption on these sites. Diffusion into the particle was described by Fick's second law of diffusion; homogeneous, spherical aggregates, and diffusion only in the aqueous phase were assumed. Figure 13.10 shows the fit of the model when sorption at all sites was controlled by intraaggregate diffusion. The fit was better when sites that had attained sorption equilibrium were included based on the assumption that there was an initial rapid sorption on external surface sites before intraaggregate diffusion.

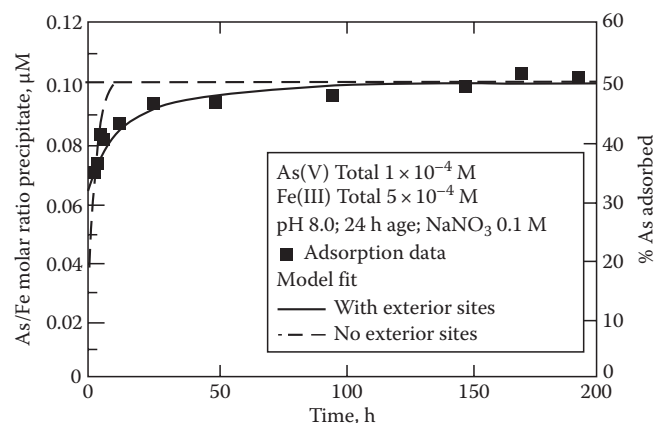


**FIGURE 13.10** Comparison of pore space diffusion model fits of As(V) sorption with experimental data (dashed curve represents sorption where all surface sites are diffusion limited and the solid curve represents sorption on equilibrium sites plus diffusion-limited sites). (Reprinted from Fuller, C.C., J.A. Davis, and G.A. Waychunas. 1993. Surface chemistry of ferrihydrite: Part 2. Kinetics of arsenate adsorption and coprecipitation. *Geochim. Cosmochim. Acta* 57:2271–2282. With permission from Elsevier.)

Pedit and Miller (1995) have developed a general multiple particle class pore diffusion model that accounts for differences in physical and sorptive properties for each particle class (Table 13.2). The model includes both instantaneous equilibrium sorption and time-dependent pore diffusion for each particle class. The pore diffusion portion of the model assumes that solute transfer between the intraparticle fluid and the solid phases is fast vis-à-vis interparticle pore diffusion processes.

Surface diffusion models, assuming a constant surface diffusion coefficient, have been used by a number of researchers (Weber and Miller, 1988; Miller and Pedit, 1992). The dual resistance model (Table 13.2) combines both pore and surface diffusion.

## 13.5 Kinetics of Important Reactions on Soils and Soil Components

In the past several decades, numerous studies have been conducted on the kinetics of metal, oxyanion, radionuclide, plant nutrient, and organic CRs on natural materials. In this section, emphasis will be placed on the kinetics of sorption/desorption, precipitation/dissolution, and oxidation/reduction reactions on soils and soil components.

### 13.5.1 Sorption/Desorption Reaction Rates

#### 13.5.1.1 Heavy Metals and Oxyanions

CRs of heavy metals and metalloids on soil components are rapid, occurring on a millisecond timescale. For such rapid reactions, chemical techniques such as pressure jump (p-jump) relaxation (Hayes and Leckie, 1986; Sparks, 1989; Sparks and Zhang, 1991; Grossl and Sparks, 1995; Sparks et al., 1996) and molecular scale methods such as ATR-FTIR and QXAS (Parikh and Chorover, 2007; Ginder-Vogel et al., 2009; Landrot et al., 2010) should be used.

The use of p-jump relaxation to measure the kinetics of ion sorption/desorption on metal oxide surfaces was pioneered by several Japanese chemists. Their research includes some of the following sorption/desorption kinetic studies: divalent metal ion (Hachiya et al., 1984), phosphate (Mikami et al., 1983a), chromate (Mikami et al., 1983c), and uranyl (Mikami et al., 1983b) sorption reactions on  $\gamma$ - $\text{Al}_2\text{O}_3$ . Hayes and Leckie (1986) were the first to use p-jump relaxation to study sorption/desorption kinetics of a metal ion contaminant ( $\text{Pb}^{2+}$ ) on goethite ( $\alpha$ - $\text{FeOOH}$ ). Other successive studies monitored the rapid sorption/desorption kinetics of molybdate (Zhang and Sparks, 1989), sulfate (Zhang and Sparks, 1990a), selenate and selenite (Zhang and Sparks, 1990b),  $\text{Cu}^{2+}$  (Grossl et al., 1994), and arsenate and chromate (Grossl et al., 1997) on goethite. Additional studies have investigated borate sorption/desorption kinetics on pyrophyllite (Keren et al., 1994) and on  $\gamma$ - $\text{Al}_2\text{O}_3$  (Toner and Sparks, 1995).

Details of many of these studies are summarized in Hayes and Leckie (1986), Sparks (1989, 1995), Sparks and Zhang (1991), and Sparks et al. (1996) and will not be detailed here. A study

of Grossl et al. (1997) will be summarized to illustrate rapid CR rates of two environmentally important oxyanions (chromate and arsenate) on goethite. A double relaxation was observed for both arsenate and chromate sorption/desorption over a pH range of 6.5–7.5 for arsenate and 5.5–6.5 for chromate, respectively (Figures 13.11 and 13.12). Based on the double relaxations, a two-step process, resulting in the formation of an inner-sphere bidentate surface complex (Figure 13.13) was proposed. The first step involves an initial ligand exchange reaction of the aqueous oxyanion ( $\text{H}_2\text{AsO}_4$  or  $\text{HCrO}_4^-$ ) with goethite, forming an inner-sphere monodentate surface complex that produces signals associated with fast  $\tau$  values. The succeeding step involves a second ligand exchange reaction, resulting in the formation of an inner-sphere bidentate surface complex that produces the signal associated with slow  $\tau$  values.

To determine if the mechanism displayed in Figure 13.13 was plausible and consistent with the kinetic data, the following linearized rate equations relating reciprocal relaxation time values ( $\tau^{-1}$ ) to the concentrations of reactive species were used:

$$\tau_{\text{fast}}^{-1} + \tau_{\text{slow}}^{-1} = k_1([\text{XOH}] + [\text{ion species}]) + k_{-1} + k_2 + k_{-2}, \quad (13.14)$$

$$\tau_{\text{fast}}^{-1} \cdot \tau_{\text{slow}}^{-1} = k_1[k_2 + k_{-2}][[\text{XOH}] + [\text{ion species}]] + k_1 k_{-2}, \quad (13.15)$$

where the ion species are  $\text{H}_2\text{AsO}_4^-$  or  $\text{HCrO}_4^-$ . The derivation of these equations was obtained from Bernasconi (1976) and is based on the two-step reaction system ( $A + B \leftrightarrow C \leftrightarrow D$ ). If the mechanism portrayed in Figure 13.13 is accurate, then a plot of  $\tau_{\text{fast}}^{-1} + \tau_{\text{slow}}^{-1}$  and  $\tau_{\text{fast}}^{-1} \cdot \tau_{\text{slow}}^{-1}$  as a function of the concentration term ( $[\text{XOH}] + [\text{ion species}]$ ) should be linear. Plots of Equations 13.14 and 13.15 were linear for both arsenate and chromate, suggesting that the proposed mechanism was plausible (Figures 13.14 and 13.15).

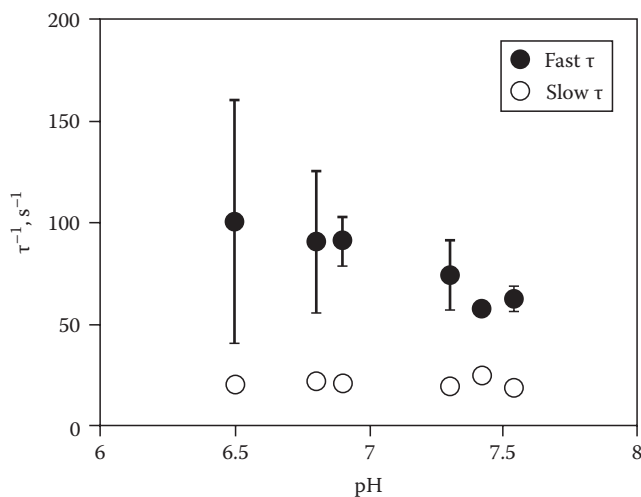


**FIGURE 13.11**  $\tau^{-1}$  Values determined from p-jump experiments for arsenate adsorption/desorption on goethite, as a function of pH. (Reprinted from Grossl, P.R., M. Eick, D.L. Sparks, S. Goldberg, and C.C. Ainsworth. 1997. Arsenate and chromate retention mechanisms on goethite. 2. Kinetic evaluation using a pressure-jump relaxation technique. Environ. Sci. Technol. 31:321–326. With permission from American Chemical Society.)

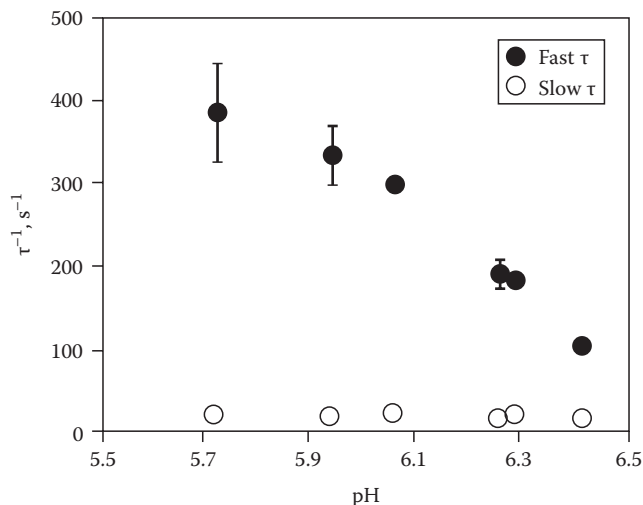


**FIGURE 13.12**  $\tau^{-1}$  Values determined from p-jump experiments for chromate adsorption/desorption on goethite, as a function of pH. (Reprinted from Grossl, P.R., M. Eick, D.L. Sparks, S. Goldberg, and C.C. Ainsworth. 1997. Arsenate and chromate retention mechanisms on goethite. 2. Kinetic evaluation using a pressure-jump relaxation technique. Environ. Sci. Technol. 31:321–326. With permission from American Chemical Society.)

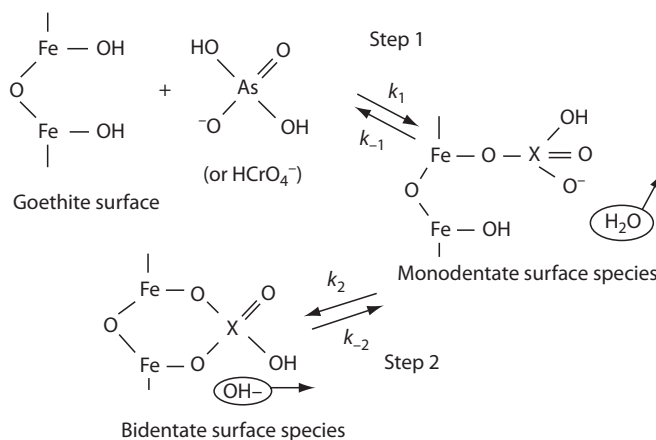


**FIGURE 13.13** Proposed mechanism for oxyanion adsorption/desorption on goethite. The X represents either As(V) or Cr(VI). (Reprinted from Grossl, P.R., M. Eick, D.L. Sparks, S. Goldberg, and C.C. Ainsworth. 1997. Arsenate and chromate retention mechanisms on goethite. 2. Kinetic evaluation using a pressure-jump relaxation technique. Environ. Sci. Technol. 31:321–326. Copyright American Chemical Society.)

From the plots in Figures 13.14 and 13.15, forward and reverse rate constants were obtained for the sorption and desorption reactions of both the monodentate and bidentate steps where  $k_1 = \text{slope}$  (Figure 13.14);  $k_{-1} = \text{intercept}$  (Figure 13.14) – slope (Figure 13.15)/slope (Figure 13.14);  $k_2 = \text{intercept}$  (Figure 13.14) –  $k_{-1} - k_{-2}$ ; and  $k_{-2} = \text{intercept}$  (Figure 13.15)/ $k_{-1}$ . The calculated rate constants for both chromate and arsenate adsorption/desorption on goethite are listed in Table 13.3.

Overall, the forward rate constants associated with the formation of the inner-sphere oxyanion/goethite surface complexes were more rapid than the reverse rate constants. Therefore, the

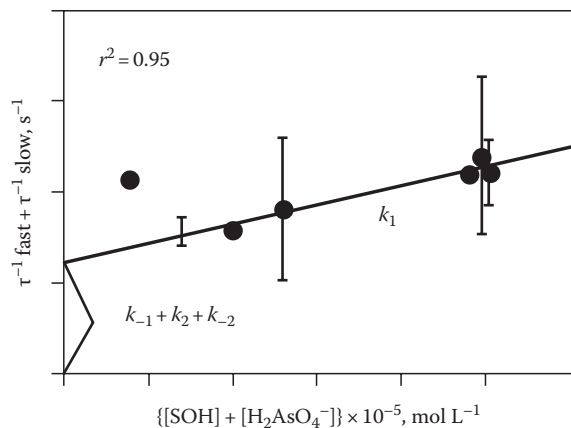


**FIGURE 13.14** Evaluation of the linearized rate Equation 13.14 for the mechanism displayed in Figure 13.13 for arsenate. (Reprinted from Grossl, P.R., M. Eick, D.L. Sparks, S. Goldberg, and C.C. Ainsworth. 1997. Arsenate and chromate retention mechanisms on goethite. 2. Kinetic evaluation using a pressure-jump relaxation technique. Environ. Sci. Technol. 31:321–326. With permission from American Chemical Society.)

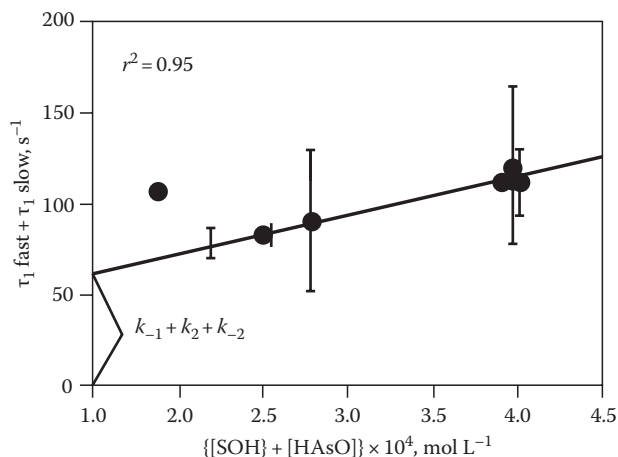


**FIGURE 13.15** Evaluation of the linearized rate Equation 13.15 for the mechanism displayed in Figure 13.13 for arsenate. (Reprinted from Grossl, P.R., M. Eick, D.L. Sparks, S. Goldberg, and C.C. Ainsworth. 1997. Arsenate and chromate retention mechanisms on goethite. 2. Kinetic evaluation using a pressure-jump relaxation technique. Environ. Sci. Technol. 31:321–326. With permission from American Chemical Society.)

rate-limiting steps were the reverse reactions. The equilibrium constants listed in Table 13.3 were calculated using the rate constants for each reaction step in the proposed mechanism (Figure 13.13) from the following relationship:

$$K_{\text{eq}} = \frac{k_1}{k_{-1}} \quad (13.16)$$

The calculated equilibrium constant for Step 1 for arsenate was  $10^{5.35}$  and for Step 2 was  $10^{0.26}$ , while the calculated  $K_{\text{eq}}$  for Step 1 for chromate was  $10^{3.7}$  and for Step 2 was  $10^{0.4}$ . The sorption of both oxyanions and subsequent formation of inner-sphere surface complexes are thermodynamically favorable, with the exception of the equilibrium constant for the second step associated

**TABLE 13.3** Calculated Rate Constants for Chromate and Arsenate Adsorption/Desorption on Goethite

	Step 1	Step 2
Arsenate	$k_f = 10^{6.3} \text{ L mol}^{-1} \text{ s}^{-1}$	$k_2 = 15 \text{ s}^{-1}$
	$k_{-1} = 8 \text{ s}^{-1}$	$k_{-2} = 8 \text{ s}^{-1}$
	$k_{\text{eq}} = 10^{5.35} \text{ L mol}^{-1} \text{ s}^{-1}$	$k_{\text{eq}} = 10^{0.26}$
Chromate	$k_1 = 10^{5.8} \text{ L mol}^{-1} \text{ s}^{-1}$	$k_2 = 16 \text{ s}^{-1}$
	$k_{-1} = 129 \text{ s}^{-1}$	$k_{-2} = 38 \text{ s}^{-1}$
	$k_{\text{eq}} = 10^{3.7} \text{ L mol}^{-1} \text{ s}^{-1}$	$k_{\text{eq}} = 10^{-0.4}$

Source: Reprinted from Grossl, P.R., M. Eick, D.L. Sparks, S. Goldberg, and C.C. Ainsworth. 1997. Arsenate and chromate retention mechanisms on goethite. 2. Kinetic evaluation using a pressure-jump relaxation technique. Environ. Sci. Technol. 31:321–326. With permission from American Chemical Society.

with chromate sorption (slightly less than 1). Thus, the monodentate chromate/goethite surface complex is slightly favored over the bidentate surface complex. This is in agreement with spectroscopic data obtained from x-ray absorption fine structure (XAFS) analyses (Fendorf et al., 1997), which indicate a mixture of both monodentate and bidentate arsenate, and chromate surface complexes; but at low-surface coverage, a greater proportion of chromate is associated with the monodentate complex than the bidentate complex. The results from both kinetic and XAFS experiments suggest that arsenate is more likely to form an inner-sphere surface complex with goethite than chromate.

While p-jump relaxation techniques are useful for measuring rapid reaction rates on soil components, the rate constants are calculated from linearized rate equations, which include parameters that are determined from equilibrium and modeling studies. Consequently, the rate “constants” are not directly determined.

The ideal way to measure rapid reaction rates that may often comprise a major portion of the total reaction process for many soil chemical processes, particularly on soil components is to use real-time molecular scale techniques such as ATR-FTIR and QXAS. With these techniques, one can not only measure reaction rates on millisecond timescales but also at the same time couple these measurements with spectroscopic analyses of the reaction mechanism (Parikh et al., 2008; Ginder-Vogel et al., 2009; Landrot et al., 2010).

While the initial sorption of heavy metals is rapid, with the CR step occurring on second or millisecond timescales, further sorption may be slow (Figure 13.16) occurring over timescales of days and longer. Such behavior has been observed for some Fe oxides. This slow sorption has been ascribed to several mechanisms, including interparticle or intraparticle diffusion in pores and solids, sites of low reactivity, and surface precipitation/nucleation (Sparks, 1998; Strawn and Sparks, 2000). With heterogeneous soils and even soil components, there may be a continuum between the three sorption mechanisms, for example, between adsorption and surface precipitation/nucleation. While it has generally been assumed that adsorption in comparison with surface precipitation/nucleation is much more rapid, recent

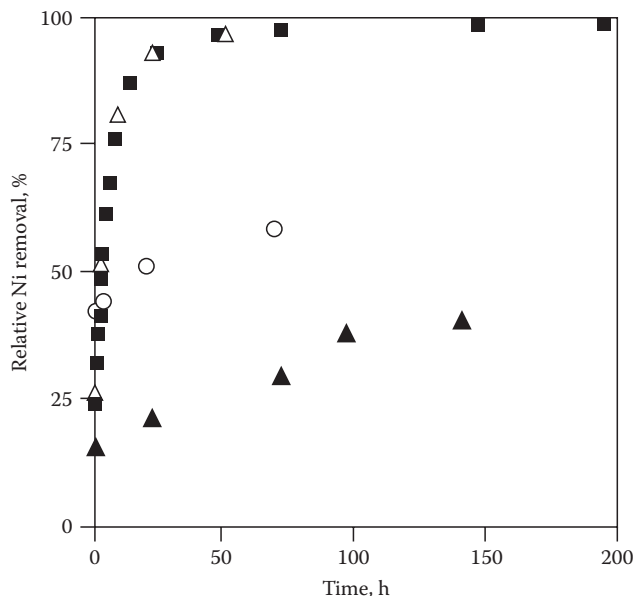


**FIGURE 13.16** Kinetics of Ni sorption [%] on pyrophyllite (■), kaolinite (Δ), gibbsite (▲), and montmorillonite (○) from a 3 mM Ni solution at pH = 7.5 and an ionic strength  $I = 0.1\text{M}$  ( $\text{NaNO}_3$ ). The last sample of each experiment was collected and analyzed by XAFS. (Reprinted from Scheidegger, A.M., G.M. Lamble, and D.L. Sparks. 1997. Spectroscopic evidence for the formation of mixed-cation hydroxide phases upon metal sorption on clays and aluminum oxides. *J. Colloid Interface Sci.* 186:118–128. With permission from Elsevier.)

studies (Scheidegger et al., 1998) that will be discussed later, have shown that surface precipitation/nucleation processes can occur on timescales as short as 15 min, which indicates that sorption and nucleation processes can occur simultaneously. However, in some cases, depending on reaction conditions and the metal involved, a particular sorption mechanism can dominate.

Obviously, an important factor affecting the degree of slow sorption/desorption of metals (and for that matter also of organic chemicals) is the time period the sorbate has been in contact with the sorbent (residence time). Bruemmer et al. (1988) studied  $\text{Ni}^{2+}$ ,  $\text{Zn}^{2+}$ , and  $\text{Cd}^{2+}$  sorption on goethite, a porous Fe oxide that has defect structures in which metals can be incorporated to satisfy charge imbalances. Bruemmer et al. (1988) found, at pH 6, that as reaction time increased from 2 h to 42 days (at 293 K), adsorbed  $\text{Ni}^{2+}$  increased from 12% to 70% of total adsorption, and total  $\text{Zn}^{2+}$  and  $\text{Cd}^{2+}$  adsorption over this time increased by 33% and 21%, respectively. The kinetic reactions could be well described using a Fickian diffusion model. Metal uptake was hypothesized to occur by a three-step mechanism: (1) adsorption of metals on external surfaces, (2) solid-state diffusion of metals from external to internal sites, and (3) metal binding and fixation at positions inside the goethite particle.

Ainsworth et al. (1994) studied the adsorption/desorption of  $\text{Co}^{2+}$ ,  $\text{Cd}^{2+}$ , and  $\text{Pb}^{2+}$  on hydrous Fe(III) as a function of aging and metal oxide residence time. Oxide aging did not cause hysteresis of metal cation sorption/desorption. Aging the oxide with the metal cations resulted in hysteresis with  $\text{Cd}^{2+}$  and  $\text{Co}^{2+}$  but little with

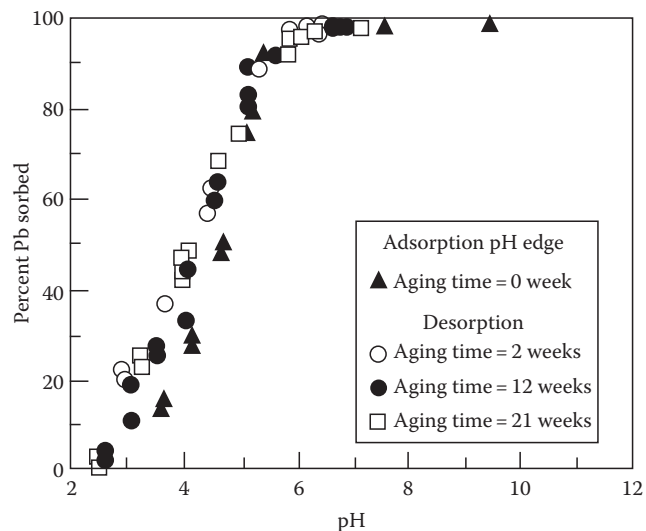


**FIGURE 13.17** Fractional sorption-desorption of  $\text{Pb}^{2+}$  to hydrous Fe(III) as a function of pH and HFO- $\text{Pb}^{2+}$  aging time. (Reprinted from Ainsworth, C.C., J.L. Pilon, P.L. Gassman, and W.G. Van Der Sluys. 1994. Cobalt, cadmium, and lead sorption to hydrous iron oxide: Residence time effect. *Soil Sci. Soc. Am. J.* 58:1615–1623. With permission from the Soil Science Society of America.)

$\text{Pb}^{2+}$ . With  $\text{Pb}^{2+}$  between pH 3 and 5.5 there was slight hysteresis over a 21 week aging process (hysteresis varied from <2% difference between sorption and desorption to ~10%). At pH 2.5,  $\text{Pb}^{2+}$  desorption was complete within a 16 h period and was not affected by aging time (Figure 13.17). However, with  $\text{Cd}^{2+}$  and  $\text{Co}^{2+}$ , extensive hysteresis was observed over a 16 week aging period and the hysteresis increased with aging time (Figures 13.18 and 13.19). After 16 weeks of aging, 20% of the  $\text{Cd}^{2+}$  and 53% of the  $\text{Co}^{2+}$  were not desorbed, and even at pH 2.5, hysteresis was observed. The extent

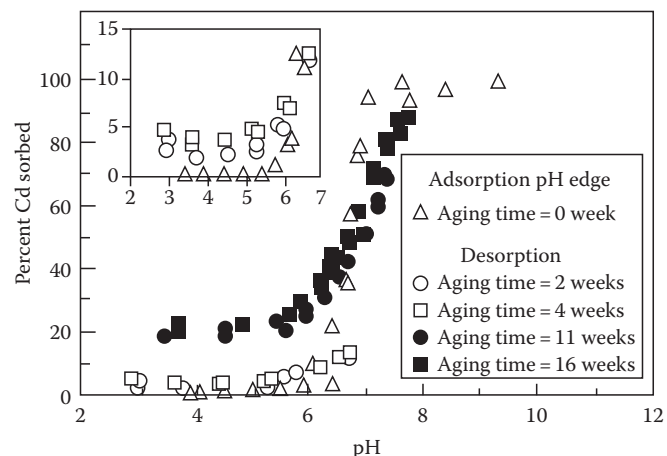


**FIGURE 13.18** Fractional sorption-desorption of  $\text{Cd}^{2+}$  to hydrous Fe oxide (HFO) as a function of pH and HFO- $\text{Cd}^{2+}$  aging time; insert shows adsorption-desorption of  $\text{Cd}^{2+}$  to HFO at 2 and 4 week aging times. (Reprinted from Ainsworth, C.C., J.L. Pilon, P.L. Gassman, and W.G. Van Der Sluys. 1994. Cobalt, cadmium, and lead sorption to hydrous iron oxide: Residence time effect. *Soil Sci. Soc. Am. J.* 58:1615–1623. With permission from the Soil Science Society of America.)

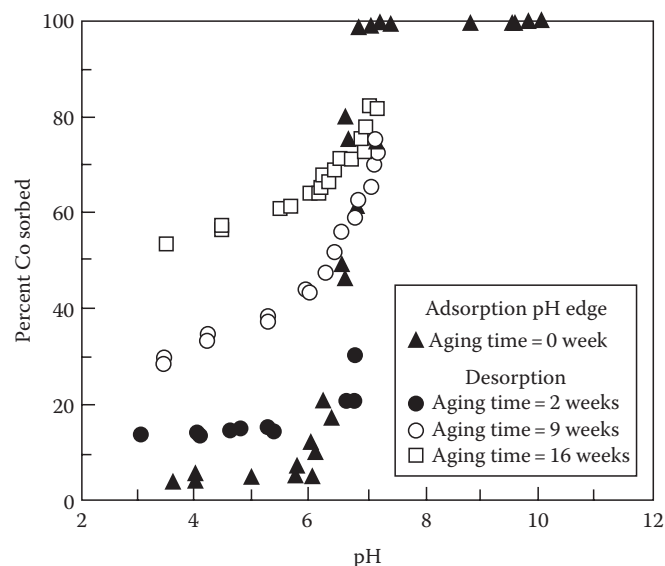


**FIGURE 13.19** Fractional adsorption of  $\text{Co}^{2+}$  to hydrous Fe oxide (HFO) as a function of pH and HFO- $\text{Co}^{2+}$  aging time. (Reprinted from Ainsworth, C.C., J.L. Pilon, P.L. Gassman, and W.G. Van Der Sluys. 1994. Cobalt, cadmium, and lead sorption to hydrous iron oxide: Residence time effect. *Soil Sci. Soc. Am. J.* 58:1615–1623. With permission from the Soil Science Society of America.)

of reversibility with aging for  $\text{Co}^{2+}$ ,  $\text{Cd}^{2+}$ , and  $\text{Pb}^{2+}$  was inversely proportional to the ionic radius of the ions, namely,  $\text{Co}^{2+} < \text{Cd}^{2+} < \text{Pb}^{2+}$ . Ainsworth et al. (1994) attributed the hysteresis to Co and Cd incorporation into a recrystallizing solid (probably goethite) by isomorphic substitution and not to micropore diffusion.

Strawn and Sparks (2000) investigated the role that residence time and organic matter content had on Pb desorption kinetics from a Matapeake soil. Residence time had little effect on the amount of Pb desorbed, but marked hysteresis was observed at all residence times, which was ascribed to diffusion of Pb into the organic matter and strong metal–soil complexes.

Fuller et al. (1993) combined kinetic sorption and desorption experiments with spectroscopic observations (Waychunas et al., 1993) to study As sorption on ferrihydrite. Using XAFS spectroscopy, they found that As was sorbed predominantly as inner-sphere bidentate complexes, regardless of whether the As was adsorbed after the mineralization of the ferrihydrite or it was present during precipitation. No As surface precipitates were observed. Slow As sorption and desorption were explained as slow diffusion of the As to or from interior surface complexation sites that exist within disordered aggregates of crystallites. The kinetic reactions could be described using a Fickian diffusion model.

Slow metal sorption/desorption has also been ascribed to conversion of the metal sorbate from a high- to a low-energy state (Kuo and Mikkelsen, 1980; Padmanabham, 1983; Schultz et al., 1987; Backes et al., 1995). Lehmann and Harter (1984) measured the kinetics of chelate-promoted  $\text{Cu}^{2+}$  release from a soil to assess the strength of the bond formed. Sorption/desorption was biphasic, which was attributed to high- and low-energy bonding sites.

With increased residence time from 30 min to 24 h, Lehmann and Harter (1984) speculated that there was a transition of Cu from low to higher energy sites (as evaluated by release kinetics). Incubations for up to 4 days showed a continued uptake of Cu and a decrease in the fraction released within the first 3 min, which was referred to as the low-energy sorbed fraction.

Recent studies particularly using surface spectroscopic and microscopic techniques such as XAS and transmission electron microscopy (TEM) have shown that the formation of polynuclear surface species (e.g., surface precipitates) on natural materials such as clay minerals, metal oxides, and in soils is an important sorption and sequestration mechanism (Charlet and Manceau, 1993; Fendorf et al., 1994; Junta and Hochella, 1994; O'Day et al., 1994a, 1994b; Wersin et al., 1994; Scheidegger et al., 1996, 1997, 1998; Towle et al., 1997; Xia et al., 1997; Elzinga and Sparks, 1999; Roberts et al., 1999; Thompson et al., 1999a, 1999b; Ford and Sparks, 2000; Nachtegaal et al., 2005; McNear et al., 2007).

The surface precipitates of Co, Cr(III), Cu, and Ni on metal oxides and clay minerals have been observed at metal surface loadings far below a theoretical monolayer coverage and in a pH range well below the pH where the formation of metal hydroxide precipitates would be expected according to the thermodynamic solubility product. In Al-bearing soil components, the precipitates are mixed metal–Al hydroxide phases of the layered double hydroxide type. Recent studies using microfocused x-ray fluorescence (micro-XRF) and x-ray absorption spectroscopy (micro-XAS) have shown that Zn–Al layered double hydroxides (LDH) (Nachtegaal et al., 2005) and Ni–Al hydroxide LDH (McNear et al., 2007) precipitates occur in field-contaminated soils.

In general, the formation of surface precipitates has been considered a slow phenomenon. However, Scheidegger et al. (1998) have demonstrated that the rate of surface precipitate formation can be quite rapid. The appearance of surface precipitates during sorption of Ni to pyrophyllite at pH 7.5 occurred over time scales less than 1 h. Similar results were observed for Ni sorption to kaolinite. However, the kinetics of Ni sorption onto gibbsite, and subsequent surface precipitate formation, were slower than for pyrophyllite (Figures 13.16 and 13.20). Time-resolved XAFS studies demonstrated continued growth of the surface precipitate during Ni uptake as the structure and Ni:Al stoichiometry of the sorption complex approached that of a takovite-like phase (Scheidegger et al., 1998).

### 13.5.1.2 Organic Contaminants

Numerous studies on the kinetics of organic chemical sorption/desorption reactions on soils and soil components have shown that sorption/desorption is characterized by a rapid, reversible stage followed by a much slower, nonreversible stage (Karickhoff et al., 1979; DiToro and Horzempa, 1982; Karickhoff and Morris, 1985; Kan et al., 1997; Xing and Pignatello, 2005), or biphasic kinetics. The rapid phase has been ascribed to retention of the organic chemical in a labile form that is easily desorbed. However, the much slower reaction phase involves the entrapment of the chemical in a nonlabile form that is difficult to desorb. The labile form of the

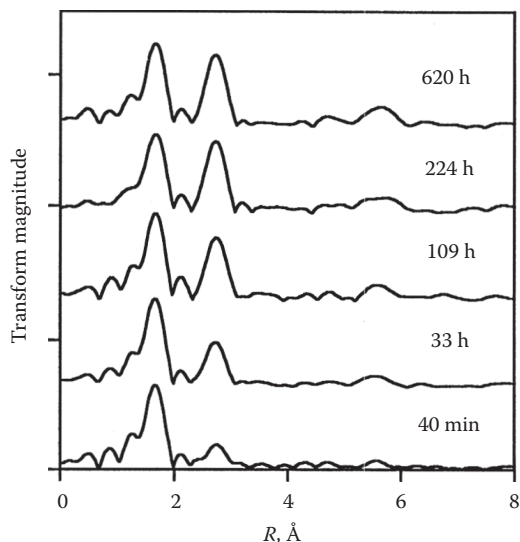


**FIGURE 13.20** Radial structure functions for Ni sorption to gibbsite for reaction times up to 620h demonstrating the appearance and growth of second shell contributions due to surface precipitation and growth of a hydroxalcite-like phase. (Reprinted from Scheidegger, A.M., D.G. Strawn, G.M. Lamble, and D.L. Sparks. 1998. The kinetics of mixed Ni–Al hydroxide formation on clay and aluminum oxide minerals: A time-resolved XAFS study. *Geochim. Cosmochim. Acta* 62:2233–2245. With permission from Elsevier.)

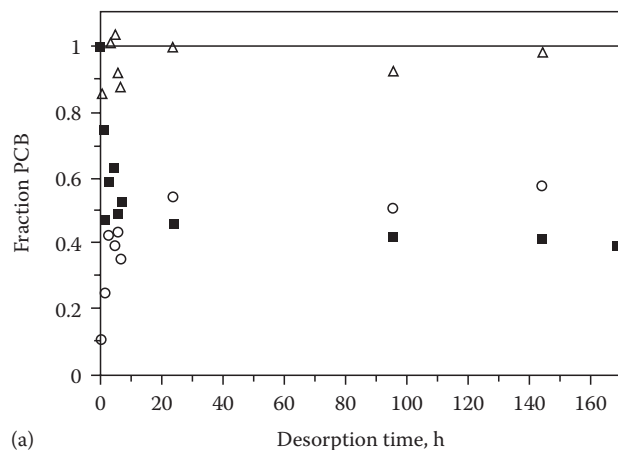
chemical is available for microbial attack, while the nonlabile portion is resistant to biodegradation.

This slower sorption/desorption reaction has been ascribed to intraparticle and interparticle diffusion of the chemical into soil organic matter (SOM) and inorganic soil components (Wu and Gschwend, 1986; Steinberg et al., 1987; Ball and Roberts, 1991).

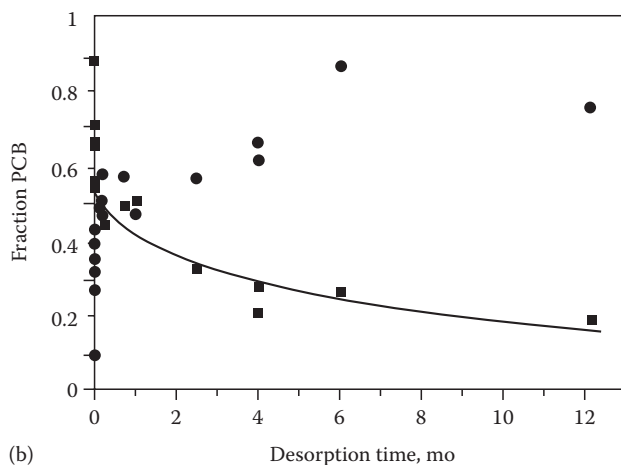
Theories proposed by a number of researchers (Weber and Huang, 1996; Xing and Pignatello, 1997; Pignatello, 2000) have explained the slow diffusion of organic chemicals into SOM by considering SOM as a combination of “rubbery” and “glassy” polymers. The rubber-like phases are characterized by an expanded, flexible, and highly solvated structure with pores of subnanometer dimensions (holes) (Xing and Pignatello, 1997; Pignatello, 1998, 2000). Sorption in the rubbery phases results in linear, noncompetitive, and reversible behavior. The glassy phases have pores that are of subnanometer size, and sorption in this phase is characterized by nonlinearity and is competitive (Xing and Pignatello, 1997). These theories, relating slow diffusion into organic matter to diffusion in polymers, are somewhat validated in some studies measuring energies of activation ( $E_a$ ) for organic chemical sorption. Cornelissen et al. (1997) studied the temperature dependence of slow adsorption and desorption kinetics of some chlorobenzenes, polychlorinated biphenyls (PCBs), and polycyclic aromatic hydrocarbons (PAHs) in laboratory- and field-contaminated sediments and obtained  $E_a$  values of 60–70 kJ mol<sup>-1</sup>, which are in the range for diffusion in polymers. These values are much higher than those for pore diffusion (20–40 kJ mol<sup>-1</sup>) suggesting that intraorganic matter diffusion may be a more important mechanism for slow organic chemical sorption than interparticle pore diffusion.

However, Chang et al. (1997) who studied sorption of toluene (TOL), *n*-hexane, and acetone on pressed humic acid disks found an insignificant amount of irreversibly bound residue with activation energies in the range of 42.3–65.8 kJ mol<sup>-1</sup>, suggesting a physical sorption process with little diffusion.

An example of the biphasic kinetics that is observed for many organic CRs in soils/sediments is shown in Figure 13.21. In this study, 55% of the labile PCB was desorbed from sediments in



(a)



(b)

**FIGURE 13.21** (a) Short-term polychlorinated biphenyl (PCB) desorption in hours (h) from Hudson River sediment contaminated with 25 mg kg<sup>-1</sup> PCB. Distribution of the PCB between the sediment (v) and XAD-4 resin (o) as well as the overall mass balance (D) is shown. The resin acts as a sink to retain the PCB that is desorbed (Carroll et al., 1994). (b) Long-term PCB desorption in months (mo) from Hudson River sediment contaminated with 25 mg kg<sup>-1</sup> PCB. Distribution of the PCB between the sediment (■) and XAD-4 resin (●) is shown. The line represents a nonlinear regression of the data by a two-site model. (Reprinted from Carroll, K.M., M.R. Harkness, A.A. Bracco, R.R. Balcarcel. 1994. Application of a permeant/polymer diffusional model to the desorption of polychlorinated biphenyls from Hudson River sediments. *Environ. Sci. Technol.* 28:253–258. With permission from American Chemical Society.)

a 24 h period, while little of the remaining 45% nonlabile fraction was desorbed in 170 h (Figure 13.21a). Over another 1 year period, ~50% of the remaining nonlabile fraction desorbed (Figure 13.21b).

Pavlostathis and Mathavan (1992) observed a biphasic desorption process for field soils contaminated with trichloroethylene (TCE), tetrachloroethylene (PCE), TOL, and xylene (XYL). A fast desorption reaction occurred in 24 h followed by a much slower desorption reaction beyond 24 h. In 24 h, 9%–29%, 14%–48%, 9%–40%, and 4%–37% of the TCE, PCE, TOL, and XYL, respectively, were released. However, the apparent irreversibility or hysteresis may be an artifact caused by not reaching a true sorption equilibrium. For example, DiVincenzo and Sparks (1997), studying pentachlorophenol sorption/desorption on a soil, found that if desorption was initiated after an apparent sorption equilibrium (i.e., slow sorption was measured) was reached, hysteresis or irreversibility was significantly reduced.

A number of studies have also shown that with aging the nonlabile portion of the organic chemical in the soil/sediment becomes more resistant to release (McCall and Agin, 1985; Steinberg et al., 1987; Pignatello and Huang, 1991; Pavlostathis and Mathavan, 1992; Scribner et al., 1992; Alexander, 1995; Loehr and Webster, 1996). However, Connaughton et al. (1993) did not observe the nonlabile fraction increasing with age for naphthalene-contaminated soils.

One way to gauge the effect of time on organic contaminant retention in soils is to compare  $K_d$  (sorption distribution coefficient) values for freshly aged and aged soil samples. In most studies,  $K_d$  values are measured based on a 24 h equilibration between the soil and the organic chemical. When these values are compared to  $K_d$  values for field soils previously reacted with the organic chemical (aged samples), the latter have much higher  $K_d$  values, indicating that much more of the organic chemical is in a sorbed state. For example, Pignatello and Huang (1991) measured  $K_d$  values in freshly aged ( $K_d$ ) and “aged” soils ( $K_{app}$ , apparent sorption distribution coefficient) reacted with atrazine and metolachlor, two widely used herbicides. The aged soils had been treated with the herbicides 15–62 months before sampling. The  $K_{app}$  values ranged from 2.3 to 42 times higher than the  $K_d$  values (Table 13.4).

Scribner et al. (1992) studying simazine (a widely used triazine herbicide for broadleaf and grass control in crops) desorption and bioavailability in aged soils found that  $K_{app}$  values were 15 times higher than  $K_d$  values. Scribner et al. (1992) also showed that 48% of the simazine added to the freshly aged soils was biodegradable over a 34-day incubation period while none of the simazine in the aged soil was biodegraded.

One of the implications of these results is that while many transport and degradation models for organic contaminants in soils and waters assume that the sorption process is an equilibrium process, the above studies clearly show that kinetic reactions must be considered when making predictions about the mobility and fate of organic chemicals. Moreover, calculation of  $K_d$  values based on a 24 h equilibration period, which are commonly used in fate and risk assessment models, can be

**TABLE 13.4** Sorption Distribution Coefficients for Herbicides in Freshly Aged and Aged Soils

Herbicide	Soil	$K_d$ (L kg <sup>-1</sup> ) <sup>a</sup>	$K_{app}$ (L kg <sup>-1</sup> ) <sup>b</sup>
Metolachlor	Cva	2.96	39
	CVb	1.46	27
	W1	1.28	49
	W2	0.77	33
Atrazine	Cva	2.17	28
	CVb	1.32	29
	W3	1.75	4

Source: Adapted from Pignatello, J.J., and L.Q. Huang. 1991. Sorptive reversibility of atrazine and metolachlor residues in field soil samples. *J. Environ. Qual.* 20:222–228. With permission of the American Society of Agronomy.

<sup>a</sup> Sorption distribution coefficient (L kg<sup>-1</sup>) of freshly aged soil based on a 24 h equilibration period.

<sup>b</sup> Apparent sorption distribution coefficient (L kg<sup>-1</sup>) in contaminated soil (aged soil) determined using a 24 h equilibration period.

inaccurate since 24 h  $K_d$  values often overestimate the amount of organic chemical in the solution phase.

The finding that many organic chemicals are quite persistent in the soil environment has both good and bad features. The beneficial aspect is that the organic chemicals are less mobile and may not be readily transported in groundwater supplies. The negative aspect is that their persistence and inaccessibility to microbes may make decontamination more difficult, particularly if in situ remediation techniques such as biodegradation are employed.

## 13.5.2 Kinetics of Mineral Dissolution

### 13.5.2.1 Rate-Limiting Steps

Dissolution of minerals involves several steps (Stumm and Wollast, 1990): (1) mass transfer of dissolved reactants from the bulk solution to the mineral surface, (2) adsorption of solutes, (3) interlattice transfer of reaction species, (4) surface CRs, (5) removal of reactants from the surface, and (6) mass transfer of products into the bulk solution. Under field conditions, mineral dissolution is slow and mass transfer of reactants or products in the aqueous phase (Steps 1 and 6) is not rate limiting. Thus, the rate-limiting steps are either transport of reactants and products in the solid phase (Step 3) or surface CRs (Step 4) and removal of reactants from the surface (Step 5).

Transport-controlled dissolution reactions or those controlled by mass transfer or diffusion can be described using a parabolic rate law given later (Stumm and Wollast, 1990):

$$r = \frac{dC}{dt} = kt^{-1/2}, \quad (13.17)$$

where

$r$  is the reaction rate

$C$  is the concentration in solution

$t$  is time

$k$  is the reaction rate constant

Integrating,  $C$  increases with  $t^{1/2}$ ,

$$C = C_0 + 2kt^{1/2}, \quad (13.18)$$

where  $C_0$  is the initial concentration in solution.

If the surface reactions are slow compared to the transport reactions, dissolution is surface controlled, which is the case for most dissolution reactions of silicates and oxides. In surface-controlled reactions, the concentrations of solutes next to the surface are equal to the bulk solution concentrations and the dissolution kinetics are zero order if steady-state conditions are operational on the surface. Thus, the dissolution rate ( $r$ ) is

$$r = \frac{dC}{dt} = kA, \quad (13.19)$$

and  $r$  is proportional to the mineral's surface area,  $A$ . Thus, for a surface-controlled reaction, the relationship between  $t$  and  $C$  should be linear. Figure 13.22 compares transport- and surface-controlled dissolution mechanisms.

Intense arguments have ensued over the years concerning the mechanism for mineral dissolution. Those that supported a transport-controlled mechanism believed that a leached layer formed as mineral dissolution proceeded and that subsequent dissolution took place by diffusion through the leached layer (Wollast, 1967; Petrovic et al., 1976). Advocates of this theory found that dissolution was described by the parabolic rate law (Equation 13.18). However, the apparent transport-controlled kinetics may be an artifact caused by dissolution of hyperfine particles formed on the mineral surfaces after grinding that are highly reactive sites or by the use of batch methods that cause reaction products to accumulate causing precipitation of secondary minerals. These experimental artifacts can cause incongruent reactions and pseudoparabolic kinetics. Studies employing x-ray photoelectron spectroscopy (XPS) and nuclear resonance profiling (Schott and Petit, 1987; Casey et al., 1989) have demonstrated

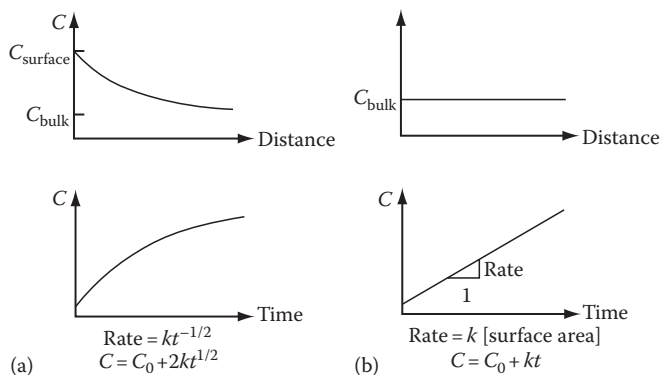


**FIGURE 13.22** (a) Transport- versus (b) surface-controlled dissolution. Schematic representation of concentration in solution,  $C$ , as a function of distance from the surface of the dissolving mineral. In the lower part of the figure, the change in concentration is given as a function of time. (Reprinted with permission from Stumm, W. 1992. *Chemistry of the solid-water interface*. Wiley, New York.)

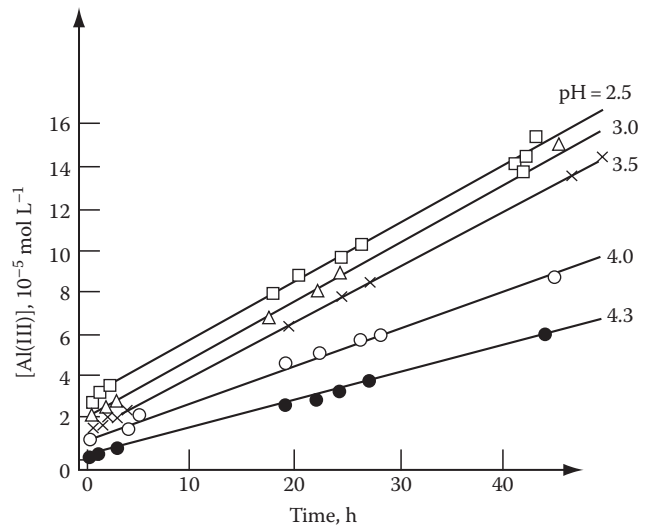


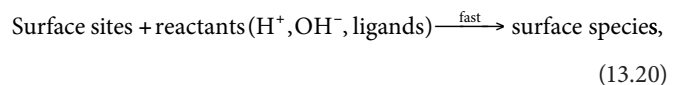
**FIGURE 13.23** Linear dissolution kinetics observed for the dissolution of  $\gamma\text{-Al}_2\text{O}_3$ . Representative of processes whose rates are controlled by a surface reaction and not by transport. (Reprinted from Furrer, G., and W. Stumm. 1986. *The coordination chemistry of weathering. I. Dissolution kinetics of  $\gamma\text{-Al}_2\text{O}_3$  and BeO*. *Geochim. Cosmochim. Acta* 50:1847–1860. Copyright 1986. With permission from Elsevier.)

that although some incongruity may occur in the initial dissolution process, which may be diffusion controlled, the overall reaction is surface controlled. Energies of activation from 60 to 86  $\text{kJ mol}^{-1}$  have been observed for dissolution of oxides and silicates, further suggesting surface-controlled dissolution (Lasaga, 1984; Jordan and Rammensee, 1996). An illustration of the surface-controlled dissolution of  $\gamma\text{-Al}_2\text{O}_3$  resulting in a linear release of  $\text{Al}^{3+}$  with time is shown in Figure 13.23. The dissolution rate ( $r$ ) can be obtained from the slope of Figure 13.23.

Scanning force microscopy (SFM), which has also been used increasingly as an in situ technique for imaging mineral surfaces immersed in aqueous solution during the course of dissolution (Hellman et al., 1992; Hillner et al., 1992a, 1992b; Johnsson et al., 1992; Bosbach and Rammensee, 1994; Maurice et al., 1995), permits a direct measure of surface-controlled dissolution rates by providing 3D data on changes in microtopography. In situ SFM has the unique ability to detect separate processes, such as dissolution and secondary phase formation, occurring simultaneously on a mineral surface (Maurice, 1998).

### 13.5.2.2 Surface-Controlled Dissolution Mechanisms

Dissolution of oxide minerals through a surface-controlled reaction by ligand- and proton-promoted processes has been described by Furrer and Stumm (1986), Zinder et al. (1986), and Stumm and Furrer (1987) using a surface coordination approach. The important reactants in these processes are  $\text{H}_2\text{O}$ ,  $\text{H}^+$ ,  $\text{OH}^-$ , ligands, and reductants and oxidants. The reaction mechanism occurs in two steps (Stumm and Wollast, 1990):





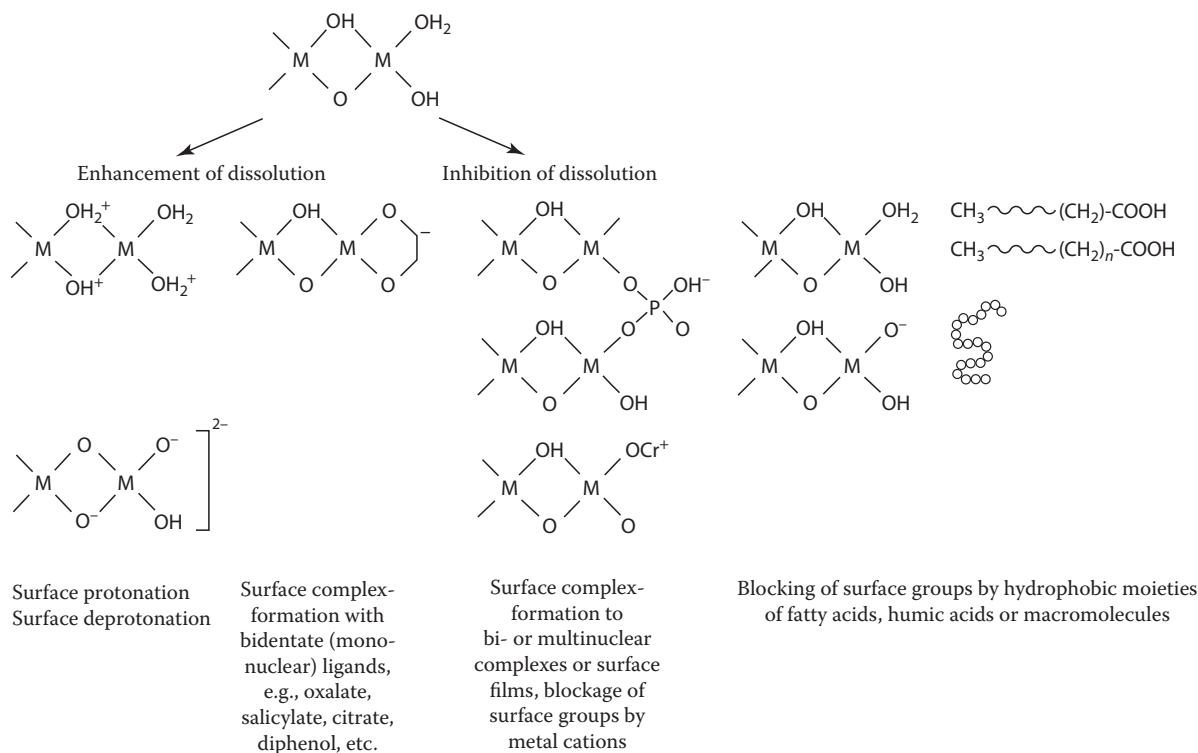
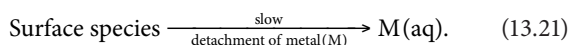


**FIGURE 13.24** The dependence of surface reactivity and of kinetic mechanisms on the coordinative environment of the surface groups. (Reprinted from Stumm, W., and R. Wollast. 1990. Coordination chemistry of weathering. Kinetics of the surface-controlled dissolution of oxide minerals. *Rev. Geophys.* 28:53–69. With permission from American Geophysical Union.)



Thus, the attachment of the reactants to the surface sites is fast, and detachment of metal species from the surface into solution is slow and rate limiting.

### 13.5.2.3 Ligand-Promoted Dissolution

Figure 13.24 shows how the surface chemistry of the mineral affects dissolution. One sees that surface protonation of the surface ligand increases dissolution by polarizing interatomic bonds close to the central surface ions that promote the release of a cation surface group into solution. Hydroxyls that bind to surface groups at higher pHs can ease the release of an anionic surface group into the solution phase.

Ligands that form surface complexes by ligand exchange with a surface hydroxyl add negative charge to the Lewis acid center coordination sphere and lower the Lewis acid acidity. This polarizes the M–O bonds causing detachment of the metal cation into the solution phase. Thus, inner-sphere surface complexation plays an important role in mineral dissolution. Ligands such as oxalate, salicylate, F<sup>-</sup>, EDTA, and NTA increase dissolution, but others, such as SO<sub>4</sub><sup>2-</sup>, CrO<sub>4</sub><sup>2-</sup>, and benzoate, inhibit dissolution. Phosphate, arsenate, and selenite enhance dissolution at low pH, and dissolution is inhibited at pH > 7 (Bondietti et al., 1993).

The reason for these differences may be that bidentate species that are mononuclear promote dissolution while binuclear bidentate species inhibit dissolution. With binuclear bidentate complexes, more energy may be needed to remove two central atoms from the crystal structure. With phosphate and arsenate, at low pH, mononuclear species are formed while at higher pH (~pH 7), binuclear or trinuclear surface complexes form. Mononuclear bidentate complexes are formed with oxalate while binuclear bidentate complexes form with CrO<sub>4</sub><sup>2-</sup>. Additionally, the electron donor properties of CrO<sub>4</sub><sup>2-</sup> and oxalate are also different. With CrO<sub>4</sub><sup>2-</sup>, a high redox potential is maintained at the oxide surface, which restricts reductive dissolution (Stumm and Wollast, 1990; Stumm, 1992). Dissolution can also be inhibited by cations such as VO<sup>2+</sup>, Cr(III), and Al(III) that block surface functional groups (Bondietti et al., 1993).

One can express the rate of the ligand-promoted dissolution ( $R_L$ ) as

$$R_L = k'_L (\equiv \text{ML}) = k'_L C_L^s, \quad (13.22)$$

where

$k'_L$  is the rate constant for ligand-promoted dissolution ( $t^{-1}$ )

ML is the metal–ligand complex

$C_L^s$  is the surface concentration of the ligand ( $\text{mol m}^{-2}$ )

Equation 13.22 adequately describes ligand-promoted dissolution of  $\gamma\text{-Al}_2\text{O}_3$  (Figure 13.25).

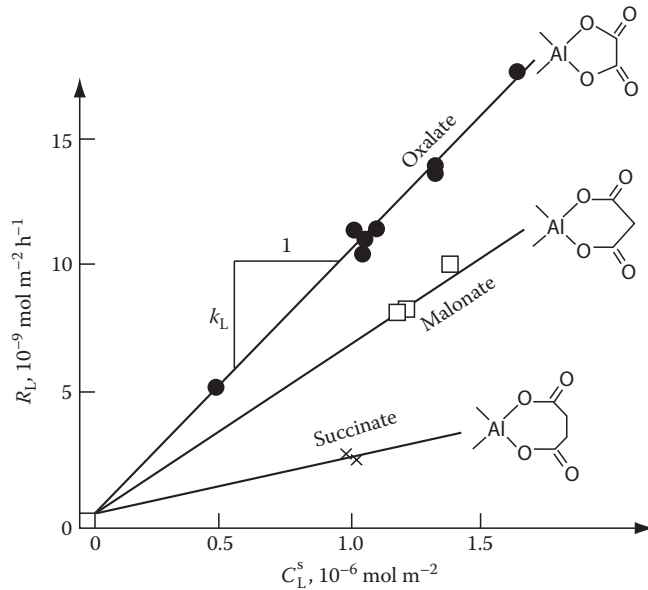


**FIGURE 13.25** The rate of ligand catalyzed dissolution of  $\gamma\text{-Al}_2\text{O}_3$  by the aliphatic ligands oxalate, malonate, and succinate,  $R_L$  ( $\text{nmol m}^{-2} \text{h}^{-1}$ ), can be interpreted as a linear dependence on the surface concentrations of the ligand complexes,  $C_L^s$ . In each case, the individual values for  $C_L^s$  were determined experimentally. (Reprinted from Furrer, G., and W. Stumm. 1986. The coordination chemistry of weathering. I. Dissolution kinetics of  $\gamma\text{-Al}_2\text{O}_3$  and BeO. *Geochim. Cosmochim. Acta* 50:1847–1860. With permission from Elsevier.)

#### 13.5.2.4 Proton-Promoted Dissolution

Under acid conditions, protons can promote mineral dissolution by binding to surface oxide ions, causing bonds to weaken which is followed by detachment of metal species into solution. The proton-promoted dissolution rate ( $R_H$ ) can be expressed as (Stumm and Wollast, 1990)

$$R_H = k'_H (\equiv\text{MOH}_2^+)^j = k'_H (C_H^s)^j, \quad (13.23)$$

where

$k'_H$  is the rate constant for proton-promoted dissolution

$\text{MOH}_2^+$  is the metal-proton complex

$C_H^s$  is the concentration of the surface-adsorbed proton complex ( $\text{mol}^{-2}$ )

$j$  corresponds to the oxidation state of the central metal ion in the oxide structure (i.e.,  $j = 3$  for Al(III) and Fe(III) in simple cases)

If dissolution occurs by only one mechanism,  $j$  is an integer. Figure 13.26 shows an application of Equation 13.23 for the proton-promoted dissolution of  $\gamma\text{-Al}_2\text{O}_3$ .

#### 13.5.2.5 Overall Dissolution Mechanisms

The rate of mineral dissolution, which is the sum of the ligand, proton, and deprotonation-promoted (or bonding of OH ligands) dissociation [ $R_{\text{OH}} = k'_{\text{OH}} (C_{\text{OH}}^s)^j$ ] rates along with the pH-independent portion of the dissolution rate ( $k'_{\text{H}_2\text{O}}$ ), which is due to hydration, can be expressed as (Stumm and Wollast, 1990)

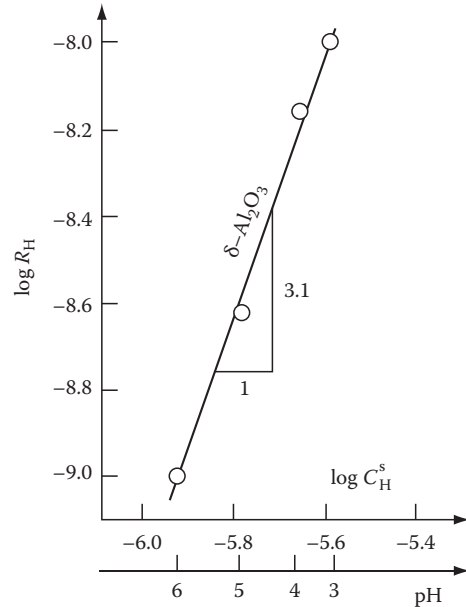


**FIGURE 13.26** The dependence of the rate of proton-promoted dissolution of  $\gamma\text{-Al}_2\text{O}_3$ ,  $R_H$  ( $\text{mol m}^{-2} \text{h}^{-1}$ ) on the surface concentration of the proton complexes,  $C_H^s$  ( $\text{mol m}^{-2}$ ). (Reprinted from Furrer, G., and W. Stumm. 1986. The coordination chemistry of weathering. I. Dissolution kinetics of  $\gamma\text{-Al}_2\text{O}_3$  and BeO. *Geochim. Cosmochim. Acta* 50:1847–1860. With permission of Elsevier Science, Amsterdam, the Netherlands.)

$$R = k'_L (C_L^s) + k'_H (C_H^s)^j + k'_{\text{OH}} (C_{\text{OH}}^s)^j + k'_{\text{H}_2\text{O}}. \quad (13.24)$$

Equation 13.24 is valid if dissolution occurs in parallel at varying metal centers (Furrer and Stumm, 1986).

#### 13.5.2.6 Dissolution Kinetics of Metal Hydroxide Precipitates

The formation of metal hydroxide surface precipitates appears to be an important way to sequester metals. As the surface precipitates age, metal dissolution is greatly reduced (Figure 13.27). Thus, the metals are less prone to leaching and being taken up by plants and microbes. Peltier et al. (2010) reacted two soils of varying mineralogy and organic matter content with 3 mM Ni at two pHs, 6 and 7.5, and evaluated Ni bioavailability using a biosensor. At pH 6, where surface precipitates did not form, 60% of the Ni was bioavailable. However, at pH 7.5, where precipitates were observed to form from XAFS analyses, Ni bioavailability was markedly reduced to 25%. Similar results were found by Everhart et al. (2006).

The decrease in metal release and bioavailability is linked to the increasing silication of the interlayer of the LDH phases with increased residence time, resulting in a mineral transformation from a LDH phase to a precursor phyllosilicate surface precipitate (Ford et al., 1999; Ford and Sparks, 2000). The mechanism for this transformation is thought to be due to diffusion of Si, originating from weathering of the sorbent, into the interlayer space

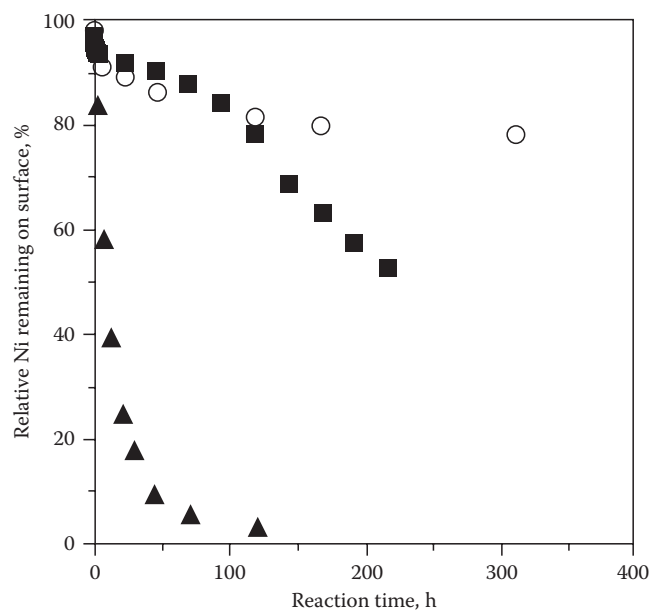
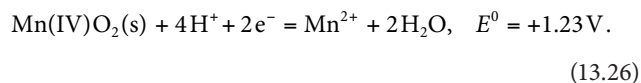
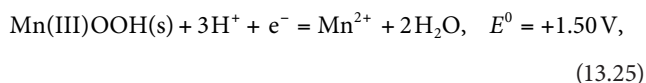


**FIGURE 13.27** Kinetics of Ni detachment from surface precipitates at pH = 4. Relative Ni remaining on the surface (%) is shown for the *conventional method* (O) and the *replenishment method* (■) as a function of the reaction time. Ninety-eight percent of the initial Ni was sorbed in the beginning of the detachment experiment. The dissolution of an equivalent amount of crystalline Ni(OH)<sub>2</sub> (in mol) at pH = 4 is given for comparison (▲). (Reprinted from Scheidegger, A.M., and D.L. Sparks. 1996a. Kinetics of the formation and the dissolution of nickel surface precipitates on pyrophyllite. *Chem. Geol.* 132:157–164. With permission of Elsevier Science, Amsterdam, the Netherlands.)

of the LDH, replacing the anions such as NO<sub>3</sub>. Polymerization and condensation of the interlayer Si slowly transform the LDH into a precursor metal–Al phyllosilicate. The metal stabilization that occurs in surface precipitates on Al-free sorbents (e.g., talc) may be due to Ostwald ripening, resulting in increased crystallization; however, microscopic analyses have shown that Ni–Al LDH phases appear to be amorphous (Livi et al., 2009). Peltier et al. (2006), using acid-solution calorimetry and results from previous calorimetry studies, showed that the enthalpy of formation of LDH phases is more exothermic, indicating great stability, on the order of Cl < NO<sub>3</sub> < SO<sub>4</sub> < CO<sub>3</sub> < Si of interlayer anionic composition, and that LDH phases were much more stable than a Ni(OH)<sub>2</sub> phase.

### 13.5.3 Redox Kinetics

It is well known that Mn(III/IV), Fe(III), Co(III), and Pb(IV) oxides/hydroxides are thermodynamically stable in oxygenated systems at neutral pH. However, under anoxic conditions, reductive dissolution of oxides/hydroxides by reducing agents occurs as shown below for MnOOH and MnO<sub>2</sub> (Stone, 1991):



Changes in the oxidation state of the metals associated with the oxides above can greatly affect their solubility and mobility in soil and aqueous environments. The reductants can be either inorganic or organic.

There are a number of natural and xenobiotic organic functional groups that are good reducers of oxides and hydroxides. These include carboxyl, carbonyl, phenolic, and alcoholic functional groups of SOM. Microorganisms in soils and sediments are also examples of organic reductants. Stone (1987a) showed that oxalate and pyruvate, two microbial metabolites, could reduce and dissolve Mn(III/IV) oxide particles. Inorganic reductants include As(III), Cr(III), and Pu(III).

#### 13.5.3.1 Mechanisms for Reductive Dissolution of Metal Oxides/Hydroxides

The reductive dissolution of metal oxides/hydroxides appears to occur in the following sequential steps (Stone, 1986, 1991): (1) diffusion of the reductant molecules to the oxide surface, (2) a surface CR, and (3) release of reaction products and diffusion away from the oxide surface. Steps (1) and (3) are transport steps. The rate-controlling step in reductive dissolution of oxides appears to be surface CR control. Reductive dissolution can be described by both inner- and outer-sphere complex mechanisms that involve (1) precursor complex formation, (2) electron transfer, and (3) breakdown of the successor complex (Figure 13.28). Inner-sphere and outer-sphere precursor complex formations are adsorption reactions that increase the density of reductant molecules at the oxide surface, which promotes electron transfer (Stone, 1991). In the inner-sphere mechanism, the reductant enters the inner coordination sphere by ligand exchange and bonds directly to the metal center prior to electron transfer. With the outer-sphere complex, the inner coordination sphere is left intact and electron transfer is enhanced by an outer-sphere precursor complex (Stone, 1986). Kinetic studies have shown that high rates of reductive dissolution are favored by high rates of precursor complex formation (i.e., large  $k_1$  and low  $k_{-1}$  values), high electron transfer rates (i.e., large  $k_2$ ), and high rates of product release (i.e., high  $k_3$ ; Figure 13.28).

Specifically, adsorbed cations and anions may reduce reductive dissolution rates by blocking oxide surface sites or by causing release of Mn(II) into solution. Stone and Morgan (1984a) showed that PO<sub>4</sub><sup>3-</sup> inhibited the reductive dissolution of Mn(III/IV) oxides by hydroquinone. Addition of 10<sup>-2</sup> M PO<sub>4</sub><sup>3-</sup> at pH 7.68 caused the dissolution rate to be only 25% of the rate when PO<sub>4</sub><sup>3-</sup> was not present. Phosphate had a greater effect than Ca<sup>2+</sup>.

#### 13.5.3.2 Oxidation of Pollutants

As mentioned earlier, Mn oxides can oxidize a number of environmentally important ions that can be toxic to humans and animals. Chromium and plutonium are similar in their chemical

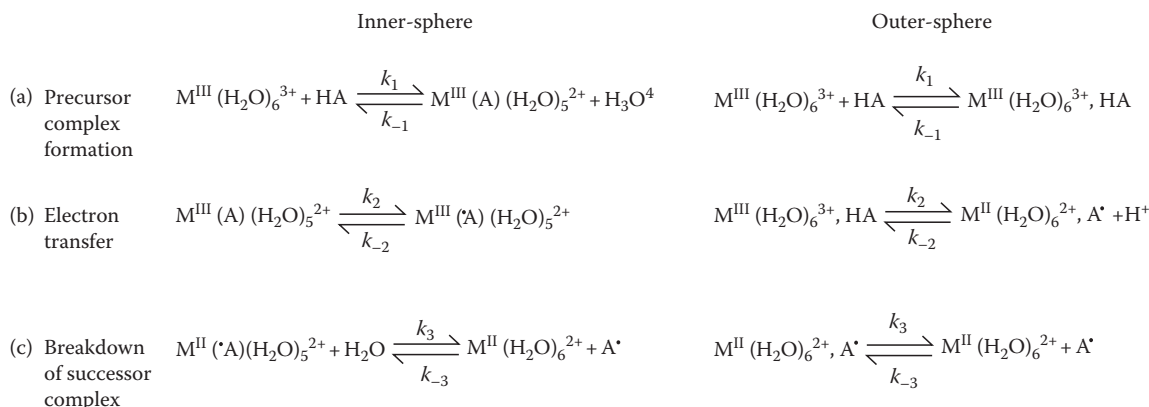


**FIGURE 13.28** Reduction of  $M(H_2O)_6^{3+}$  by phenol (HA) in homogeneous solution. (Reprinted with permission from Stone, A.T. 1986. Adsorption of organic reductants and subsequent electron transfer on metal oxide surfaces, p. 446–461. In J.A. Davis and K.F. Hayes (eds.) *Geochemical processes at mineral surfaces*. American Chemical Society, Washington, DC.)

behavior in aqueous settings (Rai and Serne, 1977; Bartlett and James, 1979). They can exist in multiple oxidation states and as both cationic and anionic species. Chromium(III) is quite stable and innocuous and occurs as  $Cr^{3+}$  and its hydrolysis products or as  $CrO_2^-$ . Chromium(III) can be oxidized to Cr(VI) by Mn(III/IV) oxides (Bartlett and James, 1979; Fendorf and Zamoski, 1992). Chromium(VI) is mobile in the soil environment and is a suspected carcinogen. It occurs as the dichromate ( $Cr_2O_7^{2-}$ ) or chromate ( $HCrO_4^-$  and  $CrO_4^{2-}$ ) anions (Huang, 1991).

Figure 13.29 shows the oxidation kinetics of Cr(III) to Cr(VI) in a soil. Most of the oxidation occurred during the

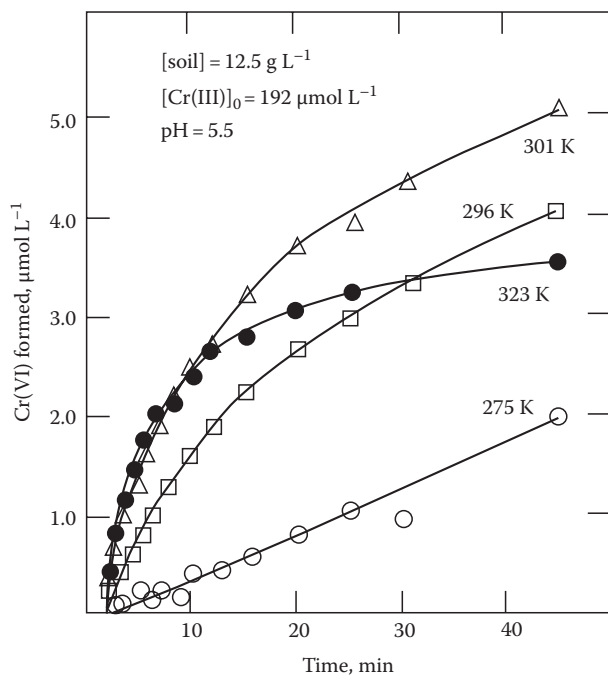
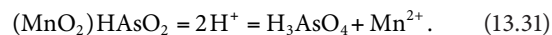
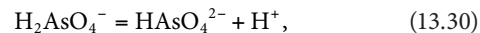
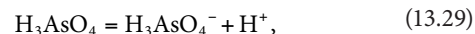
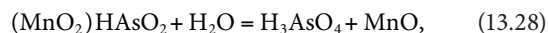
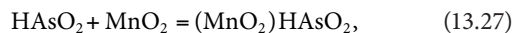


**FIGURE 13.29** Effect of temperature on the kinetics of Cr(III) oxidation in moist Hagerstown silt loam soil. (Reprinted with permission from Amacher, M.C., and D.E. Baker. 1982. Redox reactions involving chromium, plutonium, and manganese in soils. DOE/DP/04515 Pennsylvania State University, University Park, PA.)

first hour. At higher temperatures, there was a rapid oxidation rate, followed by a slower rate. Fendorf and Zamoski (1992) found that Cr(III) oxidation on  $\delta$ - $MnO_2$  was more rapid at pH 5 than pH 3 with overall production of Cr(VI) being greater at pH 3 at a Cr(III) concentration of 770  $\mu$ M. The rate and extent of Cr(III) oxidation are affected by a number of factors including formation of surface precipitates at higher pHs and Cr(III) concentrations that effectively inhibit oxidation (Fendorf et al., 1992).

Plutonium can exist in the III to VI oxidation states as  $Pu^{3+}$ ,  $Pu^{4+}$ ,  $PuO_2^{2+}$ , and  $PuO_2^{2+}$  in strongly acid solutions (Huang, 1991). Plutonium(VI), which can result from oxidation of Pu(III/IV) by Mn(III/IV) oxides (Amacher and Baker, 1982), is very toxic and mobile in soils and waters.

Arsenic (As) can exist in several oxidation states and forms in soils and waters. In waters, As can exist in the +5, +3, 0, and -3 oxidation states. Arsenite, As(III), and arsine ( $AsH_3$ , where the oxidation state of As is -3) are much more toxic to humans than arsenate, As(V). Manganese(III/IV) oxides can oxidize As(III) to As(V) as shown later where As(III) as  $HAsO_2$  is added to  $MnO_2$  to produce As(V) as  $H_3AsO_4$  (Oscarson et al., 1983):



Equation 13.28 involves the formation of an adsorbed layer. Oxygen transfer occurs and  $HAsO_2$  is oxidized to  $H_3AsO_4$  (Equation 13.28). At  $pH \leq 7$ , the predominant As(III) species is arsenious acid ( $HAsO_2$ ), but the oxidation product,  $H_3AsO_4$ , will

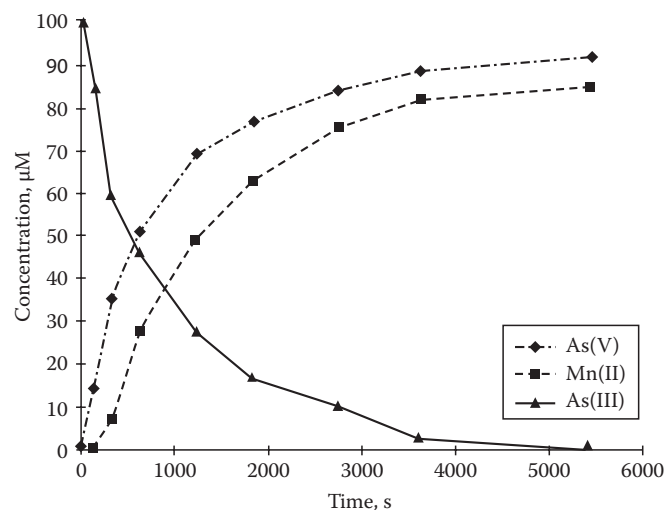


**FIGURE 13.30** Experimental behavior of aqueous As(III), As(V), and Mn(II) following 99.6 µM As(III) addition to a 0.21 g L<sup>-1</sup> of γ-MnO<sub>2</sub> particle suspension at pH 4, 25°C, and 0.1 M NaClO<sub>4</sub>. (Reprinted from Scott, M.J., and J.J. Morgan. 1995. Reactions at oxide surfaces. 1. Oxidation of As(III) by synthetic birnessite. *Environ. Sci. Technol.* 29:1898–1905. With permission from American Chemical Society.)

dissociate and form the same quantities of HAsO<sub>4</sub><sup>-</sup> and HAsO<sub>4</sub><sup>2-</sup> with little H<sub>3</sub>AsO<sub>4</sub> present at equilibrium (Equations 13.29 and 13.30). Each mole of As(III) oxidized releases about 1.5 mol H<sup>+</sup>. The H<sup>+</sup> produced after H<sub>3</sub>AsO<sub>4</sub> dissociation reacts with the adsorbed HAsO<sub>2</sub> on MnO<sub>2</sub>, forming H<sub>3</sub>AsO<sub>4</sub>, and leads to the reduction and dissolution of Mn(IV) (Equation 13.31). Thus, every mole of As(III) that is oxidized to As(V) results in 1 mol of Mn(IV) in the solid phase being reduced to Mn(II) and partially dissolved in solution (Oscarson et al., 1981).

Oscarson et al. (1980) studied the oxidation of As(III) to As(V) in sediments from five lakes in Saskatchewan, Canada. Oxidation of As(III) to As(V) occurred within 48 h. In general, >90% of the added As was sorbed on the sediments within 72 h. Scott and Morgan (1995) studied the oxidation of As(III) by synthetic birnessite. The depletion of As(III) was rapid with 50% of the initial As(III) removed from solution in 10 min, and after 90 min, the As(III) concentration was below the detection limit. Arsenic(V) was released into solution as fast as As(III) was depleted and the total concentration of aqueous As was about constant over the duration of the experiment (Figure 13.30). Scott and Morgan (1995) concluded that the process of electron transfer and release of As(V) were fast compared to the sorption of As(III), the rate-limiting step.

Recently, Parikh et al. (2008), Ginder-Vogel et al. (2009), and Landrot et al. (2010) have used real-time molecular scale ATR-FTIR and QXAS techniques to elucidate the rapid redox kinetics and mechanisms of As(III) oxidation (Parikh et al., 2008; Ginder-Vogel et al., 2009) and Cr(III) oxidation (Landrot et al., 2010) on Mn oxides. Figure 13.31 shows that the oxidation of As(III) on hydrous Mn oxide at pHs of 6–9 is extremely rapid with 50% of the reaction occurring within 1 min. Spectra for times >1 min are very similar with only small differences

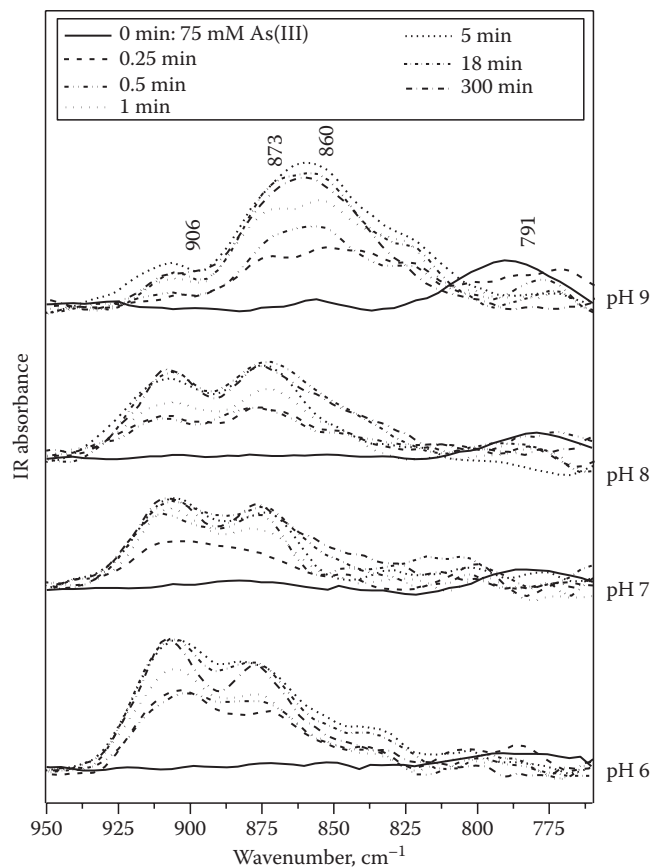


**FIGURE 13.31** ATR-FTIR spectra for HMO reacted with 75 mmol kg<sup>-1</sup> As(III) at pHs 6, 7, 8, and 9. Within 1 min of reaction, As(V) peaks (860, 873, and 906 cm<sup>-1</sup>) are observed and only minimal changes in spectra are observed in a subsequent 300 min period. (Reprinted from Parikh, S.J., B.J. Lafferty, and D.L. Sparks. 2008. An ATR-FTIR spectroscopic approach for measuring rapid kinetics at the mineral/water interface. *J. Colloid Interface Sci.* 320:177–185. With permission from Elsevier.)

in peak intensities. The reaction process is almost complete in 5 min. Figure 13.32 shows QXAS and traditional batch data for As(III) oxidation on hydrous Mn oxide. An initial concentration of 1.5 mM of As(III) was used. After 1 s of reaction, the As(V) concentration, indicating oxidation of As(III), reached 0.37 mM and continued to increase rapidly for 45 s to reach a concentration of 1 mM. The As(V) concentration continued to increase for the remainder of the reaction, reaching the initial 1.5 mM concentration after 300 s of reaction time (Ginder-Vogel et al., 2009). The initial apparent As(III) depletion rate constants ( $t < 30$  s) measured with QXAS were nearly twice as large as rate constants measured with traditional analytical techniques such as the batch method (Ginder-Vogel et al., 2009). Being able to measure the initial reaction rates with these techniques allows one to measure chemical rate constants that are independent of concentration, and, thus, important mechanistic information can be gleaned (Landrot et al., 2010).

Manganese oxides and hydroxides (e.g., Mn<sub>3</sub>O<sub>4</sub> and MnOOH) may also catalyze the oxidation of other trace metals such as Co<sup>2+</sup>,

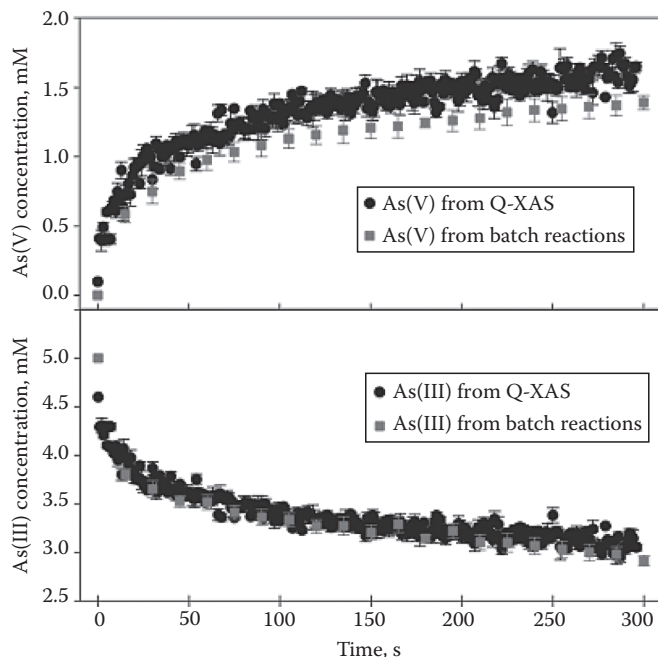
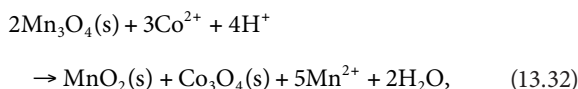


**FIGURE 13.32** As(V) and As(III) concentrations determined from traditional batch and QXAS reactions. Error bars represent the SD of three measurements made at each time point. (Reprinted from Ginder-Vogel, M., G. Landrot, J.S. Fischel, and D.L. Sparks. 2009. Quantification of rapid environmental redox processes with quick-scanning X-ray absorption spectroscopy (Q-XAS). *Proc. Natl Acad. Sci. U. S. A.* 106:16124–16128. With permission National Academy of Sciences, USA.)

$\text{Co}^{3+}$ ,  $\text{Cu}^{2+}$ ,  $\text{Ni}^{2+}$ ,  $\text{Ni}^{3+}$ , and  $\text{Pb}^{2+}$  by disproportionation to  $\text{Mn}^{2+}$  and  $\text{MnO}_2$  (Hem, 1978). The disproportionation results in vacancies in the Mn oxide structure. Since the  $\text{Mn}^{2+}$  and  $\text{Mn}^{3+}$  in the oxides have similar physical sizes as  $\text{Co}^{2+}$ ,  $\text{Co}^{3+}$ ,  $\text{Cu}^{2+}$ ,  $\text{Ni}^{2+}$ ,  $\text{Ni}^{3+}$ , and  $\text{Pb}^{2+}$ , these metals can occupy the vacancies in the Mn oxide and become part of the structure. With disproportionation or with other redox processes involving the Mn oxides, the solubility of the metals can be affected. For example, if during the disproportionation process  $\text{Co}_3\text{O}_4$ , the oxidized form of the metal forms from  $\text{Co}^{2+}$ , the reaction can be expressed as (Hem, 1978)



and the equilibrium constant ( $K^\circ$ ) is (Hem, 1978)

$$\frac{(\text{Mn}^{2+})^5}{(\text{Co}^{2+})^3(\text{H}^+)^4} = 10^{18.73}. \quad (13.33)$$

Thus, the oxidation of Co(II) to Co(III) reduces its solubility and mobility in the environment. Using XPS analyses (Murray and Dillard, 1979), this reaction has been shown to occur. More recent evidence for heterogeneous redox reactions of trace metals is discussed in Chapter 19. Scott and Morgan (1996) studied the

**TABLE 13.5** Inorganic Redox Reactions with Manganese Dioxides

System	Time to Oxidize 50%	Driving Force at pH 4 $\Delta e^\circ$ (V) <sup>a</sup>	Source
$\delta\text{-MnO}_2$ ; As(III) $\rightarrow$ As(V) pH 4, 25°C, 14 m <sup>2</sup> L <sup>-1</sup>	10 min	+0.529	Scott and Morgan (1995)
$\delta\text{-MnO}_2$ ; Se(IV) $\rightarrow$ Se(VI) pH 4, 35°C, 14 m <sup>2</sup> L <sup>-1</sup>	10 days		
pH 4, 25°C, 28 m <sup>2</sup> L <sup>-1</sup>	16 days	+0.092	
pH 4, 25°C, 14 m <sup>2</sup> L <sup>-1</sup>	30 days		
$\beta\text{-MnO}_2$ ; Cr(III) $\rightarrow$ Cr(VI) pH 4, 25°C, 71 m <sup>2</sup> L <sup>-1</sup>	95 days	+0.011	Eary and Rai (1987)

Source: Reprinted from Scott, M.J., and J.J. Morgan. 1995. Reactions at oxide surfaces. 1. Oxidation of As(III) by synthetic birnessite. *Environ. Sci. Technol.* 29:1898–1905. With permission American Chemical Society.

<sup>a</sup> The activity ratio for each oxidant/reductant pair is taken as unity.

oxidation of Se(IV) by synthetic birnessite. Se(IV) was oxidized to Se(VI) with Se(VI) first appearing in the aqueous suspension after 12 h and was produced at a constant rate over the duration of the experiment (28 days). Scott and Morgan (1996) suggested the following oxidation mechanisms: (1) birnessite directly oxidized Se(IV) through a surface complex mechanism; (2) the rate-limiting step in the production of Se(VI) was the electron transfer step involving a transfer of two electrons from the anion to the metal ion, breaking of two Mn–O bonds, and addition of an O from water to Se(VI); and (3) the reaction products Se(VI) and Mn(II) were released from the surface by different steps.

Scott and Morgan (1996) compared their results with those of Eary and Rai (1987) who studied Cr(III) oxidation by pyrolusite ( $\beta\text{-MnO}_2$ ) between pH 3.0 and 4.7 and Scott and Morgan (1995) who studied As(III) oxidation by birnessite ( $\delta\text{-MnO}_2$ ) at pH values between 4.0 and 8.2 (Table 13.5). The Cr(III) redox transformation on pyrolusite was slowest which Scott and Morgan (1996) attributed to unfavorable adsorption on both a positively charged surface and aqueous species and the small thermodynamic driving force. Also, the transfer of three electrons from Cr(III) to Mn(IV) requires the involvement of more than one Mn(IV) atom per Cr(III) atom.

Manganese oxides also appear to play an important role in ligand-facilitated metal transport. Using soil columns that consisted of fractured saprolite coated with amorphous Fe and Mn oxides, Jardine et al. (1993) studied the transport of Co(II)  $\text{EDTA}^{2-}$ , a mixture of Co(II)  $\text{EDTA}^{2-}$  and Co(III)  $\text{EDTA}^-$  and Sr  $\text{EDTA}^{2-}$ . The Mn oxides oxidized Co(II)  $\text{EDTA}^{2-}$  into Co(III)  $\text{EDTA}^-$ , a very stable complex (log  $K$  value of 41.4; Xue and Traina, 1996). The formation of this complex resulted in enhanced transport of Co.

Xue and Traina (1996) found that an aerobic goethite suspension catalyzed oxidation of Co(II)  $\text{EDTA}^{2-}$  to Co(III)  $\text{EDTA}^-$  by dissolved  $\text{O}_2$ . The kinetics were described using a pseudo-first-order rate constant,  $k_1$  of  $0.0078 \pm 0.0002 \text{ h}^{-1}$  at pH 5 and a goethite concentration of  $3.09 \text{ g L}^{-1}$ .

A number of investigators have studied the reductive dissolution of Mn oxides by organic pollutants such as hydroquinone (Stone and Morgan, 1984a), substituted phenols (Stone, 1987b), and other organic compounds (Stone and Morgan, 1984b). With substituted phenols, the rate of dissolution was proportional to substituted phenol concentration and the rate increased as pH decreased (Stone, 1987b). Phenols containing alkyl, alkoxy, or other electron-donating substituents were more slowly degraded; *p*-nitrophenol reacted slowly with Mn(III/IV) oxides. The increased rate of reductive dissolution at lower pH may be due to more protonation reactions that enhance the creation of precursor complexes or increases in the protonation level of the surface precursor complexes that increase electron transfer rates (Stone, 1987b). Further discussions on this topic can be found in Chapter 19.

### 13.6 Conclusions

Research on the kinetics and mechanisms of soil CRs will be a common theme in soil and environmental sciences for decades to come. This research emphasis is in large part due to the need to more accurately understand and predict the long-term fate and transport of contaminants in the subsurface environment. Without such data, economically sound decisions about soil remediation cannot be made and risk assessment models are incomplete and most probably inaccurate.

While some very fine and informative research on rates and mechanisms of soil CRs/processes has been conducted in the past few decades, there are many gaps that need to be filled. The following research is needed: (1) more accurate kinetic models that describe reactions on multireactive, heterogeneous particle surfaces; (2) long-term sorption and particularly, desorption rate studies; (3) a better understanding of residence time effects on plant nutrient, radionuclide, metal, and organic retention/release mechanisms on soils and other natural materials; (4) an increased knowledge of nucleation/precipitation and dissolution reaction rate phenomena at the mineral/water interface and their effect on nutrient/contaminant mobility and bioavailability in the soil environment; (5) more studies on the kinetics and mechanisms of redox processes in soils, particularly the role that soil components such as Mn oxides have on oxidation/reduction of inorganic and organic pollutants; and (6) increased use of real-time molecular scale in situ spectroscopic and microscopic techniques to confirm reaction mechanisms.

### References

- Aharoni, C. 1984. Kinetics of adsorption: The S-shaped Z(t) plot. *Adsorp. Sci. Technol.* 1:1–29.
- Aharoni, C., and D.L. Sparks. 1991. Kinetics of soil chemical reactions: A theoretical treatment, p. 1–18. *In* D.L. Sparks and D.L. Suarez (eds.) Rates of soil chemical processes. SSSA, Madison, WI.
- Aharoni, C., and Y. Suzin. 1982a. Application of the Elovich equation to the kinetics of occlusion: Part 1. Homogenous micro-porosity. *J. Chem. Soc., Faraday Trans. 1* 78:2313–2320.
- Aharoni, C., and Y. Suzin. 1982b. Application of the Elovich equation to the kinetics of occlusion: Part 3. Heterogenous micro-porosity. *J. Chem. Soc., Faraday Trans. 1* 78:2329–2336.
- Aharoni, C., and M. Ungarish. 1976. Kinetics of activated chemisorption. Part 1. The non-Elovichian part of the isotherm. *J. Chem. Soc., Faraday Trans. 1* 72:400–408.
- Ainsworth, C.C., J.L. Pilon, P.L. Gassman, and W.G. Van Der Sluys. 1994. Cobalt, cadmium, and lead sorption to hydrous iron oxide: Residence time effect. *Soil Sci. Soc. Am. J.* 58:1615–1623.
- Alexander, M. 1995. How toxic are toxic-chemicals in soil. *Environ. Sci. Technol.* 29:2713–2717.
- Allen, E.R., D.W. Ming, L.R. Hossner, and D.L. Henninger. 1995. Modeling transport kinetics in clinoptilolite–phosphate rock systems. *Soil Sci. Soc. Am. J.* 59:248–255.
- Amacher, M.C. 1991. Methods of obtaining and analyzing kinetic data, p. 19–59. *In* D.L. Sparks and D.L. Suarez (eds.) Rates of soil chemical processes. SSSA, Madison, WI.
- Amacher, M.C., and D.E. Baker. 1982. Redox reactions involving chromium, plutonium, and manganese in soils. DOE/DP/04515 Pennsylvania State University, University Park, PA.
- Atkinson, R.J., F.J. Hingston, A.M. Posner, and J.P. Quirk. 1970. Elovich equation for the kinetics of isotope exchange reactions at solid–liquid interfaces. *Nature* 226:148–149.
- Backes, E.A., R.G. McLaren, A.W. Rate, and R.S. Swift. 1995. Kinetics of cadmium and cobalt desorption from iron and manganese oxides. *Soil Sci. Soc. Am. J.* 59:778–785.
- Ball, W.P., and P.V. Roberts. 1991. Long-term sorption of halogenated organic chemicals by aquifer material: 1. Equilibrium. *Environ. Sci. Technol.* 25:1223–1237.
- Bartlett, R., and B. James. 1979. Behavior of chromium in soils. III. Oxidation. *J. Environ. Qual.* 8:31–35.
- Bernasconi, C.F. 1976. Relaxation kinetics. Academic Press, New York.
- Bondiotti, G., J. Sinniger, and W. Stumm. 1993. The reactivity of Fe(III) (hydr)oxides: Effects of ligands in inhibiting the dissolution. *Colloids Surf. A* 79:157–167.
- Borda, M.J., and D.L. Sparks. 2008. Kinetics and mechanisms of sorption–desorption in soils: A multiscale assessment, p. 97–124. *In* A. Violante, P.M. Huang, and G.M. Gadd (eds.) Biophysico-chemical processes of heavy metals and metalloids in soil environments. John Wiley & Sons, Inc., New York.
- Bosbach, D., and W. Rammensee. 1994. In situ investigation of growth and dissolution on the (010) surface of gypsum by scanning force microscopy. *Geochim. Cosmochim. Acta* 58:843–849.
- Bruemmer, G.W., J. Gerth, and K.G. Tiller. 1988. Reaction kinetics of the adsorption and desorption of nickel, zinc and cadmium by goethite: I. Adsorption and diffusion of metals. *J. Soil Sci.* 39:37–52.
- Brusseau, M.L., and P.S.C. Rao. 1989. Sorption non-ideality during organic contaminant transport in porous media. *CRC Crit. Rev. Environ. Control* 19:33–99.
- Bunnett, J.F. 1986. Kinetics in solution, p. 171–250. *In* C.F. Bernasconi (ed.) Investigations of rates and mechanisms of reactions. Wiley, New York.

- Bunzl, K., W. Schmidt, and B. Sansoni. 1976. Kinetics of ion exchange in soil organic matter. IV. Adsorption and desorption of  $Pb^{2+}$ ,  $Cu^{2+}$ ,  $Zn^{2+}$ , and  $Ca^{2+}$  by peat. *J. Soil. Sci.* 27:32–41.
- Carroll, K.M., M.R. Harkness, A.A. Bracco, R.R. Balcarcel. 1994. Application of a permeant/polymer diffusional model to the desorption of polychlorinated biphenyls from Hudson River sediments. *Environ. Sci. Technol.* 28:253–258.
- Casey, W.H., H.R. Westrich, G.W. Arnold, and J.F. Banfield. 1989. The surface chemistry of dissolving labradorite feldspar. *Geochim. Cosmochim. Acta* 53:821–832.
- Chang, M.L., S.C. Wu, and C.Y. Chen. 1997. Diffusion of volatile organic compounds in pressed humic acid disks. *Environ. Sci. Technol.* 31:2307–2312.
- Charlet, L., and A. Manceau. 1993. Structure, formation, and reactivity of hydrous oxide particles: Insights from X-ray absorption spectroscopy, p. 117–164. *In* J. Buffle and H.P. van Leeuwen (eds.) *Environmental particles*. Lewis Publishers, Boca Raton, FL.
- Chien, S.H., and W.R. Clayton. 1980. Application of Elovich equation to the kinetics of phosphate release and sorption in soils. *Soil Sci. Soc. Am. J.* 44:265–268.
- Chute, J.H., and J.P. Quirk. 1967. Diffusion of potassium from mica-like materials. *Nature* 213:1156–1157.
- Comans, R.N.J., and D.E. Hockley. 1992. Kinetics of cesium sorption on illite. *Geochim. Cosmochim. Acta* 56:1157–1164.
- Connaughton, D.F., J.R. Stedinger, L.W. Lion, and M.L. Shuler. 1993. Description of time-varying desorption kinetics: Release of naphthalene from contaminated soils. *Environ. Sci. Technol.* 27:2397–2403.
- Cornelissen, G., P.C.M. van Noort, J.R. Parsons, and H.A.J. Govers. 1997. Temperature dependence of slow adsorption and desorption kinetics of organic compounds in sediments. *Environ. Sci. Technol.* 31:454–460.
- Crank, J. 1976. *The mathematics of diffusion*. 2nd edn. Oxford University Press (Clarendon), London, U.K.
- DiToro, D.M., and L.M. Horzempa. 1982. Reversible and resistant components of PCB adsorption–desorption: Isotherms. *Environ. Sci. Technol.* 16:594–602.
- Divincenzo, J.P., and D.L. Sparks. 1997. Slow sorption kinetics of pentachlorophenol on soil: Concentration effects. *Environ. Sci. Technol.* 31:977–983.
- Eary, L.E., and D. Rai. 1987. Kinetics of chromium(III) oxidation to chromium(VI) by reaction with manganese dioxide. *Environ. Sci. Technol.* 21:1187–1193.
- Elzinga, E.J., and D.L. Sparks. 1999. Nickel sorption mechanisms in a pyrophyllite–montmorillonite mixture. *J. Colloid Interface Sci.* 213:506–512.
- Everhart, J.L., D. McNear Jr., E. Peltier, D. van der Lelie, R.L. Chaney, and D.L. Sparks. 2006. Assessing nickel bioavailability in smelter-contaminated soils. *Sci. Total Environ.* 367:732–744.
- Fendorf, S., M.J. Eick, P. Grossl, and D.L. Sparks. 1997. Arsenate and chromate retention mechanisms on goethite. 1. Surface structure. *Environ. Sci. Technol.* 31:315–320.
- Fendorf, S.E., M. Fendorf, D.L. Sparks, and R. Gronsky. 1992. Inhibitory mechanisms of Cr(III) oxidation by  $\delta$ - $MnO_2$ . *J. Colloid Interface Sci.* 153:37–54.
- Fendorf, S.E., G.M. Lamble, M.G. Stapleton, M.J. Kelley, and D.L. Sparks. 1994. Mechanisms of chromium(III) sorption on silica: 1. Cr(III) surface structure derived by extended X-ray absorption fine structure spectroscopy. *Environ. Sci. Technol.* 28:284–289.
- Fendorf, S.E., and R.J. Zasoski. 1992. Chromium(III) oxidation by  $\delta$ - $MnO_2$ . 1. Characterization. *Environ. Sci. Technol.* 26:79–85.
- Fendorf, S.E. et al. 1993. *Soil Sci. Soc. Am. J.*, 57:57–62.
- Ford, R.G., A.C. Scheinost, K.G. Scheckel, and D.L. Sparks. 1999. The link between clay mineral weathering and the stabilization of Ni surface precipitates. *Environ. Sci. Technol.* 33:3140–3144.
- Ford, R.G., and D.L. Sparks. 2000. The nature of Zn precipitates formed in the presence of pyrophyllite. *Environ. Sci. Technol.* 34:2479–2483.
- Fuller, C.C., J.A. Davis, and G.A. Waychunas. 1993. Surface chemistry of ferrihydrite: Part 2. Kinetics of arsenate adsorption and coprecipitation. *Geochim. Cosmochim. Acta* 57:2271–2282.
- Furrer, G., and W. Stumm. 1986. The coordination chemistry of weathering. I. Dissolution kinetics of  $\gamma$ - $Al_2O_3$  and BeO. *Geochim. Cosmochim. Acta* 50:1847–1860.
- Gardiner, W.C., Jr. 1969. *Rates and mechanisms of chemical reactions*. Benjamin, New York.
- Ginder-Vogel, M., G. Landrot, J.S. Fischel, and D.L. Sparks. 2009. Quantification of rapid environmental redox processes with quick-scanning X-ray absorption spectroscopy (Q-XAS). *Proc. Natl Acad. Sci. U. S. A.* 106:16124–16128.
- Grossl, P.R., M. Eick, D.L. Sparks, S. Goldberg, and C.C. Ainsworth. 1997. Arsenate and chromate retention mechanisms on goethite. 2. Kinetic evaluation using a pressure-jump relaxation technique. *Environ. Sci. Technol.* 31:321–326.
- Grossl, P.R., and D.L. Sparks. 1995. Evaluation of contaminant ion adsorption/desorption on goethite using pressure-jump relaxation kinetics. *Geoderma* 67:87–101.
- Grossl, P.R., D.L. Sparks, and C.C. Ainsworth. 1994. Rapid kinetics of Cu(II) adsorption/desorption on goethite. *Environ. Sci. Technol.* 28:1422–1429.
- Hachiya, K., M. Sasaki, I. Ikeda, N. Mikami, and T. Yasunaga. 1984. Static and kinetic studies of adsorption–desorption of metal ions on a  $\gamma$ - $Al_2O_3$  surface. 2. Kinetic studies by means of pressure-jump technique. *J. Phys. Chem.* 88:27–31.
- Hamaker, J.W., and J.M. Thompson. 1972. Adsorption, p. 39–151. *In* C.A.I. Goring and J.W. Hamaker (eds.) *Organic chemicals in the environment*. Marcel Dekker, New York.
- Harmon, T.C., L. Semprini, and P.V. Roberts. 1992. Simulating solute transport using laboratory-based sorption parameters. *J. Environ. Eng.* 118:666–689.
- Havlin, J.L., and D.G. Westfall. 1985. Potassium release kinetics and plant response in calcareous soils. *Soil Sci. Soc. Am. J.* 49:366–370.



- Hayes, K.F., and J.O. Leckie. 1986. Mechanism of lead ion adsorption at the goethite-water interface. *ACS Symp. Ser.* 323:114-141.
- Hellman, R., B. Drake, and K. Kjoller. 1992. Using atomic force microscopy to study the structure, topography and dissolution of albite surfaces, p. 149-152. *In* Y.K. Kharaka and A.S. Maest (eds.) *Water-rock interaction VII*. A.A. Balkema, Rotterdam, the Netherlands.
- Hem, J.D. 1978. Redox processes at the surface of manganese oxide and their effects on aqueous metal ions. *Chem. Geol.* 21:199-218.
- Hillner, P.E., A.J. Gratz, S. Manne, and P.K. Hansma. 1992a. Atomic-scale imaging of calcite growth and dissolution in real-time. *Geology* 20:359-362.
- Hillner, P.E., S. Manne, A.J. Gratz, and P.K. Hansma. 1992b. AFM images of dissolution and growth on a calcite crystal. *Ultramicroscopy* 44:1387-1393.
- Huang, P.M. 1991. Kinetics of redox reactions on manganese oxides and its impact on environmental quality, p. 191-230. *In* D.L. Sparks and D.L. Suarez (eds.) *Rates of soil chemical processes*. SSSA, Madison, WI.
- Jardine, P.M., F.M. Dunnivant, H.M. Selim, and J.F. McCarthy. 1992. Comparison of models for describing the transport of dissolved organic carbon in aquifer columns. *Soil Sci. Soc. Am. J.* 56:393-401.
- Jardine, P.M., G.K. Jacobs, and J.D. Odell. 1993. Unsaturated transport processes in undisturbed heterogeneous porous-media. 2. Cocontaminants. *Soil Sci. Soc. Am. J.* 57:954-962.
- Jardine, P.M., and D.L. Sparks. 1984. Potassium-calcium exchange in a multireactive soil system. I. Kinetics. *Soil Sci. Soc. Am. J.* 48:39-45.
- Johnsson, P.A., M.F. Hochella, Jr., G.A. Parks, A.E. Blum, and G. Sposito. 1992. Direct observation of muscovite basal-plane dissolution and secondary phase formation: An XPS, LEED, and SFM study, p. 159-162. *In* Y.K. Kharaka and A.S. Maest (eds.) *Water-rock interaction VII*. A.A. Balkema, Rotterdam, the Netherlands.
- Jordan, G., and W. Rammensee. 1996. Dissolution rates and activation energy for dissolution of brucite(001): A new method based on the microtopography of crystal surfaces. *Geochim. Cosmochim. Acta* 60:5055-5062.
- Junta, J.L., and M.F. Hochella, Jr. 1994. Manganese(II) oxidation at mineral surfaces: A microscopic and spectroscopic study. *Geochim. Cosmochim. Acta* 58:4985-4999.
- Kan, A.T., G.M. Fu, M.A. Hunter, and M.B. Tomson. 1997. Irreversible adsorption of naphthalene and tetrachlorobiphenyl to Lula and surrogate sediments. *Environ. Sci. Technol.* 31:2176-2185.
- Karickhoff, S.W. 1980. Sorption kinetics of hydrophobic pollutants in natural sediments, p. 193-205. *In* R.A. Baker (ed.) *Contaminants and sediments*. Ann Arbor Science, Ann Arbor, MI.
- Karickhoff, S.W., D.S. Brown, and T.A. Scott. 1979. Sorption of hydrophobic pollutants on natural sediments. *Water Res.* 13:241-248.
- Karickhoff, S.W., and K.R. Morris. 1985. Sorption dynamics of hydrophobic pollutants in sediment suspensions. *Environ. Toxicol. Chem.* 4:469-479.
- Keren, R., P.R. Grossl, and D.L. Sparks. 1994. Equilibrium and kinetics of borate adsorption-desorption on pyrophyllite in aqueous suspensions. *Soil Sci. Soc. Am. J.* 58:1116-1122.
- Krishnamurti, G.S.R., G. Cieslinski, P.M. Huang, and K.C.J. VanRees. 1997. Kinetics of cadmium release from soils as influenced by organic acids: Implication in cadmium availability. *J. Environ. Qual.* 26:271-277.
- Krishnamurti, G.S.R., and P.M. Huang. 1992. Dynamics of potassium chloride induced manganese release in different soil orders. *Soil Sci. Soc. Am. J.* 56:11115-11123.
- Kuo, S., and E.G. Lotse. 1974. Kinetics of phosphate adsorption and desorption by lake sediments. *Soil Sci. Soc. Am. Proc.* 38:50-54.
- Kuo, S., and D.S. Mikkelsen. 1980. Kinetics of zinc desorption from soils. *Plant Soil* 56:355-364.
- Landrot, G., M. Ginder-Vogel, and D.L. Sparks. 2010. Kinetics of chromium(III) oxidation by manganese(IV) oxides using quick scanning X-ray absorption fine structure spectroscopy (Q-XAFS). *Environ. Sci. Technol.* 44:143-149.
- Lasaga, A.C. 1984. Chemical-kinetics of water-rock interactions. *J. Geophys. Res.* 89:4009-4025.
- Lee, L.S., P.S.C. Rao, M.L. Brusseau, and R.A. Ogwada. 1988. Nonequilibrium sorption of organic contaminants during flow through columns of aquifer materials. *Environ. Toxicol. Chem.* 7:779-793.
- Leenheer, J.A., and J.L. Ahrlichs. 1971. A kinetic and equilibrium study of the adsorption of carbaryl and parathion upon soil organic matter surfaces. *Soil Sci. Soc. Am. Proc.* 35:700-704.
- Lehmann, R.G., and R.D. Harter. 1984. Assessment of copper-soil bond strength by desorption kinetics. *Soil Sci. Soc. Am. J.* 48:769-772.
- Livi, K.J.T., G.S. Senesi, A.C. Scheinost, and D.L. Sparks. 2009. Microscopic examination of nanosized mixed Ni-Al hydroxide surface precipitates on pyrophyllite. *Environ. Sci. Technol.* 43:1299-1304.
- Loehr, R.C., and M.T. Webster. 1996. Behavior of fresh vs aged chemicals in soil. *J. Soil Contam.* 5:361-383.
- Lövgren, L., S. Sjöberg, and P.W. Schindler. 1990. Acid/base reactions and Al(III) complexation at the surface of goethite. *Geochim. Cosmochim. Acta* 54:1301-1306.
- Low, M.J.D. 1960. Kinetics of chemisorption of gases on solids. *Chem. Rev.* 60:267-312.
- Matocha, C.J., K.G. Scheckel, and D.L. Sparks. 2005. Kinetics and mechanisms of soil biogeochemical processes, p. 309-342. *In* M.A. Tabatabai and D.L. Sparks (eds.) *Chemical processes in soils*. SSSA, Madison, WI.
- Maurice, P.A. 1998. Scanning probe microscopy of environmental surfaces, p. 109-154. *In* P.M. Huang, N. Senesi, and J. Buffle (eds.) *Structure and surface reactions of soil particles*. Vol. 4. John Wiley & Sons, New York.

- Maurice, P.A., M.F. Hochella, Jr., G.A. Parks, G. Sposito, and U. Schwertmann. 1995. Evolution of hematite surface microtopography upon dissolution by simple organic acids. *Clays Clay Miner.* 43:29–38.
- McCall, P.J., and G.L. Agin. 1985. Desorption kinetics of picloram as affected by residence time in the soil. *Environ. Toxicol. Chem.* 4:37–44.
- McNear, D.H., R.L. Chaney, and D.L. Sparks. 2007. The effects of soil type and chemical treatment on nickel speciation in refinery enriched soils: A multi-technique investigation. *Geochim. Cosmochim. Acta* 71:2190.
- Mikami, N., M. Sasaki, K. Hachiya, R.D. Ikeda, and T. Yasunaga. 1983a. Kinetics of the adsorption of  $\text{PO}_4$  on the  $\gamma\text{-Al}_2\text{O}_3$  surface using the pressure-jump technique. *J. Phys. Chem.* 87:1454–1458.
- Mikami, N., M. Sasaki, K. Hachiya, and T. Yasunaga. 1983b. Kinetic study of the adsorption–desorption of the uranyl ion on a  $\gamma\text{-Al}_2\text{O}_3$  surface using the pressure-jump technique. *J. Phys. Chem.* 87:5478–5481.
- Mikami, N., M. Sasaki, T. Kikuchi, and T. Yasunaga. 1983c. Kinetics of the adsorption–desorption of chromate on  $\gamma\text{-Al}_2\text{O}_3$  surfaces using the pressure-jump technique. *J. Phys. Chem.* 87:5245–5248.
- Miller, C.T., and J. Pedit. 1992. Use of a reactive surface–diffusion model to describe apparent sorption–desorption hysteresis and abiotic degradation of lindane in a subsurface material. *Environ. Sci. Technol.* 26:1417–1427.
- Murray, J.W., and J.G. Dillard. 1979. The oxidation of cobalt(II) adsorbed on manganese dioxide. *Geochim. Cosmochim. Acta* 43:781–787.
- Nachtegaal, M., M.A. Marcus, J.E. Sonke, J. Vangronsveld, K.J.T. Livi, D. Van der Lelie, and D.L. Sparks. 2005. Effects of in situ remediation on the speciation and bioavailability of zinc in a smelter contaminated soil. *Geochim. Cosmochim. Acta* 69:4649–4664.
- Nkedi-Kizza, P., J.W. Biggar, H.M. Selim, M.Th. van Genuchten, P.J. Wierenga, J.M. Davidson, and D.R. Nielsen. 1984. On the equivalence of two conceptual models for describing ion exchange during transport through an aggregated oxid. *Water Resour. Res.* 20:1123–1130.
- O'Day, P.A., G.E. Brown, and G.A. Parks. 1994a. X-Ray absorption spectroscopy of cobalt(II) multinuclear surface complexes and surface precipitates on kaolinite. *J. Colloid Interface Sci.* 165:269–289.
- O'Day, P.A., G.A. Parks, and G.E. Brown, Jr. 1994b. Molecular structure and binding sites of cobalt(II) surface complexes on kaolinite from X-ray absorption spectroscopy. *Clays Clay Miner.* 42:337–355.
- Onken, A.B., and R.L. Matheson. 1982. Dissolution rate of EDTA-extractable phosphate from soils. *Soil Sci. Soc. Am. J.* 46:276–279.
- Oscarson, D.W., P.M. Huang, C. Defosse, and A. Herbillon. 1981. The oxidative power of Mn(IV) and Fe(III) oxides with respect to As(III) in terrestrial and aquatic environment. *Nature* 291:50–51.
- Oscarson, D.W., P.M. Huang, and U.T. Hammer. 1983. Oxidation and sorption of arsenite by manganese dioxide as influenced by surface coatings of iron and aluminum oxides and calcium carbonate. *Water Air Soil Pollut.* 20:233–244.
- Oscarson, D.W., P.M. Huang, and W.K. Liaw. 1980. The oxidation of arsenite by aquatic sediments. *J. Environ. Qual.* 9:700–703.
- Padmanabham, M. 1983. Adsorption–desorption behavior of copper(II) at the goethite–solution interface. *Aust. J. Soil Res.* 21:309–320.
- Parikh, S.J., and J. Chorover. 2007. Infrared spectroscopy studies of cation effects on lipopolysaccharides in aqueous solution. *Colloids Surf. B* 55:241–250.
- Parikh, S.J., B.J. Lafferty, and D.L. Sparks. 2008. An ATR–FTIR spectroscopic approach for measuring rapid kinetics at the mineral/water interface. *J. Colloid Interface Sci.* 320:177–185.
- Pavlostathis, S.G., and G.N. Mathavan. 1992. Desorption kinetics of selected volatile organic compounds from field contaminated soils. *Environ. Sci. Technol.* 26:532–538.
- Pedit, J.A., and C.T. Miller. 1995. Heterogenous sorption processes in subsurface systems. 2. Diffusion modeling approaches. *Environ. Sci. Technol.* 29:1766–1772.
- Peltier, E., R. Allada, A. Navrotsky, and D.L. Sparks. 2006. Nickel solubility and precipitation in soils: A thermodynamic study. *Clays Clay Miner.* 54:153–164.
- Peltier, E., D. van der Lelie, and D.L. Sparks. 2010. Formation and stability of Ni–Al hydroxide phases in soils. *Environ. Sci. Technol.* 44:302–308.
- Petrovic, R., R.A. Berner, and M.B. Goldhaber. 1976. Rate control in dissolution of alkali feldspars. I. Study of residual feldspar grains by X-ray photoelectron spectroscopy. *Geochim. Cosmochim. Acta* 40:537–548.
- Pignatello, J.J. 1998. Soil organic matter as a nanoporous sorbent of organic pollutants. *Adv. Colloid Interface Sci.* 76:445–467.
- Pignatello, J.J. 2000. The measurement and interpretation of sorption and desorption rates for organic compounds in soil media. *Adv. Agron.* 69:1–73.
- Pignatello, J.J., F.J. Ferrandino, and L.Q. Huang. 1993. Elution of aged and freshly added herbicides from a soil. *Environ. Sci. Technol.* 27:1563–1571.
- Pignatello, J.J., and L.Q. Huang. 1991. Sorptive reversibility of atrazine and metolachlor residues in field soil samples. *J. Environ. Qual.* 20:222–228.
- Polyzopoulos, N.A., V.Z. Keramidas, A. Pavlatou. 1986. On the limitations of the simplified Elovich equation in describing the kinetics of phosphate sorption and release from soils. *J. Soil Sci.* 37:81–87.
- Rai, E., and R.J. Serne. 1977. Plutonium activities in soil solutions and the stability and formation of selected plutonium minerals. *J. Environ. Qual.* 6:89–95.
- Roberts, D.R., A.M. Scheidegger, and D.L. Sparks. 1999. Kinetics of mixed Ni–Al precipitate formation on a soil clay fraction. *Environ. Sci. Technol.* 33:3749–3754.

- Scheidegger, A.M., G.M. Lamble, and D.L. Sparks. 1996. Investigation of Ni sorption on pyrophyllite: An XAFS study. *Environ. Sci. Technol.* 30:548–554.
- Scheidegger, A.M., G.M. Lamble, and D.L. Sparks. 1997. Spectroscopic evidence for the formation of mixed-cation hydroxide phases upon metal sorption on clays and aluminum oxides. *J. Colloid Interface Sci.* 186:118–128.
- Scheidegger, A.M., and D.L. Sparks. 1996a. Kinetics of the formation and the dissolution of nickel surface precipitates on pyrophyllite. *Chem. Geol.* 132:157–164.
- Scheidegger, A.M., and D.L. Sparks. 1996b. A critical assessment of sorption–desorption mechanisms at the soil mineral/water interface. *Soil Sci.* 161:813–831.
- Scheidegger, A.M., D.G. Strawn, G.M. Lamble, and D.L. Sparks. 1998. The kinetics of mixed Ni–Al hydroxide formation on clay and aluminum oxide minerals: A time-resolved XAFS study. *Geochim. Cosmochim. Acta* 62:2233–2245.
- Schott, J., and J.C. Petit. 1987. New evidence for the mechanisms of dissolution of silicate minerals, p. 293–312. *In* W. Stumm (ed.) *Aquatic surface chemistry*. Wiley Interscience, New York.
- Schultz, M.F., M.M. Benjamin, and J.F. Ferguson. 1987. Adsorption and desorption of metals on ferrihydrite—Reversibility of the reaction and sorption properties of the regenerated solid. *Environ. Sci. Technol.* 21:863–869.
- Schwarzenbach, R.T., P.M. Gschwend, and D.M. Boden. 1993. *Environmental organic chemistry*. Wiley, New York.
- Scott, M.J., and J.J. Morgan. 1995. Reactions at oxide surfaces. 1. Oxidation of As(III) by synthetic birnessite. *Environ. Sci. Technol.* 29:1898–1905.
- Scott, M.J., and J.J. Morgan. 1996. Reactions at oxide surfaces. 2. Oxidation of Se(IV) by synthetic birnessite. *Environ. Sci. Technol.* 30:1990–1996.
- Scribner, S.L., T.R. Benzing, S. Sun, and S.A. Boyd. 1992. Desorption and bioavailability of aged simazine residues in soil from a continuous corn field. *J. Environ. Qual.* 21:115–120.
- Sharpley, A.N. 1983. Effect of soil properties on the kinetics of phosphorus desorption. *Soil Sci. Soc. Am. J.* 47:462–467.
- Skopp, J. 1986. Analysis of time dependent chemical processes in soils. *J. Environ. Qual.* 15:205–213.
- Sparks, D.L. 1989. *Kinetics of soil chemical processes*. Academic Press, San Diego, CA.
- Sparks, D.L. 1991. Chemical kinetics and mass transfer processes in soils and soil constituents, p. 585–637. *In* J. Bear and M.Y. Corapcioglu (eds.) *Transport processes in porous media*. Kluwer Academic Publishers, Dordrecht, the Netherlands.
- Sparks, D.L. 1995. *Environmental soil chemistry*. Academic Press, San Diego, CA.
- Sparks, D.L. 1998. Kinetics of sorption/release reactions on natural particles, p. 413–448. *In* P.M. Huang, N. Senesi, and J. Buffle (eds.) *Structure and surface reactions of soil particles*. John Wiley & Sons, New York.
- Sparks, D.L. 1999a. Kinetics and mechanisms of chemical reactions at the soil mineral/water interface, p. 135–192. *In* D.L. Sparks (ed.) *Soil physical chemistry*. CRC Press, Boca Raton, FL.
- Sparks, D.L. 1999b. Kinetics of soil chemical phenomena: Future directions, p. 81–102. *In* P.M. Huang, D.L. Sparks, and S.A. Boyd (eds.) *Future prospects for soil chemistry*. SSSA, Madison, WI.
- Sparks, D.L. 2002. *Environmental soil chemistry*. 2nd edn. Academic Press, San Diego, CA.
- Sparks, D.L. 2005. Sorption–desorption, kinetics, p. 556–561. *In* D. Hillel et al. (eds.) *Encyclopedia of soils in the environment*. Elsevier Ltd., Oxford, U.K.
- Sparks, D.L., S.E. Fendorf, C.V. Toner, IV, and T.H. Carski. 1996. Kinetic methods and measurements, p. 1275–1307. *In* D.L. Sparks (ed.) *Methods of soil analysis: Chemical methods*. SSSA, Madison, WI.
- Sparks, D.L., S.E. Fendorf, P.C. Zhang, and L. Tang. 1993. Kinetics and mechanisms of environmentally important reactions on soil colloidal surfaces, p. 141–168. *In* D. Petruzzelli and F.G. Helfferich (eds.) *Migration and fate of pollutants in soils and subsoils*. Springer-Verlag, Berlin, Germany.
- Sparks, D.L., and P.M. Jardine. 1984. Comparison of kinetic equations to describe K–Ca exchange in pure and in mixed systems. *Soil Sci.* 138:115–122.
- Sparks, D.L., and D.L. Suarez (eds.). 1991. *Rates of soil chemical processes*. SSSA, Special Publication No. 27, Madison, WI.
- Sparks, D.L., and P.C. Zhang. 1991. Relaxation methods for studying kinetics of soil chemical phenomena, p. 61–94. *In* D.L. Sparks and D.L. Suarez (eds.) *Rates of soil chemical processes*. SSSA, Madison, WI.
- Sposito, G. 1994. *Chemical equilibria and kinetics in soils*. Wiley, New York.
- Steinberg, S.M., J.J. Pignatello, and B.L. Sawhney. 1987. Persistence of 1,2 dibromoethane in soils: Entrapment in intra particle micropores. *Environ. Sci. Technol.* 21:1201–1208.
- Stone, A.T. 1986. Adsorption of organic reductants and subsequent electron transfer on metal oxide surfaces, p. 446–461. *In* J.A. Davis and K.F. Hayes (eds.) *Geochemical processes at mineral surfaces*. American Chemical Society, Washington, DC.
- Stone, A.T. 1987a. Microbial metabolites and the reductive dissolution of manganese oxides: Oxalate and pyruvate. *Geochim. Cosmochim. Acta* 51:919–925.
- Stone, A.T. 1987b. Reductive dissolution of manganese(III/IV) oxides by substituted phenols. *Environ. Sci. Technol.* 21:979–988.
- Stone, A.T. 1991. Oxidation and hydrolysis of ionizable organic pollutants at hydrous metal oxide surfaces, p. 231–254. *In* D.L. Sparks and D.L. Suarez (eds.) *Rates of soil chemical processes*. SSSA, Madison, WI.
- Stone, A.T., and J.J. Morgan. 1984a. Reduction and dissolution of manganese (III) and manganese (IV) oxides by organics. 1. Reaction with hydroquinone. *Environ. Sci. Technol.* 18:450–456.
- Stone, A.T., and J.J. Morgan. 1984b. Reduction and dissolution of manganese (III) and manganese (IV) oxides by organics. 2. Survey of the reactivity of organics. *Environ. Sci. Technol.* 18:617–624.

- Strawn, D.G., and D.L. Sparks. 2000. Effects of soil organic matter on the kinetics and mechanisms of Pb(II) sorption and desorption in soil. *Soil Sci. Soc. Am. J.* 64:144–156.
- Stumm, W. 1992. *Chemistry of the solid–water interface*. Wiley, New York.
- Stumm, W., and G. Furrer. 1987. The dissolution of oxides and aluminum silicates: Examples of surface-coordination-controlled kinetics, p. 197–219. *In* W. Stumm (ed.) *Aquatic surface chemistry*. Wiley Interscience, New York.
- Stumm, W., and R. Wollast. 1990. Coordination chemistry of weathering. Kinetics of the surface-controlled dissolution of oxide minerals. *Rev. Geophys.* 28:53–69.
- Tang, L.Y., and D.L. Sparks. 1993. Cation-exchange kinetics on montmorillonite using pressure-jump relaxation. *Soil Sci. Soc. Am. J.* 57:42–46.
- Thompson, H.A., G.A. Parks, and G.E. Brown. 1999a. Dynamic interactions of dissolution, surface adsorption, and precipitation in an aging cobalt(II)–clay–water system. *Geochim. Cosmochim. Acta* 63:1767–1779.
- Thompson, H.A., G.A. Parks, and G.E. Brown. 1999b. Ambient-temperature synthesis, evolution, and characterization of cobalt–aluminum hydroxalite-like solids. *Clays Clay Miner.* 47:425–438.
- Toner, C.V., IV, and D.L. Sparks. 1995. Chemical relaxation and double-layer model analysis of Boron adsorption on alumina. *Soil Sci. Soc. Am. J.* 59:395–404.
- Towle, S.N., J.R. Bargar, G.E. Brown, Jr., and G.A. Parks. 1997. Surface precipitation of Co(II) (aq) on Al<sub>2</sub>O<sub>3</sub>. *J. Colloid Interface Sci.* 187:62–82.
- van Genuchten, M.Th., and R.J. Wagenet. 1989. Two-site/two-region models for pesticide transport and degradation: Theoretical development and analytical solutions. *Soil Sci. Soc. Am. J.* 53:1303–1310.
- Waychunas, G.A., B.A. Rea, C.C. Fuller, and J.A. Davis. 1993. Surface chemistry of ferrihydrite: Part 1. EXAFS studies of the geometry of coprecipitated and adsorbed arsenate. *Geochim. Cosmochim. Acta* 57:2251–2269.
- Weber, W.J., Jr., and J.P. Gould. 1966. Sorption of organic pesticides from aqueous solution. *Adv. Chem. Ser.* 60:280–305.
- Weber, W.J., and W.L. Huang. 1996. A distributed reactivity model for sorption by soils and sediments. 4. Intraparticle heterogeneity and phase-distribution relationships under non-equilibrium conditions. *Environ. Sci. Technol.* 30:881–888.
- Weber, W.J., Jr., and C.T. Miller. 1988. Modeling the sorption of hydrophobic contaminants by aquifer materials. 1. Rates and equilibria. *Water Res.* 22:457–464.
- Wersin, P., M.F. Hochella, Jr., P. Persson, G. Redden, J.O. Leckie, and D.W. Harris. 1994. Interaction between aqueous uranium (VI) and sulfide minerals: Spectroscopic evidence for sorption and reduction. *Geochim. Cosmochim. Acta* 58:2829–2843.
- Wollast, R. 1967. Kinetics of the alteration of K-feldspar in buffered solutions at low temperature. *Geochim. Cosmochim. Acta* 31:635–648.
- Wu, S., and P.M. Gschwend. 1986. Sorption kinetics of hydrophobic organic compounds to natural sediments and soils. *Environ. Sci. Technol.* 20:717–725.
- Xia, K., A. Mehadi, R.W. Taylor, and W.F. Bleam. 1997. X-ray absorption and electron paramagnetic resonance studies of Cu(II) sorbed to silica: Surface-induced precipitation at low surface coverages. *J. Colloid Interface Sci.* 185:252–257.
- Xing, B., and J.J. Pignatello. 1997. Dual-mode sorption of low-polarity compounds in glassy poly (vinyl chloride) and soil organic matter. *Environ. Sci. Technol.* 31:792–799.
- Xing, B., and J.J. Pignatello. 2005. Sorption of organic chemicals. *In* D. Hillel (ed.) *Encyclopedia of soils in the environment*, p. 537–548. Vol. 3. Elsevier Ltd., Oxford, U.K.
- Xue, Y., and S.J. Traina. 1996. Oxidation kinetics of Co(II)-EDTA in aqueous and semi-aqueous goethite suspensions. *Environ. Sci. Technol.* 30:1975–1981.
- Zhang, P.C., and D.L. Sparks. 1989. Kinetics and mechanisms of molybdate adsorption/desorption at the goethite/water interface using pressure-jump relaxation. *Soil Sci. Soc. Am. J.* 53:1028–1034.
- Zhang, P.C., and D.L. Sparks. 1990a. Kinetics and mechanisms of sulfate adsorption/desorption on goethite using pressure-jump relaxation. *Soil Sci. Soc. Am. J.* 54:1266–1273.
- Zhang, P.C., and D.L. Sparks. 1990b. Kinetics of selenate and selenite adsorption/desorption at the goethite/water interface. *Environ. Sci. Technol.* 24:1848–1856.
- Zinder, B., G. Furrer, and W. Stumm. 1986. The coordination chemistry of weathering. II. Dissolution of Fe(III) oxides. *Geochim. Cosmochim. Acta* 50:1861–1869.

# Oxidation–Reduction Phenomena

14.1	Concepts, Principles, and Theories.....	14-1
	Nature of the Electron and Proton in Soil Solutions • Thermodynamic Relationships for Electron Activity in Soils • Kinetic Derivation of Thermodynamic Parameters for Redox • Microbiological and Enzymatic Controls for Redox State and Processes in Soils	
14.2	Methods and Procedures.....	14-12
	Uses of pe–pH Thermodynamic Information • Use of pe–pH Diagrams • Measurement of Soil Redox and Acid–Base Status • Proposed Alternative Strategies for More Accurate Measurement of Soil Redox Status	
14.3	Applications of Redox Methods and Concepts to Ecological, Engineered, and Agricultural Soil Systems .....	14-17
	Rhizosphere Processes • Soil Remediation and Pollutant Speciation • Soil Fertility and Nutrient Cycling • Soil Organic C Dynamics and Climate Change • Wetland Delineation and Function • Riparian Soil–Vegetation Systems and Groundwater Nitrate Concentrations	
14.4	Earlier Reviews and Prescient Work on Oxidation–Reduction Processes in Soils.....	14-19
	References.....	14-20

Bruce R. James  
*University of Maryland*

Dominic A. Brose  
*University of Maryland*

## 14.1 Concepts, Principles, and Theories

### 14.1.1 Nature of the Electron and Proton in Soil Solutions

Electrons are subatomic particles with wave-like properties that have defied exact characterization since their discovery in 1897, despite their central role in chemical reactions (Castellan, 1983). Electrons are considered fundamental subatomic particles, but recent findings suggest that they may possess a substructure of leptiquarks, that electron orbitals do not exist, and that the role of electrons in predicting periodicity of the elements is only approximate (Scerri, 1997). In addition, new frontiers are expanding to explain electron-transfer processes at interfaces (Tributsch and Pohlmann, 1998). Studying and understanding electron-transfer processes in soils, therefore, is challenging and must be based on sources of information from relatively simple aqueous systems and natural waters, as well as on a large base of empirical studies using soils. Electron-transfer processes in microbial cells are central to nutrient and pollutant chemical reactions, especially oxidation state changes governed by intra- and extracellular enzymes (Paul, 2007). Recent developments in environmental microbiology have found that bacteria form biofilms almost ubiquitously in aqueous and colloidal environments, such as natural waters, soils, and the human body (Stoodley et al., 2004). Therefore, understanding the role of microbes in controlling redox processes in soils requires an appreciation of such “matrix enclosed accretions that adhere to biological and nonbiological surfaces” (Stoodley et al., 2004).

To understand and characterize the nature of “electron activity” and oxidation–reduction reactions in biotic and abiotic, heterogeneous, multiphase soils and soil solutions, an appreciation of the characteristics of electrons and closely allied protons is needed (James, 1989; Stumm and Morgan, 1996; Bartlett, 1998; Bartlett and Ross, 2005). An examination of the complementary nature of electrons and protons affirms the importance of hydrogen ion and electron activities as master variables in soils (Sillén, 1967).

The H atom comprises one proton and one electron, and it may be visualized as a spherical puff of cotton candy with a radius of approximately 10 cm and a proton nucleus with a radius of 5 μm; essentially an invisible fleck of unspun sugar in the center. The remaining volume of the atom is occupied by the electron and the density of the spun sugar represents the probability of finding the electron in any one location. It becomes increasingly less dense (less probable) with distance away from the positively charged proton (Castellan, 1983). The radius of the H atom (0.3 Å), therefore, is approximately 20,000 times greater than that of the proton (~1.5 × 10<sup>-5</sup> Å). The proton also may be visualized as the size of a 0.1 μm colloidal clay particle, compared to a 2000 μm sand grain in a soil. In contrast to the large proportion of the volume of the H atom occupied by the negatively charged, wave-like electron, the electron has only negligible mass equal to approximately 550 μg mol<sup>-1</sup>, 1/1836 of the mass of the H atom (10<sup>6</sup> μg mol<sup>-1</sup>).

The tiny, heavy proton persists in hydrated form in aqueous media as H<sub>3</sub>O<sup>+</sup>, the hydroxonium or hydronium ion. The H atom

can only form the  $H^+$  ion when its compounds are dissolved in media that solvate protons, so the  $H^+$  cannot exist in solid phases (Cotton and Wilkinson, 1980). The solvation enthalpy of  $-1091 \text{ kJ mol}^{-1}$  provides the energy for bond rupture. Protons migrate rapidly between water molecules, and an individual  $H_3O^+$  ion has a lifetime of approximately  $10^{-13} \text{ s}$ . Its concentration and activity can, therefore, be measured and understood in terms of the hydration of a cation in solution. The single ion activity coefficient can be calculated based on ionic strength, temperature, effective diameter, and solvent characteristics; and  $H^+$  activity can be calculated or measured (Westcott, 1978; Bates, 1981).

The extremely large “charge-to-size ratio” of the electron prevents it from persisting in free form in aqueous systems, as does the solvated  $H^+$ . The ephemeral “hydrated electron” is a powerful reducing agent with a potential of  $-2.7 \text{ V}$  relative to the  $H^+/H_2$  reference potential of  $0.0 \text{ V}$  and has a half-life of  $<1 \text{ ms}$ . It reacts rapidly with second-order rate constants of  $10^8$ – $10^{10} \text{ M}^{-1} \text{ s}^{-1}$ , near the diffusion-controlled limit (Sullivan et al., 1976). Hydrated electrons may be transferred to aqueous solution from photoexcited hydrocarbons as  $\bullet e_{\text{aq}}^-$ . Such “free” or “aqueous” electrons react with  $H_2O$  and  $H_3O^+$  at femtosecond rates ( $10^{-15} \text{ s}$ ) to form the “conjugate acid” of the electron,  $H^\bullet$ , and the reaction with  $H_3O^+$  is approximately  $10^7$  times faster than with water (Leffler, 1993). The role of such aqueous electrons in soils remains unstudied, and photochemical studies of soils may reveal their presence and importance.

In soil chemical calculations and theory, one considers the electron as a “species,” designated “ $e^-$ ,” with negligible mass and thermodynamically as a ligand, reactant, and product (Sposito, 1981). The electron is not ionic, but it is “negatively charged” as the carrier of negative electricity (Thompson, 1923). Its “activity” is conceptually analogous to that of  $H^+$ , but its concentration in “ $\text{mol L}^{-1}$ ” is undefined. All these caveats about the electron require that one understand that electron activity in soils and natural waters should be regarded as related strictly to energy functions. Such functions can be described simply as “the ability to do work,” “electrochemical potential,” and more colloquially, “electron pressure.”

Generically, for a reduction half-reaction:  $\text{ox} + ne^- = \text{red}$ , the electron activity, ( $e^-$ ), equals  $[(\text{red})/K(\text{ox})]^{1/n}$ , in which “ox” is the oxidized species, “red” is the reduced species,  $n$  is the number of moles of electrons, and  $K$  is the equilibrium constant. Therefore, electron activity is a function of the ratio of reduced-to-oxidized species activities and of the equilibrium constant [or Gibbs free energy for the reaction, since  $\Delta G_r^\circ = -RT \ln K$ , where  $R$  is the gas law constant ( $8.313 \text{ J K}^{-1} \text{ mol}^{-1}$ ) and  $T$  is the absolute temperature measured in Kelvin ( $298 \text{ K}$  under standard conditions)]. A “favorable reaction” with a large positive value for  $K$  (or large negative  $\Delta G_r^\circ$ ) will therefore be associated with low electron activity. For example, a value of the equilibrium constant,  $K = 6 \times 10^8$ , corresponds to  $\Delta G_r^\circ = -50 \text{ kJ mol}^{-1}$  and  $K = 57$  corresponds to  $-10 \text{ kJ mol}^{-1}$  (Compton and Sanders, 1996). That is, such reactions will proceed spontaneously at relatively low electron activities or pressures, corresponding to positive electrode voltages. In these examples, since  $\Delta G_r^\circ = -nFE^\circ$ , the voltages

( $E^\circ$ ) associated with the electron transfers are  $+5.2$  and  $+1.04 \text{ V}$ , respectively, where  $n$  is the number of moles of electrons and  $F$  is the Faraday constant [ $96,487 \text{ C (coulombs) mol}^{-1}$  or  $\text{J V}^{-1} \text{ mol}^{-1}$ ].

The concept of  $H^+$  activity and pH also can be described in terms of thermodynamic work ( $\Delta w$ ) defined as the product of an intensive property and extensive variation, such as  $P(\Delta V)$ , where  $P$  is pressure and  $\Delta V$  is change in volume (Stumm and Morgan, 1996). Similarly, electron activity may be defined as  $E(\Delta e)$ , where  $E$  is potential and  $\Delta e$  is change in charge of the system. Proton and electron activities also may be defined as chemical work,  $\mu(\Delta n)$ , where  $\mu$  is chemical potential and  $\Delta n$  is change in moles (Sposito, 1981).

Viewing the sibling concepts of “proton activity” and “electron activity” in soils, they must not be considered twins. Recognition must be given to similarities and differences in the formulation of conceptual and operational definitions for these key variables, and such comparisons are based on the differences in the nature of the proton and electron, as described above. In both cases, however, their thermodynamic activities in a given system are relative to their activities under standard-state conditions. In the case of the  $e^-$ , the standard state is at  $(H^+) = 1 \text{ M}$ , a partial pressure of  $H_2 = 1 \text{ atm}$ , and a temperature of  $298 \text{ K}$ , characteristics of the standard hydrogen electrode (SHE) with  $0 \text{ V}$  under these conditions (Lindsay, 1979; Compton and Sanders, 1996; Stumm and Morgan, 1996). For  $H^+$  activity, the reference state is  $1 \text{ M}$  or  $\text{pH } 0$  (Bates, 1981).

The familiar concept of buffer capacity for pH is defined as the change in acid or base added (capacity factor) to effect a one unit change in pH (intensive variable; Stumm and Morgan, 1996). Similarly, the “capacity factor” in redox is referred to as poise and is defined as the change in added equivalents of reductant or oxidant to bring about a one unit change in  $p_e$  ( $-\log$  of electron activity) or an  $E_h$  (voltage relative to the SHE) change of  $59 \text{ mV}$ , as discussed in Section 14.1.2. Poise in soils and natural waters has been less intensively studied than pH buffering, but it is a central concept governed by reductant and oxidant activities and microbial processes.

The choice of oxidant or reductant to add in a redox titration will affect the calculated poise (resistance to change in  $p_e$  as measured by the Pt electrode), and poise will be operationally defined by the couple interacting with the Pt wire. For instance, if the soil is titrated with Cr(VI), the Cr(VI)–Cr(III) couple will be potential determining, so the poise will reflect that  $p_e$  range. If Fe(II) were added, the Fe(III)–Fe(II) couple would set a lower  $p_e$  range than would Cr(VI)–Cr(III). Heron et al. (1994) titrated aquifer sediments with the reducing agent,  $\text{Ti}^{3+}$  EDTA, to determine the poise associated with oxidants, such as Fe(III) and Mn(III,IV) (hydr)oxides. Barcelona and Holm (1991) titrated with  $\text{Cr}^{2+}$  to quantify poise due to oxidants, and with  $\text{Cr}_2\text{O}_7^{2-}$  to determine poise governed by reductants in the soil, respectively. Bauer et al. (2007) measured electron-transfer capacities and reaction kinetics of peat-dissolved organic matter, an organic matter analog for soil C. They used Zn and  $\text{H}_2\text{S}$  oxidation and complexed Fe(III) reduction to show that dissolved organic matter is a redox poisoning system between  $-0.9$  and  $1.0 \text{ V}$ .

Redox intensity measurements ( $E_h$  or  $p_e$ ) and estimates of poise as the redox capacity of soils and sediments are also distinguished from those only associated with  $H^+$  in that microbial

catalysis controls the rates of many of the oxidation and reduction reactions governing soil redox status (Russell, 1973; Banerjee, 2008). Also, the adaptation and growth of higher plants and algae in soils affects redox intensity and capacity. Examples of such microbial processes governing redox in soils include Fe(III) and  $\text{SO}_4^{2-}$  reduction in sediments (Coleman et al., 1993), denitrification in soil microenvironments (Højberg et al., 1994),  $\text{N}_2$  fixation in flooded soils (e.g., due to pH and pe changes by the *Anabaena–Azolla* symbiosis in rice or that of the *Frankia* sp. actinomycete infection of alder (*Alnus* spp.; Buresh et al., 1980; Madigan and Martinko, 2006), methane oxidation in flooded rice soils (Wang et al., 1997), the reactions of  $\text{H}_2$  in anoxic groundwater (Lovley et al., 1994), methanogenesis (Welsch and Yavitt, 2007; Goldhammer and Blodau, 2008; Saggar et al., 2008), and the formation of oxidized root channels (rhizospheres) in soils (Mendelsohn et al., 1995).

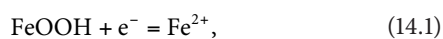
The poise and pe of soils also differ from natural waters in that the solids-to-solution ratio is high; and subsequently, redox reactions across colloid–solution interfaces are centrally important. Biofilm–water interfaces may be especially important in the case of microbially governed redox processes. Relatively few studies have been reported on redox reactions across soil colloid–water interfaces, but this area is critically important for predicting oxidation state and potential mobility of nutrients and pollutants in soil environments. Examples include reductive dissolution of Fe(III) and Mn(III,IV) (hydr)oxides and redox reactions on such surfaces or with constituent ions (Bartlett and James, 1979; Stone and Morgan, 1987; Suter et al., 1991; Stumm and Sulzberger, 1992; Postma and Jakobsen, 1996; White and Peterson, 1996).

### 14.1.2 Thermodynamic Relationships for Electron Activity in Soils

Since electrons are transferred from reductants ( $e^-$  donors or reducing agents) to oxidants ( $e^-$  acceptors or oxidizing agents) and do not persist free in soil solution, reduction reactions must be coupled to oxidation reactions to describe complete oxidation–reduction processes (redox reactions). By convention, reduction half-reactions can be written and thermodynamic relationships derived from them, despite the fact that they do not occur in isolation. The log K values (where K is the equilibrium constant for the half-reaction) for the coupled reactions may be compared to predict the likelihood of a reaction occurring spontaneously as written.

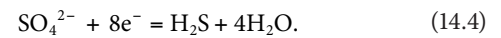
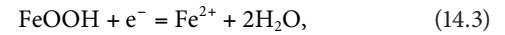
For example, development of reduction half-reactions to predict whether gaseous  $\text{H}_2\text{S}$  could reduce colloidal FeOOH across a sulfidic–aerobic interface in a wetland soil may be completed in the following manner:

1. Write the oxidized and reduced species on the left and right sides of the equation, respectively, with the appropriate number of electrons per mole of oxidant written on the left side. Balance moles of elements other than O and H:

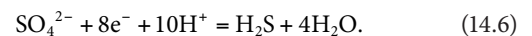
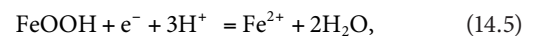


The number of electrons needed for reduction is calculated from the oxidation numbers or states of the elements in the oxidized and reduced species (Vincent, 1985). In this example, the oxidation numbers are III+ and VI+ for Fe and S in FeOOH and  $\text{SO}_4^{2-}$ , respectively.

2. Add  $\text{H}_2\text{O}$  to the equation (usually to the right side) to balance the moles of O:



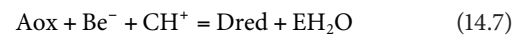
3. Then add  $\text{H}^+$  to balance moles of H, usually on the left side of the equation:



4. Check charge and mass balances for the equations.

These equations can now be used to develop expressions for electron activity based on equilibrium expressions and free energy of formation ( $\Delta G_f^\circ$ ) data.

The principles for doing this can be understood by starting with a generic reduction half-reaction:



where A, B, C, D, and E are the stoichiometric coefficients. The expression for the equilibrium constant (K) is as follows:

$$K = \frac{[(\text{red})^D (\text{H}_2\text{O})^E]}{[(\text{ox})^A (e^-)^B (\text{H}^+)^C]} \quad (14.8)$$

where

- ( ) denotes activity
- ( $\text{H}_2\text{O}$ ) has a value of 1, by convention

Taking the log of both sides of the equation,

$$\log K = \log \left[ \frac{(\text{red})^D}{(\text{ox})^A} \right] + \log \left[ \frac{1}{(e^-)^B} \right] + \log \frac{1}{(\text{H}^+)^C} \quad (14.9)$$

and

$$\log K = D \log(\text{red}) - A \log(\text{ox}) + Bpe + CpH \quad (14.10)$$

where

- pe and pH are defined as  $-\log$  electron activity
- $\text{H}^+$  activity, respectively.

The “p” notation means power and denotes the exponent for the  $\text{H}^+$  activity (pH 4 or  $10^{-4}$  mol  $\text{H}^+$   $\text{kg}^{-1}$  water). Therefore,  $(\text{H}^+) = 10^{-\text{pH}}$ . In contrast, the exponent for  $e^-$  activity is not  $10^{-\text{pe}}$ , since the electron

activity is not defined in terms of "mol e<sup>-</sup> L<sup>-1</sup>." Both pe and pH are analogous, though, if viewed as related to the ability of e<sup>-</sup> and H<sup>+</sup> to do thermodynamic work (Section 14.1.1).

Further rearrangement of Equation 14.10 yields a pe–pH relationship of the following form:

$$\left[ \left( \frac{1}{B} \right) \log K - \left( \frac{D}{B} \right) \log(\text{red}) + \left( \frac{A}{B} \right) \log(\text{ox}) \right] - \left( \frac{C}{B} \right) \text{pH} = \text{pe}, \quad (14.11)$$

which gives a straight line with slope C/B and the intercept in square brackets that is a function of log K for the half-reaction and the activities of the oxidized and reduced species.

For a one-electron transfer (B = 1) coupled with one-proton consumption (C = 1), and when D = A and (red) = (ox),

$$\text{pe} + \text{pH} = \log K. \quad (14.12)$$

And when pH = 0 (standard state),

$$\text{pe} = \log K. \quad (14.13)$$

Knowledge of pe and pH is pertinent to describing the equilibrium condition of a soil as defined by the master variables, pe, pH, and their sum (Lindsay, 1979). The concepts of electron activity and hydrogen ion activity are closely coupled and cannot be separated in assessing the oxidation–reduction status of a soil system. The pe + pH parameter has been described metaphorically by Bartlett (1998) as a seesaw with a hungry baby bird on one side (the electron-deficient player) and earthworms on the other (the electron-rich source). The parent bird carries the earthworms to the baby, representing electron transfer and causing a shift in the position of the seesaw, quantified by the pe–pH balance. As worms are transferred, the pe increases and the pH decreases, counteracting and interacting controls on the redox equilibrium. As the worms are consumed by the baby, the seesaw shifts back again, representing a dynamic, metastable system governed by the flow of energy and the cycling of nutrients, characteristics of ecosystems. The position of the seesaw governed by pe and pH reflects the equilibrium condition of a soil, and the values of pe and pH are intensity measures of redox status. The change in measured pe and pH per mole of electrons plus H<sup>+</sup> (H atoms in principle) transferred reflects the buffer capacity or poise of the system,  $\Delta(\text{pe} + \text{pH})/\Delta(\text{mol H atoms transferred})$ .

To relate the concept of log K to the Gibbs free energy change ( $\Delta G_r^\circ$ ) for a given half-reaction in the soil, the following expressions are pertinent:

$$\Delta G_r^\circ = -RT \ln K \quad (14.14)$$

where

$\Delta G_r^\circ$  is Gibbs free energy of reaction under standard conditions (298 K and 1 atm)

R is the universal gas law constant (0.00831 kJ K<sup>-1</sup> mol<sup>-1</sup>)

T is absolute temperature (298 K)

Converting to log<sub>10</sub> (ln K = 2.303 log K) yields the following:

$$\frac{\Delta G_r^\circ}{-5.70} = \log K. \quad (14.15)$$

log K may therefore be estimated simply from knowledge of free energies of formation of H<sub>2</sub>O, the red, and the ox; since those of H<sup>+</sup> and e<sup>-</sup> are zero, by convention. To relate log K directly to pe as defined by Equation 14.11 for one-electron transfers, log K values must be divided by B, the mol of e<sup>-</sup> consumed in the reaction. Therefore, pe at a given pH and other defined conditions is equivalent to log K, and the parameter pe + pH couples the master variables in defining the equilibrium redox state of a soil–water system.

Log K values also are related to thermodynamic electrochemical potentials (Eh) according to the following expressions (Compton and Sanders, 1996):

$$\Delta G_r^\circ = -nFEh \quad (14.16)$$

where

n is the number of e<sup>-</sup> transferred mol<sup>-1</sup>

F is the Faraday constant (96.5 kJ V<sup>-1</sup> equivalent<sup>-1</sup> or 96,487 C mol<sup>-1</sup> where C is coulombs, derived from 1.60 × 10<sup>-19</sup> C/e<sup>-</sup> × 6.02 × 10<sup>23</sup> e<sup>-</sup>/mol)

Since both Equations 14.16 and 14.14 are expressions for  $\Delta G_r^\circ$ ,

$$-nFEh = -RT \ln K \quad (14.17)$$

and, when T = 298 K,

$$Eh = \frac{RT \cdot 2.303 \log K}{nF} = 0.0592 \log K. \quad (14.18)$$

If n = 1, (red) = (ox), and pe = log K at a given pH (Equation 14.12), then

$$Eh (\text{V}) = 0.0592 \text{ pe} \quad (14.19)$$

or

$$\frac{Eh}{0.0592} = \text{pe}. \quad (14.20)$$

Therefore, calculating or interpreting Eh values rigorously and linking soil measurements to thermodynamics require knowledge of the pH of the soil–water system.

Applying these principles to the H<sub>2</sub>S–FeOOH problem above (Equations 14.5 and 14.6), the following pe–pH expressions can be derived:

For FeOOH–Fe<sup>2+</sup>:

$$\text{pe} = \log K_{\text{Fe}} - \log(\text{Fe}^{2+}) - 3\text{pH} \quad (14.21)$$



where activity of FeOOH is assumed to be 1, an assumption that may or may not be valid for redox processes (Stumm, 1993; White and Peterson, 1996).

For  $\text{SO}_4^{2-}$ – $\text{H}_2\text{S}$ :

$$pe = \frac{1}{8} \log K_S - \frac{1}{8} \log \left[ \frac{P_{\text{H}_2\text{S}}}{\text{SO}_4^{2-}} \right] - \frac{5}{4} \text{pH} \quad (14.22)$$

where

$K_{\text{Fe}}$  and  $K_S$  are the equilibrium constants for the FeOOH and  $\text{SO}_4^{2-}$  reduction half-reactions

$P_{\text{H}_2\text{S}}$  is the partial pressure of  $\text{H}_2\text{S}$

Calculating log K values and substituting into Equations 14.21 and 14.22 yield the following:

$$pe = 13.0 - \log(\text{Fe}^{2+}) - 3\text{pH} \quad (14.23)$$

and

$$pe = 5.21 - \left(\frac{1}{8}\right) \log \left[ \frac{P_{\text{H}_2\text{S}}}{\text{SO}_4^{2-}} \right] - \left(\frac{5}{4}\right) \text{pH}. \quad (14.24)$$

At defined activities for the ions and partial pressure for  $\text{H}_2\text{S}$ , pe may be calculated, and if pe for Fe(III) reduction > pe for  $\text{SO}_4^{2-}$  reduction, then FeOOH will be reduced to  $\text{Fe}^{2+}$  and  $\text{H}_2\text{S}$  oxidized to  $\text{SO}_4^{2-}$  at equilibrium and at the hypothetical soil interface. The same result will be obtained if after subtracting the log K value for S from that for Fe, a positive answer is obtained.

The Equations 14.23 and 14.24 can be plotted on an  $x$ - $y$ -graph called a pe–pH diagram (Figure 14.1). In this graph, each reduction half-reaction is plotted for (red)/(ox) = 1 and  $10^{-4}$ . Note that

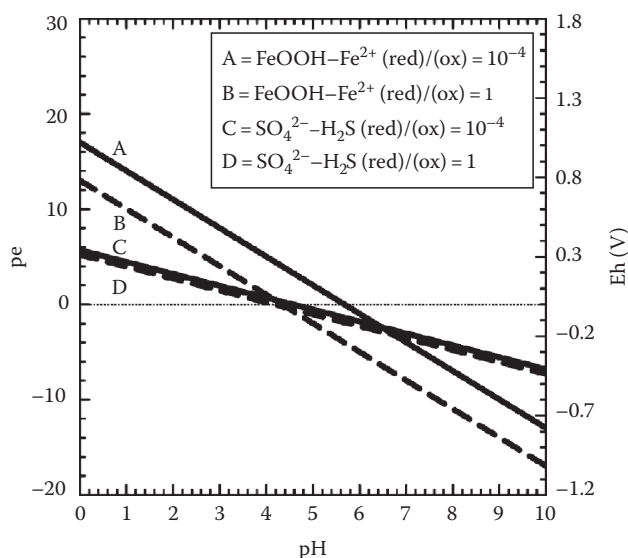


FIGURE 14.1 pe–pH diagram for FeOOH– $\text{Fe}^{2+}$  and  $\text{SO}_4^{2-}$ – $\text{H}_2\text{S}$  equilibria at two activity ratios.

the positions of the lines are shifted to higher pe values for the lower activities of the reduced species; the effect being greater for the FeOOH– $\text{Fe}^{2+}$  couple than for  $\text{SO}_4^{2-}$ – $\text{H}_2\text{S}$ , due to the greater oxidation state change per mole for S than for Fe. This effect of changing the activity ratio on pe values is an easy way to perform a sensitivity analysis for these thermodynamic models and to plot a family of curves representative of a range of activities relevant to any soil system or conditions. Similar calculations can be performed for variations in the values of  $\square G_f^\circ$ , since the conditions (e.g., temperature, pressure, and ionic strength) under which these values are determined may result in a range of values of up to 10 or more  $\text{kJ mol}^{-1}$ . The  $\square G_f^\circ$  values tabulated by Lindsay (1979) were reviewed and selected for their accuracy and their relevance to soils and natural waters.

An important use of pe–pH diagrams is for predicting thermodynamically whether or not the oxidized species in one reduction half-reaction will oxidize the reduced species in a second reduction half-reaction (i.e., when the second half-reaction is reversed to become the oxidation half-reaction and is added to the first reduction half-reaction). When the line for a pe–pH couple is above another over a pH range, the calculated  $\Delta pe$  or  $\Delta Eh$  values will be >0 (and corresponding  $\square G_r^\circ$  values <0), signifying that the reaction is spontaneous as written. In the above example, FeOOH is expected to oxidize  $\text{H}_2\text{S}$  over the pH range 0–6.6 for the activity ratio = 1 but only up to pH 4.6 for the activity ratio =  $10^{-4}$ . Theoretically, above the crossover pH values,  $\text{SO}_4^{2-}$  would be expected to oxidize  $\text{Fe}^{2+}$  to FeOOH, while being reduced to  $\text{H}_2\text{S}$ ; the opposite of the reaction at pHs < the crossover value.

Calculations of myriad pe–pH relationships are conveniently performed using a spreadsheet template that incorporates balanced half-reactions, appropriate  $\square G_f^\circ$  values to calculate log K, chosen activity ratios, and Equation 14.11. Using such a spreadsheet, numerous pe values for common reduction half-reactions pertinent to soil chemical and biochemical processes were calculated and are presented in Table 14.1. Table 14.1 also includes numerous pe values derived from Eh data in various published databases, especially for coenzymes and some intermediates governing microbial respiration. This list provides a quick, semi-quantitative means of assessing what the products of selected, coupled reduction and oxidation half-reactions are likely to be.

The U.S. Environmental Protection Agency developed MINTEQA2 (for “Mineral Thermal Equilibria”), a DOS-based computer program that calculates the distribution of myriad species based on minimizing the Gibbs free energy of a system of multiple chemical equilibria. Different from earlier such programs, such as GEOCHEM, it incorporates algorithms for redox reactions and allows the estimation of pe, pH, and reductant and oxidant activities in conjunction with dissolution and exchange equilibria. The use of MINTEQA2 also permits an easy way to conduct a sensitivity analysis for estimated pe, pH, or ion activities when just one value for a given parameter is varied (Allison and Brown, 1995). Visual MINTEQA2 was written and is updated for Microsoft Windows by J.P. Gustafsson, and version 3.0 (as of August 2010) is now available free online at <http://www.lwr.kth.se/English/OurSoftware/vminteq/>

TABLE 14.1 Reduction Half-Reactions for Soils

	Log K <sup>a</sup>	pe <sup>b</sup>	
	(pe at pH 0)	pH 5	pH 7
<i>Nitrogen species</i>			
$\frac{1}{2}\text{N}_2\text{O} + \text{e}^- + \text{H}^+ = \frac{1}{2}\text{N}_2 + \frac{1}{2}\text{H}_2\text{O}$	29.8	22.9	20.9
$\text{NO} + \text{e}^- + \text{H}^+ = \frac{1}{2}\text{N}_2\text{O} + \frac{1}{2}\text{H}_2\text{O}$	26.8	19.8	17.8
$\frac{1}{2}\text{NO}_2^- + \text{e}^- + \frac{3}{2}\text{H}^+ + \frac{1}{4}\text{N}_2\text{O} + \frac{3}{4}\text{H}_2\text{O}$	23.6	15.1	12.1
$\frac{1}{5}\text{NO}_3^- + \text{e}^- + \frac{9}{5}\text{H}^+ = \frac{1}{10}\text{N}_2 + \frac{3}{5}\text{H}_2\text{O}$	21.1	14.3	11.9
$\text{NO}_2^- + \text{e}^- + 2\text{H}^+ = \text{NO} + \text{H}_2\text{O}$	19.8	9.8	5.8
$\frac{1}{4}\text{NO}_3^- + \text{e}^- + \frac{3}{4}\text{H}^+ = \frac{1}{8}\text{N}_2\text{O} + \frac{5}{8}\text{H}_2\text{O}$	18.9	12.1	9.6
$\frac{1}{6}\text{NO}_2^- + \text{e}^- + \frac{4}{3}\text{H}^+ = \frac{1}{6}\text{NH}_4^+ + \frac{1}{3}\text{H}_2\text{O}$	15.1	8.4	5.7
$\frac{1}{8}\text{NO}_3^- + \text{e}^- + \frac{5}{4}\text{H}^+ = \frac{1}{8}\text{NH}_4^+ + \frac{3}{8}\text{H}_2\text{O}$	14.9	8.6	6.1
$\frac{1}{2}\text{NO}_3^- + \text{e}^- + \text{H}^+ = \frac{1}{2}\text{NO}_2^- + \frac{1}{2}\text{H}_2\text{O}$	14.1	9.1	7.1
$\frac{1}{6}\text{NO}_3^- + \text{e}^- + \frac{7}{6}\text{H}^+ = \frac{1}{6}\text{NH}_2\text{OH} + \frac{1}{3}\text{H}_2\text{O}$	11.3	5.4	3.1
$\frac{1}{6}\text{N}_2 + \text{e}^- + \frac{4}{3}\text{H}^+ = \frac{1}{3}\text{NH}_4^+$	4.6	-0.7	-3.3
<i>Oxygen species</i>			
$\text{OH}^\bullet + \text{e}^- + \text{H}^+ = \text{H}_2\text{O}$	—	—	36.8
$\text{O}_3^{\bullet-} + \text{e}^- + 2\text{H}^+ = \text{H}_2\text{O} + \text{O}_2$	— <sup>c</sup>	—	30.5 <sup>d</sup>
$\frac{1}{2}\text{O}_3 + \text{e}^- + \text{H}^+ = \frac{1}{2}\text{O}_2 + \frac{1}{2}\text{H}_2\text{O}$	35.1	28.4	26.4
$\text{OH}^\bullet + \text{e}^- = \text{OH}^-$	33.6	33.6	33.6
$\text{O}_2^- + \text{e}^- + 2\text{H}^+ = \text{H}_2\text{O}_2$	32.6	22.6	18.6
$\frac{1}{2}\text{H}_2\text{O}_2 + \text{e}^- + \text{H}^+ = \text{H}_2\text{O}$	30.0	23.0	21.0
$\text{HO}_2^\bullet + \text{e}^- + \text{H}^+ = \text{H}_2\text{O}_2$	—	—	17.9 <sup>d</sup>
$\text{O}_3 + \text{e}^- = \text{O}_3^{\bullet-}$	—	—	15.1 <sup>d</sup>
$^1\text{O}_2 + \text{e}^- = \text{O}_2^{\bullet-}$ (singlet)	—	—	14.1 <sup>d</sup>
$\frac{1}{4}\text{O}_2 + \text{e}^- + \text{H}^+ = \frac{1}{2}\text{H}_2\text{O}$	20.8	15.6	13.6
$\text{H}_2\text{O}_2 + \text{e}^- + \text{H}^+ = \text{OH}^\bullet + \text{H}_2\text{O}$	—	—	7.8
$\frac{1}{2}\text{O}_2 + \text{e}^- + \text{H}^+ = \frac{1}{2}\text{H}_2\text{O}_2$	11.6	8.2	6.2
$^3\text{O}_2 + \text{e}^- = \text{O}_2^{\bullet-}$ (triplet, ground state)	-9.5	-6.2	-6.2
$^3\text{O}_2 + \text{e}^- + \text{H}^+ = \text{HO}_2^\bullet$ (triplet, ground state)	—	—	-7.8
<i>Sulfur species</i>			
$\frac{1}{8}\text{SO}_4^{2-} + \text{e}^- + \frac{5}{4}\text{H}^+ = \frac{1}{8}\text{H}_2\text{S} + \frac{1}{2}\text{H}_2\text{O}$	5.2	-1.0	-3.5
$\frac{1}{6}\text{SO}_4^{2-} + \text{e}^- + \frac{4}{3}\text{H}^+ = \frac{1}{6}\text{S} + \frac{2}{3}\text{H}_2\text{O}$	5.3	-1.4	-4.0
$\frac{1}{2}\text{S} + \text{e}^- + \text{H}^+ = \frac{1}{2}\text{H}_2\text{S}$	4.9	-0.1	-2.1
$\frac{1}{2}\text{SO}_4^{2-} + \text{e}^- + 2\text{H}^+ = \frac{1}{2}\text{SO}_2 + \text{H}_2\text{O}$	2.9	-7.1	-11.1
<i>Iron and manganese compounds</i>			
$\frac{1}{2}\text{Mn}_3\text{O}_4 + \text{e}^- + 4\text{H}^+ = \frac{3}{2}\text{Mn}^{2+} + 2\text{H}_2\text{O}$	30.7	16.7	8.7
$\frac{1}{2}\text{Mn}_2\text{O}_3 + \text{e}^- + 3\text{H}^+ = \text{Mn}^{2+} + \frac{3}{2}\text{H}_2\text{O}$	25.7	14.7	8.7
$\text{Mn}^{3+} + \text{e}^- = \text{Mn}^{2+}$	25.5	25.5	25.5
$\gamma\text{-MnOOH} + \text{e}^- + 3\text{H}^+ = \text{Mn}^{2+} + 2\text{H}_2\text{O}$	25.4	14.4	8.4
$0.62\text{MnO}_{1.8} + \text{e}^- + 2.2\text{H}^+ = 0.62\text{Mn}^{2+} + 1.1\text{H}_2\text{O}$	22.1	13.4	8.9
$\frac{1}{2}\text{Fe}_3(\text{OH})_8 + \text{e}^- + 4\text{H}^+ = \frac{3}{2}\text{Fe}^{2+} + 4\text{H}_2\text{O}$	21.9	7.9	-0.1
$\frac{1}{2}\text{MnO}_2 + \text{e}^- + 2\text{H}^+ = \frac{1}{2}\text{Mn}^{2+} + \text{H}_2\text{O}$	20.8	12.8	8.8
$[\text{Mn}^{3+}(\text{PO}_4)_2]^{3-} + \text{e}^- = [\text{Mn}^{2+}(\text{PO}_4)_2]^{4-}$	20.7	20.7	20.7
$\text{Fe}(\text{OH})_2^+ + \text{e}^- + 2\text{H}^+ = \text{Fe}^{2+} + 2\text{H}_2\text{O}$	20.2	10.2	6.2
$\frac{1}{2}\text{Fe}_3\text{O}_4 + \text{e}^- + 4\text{H}^+ = \frac{3}{2}\text{Fe}^{2+} + 2\text{H}_2\text{O}$	17.8	3.9	-4.1
$\text{MnO}_2 + \text{e}^- + 4\text{H}^+ = \text{Mn}^{3+} + 2\text{H}_2\text{O}$	16.5	0.54	-7.5

TABLE 14.1 (continued) Reduction Half-Reactions for Soils

	Log K <sup>a</sup>	pe <sup>b</sup>	
	(pe at pH 0)	pH 5	pH 7
$\text{Fe}(\text{OH})_3 + \text{e}^- + 3\text{H}^+ = \text{Fe}^{2+} + 3\text{H}_2\text{O}$	15.8	4.8	-1.2
$\text{FeOH}^{2+} + \text{e}^- + \text{H}^+ = \text{Fe}^{2+} + \text{H}_2\text{O}$	15.2	10.2	8.2
$\frac{1}{2}\text{Fe}_2\text{O}_3 + \text{e}^- + 3\text{H}^+ = \text{Fe}^{2+} + \frac{3}{2}\text{H}_2\text{O}$	13.4	2.4	-3.6
$\text{FeOOH} + \text{e}^- + 3\text{H}^+ = \text{Fe}^{2+} + 2\text{H}_2\text{O}$	13.0	2.0	-4.0
$\text{Fe}^{3+} + \text{e}^- = \text{Fe}^{2+}$ (phenanthroline)	18.0	— <sup>c</sup>	—
$\text{Fe}^{3+} + \text{e}^- = \text{Fe}^{2+}$ ( $\text{H}_2\text{O}$ only)	13.0	13.0	13.0
$\text{Fe}^{3+} + \text{e}^- = \text{Fe}^{2+}$ (acetate)	—	5.8	—
$\text{Fe}^{3+} + \text{e}^- = \text{Fe}^{2+}$ (malonate), pH 4	—	4.4	—
$\text{Fe}^{3+} + \text{e}^- = \text{Fe}^{2+}$ (salicylate), pH 4	—	4.4	—
$\text{Fe}^{3+} + \text{e}^- = \text{Fe}^{2+}$ (hemoglobin)	—	—	2.4
$\text{Fe}^{3+} + \text{e}^- = \text{Fe}^{2+}$ (EDTA)	—	—	2.0 <sup>d</sup>
$\text{Fe}^{3+} + \text{e}^- = \text{Fe}^{2+}$ cyt b <sub>3</sub> (plants)	—	—	0.68
$\text{Fe}^{3+} + \text{e}^- = \text{Fe}^{2+}$ (DTPA)	—	—	0.51
$\text{Fe}^{3+} + \text{e}^- = \text{Fe}^{2+}$ (oxalate)	—	—	0.034
$\text{Fe}^{3+} + \text{e}^- = \text{Fe}^{2+}$ (pyrophosphate)	-2.4	—	—
$\text{Fe}^{3+} + \text{e}^- = \text{Fe}^{2+}$ (peroxidase)	—	—	-4.6
$\text{Fe}^{3+} + \text{e}^- = \text{Fe}^{2+}$ (spinach ferredoxin)	—	—	-7.3
$\text{Fe}^{3+} + \text{e}^- = \text{Fe}^{2+}$ (ferritin)	—	—	-3.2 <sup>d</sup>
$\frac{1}{3}\text{KFe}_3(\text{SO}_4)_2(\text{OH})_6 + \text{e}^- + 2\text{H}^+ = \text{Fe}^{2+} + 2\text{H}_2\text{O} + \frac{2}{3}\text{SO}_4^{2-} + \frac{1}{3}\text{K}^+$	8.9	6.9	2.9
$[\text{Fe}(\text{CN})_6]^{3-} + \text{e}^- = [\text{Fe}(\text{CN})_6]^{4-}$	—	—	6.1
<i>Carbon species</i>			
$\text{CH}_3\text{CH}_2^\bullet + \text{e}^- + \text{H}^+ = \text{CH}_3\text{CH}_3$	—	—	32.2 <sup>d</sup>
$\text{RO}^\bullet + \text{e}^- + \text{H}^+ = \text{ROH}$ (aliphatic)	—	—	27.1 <sup>d</sup>
$\text{CO}_3^{\bullet-} + \text{e}^- + \text{H}^+ = \text{CO}_3^{2-}$	—	—	25.1 <sup>d</sup>
Tryptophan <sup>•</sup> + H <sup>+</sup> + e <sup>-</sup> = tryptophan	—	—	16.9
Catechol-O <sup>•</sup> + e <sup>-</sup> + H <sup>+</sup> = catechol	—	—	9.0 <sup>d</sup>
Benzosemiquinone + e <sup>-</sup> + H <sup>+</sup> = hydroquinone	—	—	7.8 <sup>d</sup>
$\frac{1}{2}\text{Ubiquinone} + \text{H}^+ + \text{e}^- = \text{ubiquinone-H}_2$	—	—	1.7
$\frac{1}{2}o\text{-quinone} + \text{e}^- + \text{H}^+ = \frac{1}{2}\text{diphenol}$	—	—	5.9
$\frac{1}{2}p\text{-quinone} + \text{e}^- + \text{H}^+ = \frac{1}{2}\text{hydroquinone}$	—	—	4.7
$\text{Cu}^{2+} + \text{H}^+ + \text{e}^- = \text{Cu}^+$ (superoxide dismutase)	—	—	7.1
$\text{Mn}^{3+} + \text{H}^+ + \text{e}^- = \text{Mn}^{2+}$ (superoxide dismutase)	—	—	5.2
$\text{Fe}^{3+} + \text{H}^+ + \text{e}^- = \text{Fe}^{2+}$ (superoxide dismutase)	—	—	4.7
$\frac{1}{2}\text{CH}_3\text{OH} + \text{e}^- + \text{H}^+ = \frac{1}{2}\text{CH}_4 + \frac{1}{2}\text{H}_2\text{O}$	9.9	4.9	2.9
$\frac{1}{12}\text{C}_6\text{H}_{12}\text{O}_6 + \text{e}^- + \text{H}^+ = \frac{1}{4}\text{C}_2\text{H}_5\text{OH} + \frac{1}{4}\text{H}_2\text{O}$	4.4	—	-1.9
$\frac{1}{8}\text{CO}_2 + \text{e}^- + \text{H}^+ = \frac{1}{8}\text{CH}_4 + \frac{1}{8}\text{H}_2\text{O}$	2.9	-2.1	-4.1
$\frac{1}{2}\text{CH}_2\text{O} + \text{e}^- + \text{H}^+ = \frac{1}{2}\text{CH}_3\text{OH}$	2.1	-2.9	-4.9
$\frac{1}{2}\text{HCOOH} + \text{e}^- + \text{H}^+ = \frac{1}{2}\text{CH}_2\text{O} + \frac{1}{2}\text{H}_2\text{O}$	1.5	-3.5	-5.5
$\frac{1}{4}\text{CO}_2 + \text{e}^- + \text{H}^+ = \frac{1}{24}\text{C}_6\text{H}_{12}\text{O}_6 + \frac{1}{4}\text{H}_2\text{O}$	-0.21	-5.9	-7.9
$\frac{1}{2}\text{Dehydroascorbate} + \text{e}^- + \text{H}^+ = \frac{1}{2}\text{ascorbic acid}$	1.0	-3.5	-5.5
$\frac{1}{2}\text{Methylene blue(ox)} + \text{H}^+ + \text{e}^- = \frac{1}{2}\text{methylene blue(red)}$	—	—	0.2
$\text{FAD} + \text{H}^+ + \text{e}^- = \frac{1}{2}\text{FADH}_2$	—	—	-3.0
$\frac{1}{2}\text{Pyruvate} + \text{H}^+ + \text{e}^- = \frac{1}{2}\text{lactate}$	—	—	-3.2
$\frac{1}{2}\text{NAD}^+ + \text{H}^+ + \text{e}^- = \frac{1}{2}\text{NADH} + \frac{1}{2}\text{H}^+$	—	—	-5.4

(continued)

TABLE 14.1 (continued) Reduction Half-Reactions for Soils

	Log K <sup>a</sup>	pe <sup>b</sup>	
	(pe at pH 0)	pH 5	pH 7
$\frac{1}{2}$ Pyruvate + $\frac{1}{2}$ CO <sub>2</sub> + H <sup>+</sup> + e <sup>-</sup> = $\frac{1}{2}$ malate	—	—	-5.6
Ferredoxin-Fe <sup>3+</sup> + e <sup>-</sup> = ferredoxin-Fe <sup>2+</sup>	—	—	-7.3
$\frac{1}{4}$ CO <sub>2</sub> + e <sup>-</sup> + H <sup>+</sup> = $\frac{1}{4}$ CH <sub>2</sub> O + $\frac{1}{4}$ H <sub>2</sub> O	-1.2	-6.1	-8.1
$\frac{1}{2}$ CO <sub>2</sub> + e <sup>-</sup> + H <sup>+</sup> = $\frac{1}{2}$ HCOOH	-1.9	-6.7	-8.7
$\frac{1}{2}$ Acetate + H <sup>+</sup> + e <sup>-</sup> = $\frac{1}{2}$ acetaldehyde	—	—	-10.1
$\frac{1}{2}$ Acetate + CO <sub>2</sub> + H <sup>+</sup> + e <sup>-</sup> = $\frac{1}{2}$ pyruvate	—	—	-11.8
CO <sub>2</sub> + e <sup>-</sup> = CO <sub>2</sub> <sup>•-</sup>	—	—	-30.5
<i>Pollutant/nutrient group</i>			
Co <sup>3+</sup> + e <sup>-</sup> = Co <sup>2+</sup>	30.6	30.6	30.6
$\frac{1}{2}$ NiO <sub>2</sub> + e <sup>-</sup> + 2H <sup>+</sup> = $\frac{1}{2}$ Ni <sup>2+</sup> + H <sub>2</sub> O	29.8	21.8	17.8
PuO <sub>2</sub> <sup>+</sup> + e <sup>-</sup> = PuO <sub>2</sub>	26.0	22.0	22.0
$\frac{1}{2}$ PbO <sub>2</sub> + e <sup>-</sup> + 2H <sup>+</sup> = $\frac{1}{2}$ Pb <sup>2+</sup> + H <sub>2</sub> O	24.8	16.8	12.8
PuO <sub>2</sub> + e <sup>-</sup> + 4H <sup>+</sup> = Pu <sup>3+</sup> + 2H <sub>2</sub> O	9.9	-6.1	-14.1
$\frac{1}{3}$ HCrO <sub>4</sub> <sup>-</sup> + e <sup>-</sup> + $\frac{4}{3}$ H <sup>+</sup> = $\frac{1}{3}$ Cr(OH) <sub>3</sub> + $\frac{1}{3}$ H <sub>2</sub> O	18.9	10.9	8.2
$\frac{1}{2}$ H <sub>2</sub> AsO <sub>4</sub> <sup>-</sup> + e <sup>-</sup> + $\frac{3}{2}$ H <sup>+</sup> = $\frac{1}{2}$ H <sub>3</sub> AsO <sub>3</sub> + $\frac{1}{2}$ H <sub>2</sub> O	11.2	3.7	0.7
Hg <sup>2+</sup> + e <sup>-</sup> = $\frac{1}{2}$ Hg <sub>2</sub> <sup>2+</sup>	15.4	13.4	13.4
$\frac{1}{2}$ MoO <sub>4</sub> <sup>2-</sup> + e <sup>-</sup> + 2H <sup>+</sup> = $\frac{1}{2}$ MoO <sub>2</sub> + H <sub>2</sub> O	15.0	3.0	-1.0
$\frac{1}{2}$ SeO <sub>4</sub> <sup>2-</sup> + e <sup>-</sup> + H <sup>+</sup> = $\frac{1}{2}$ SeO <sub>3</sub> <sup>2-</sup> + $\frac{1}{2}$ H <sub>2</sub> O	14.9	9.9	7.9
$\frac{1}{4}$ SeO <sub>3</sub> <sup>2-</sup> + e <sup>-</sup> + $\frac{3}{2}$ H <sup>+</sup> = $\frac{1}{4}$ Se + $\frac{3}{4}$ H <sub>2</sub> O	14.8	6.3	3.3
$\frac{1}{6}$ SeO <sub>3</sub> <sup>2-</sup> + e <sup>-</sup> + $\frac{4}{3}$ H <sup>+</sup> = $\frac{1}{6}$ H <sub>2</sub> Se + $\frac{1}{2}$ H <sub>2</sub> O	7.62	1.0	-1.7
$\frac{1}{2}$ VO <sub>2</sub> <sup>+</sup> + e <sup>-</sup> + $\frac{1}{2}$ H <sub>3</sub> O <sup>+</sup> = $\frac{1}{2}$ V(OH) <sub>3</sub>	6.9	2.4	1.4
Cu <sup>2+</sup> + e <sup>-</sup> = Cu <sup>+</sup>	2.6	2.6	2.6
PuO <sub>2</sub> + e <sup>-</sup> + 3H <sup>+</sup> = PuOH <sup>2+</sup> + H <sub>2</sub> O	2.9	-8.1	-14.1
Paraquat + e <sup>-</sup> = paraquat <sup>•-</sup>	—	—	-7.6
<i>Analytical couples</i>			
CeO <sub>2</sub> + e <sup>-</sup> + 4H <sup>+</sup> = Ce <sup>3+</sup> + 2H <sub>2</sub> O	47.6	31.6	23.6
$\frac{1}{2}$ ClO <sup>-</sup> + e <sup>-</sup> + H <sup>+</sup> = $\frac{1}{2}$ Cl <sup>-</sup> + $\frac{1}{2}$ H <sub>2</sub> O	29.0	24.0	22.0
HClO + e <sup>-</sup> + H <sup>+</sup> = $\frac{1}{2}$ Cl <sub>2</sub> + H <sub>2</sub> O	27.6	20.6	18.6
$\frac{1}{2}$ Cl <sub>2</sub> + e <sup>-</sup> = Cl <sup>-</sup>	23.0	25.0	25.0
$\frac{1}{6}$ IO <sub>3</sub> <sup>-</sup> + e <sup>-</sup> + H <sup>+</sup> = $\frac{1}{6}$ I <sup>-</sup> + $\frac{1}{2}$ H <sub>2</sub> O	18.6	13.6	11.6
$\frac{1}{2}$ Pt(OH) <sub>2</sub> + e <sup>-</sup> + H <sup>+</sup> = $\frac{1}{2}$ Pt + H <sub>2</sub> O	16.6	11.6	9.6
$\frac{1}{2}$ I <sub>2</sub> + e <sup>-</sup> = I <sup>-</sup>	9.1	11.1	11.1
$\frac{1}{2}$ Hg <sub>2</sub> Cl <sub>2</sub> + e <sup>-</sup> = Hg + Cl <sup>-</sup>	4.5	3.9	3.9
AgCl + e <sup>-</sup> = Ag + Cl <sup>-</sup>	3.8	3.2	3.2 <sup>c</sup>
e <sup>-</sup> + H <sup>+</sup> = $\frac{1}{2}$ H <sub>2</sub>	0	-5	-7
$\frac{1}{2}$ PtS + e <sup>-</sup> + H <sup>+</sup> = $\frac{1}{2}$ Pt + $\frac{1}{2}$ H <sub>2</sub> S	-5.0	-10.0	-12.0

<sup>a</sup> Calculated for reaction as written according to Equation 14.14. Free energy of formation data were taken from Lindsay (1979) as a primary source, and when not available from that source, from Garrels and Christ (1965) and Loach (1976).

<sup>b</sup> Calculated using tabulated log K values, (red) and (ox) = 10<sup>-4</sup> mol/L soluble ions and molecules, activities of solid phases = 1, and partial pressures for gases that are pertinent to soils: 10<sup>-4</sup> atm for trace gases, 0.21 atm for O<sub>2</sub>, 0.78 for N<sub>2</sub>, and 0.00032 for CO<sub>2</sub>. Note: pe × 59.2 = Eh (mV) at the specified pH.

<sup>c</sup> Values not listed by Loach (1976) or Larson (1997).

<sup>d</sup> Values from Larson (1997).

<sup>e</sup> Value for 4 M Cl<sup>-</sup> in Ag/AgCl reference electrode.

### 14.1.3 Kinetic Derivation of Thermodynamic Parameters for Redox

This thermodynamic derivation of  $\log K$  and its relationship to  $p_e$  and  $pH$  of soils is based on free energy of formation data for oxidants and reductants, and it is not related to reaction mechanisms or rates. An alternate procedure to obtain  $\log K$  values, in theory, is the kinetic approach suggested by Sparks (1985) for cation exchange and by Harter and Smith (1981) for adsorption processes. This approach has been little used in redox soil chemistry, probably due to difficulties in obtaining rate coefficients for many electron-transfer processes in soils and due to the irreversibility of most redox reactions. The application of such approaches should, however, be appropriate for certain reversible redox reactions in soils, especially in situations where metastability and lack of chemical equilibrium prevail or when accurate free energy of formation data is unavailable for oxidants and reductants.

In principle, this is the method for calculating kinetic parameters: the equilibrium constant ( $K$ ) for redox equilibria can be estimated from the ratio of forward and reverse rate coefficients for a given reversible reaction in soils:

$$K = \frac{k_f}{k_r} \quad (14.25)$$

where  $k_f$  and  $k_r$  are the rate constants for forward and reverse reactions, respectively. The standard Gibbs free energy for the reaction then can be calculated by substituting  $\ln K$  into Equation 14.14. Preparation of Arrhenius plots of the rate coefficients as a function of  $1/T$  permits estimation of activation energies for the forward and reverse reactions, and standard enthalpies for the reactions can be calculated as

$$\Delta H^\circ = E_f^* - E_r^* \quad (14.26)$$

where

$\Delta H^\circ$  is enthalpy for the redox reaction

$E_f^*$  and  $E_r^*$  are the activation energies for the forward and reverse reactions

With knowledge of  $\Delta G^\circ$  and  $\Delta H^\circ$ , standard entropy of the reaction can be calculated as

$$\Delta S^\circ = \frac{\Delta H^\circ - \Delta G^\circ}{T} \quad (14.27)$$

Since the  $e^-$  and  $H^+$  are key reactants and products in the thermodynamic sense, a refined knowledge of mechanisms for particular redox reactions is needed because of our current limitations in understanding how similar or different  $e^-$  and  $H^+$  reactions are in soils and natural waters. Knowledge of thermodynamic stability for a redox system does not necessarily predict kinetic lability, a concept directly pertinent to reactivity of different types of complexes (Cotton and Wilkinson, 1980). The kinetic lability of redox processes in soils has not been compared systematically with predictions of stability based on thermodynamic data,

but linear free energy relationships (LFERs) are useful plots of observed rate constants versus equilibrium constants or  $E_h$  values (Stumm and Morgan, 1996; Burge and Hug, 1997). Such information could affirm the reliability of using thermodynamic data to predict bioavailability of nutrients and pollutants, and to estimate true reactivity of electron donors and acceptors in nonequilibrium, kinetically governed soil chemical and microbial environments.

Given the constraining limitation of irreversibility of most redox reactions in soils, especially microbial ones, for using experimental data to calculate values for thermodynamic parameters, the use of kinetic knowledge on soil redox processes is less widely used than are  $p_e$  (and  $E_h$ ) and  $pH$  for assessing equilibrium conditions of soils. Empirical studies in relatively pure, aqueous systems, and complex soil suspensions have, however, provided pertinent information on the kinetics of redox processes and their relation to thermodynamic parameters and reaction pathways (Stumm, 1992, 1993; Stumm and Morgan, 1996; Hug et al., 1997; Typrin, 1998).

### 14.1.4 Microbiological and Enzymatic Controls for Redox State and Processes in Soils

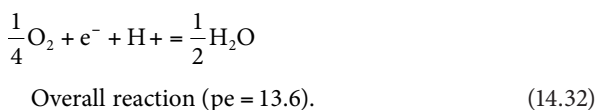
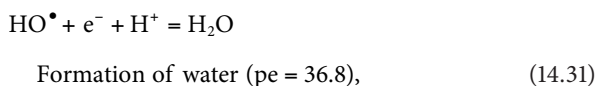
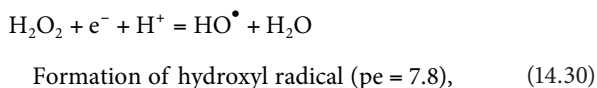
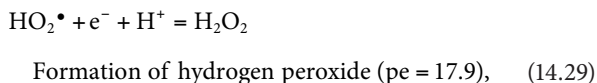
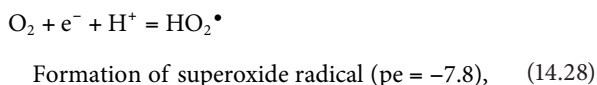
Bacterial metabolism, the process of producing adenosine triphosphate (ATP) through a series of catabolic reactions and building cell constituents with anabolic reactions, requires energy, electrons, nutrients, and either oxygen or another highly oxidized compound to serve as a terminal electron acceptor (TEA; Sylvia et al., 2005). Bacteria that use  $O_2$  as the electron acceptor are aerobic, those that utilize another oxidized compound in the absence of oxygen are anaerobic, and those capable of both are facultative anaerobes. The use of external TEAs intricately links bacteria to important geochemical processes, such as denitrification, methane production, and metal reduction (Salminen et al., 2006; Banerjee, 2008).

The metabolic classification of bacteria is based on the energy source, electron source (reducing equivalents), and carbon source used in catabolic and anabolic processes. Bacteria can derive energy from natural sunlight or from chemical reactions. Phototrophy is the process of using natural light for energy, as employed by photosynthesizing algae or cyanobacteria, whereas chemotrophy requires a chemical reaction for metabolic growth (Madigan and Martinko, 2006). All nonphotosynthetic cellular organisms utilize this pathway to derive the energy needed for metabolic reactions. Electrons (reducing equivalents) can be derived from either organic or inorganic compounds. Organotrophy is the process of using organic compounds, and lithotrophy is that of using inorganic compounds. Organotrophic bacteria are generally associated with chemotrophy; however, lithotrophic bacteria can be either phototrophs or chemotrophs. Cellular C needed for metabolic processes can be derived from organic compounds, which is referred to as heterotrophy, or from  $CO_2$  (dissolved  $CO_2$ ,  $H_2CO_3$ ,  $HCO_3^-$ , or  $CO_3^{2-}$  in natural waters and soil solution; the predominant

species depending on pH), which is autotrophy. Autotrophy is generally linked with lithotrophy, and heterotrophy is associated with organotrophy (Sylvia et al., 2005).

The oxidation of an organic or inorganic compound and reduction of  $O_2$  or other oxidized species during bacterial metabolism is the coupling of oxidation–reduction half-reactions (redox processes) and is the basis for bioenergetics. Biologically mediated redox reactions in soils are linked to metabolic processes and will follow a thermodynamic sequence based on the energetic possibility of the reaction (Stumm and Morgan, 1996). Aerobic chemoorganoheterotrophs use organic C compounds as a source of energy, electrons, and C; and they use  $O_2$  as the TEA. The half-reactions for the reduction of  $O_2$  and oxidation of an organic compound (generally represented by  $CH_2O$  with the oxidation state of C = 0) from Table 14.1 can be coupled to show that the overall  $\Delta G_r^\circ = -130 \text{ kJ mol}^{-1}$ . An anaerobic chemoorganoheterotroph present in an  $O_2$ -depleted environment, such as a wetland soil, can utilize the same C source but would require another TEA. Using  $Fe(OH)_3$  instead of  $O_2$  from Table 14.1 would result in an overall  $\Delta G_r^\circ = -102 \text{ kJ mol}^{-1}$ . This example illustrates how the use of  $O_2$ , when available, is thermodynamically more favorable for metabolic growth than other oxidized species.

The reduction of  $O_2$  to  $H_2O$  in aerobic respiration involves four, one-electron reduction steps, shown with pe values at pH 7:



An examination of the pe values for the stepwise reduction of  $O_2$  to  $H_2O$  demonstrates that even though the overall reaction has a pe = 13.6 (confirming that it is a good oxidizing agent), superoxide, hydrogen peroxide, and hydroxyl radical intermediates are more powerful oxidants than  $O_2$ . Superoxide dismutase or reductase, catalase or peroxidase, and glucose-6-dehydrogenase are essential enzymes used by aerobic cells. They dismutate superoxide and hydrogen peroxide and subsequently reduce hydroxyl radicals more rapidly than the reactive oxygen

species can react with cell constituents, thereby allowing aerobic respiration to proceed. Hydroxyl radicals are rarely formed in microbial cells due to the efficiency of  $H_2O_2$  dismutation to  $H_2O$  and  $O_2$ , following reduction of  $HO_2^\bullet$ . Deficiencies of some or all of these enzymes render soil microbes incapable of respiration under fully aerobic conditions but better adapted to microaerophilic or anaerobic conditions (Madigan and Martinko, 2006).

In aerobic respiration, the coupling of C oxidation to  $O_2$  reduction occurs within the bacterial cell either by substrate-level phosphorylation or oxidative phosphorylation, which is carried out by an intermediate compound such as the coenzyme nicotinamide adenine dinucleotide ( $NAD^+$ ) or nicotinamide adenine dinucleotide phosphate ( $NADP^+$ ) Madigan and Martinko, 2006). Although intermediaries are utilized in oxidative phosphorylation, the overall net change in energy is the difference in reduction potential between the primary electron donor and TEA. The electron-carrying coenzyme NADH or NADPH transfers electrons to a series of four complexes of the mitochondrial respiratory chain, which conserves energy by proton pumping, which further drives the synthesis of ATP (Banerjee, 2008). It is at complex IV, the final complex of electron transfer in oxidative phosphorylation, that oxygen is reduced to water by cytochrome c oxidase in a four-electron, one-step reaction (Equations 14.28 through 14.31). In substrate-level phosphorylation, ATP is directly produced in the enzymatic oxidation of an organic substance but with much lower yields than obtained via oxidative phosphorylation (Madigan and Martinko, 2006).

Calculating the Gibbs free energy of a reaction may indicate that the use of an electron donor and acceptor in a reaction is thermodynamically favorable, but it does not indicate at what rate the reaction would occur. The use of a substrate, although energetically favorable, may not occur at a biologically relevant rate without the catalytic action of an enzyme. Enzymes are proteins configured in secondary, tertiary, or quaternary structures that allow for specific binding properties and often contain non-protein prosthetic groups, cofactors, and coenzymes that participate in the catalytic functions of the enzyme (Madigan and Martinko, 2006). In order to obtain substrates located outside of the cell, enzymes (e.g., hydrolases) can be excreted to break down insoluble polymers such as cellulose, starch, and proteins. These degraded macromolecules are then transported into the cell for use in metabolic reactions (Sylvia et al., 2005). Soil microorganisms using extracellular enzymes are important in the initial depolymerization of cellulose. White rot and brown rot fungi are key microorganisms in the breakdown of cellulose, hemicellulose, and lignin in woody plant tissue in contact with soil.

Either through intracellular or extracellular mechanisms, once substrates are in the cell; oxidative phosphorylation requires a TEA, and in oxygen-depleted environments, bacteria must use alternative oxidized species. Nitrate ( $NO_3^-$ ), Fe(III) (hydr)oxides, Mn(III,IV) (hydr)oxides,  $SO_4^{2-}$ , and  $CO_2$  are oxidized species found in soil, which can be reduced in the terminal step of oxidative phosphorylation, and the reduced forms are excreted from the cell (Sylvia et al., 2005). The reduction of

nitrate coupled to the oxidation of pyrite in anoxic groundwater sediments was recently demonstrated to be a biologically driven redox process (Jorgensen et al., 2009).

In addition to soluble constituents, such as  $\text{NO}_3^-$  or  $\text{SO}_4^{2-}$ , as TEAs, the use of less soluble minerals, such as Fe(III) (hydr)oxides or Mn(III,IV) (hydr)oxides, can also be accomplished. The mechanism by which microbial cells interact with the molecular lattice of minerals is yet to be fully understood. It is speculated that structural or chemical defects, or points in the solid where energy has been perturbed, can serve as regions of reactivity or possibly access sites for organisms (Fredrickson and Zachara, 2008).

Nonenzymatic, extracellular strategies for moving electrons from inside the cell to the outside in electron-transfer processes have been observed. One such strategy is the use of a protein on the cell wall surface that extends away from the cell or a molecule that passes between the cell and substrate when a bacterium lacks the c-type cytochrome necessary to reduce a metal internally (Rawlings, 2005; Gralnick and Newman, 2007; Dittrich and Lutge, 2008). When at a distance from a mineral, *Geobacter sulfurreducens* develops pili, or nanowires, which are localized to one side of the cell wall, and extend out to allow electron transfers to the mineral surface of Fe(III) (hydr)oxides (Reguera et al., 2005).

In addition to localizing proteins to the exterior of the outer membrane, another strategy bacteria use in extracellular respiration is to utilize small organic shuttles to transfer electrons to substrates at a distance from the cell. Quinones are ubiquitous structures found in nature and are principal constituents of soil organic matter (SOM). In the human body, coenzyme Q or ubiquinone is present in every cell, and the ubiquinone/ubiquinol redox couple plays a role in shuttling electrons between complex II and III of the mitochondrial electron transport chain during oxidative phosphorylation (Table 14.1; Banerjee, 2008). Ubiquinone also acts as a lipid-soluble antioxidant by accepting one electron and forming a stable radical anion semiquinone.

This same quinone structure is present in soils and natural waters as the primary abiotic electron-donating and accepting moiety of humic and fulvic acids in natural organic matter (Scott et al., 1998; Ratasuk and Nanny, 2007).

Phenolic groups are abundant in natural organic matter and are important in complexation reactions with metals. Phenolic groups can be biologically oxidized by the enzymes phenolase and laccase to produce quinones (Tan, 2003). Converse to this oxidation, a one-electron transfer to quinone forms the same, highly reactive intermediate semiquinone as with ubiquinone and then the second electron transfer forms hydroquinone (Larson, 1997). Hydroquinone is then capable of donating its two electrons in further reduction reactions, making the quinone–hydroquinone species a very dynamic redox constituent in soils. The natural reducing capacities of International Humic Substance Society (IHSS) humic acids were shown to increase several-fold following microbial reduction and were significant even under aerobic conditions (Peretyazhko and Sposito, 2006).

The electron-donating kinetics of dissolved organic matter in aquatic systems was shown to occur within the course of 1 day and capable of shuttling electrons to  $\text{SO}_4^{2-}$  and Fe(III) (Bauer et al., 2007).

Quinone moieties in natural organic matter can serve as TEAs in microbial respiration, cycling electrons from bacteria to mineral surfaces (Lovley et al., 1996; Bond and Lovley, 2002). Soil bacteria reduced the humic acid analog, anthraquinone-2,6-disulfonate (AQDS), which then shuttled electrons to reduce Fe(III) (Fredrickson et al., 1998; Kappler et al., 2004). The shuttling activity of AQDS was demonstrated further with *G. sulfurreducens* shuttling electrons to ferrihydrite in solution (Straub and Schink, 2003). This use of humic substances as a TEA may allow for more efficient respiration than directly using a mineral. The rate of electron transfer between reduced humic substances to ferrihydrite is approximately 27 times faster than the rate of *G. sulfurreducens* directly transferring electrons to ferrihydrite (Jiang and Kappler, 2008).

The biological reduction of electron shuttles, such as soluble humic acids, is important in soils, but abiotic reduction pathways also significantly contribute to the natural redox cycling of metals and nutrients. Lactic acid, tartaric acid, and citric acid were shown to reduce AQDS, which then shuttled electrons to enhance the reduction of Cr(VI) in solution (Brose and James, 2010). Low-molecular-weight organic acids, such as these, are produced naturally by microbial activity or plant root exudates and can be important reducing agents for quinone moieties in soils and soluble humic acids, thus further contributing to natural redox process in soils. Figure 14.2 illustrates the conceptual model of how citric acid reduces the electron shuttle AQDS to  $\text{AH}_2\text{DS}$ , which ultimately reduces Cr(VI) to Cr(III).

Electrons are in constant flux in soils, being transferred from electron donors to electron acceptors, often mediated by soil microorganisms, which results in metastable redox conditions in soils. Though thermodynamic equilibrium models may predict steady-state conditions, in reality, a dynamic nonequilibrium state is a more accurate representation of natural systems (Stumm and Morgan, 1996). Often, redox reactions in soils are moving

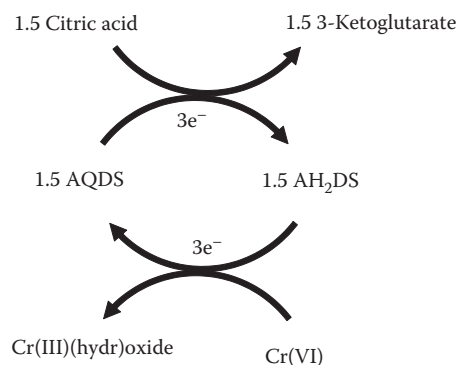


**FIGURE 14.2** The stoichiometric transfer of electrons from citric acid to AQDS, reducing it to the hydroquinone form  $\text{AH}_2\text{DS}$ , which ultimately reduces Cr(VI) to Cr(III).

toward equilibrium, but the reactions are constantly being perturbed by the influx and efflux of chemical species and soil biota, thus shifting activities and reestablishing new, partial equilibria. Dioxide is the most ubiquitous electron acceptor in natural systems, when available, and the electron activity and type of microorganisms present in a soil depend, in part, on its presence.

Because a saturated soil restricts the diffusion of  $O_2$ , saturated soils allow for more electron flow to other electron acceptors, such as Fe(III) (hydr)oxides and  $SO_4^{2-}$  (Bartlett and James, 1993). When a soil becomes submerged, pe decreases, and the rate of decrease will be a function of easily oxidized SOM, temperature, time submerged, and nature of available electron acceptors (Sparks, 2003), which are also important metabolic requirements of soil microorganisms. Though soils host a variety of microorganisms using a diverse array of electron acceptors for respiration, such as Fe(III) (hydr)oxides in anoxic sediments, SOM is the dominant electron donor and can be fully oxidized to  $CO_2$  (Lovley, 2000), or partially to organic acids. Aerobic microorganisms will thrive until  $O_2$  is depleted, and then facultative and obligate anaerobic microorganisms will be the dominant biological mediators.

Bacteria and their electron-shuttling systems are widely used in remediation strategies for organic and inorganic pollutants. Humus and other quinone analogs were used in the reductive biotransformation of nitroaromatic compounds and to dechlorinate organic pollutants (Field et al., 2000; Becker, 2006). In the anaerobic oxidation of phenol and *p*-cresol, it was shown that the addition of the quinone analog AQDS diverted electrons from methanogenesis to quinone reduction, a more thermodynamically favorable reaction (Cervantes et al., 2000).

The bioremediation of metals, such as Cr(VI) and U(VI) has also proven to be an effective strategy for treating contaminated soils and groundwater (Gu and Chen, 2003; Nyman et al., 2007; Wu et al., 2007). The cell wall of *Arthrobacter oxydans* contains an acid-soluble protein with a positive charge, as shown by electrophoresis, capable of reducing Cr(VI) to an insoluble Cr(III) (hydr)oxide (Asatiani et al., 2004). Bacteria can transform Hg compounds to either less toxic or less bioavailable species. *Desulfovibrio desulfuricans* API strain degrades  $CH_3Hg^+$  by producing  $H_2S$  that reacts with  $CH_3Hg^+$  forming the insoluble species  $(CH_3Hg)_2S$  (Hobman et al., 2000). The dissimilative reduction of Se(VI), a soluble, toxic form of Se, to the insoluble Se(0) by anaerobic bacteria in anoxic environments has important implications for the continued irrigation of seleniferous soils and industrial applications such as the production of pesticides and semiconductors (Oremland and Stolz, 2000).

As bacterial metabolic activities are continually studied, more ways will be discovered to apply the use of microorganisms to transform pollutants to less toxic or less bioavailable forms. The adaptation of bacteria to a wide variety of electron donors and acceptors provides almost unlimited application of biologically mediated redox reactions. Understanding how bacteria link the oxidation of electron donors to the reduction of electron acceptors will provide insight into further utilizing these mediated reactions to improve ecosystems and natural waters.

## 14.2 Methods and Procedures

### 14.2.1 Uses of pe–pH Thermodynamic Information

Values of log K derived from Gibbs free energy of formation data or kinetic evaluations of redox reactions provide tools for predicting if a reduction half-reaction coupled with an oxidation half-reaction will allow the spontaneous transfer of electrons from reductant to oxidant. Since soils are only metastable and highly heterogeneous in nature, such predictive capability is necessary to formulate hypotheses for many processes that may occur in the field, even if they require microbial catalysis or other coupled reactions to occur at ambient temperatures and pressures of soil–water–plant systems.

The reduction half-reactions listed in Table 14.1 are biological and abiotic species of N, O, Mn, Fe, S, C, various pollutants sensitive to redox conditions in soils and several reactions pertinent to the analysis or characterization of redox conditions. Within groups, the half-reactions are arranged in descending order of log K values, calculated as described above. These values are pe at pH = 0 when activities of oxidant and reductant are 1 and may be considered standard, reference pe values for the reactions (formal potentials). The pe values listed at pH 5 and 7 are calculated to represent typical activities of ions and partial pressures of gases in soil environments.

Higher log K or pe values indicate greater “ease of reduction” of an oxidant (left side of equation) to its reduced form than do lower values. This means that for predictive purposes, an oxidant in a particular reduction half-reaction is able to oxidize the reductant in another half-reaction with a lower pe, at a specified pH, as demonstrated quantitatively for the  $FeOOH-Fe^{2+}$  and  $SO_4^{2-}-H_2S$  couples. Another example shows Mn(III,IV) (hydr)oxides would be expected to oxidize Cr(OH)<sub>3</sub> to Cr(VI) at pH 5 since the range of pe values for reduction of Mn (12.8–16.7) is greater than that for Cr(VI) reduction (10.9). This has been demonstrated to occur in most field-moist soils in the pH range of 4–7 containing oxides of Mn(III,IV) (Bartlett and James, 1979; James and Bartlett, 1983). Conversely, these oxides would not be expected to oxidize  $N_2$  to  $N_2O$  (pe at pH 5 = 22.9).

Even though the log K or pe for one reduction half-reaction is less than that for a second half-reaction, the reduced form in the first reaction may still be oxidized by the oxidized species in the second half-reaction (the reverse of the above concept). For example, the pe at pH 5 for reduction of  $CO_2$  to  $C_6H_{12}O_6$  is –5.9 and that for reduction of  $O_2$  to  $H_2O$  is 15.6. Based on this difference, one would predict that reduction of  $O_2$  to  $H_2O$  would be coupled to oxidation of  $C_6H_{12}O_6$  to  $CO_2$ , and coupling oxidation of  $H_2O$  to  $O_2$  with reduction of  $CO_2$  to  $C_6H_{12}O_6$  would not be thermodynamically probable. In fact, both respiration (the predicted reaction) and photosynthesis (the second, “improbable” reaction) occur together, and the balance of the two is responsible for the existence of the aerobic lifestyle and the persistence of SOM. Photosynthesis (represented simply as  $CO_2 \rightarrow C_6H_{12}O_6$ ) is made possible by a complex series of coupled reactions that



make an overall thermodynamically improbable reaction occurring rapidly in sunlight.

Similarly, a reaction predicted to be thermodynamically probable may not occur at any appreciable rate under natural conditions. The pe for  $\text{NO}_3^-$  reduction to  $\text{N}_2$  at pH 5 (14.3) is greater than that for  $\text{HCrO}_4^-$  reduction to  $\text{Cr}(\text{OH})_3$  (10.9), but this  $\text{NO}_3^-$  oxidation of Cr(III) has not been demonstrated in soils or plants, probably because the reduction of  $\text{NO}_3^-$  requires enzymatic catalysis to lower the energy of activation at such a high pH.

The order of log K values for reduction half-reactions also has been used to predict the sequence of reduction reactions carried out by respiring soil microorganisms following saturation of a soil (Ponnamperuma, 1972). The descending order of preference (pe) for the electron acceptors at pH 7 (proportional to free energy derived from the reduction) is  $\text{O}_2$ – $\text{H}_2\text{O}$  (13.6),  $\text{NO}_3^-$ – $\text{N}_2$  (11.9),  $\text{MnO}_2$ – $\text{Mn}^{2+}$  (8.8),  $\text{Fe}(\text{OH})_3$ – $\text{Fe}^{2+}$  (–1.2),  $\text{SO}_4^{2-}$ – $\text{H}_2\text{S}$  (–3.5), and  $\text{CO}_2$ – $\text{CH}_4$  (–4.1). Heterotrophic bacteria are using organic compounds as the electron donors and their energy source (chemoorganoheterotrophs) in their respiration to produce  $\text{CO}_2$  or organic acids (pe range at pH 7 of –8.7 to –3.1), so most of the organic compounds can be used throughout the reduction sequence following depletion of atmospheric  $\text{O}_2$ .

## 14.2.2 Use of pe–pH Diagrams

### 14.2.2.1 Oxygen Species

While the pe for reduction of  $\text{O}_2$  to  $\text{H}_2\text{O}$  ranges from 20.8 at pH 0 to 13.6 at pH 7 (Table 14.1), the intermediates associated with one-electron transfers show a wide fluctuation in their oxidizing power (Equations 14.28 through 14.32), a property of  $\text{O}_2$  that is pertinent to understanding the transition in soils from “aerobic” to “anaerobic” conditions. Anaerobic respiratory enzymes are typically produced when  $P_{\text{O}_2}$  reaches approximately 1% of atmospheric levels (0.0021 atm). The data in Table 14.2 also indicate that the pe for reduction of  $\text{O}_2$  is relatively insensitive to the  $\text{O}_2$  partial pressure in this range.

Ozone ( $\text{O}_3$ ) and the hydroxyl free radical ( $\text{HO}^\bullet$ ) are the most powerful oxidants among the oxygen species (Table 14.1), and the latter may be formed during stepwise, four-electron reduction of  $\text{O}_2$  to  $\text{O}_2^-$ ,  $\text{H}_2\text{O}_2$ , and  $\text{H}_2\text{O}$  (Fridovich, 1978; Equations 14.28 through 14.32). The high and low pe values for superoxide reduction to  $\text{H}_2\text{O}_2$  and for superoxide oxidation to  $\text{O}_2$  indicate that both a powerful oxidant and a powerful reductant agent are formed in the first of four, one-electron steps in the reduction of  $\text{O}_2$  to  $\text{H}_2\text{O}$ . The enzyme superoxide dismutase scavenges superoxide in living cells using  $\text{O}_2$  as the TEA (respiring aerobically), but relatively little is known about its reactivity in biological and chemical processes in soils that may be pertinent to our understanding of the formation of highly reduced components such as SOM and highly oxidized species such as  $\text{NO}_3^-$  that coexist in soil under non- or quasi-equilibrium conditions.

The wide range of reduction potentials for  $\text{O}_2$  and its partially reduced intermediates, coupled with biological processes controlling the partial pressure of this gas in soil solution, create

**TABLE 14.2** Sensitivity of Calculated pe at pH 0 to Variation in  $\square G_f^\circ$  and Activities of Oxidant and Reductant in Selected Half-Reactions Pertinent to Soils

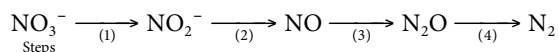
Couple	–log Activity		$\square G_f^\circ$		pe	$\Delta\text{pe}^a$
	Ox	Red	Ox	Red		
$\text{O}_2/\text{H}_2\text{O}$	0.68	0	0.00	–237.01	20.61	
	2.68	0	0.00	–237.01	20.11	–0.50
	0.68	0	0.00	–278.81	24.20	3.59
$\text{NO}_3^-/\text{N}_2$	4	0.11	–110.48	0.00	20.30	
	6	0.11	–110.48	0.00	19.90	–0.40
	4	0.11	–152.28	0.00	18.80	–1.50
$\text{Mn}_3\text{O}_4/\text{Mn}^{2+}$	0	4	–1279.92	–227.39	36.70	
	0	6	–1279.92	–227.39	39.70	3.00
	0	4	–1321.72	–227.39	33.00	–3.70
$\text{MnO}_2/\text{Mn}^{2+}$	0	4	–464.40	–227.39	22.80	
	0	6	–464.40	–227.39	23.80	1.00
	0	4	–506.20	–227.39	19.10	–3.70
$\text{MnOOH}/\text{Mn}^{2+}$	0	4	–556.36	–227.39	29.40	
	0	6	–556.36	–227.39	31.40	2.00
	0	4	–598.16	–227.39	22.10	–7.30
$\text{CO}_2/\text{C}_6\text{H}_{12}\text{O}_6$	3.5	4	–394.01	–913.66	–0.91	
	3.5	6	–394.01	–913.66	–0.83	0.08
	3.5	4	–394.01	–955.46	–0.60	–0.31
$\text{Fe}(\text{OH})_3/\text{Fe}^{2+}$	0	4	–712.27	–91.12	19.80	
	0	6	–712.27	–91.12	21.80	2.00
	0	4	–754.07	–91.12	12.40	–7.40
$\text{Fe}_2\text{O}_3/\text{Fe}$	0	4	–740.28	–91.12	17.40	
	0	6	–740.28	–91.12	19.40	2.00
	0	4	–782.08	–91.12	13.70	–3.70
$\text{SO}_4^{2-}/\text{H}_2\text{S}$	4	4	–743.83	–33.52	5.20	
	6	4	–743.83	–33.52	5.50	0.30
	4	4	–702.03	–33.52	6.10	0.90

<sup>a</sup> Change in calculated pe resulting from a change in activity of the ox or red species (column 1 or 2) or resulting from use of a  $\square G_f^\circ$  value that is 44 kJ mol<sup>–1</sup> (10 kcal) different from the published value (first row, column 3 or 4).

conditions under which the  $\text{O}_2$ – $\text{H}_2\text{O}$  system may rarely attain equilibrium. Therefore, only metastable conditions and a slow approach to chemical equilibrium characterize  $\text{O}_2$  behavior, making thermodynamic predictions difficult for aerobic soils (Bartlett, 1981).

### 14.2.2.2 Nitrogen Species

Most reduction reactions of N species (Table 14.1) are not reversible, are biologically mediated, and therefore are not well defined by thermodynamic pe–pH relationships. The series of half-reactions composing the process of denitrification, though, is instructive in that it identifies the wide range in pe for reduction of each of the intermediates believed to form in the sequence of electron acceptors used by microbes:



Step (1) of the sequence occurs at  $pe$  values less than those for reduction of  $O_2$  to  $H_2O$ , while those for steps (2), (3), and (4) are increasingly higher. The overall reduction of  $NO_3^-$  to  $N_2$  is almost identical to that for the  $O_2$ - $H_2O$  couple. The similar  $pe$  range for the  $O_2$  and  $NO_3^-$  reduction intermediates indicates that denitrification and aerobic respiration may occur at the same time under certain conditions when organic C is used as the electron donor. They may not be mutually exclusive as predicted from  $\log K$  values for the overall reactions,  $O_2$  to  $H_2O$  and  $NO_3^-$  to  $N_2$ .

#### 14.2.2.3 Manganese Oxide Species

Manganese exists in soils in the II+, III+, and IV+ oxidation states, and the latter two are most stable as oxides or oxyhydroxides. Trivalent Mn may exist as  $Mn(H_2O)_6^{3+}$ , especially if stabilized by ligands, such as pyrophosphate or citrate. The  $pe$  values (Table 14.1) predict that different oxidation states of Mn in  $Mn_3O_4$ ,  $MnOOH$ , and  $MnO_2$  affect the  $pe$  at which  $Mn^{2+}$  would be expected to form at pH 5 ( $pe$  values of 16.7, 14.4, and 12.8, respectively), but they are all similar at pH 7 (8.7, 8.4, and 8.8). The  $Mn^{3+}$ - $Mn^{2+}$  couple indicates that at pH  $\approx$  5,  $Mn^{3+}$  is a powerful oxidant ( $pe$  25.5) similar to superoxide ( $pe$  22.6) if in equilibrium with  $Mn^{2+}$ . At pH  $\approx$  6.5,  $Mn^{3+}$  in equilibrium with  $MnO_2$  is a powerful reductant similar to  $H_2$  and again, superoxide. This predicted reducing energetics of  $Mn^{3+}$  may be pertinent to anaerobic soils that are exposed to  $O_2$ , and in which  $Mn^{2+}$  is oxidizing to form Mn(III,IV) (hydr)oxides via  $Mn^{3+}$ . In oxidized soils containing  $MnO_2$ , flooding and the process of becoming reduced may produce  $Mn^{3+}$ , which is a powerful reducing agent. The trivalent Mn species may be ephemeral intermediates in such processes at redox interfaces, such as in the rhizosphere of plant roots or between the vadose zone and groundwater.

Since many Mn(III,IV) (hydr)oxides are nonstoichiometric and no compound with the exact composition of  $MnO_2$  is known (Arndt, 1981), predictions of their redox properties as a function of mineralogy or oxidation state in heterogeneous soils may be hard to formulate. Despite the uncertainty of thermodynamic predictions for the redox behavior of Mn, the chemistry of this element is pertinent to a number of processes governing speciation and oxidation state of trace elements and pollutants found in soils (Bartlett and Ross, 2005). The  $pe$ -pH data indicate that oxides of Mn may oxidize Pu(III) to Pu(IV), V(III) to V(V), As(III) to As(V), Se(IV) to Se(VI), N(III) to N(V), and Cr(III) to Cr(VI) since the  $pe$  for each of these couples falls below that for Mn oxides (Table 14.1). The oxidations of Pu(III), As(III), Se(IV), N(III), and Cr(III) all have been demonstrated to occur in soils containing Mn(III,IV) (hydr)oxides or by synthetic Mn(III,IV) (hydr)oxides (Bartlett and James, 1979; Amacher and Baker, 1981; Bartlett, 1981; Moore et al., 1990; Blaylock and James, 1994).

The instability of  $Mn^{3+}$  and its ability to dismutate, similar to  $H_2O_2$  and superoxide, mean that kinetic constraints and very low steady-state concentrations in soil solution may be particularly important in understanding the redox behavior of Mn in soils undergoing transitions between anaerobic and

aerobic conditions. The kinetic lability of these species is poorly understood and new knowledge could contribute significantly to predictions of bioavailability and toxicity of numerous plant nutrients and pollutants in a range of soil types from rice paddies and wetlands to well-drained agricultural and forest soils.

#### 14.2.2.4 Iron Species

While predictions of redox behavior of Fe(II) and Fe(III) species indicate that they fall below most Mn(III,IV) (hydr)oxide species (lower  $pe$  values and less free energy released per equivalent upon reduction), intermediate hydrolysis products, such as  $Fe(OH)_2^+$ , theoretically can oxidize Cr(III) to Cr(VI) at pH values  $<4$  (Table 14.1). In addition, thermodynamically more stable complexation of  $Fe^{3+}$  by organic and inorganic ligands such as  $OH^-$ , relative to complexation of  $Fe^{2+}$ , lowers the  $pe$  at which  $Fe^{3+}$  is reduced to  $Fe^{2+}$ . These Fe(II)-Fe(III)-ligand reduction potentials are similar to those of Fe(III) (hydr)oxides in the pH range 5-7 (Table 14.1). This phenomenon suggests that Fe(II)-Fe(III)-ligand systems create Fe(II) species that are more powerful reductants than hexaquo  $Fe^{2+}$  if the Fe(III)-ligand complex is more thermodynamically stable than the Fe(II)-ligand complex. Conversely, if the complex with Fe(II) is more stable than that with Fe(III) (e.g., with phenanthroline), the Fe(II) becomes a less powerful reductant than hexaquo  $Fe^{2+}$ . This may explain the ability of a Fe(II,III) system to act as a cofactor in enzymes involved in redox processes, such as peroxidases and superoxide dismutases. These enzymes reduce or dismutate  $H_2O_2$  and superoxide. The application of such concepts to abiotic redox processes in soils remains a key area for future research.

#### 14.2.2.5 Carbon and Sulfur Species

Reduced forms of C and S are normally viewed as reductants in soils, either in abiotic or biological processes. Thermodynamic predictions support this idea for carbohydrates produced in photosynthesis,  $CH_4$  from methanogenesis, and  $H_2S$  from reduction of  $SO_4^{2-}$  (Table 14.1). The reduction reactions of *o*- and *p*-quinone, suggest that these compounds may be reduced at higher  $pe$  values than are  $CO_2$  and  $SO_4^{2-}$ . These  $pe$  values, however, coincide with the  $MnO_2/Mn^{3+}$  couple at pH 7, suggesting that  $Mn^{3+}$  may act as a reducing agent for certain organic species in near neutral soils. The coupling of reduction of the organic species with oxidation of Mn may result in formation of free radical species. This is pertinent to understanding the formation and persistence of SOM in high pH soils that may contain reactive forms of Mn(III,IV) (hydr)oxides (Bartlett and Ross, 2005).

Reactions of  $H_2S$  and  $H_2Se$  are predicted to be similar with respect to  $SO_4^{2-}$  and  $SeO_3^{2-}$  formation (Table 14.1). While  $SeO_4^{2-}$  and  $SO_4^{2-}$  are similar chemically, the oxidation of  $SeO_3^{2-}$  to  $SeO_4^{2-}$  is predicted to occur at higher  $pe$  values than that of  $H_2S$  to  $SO_4^{2-}$  (Table 14.1). Blaylock and James (1994) observed that Mn(III,IV) (hydr)oxides in soils or in pure form will oxidize  $SeO_3^{2-}$  to  $SeO_4^{2-}$ , as predicted by thermodynamics. They also observed that adding reducing phenolic acids, such as gallic and ascorbic acids, actually enhanced this oxidation reaction of  $SeO_3^{2-}$ . They hypothesized that partial reduction of  $MnO_2$

in soils converted the Mn(IV) (hydr)oxide into a Mn(III) (hydr)oxide or ion that is a more powerful oxidant for  $\text{SeO}_3^{2-}$  than is Mn(IV) oxide. Such a hypothesis is supported by the relative oxidizing power of  $\text{MnO}_2$ ,  $\text{MnOOH}$ , and  $\text{Mn}_3\text{O}_4$ , where the latter two oxides contain Mn(III) (Table 14.1).

### 14.2.3 Measurement of Soil Redox and Acid–Base Status

The most common method for quantifying electron activity of soils and natural waters is to measure the potential difference between a Pt indicator electrode and a calomel or Ag/AgCl reference electrode, both connected to a voltmeter or a pH meter (Pearsall and Mortimer, 1939; Patrick and DeLaune, 1972; Rowell, 1981; Bricker, 1982; Patrick et al., 1996; Rabenhorst et al., 2009). In this method, the Pt electrode is presumed to be inert and does not react chemically while coming into equilibrium with electroactive species in soil solution and on soil colloids (Compton and Sanders, 1996). Figure 14.3 illustrates how a Pt electrode establishes an equilibrium condition with soil solution. When the electrode contacts the soil solution (and while coupled to a reference electrode), a tiny quantity of electrons jumps either from the soil solution to the electrode (when soil is more reduced than the electrode) or in the opposite direction when the soil solution is more oxidized. In the first case, the Pt electrode becomes more negative relative to the soil, and this lowers the voltage at the electrode–soil solution interface. In the second, the electrode surface and the potential become more positive.

A high input impedance ( $\geq 20 \text{ m}\Omega$ ) is needed to obtain precise and accurate electrode potentials, because if current flows under

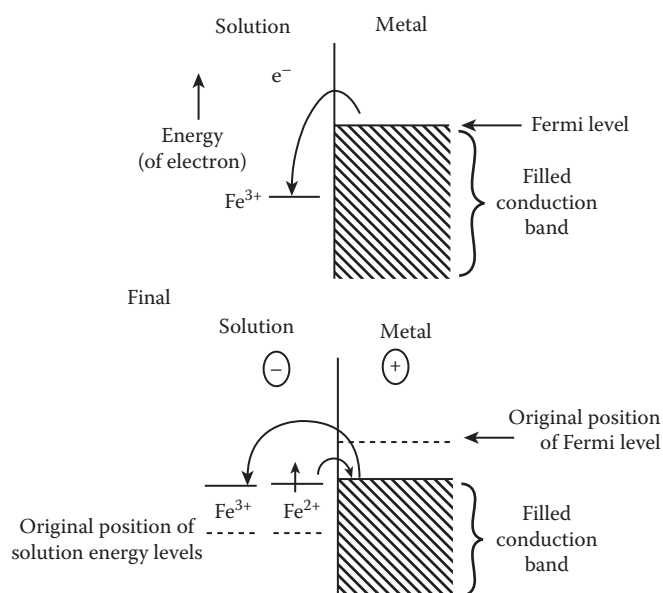


**FIGURE 14.3** The energy of electrons in ions in solution and in the Pt electrode. (Taken from Compton, R.G., and G.H.W. Sanders. 1996. *Electrode potentials*. Oxford Science Publications, Oxford, U.K. p. 4, Fig. 1.2.)

low impedance, drift will be observed in the voltage readings (Rabenhorst et al., 2009), and redox reactions may take place at the electrode–soil solution interface. Such reactions may form interfering redox couples on the Pt metal (e.g.,  $\text{Pt}(\text{OH})_2$ –Pt or PtS–Pt; see Table 14.1). Commercially available pH meters typically have high input impedance, but inexpensive voltmeters that are sometimes used in field studies with multiple Pt electrodes do not.

Generally, Pt electrode measurements are only semiquantitative for assessments of redox status, especially of aerobic soils in the field (Whitfield, 1974; Bartlett, 1981; Grenthe et al., 1992; Hostettler, 1992; Grundl, 1994). Other methods that employ analysis of soil solution analytes indicative of redox status, along with thermodynamic half-reactions, as discussed above, may prove more reliable for calculating pe ranges for aerobic and anaerobic soil systems (Peiffer et al., 1992; Kludze et al., 1994; Lovley et al., 1994; Stumm and Morgan, 1996; Typrin, 1998).

#### 14.2.3.1 Construction and Use of Pt Electrodes

Platinum and suitable reference electrodes are relatively easy and inexpensive to construct (Mueller et al., 1985; Farrell et al., 1991), but measurement technique may significantly alter measured voltages (Bartlett, 1981; Bricker, 1982; Matia et al., 1991). These researchers have described several aspects of electrode use and misuse with respect to the reliability of recorded voltages for natural systems. Comparisons have been made between  $\text{H}_2$  and Eh measurements for redox status in a contaminated aquifer (Chapelle et al., 1996). Quantification of  $\text{H}_2$  was more reliable than Eh measurements for identifying anoxic redox process, especially when considered with respect to electron acceptor availability. The limits and limitations of Eh measurements have been described for natural systems, especially with respect to how long the electrodes may be left in place in the soil or water (Mansfeldt, 1993; Norrström, 1994) and with respect to interpreting the Eh values obtained (Baas-Becking et al., 1960; Whitfield, 1974; Lindberg and Runnells, 1984; Yu, 1992). Platinum electrode systems also have been incorporated into potential-controlling systems for long-term laboratory studies (Patrick, 1966; Petrie et al., 1998).

#### 14.2.3.2 Inadequacies of Pt Electrode Potentials

Assessing “electron activity” in soils relates strictly to an evaluation of the ability of the electron to be transferred, or do thermodynamic work, and not of its concentration or activity in soil solution, as can be defined for  $\text{H}^+$ . Because of the nature of the electron and its differences from  $\text{H}^+$ , a number of caveats must be described and recognized when evaluating Pt electrode potentials.

##### 14.2.3.2.1 Dissolved Oxygen Status

While a stable potential can be obtained for a Pt-reference electrode pair immersed in an oxygenated soil suspension, this potential is unreliable as a measure of dissolved oxygen status (Bricker, 1982; Stumm and Morgan, 1996). The Pt surface may

react with  $O_2$  to form  $Pt(OH)_2$  that develops a potential with elemental Pt with a pe of 9.6 at pH 7 (Table 14.1). In addition, the measurement may not be that of the  $O_2$ - $H_2O$  couple but may be responding to  $O_2$  reduction intermediates, such as  $H_2O_2$  and superoxide (Bricker, 1982). In addition, predicted pe values are relatively insensitive to changes in dissolved  $O_2$  between 0.21 and 0.0021 atm (Table 14.2), the range of  $O_2$  partial pressures in which aerobic respiration occurs (Russell, 1973). For these reasons, Pt electrode potentials cannot be used reliably as a measure of redox status for aerobic soils, but empirical values for pe may be obtained for comparison purposes (Bartlett, 1981, 1998).

While more faith is placed in measurements of soil pH, it also should be considered an empirical measurement because of uncertainty about the form of the  $H^+$  ion in colloidal environments and about the behavior of the glass electrode in such systems. For these reasons, both pe and pH measured with electrodes in soils may be very uncertain for accurate descriptions of the redox status of soil environments containing air-filled pores.

#### 14.2.3.2.2 Irreversibility of Redox Couples

Many of the important redox processes involving C, H, N, O, and S (the “light” elements, relative to the “heavy” metals) are irreversible in the thermodynamic sense, and nonelectroactive gases and molecules may be consumed or formed. As a result, potentials generated by redox couples for these elements are difficult to obtain and interpret using a Pt electrode. In addition, many of these reactions do not reach true chemical equilibrium, and activities measured in soil solution may be kinetically constrained (Liu and Narasimhan, 1989). Since soil redox status is often set by “microbial potentials,” as discussed earlier, consuming or producing compounds or ions containing one or more of these elements may render Pt electrode measurements inaccurate.

#### 14.2.3.2.3 Mixed Potentials

Measured redox potentials in soils normally are governed by more than one redox couple (“mixed potentials”), and these couples usually are not at true chemical equilibrium. Therefore, thermodynamic interpretations of measured Pt electrode potentials in soil suspensions need to consider several couples, and analyses of soil solution concentrations of redox active species may be indicative of the couples controlling the potential at the Pt surface (Typrin, 1998). For example, a  $Fe^{2+}$ - $Fe^{3+}$  couple at activities greater than  $10^{-5}$  M generates sufficient anodic and cathodic currents to obtain a measurable voltage for the system, and this may coexist with the relatively nonelectroactive couple,  $O_2$ - $H_2O$  in heterogeneous soils.

The establishment of a measurable balance between the cathodic and anodic current at the Pt electrode at the point of zero applied voltage requires activities of  $>10^{-5}$  M, a condition that may not exist for many redox active species of interest in soils. Activities  $<10^{-6}$  M may be common, especially for certain plant nutrients and soil pollutants. For this reason, application of measured Pt electrode potentials to predicting soil composition may not be possible.

#### 14.2.3.2.4 Coupling of pH and pe

Based on the complementary nature of pH and pe (Stumm and Morgan, 1996) summing pe + pH to describe log K for soils is possible theoretically, as described above. Due to the fact that the Pt electrode responds to pH (almost in Nernstian fashion) as well as to electron activity, pH should always be measured and reported with pe. The negative slopes of the pe-pH relationships (Figure 14.1) of many of the reduction half-reactions also indicate that the energy change associated with a particular reduction reaction decreases with increasing pH. Therefore, an Eh measurement cannot be used to predict the presence of a particular redox couple unless pH is known. Since higher pe values at lower pHs correspond to larger releases of free energy, reduction reactions are expected to be more likely to occur at lower pH. That is, such systems are ones in which “reduction is favored.” In contrast, loss of electrons from reductants of a particular couple is favored at higher pH, or the system is more “prone to oxidation.”

### 14.2.4 Proposed Alternative Strategies for More Accurate Measurement of Soil Redox Status

#### 14.2.4.1 Using Electrochemical Relations in Reverse

Given the uncertainty associated with measured Pt electrode potentials in soils to quantify Eh or pe, actual measurements of reductant and oxidant activities, along with a reliable pH measurement, may be a better approach (Stumm and Morgan, 1996; Typrin, 1998). The activities are substituted into appropriate half-reactions relating pe and pH, and pe is thereby obtained by calculation.

As shown in Table 14.2, the pe predicted by such a technique will be inaccurate to different degrees for different half-reactions. For example, an error of two log units for  $H_2S$  or  $O_2$  partial pressures will only produce errors of 0.3–0.5 pe units. In contrast, similar errors in measurement of  $Mn^{2+}$  or  $Fe^{2+}$  will result in pe errors of 1.0–3.0 pe units. Since Mn and Fe are relatively easy to measure accurately by atomic absorption or colorimetric methods and mineralogy of associated oxides can be made with infrared or x-ray techniques, assessing pe for Mn and Fe oxide-dominated systems could be reliable. Detailed research is needed to prove this hypothesis. In contrast, dissolved gases are harder to measure accurately, and qualitative estimates may be sufficient to obtain accurate evaluations of pe.

If calculated pe values obtained with this “reverse electrochemical technique” are equal for two different reduction half-reactions, then chemical equilibrium may be assumed to exist. If the pe values are unequal, then disequilibrium and a metastable, kinetically limited soil system probably exists. This latter condition is common in soils due to spatial heterogeneity of soil solution, oxide mineralogy, organic matter reactivity, and microbial controls on key reactions. New thinking and hands-on research are needed to provide new ideas for evaluation of the “electron activity” for soils by this combination of analytical and thermodynamic approaches. A key to its accuracy is knowing what

redox couples are contributing to the electron activity, assumed to exist as a quantifiable parameter at chemical equilibrium.

#### 14.2.4.2 Redox Ranges for Empirical pe Values

These limitations to assessing soil pe based on Pt electrode and reverse electrochemical methods indicate that our sense of accuracy for soil redox status must be modified. If we surrender in our efforts to conceptualize and operationally define soil redox status, we will have lost a challenging scientific crusade. This means that while new ideas are being developed, we accept a lack of knowledge of pe values more accurate than ranges bracketed by whole numbers.

Liu and Narasimhan (1989) have described “redox zones” in which a range in Eh or pe defines an electron activity condition. The oxygen–nitrogen range is defined by Eh values of +250 to +100 mV, the iron range is +100 to 0.0 mV, the sulfate range is 0.0 to –200 mV, and that for methane–hydrogen is defined at < –200 mV. Sposito (1989) proposed “oxic” soils as those with pe > 7, “suboxic” ones in the range of pe between +2 and +7, and “anoxic” soils with pe < +2; all at pH 7. These ranges correspond roughly to redox control by oxygen–nitrogen, manganese–iron, and sulfur couples.

Berner (1981) proposed categories for redox named “oxic, postoxic, sulfidic, and methanic” controlled by transformations of oxygen/nitrogen, iron, sulfur, and methane–hydrogen, respectively. James (1989) has proposed these names be assigned to ranges in EMpe (empirical pe; Bartlett, 1981, 1998) of +7 to +13, +2 to +7, –2 to +2, and –6 to –2 (at pH 7). The appropriateness of these categories and names will require further evaluation of new operational definitions for the concept of “redox status” in soils.

Bartlett and James (1995) proposed a new system for categorizing soil redox status using chemical field tests such as tetramethylbenzidine for Mn status, Cr oxidation–reduction reactions, Fe speciation, sulfide levels, and pH. They proposed the following categories: superoxic, manoxic, suboxic, redoxic, anoxic, and sulfidic, which relate to electron lability in heterogeneous soil systems under field conditions. Bartlett (1998) has refined this system of redox classification and applied it to interfacial processes in soils pertinent to wetlands, hydric soils, and other soil–water systems containing contrasting zones of redox status.

#### 14.2.4.3 Use of “Indicator of Reduction in Soils” (IRIS) Tubes

A novel method for assessing whether or not a soil may become reducing for Fe(III) (hydr)oxides to Fe(II) is to coat 21 mm, polyvinyl chloride (PVC) tubes with paints made from Fe(III) (hydr)oxide suspensions of known mineralogy. The coated tubes are placed in soil columns in the laboratory or in the field, and after a period of incubation, the extent of removal of Fe(III) from the tubes by reduction to Fe(II) is quantified by image processing (Rabenhorst et al., 2008 and references therein). Such in situ, empirical methods may prove useful in delineating wetlands, hydric soils, and the extent of reducing conditions for Fe(III) under various soils conditions.

## 14.3 Applications of Redox Methods and Concepts to Ecological, Engineered, and Agricultural Soil Systems

The principles and theories of oxidation–reduction processes in soils, and methods for defining them operationally, have many applications that relate to root–soil interactions in the rhizosphere, to pollutant oxidation state in and remediation of contaminated soils, to nutrient management and soil fertility in agricultural and wild ecosystems, to the role of soils in global C balances affecting the earth’s climate, to the study of wetlands and hydric soils, and to understanding groundwater chemical composition at the interface with surface waters. A brief discussion of each of these applications follows, coupled to specific examples.

### 14.3.1 Rhizosphere Processes

Root exudates (rhizodeposition), especially those containing C compounds, are key constituents that influence microbial metabolism and chemical processes in the rhizosphere (Jones et al., 2009). These exudates may be the result of cell sloughing, establishment and maintenance of microsymbionts, gaseous loss (e.g., O<sub>2</sub> and CO<sub>2</sub>), and mucilage production. Carbon compounds typically act as electron donors (and in the case of quinone functional groups as electron acceptors) for heterotrophic microbes, and HCO<sub>3</sub><sup>–</sup> acts as the C source for autotrophs.

The diffusion of O<sub>2</sub> from the atmosphere through aerenchyma tissue formed in stems and roots in response to the development of anaerobic soil conditions favors the formation of oxidized rhizospheres in plants adapted to grow in anaerobic soils. Examples are rice paddies, freshwater and tidal wetlands, and other poorly drained soils (Marschner, 1995). In plants poorly adapted to growth in anaerobic soils, redox changes related to denitrification, reductive dissolution of Mn(III,IV) (hydr)oxides and Fe(III) (hydr)oxides, sulfate reduction, and methanogenesis can significantly affect plant growth, the maintenance of a symbiotic relationship with N<sub>2</sub>-fixing bacteria and mycorrhizal fungi (Marschner, 1995).

The formation of the products of organic matter decomposition and fermentation of glucose to lactate or ethanol can affect rhizosphere chemistry and microbial activity. Formation of ethylene, volatile fatty acids, and phenolic compounds activity affects vascular tissue conductivity and root growth (Marschner, 1995). Ethylene production in root tissues in response to water logging is responsible for the formation of aerenchyma tissue in plants tolerant of anaerobic soil conditions.

The rhizosphere is a soil environment that is hard to study in situ but one that is critically important in plant nutrition, soil fertility, plant pathology, soil biochemistry, microbial ecology, and pedology. The August, 2009 issue of *Plant and Soil* comprises 21 articles dedicated to reviewing current knowledge of rhizosphere processes, many of which are redox based (Dessaux et al., 2009).

### 14.3.2 Soil Remediation and Pollutant Speciation

In recent years, much emphasis has been placed on the remediation of soils contaminated with organic or inorganic industrial waste products (Clapp et al., 2001). Examples of these contaminants are synthetic organic chemicals, such as dense nonaqueous phase liquids (DNAPLs); benzene, toluene, ethylbenzene, and xylenes (BTEX); and pesticides (herbicides, insecticides, and fungicides) (Schwarzenbach et al., 1993). The oxidation or reduction of functional groups, aliphatic chains, and aromatic rings results in changes in solubility and toxicity (Schwarzenbach et al., 1993; Clapp et al., 2001).

The oxidation state of contaminant metals and metalloids can be transformed through microbiological or chemical redox processes. Such redox-based remediation changes their speciation, solubility, bioavailability, and toxicity (Sauvé and Parker, 2005). In such cases, the total, unspicated concentration of the element in question remains the same; only the oxidation state is changed. In these cases, the development of new methods for speciation and fractionation (Sauvé and Parker, 2005) based on oxidation state of the element has contributed to novel methods for remediation that do not involve removal of the element from the soil and that allow novel, in situ methods of remediation (James, 1996).

An example of an ongoing remediation-by-reduction are soils contaminated with chromate [Cr(VI)] from industrial plating operations and chromite ore processing residue (James, 1996). In situ or *ex situ* conversion of toxic, soluble Cr(VI) to much less toxic and insoluble Cr(III) species has been effective in laboratory, pilot, and field-scale studies. Methods studied have included elemental Fe in permeable reactive barriers (PRBs; Rivero-Huguet and Marshall, 2009), steel wool (James, 1994), ascorbic acid (Xu et al., 2005), animal manures (Bartlett and Kimble, 1975), polysulfides (Graham et al., 2005), and FeSO<sub>4</sub> (Geelhoed et al., 2003). Central to the acceptance of these methods by government regulatory agencies has been the refinement of an analytical method for soils that selectively dissolves Cr(VI) from the solid matrix without reducing it and without method-induced oxidation of Cr(III) in the soil (Vitale et al., 1997).

### 14.3.3 Soil Fertility and Nutrient Cycling

Redox transformations are central to the biological controls of the N cycle, including N<sub>2</sub> fixation (N<sub>2</sub> to NH<sub>4</sub><sup>+</sup>), nitrification (NH<sub>4</sub><sup>+</sup> to NO<sub>3</sub><sup>-</sup>), denitrification (NO<sub>3</sub><sup>-</sup> to N<sub>2</sub>O and N<sub>2</sub>). These processes govern the speciation of N in all ecosystems, whether in wild biomes, engineered soils, or domesticated agricultural ecosystems. Redox processes also govern speciation, bioavailability, and solubility of Mn, Fe, C and S, cofactors in many of the enzymes that catalyzed these N redox changes (Sylvia et al., 2005).

In soils and natural waters, high levels of P contribute to the growth of cyanobacteria and are therefore a concern related to eutrophication of freshwaters (Howarth, 1988). The oxidation

state under ambient biological temperatures and pressures remains V+, but reduction of Fe(III) (hydr)oxides and the oxidation of Fe(II) control, in complex ways, the presence of an important sorbent for orthophosphate in soils (H<sub>2</sub>PO<sub>4</sub><sup>-</sup> and HPO<sub>4</sub><sup>2-</sup>, the dominant inorganic forms of P between pH 4 and 9; Young and Ross, 2001; Sims and Pierzynski, 2005).

### 14.3.4 Soil Organic C Dynamics and Climate Change

The oxidation state of C varies from IV- to IV+ in natural environments, and enzymatic processes govern transformations among them. Examples of the classes of C compounds representing the range of oxidation states are alkanes (IV- in methane, CH<sub>4</sub>), alcohols (II- in methanol, CH<sub>3</sub>OH), aldehydes (0 in form-aldehyde or general representations of SOM, CH<sub>2</sub>O), carboxylic acids (II+ in formic acid, HCOOH, i.e., hydrated CO), and carbon dioxide (IV+ in CO<sub>2</sub>; and when hydrated as H<sub>2</sub>CO<sub>3</sub>, HCO<sub>3</sub><sup>-</sup>, and CO<sub>3</sub><sup>2-</sup>, depending on pH). The speciation of C in soils is governed by myriad anabolic and catabolic processes in cells (Clapp et al., 2005; Table 14.3).

The knowledge of C speciation and the reactions governing it are central to many contemporary environmental, engineering, and agricultural concerns. Greenhouse gas and particulate releases into the atmosphere (CO<sub>2</sub>, CH<sub>4</sub>, black C and other C-rich particulates) has encouraged research on C sequestration related to balances between methanogenesis and methanotrophy (Sylvia et al., 2005). Concern about climate change due to greenhouse gas releases is linked to the kinetics of formation and degradation of SOM and to effects of tillage practices and plant and animal waste decomposition dynamics (Ussiri and Lal, 2009). Balances between sources of SOM (via photosynthesis and oxidation polymerization processes) and its decomposition to simple organic acids and CO<sub>2</sub> are keys to how soils may sequester organic C.

Clapp et al. (2005) provide an encyclopedic treatise on SOM, its structure, reactions, and roles in soils as a base for understanding organic matter and C dynamics. Lal (1999) provides a brief description, with examples, of the role of soils in the greenhouse effect. He includes relevant information on greenhouse emissions, with particular reference to rice paddies and organic soils. Falkowski et al. (2008) provide excellent perspective on the microbial redox processes that govern nonequilibrium biological systems, using what they call “nanobiological machines.” They also describe how redox processes integrate sediments, water, and the atmosphere through interconnected, biologically mediated cycles for H, C, N, O, S, and Fe.

### 14.3.5 Wetland Delineation and Function

The delineation and redox-based functioning of freshwater and tidal wetlands (and their constituent hydric soils) are current challenges as a result of increasing interest in preventing loss of wetlands due to human development and sea level rise linked to global climate change and crustal subsidence (Hurt and Vasilas, 2006).

**TABLE 14.3** Reduction Half-Reactions for Environmentally Relevant Species

Species	Equations	E° (V)	Log K	ΔG <sub>r</sub> ° (kJ/eq)
A	$\gamma\text{-MnOOH} + e^- + 3\text{H}^+ \rightarrow \text{Mn}^{2+} + 2\text{H}_2\text{O}$	1.50	25.4	-145.0
B	$\text{CrO}_4^{2-} + e^- + 5/3\text{H}^+ \rightarrow 1/3\text{Cr}(\text{OH})_3 + 1/3\text{H}_2\text{O}$	1.24	21.0	-119.9
C	$\text{MnO}_2 + e^- + 2\text{H}^+ \rightarrow 1/2\text{Mn}^{2+} + \text{H}_2\text{O}$	1.23	20.8	-118.8
D	$\text{HCrO}_4^- + e^- + 4/3\text{H}^+ \rightarrow 1/3\text{Cr}(\text{OH})_3 + 1/3\text{H}_2\text{O}$	1.11	18.9	-107.9
E	$\text{AQDS} + e^- + \text{H}^+ \rightarrow 1/2\text{AH}_2\text{DS}$	0.22	3.9	-22.3
F	$1/2\text{Pyruvate} + e^- + \text{H}^+ \rightarrow 1/2\text{lactate}$	0.23	3.9	-22.3
G	$\text{CH}_2\text{O} + e^- + \text{H}^+ \rightarrow 1/4\text{CH}_2\text{O} + 1/4\text{H}_2\text{O}$	-0.07	-1.2	6.9
<i>Examples</i>				
	$\gamma\text{-MnOOH}$ reduction by $\text{AH}_2\text{DS}$ (A and E)		21.5	-122.8
	$\text{HCrO}_4^-$ reduction by $\text{CH}_2\text{O}$ (D and G)		20.1	-114.8
	$\text{HCrO}_4^-$ reduction by lactate (D and F)		15.0	-85.7
	$\text{HCrO}_4^-$ reduction by $\text{AH}_2\text{DS}$ (D and E)		15.0	-85.7
	$\text{Cr}(\text{OH})_3$ oxidation by $\gamma\text{-MnOOH}$ (A and D)		6.5	-37.1
	AQDS reduction by $\text{CH}_2\text{O}$ (E and G)		5.1	-29.1
	AQDS reduction by lactate (E and F)		0.0	0.0

*Sources:* Data from Bartlett, R.J., and B.R. James. 2000. Redox phenomena, p. 169–193. In M.E. Sumner (ed.) Handbook of soil science, 1st Ed. CRC Press, Washington, DC; Milazzo, G., V.K. Sharma, and S. Caroli. 1978. Tables of standard electrode potentials. Wiley, New York; Loach, P.A. 1976. Oxidation–reduction potentials, absorbency bands, and molar absorbency of compounds used in biochemical studies, p. 122–130. In G. Fasman (ed.) Handbook of biochemistry and molecular biology. Chemical Rubber Co., Cleveland, OH.

These reactions can be combined to form redox reactions, many of which are energetically favorable as indicated by negative  $G_r$  values in the given examples.

The definition of hydric soils (Hurt and Vasilas, 2006) and wetlands are linked to redox conditions and dynamics associated with the position and fluctuations of the water table. A so-called technical standard for defining wetlands is based on Eh and pH measurements associated with the oxidation and reduction of Fe(II,III) (Rabenhorst and Castenson, 2005; Hurt and Vasilas, 2006; NTCHS, 2007). Recent research on IRIS tubes and the concept of “biological zero” have contributed new methods and conceptual thinking on this technical standard and how to define a wetland (Rabenhorst, 2005; Rabenhorst et al., 2008).

The chemistry of tidal marshes that are diurnally inundated with  $\text{SO}_4^{2-}$ -rich seawater leads to the accumulation of numerous iron sulfide minerals, including iron monosulfides (e.g., FeS) and pyrite ( $\text{FeS}_2$ ) (Rabenhorst and James, 1992). In addition, the dynamics of organic C accumulation, methanogenesis and methane oxidation are important applications of redox concepts because of the importance of  $\text{CH}_4$  as a greenhouse gas (Liverman, 2007).

### 14.3.6 Riparian Soil-Vegetation Systems and Groundwater Nitrate Concentrations

Redox transformations of  $\text{NO}_3^-$  in groundwater have been major societal concerns due to the potential for eutrophication of natural waters, especially of by non- $\text{N}_2$  fixing, green algae in saline waters of estuaries, such as the Chesapeake Bay of the Coastal Plain of the United States (James et al., 1991). The reduction of N in  $\text{NO}_3^-$  (oxidation state V+) to  $\text{N}_2\text{O}$  (oxidation state I+) and  $\text{N}_2$  (oxidation state 0) via denitrification in riparian ecosystems has been extensively studied (Lowrance et al., 1984; Peterjohn and

Correll, 1984; Allan et al., 2008). The role of trees, understory vegetation, and planted grasses in riparian ecosystems has shown that black locust trees (*Pseudoacacia* spp.) act as a source of  $\text{NO}_3^-$  in groundwater that occurs following  $\text{N}_2$  fixation,  $\text{NH}_4^+$  release into the soil, and nitrification. When black locust trees were cut and replaced with planted tall fescue,  $\text{NO}_3^-$  concentrations in groundwater beneath the riparian zones decreased, whereas when non-leguminous trees (red oak, loblolly pine, and sassafras) were cut,  $\text{NO}_3^-$  concentrations increased. These results demonstrated the important roles played by vegetation–microbe–soil–groundwater interactions affecting N speciation (James et al., 1991).

## 14.4 Earlier Reviews and Prescient Work on Oxidation–Reduction Processes in Soils

There are numerous general reviews and examples of redox measurements, processes, applications, and data in soils and natural waters. Interested readers are referred to the following sources: Lindsay (1979), Buxton et al. (1988), Neta et al. (1988), Wardman (1989), Sawyer (1991), Bartlett and James (1993), Schwarzenbach et al. (1993), Helz et al. (1994), Blough and Zepp (1995), Compton and Sanders (1996), Stumm and Morgan (1996), Bartlett (1998).

Bartlett and Ross (2005) provide novel and heuristic ideas surrounding a central role played by Mn in soil redox processes, including formation of humic compounds, free radical reactions, nutrient cycling, rhizosphere chemistry, photochemistry, and wetlands. Other chapters in this book tie in soil acidity, chemical kinetics, and other topics related to oxidation–reduction.

Extensive redox-based research conducted by the late William Patrick and coworkers at the Wetland Biogeochemistry Institute at Louisiana State University (Baton Rouge, LA) has been central to much of current knowledge related to Eh and pH as master variables controlling the chemistry and biochemistry of tidal marshes and freshwater wetlands.

Remarkable, almost prescient, insight is provided in several references on electron activity and its measurement by the Pt electrode in the first four decades of the twentieth century following the discovery of the electron in 1897 (Gillespie, 1920; Willis, 1932; Pearsall and Mortimer, 1939). These researchers linked thermodynamic theory, biological processes in soils, and applications of redox chemistry to societal needs of their times—an accomplishment that can serve as a guide for future studies on the elusive electron in soil environments. Research and teaching related to oxidation–reduction processes in myriad soil environments remains a vital and dynamic field of study with many applications for future soil chemists and environmental scientists interested in addressing complex biological and chemical systems.

## References

- Allan, C.J., P. Vidon, and R. Lowrance. 2008. Frontiers in riparian zone research in the 21st century. *Hydrol. Process.* 22:3221–3222.
- Allison, J.D., and D.S. Brown. 1995. MINTEQA2/PRODEFA2—A geochemical speciation model and interactive processor, p. 241–252. *In* R.H. Loeppert et al. (eds.) *Chemical equilibria and reaction models*. Soil Science Society of America Special Publication. SSSA, Madison, WI.
- Amacher, M.C., and D.E. Baker. 1981. Redox reactions involving chromium, plutonium, and manganese in soils. Final Rep. Div. Energy Tech. US Dep. Energy DOE/DP/0415-1. Washington, DC.
- Arndt, D. 1981. Manganese compounds as oxidizing agents in organic chemistry. Open Court Publishing Co., La Salle, IL.
- Asatiani, N.V., M.K. Abuladze, T.M. Kartvelishvili, N.G. Bakradze, N.A. Sapojnikova, N.Y. Tsibakhashvili, L.V. Tabatadze, L.V. Lejava, L.L. Asanishvili, and H.Y. Holman. 2004. Effect of chromium(VI) action on *Arthrobacter oxydans*. *Curr. Microbiol.* 49:321–326.
- Baas-Becking, L.G.M., I.R. Kaplan, and D. Moore. 1960. Limits of the natural environment in terms of pH and oxidation–reduction potentials. *J. Geol.* 68:243–284.
- Banerjee, R. 2008. Redox metabolism and life, p. 1–10. *In* R. Banerjee et al. (eds.) *Redox biochemistry*. John Wiley & Sons Inc., Hoboken, NJ.
- Barcelona, M.J., and T.R. Holm. 1991. Oxidation–reduction capacities of aquifer solids. *Environ. Sci. Technol.* 25:1565–1572.
- Bartlett, R.J. 1981. Oxidation–reduction status of aerobic soils, p. 77–102. *In* D. Baker (ed.) *Chemistry in soil environments*. SSSA, Madison, WI.
- Bartlett, R.J. 1998. Characterizing soil redox behavior, p. 371–397. *In* D.L. Sparks (ed.) *Soil physical chemistry*, 2nd Ed. CRC Press, Boca Raton, FL.
- Bartlett, R., and B. James. 1979. Behavior of chromium in soils. III. Oxidation. *J. Environ. Qual.* 8:31–35.
- Bartlett, R.J., and B.R. James. 1993. Redox chemistry of soils. *Adv. Agron.* 50:151–208.
- Bartlett, R.J., and B.R. James. 1995. System for categorizing soil redox status by chemical field testing. *Geoderma* 68:211–218.
- Bartlett, R.J., and B.R. James. 2000. Redox phenomena, p. 169–193. *In* M.E. Sumner (ed.) *Handbook of soil science*, 1st Ed. CRC Press, Washington, DC.
- Bartlett, R.J., and J.M. Kimble. 1975. Behavior of chromium in soils. II. Hexavalent forms. *J. Environ. Qual.* 5:383–386.
- Bartlett, R.J., and D.S. Ross. 2005. Chemistry of redox processes in soils, p. 461–487. *In* M.A. Tabatabai and D.L. Sparks (eds.) *Chemical processes in soils*. Soil Sci. Soc. Am. Book Ser. 8. SSSA, Madison, WI.
- Bates, R.G. 1981. The modern meaning of pH. *Crit. Rev. Anal. Chem.* 10:247–278.
- Bauer, M., T. Heitmann, D.L. Macalady, and C. Blodau. 2007. Electron transfer capacities and reaction kinetics of peat dissolved organic matter. *Environ. Sci. Technol.* 41:139–145.
- Becker, J.G. 2006. A modeling study and implications of competition between *Dehalococcoides ethenogenes* and other tetrachloroethene-respiring bacteria. *Environ. Sci. Technol.* 40:4473–4480.
- Berner, R.A. 1981. A new geochemical classification of sedimentary environments. *J. Sediment. Petrol.* 51:359–365.
- Blaylock, M.J., and B.R. James. 1994. Redox transformations and plant uptake of selenium resulting from root–soil interactions. *Plant Soil* 158:1–12.
- Blough, N.V., and R.G. Zepp. 1995. Reactive oxygen species in natural waters, p. 280–332. *In* C.S. Foote et al. (eds.) *Active oxygen in chemistry*. Chapman & Hall, New York.
- Bond, D.R., and D.R. Lovley. 2002. Reduction of Fe(III) oxide by methanogens in the presence and absence of extracellular quinones. *Environ. Microbiol.* 4:115–124.
- Bricker, O.P. 1982. Redox measurement: Its measurement and importance in water systems. *Water Analysis*, Vol. 1. Academic Press, Orlando, FL.
- Brose, D.A. and B.R. James, 2010. Oxidation–reduction transformations of chromium in aerobic soils: Role of electron-shuttling quinones. *Environ. Sci. Technol.* 44:9438–9444.
- Buresh, R.J., M.E. Casselman, and W.H. Patrick, Jr. 1980. Nitrogen fixation in flooded soil systems: A review. *Adv. Agron.* 33:149–192.
- Bürge, I., and S. Hug. 1997. Kinetics and pH dependence of chromium(VI) reduction by iron(II). *Environ. Sci. Technol.* 31:1426–1432.
- Buxton, G.V., C.L. Greenstock, W.P. Helman, and A.B. Ross. 1988. Critical review of rate constants for reactions of hydrated electrons, hydrogen atoms, and hydroxyl radicals ( $\bullet\text{OH}/\bullet\text{OH}^-$ ) in aqueous solution. *J. Phys. Chem. Ref. Data* 17:513–886.
- Castellan, G.W. 1983. *Physical chemistry*, 3rd Ed. Addison-Wesley Publishing Co., Reading, MA.



- Cervantes, F.J., S. van der Velde, G. Lettinga, and J.A. Field. 2000. Quinones as terminal electron acceptors for anaerobic microbial oxidation of phenolic compounds. *Biodegradation* 11:313–321.
- Chapelle, F.H., S.K. Haack, P. Adriaens, M.A. Henry, and P.M. Bradley. 1996. Comparison of Eh and H<sub>2</sub> measurements for delineating redox processes in a contaminated aquifer. *Environ. Sci. Technol.* 30:3565–3569.
- Clapp, C.E. et al. (eds.). 2001. Humic substances and chemical contaminants. SSSA, Madison, WI.
- Clapp, C.E., M.H.B. Hayes, A.J. Simpson, and W.L. Kingery. 2005. Chemistry of soil organic matter, p. 1–150. *In* M.A. Tabatabai and D.L. Sparks (eds.) *Chemical processes in soils*. SSSA Book Series 8. SSSA, Madison, WI.
- Coleman, M.L., D.B. Hedrick, D.R. Lovley, D.C. White, and K. Pyle. 1993. Reduction of Fe(III) in sediments by sulphate-reducing bacteria. *Nature* 361:436–438.
- Compton, R.G., and G.H.W. Sanders. 1996. *Electrode potentials*. Oxford Science Publications, Oxford, U.K.
- Cotton, F.A., and G. Wilkinson. 1980. *Advanced inorganic chemistry*. John Wiley & Sons, New York.
- Dessaux, Y., P. Hinsinger, and P. Lemanceau. 2009. Rhizosphere: So many achievements and even more challenges. *Plant Soil* 321:1.
- Dittrich, M., and A. Luttge. 2008. Microorganisms, mineral surfaces, and aquatic environments: Learning from the past for future progress. *Geobiology* 6:201–213.
- Falkowski, P.G., T. Fenchel, and E.F. DeLong. 2008. The microbial engines that drive earth's biogeochemical cycles. *Science* 320:1034–1039.
- Farrell, R.E., G.D.W. Swerhone, and C. van Kessel. 1991. Construction and evaluation of a reference electrode assembly for use in monitoring in situ soil redox potentials. *Comm. Soil Sci. Plant Anal.* 22:1059–1068.
- Field, J.A., F.J. Cervantes, F.P. van der Zee, and G. Lettinga. 2000. Role of quinones in the biodegradation of priority pollutants: A review. *Water Sci. Technol.* 42:215–222.
- Fredrickson, J.K., and J.M. Zachara. 2008. Electron transfer at the microbe–mineral interface: A grand challenge in biogeochemistry. *Geobiology* 6:245–253.
- Fredrickson, J.K., J.M. Zachara, D.W. Kennedy, H. Dong, T.C. Onstott, N.W. Hinman, and S. Li. 1998. Biogenic iron mineralization accompanying the dissimilatory reduction of hydrous ferric oxide by a groundwater bacterium. *Geochim. Cosmochim. Acta* 62:3239–3257.
- Fridovich, I. 1978. The biology of oxygen radicals. *Science* 201:875–880.
- Garrels, R.M., and C.L. Christ. 1965. *Solutions, minerals, and equilibria*. Freeman, Cooper, & Co., San Francisco, CA.
- Geelhoed, J.S., J.C.L. Meeussen, M.J. Roe, S. Hillier, R.P. Thomas, J.G. Farmer, and E. Paterson. 2003. Chromium remediation or release? Effect of iron(II) sulfate addition on chromium(VI) leaching from columns of chromite ore processing residue. *Environ. Sci. Technol.* 37:3206–3213.
- Gillespie, L.J. 1920. Reduction potentials of bacterial cultures and of water-logged soils. *Soil Sci.* 9:199–216.
- Goldhammer, T., and C. Blodau. 2008. Desiccation and product accumulation constrain heterotrophic anaerobic respiration in peats of an ombrotrophic temperate bog. *Soil Biol. Biochem.* 40:2007–2015.
- Graham, M.C., J.G. Farmer, P. Anderson, E. Paterson, S. Hillier, D.G. Lumsdon, and R.J.F. Bewley. 2005. Calcium polysulfide remediation of hexavalent chromium contamination from chromite ore processing residue. *Sci. Total Environ.* 364:32–44.
- Gralnick, J.A., and D.K. Newman. 2007. Extracellular respiration. *Mol. Microbiol.* 65:1–11.
- Grenthe, I., W. Stumm, M. Laaksuharju, A.C. Nilsson, and P. Wikberg. 1992. Redox potentials and redox reactions in deep groundwater systems. *Chem. Geol.* 98:131–150.
- Grundl, T. 1994. A review of the current understanding of redox capacity in natural, disequilibrium systems. *Chemosphere* 28:613–626.
- Gu, B.H., and J. Chen. 2003. Enhanced microbial reduction of Cr(VI) and U(VI) by different natural organic matter fractions. *Geochim. Cosmochim. Acta Suppl.* 67:3575–3582.
- Harter, R.D., and G. Smith. 1981. Langmuir equation and alternate methods for studying “adsorption” reactions in soils, p. 167–182. *In* D. Baker (ed.) *Chemistry in soil environments*. SSSA, Madison, WI.
- Helz, G.R., R.G. Zepp, and D.G. Crosby (eds.). 1994. *Aquatic and surface photochemistry*. Lewis Publishers, Boca Raton, FL.
- Heron, G., T.H. Christensen, and J.C. Tjell. 1994. Oxidation capacity of aquifer sediments. *Environ. Sci. Technol.* 28:153–158.
- Hobman, J.L., J.R. Wilson, and N.L. Brown. 2000. Microbial mercury reduction. *In* D.R. Lovley (ed.) *Environmental microbe–metal interactions*. ASM Press, Washington, DC.
- Højberg, O., N.P. Revsbech, and J.M. Tiedje. 1994. Denitrification in soil aggregates analyzed with microsensors for nitrous oxide and oxygen. *Soil Sci. Soc. Am. J.* 58:1691–1698.
- Hostettler, J.D. 1992. The physical basis of Eh related to Eh measurements in natural waters. Preprint extended abstract. American Chemical Society Meetings, San Francisco, CA.
- Howarth, R.W. 1988. Nutrient limitation of net primary production in marine ecosystems. *Annu. Rev. Ecol.* 19:89–110.
- Hug, S.J., B.R. James, and H.U. Laubscher. 1997. Iron(III) catalyzed photochemical reduction of chromium(VI) by oxalate and citrate in aqueous solutions. *Environ. Sci. Technol.* 31:160–170.
- Hurt, G.W., and L.M. Vasilas. 2006. Field indicators of hydric soils in the United States: A guide for identifying and delineating hydric soils, Version 6.0. USDA–NRCS, Washington, DC.
- James, B.R. 1989. Electron activity in soils: A key master variable, p. 201. *Agronomy abstract*. ASA, Madison, WI.
- James, B.R. 1994. Hexavalent chromium solubility and reduction in alkaline soils enriched with chromite ore processing residue. *J. Environ. Qual.* 23:227–233.
- James, B.R. 1996. The challenge of remediating chromium-contaminated soil. *Environ. Sci. Technol.* 30:248–251.

- James, B.R., B.B. Bagley, and P.H. Gallagher. 1991. Riparian zone vegetation effects on concentrations of nitrate in shallow groundwater, p. 605–611. *In* J.A. Mihursky and A. Chaney (eds.) *New perspectives in the Chesapeake system: A research and management partnership*. Proc. Conf. Chesapeake Res. Consort. Publ. 137. December 4–6, 1990. Baltimore, MD.
- James, B.R., and R.J. Bartlett. 1983. Behavior of chromium in soils. VI. Interactions between oxidation–reduction and organic complexation. *J. Environ. Qual.* 12:173–176.
- Jiang, J., and A. Kappler. 2008. Kinetics of microbial and chemical reduction of humic substances: Implications for electron shuttling. *Environ. Sci. Technol.* 42:3563–3569.
- Jones, D.L., C. Nguyen, and R.D. Finlay. 2009. Carbon flow in the rhizosphere: Carbon trading at the soil–root interface. *Plant Soil* 321:4–33.
- Jorgensen, C.J., O.S. Jacobsen, B. Elberling, and J. Aamand. 2009. Microbial oxidation of pyrite coupled to nitrate reduction in anoxic groundwater sediment. *Environ. Sci. Technol.* 43:4851–4857.
- Kappler, A., M. Benz, B. Schink, and A. Brune. 2004. Electron shuttling via humic acids in microbial iron(III) reduction in a freshwater sediment. *FEMS Microbiol. Ecol.* 47:85–92.
- Kludze, H.K., R.D. DeLaune, and W.H. Patrick, Jr. 1994. A colorimetric method for assaying dissolved oxygen loss from container-grown rice roots. *Soil Sci. Soc. Am. J.* 86:483–487.
- Lal, R. 1999. Soil processes and greenhouse effect, p. 199–212. *In* R.L. Lal et al. (eds.) *Methods for assessment of soil degradation: Advances in soil science*. CRC Press, Boca Raton, FL.
- Larson, R.A. 1997. *Naturally occurring antioxidants*. Lewis Publishers, Boca Raton, FL.
- Leffler, J.E. 1993. *An introduction to free radicals*. John Wiley & Sons, New York.
- Lindberg, R.D., and D.D. Runnells. 1984. Ground water redox reactions: An analysis of equilibrium state applied to Eh measurements and geochemical modeling. *Science* 225:925–927.
- Lindsay, W.L. 1979. *Chemical equilibria in soils*. Wiley-Interscience, New York.
- Liu, C.W., and T.N. Narasimhan. 1989. Redox-controlled multiple-species reactive chemical transport. 1. Model development. *Water Resour. Res.* 25:869–882.
- Liverman, D. 2007. From uncertain to unequivocal—The IPCC Working Group I Report: Climate change 2007—The physical science basis. *Environment* 49:28–32.
- Loach, P.A. 1976. Oxidation–reduction potentials, absorbency bands, and molar absorbency of compounds used in biochemical studies, p. 122–130. *In* G. Fasman (ed.) *Handbook of biochemistry and molecular biology*. Chemical Rubber Co., Cleveland, OH.
- Lovley, D.R. 2000. Fe(III) and Mn(IV) reduction, p. 3–30. *In* D.R. Lovley (ed.) *Environmental microbe–metal interactions*. ASM Press, Washington, DC.
- Lovley, D.R., F.H. Chappelle, and J.C. Woodward. 1994. Use of dissolved  $H_2$  concentrations to determine distribution of microbially catalyzed redox reactions in anoxic groundwater. *Environ. Sci. Technol.* 28:1205–1210.
- Lovley, D.R., J.D. Coates, E.L. Blunt-Harris, E.J.P. Phillips, and J.C. Woodward. 1996. Humic substances as electron acceptors for microbial respiration. *Nature* 382:445–448.
- Lowrance, R.R., R.L. Todd, and L.E. Asmussen. 1984. Nutrient cycling in an agricultural watershed I. Phreatic movement. *J. Environ. Qual.* 13:22–27.
- Madigan, M.T., and J.M. Martinko. 2006. *Brock biology of microorganisms*, 11th Ed. Pearson Prentice Hall, Upper Saddle River, NJ.
- Mansfeldt, T. 1993. Redoxpotentialmessungen mit dauerhaft installierten Platinelektroden unter reduzierenden Bedingungen. *J. Plant Nutr. Soil Sci.* 156:287–292.
- Marschner, H. 1995. *Mineral nutrition of higher plants*, 2nd Ed. Academic Press, London, U.K.
- Matia, L., G. Rauret, and R. Rubio. 1991. Redox potential measurement in natural waters. *Fresen. J. Anal. Chem.* 339:455–462.
- Mendelssohn, I.A., B.A. Kleiss, and J.S. Wakeley. 1995. Factors controlling the formation of oxidized root channels: A review. *Wetlands* 15:37–46.
- Milazzo, G., V.K. Sharma, and S. Caroli. 1978. *Tables of standard electrode potentials*. Wiley, New York.
- Mueller, S.C., L.H. Stolzy, and G.W. Fick. 1985. Constructing and screening platinum microelectrodes for measuring soil redox potential. *Soil Sci.* 139:558–560.
- Moore, J.N., J.R. Walker, and T.H. Hayes. 1990. Reaction scheme for the oxidation of As(III) to As(V) by birnessite. *Clay. Clay Miner.* 38:549–555.
- Neta, P., R.E. Huie, and A.B. Ross. 1988. Rate constants for reactions of inorganic radicals in aqueous solution. *J. Phys. Chem. Ref. Data* 17:1027–1284.
- Norrström, A.C. 1994. Field-measured redox potentials in soils at the groundwater–surface–water interface. *Eur. J. Soil Sci.* 45:31–36.
- NTCHS. 2007. The hydric soil technical standard. Deliberations of the National Tech. Comm. Hydric Soils. Available online at [http://soils.usds.gov/use/hydric/ntchs/tech\\_notes/index.html](http://soils.usds.gov/use/hydric/ntchs/tech_notes/index.html) (October 15, 2009).
- Nyman, J., M. Gentile, and C. Criddle. 2007. Sulfate requirement for the growth of U(VI)-reducing bacteria in an ethanol-fed enrichment. *Bioremediation J.* 11:21–32.
- Oremland, R.S., and J. Stolz. 2000. Dissimilatory reduction of selenate and arsenate in nature, p. 199–224. *In* D.R. Lovley (ed.) *Environmental microbe–metal interactions*. ASM Press, Washington, DC.
- Patrick Jr., W.H. 1966. Apparatus for controlling the oxidation–reduction potential of waterlogged soils. *Nature* 212:1278–1279.
- Patrick Jr., W.H., and R.D. DeLaune. 1972. Characterization of the oxidized and reduced zones in flooded soils. *Soil Sci. Soc. Am. Proc.* 36:573–576.

- Patrick, W.H., R.P. Gambrell, and S.P. Faulkner. 1996. Redox measurements of soils, p. 1255–1273. *In* D.L. Sparks (ed.) *Methods of soil analysis. Part 3.* SSSA, Madison, WI.
- Paul, E. (ed.) 2007. *Soil microbiology, ecology, and biochemistry*, 3rd Ed. Elsevier, Amsterdam, the Netherlands.
- Pearsall, W.H., and C.H. Mortimer. 1939. Oxidation–reduction potentials in waterlogged soils, natural waters, and muds. *J. Ecol.* 27:483–501.
- Peiffer, S., O. Klemm, K. Pecher, and R. Hollerung. 1992. Redox measurements in aqueous solutions: A theoretical approach to data interpretation, based on electrode kinetics. *J. Contam. Hydrol.* 10:1–18.
- Peretyazhko, T., and G. Sposito. 2006. Reducing capacity of terrestrial humic acids. *Geoderma* 137:140–146.
- Peterjohn, W.T., and D.L. Correll. 1984. Nutrient dynamics in an agricultural watershed: Observations on the role of a riparian forest. *Ecology* 65:1466–1475.
- Petrie, R.A., P.R. Grossl, and R.C. Sims. 1998. Controlled environment potentiostat to study solid–aqueous systems. *Soil Sci. Soc. Am. J.* 62:379–382.
- Ponnamperuma, F.N. 1972. The chemistry of submerged soils. *Adv. Agron.* 24:29–96.
- Postma, D., and R. Jakobsen. 1996. Redox zonation: Equilibrium constraints on the Fe(III)/SO<sub>4</sub><sup>2-</sup> reduction interface. *Geochim. Cosmochim. Acta* 60:3169–3175.
- Rabenhorst, M.C. 2005. Biologic zero: A soil temperature concept. *Wetlands* 25:616–621.
- Rabenhorst, M.C., R.R. Bourgault, and B.R. James. 2008. Iron oxyhydroxide reduction in simulated wetland soils: Effects of mineralogical composition of IRIS paints. *Soil Sci. Soc. Am. J.* 72:1838–1842.
- Rabenhorst, M.C., and K.L. Castenson. 2005. Temperature effects on iron reduction in a hydric soil. *Soil Sci.* 170:734–742.
- Rabenhorst, M.C., W.D. Hively, and B.R. James. 2009. Measurements of soil redox potential. *Soil Sci. Soc. Am. J.* 73:668–674.
- Rabenhorst, M.C., and B.R. James. 1992. Iron sulfidization in tidal marsh soils, p. 203–217. *In* H.C.W. Skinner and R.W. Fitzpatrick (eds.) *Biomining processes of iron and manganese.* Catena Supplement 21. Catena Verlag, Destedt, Germany.
- Ratasuk, N., and M.A. Nanny. 2007. Characterization and quantification of reversible redox sites in humic substances. *Environ. Sci. Technol.* 41:7844–7850.
- Rawlings, D.E. 2005. Characteristics and adaptability of iron- and sulfur-oxidizing microorganisms used for the recovery of metals from minerals and their concentrates. *Microb. Cell Fact.* 4:13.
- Reguera, G., K.D. McCarthy, T. Mehta, J.S. Nicoll, M.T. Tuominen, and D.R. Lovley. 2005. Extracellular electron transfer via microbial nanowires. *Nature* 435:1098–1101.
- Rowell, D.L. 1981. Oxidation and reduction, p. 401–461. *In* D.J. Greenland and M.H.B. Hayes (eds.) *The chemistry of soil processes.* John Wiley & Sons, Cleveland, OH.
- Rivero-Huguet, M., and W.D. Marshall. 2009. Influence of various organic molecules on the reduction of hexavalent chromium mediated by zero valent iron. *Chemosphere* 76:1240–1248.
- Russell, E.W. 1973. *Soil conditions and plant growth*, 10th Ed. Longman, London, U.K.
- Saggar, S., K.R. Tate, D.L. Giltrap, and J. Singh. 2008. Soil–atmosphere exchange of nitrous oxide and methane in New Zealand terrestrial ecosystems and their mitigation options: A review. *Plant Soil* 309:25–42.
- Salminen, J.M., P.J. Hanninen, J. Leveinen, P.T.J. Lintinen, and K.S. Jorgensen. 2006. Occurrence and rates of terminal electron-accepting processes and recharge processes in petroleum hydrocarbon-contaminated subsurface. *J. Environ. Qual.* 35:2273–2282.
- Sauvé, S., and D.R. Parker. 2005. Chemical speciation of trace elements in soil solution, p. 655–688. *In* M.S. Tabatabai and D.L. Sparks (eds.) *Chemical processes in soils.* SSSA Book Series 8. SSSA, Madison, WI.
- Sawyer, D.T. 1991. *Oxygen chemistry.* Oxford University Press, New York.
- Scerri, E.R. 1997. The periodic table and the electron. *Am. Sci.* 85:546–553.
- Schwarzenbach, R.P., P.M. Gschwend, and D.M. Imboden. 1993. *Environmental organic chemistry.* John Wiley & Sons, New York.
- Scott, D.T., D.M. McKnight, E.L. Blunt-Harris, S.E. Kolesar, and D.R. Lovley. 1998. Quinone moieties act as electron acceptors in the reduction of humic substances by humics-reducing microorganisms. *Environ. Sci. Technol.* 32:2984–2989.
- Sillén, L.G. 1967. Master variables and activity scales, p. 45–56. *In* W. Stumm (ed.) *Equilibrium concepts in natural water systems.* Advances in Chemistry Series 67. Am. Chem. Soc., Washington, DC.
- Sims, J.T., and G.M. Pierzynski. 2005. Chemistry of phosphorus in soils, p. 151–192. *In* M.A. Tabatabai and D.L. Sparks (eds.) *Chemical processes in soils.* SSSA Book Series 8. SSSA, Madison, WI.
- Sparks, D.L. 1985. Kinetics of ionic reactions in clay minerals and soils. *Adv. Agron.* 38:231–265.
- Sparks, D.L. 2003. *Environmental soil chemistry*, 2nd Ed. Academic Press, Amsterdam, the Netherlands.
- Sposito, G. 1981. *The thermodynamics of soil solutions.* Oxford University Press, New York.
- Sposito, G. 1989. *The chemistry of soils.* Oxford University Press, New York.
- Stone, A.T., and J.J. Morgan. 1987. Reductive dissolution of metal oxides, p. 221–254. *In* W. Stumm (ed.) *Aquatic surface chemistry.* John Wiley & Sons, New York.
- Stoodley, L.H., J.W. Costerton, and P. Stoodley. 2004. Bacterial biofilms: From the natural environment to infectious diseases. *Nat. Rev. Microbiol.* 2:95–108.
- Straub, K.L., and B. Schink. 2003. Evaluation of electron-shuttling compounds in microbial ferric iron reduction. *FEMS Microbiol. Lett.* 220:229–233.

- Stumm, W. 1992. Chemistry of the solid–water interface. Wiley-Interscience, New York.
- Stumm, W. 1993. Aquatic colloids as chemical reactants: Surface structure and reactivity. *Colloids Surf. A* 73:1–18.
- Stumm, W., and J.J. Morgan. 1996. Aquatic chemistry, 3rd Ed. Wiley-Interscience, New York.
- Stumm, W., and B. Sulzberger. 1992. The cycling of iron in natural environments: Considerations based on laboratory studies of heterogeneous redox processes. *Geochim. Cosmochim. Acta* 56:3233–3258.
- Sullivan, J.C., S. Gordan, D. Cohen, W. Mulac, and K.H. Schmidt. 1976. Pulse radiolysis studies of uranium(VI), neptunium(VI), neptunium(V), and plutonium(VI) in aqueous perchlorate media. *J. Phys. Chem.* 8:1684–1686.
- Suter, D., S. Banwart, and W. Stumm. 1991. Dissolution of hydrous iron(III) oxides by reductive mechanism. *Langmuir* 7:809–813.
- Sylvia, D.M., P.G. Hartel, J.J. Fuhrmann, and D.A. Zuberer. 2005. Principles and application of soil microbiology, 2nd Ed. Pearson Prentice Hall, Upper Saddle River, NJ.
- Tan, K.H. 2003. Humic matter in soil and the environment: Principles and controversies. Marcel Dekker, Inc., New York.
- Thompson, J.J. 1923. The electron in chemistry. Franklin Institute Press, Philadelphia, PA.
- Tributsch, H., and L. Pohlmann. 1998. Electron transfer: Classical approaches and new frontiers. *Science* 279:1891–1895.
- Typrin, L.R. 1998. Using a thermodynamically-based approach to assess the redox status and predict the valence state of chromium in simple, aqueous systems and chromium-enriched soils. MS thesis. University of Maryland. College Park, MD.
- Ussiri, D.A.N., and R. Lal. 2009. Long-term tillage effects on soil carbon storage and carbon dioxide emissions in continuous corn cropping system from an alfisol in Ohio. *Soil Tillage Res.* 104:39–47.
- Vincent, A., 1985. Oxidation and reduction in inorganic and analytical chemistry. John Wiley & Sons, Chichester, U.K.
- Vitale, R. J., G.R. Mussoline, J.C. Petura, and B.R. James. 1997. Cr(VI) soil analytical method: A reliable analytical method for extracting and quantifying Cr(VI) in soils. *J. Soil Contam.* 6:581–593.
- Wang, Z.P., D. Zeng, and W.H. Patrick, Jr. 1997. Characteristics of methane oxidation in a flooded rice profile. *Nutr. Cycl. Agroecosyst.* 49:97–103.
- Wardman, P. 1989. Reduction potentials of one-electron couples involving free radicals in aqueous solution. *J. Phys. Chem. Ref. Data* 18:1637–1756.
- Welsch, M., and J.B. Yavitt. 2007. Microbial CO<sub>2</sub> production, CH<sub>4</sub> dynamics and nitrogen in a wetland soil (New York State, USA) associated with three plant species (*Typha*, *Lythrum*, and *Phalaris*). *Eur. J. Soil Sci.* 58:1493–1505.
- Westcott, C.C., 1978. pH measurements. Academic Press, New York.
- White, A.F., and M.L. Peterson. 1996. Reduction of aqueous transition metal species on the surfaces of Fe(II)-containing oxides. *Geochim. Cosmochim. Acta* 60:3799–3814.
- Whitfield, M. 1974. Thermodynamic limitations on the use of the platinum electrode in Eh measurements. *Limnol. Oceanogr.* 19:857–865.
- Willis, L.G. 1932. Oxidation–reduction potentials and the hydrogen ion concentration of a soil. *J. Agric. Res.* 45:571–575.
- Wu, W.-M., J. Carley, J. Luo, M. Ginder-Vogel, E. Cardanans, M.B. Leigh, C. Hwang, S.D. Kelly, C. Ruan, L. Wu, T. Gentry, K. Lowe, T. Mehlhorn, S.L. Carroll, M.W. Fields, B. Gu, D. Watson, K.M. Kemner, T.L. Marsh, J.M. Tiedje, J. Zhou, S. Fendorf, P. Kitanidis, P.M. Jardine, and C. Criddle 2007. In situ bioreduction of uranium(VI) to submicromolar levels and reoxidation by dissolved oxygen. *Environ. Sci. Technol.* 41:5716–5723.
- Xu, X., H. Li, J. Gu, and X. Li. 2005. Kinetics of the reduction of chromium(VI) by vitamin C. *Environ. Toxicol. Chem.* 24:1310–1314.
- Young, E.O., and D.S. Ross. 2001. Phosphate release from seasonally flooded soils: A laboratory microcosm study. *J. Environ. Qual.* 30:91–101.
- Yu, T.R. 1992. Electrochemical techniques for characterizing soil chemical properties. *Adv. Agron.* 48:205–250.

Sabine Goldberg

*United States Department  
of Agriculture*

Inmaculada Lebron

*Centre for Ecology & Hydrology*

John C. Seaman

*University of Georgia*

Donald L. Suarez

*United States Department  
of Agriculture*

15.1 Nature of Soil Colloids.....	15-1
Significance of Colloidal Phenomena • Types of Soil Colloids • Properties of Soil Colloids • Thermodynamics of Colloid Surfaces	
15.2 Interparticle Forces .....	15-16
Electrical Double Layer • Attractive Force • Repulsive Force	
15.3 Colloidal Stability .....	15-18
Flocculation and Dispersion • Factors Affecting Colloidal Stability • Measurement of Colloidal Stability	
15.4 Colloid Transport .....	15-25
Colloid Transport Modeling • Colloid-Mediated Contaminant Transport • Effect of Colloid Transport on Hydraulic Conductivity and Soil Formation	
References.....	15-30

## 15.1 Nature of Soil Colloids

### 15.1.1 Significance of Colloidal Phenomena

The importance of colloids in soil science has been appreciated for many years. However, recent understanding that organic and inorganic contaminants are often transported via colloidal particles has increased interest in colloid science. Essentially, all chemicals and individual species are to some extent reactive with soils, including species such as chloride ions, which undergo repulsion from negatively charged surfaces. With few exceptions, soil chemistry is primarily the chemistry of colloids and surfaces. The primary importance of colloids in soil science stems from their surface reactivity and charge characteristics. The overwhelming majority of surface area and electrostatic charge in a soil resides in the less than 1  $\mu\text{m}$  size fraction with particles with radii between 20 and 1000 nm constituting the major part of the soil surface area (Borkovec et al., 1993). A significant fraction of reactive soil colloidal material falls within the <100 nm size range and thus is relevant to the growing interest in the properties and behavior of nanoparticles. Furthermore, soil is often the ultimate repository for anthropogenic nanomaterials of environmental concern (Hochella, 2008; Theng and Yuan, 2008; Waychunas and Zhang, 2008). The unique aspects of “nanoscience” as a discipline separate from colloid science reflect deviations in material properties in the nanoparticle size range, especially for materials <10 nm, and in many cases the lack of a natural bulk analog in the larger size fractions, for example, ferrihydrite (Hochella, 2008; Waychunas and Zhang, 2008).

Characterizations of size, shape, surface area, surface charge density, and changes in surface charge are required for

understanding the processes of adsorption, flocculation, dispersion, and transport in soils and the resultant changes in soil hydraulic properties, as well as chemical migration. Since the major part of the surface area is in the colloidal fraction of the soil, almost all surface-controlled processes including adsorption reactions, nucleation, precipitation, and dissolution involve colloids. Colloids are reactive not only because of their total surface area but also because of enhanced reactivity related to rough surfaces and highly energetic sites, as well as the effects of electrostatic charge. Colloid charge is associated with substitution of lower charge cations for those of higher charge in the mineral lattice (which results in a net permanent charge) as well as surface charge associated with broken bonds. The charge associated with broken bonds is characterized as variable charge in as much as the solution influences the surface speciation (Chapter 16). In addition to these chemical processes, colloids are mobile in soils and thus not only affect the chemical transport of otherwise immobile chemicals but also exert a strong influence on soil hydraulic properties.

### 15.1.2 Types of Soil Colloids

Colloidal particles are defined as having an equivalent spherical radius smaller than 1  $\mu\text{m}$  (van Olphen, 1977). A homogeneous dispersion of colloidal particles in a liquid is called a colloidal dispersion. If the particles are large and settle rapidly, the dispersion is called a suspension. A colloidal dispersion is defined as a system where particles of colloidal dimensions are dispersed in a continuous phase of a different composition (van Olphen, 1977).

### 15.1.2.1 Oxides

Oxides, including hydroxides and oxyhydroxides, are ubiquitous constituents of soils, occurring as both discrete particles and as coatings on other soil surfaces. Oxide minerals that are commonly found in the soil clay fraction are discussed in Chapter 22.

Hydroxylation of oxide minerals can either be structural and/or occur by chemisorption of water in an aqueous medium (Schwertmann and Taylor, 1977). Edge hydroxyl groups on oxides and clay minerals represent the most abundant and reactive surface functional groups in soils (Sposito, 1984). Any one type of oxide mineral contains various groups of surface hydroxyls that are distinguishable by crystal plane location and/or extent of coordination to the cations of the bulk structure. However, as a simplification, it is often assumed that each oxide mineral has a single set of homogeneous reactive functional groups. Surface hydroxyl groups on most oxide minerals are amphoteric, exhibiting positive charge at low pH and negative charge at high pH. For this reason, oxide minerals are often referred to as variable charge soil minerals. Table 15.1 provides densities of surface hydroxyl groups for some common oxide minerals in soils.

Boehmite and gibbsite are the only crystalline Al oxides common in soils. Aluminum oxides are the products of intense weathering of aluminosilicate minerals and are most abundant in tropical soils. Gibbsite can also be found in volcanic ash soils of humid regions (Brown et al., 1978). Noncrystalline Al oxides, which have similar structure and chemical characteristics but smaller particle size than crystalline varieties, often dominate the chemical reactions with anions in soils (Hsu, 1977). Aluminum oxides play an important role in ion adsorption, stabilization of soil aggregates, and flocculation of soil particles.

Iron oxides are found in most soils and provide soil horizons with their red, yellow, and brown colors (Brown et al., 1978). Most iron oxides are the weathering products of iron-containing silicates. Goethite, which is the most common Fe oxide in temperate, subtropical, and tropical soils, is usually thermodynamically the most stable (Schwertmann and Taylor, 1977). Soil goethites are usually fine grained and contain appreciable substituted Al. Lepidocrocite is a minor constituent of waterlogged temperate soils undergoing alternating oxidizing and reducing conditions, whereas hematite is a common soil mineral that can

be inherited from parent materials or formed pedogenically in warm climatic regions (Brown et al., 1978). The two magnetic Fe minerals, magnetite and maghemite, occur in soils; the former is inherited from parent rock, while the latter is formed pedogenically in highly weathered soils (Brown et al., 1978). Ferrihydrites are poorly crystalline, have indefinite composition, and occur as very small particles with high surface area (Schwertmann and Taylor, 1977). Ilmenite is an uncommon mineral usually inherited from igneous or metamorphic parent rocks (Brown et al., 1978). Iron oxides play an important role in ion adsorption and in aggregation and cementation of soil particles.

Manganese oxides occur widely in soils as minor constituents, mainly as dark coatings on particle surfaces. Manganese oxides are chemically complex, existing as a continuous range of compositions between MnO and MnO<sub>2</sub> (Brown et al., 1978). Birnessite, vernadite, lithiophorite, and hollandite are the most common crystalline manganese minerals in soils (McKenzie, 1989). Birnessite occurs in both acid and alkaline soils, while lithiophorite occurs mainly in neutral to acid soils (Brown et al., 1978). These oxides supply Mn for plant nutrition. Manganese oxides exhibit a strong adsorption capacity for metal cations, especially copper, due to their pH-dependent charge, small particle size, and large surface area (McKenzie, 1989).

Rutile and anatase are the common titanium oxides occurring in soils. Rutile is a high-temperature form occurring in igneous and metamorphic rocks (Hutton, 1977). Anatase is a low-temperature form occurring as an alteration product of titanium containing minerals such as ilmenite and is much less abundant than rutile (Brown et al., 1978). Titanium oxides are present in both the coarse and fine fractions of soils and are very insoluble (Hutton, 1977).

Quartz is not only the most abundant silicon oxide but also the most abundant mineral in most soils. Most quartz is found predominantly in the sand, silt, and coarse clay fractions of soils (Wilding et al., 1977). Silicon oxides are generally considered inert having a small surface area and little surface charge.

### 15.1.2.2 Clay Minerals

The clay fraction of most soils is dominated by various layer silicate clay minerals. Layer silicate clay minerals are classified as 1:1 where each layer consists of one tetrahedral silica sheet and one octahedral alumina sheet, 2:1 where each layer consists of one octahedral sheet sandwiched between two tetrahedral sheets, or 2:1:1 where a metal hydroxide sheet is sandwiched between the 2:1 layers. Layer silicate minerals common in soils are discussed in Chapter 21. A discussion of silicate structures is provided by Schulze (2002).

Layer silicate clay minerals are characterized by isomorphic substitution of lower valence cations in either or both the tetrahedral and the octahedral sheets. This excess of negative charge is balanced by other cations, either inside the crystal or on the external surfaces (McBride, 1994). Layer charge is an electrostatic charge balanced outside of the structural unit and determines the strength and type of bonding occurring between the basal planes. Charge arising from isomorphic substitution is

**TABLE 15.1** Densities of Surface Hydroxyl Groups on Oxide Minerals

Solid	Site Density Range (Sites nm <sup>-2</sup> )
Gibbsite	2–12
Goethite	2.6–16.8
Hematite	5–22
Ferrihydrite	1.1–10.1
MnO <sub>2</sub>	6.2
TiO <sub>2</sub>	2–12
Amorphous SiO <sub>2</sub>	4.5–12

Source: Adapted from Davis, J.A., and D.B. Kent. 1990. Surface complexation modeling in aqueous geochemistry. *Rev. Mineral. Geochem.* 23:177–260.

**TABLE 15.2** Charge Characteristics and Cation Exchange Capacities of Clay Minerals

Solid	Charge per Unit Half Cell		Cation Exchange Capacity (cmol <sub>c</sub> kg <sup>-1</sup> )
	Tetrahedral	Octahedral	
Kaolinite	0	0	1–10
Smectite			80–120
Montmorillonite	0	–0.33	
Beidellite	–0.5	0	
Vermiculite	–0.85	+0.23	120–150
Mica			20–40
Muscovite	–0.89	–0.05	
Chlorite			10–40

Sources: Bohn, H.L., B.L. McNeal, and G.A. O'Connor. 1985. Soil chemistry. John Wiley & Sons, New York; McBride, M.B. 1994. Environmental chemistry of soils. Oxford University Press, New York.

called permanent charge because it is independent of solution pH. Layer silicate clay minerals also possess variable charge located at the broken edges of the particles. At the edges of the octahedral sheet, hydroxyl ions attached to Al cations are called aluminol groups. Similar to the hydroxyl groups on oxide minerals, aluminol groups are amphoteric. At the edges of the tetrahedral sheet, hydroxyl groups attached to Si cations are called silanol groups. Silanol groups do not undergo protonation, but dissociate and become negatively charged at high pH. Adsorbed cations on clay minerals balance both pH dependent and permanent charges. Table 15.2 provides charge characteristics and cation exchange capacities (CEC) for some common clay minerals in soils.

Kaolinite is one of the most widespread clay minerals in soils, being most abundant in soils of warm moist climates (Dixon, 1977); while halloysite is formed through acid weathering and in soils of volcanic origin. The halloysite structure is the same as the kaolinite structure but contains a sheet of water molecules between the layers. Both minerals have low colloidal activity, low surface area, and low CEC and anion exchange capacity (AEC) (Dixon, 1977). The CEC and AEC of the 1:1 minerals are predominantly pH dependent (McBride, 1994).

Micas are abundant in soils, occurring as primary minerals inherited from soil parent materials. Micas strongly retain interlayer potassium ions, rendering them nonexchangeable and reducing the CEC of these minerals. Through weathering, micas release K and provide an important natural source of this plant nutrient (Fanning and Keramidas, 1977). Illite is a secondary mineral that is less crystalline, contains less K, and contains more water than muscovite mica (McBride, 1994). Micas and illites are nonswelling minerals.

Smectites constitute an important group of 2:1 clay minerals. Members that are important in soils include montmorillonite, beidellite, and nontronite. Smectites are most significant in moderately weathered soils and have high colloidal activity and high surface area. Smectites are responsible for a large part of the CEC and the majority of the shrink/swell properties of smectitic soils (Borchardt, 1977).

Vermiculite is an important clay mineral in soils that is formed as an alteration product of muscovite and biotite micas (Douglas, 1977). Vermiculite is widely distributed and has a wide particle size range. Vermiculites contain hydrated magnesium cations that can be readily exchanged by K and ammonium ions, resulting in collapse of the clay layers and fixation of these nutrient ions. Vermiculites have high CEC and high surface area but exhibit limited swelling.

Chlorites are 2:1:1 layer silicates that occur extensively in soils. The hydroxide interlayer sheet is usually dominated either by brucite [Mg(OH)<sub>2</sub>] or by gibbsite [Al(OH)<sub>3</sub>]. This interlayer sheet restricts swelling, decreases effective surface area, and decreases effective CEC (McBride, 1994). Chlorites are non-swelling silicates.

### 15.1.2.3 Organic Matter

Soil organic matter (SOM) refers to the mixture of products resulting from microbial and chemical transformations of organic residues and is discussed in Chapter 11. An important component of SOM is called humus, a complex and microbially resistant mixture of amorphous and colloidal substances. These substances are the result of modifications of original tissues or synthesis by soil microorganisms. Humic substances are subdivided into humic acid, fulvic acid, and humin using a separation scheme based on solubility in strong acid and base (McBride, 1994). The structure and composition of humus are complex and incompletely known. The structure contains a variety of reactive functional groups including carboxyl R–COOH, phenol C<sub>6</sub>H<sub>5</sub>OH, alcohol R–CH<sub>2</sub>OH, enol R–CH=CH–OH, ketone R–CO–R', quinone O=C<sub>6</sub>H<sub>4</sub>=O, ether R–CH<sub>2</sub>–O–CH<sub>2</sub>–R', and amino R–NH<sub>2</sub> (Stevenson, 1982). Humus is amorphous and highly colloidal; its surface area, ion adsorption, and CEC are greater than those of layer silicate clay minerals (McBride, 1994). The presence of humus usually promotes aggregation of soil particles.

## 15.1.3 Properties of Soil Colloids

### 15.1.3.1 Particle Size and Shape

Colloids in natural systems are characterized by a continuous particle size distribution (PSD; polydispersivity) of extreme complexity and diversity. Organisms, organic macromolecules, minerals, clays, oxides, and combinations of any of them constitute the colloidal fraction in soils. The distribution of shapes, densities, surface chemical properties, and chemical composition vary widely with size. Some fractions of the size spectrum may be living, and all particulates are subject to diverse physical, chemical, and biological processes that can alter size distribution, shape, or chemical composition (Kavanaugh and Leckie, 1980).

Colloids are dynamic particles, subject to constant alteration; the distribution of particle sizes in natural systems is the result of a number of processes, which either bring the particles together (coagulation) or disrupt existing aggregates (dispersion) (Filella and Buffle, 1993; Buffle and Leppard, 1995a, 1995b). Particle size is an important parameter in the characterization

of colloids. Sequential gravimetric sedimentation has been the classical method for measuring PSDs in soils. However, this technique has proven to be unreliable for particle sizes in the colloidal range (1–1000 nm). The reason for the lack of reliability is the combination of Brownian motion and convection currents, which each exert a significant influence on settling at diameters below  $\sim 1 \mu\text{m}$  in water.

Awareness of the environmental importance of colloids, for example, remediation schemes using engineered nanoparticles, and studies on the ecotoxicology of the products created by the emerging nanotechnology industry have accelerated the development of analytical techniques for nanoscale research (Wilkinson and Lead, 2007). These analytical techniques provide quantification, analyses, and characterization of the size, shape, and distribution of colloids in polydisperse systems within the environment (Handy et al., 2008). Some of the techniques more commonly used in soil science for colloid characterization and determination of PSD are reviewed in the following section. These include centrifugation, particle size analysis using the Coulter principle, field flow fractionation (FFF), atomic force microscopy (AFM), electron microscopy (EM), and acoustic spectroscopy. A recent publication by the International Union of Pure and Applied Chemistry (IUPAC) Wilkinson and Lead (2007) provides more detailed information on the various techniques.

It is important to consider that each particle size measurement technique has different accuracy and precision. In other words, detection limits and detection windows, corresponding to different size ranges, are technique dependent (Table 15.3). Not all

techniques are able to accurately measure the full scale of size ranges for colloids in polydisperse samples. Furthermore, most of the colloidal-sizing techniques do not measure size directly, but rather determine a physicochemical property from which the size is calculated (Lead and Wilkinson, 2007). For example, scanning and transmission electron microscopic techniques determine the physical dimensions of the projected area of the particles (Lebron et al., 1999), light scattering and flow-FFF generally determine the diffusion coefficients (Lead et al., 2000; Hasselov et al., 2007), and sedimentation-FFF (Sd-FFF) and other centrifugation-based techniques measure the buoyant mass (Hasselov et al., 2007). Although particle size can be estimated from projected areas, diffusion coefficients, and buoyant mass, the calculations are based on a number of assumptions, which if not met, will reduce the quality of the results (i.e., sphericity, homogeneous charge distribution, absence of coulombic interactions among particles). Therefore, it is not uncommon to obtain different PSDs for the same sample when using different techniques (Lead and Wilkinson, 2007). Even more direct techniques like scanning electron microscopy (SEM) and environmental scanning electron microscopy (ESEM) have their limitations. Doucet et al. (2004) observed differing colloidal morphologies in preparations obtained from the same sample with SEM and AFM. They attributed these differences to the sample preparation required for each technique. The difficulty in obtaining similar PSDs using different techniques indicates the limitation of the individual techniques. Therefore, it is good practice to use the results of several characterization techniques simultaneously (Lead and Wilkinson, 2007; Hasselov et al., 2008).

**TABLE 15.3** Operational Range of Colloid Particle Size Characterization for a Variety of Analytical Techniques and the Inferred Colloidal Dimension Quantified by Each Technique

Analytical Technique	Quantified Parameter	Approximate Analysis Size Range (nm)
Filtration	Equivalent pore size diameter	100–>1000
Ultrafiltration	Equivalent molar mass	1–100
Centrifugation	Equivalent spherical volume diameter	10–>1000
Dialysis	Equivalent molar mass	0.5–100
ESEM	Projected area	40–>1000
SEM	Projected area	10–>1000
TEM	Projected area	1–>1000
AFM	Three dimensions	0.5–>1000
Fl-FFF	Hydrodynamic diameter	1–1000
Sd-FFF	Equivalent spherical volume diameter	50–1000
DLS	Hydrodynamic diameter	3–>1000
Acoustic spectroscopy	Equivalent particle diameter	5–>1000

Source: Adapted from Hasselov, M., J.W. Readman, J.F. Ranville, and K. Tiede. 2008. Nanoparticle analysis and characterization methodologies in environmental risk assessment of engineered nanoparticles. *Ecotoxicology* 17:344–361.

#### 15.1.3.1.1 Measurement Methodology

Minimization of sample handling and processing is recommended when analyzing colloidal systems. Currently, no in situ technique allows direct measurement of the PSD for soils. Furthermore, measurement of colloid particles cannot be compared to standard samples to evaluate the quality of measurements made because there are no accepted standards or reference materials for natural colloids (Lead and Wilkinson, 2007).

#### 15.1.3.1.2 Electron Microscopy

EM is one of the few techniques capable of measuring the size of particles across the entire colloidal range (Table 15.3). Both transmission electron microscopy (TEM) and SEM require deposition of aqueous suspensions, sample evacuation, and in the case of SEM, sample coating with a conducting material, typically graphite or gold, to reduce charging from the beam. Hence sample preparation can, and most likely will, alter the original particle morphology and size distribution (Buffle and Leppard, 1995a, 1995b; Chanudet and Filella, 2006). However, new sample preparation techniques are constantly being developed to counteract artifacts generated by dehydration. For example, freeze-drying techniques or the use of hydrophilic resins and multimethod TEM sample generation techniques can be used to stabilize the three-dimensional structure of colloids (Mavrocordatos et al., 2007).



ESEM can, in theory, be used to quantify colloids under ambient conditions, as can AFM that is generally used only to determine the dimensions and characteristics of individual colloids. While minimal sample manipulation is an advantage, the disadvantage is a reduction in the resolution of the techniques; both ESEM and AFM produce much better resolution at lower relative humidity. Another serious problem in AFM imaging of liquids is the alteration of the AFM-derived signal due to the uptake of nanoparticles onto the AFM cantilever (Lead et al., 2005). Applications and new sample preparation techniques for environmental colloids using AFM are discussed by Balnois et al. (2007). Force-volume mode AFM has been used to evaluate the heterogeneous distribution of charge on clay surfaces (Taboada-Serrano et al., 2005).

Microscopy, despite being a very powerful technique, is not widely used for routine particle size analysis. The reasons for its limited use are the high cost of the equipment and the small sample volumes that can be scanned at any given magnification. Image analysis software facilitates the quantification of the different particle metrics in the micrographs. However, obtaining sufficient particles to allow representative and robust statistics requires the scanning of many micrographs of the specimen. Nevertheless, the determination of morphology and particle shape factor still remains the strength of microscopic techniques. Automated instrumental analysis routines that take advantage of enhanced beam stability combined with image analysis software, and greater computing capacity have the potential to address such limitations (Seaman, 2000; Laskin and Cowin, 2001). Additionally, SEM, ESEM, and TEM coupled with energy dispersive x-ray (EDX) spectroscopy can provide valuable chemical information about individual particles. It must be recognized that the resulting x-ray signal in SEM may be generated from a sample region larger than the particle of interest (Goldstein et al., 1992; Seaman, 2000). Furthermore, TEM can also, by measuring the x-ray spectra emitted by the specimen, resolve crystal spacing. Selective area electron diffraction can be used to identify colloidal minerals and to determine their degree of colloid crystallinity.

### 15.1.3.1.3 Centrifugation

A particle falling through an infinite fluid will eventually travel at a terminal constant velocity determined by the size of the particle and the resistance offered by the fluid. The terminal velocity in a centrifugal field is not constant, but rather a function of distance from the axis of rotation. Measurement of this radius is necessary in order to calculate the particle size. The relationship between the movement of the particle and the movement of fluid around that particle may be reduced to the Stokes equation. For fluid moving past a particle of diameter ( $d_p$ ), the ratio of the inertial transfer is described by the dimensionless parameter, the Reynolds number ( $R_E$ ):

$$R_E = \frac{\rho_0 u d_p}{\eta} \quad (15.1)$$

where  $u$  is the velocity. If  $R_E \leq 0.2$ , the fluid conditions are described as streamlined or laminar, and the drag on the particle is due mainly to viscous force within the fluid. Particles with high densities or large particle diameters may be moving with velocities that exceed  $R_E = 0.2$ , and in this situation, they are likely to enter the region of turbulent flow, where velocities are more difficult to calculate. In a centrifugal field, Stokes' equation has the form:

$$u = \frac{(\rho - \rho_0)\omega^2 d_p^2}{18\eta} = \frac{\ln(r/s_0)}{t} \quad (15.2)$$

where

$\omega$  is the rotational velocity (rad s<sup>-1</sup>)

$t$  is the time (s) required for a particle of diameter  $d_p$  to move from its starting point radius ( $s_0$ ) to the analytical radius ( $r$ )

Application of the Stokes equation requires certain assumptions that are not always achieved. All of these assumptions are critical to the measurement of the size of the sedimenting particles. The first assumption is that the particles are spherical, smooth, and rigid. Since this assumption is almost never valid, the diameter calculated is an equivalent or Stokes diameter ( $d_{st}$ ). It is assumed that the particle terminal velocity is reached instantly, although calculations show that a finite but small time is actually required before this condition is reached. The particle is assumed to be moving without interference or interaction from other particles in the system. This assumption is only true at high dilutions (<1%) that ensure considerable separation between particles. Also, it is assumed that inertial effects are not present and that the fluid exhibits only Newtonian flow properties. Since water is generally the dilution medium in soils and colloidal particles are <1  $\mu\text{m}$ , these assumptions are usually valid. A more detailed analysis of the methodology as well as a description of different centrifugation methods is provided by Bunville (1984), Groves (1984), Koehler et al. (1987), Holsworth et al. (1987), and Coll and Oppenheimer (1987).

### 15.1.3.1.4 Coulter Effect

The increase in the resistance across a small aperture produced by a nonconducting particle in a conducting medium is called the Coulter effect. The magnitude of this increase in resistance ( $\Delta R$ ) for a spherical particle of diameter ( $d_p$ ) suspended in an aperture of diameter ( $D_a$ ) is

$$\Delta R = \frac{8P_f d_p}{3\pi D_a^4} \left[ 1 + \frac{4}{5} \left( \frac{d_p}{D_a} \right)^2 + \frac{24}{35} \left( \frac{d_p}{D_a} \right) + \dots \right] \quad (15.3)$$

where  $P_f$  is the resistivity of the conducting medium. This resistance pulse ( $\Delta R$ ) results in a voltage pulse ( $i\Delta R$ ) for a sphere

of diameter  $d_p$ , where  $i$  is the current across the aperture. The resulting voltage pulses are counted and scaled using a multi-channel analyzer.

Instruments utilizing the resistive pulse technique require calibration using standard particles with known diameter to assign a particle size to each of the thresholds. This procedure takes into account the dimensions and electrical characteristics of the aperture and the conducting medium.

The advantage of the resistive pulse technique is that no other properties of the particle, such as refractive index or specific gravity, are required for the interpretation of the data in terms of a PSD. Developments in instrumentation for particle size analysis using the resistive pulse technique allow the analysis of particle sizes  $<1\ \mu\text{m}$  but the range is limited (typically  $0.4\text{--}<1\ \mu\text{m}$ ) (Bunville, 1984).

#### 15.1.3.1.5 Dynamic Light Scattering or Photon Correlation Spectroscopy

Dynamic light scattering (DLS), also called photon correlation spectroscopy, or quasielastic light-scattering measures the fluctuation in scattered intensity of a laser beam over small-time intervals when it passes through a small volume of particles under Brownian motion. These fluctuations are dependent on the diffusion coefficient of the particles.

When the particles have a regular shape other than spherical, the depolarized component can be used to study the particle rotational diffusion coefficient. The rotational and translational diffusion coefficients obtained in conjunction with theoretical, hydrodynamic relationships contain information about the particle dimensions. For a nonspherical particle larger than the incident wavelength, light is scattered from different parts of the same particle producing interferences, which are dependent on the angle of the scattered intensity and characteristic of a particular particle shape (Pecora, 1983).

Limitations of DLS are due to the assumptions made in calculating the particle radius from the diffusion coefficients. These assumptions include sphericity, nonpenetrable spheres, and non-coulombic forces existing among the particles. A more major limitation, when applied to colloidal systems, is the strong particle size dependence of the scattered light intensity. Larger particles have a much larger influence than smaller particles, biasing size quantification toward larger particle sizes. Consequently, previous sample fractionation is advised, since small fractions of dust or other micrometer-sized particles will overshadow the signal of the particles in the colloidal range (Hasselov et al., 2008). Despite limitations, DLS is quick and easy to use, is available in most laboratories, and is very useful for monitoring changes in colloid aggregation. It has been applied successfully to measure particle sizes of colloids in natural systems (Rees, 1990; Ryan and Gschwend; 1990; Lebron et al., 1993; Ledin et al., 1993, 1994; Finsy, 1994; Perret et al., 1994; Newman et al., 1994; Filella et al., 1997).

#### 15.1.3.1.6 Field-Flow Fractionation

FFF is a group of separation techniques capable of fractionating and characterizing the PSD of colloids in the range  $0.01\text{--}1\ \mu\text{m}$ .

Like chromatography, FFF is an elution methodology in which constituents are differentially retained, and thus separated in a flow channel (Beckett et al., 1997). With this technique, a colloidal sample is introduced into a stream of liquid and subjected to a field (such as gravitational, centrifugal, third cross-flow, thermal gradient, electrical, or magnetic) acting perpendicular to the stream direction (Beckett and Hart, 1993). According to theory, the rate at which particles are displaced downstream, measured as emergence times, can be related exactly to particle properties such as mass, size, and density. However, since different kinds of particles move at different velocities in this system, broad particle populations are sorted into graded size (or mass) distributions along the length of the flow channel. Observation of the shape of the emerging distribution, combined with theory, yields PSD curves called fractograms.

If applied as indicated above, FFF provides highly detailed size distribution curves and is a very flexible technique that can be adapted to different particle types in almost any suspending medium. The more commonly used FFFs in environmental applications are Sd-FFF and flow-FFF (FI-FFF). Sd-FFF uses a centrifugal field to aid the separation of the colloids, while FI-FFF uses a cross flow. For detailed information about FFF, Giddings (1993) provides a detailed explanation of this family of techniques and Hasselov et al. (2007) highlight the latest accomplishments of FFF for aquatic colloids and macromolecules.

Detection limits for colloid chemical analyses have been limited using traditional analytical techniques because the amount of colloids collected for analysis is generally limited. Presently, with the availability of low detection limit chemical analysis instrumentation such as graphite furnace atomic absorption spectrometer (GFAAS) and inductively coupled plasma-mass spectrometry (ICP-MS), concurrent particle size determination and chemical analyses can be conducted. Instruments can be assembled either off-line (disconnected) or online (connected) to achieve a more complete description of the colloid nature. Blo et al. (1995) used GFAAS as an off-line detector for Sd-FFF, while Contado et al. (1997) coupled online GFAAS to Sd-FFF to characterize suspended particulate matter from rivers. When analyzing colloidal fractions, techniques like inductively coupled optical emission spectrometry (ICP-OES) or ICP-MS that allow the simultaneous collection of multiple element signals are preferable. Sd-FFF was coupled with ICP-MS for the first time by Beckett (1991). Since then, many scientists have produced detailed chemical information about colloidal size fractions and associated elements (Murphy et al., 1993; Ranville et al., 1999). As per Table 15.3, Sd-FFF is only capable of separating particles down to  $\sim 50\ \text{nm}$ . Since many colloids of interest are smaller, Chittleborough et al. (2004) developed the FI-FFF-ICP-MS technique that can operate across the entire colloidal size range.

#### 15.1.3.1.7 Acoustic Spectroscopy

Acoustic spectroscopy methods measure the propagation velocity and attenuation of sound waves (i.e.,  $1\text{--}100\ \text{MHz}$ ) passing through a colloidal suspension, providing information about the PSD, rheology, and electrokinetic behavior of the suspension.

Dukhin and Goetz (2002) provide a thorough discussion of acoustic methods and the six mechanisms of acoustic attenuation associated with a colloidal suspension: viscous, thermal, scattering, intrinsic, electrokinetic, and structural signal dissipation. The application of acoustic spectroscopy to colloid characterization assumes that each attenuation process functions independently and that the overall attenuation is the summation of the independent processes.

Viscous and thermal dissipation are the most important because colloids mainly interact with sound waves hydrodynamically through the generation of oscillating shear waves and thermodynamically through temperature losses. The resulting acoustic spectra are generally insensitive to the electrical conductivity of the solution and the charge of suspended particles and provide no information concerning particle morphology (Dukhin and Goetz, 2002; Seaman et al., 2003).

Acoustic attenuation attributed to the suspension is generally determined by measuring the relative change in signal at each frequency with precise changes in gap distance or sample path length in spectroscopic terms. Thermal losses dominate in emulsions and low-density dispersions, so that viscous losses may be neglected. For rigid submicron particles (i.e., soil clays, oxides), viscous attenuation dominates and limited information regarding composition of the particles (density), the media (solution density and shear viscosity), and the relative volume fraction of the two phases is required for estimating particle size, providing a minimum detectable particle size of approximately 10 nm. For complex environmental samples, however, such information may be lacking. Acoustic scattering becomes more important with increasing particle size, and sound speed must also be considered. When characterizing “soft” particles having a limited density contrast compared to the suspending solution, such as latex particles and polymers, additional information concerning their thermal expansion properties is required for interpretation of the attenuation spectra (Dukhin and Goetz, 1996, 1998, 2002).

Acoustic methods offer several advantages compared to other instrumental techniques for evaluating colloid size and surface charge properties. Ultrasound can propagate through suspensions to a much greater degree than light. Therefore, acoustic analysis can be conducted at relatively high solid to solution ratios (up to 30% solids by volume) that are more analogous to soil conditions in the field. However, the analysis may require more colloidal material than may be readily available. Analysis may be indicative of particle interaction within the intact suspension, lessening the impact of trace artifacts, that is, dust, bubbles, suspension heterogeneity due to particle segregation, and filtration artifacts that can bias sizing methods such as SEM and DLS. The applicable sizing range is much larger than light-scattering methods, that is,  $\approx 5$  nm–1000  $\mu$ m. It is also less biased with respect to larger particles, making it more suitable for complex polydisperse systems. Acoustic methods are insensitive to sample convection, allowing stirring or agitation of the sample during analysis as required for reactive titration (e.g., Sun et al., 2006) or for the characterization of low charge,

inherently unstable suspensions, such as materials close to their zero point of charge (ZPC) and/or critical coagulation concentration (CCC) (Babick et al., 2000; Dukhin and Goetz, 2002; Kosmulski et al., 2002; Guerin and Seaman, 2004; Guerin et al., 2004; Delgado et al., 2005). Furthermore, the relatively large sample volume allows for the collection of subsamples throughout acoustic analysis for characterization by other analytical methods (Seaman et al., 2003).

Acoustic spectrometers for use in characterizing colloidal suspensions became commercially available in the 1990s. Despite several advantages when compared to light-scattering techniques, the application of acoustic-based methods to the study of soil colloids has generally been restricted to the characterization of mineral standards or synthesized mineral analogs, such as goethite and hematite (Gunnarsson et al., 2001; Kosmulski, 2002; Kosmulski et al., 2002, 2003; Appel et al., 2003; Guerin and Seaman, 2004; Guerin et al., 2004; Delgado et al., 2005). However, acoustic methods of suspension characterization rely on the interpretation of macroscopic sample properties, that is, the acoustic attenuation spectrum of a suspension, using idealized model algorithms with various simplifying assumptions and a few known system parameters, such as suspension concentration and particle density. The limited information can often result in systems that are “ill defined” and can be described by multiple answers, that is, PSDs (Dukhin and Goetz, 2001; Babick and Ripperger, 2002), a problem that also plagues light-scattering techniques (Schurtenberger and Newman, 1993). As such, acoustic methods are most suitable for evaluating relative changes in colloid aggregation and surface charge for suspensions in response to known changes in solution chemistry rather than for comparing subtle differences between poorly defined environmental samples.

#### 15.1.3.1.8 Applications of Particle Size Methods

PSD is a fundamental soil property, affecting soil surface area, bulk density, porosity, water retention, and hydraulic behavior. Furthermore, precise information about colloidal size and shape is important because submicron-size colloids often act as vehicles that control the transport and fate of adsorbed pollutants (hydrophobic organic compounds, toxic trace metals, and radionuclides [de Jonge et al., 2004a]). Bacteria and viruses are part of the colloidal pool in natural environments; their characterization and transport are significant for understanding biogeochemical processes (Rockhold et al., 2004), epidemic evolution (Bertuzzo et al., 2008), and the spread of diseases in general (Khilar and Fogler, 1984; McDowell-Boyer et al., 1986; Kia et al., 1987; Ryan and Elimelech, 1996; Kretzschmar et al., 1999; de Jonge et al., 2004a; McCarthy and McKay, 2004; Tufenkji, 2007). Submicron-size colloids have been insufficiently studied in the past because methods for their isolation, detection, and characterization have been inadequate, with the exception of a few examples (Kaplan et al., 1993; Kretzschmar et al., 1993; Chanudet and Filella, 2006). However, with the new fractionation methods and the coupling with low detection limit analytical instruments (FFF-ICP-MS), a new era in the characterization of soil colloids

is commencing (Chittleborough et al., 2004; Ranville et al., 2005; Lead and Wilkinson, 2007).

Despite the new advances in the characterization and analysis of colloids, many unanswered questions exist in regard to in situ colloidal behavior in natural environments, in particular, the chemical nature of colloids present and their structure, size, and shape distributions (Filella et al., 1997; Lead and Wilkinson, 2007). New methods of in situ visualization of colloids in porous media are the research focus of several recent publications; light transmission and epifluorescent microscopy are some of the new techniques developed by Crist et al. (2004) and Baumann and Werth (2004) for the observation and modeling of colloidal transport in porous media.

### 15.1.3.2 Surface Area

Surface area must be regarded as a relative term, in as much as it is scale dependent, as well as often dependent on the chemical and physical conditions of a system. Determinations of surface area range from particle size calculations assuming smooth surfaces and simplified geometry, generally termed geometric surface area, to possible molecular level calculations based on the distances between surface ions in a mineral structure. Because the measurement is scale and system dependent, there is no universally accepted way to measure surface area. Determination as to which measurement system to utilize should consider the scale and chemical conditions required by the application. Kinetic reactions that are diffusion controlled should likely consider geometric surface area, while surface-controlled reactions (such as some adsorption and some dissolution/precipitation reactions) should consider surface area at the scale of the reacting molecule. In most instances, surface area is related to surface reactivity, either adsorption or surface-controlled kinetic processes.

#### 15.1.3.2.1 Measurement Methodology

The results of surface area determinations must be interpreted within the context of the size and orientation of the adsorbate, as well as the attractive forces between the surface and the adsorbate. This distinction is particularly important for clays such as smectites, which can be considered to have internal as well as external surface area. Internal surface area is representative of the surface area of the interlayers. Inert gases such as  $N_2$  are not able to enter the interlayer positions, and thus, measure only external surface area of clay particles. In contrast, polar molecules such as ethylene glycol, ethylene glycol monoethyl ether (EGME), and water are able to cause expansion of the layers and penetrate into interlayer positions. Use of such molecules results in measurement of internal and external surface area. Since water is the solvent in environmental systems, these total surface area measurements are appropriate for adsorption studies. Soil surface area measurements obtained using  $N_2$ , water, and EGME were highly correlated with each other and with clay content when considering soils with similar mineralogy but not for soils with differing mineralogy (de Jong, 1999).

To characterize adsorption methods of surface area determination, it is useful to distinguish between chemical and

physical adsorption. Physical adsorption is characterized by low heats of adsorption without structural changes at the surface, fully reversible and rapid reactions since no activation energy is required, coverage of the entire surface rather than specific sites, little or no adsorption at elevated temperatures, and potential coverage by more than one layer of adsorbate (Lowell, 1979). Chemisorption is characterized by high heats of adsorption, localization of adsorption at specific surface sites, and irreversible reaction. The term "specific surface area" has been used to denote the surface area of a material expressed on a mass basis ( $m^2 g^{-1}$ ).

#### 15.1.3.2.2 Gas Adsorption Using the BET Equation

The BET equation is commonly used in conjunction with physical gas adsorption to measure surface area. The BET equation is named after Brunauer, Emmett, and Teller (1938), who extended the Langmuir theory for monolayer gas adsorption to multilayer adsorption. The Langmuir equation (Langmuir, 1918) is given by:

$$\frac{P}{V} = \frac{1}{kV_m} + \frac{P}{V_m} \quad (15.4)$$

where

$P$  is the pressure

$V$  is the volume of gas adsorbed per kilogram of adsorbent at that pressure

$k$  is a constant

$V_m$  is the volume of gas adsorbed per kilogram of adsorbent at monolayer surface coverage

The surface area is obtained by determination of  $1/V_m$ , which is the slope of the  $P/V$  versus  $P$  plot. The specific surface area is then equal to  $1/V_m$  multiplied by the cross-sectional area of the adsorbate and the number of molecules in volume  $V_m$ .

The BET relation assumes that there is a dynamic equilibrium between the molecules in the various layers such that the number of molecules in each layer remains constant, although different sites may or may not be occupied at any given time. Use of the equation enables calculation of the number of molecules in a monolayer despite the fact that complete monolayer coverage may not have occurred. The BET equation is written as (Lowell, 1979):

$$\frac{1}{W[P_0/P]} = \frac{1}{W_m C} + \frac{C-1}{W_m C} \frac{P}{P_0} \quad (15.5)$$

where

$P$  is the adsorbate gas pressure

$P_0$  is the adsorbate pressure at saturation for the temperature of the experiment

$W$  is the weight adsorbed in the monolayer

$W_m$  is the weight adsorbed in the complete monolayer

$C$  is the BET constant

Multipoint BET plots are created by plotting  $1/(W(P_0/P - 1))$  on the  $y$  axis and  $P/P_0$  on the  $x$  axis. The value of  $W_m$  is calculated from the slope and intercept. The specific surface area is determined by dividing the total surface area by the sample weight. The region of  $P/P_0$  between 0.05 and 0.35 is usually linear and within the region of pressures corresponding to sufficient adsorption to complete monolayer coverage, and thus, best suited for determination of  $W_m$  (Lowell, 1979).

Often the BET surface area can be determined from a single pressure measurement without much loss of accuracy. For relatively high values of  $C$ , the intercept value is small relative to the slope and can be approximated by zero. The BET equation is thus reduced to (Lowell, 1979):

$$W_m = W \left( 1 - \frac{P}{P_0} \right) \quad (15.6)$$

Soil and mineral surface areas are most commonly measured by  $N_2$  adsorption, using the BET equation. The calculation is made using the  $N_2$  cross-sectional area of  $0.162 \text{ nm}^2$  (Gregg and Sing, 1982). Often this area is referred to as the effective or occupied area. Alternatively for surface area  $< 1 \text{ m}^2 \text{ g}^{-1}$  the use of Kr is recommended.

Most commonly, the BET method consists of adsorption of  $N_2$  at a fixed partial pressure  $P$  in a He- $N_2$  mixture and measurement of the desorbed  $N_2$  in a pure He gas stream using gas chromatography. Alternative methods include measurement of the mass of  $N_2$  adsorbed. In this method, the sample is evacuated to high vacuum, heated, then cooled to liquid  $N_2$  temperature, and weighed. Quantities of  $N_2$  are then added to the system and a series of weighings is made at various pressures. In this instance, the  $N_2$  partial pressures are equal to the total pressure in the system.

Surface area can also be determined from the sorption of water at one or more vapor pressures (Newman, 1983). In this instance, air-dried samples are reacted in evacuated desiccators containing saline solutions with relative vapor pressures on the order of 0.2–0.4. Samples are equilibrated until there is no further weight change, then samples are dried at  $105^\circ\text{C}$  and weighed again. Sorbed water is taken as the difference between the oven-dry weight and the desiccator-equilibrated weight. Surface area is then calculated as with  $N_2$ , using Equation 15.5. This method gives values comparable to EGME values for nonexpanding clays but underestimates surface area for smectites due to limited water uptake in the interlayers (de Jong, 1999). For smectitic soils, de Jong (1999) recommended using the Langmuir equation (monolayer) for water sorption indicating that the reduced BET equation (Equation 15.6) is not applicable because interlayer water uptake is limited. de Jong (1999) demonstrated a correspondence close to 1:1 between surface area determined with EGME using the BET equation and with water using the Langmuir expression. It can be argued that water sorption values may be more realistic than EGME values (Pennell et al., 1995), since the interlayer spaces of smectites are not accessible

to nonpolar molecules until at least two layers of water are present (Quirk and Murray, 1991).

#### 15.1.3.2.3 Organic Molecules

**15.1.3.2.3.1 Ethylene Glycol** Ethylene glycol was utilized by Dyal and Hendricks (1950) for determination of total surface area of clays. The method consists of adding excess ethylene glycol to soil or clays and allowing the excess to evaporate under vacuum. It is assumed that when the rate of weight loss of the sample decreases, only a monolayer of ethylene glycol remains. Dyal and Hendricks (1950) calibrated the method assuming a bentonite surface area of  $810 \text{ m}^2 \text{ g}^{-1}$  and calculated that  $0.31 \text{ mg}$  of adsorbed ethylene glycol corresponded to each square meter of surface area. The method was modified by Bower and Goertzen (1959) using  $\text{CaCl}_2$ -monoglycolate to maintain an ethylene glycol vapor pressure just below that of the saturation vapor pressure. In this method, the sample and the liquid are placed in separate open vessels in an evacuated system and the sample is weighed until it is in equilibrium with the vapor pressure of the ethylene glycol.

**15.1.3.2.3.2 Ethylene Glycol Monoethyl Ether** Ethylene glycol monoethyl ether (EGME) has replaced ethylene glycol as the polar solvent of choice for determination of surface area. Since EGME has a higher vapor pressure than ethylene glycol, it requires a shorter reaction time to equilibrate the sample (Carter et al., 1986). A solvate of EGME and  $\text{CaCl}_2$  is used in the evacuated chamber to lower the vapor pressure of EGME to just below the saturation pressure. Open vessels of EGME/ $\text{CaCl}_2$  and soil are placed in the chamber and the soil is periodically weighed until no further weight gain is observed. It is assumed that the EGME surface coverage is  $5.2 \times 10^{-19} \text{ m}^2$  per molecule and that  $0.286 \text{ mg}$  adsorbed corresponds to  $1 \text{ m}^2$  of surface area (Carter et al., 1986). The method is limited in that the EGME affinity for cations results in greater than monolayer coverage at those sites, the assumption that EGME covers all surfaces cannot be properly evaluated, and the large size of the molecule may prevent coverage in small surface voids. A serious reservation of the procedure is the assumption that the average EGME occupancy of smectite surface applies equally well to all soil surfaces, regardless of mineralogy (Tiller and Smith, 1990). These authors found that more EGME was retained per unit area by nonexpanding soil clays such as illites and kaolinites than by smectites resulting in an overestimation in surface area of 50%–100% when using smectite as a reference. Measurement of total surface area of soils with mixed mineralogy using EGME and a single conversion factor based on smectite leads to significant under- and overestimation of surface area of many soils, even including smectitic soils (Tiller and Smith, 1990).

**15.1.3.2.3.3 Methylene Blue** Methylene blue, an organic cation, is reacted at various concentrations with soil suspensions (typically with organic material removed) under pH-buffered conditions. Measurement of methylene blue concentration before and after reaction with soil is made spectrophotometrically at a wavelength of  $665 \text{ nm}$ . The adsorbed concentration of methylene

blue is used to calculate surface area assuming an area of  $1.3 \text{ nm}^2$  per methylene blue molecule (Hang and Brindley, 1970). This surface area corresponds to the molecule attaching parallel to its long axis. This method can only be used in hydrated systems. Aringhieri et al. (1992) found surface areas determined with methylene blue to be unrealistically lower than those obtained with water adsorption and suggested that the major limitation of the method is its dependence on the soil surface charge characteristics. Alternatively, Borkovec et al. (1993) obtained relatively good agreement between methylene blue and  $\text{N}_2$  BET surface areas for four soil samples assuming a methylene blue surface area of  $0.247 \text{ nm}^2$ , corresponding to a molecular attachment of methylene blue perpendicular to its long axis. Orientation of the organic molecules may be related to surface site characteristics, as well as concentration of adsorbing molecules. These differences illustrate one of the disadvantages of using charged molecules for surface area determination; their use is not recommended.

#### 15.1.3.2.4 Electron Microscopy Image Analysis

Transmission electron microscopy as well as SEM can be used for determination of geometric surface area using a variety of methods, including calculation of planar surface area and assumptions regarding geometry to calculate total external surface area. With this method, only edge roughness can be measured. The SEM method, which offers the possibility of measuring the external surface roughness, consists of collecting two images at different sample tilt angles and constructing a three-dimensional representation of the surface. Surface area is calculated within a grid of fixed lines by summation of the planar surfaces in the grid. The ratio of the calculated surface to the area within the grid gives a measure of surface roughness. Measurements can also be made at different scales, providing information about the size distribution of the surface features. Since these measurements are typically made at the micrometer scale, and measure external surface area, it is not surprising that the values are intermediate between geometric surface areas based on particle size and BET values. Determination of specific surface area requires conversion of particle surface area to a mass basis using the particle density. The assumption that the particle density is equal to the density of specimen samples of the mineral is reasonable and introduces relatively minor errors in comparison to other assumptions made in the calculation. Increasing computer capacity and suitable software makes this method the most useful of the geometric methods.

#### 15.1.3.2.5 Small Angle X-Ray Scattering

In this application,  $K\alpha$  radiation from a conventional x-ray tube is scattered by freeze-dried samples in glass capillary tubes. The background-corrected x-ray-scattering intensity is plotted against the scattering vector ( $q$ ) to obtain the apparent surface fractal dimension ( $D_s$ ) using the relation (Borkovec et al., 1993):

$$I_q = Aq^{D_s-5} + B \quad (15.7)$$

where

- $I_q$  is the scattering intensity
- $A$  is a proportionality constant
- $B$  is the background correction

Values of  $D_s$  obtained for soils using this method are in relatively good agreement with values calculated from gas adsorption surface area ( $a$ ) for soil particle radii ( $r$ ) using the relation (Borkovec et al., 1993):

$$a = C\lambda^{2-D_s} r^{D_s-3} \quad (15.8)$$

where

- $\lambda$  is the size of the probing molecules
- $C$  is the proportionality constant

#### 15.1.3.2.6 Negative Adsorption

Negative adsorption refers to a deficiency in the concentration of an ion in solution adjacent to a solid surface relative to the concentration of the ion in the bulk solution. The deficit is caused by electrostatic repulsion between ions and surfaces of similar charge. Since most charged surfaces in soils are negatively charged, negative adsorption usually relates to solution anion concentrations and negative surfaces. For a 1:1 electrolyte, the diffuse double layer model produces the following approximation (Sposito, 1984):

$$d_e \approx \frac{2}{\sqrt{\beta c}} - \delta \quad (15.9)$$

where

- $d_e$  is the exclusion distance
- $c$  is the concentration of the bulk electrolyte
- $\beta$  is a constant equal to  $1.08 \times 10^{16} \text{ m mol}^{-1}$
- $\delta$  is the distance between two planes

The exclusion volume and area ( $S_e$ ) are related by

$$V_e = S_e d_e \quad (15.10)$$

where  $V_e$  is the exclusion volume (the hypothetical volume from which the ion is completely excluded). Substituting into Equation 15.9 yields

$$V_e \approx \frac{2S_e}{\sqrt{\beta c}} - \delta S_e \quad (15.11)$$

The exclusion volume is calculated by first removing the bulk solution, determining the remaining liquid volume, displacing the liquid, and analyzing for the bulk solution and extract concentration. The exclusion volume is then equal to the mass deficit in the extract divided by the concentration in the bulk solution.

A plot of  $V_e$  vs.  $c^{-0.5}$  should yield a straight line whose slope is proportional to the exclusion specific surface area as shown by inspection of Equation 15.11.

This method was first described by Schofield (1949), who used it to determine montmorillonite surface area from reactions with NaCl, NaNO<sub>3</sub>, and Na<sub>2</sub>SO<sub>4</sub> solutions. Subsequent work by Edwards et al. (1965a, 1965b) demonstrated that the specific surface area determined with this method varied with cation selected. Calculated values for illites ranged from values close to the N<sub>2</sub> BET values with Li to 0 with Cs. In contrast, for montmorillonite, LiCl exclusion volumes were 10 times greater than N<sub>2</sub> BET surface areas, while Cs values were comparable to those obtained by N<sub>2</sub> BET. Trends in surface area values measured using anion exclusion for Li, Na, K, NH<sub>4</sub>, Cs, and Ca-montmorillonites were in agreement with those calculated from a tactoid model (Schramm and Kwak, 1982a, 1982b).

#### 15.1.3.2.7 Applications

Surface area measurements are required for a variety of calculations. In most soils, the bulk soil surface area is dominated by the surface area of the clay minerals. Surface charge density, which requires measurement of both surface area and particle charge, has been related to cation exchange selectivity. As expected, increasing surface charge density favors adsorption of the higher valence cation in heterovalent exchange (Maes and Cremers, 1977). Surface charge density is also required for calculation of double layer thickness and for use in a variety of adsorption relationships. Determination of specific surface area is required for chemical studies on many different minerals. In this case, bulk surface area is not appropriate. Controlled laboratory studies are often performed using addition of quantities of a well-characterized mineral having a known surface area. This method is used to study a variety of chemical reactions, such as kinetics of calcite, gypsum, and dolomite dissolution, surface area of calcite for prediction of phosphate adsorption, and addition of various Fe or Mn oxides for study of adsorption and redox processes. Among the various applications of the EGME method, Ross (1978) related shrink/swell properties of soils to surface area and Supak et al. (1978) related the specific surface area of clays to the adsorption of the pesticide aldicarb.

#### 15.1.3.3 Surface Charge

The total net surface charge on a particle ( $\Phi_p$ ) is

$$\sigma_p = \sigma_s + \sigma_H + \sigma_{is} = \sigma_{os} - \sigma_d \quad (15.12)$$

where

- $\sigma_s$  is the permanent structural charge
- $\sigma_H$  is the proton surface charge resulting from the specific adsorption of protons and hydroxyl ions
- $\sigma_{is}$  is the inner-sphere complex charge resulting from specific ion adsorption
- $\sigma_{os}$  is the outer-sphere complex charge resulting from non-specific adsorption
- $\sigma_d$  is the dissociated charge

This definition is similar to the one provided by Sposito (1984) with the exception that total net surface charge results from isomorphic substitution and is generated by specifically adsorbing ions (Hunter, 1981). An inner-sphere surface complex contains no water between the adsorbing ion and the surface functional group; while an outer-sphere surface complex contains at least one water molecule between the adsorbing ion and the surface functional group (Sposito, 1984). Examples of surface functional groups are reactive surface hydroxyl groups on oxide minerals, aluminol and silanol groups on clay minerals, and carboxyl and phenol groups on SOM.

#### 15.1.3.3.1 Measurement Methodology

The total net surface charge can be measured directly using electrokinetic experiments. The point of zero charge (p.z.c.) of a particle is the solution pH value where total net particle charge is zero. The p.z.c. can be measured directly using electrokinetic experiments or indirectly from potentiometric titrations under certain experimental conditions (Sposito, 1984).

Electrokinetic phenomena are processes where a relative velocity exists between two parts of the electrical double layer (Hiemenz, 1977; Hiemenz and Rajagopalan, 1997). In this motion, a thin layer of liquid remains with the solid and a shear plane is located between the solid and liquid phases at some distance from the solid surface (van Olphen, 1977). The electric double layer potential at the shear plane is called the zeta potential ( $\zeta$ ). The assumption that  $\zeta$  is equal to or very close to the diffuse double layer potential ( $\psi_d$ ) is supported indirectly by a large body of data on a variety of surfaces (Hunter, 1981, 1989). The principle electrokinetic phenomena that measure zeta potential are discussed later.

#### 15.1.3.3.2 Electrophoresis

Electrophoresis measures the movement of a suspended charged particle in response to an applied electric field. This movement is called electrophoretic mobility ( $\mu_E$ ) and is given by the Smoluchowski equation (Hunter, 1989):

$$\mu_E = \frac{\epsilon \zeta}{\eta} \quad (15.13)$$

where

- $\epsilon$  is the relative permittivity
- $\eta$  is the viscosity

The Smoluchowski equation applies when the particle dimensions are much greater than the double layer thickness (Hunter, 1987). The complete formula relating  $\zeta$  and  $\mu_E$  is derived by the theoretical evaluation of the electric force on the charged particle ( $f_1$ ), the hydrodynamic frictional force on the particle by the liquid ( $f_2$ ), the electrophoretic retardation force ( $f_3$ ), a frictional force resulting from the movement of water with the counterions, and the relaxation force ( $f_4$ ), caused by distortion of the double layer around the particle (van Olphen, 1977). Additional considerations arise

for nonspherical particles and those carrying two double layers such as clays. For these reasons, the Smoluchowski equation is, in general, only approximate and it is advisable to report electrophoresis results as electrophoretic mobility rather than to attempt to convert to zeta potential (van Olphen, 1977).

Electrophoresis is the most common method of determining zeta potential. For colloidal systems, the most appropriate technique is microelectrophoresis where the movement of individual particles is followed directly by microscopy (Hunter, 1981). Microelectrophoresis is only applicable at very low particle concentrations. Electrophoresis can also be studied using laser Doppler velocimetry and photon correlation spectroscopy. The mass transport mobility apparatus measures electrophoretic mobility from the mass of colloids transported to a suitable electrode compartment (Hunter, 1981). This apparatus can be used at much higher particle concentrations than microelectrophoresis.

#### 15.1.3.3.3 Electroosmosis

Electroosmosis measures the movement of the liquid adjacent to a flat, charged surface in response to an electric field applied parallel to the surface. This movement is called electroosmotic velocity ( $v_{eo}$ ) and is also obtained from the Smoluchowski equation (Hunter, 1987):

$$v_{eo} = \frac{-\epsilon\zeta E}{\eta} \quad (15.14)$$

where  $E$  is the electric field strength. While it is possible to measure electroosmotic velocity directly using microscopy, it is more common to measure the volume of liquid transported per unit time (Hunter, 1981):

$$\frac{V}{i} = \frac{\epsilon\zeta}{\eta\lambda_0} \quad (15.15)$$

where

$V$  is volume

$i$  is the electric current

$\lambda_0$  is the electrical conductivity

The material whose zeta potential is being measured is formed into a porous plug and the transport of liquid across a tube in response to an electric field may be obtained by measuring the movement of an air bubble in the capillary providing the return path (Adamson, 1976). It is also possible to measure the electroosmotic flow by applying a counter pressure until the flow is exactly compensated (Hunter, 1981).

#### 15.1.3.3.4 Electroacoustic Spectroscopy

A general discussion of the application of acoustic spectroscopy for characterizing colloidal suspensions was presented earlier in this chapter (Section 15.1.3.1). Both acoustic and electroacoustic spectrometers are commercially available separately or combined in a single instrument. In electroacoustic spectroscopy,

one measures either (1) the colloid vibration potential (CVP) or colloid vibration current (CVI), the induced dipole moment created by the displacement or polarization of the electrical double layer in response to an acoustic wave, or (2) the electrokinetic sonic amplitude (ESA) generated by the movement of a charged particle in response to an electrical field as indicators of colloidal zeta potential. The individual dipole moments created by the interaction of sound waves with a colloidal suspension can be measured as an alternating electrical field that varies with the amplitude of the sound wave. Conversely, the electrophoretic movement of charged particles in response to an applied electrical field gives rise to sound waves, known as the ESA effect. Although electroacoustic spectroscopy can provide PSD, such information is best derived from the conventional acoustic spectra (Dukhin and Goetz, 2002; Seaman et al., 2003).

In contrast to microelectrophoretic light-scattering methods, electroacoustic measurement of zeta potential can be conducted at much higher suspension concentrations (30%–50% solids), an obvious advantage given that sample dilution and changes in solution chemistry can impact the expression of zeta potential and apparent particle size (Dukhin et al., 2001; Dukhin and Goetz, 2002; Delgado et al., 2005). Acoustic methods have been used to evaluate shifts in the isoelectric point (IEP) of materials at high-ionic strengths as indicators of specific and nonspecific sorption mechanisms (Kosmulski, 2002; Kosmulski et al., 2002; Greenwood, 2003). Such applications are best used in combination with other surface active spectroscopic methods for determining sorption mechanisms. In comparing various techniques for evaluating the IEP and p.z.c. of Fe (hydr)oxides, Kosmulski et al. (2003) noted that electroacoustic methods produced higher IEP values than observed for potentiometric titration methods. The cause of the discrepancy was not discussed.

#### 15.1.3.3.5 Streaming Potential

The streaming potential is an electric potential difference generated when liquid adjacent to a charged surface is set in motion by an applied pressure gradient (Hunter, 1987). The streaming potential ( $\Phi_{st}$ ) is also governed by the Smoluchowski equation and given by (Sposito, 1984)

$$\Phi_{st} = \frac{\epsilon\zeta}{\lambda_0\eta} \Delta P \quad (15.16)$$

where  $\Delta P$  is the applied pressure difference. The streaming potential can be measured in similar fashion as the electroosmotic velocity. Liquid is forced under pressure through a porous plug and  $\Phi_{st}$  is measured by electrodes in the solution on either end (Adamson, 1976).

#### 15.1.3.3.6 Sedimentation Potential

When particles having charged surfaces settle in a liquid under the force of gravity, a plane of shear is developed. As the particles settle, the interfacial charge is separated since a portion inside the shear plane moves with the particle and the remainder is left behind (Sposito, 1984). An electric potential difference arises



from the separation of charge called the sedimentation potential. The gradient for the sedimentation potential,  $d\Phi_{sed}$ , is given by (Sposito, 1984)

$$\frac{d\Phi_{sed}}{dz} = \frac{\epsilon\zeta}{\lambda_0\eta} n\Delta\rho g \quad (15.17)$$

where

- $n$  is the number of particles per unit volume
- $\Delta\rho$  is the difference in mass density between the particles and the liquid phase
- $g$  is gravitational acceleration
- $z$  is distance

The potential difference is measured by inserting reversible electrode probes at two different heights in the column of settling particles (Hunter, 1981). For low particle concentration, the sedimentation potential is also governed by the Smoluchowski equation (Hunter, 1981).

#### 15.1.3.3.7 Potentiometric Titration

Potentiometric titration measures the surface density of proton surface charge ( $\sigma_H$ ) defined as (Sposito, 1984)

$$\sigma_H = \frac{F}{A} (q_H - q_{OH}) \quad (15.18)$$

where

- $F$  is the Faraday constant
- $A$  is the specific surface area
- $q_H$  is the complexed proton charge (mol)
- $q_{OH}$  is the complexed hydroxyl charge (mol) per unit mass of solid

Titration data consist of pH readings obtained while known amounts of acid or base are added to a solid suspension. A net titration curve is obtained by subtracting a calibration curve obtained by titrating the equivalent supernatant solution. The values of  $q_H - q_{OH}$  are given by (Sposito, 1984)

$$q_H - q_{OH} = \frac{C_A - C_B - [H^+] + [OH^-]}{C_s} \quad (15.19)$$

where

- $C_A$  is the molar concentration of acid added
- $C_B$  is the molar concentration of base added
- $[H^+]$  is the molar proton concentration
- $[OH^-]$  is the molar hydroxyl concentration obtained from pH measurement
- $C_s$  is the particle concentration

In order for Equation 15.19 to be valid, added protons and hydroxyl ions must only react with surface-reactive functional groups whose charge is pH dependent. Usually, other reactions that are also pH dependent occur, such as soluble complex formation,

dissolution of solid phases, or complexation with surfaces whose charge is not pH dependent (Parker et al., 1979). Without these corrections, no surface chemical significance can be provided by Equation 15.19. A detailed description of the use of potentiometric titration to determine surface charge is provided by Huang (1981).

#### 15.1.3.3.8 Applications

One of the most important applications of electrokinetic experiments and potentiometric titrations is the determination of the p.z.c. A characteristic of variable charge minerals is the p.z.c. obtained in the presence of an inert electrolyte. This p.z.c. is determined electrokinetically as the pH value where the zeta potential is zero or indirectly from the point of zero net proton charge (p.z.n.p.c.) or from the point of zero salt effect (p.z.s.e.) obtained potentiometrically. The p.z.n.p.c. and the p.z.s.e. are discussed in detail in Chapter 16. The p.z.n.p.c. and the p.z.s.e. are equivalent to the p.z.c. in the absence of surface complex formation. Table 15.4 provides characteristic values of p.z.c. obtained using electrokinetic experiments and potentiometric titrations for a variety of variable charge minerals.

**TABLE 15.4** Representative Points of Zero Charge for Various Minerals

Solid	p.z.c.
<i>Electrophoresis</i>	
Goethite	8.8
Hematite	8.5
Magnetite	6.9
Amorphous iron oxide	8.0
Gibbsite	9.8
Bayerite	9.2
Boehmite	9.4
Pseudoboehmite	9.2
Amorphous aluminum oxide	9.3
$\delta$ -MnO <sub>2</sub>	2.3
Rutile	4.8
Anatase	5.9
Kaolinite	2.9
<i>Streaming potential</i>	
$\gamma$ -Al <sub>2</sub> O <sub>3</sub>	9.1
$\alpha$ -Al <sub>2</sub> O <sub>3</sub>	9.2
<i>Titration</i>	
Goethite	8.7
Hematite	8.6
Magnetite	6.9
Gibbsite	9.8
Boehmite	8.5
Pseudoboehmite	9.3
Amorphous aluminum oxide	9.5
$\delta$ -MnO <sub>2</sub>	3.6
SiO <sub>2</sub>	3.0
Rutile	5.8
Anatase	6.0
Kaolinite	2.9

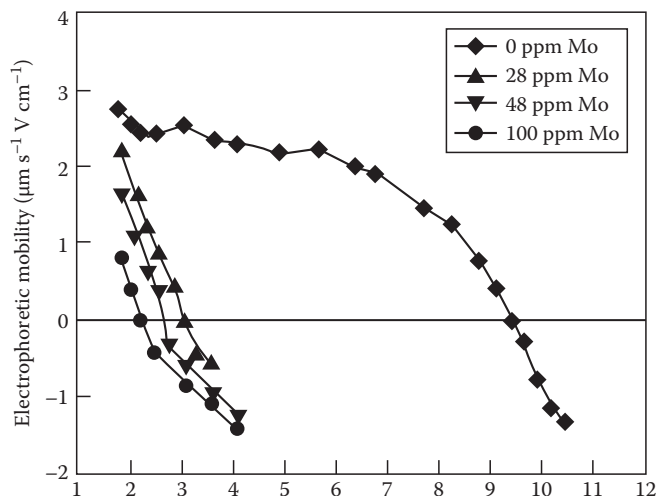


**FIGURE 15.1** Shifts in p.z.c. and charge reversal of gibbsite in the presence of molybdate. (Adapted from Goldberg, S., H.S. Forster, and C.L. Godfrey. 1996. Molybdenum adsorption on oxides, clay minerals, and soils. *Soil Sci. Soc. Am. J.* 60:425–432.)

Electrokinetic experiments and potentiometric titrations can be used to infer adsorption mechanisms for adsorbing ions on surfaces. Adsorption of ions that form inner-sphere surface complexes is characterized by shifts in the p.z.c. of the particles and reversals of their electrophoretic mobility with increasing ion concentration (Hunter, 1981). Adsorption of ions that form outer-sphere surface complexes does not produce p.z.c. shifts since they are assumed to lie outside the shear plane. Figure 15.1 presents the shifts in p.z.c. and charge reversals observed for gibbsite upon the specific adsorption of increasing amounts of molybdate. These results are indirect evidence for inner-sphere surface complexation of this ion.

Net particle surface charge is a primary factor in dispersion of clay minerals. Zeta potential as a measure of particle surface charge was also related to percentage of dispersible clay (Chorom and Rengasamy, 1995). Figure 15.2 indicates the relationship between zeta potential measured using electrophoresis, and dispersible clay for Na-saturated kaolinite, montmorillonite, and illite.

The plane interface technique determines the electroosmotic velocity at large plane interfaces and can be used to determine the zeta potential of two different surfaces at the same time under the same conditions (Nishimura et al., 1992). These authors used the plane interface technique to simultaneously study silica plates and muscovite mica basal planes. The zeta potential values for silica presented in Figure 15.3 indicate that the asymmetric silica–mica cell provides results comparable to those of the symmetrical silica–silica cell.

Zeta potentials of clay minerals have also been determined using a flat plate streaming potential apparatus for muscovite mica (Scales et al., 1990), saponite, and hectorite (Nishimura et al., 2002a). Zeta potential of clays becomes less negative with increasing electrolyte concentration as a result of double layer compression (Figure 15.4). The resulting charge reduction causes clay flocculation. Streaming potential measurements of sodium montmorillonite using a flexible wall permeameter were

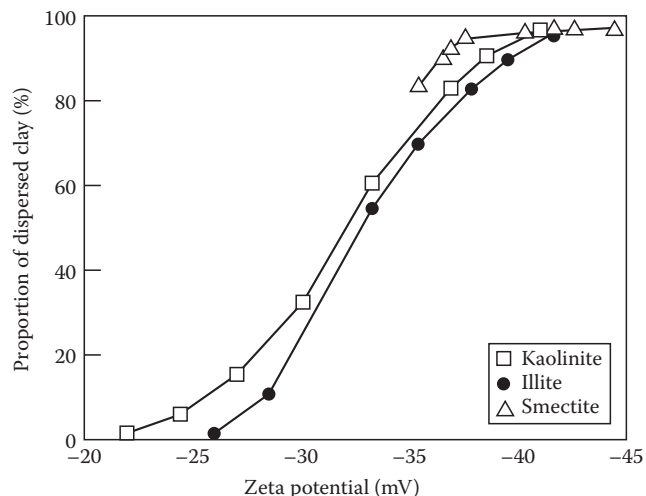


**FIGURE 15.2** Relation between zeta potential and dispersible clay of Na-clay minerals obtained using electrophoresis. (Reprinted from Chorom, M., and P. Rengasamy. 1995. Dispersion and zeta potential of pure clays as related to net particle charge under varying pH, electrolyte concentration and cation type. *Eur. J. Soil Sci.* 46:657–665. With permission of Blackwell Science Ltd.)

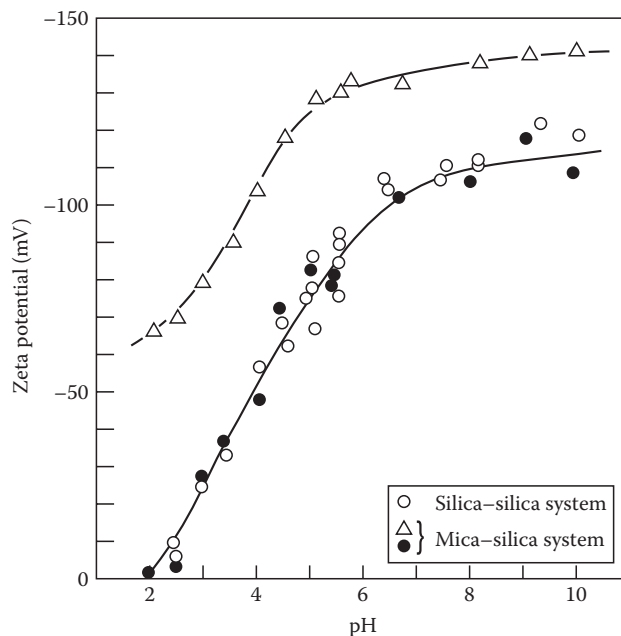


**FIGURE 15.3** Zeta potentials as a function of solution pH for muscovite mica basal plane- and silica plate–aqueous solution interfaces obtained using electroosmosis. (Reprinted from Nishimura, S., H. Tateyama, K. Tsunematsu, and K. Jinnai. 1992. Zeta potential measurement of muscovite mica basal plane–aqueous solution interface by means of plane interface technique. *J. Colloid Interface Sci.* 152:359–367. With permission of Academic Press, Inc.)

found to be dependent on the salt concentration of the permeating solution (Heister et al., 2005).

A vastly different application of electrokinetic experiments is the application to dewatering and decontamination of soils

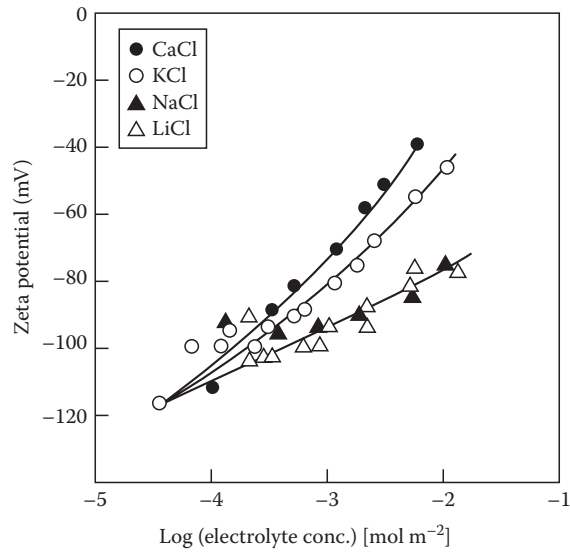


**FIGURE 15.4** Relation between zeta potential and electrolyte concentration for various 1:1 electrolytes obtained from streaming potential. (Reprinted with permission from Scales, P.J., F. Grieser, and T.W. Healy. 1990. Electrokinetics of the muscovite mica–aqueous solution interface. *Langmuir* 6:582–589. Copyright 1990 American Chemical Society.)

and clays. For example, electroosmosis has been used for removing organic contaminants from kaolinite and soil clays (Shapiro and Probstein, 1993; Schultz, 1997; Kim et al., 2001). These authors present applications for in situ hazardous waste remediation of soils. Economic analysis indicated that electroosmosis compared favorably with the cost of excavation and ex situ treatment (Schultz, 1997).

A potentiometric titration method has been developed to account for changes in solubility of the solid with changes in pH (Schulthess and Sparks, 1986). This is a batch method where the reference for each sample is the supernatant specific to that sample back titrated to pH 7. This method is considered to account for all sources of proton consumption (Schulthess and Sparks, 1986).

#### 15.1.4 Thermodynamics of Colloid Surfaces

To develop the thermodynamic treatment of the surface region, a few definitions are useful. The interfacial region is a space between two adjoining phases (gas–liquid, gas–solid, liquid–liquid, liquid–solid, solid–solid), which is characterized by inhomogeneity in its properties. The Gibbs surface is a mathematical dividing surface, without volume, drawn parallel to the boundaries of the interfacial region, which is used to define the volumes of the two adjoining bulk phases. A schematic of the interfacial region and the Gibbs surface is presented in Figure 15.5. The actual values for the system as a whole will differ from the sum of the values for the bulk phases by an excess or deficiency due to the Gibbs surface (Adamson, 1976). The following relations hold for the variables of state:

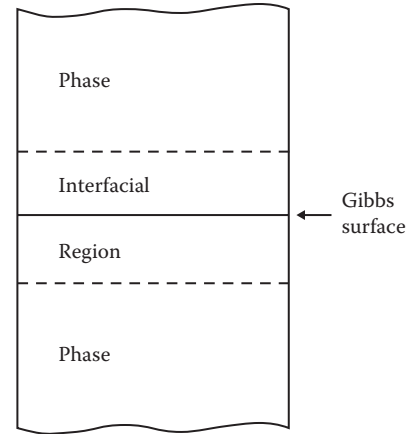


**FIGURE 15.5** Representation of the interfacial region and the Gibbs surface.

$$\text{Volume: } V = V^\alpha - V^\beta$$

$$\text{Internal Energy: } E = E^\alpha + E^\beta + E^\sigma \quad (15.20)$$

$$\text{Entropy: } S = S^\alpha + S^\beta + S^\sigma$$

$$\text{Moles: } n_i = n_i^\alpha + n_i^\beta + n_i^\sigma$$

where

$\alpha$  and  $\beta$  denote the bulk phases

$\sigma$  denotes the Gibbs surface (Adamson, 1976)

Additional variables of state are defined as the surface tension or surface free energy ( $\gamma$ ) and the area of the Gibbs surface ( $A$ ).

The three fundamental thermodynamic relationships of surface chemistry are the Young–Laplace equation, the Kelvin equation, and the Gibbs equation (Adamson, 1976). The Young–Laplace equation is the fundamental equation of capillarity for a curved Gibbs surface:

$$P^\beta - P^\alpha = \gamma \left( \frac{1}{r_1} + \frac{1}{r_2} \right) \quad (15.21)$$

where

$P^\beta - P^\alpha$  is the capillary pressure

$r_1$  and  $r_2$  are the radii of curvature

The Kelvin equation gives the effect of surface curvature on the molar free energy of a substance. The free energy of a substance can be related to its vapor pressure assuming the vapor to be ideal (Adamson, 1976). The Kelvin equation is

$$\ln \left( \frac{P}{P_0} \right) = \frac{\gamma V}{RT} \left( \frac{1}{r_1} + \frac{1}{r_2} \right) \quad (15.22)$$

where

$P_0$  is the normal vapor pressure of the liquid

$P$  is the vapor pressure observed over the curved surface

$R$  is the molar gas constant

$T$  is temperature

For a small, reversible change  $dE$  in the energy of the system (Adamson, 1976)

$$\begin{aligned}
 dE &= dE^\alpha + dE^\beta + dE^\sigma \\
 &= TdS^\alpha + \sum \mu_i dn_i^\alpha - P^\alpha dV^\alpha + TdS^\beta \\
 &\quad + \sum \mu_i dn_i^\beta - P^\beta dV^\beta + TdS^\sigma + \sum \mu_i dn_i^\sigma - P^\sigma dV^\sigma + \gamma dA
 \end{aligned}
 \tag{15.23}$$

where  $\mu_i$  is chemical potential. Substituting for  $dE^\alpha$  and  $dE^\beta$  and manipulating the equation for  $dE^\sigma$  lead to the expression (Adamson, 1976)

$$S^\sigma dT = A d\gamma + \sum n_i^\sigma d\mu_i = 0 \tag{15.24}$$

At constant  $T$  and  $A$ , the Gibbs equation is

$$-d\gamma = \sum \frac{n_i^\sigma}{A} d\mu_i = \sum \Gamma_i^\sigma d\mu_i \tag{15.25}$$

where  $\Gamma_i^\sigma$  is a surface excess concentration per unit area defined as  $\Gamma_i^\sigma = n_i^\sigma/A$ . The Gibbs equation can be applied to liquid-liquid and liquid-vapor interfaces where the surface tension can be measured to calculate the surface concentration of the adsorbed species causing the surface tension change. Similarly, if the surface concentration can be measured directly but the surface tension cannot, the Gibbs equation can be used to calculate the lowering of  $\gamma$  from the measured adsorption in solid-gas and solid-liquid systems (Hunter, 1987).

## 15.2 Interparticle Forces

### 15.2.1 Electrical Double Layer

Double layer theory describes the distribution of ionic concentrations near electrostatically charged particles. The charge on the colloidal particles is due to isomorphic substitution in the particle lattices or arises from the preferential adsorption of one ionic species from the solution phase (Babcock, 1963). Such a charge requires the presence of a layer of ions of opposite charge. The double layer consists of an excess of ions of opposite sign and a deficiency of ions of the same sign that are electrostatically repelled by the particle. Double layer theory assumes that the surface of the colloidal particles is represented by an infinite flat surface having continuous and uniform electrostatic charge density immersed in an electrolyte with a uniform dielectric constant (Babcock, 1963). All electrolyte ions are assumed to be point charges. The electrical potential, ion charge, and ion distributions can be calculated from the Poisson-Boltzmann equation:

$$\frac{d^2\psi}{dx^2} = -\frac{1}{\epsilon_0 D} \sum c F z_i \exp(-z_i F \psi(x)/RT) \tag{15.26}$$

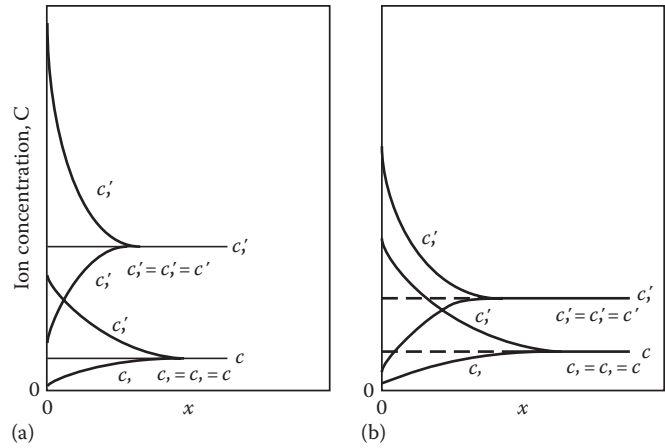


**FIGURE 15.6** Distribution of ions in the electric double layer at two electrolyte concentrations ( $c' > c$ ). (a) Constant potential surface. (b) Constant surface charge. (Adapted from van Olphen, H. 1977. An introduction to clay colloid chemistry, 2nd Ed. John Wiley & Sons, New York.)

where

- $\psi(x)$  is the inner potential at a distance  $x$  from the surface
- $\epsilon_0$  is the permittivity of free space
- $D$  is the dielectric constant of water
- $c$  is the concentration
- $R$  is the gas constant
- $T$  is the temperature (K)
- $F$  is the Faraday constant
- $z_i$  is the valence of the charged species (Sposito, 1984)

Figures 15.6 and 15.7 present the ion distribution and the electric potential distribution, respectively, in the double layer at two electrolyte concentrations. The extent of the double layer is given by the distance  $(1/\kappa)$  in units of meters:

$$\frac{1}{\kappa} = \sqrt{\frac{\epsilon_0 RT}{2000 F^2 I}} \tag{15.27}$$

where  $I$  is the ionic strength ( $=1/2 \sum c_i z_i^2$ ). Important findings of diffuse double layer theory are (1) the excess cations near the negative surface neutralize more of the charge than the anion deficit, (2) the electric potential decreases as the electrolyte concentration increases, and (3) the double layer distance  $(1/\kappa)$  decreases as the electrolyte concentration increases. Some important limitations of double layer theory are that it applies only to infinitely dilute suspensions and to low surface charge densities (Babcock, 1963).

### 15.2.2 Attractive Force

The attractive force acting on colloidal particles is called the van der Waals force and acts to bring particles closer together. The basis of the attractive force is that the fluctuating dipole of one atom polarizes another one and the two atoms attract

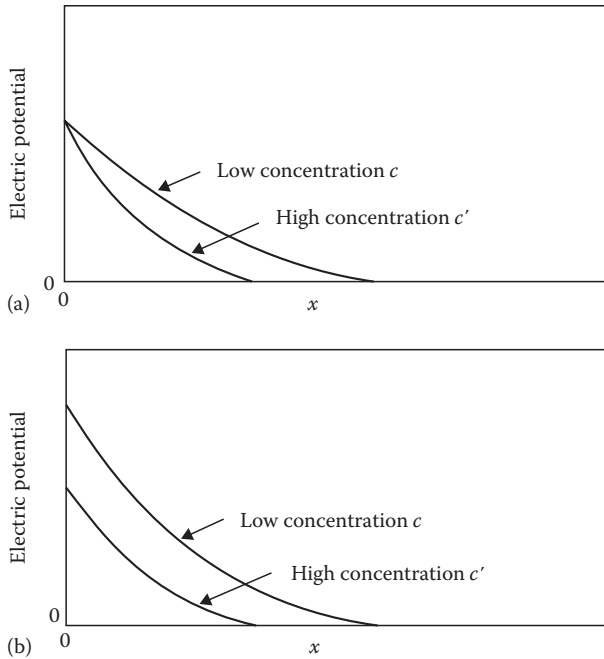


**FIGURE 15.7** Electric potential distribution in the electric double layer at two electrolyte concentrations. (a) Constant potential surface. (b) Constant surface charge. (Adapted from van Olphen, H. 1977. An introduction to clay colloid chemistry, 2nd Ed. John Wiley & Sons, New York.)

each other. This attraction between atom pairs is additive, and, therefore, the energy of interaction between particles decreases much more slowly with distance than that between individual atoms (Quirk, 1994). The interaction energy per unit area between two opposing planar solids for the van der Waals force ( $\Phi_{vdW}$ ) is (Israelachvili, 1992)

$$\Phi_{vdW} = -\frac{A_H}{12\pi d^2} \quad (15.28)$$

where

- $A_H$  is the Hamaker constant
- $d$  is the distance separating the solid surfaces

At distances  $>5$  nm, the correlations between the induced dipole distributions weaken and the interaction energy per unit area corresponds to the retarded van der Waals force ( $\Phi_{RvdW}$ ):

$$\Phi_{RvdW} = -\frac{B_{rH}}{3d^3} \quad (15.29)$$

where  $B_{rH}$  is the retarded Hamaker constant. Figure 15.8 shows values of the van der Waals force obtained experimentally between two mica surfaces. Attractive forces were observed between mica particles in the range of 0.6–2 nm in  $\text{CaCl}_2$  solution both experimentally and theoretically with statistical mechanics and Monte Carlo simulations (Kjellander et al., 1990).

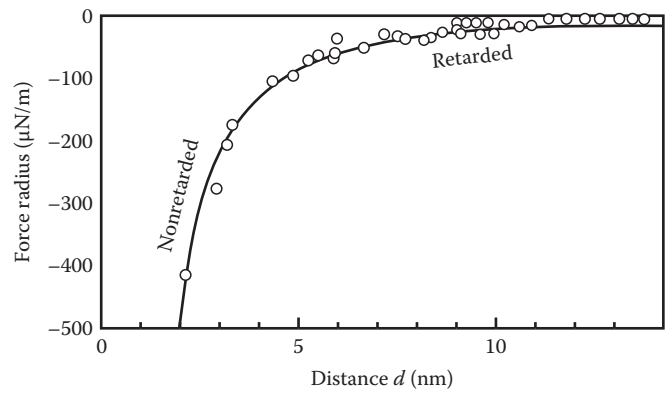


**FIGURE 15.8** van der Waals forces between two mica surfaces in aqueous electrolyte solutions. The measured Hamaker constant is  $A = 2.2 \times 10^{-20}$  J. Retarded van der Waals forces are observed above 5 nm. (Reprinted from Israelachvili, J.N. 1992. Intermolecular and surface forces, 2nd Ed. Academic Press, San Diego, CA. With permission of Academic Press Ltd.)

### 15.2.3 Repulsive Force

The electrostatic force results from the charge on the colloidal particles and acts to repel them. A force operates on charged surfaces as a result of their interacting double layers. This force is repulsive if the charges on the particles are the same. The repulsion described in terms of interaction energy per unit area ( $\Phi_R$ ) is given by the force times the distance through which it operates (Hiemenz, 1977; Sposito, 1984; Hiemenz and Rajagopalan, 1997):

$$\Phi_R = -\frac{64a^2}{z} cRT \exp(-z\kappa d) \quad (15.30)$$

where

- $a = \tanh(z\psi_0/4RT)$
- $z$  is the charge on the electrolyte ions
- $c$  is the concentration of the electrolyte ions
- $\kappa$  is the inverse double layer distance
- $d$  is half of the surface separation

This equation is valid only when the surface separation  $2d \gg 1/\kappa$  and  $a \approx 1$ . The electrostatic force between two plates for different electrolyte concentrations is presented in Figure 15.9.

When surfaces are brought closer together, an additional repulsive force becomes important. This force is called the solvation force or, when water is the medium, the hydration force. Solvation forces are of short range and oscillatory and arise whenever liquid molecules are induced to order between surfaces. Between colloid surfaces, repulsive hydration forces arise when water molecules strongly bind to hydrogen bonding surface groups such as hydrated ions or hydroxyl groups (Israelachvili, 1992). The effective range of hydration forces in clays and silicas is 3–5 nm. The interaction of mica surfaces in dilute solution obeys double layer theory, but at higher electrolyte concentration, a hydration force

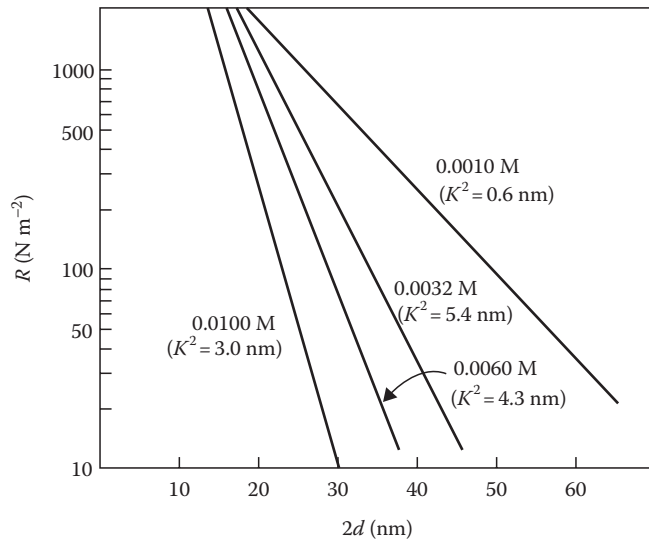


**FIGURE 15.9** Repulsive force between two plates for different concentrations of a 1:1 electrolyte where  $\kappa$  is the inverse double layer distance. (Reprinted from Hiemenz, P.C. 1977. Principles of colloid and surface chemistry. Marcel Dekker Inc., New York. With permission of Marcel Dekker, Inc.)

develops due to the energy needed to dehydrate surface-bound cations. The strength of the hydration force, which increases with the hydration number of the cation:  $\text{Mg}^{2+} > \text{Ca}^{2+} > \text{Li}^+ \approx \text{Na}^+ > \text{K}^+ > \text{Cs}^+$  (Pashley and Quirk, 1984; Israelachvili, 1992), is illustrated for two mica surfaces in Figure 15.10.

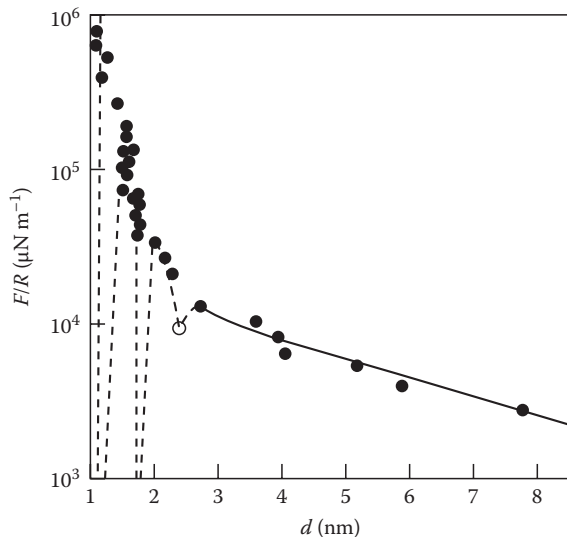


**FIGURE 15.10** Forces between two mica surfaces in 7 mmol L<sup>-1</sup> NaCl electrolyte.  $F$  is the total force scaled by the radius ( $R$ ) of the curved surfaces. At distances  $> 1.5$  nm, the forces are described by double layer theory. Hydration forces are observed at distances  $< 1.5$  nm. (Reprinted with permission from Ducker, W.A., and R.M. Pashley. 1992. Forces between mica surfaces in the presence of rod-shaped divalent counterions. *Langmuir* 8:109–112. Copyright 1992 American Chemical Society.)

Clay swelling is the result of double layer repulsion between the surfaces of individual particles. Under confining conditions, a fluid pressure or swelling pressure is created that is a direct measure of the balance of forces between particles (van Olphen, 1977). The swelling pressure is obtained by measuring the confining force that must be applied to keep the clay layers at a given distance. The swelling pressure ( $\Pi$ ) is

$$\Pi = P_{vdW} + P_R \quad (15.31)$$

where

$P_{vdW}$  is the van der Waals force

$P_R$  is the electrostatic force (Greathouse et al., 1994)

At short distances, hydration forces become significant in the swelling pressure. At greater distances, measured swelling pressures are of similar magnitude to calculated double layer repulsions (van Olphen, 1977).

Interparticle forces can be measured experimentally using the surface force apparatus (SFA), total internal reflectance microscopy, and the AFM (Israelachvili, 1992). The SFA can measure forces between surfaces at the  $10^{-10}$  m level of resolution. This apparatus has been used to measure attractive van der Waals forces, repulsive double layer forces, and repulsive hydration forces in aqueous solutions (Israelachvili, 1992). Because of its smooth surface and ease of handling, mica has been the primary solid used in SFA studies. Total internal reflection microscopy has been used to study forces between a surface and an individual colloidal particle. AFM has been used to measure both short- and long-range forces (Ducker et al., 1991; Nishimura et al., 2002b; Zhao et al., 2008). Interactions between charged mica surfaces have been investigated using a combination of SFA and AFM experiments. Results from both methods agree with theoretical predictions (Kékicheff et al., 1993).

## 15.3 Colloidal Stability

### 15.3.1 Flocculation and Dispersion

The International Union of Pure and Applied Chemistry defines flocculation as “a process of contact and adhesion whereby the particles of a dispersion form larger-size clusters,” other terms used interchangeably with flocculation are agglomeration and coagulation (IUPAC, 2009). The stability of colloidal suspensions is a balance between repulsive and attractive forces acting among the suspended particles. If net repulsive forces predominate, particles do not coagulate and remain dispersed. When the attractive forces are dominant, interacting particles coagulate and the resulting flocs settle more rapidly from the suspension than the smaller dispersed particles. Different theories in the literature attempt to describe colloid behavior (Sogami and Ise, 1984; Smalley, 1990; Ise and Smalley, 1994; McBride and Baveye, 2002). A classical continuum scale theory of the forces between particles is the DLVO theory named after Derjaguin, Landau, Verwey, and Overbeek, largely responsible

for its development (Hunter, 1987). Through the use of the SFA, it has been shown that the DLVO theory is an oversimplification of the forces acting at the mineral surface. For example, DLVO theory does not take into account short-range solvation forces (Israelachvili, 1992).

Continuum DLVO theory provides a simplified assumption of a phyllosilicate surface with permanent negative charge. Conceptually, the negative charge is developed from isomorphous substitution of lower valent cations for higher valent cations in either the tetrahedral or octahedral layers of the crystal. With regard to soils, a further complication exists in terms of mineral/organic interaction. Mounting evidence suggests that the primary reactive phases in soils are complex mineral assemblages where phyllosilicates are coated by natural organic matter and Fe-oxyhydroxide phases (Bertsch and Seaman, 1999). In this case, the theoretical models are too simplified to provide a good representation of natural colloids. Advanced computer molecular simulations must be used to begin to understand the complexities of mineral/fluid and mineral/mineral interaction, even for clean systems, for surface force behavior on the colloidal scale (Hsu, 1999). Consequently, DLVO theory, acknowledging its simplifications, will be used as a frame of reference for the discussion of flocculation dispersion.

Flocculation is a thermodynamically favorable process; however, the kinetics of coagulation determine the stability of colloidal suspensions. Generally, all colloidal suspensions will spontaneously flocculate given sufficient time, but potential energy barriers retard the rate of flocculation. These barriers are analogous to activation energies considered in chemical kinetics (Hiemenz and Rajagopalan, 1997). Particles in a primary minimum are adhesive and are not readily separated. In contrast, the dispersion/flocculation transition is the result of a secondary minimum, involves card-house type structures (Figure 15.11), and is readily reversible (Quirk, 1994).

There are many examples in the literature showing that DLVO theory can account for the observed kinetic behavior of dispersed colloidal systems (e.g., Napper and Hunter, 1974). However, this theory must be applied with caution since it treats ions exclusively as point charges ignoring their surface chemical

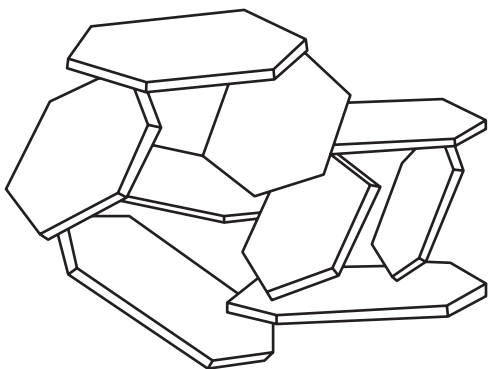


**FIGURE 15.11** Representation of card-house structure. (Reprinted from Hunter, R.J. 1987. Foundations of colloid science, Vol. 1. Oxford University Press, New York by permission of Oxford University Press.)

properties and geometry, and should only be applied to dilute systems (Sogami and Ise, 1984).

The potential barrier preventing particles from coagulating is defined by the stability ratio ( $W$ ), which is the fraction of the total number of collisions between particles that result in coagulation. The rate of coagulation in the absence of a potential barrier or rapid coagulation ( $R_f$ ) is limited only by the rate of diffusion of the particles toward one another. When the particles have a potential barrier to overcome, the rate of coagulation ( $R_s$ ) is slow and is related to  $R_f$  by

$$R_s = \frac{R_f}{W} \quad (15.32)$$

Rapid coagulation occurs when no significant repulsive forces act between particles and van der Waals or long-range coulombic attractions predominate. The quantification of the coagulation rate under these conditions was examined by von Smoluchowski (1916, 1917) and is discussed by Overbeek (1952).

Slow coagulation occurs over distances of the order of 1–100 nm when the approaching particles experience a barrier as their double layers overlap. Diffusion over this distance results from many individual Brownian events, some of which bring the particles closer together and some of which take them further apart. Since the rates of rapid and slow coagulation are directly proportional to the number of particles diffusing in the direction of a central particle ( $J$ ), it follows from Equation 15.32 that the stability ratio is given by

$$W = \frac{R_f}{R_s} = \frac{J_f}{J_s} = 2r \int_{2r}^{\infty} \exp\left(\frac{E_T}{K_B T}\right) \frac{dr}{d^2} \quad (15.33)$$

where

$r$  is the particle radius

$d \cong 2r$

Verwey and Overbeek (1948) showed that  $W$  was determined almost entirely by the value of the total potential energy ( $E_T$ ) at the maximum (Figure 15.12). In Figure 15.12  $E_R$  and  $E_A$  are the potential energies due to repulsive and attractive forces. A more complete analysis of the kinetics of colloid flocculation is presented in Hunter (1987).

Gravity removes suspended particles by sedimentation while inducing differential sedimentation coagulation, thereby decreasing Brownian coagulation rates. Ultimately, sedimentation limits the time of a flocculation series test. The test should be long enough to detect relative changes in suspended particle numbers, but not so long that all dispersed particles settle from a stable suspension (Hesterberg and Page, 1990a).

The reverse of flocculation is called dispersion. Ideally, the amount of energy required to separate two particles coagulated into a potential energy minimum is approximately equal to the difference between the interaction energy at the minimum and that at the adjacent maximum (van Olphen, 1977).

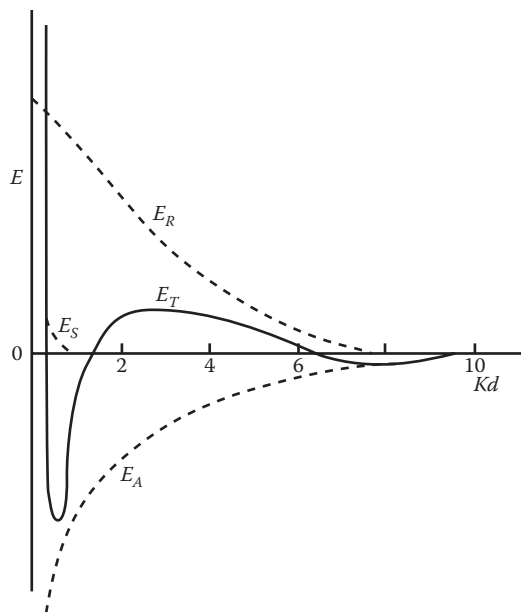


**FIGURE 15.12** Total potential energy of interaction of two colloidal particles.  $E_T = E_S + E_R + E_A$ , where  $E_S$  is the potential energy of repulsion due to the solvent layers,  $E_R$  is the potential energy due to the repulsive forces,  $E_A$  is the potential energy due to the attractive forces, and  $\kappa d$  is particle separation. (Reprinted from Hunter, R.J. 1987. Foundations of colloid science, Vol. 1. Oxford University Press, New York by permission of Oxford University Press.)

Under constant chemical conditions, separation of particles could presumably be induced by an input of kinetic energy (e.g., thermal or mechanical shear). Alternatively, changing the chemical conditions of the bulk solution surrounding coagulated particles could provide chemical and/or electrochemical energy to produce dispersion.

### 15.3.1.1 Modes of Particle Association

#### 15.3.1.1.1 Edge-Edge, Edge-Face, Face-Face

Clay crystals have a net negative surface charge as a consequence of isomorphous substitutions of electropositive ions for ions with a lower valence. This negative charge generates an ionic reorganization in the solution medium that has been described above as the diffuse double layer. Clay particles also have edge surfaces with atomic structure different from the faces. At the edge of the platelet, the tetrahedral layer of Si and the octahedral layer of Al exhibit broken bonds, which, in turn, generate another electric double layer.

Double layer theory assumes that the surfaces of the clay minerals are of semi-infinite spatial extent and show no edge effects, a simplification that is not always satisfactory. Clay mineral particles have finite dimensions. Below the p.z.c., edge surfaces carry a positive charge due to specific adsorption of protons. Using the Poisson-Boltzmann equation, Secor and Radke (1985) calculated the effect of edge-face corners on the electrical potential distribution around an idealized, symmetrical montmorillonite disk. Spillover of the negative electrical potential from the particle faces into the edge region can result in a negative potential everywhere around the particle.

The electrical potential at the edge surface strongly depends on the electrolyte concentration and the ratio of the face to edge charge density. The extent of spillover also is a weak function of the particle shape (Secor and Radke, 1985). This study implies that attraction between positively charged edges and negatively charged faces of phyllosilicate mineral particles will depend on the extent of the edge protonation, electrolyte concentration, and shape of the particle. A phyllosilicate structure that is collapsed in the  $c$ -dimension, such as mica, should be able to acquire a larger edge surface charge density than a layer silicate like smectite where structural expansion increases the distance between edge surface aluminol groups (Hesterberg, 1988).

When there is a reduction in the thickness of the double layer, particles can associate among themselves in three different ways: face-face, face-edge, or edge-edge. Face-face association is also called parallel aggregation and does not produce flocs, while the other two associations do produce three-dimensional structures called card houses (see Figure 15.11).

In concentrated suspensions of clay, the edge-edge and edge-face associations form a continuum, with chains of particles in the card-house structures mentioned above. The rigidity of the gel depends on the number and strength of the bonds in the continuum structure. Some attempts to characterize the gel structure using freeze-drying techniques have been made (Norrish and Rausell-Colom, 1961). When the water is eliminated from the suspension, the volume of the system does not change and the final product is a dry clay structure with some strength that has been called aerogel (van Olphen, 1977).

#### 15.3.1.1.2 Domains and Quasicrystals

Some colloidal systems may, under certain circumstances, show a reversible clustering among particles. The earliest reported example is the Fe-hydroxide sol described by Cotton and Mouton (1907). The term tactoid was first used by Freundlich (1932) and was more precisely defined by Overbeek (1952) as the association of particles at a certain distance affected by electrolyte concentration and pH. Quirk and Aylmore (1971) proposed the term quasicrystal to describe the regions of parallel alignment of individual aluminosilicate lamellae in montmorillonite and the term domain to describe the regions of parallel alignment of crystals for illite. This terminology is adopted in the present chapter.

The distribution model of adsorbed ions in mixed mono- and divalent systems for smectite quasicrystals was described by Shainberg and Otoh (1968) and Bar-on et al. (1970). According to this theory, called the ion demixing model, when Na is added to Ca saturated montmorillonite, most of the adsorbed Na will concentrate on the external surfaces of the quasicrystals until 10% of the adsorbed Ca has been replaced by Na. Initially, the size and shape of the particles are not altered by the addition of adsorbed Na. As further Na is added to the system, Na penetrates into the quasicrystals and brings about disintegration of the clay packets (Bar-on et al., 1970).

Lebron and Suarez (1992a) used electrophoretic mobility experiments to show that the demixing model can be applied to micaceous clays. The electrophoretic mobility of micaceous



**TABLE 15.5** Critical Coagulation Concentrations of Phyllosilicates under Various Conditions

Mineral	CCC (mol <sub>c</sub> L <sup>-1</sup> )	Background Electrolyte	pH	Solids Concentration (g kg <sup>-1</sup> )
Kaolinite-4	2–40	NaNO <sub>3</sub>	4–10	0.025
Kaolinite-9	8, 30	NaHCO <sub>3</sub> , Na <sub>2</sub> CO <sub>3</sub>	8.3, 9.5	0.6–0.9
Kaolinite (Georgia)	5, 245, 75	NaCl, NaHCO <sub>3</sub> , Na <sub>2</sub> CO <sub>3</sub>	7, 8.3, 9.5	0.6–0.9
Kaolinite (KGa-1)	<0.19–54.6	NaCl	5.8–9.1	0.67
Kaolinite-4	0.1–0.3	Ca(NO <sub>3</sub> ) <sub>2</sub>	4–10	0.025
Kaolinite (KGa-1)	<0.19–0.85	CaCl <sub>2</sub>	5.5–9.3	0.67
Montmorillonite-23	1–10	NaNO <sub>3</sub>	3.8–10	0.25
Montmorillonite-23	20, 48, 68	NaCl, NaHCO <sub>3</sub> , Na <sub>2</sub> CO <sub>3</sub>	7, 8.3, 9.5	0.6–0.9
Montmorillonite-27	14, 47, 17	NaCl, NaHCO <sub>3</sub> , Na <sub>2</sub> CO <sub>3</sub>	7, 8.3, 9.5	0.6–0.9
Montmorillonite (SAZ-1)	14–28	NaCl	6.4–9.4	0.67
Montmorillonite (SAZ-1)	1.09, 1.56	CaCl <sub>2</sub>	6.1, 7.6	0.67
Montmorillonite (SAZ-1)	0.93, 2.02, 0.88	MgCl <sub>2</sub>	6.1, 8.4, 9.0	0.67
Vermiculite	38, 58, 30	NaCl, NaHCO <sub>3</sub> , Na <sub>2</sub> CO <sub>3</sub>	7, 8.3, 9.5	0.6–0.9
Illite-36	9, 185, 95	NaCl, NaHCO <sub>3</sub> , Na <sub>2</sub> CO <sub>3</sub>	7, 8.3, 9.5	0.6–0.9
Illite (Grundy)	7.24	NaCl	–6	1
Illite (Grundy)	0.2	CaCl <sub>2</sub>	–6	1

Source: Adapted from Hesterberg, D.L. 1988. Critical coagulation concentrations and rheological properties of illite. Ph.D. Thesis. University of California, Riverside, CA by Oxford University Press.

domains increased when the sodium adsorption ratio (SAR) increased from 5 to approximately 10.

### 15.3.1.2 Critical Coagulation Concentration

The CCC, sometimes called the critical flocculation concentration (CFC), is the minimum concentration of indifferent electrolyte that induces rapid coagulation. The CCC is strongly dependent on counterion valence (Table 15.5). This observation is known as the Schulze–Hardy rule. An estimate of the CCC (mol L<sup>-1</sup>) is given by (Hunter, 1987)

$$CCC = \frac{0.107\epsilon^3(k_B T)^5 Z^4}{N_A A_H^2 (ze)^6} \quad (15.34)$$

where

$$Z = \tanh(ze\psi_0/4k_B T)$$

$N_A$  is Avogadro's number

$A_H$  is the Hamaker constant

$\epsilon$  is the relative dielectric constant

$k_B$  is the Boltzmann constant

$e$  is the proton charge

The variation of CCC with counterion valence depends approximately on the inverse sixth power of  $z$ . At 25°C in water, using the experimental observation that coagulation usually occurs between low-potential surfaces, the result is

$$CCC \propto \frac{\psi_0^4}{z^2} \quad (15.35)$$

where now the CCC depends on the inverse of the square of the valence. However, the CCC calculated with Equation 15.35

agrees well with experimental results if  $\psi_0 \propto 1/z$ . When calculating the CCC in soils, one must consider that soils consist of mixtures of permanent and variable charge minerals. The net surface charge, and consequently, the electrical potential around the mixture of particles are dependent upon variables such as pH, specifically adsorbed ions, ionic strength, and mineralogy. A more detailed evaluation of the effect of these variables on the stability of colloids is presented below.

## 15.3.2 Factors Affecting Colloidal Stability

### 15.3.2.1 Solution Composition

The magnitude of the repulsion barrier is determined by the nature of the material adsorbed on the particle surface. In the case of a charged colloid, repulsion depends on the magnitude of the surface charge and on the extent of the electrical double layer, which, in turn, depends on the total electrolyte concentration. It is necessary here to distinguish between the concentration of the potential determining ions and that of other ions that have no direct interaction with the surface. If the surface potential of the particles is determined by the concentration of potential determining ions, the magnitude of this potential is not affected by the addition of an indifferent electrolyte. For this type of double layer, when salt concentration increases, the double layer thickness decreases, the surface charge of the particles increases, and the surface potential remains constant (Figure 15.7a).

If the surface charge of the particle is determined by isomorphic substitution, the surface charge does not change with increasing electrolyte concentration. The diffuse double layer compresses, but in this case, the surface potential decreases with increasing electrolyte concentration (Figure 15.7b) (van Olphen, 1977).

### 15.3.2.2 Exchange Complex Composition

As explained above, clay particles are surrounded by cations as a consequence of the net negative electrical charge on the surface. Cations bonded to the surface can be exchanged for other cations in solution. Consequently, the cations on the exchange complex are dependent on the solution composition.

There is an equilibrium between the cations on the exchange complex and the cations in the solution. Not all cations are adsorbed with the same affinity. Cations with larger hydrated radii are less strongly adsorbed than those with smaller hydrated radii. In solutions with equal initial concentration of different cations, the amounts of Ca and Mg adsorbed are several times greater than the amount of Na adsorbed. In general, polyvalent cations are adsorbed more strongly than monovalent cations and are not easily displaced by other cations. The order of adsorption strength is  $Al > Ca > Mg > H > K > Na$  (Duchaufour, 1970).

The flocculation/dispersion behavior of soil colloids depends on salt concentration, exchange complex cation, cation valence, and dominant clay mineralogy. In general, divalent cations are more effective in flocculating colloids than monovalent cations. For example, Quirk and Schofield (1955) found that the flocculating power of  $CaCl_2$  is 50–100 times higher than that of NaCl. For monovalent cations, there is also a difference, with KCl showing greater flocculation power than NaCl (Pashley, 1981).

### 15.3.2.3 pH

The pH is an important determinant of the electrical potential of the clay surface. Changes in pH affect the edge charge on clays and the surface charge of variable charge minerals such as Fe and Al oxides. There is considerable variability depending on structural composition and degree of crystallinity, but Fe and Al oxides generally undergo a surface charge reversal around pH 7–9 (positively charged below that pH and negatively charged above). This is also the region in which kaolinite exhibits its edge charge reversal as evidenced by  $Cl^-$  adsorption studies (Schofield and Samson, 1954). Soil colloids consist of a mixture of minerals, each with a different p.z.c. At low pH, edge to face bonding, as well as bonding of positive Fe and Al oxides to negative clay surfaces, is expected to occur (van Olphen, 1977; Kretschmar et al., 1993, 1997). This type of bonding should hinder dispersion and should thus result in flocculation. With increasing pH, as the p.z.c. is approached, edge to face clay bonding decreases and Fe and Al oxide bonding to clays is also expected to decrease (Suarez et al., 1984). In variable charge systems, flocculation is at a maximum at the p.z.c.

CCC increased at high SAR values with increasing pH for three soil clays whose clay mineralogy was dominantly kaolinite, montmorillonite, or illite (Goldberg and Forster, 1990). Hesterberg and Page (1990b) also found an increase in CCC for a Na- and a K-illite with increasing pH. Similar results were found for illite and three micaceous soil clays when  $SAR > 15$  (Lebron and Suarez, 1992a, 1992b). The electrophoretic mobility of these materials increased when the SAR was greater than 20 and the pH was above the p.z.c. No pH effect was observed at  $SAR < 15$  for either mobility or CCC.

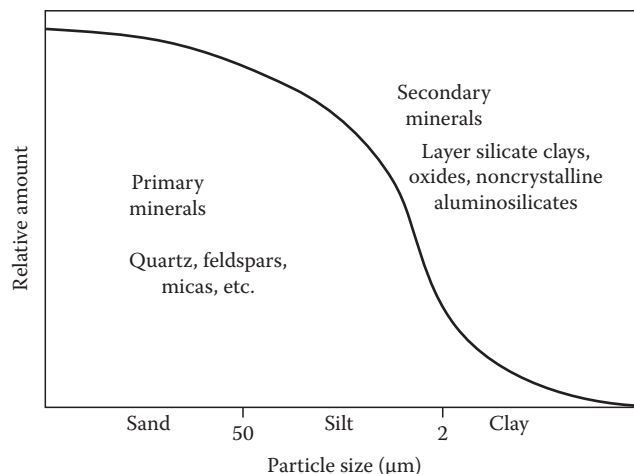


**FIGURE 15.13** Typical abundance of primary and secondary minerals in different size fractions of the soil. (Reprinted from McBride, M.B. 1994. *Environmental chemistry of soils*. Oxford University Press, New York by permission of Oxford University Press.)

### 15.3.2.4 Mineralogy

The colloidal fraction of a soil consists primarily of secondary minerals (Figure 15.13). Layer silicate minerals differ in chemical composition and charge characteristics leading to different physicochemical behavior (Table 15.5). The stoichiometry of each mineral varies due to isomorphic substitutions in the crystal lattice during the formation or evolution of the mineral structure.

The siloxane (Si–O–Si) surfaces of 2:1 layer silicates without structural charge are hydrophobic. Therefore, the surface oxygens coordinated to Si show little tendency to hydrogen bond with water molecules. Smectites, such as montmorillonite, form weak hydrogen bonds between structural charge located mainly in the octahedral sheet and water. Such bonds are the result of the delocalization of some structural charge into the surface oxygens (Farmer, 1978). Smectites, such as beidellite, with a high proportion of charge in the tetrahedral sheet, form stronger hydrogen bonds. The siloxane surfaces of vermiculite are the most hydrophilic of the 2:1 layer silicate clays because they possess a large tetrahedral charge partially distributed onto surface oxygens (Farmer, 1978). Tetrahedral charge is much more localized on fewer surface oxygens than octahedral charge, explaining the stronger hydrogen bonding of adsorbed water on vermiculite (McBride, 1989). An extensive study of the structural characteristics of soil minerals can be found in Dixon and Weed (1989).

An example of how these mineral differences affect the flocculation/dispersion behavior of soil colloids is shown in Table 15.5. An overview of the data reveals that reported CCC values of kaolinite, montmorillonite, vermiculite, and illite are quite variable within and between these mineral groups.

Many of the differences in Table 15.5 are due to differences in methodology in the determination of CCC and/or differences in the stoichiometry of the silicate minerals. However, these factors do not account for all of the variability. Lebron and Suarez

(1992a) found substantial differences in CCC within samples from the same soil type. Differences in content of organic matter and other minerals can drastically change the behavior of soil colloids. Consequently, general guidelines for reclamation of agricultural land or the use of amendments to maintain colloids in a flocculated state must be implemented with caution because soils usually require higher electrolyte concentrations than the corresponding pure clay minerals to maintain a flocculated condition.

### 15.3.2.5 Organic Matter

Organic matter constitutes a small portion of the soil mass (0.5%–10%) but is intimately associated with inorganic particles and plays an important role in the improvement of soil structure (Nelson and Oades, 1998). Aeration, water-holding capacity, and permeability increase with increasing soil SOM content. However, adsorbed organic matter can promote dispersion of soil particles. Organic coatings, under certain conditions, maintain a dispersed state for soil colloids in suspension through a combination of electrostatic and steric mechanisms (Stevenson, 1982). Table 15.6 shows the spatial extensions for nonionic polymer molecules of different molecular weights. Like electrical double layers, macromolecules of at least a few thousand molecular weight also extend in space over distances comparable to, or greater than, the van der Waals attraction. In general, it has been shown that organic matter coatings modify the surface properties of minerals, increasing their CEC, generating hydrophobic and hydrophilic surfaces (Hunter, 1987), and significantly altering the point of zero net charge (p.z.n.c., pH at which the CEC and AEC are equal) (Heil and Sposito, 1993; Kaplan et al., 1997; Kretzschmar et al., 1997; Bertsch and Seaman, 1999).

Goldberg and Forster (1990) and Kretzschmar et al. (1993) found that the removal of SOM enhanced soil flocculation (decreased the CCC). Similarly, addition of small amounts of organic material substantially increased dispersion of Na-saturated soil or clay in the order: humic acid > soil polysaccharide  $\geq$  anionic polysaccharide (Gu and Doner, 1993; Kretzschmar et al., 1997). Using smectite, kaolinite, and three soils whose clay fractions were dominated by one of these minerals, Frenkel et al. (1992) showed that the CCC values of Na-soils were much higher, and much more affected by organic matter than those of Ca-soils.

**TABLE 15.6** Spatial Extensions of Electrical Double Layers and Polymers of Different Molecular Weight

1:1 Electrolyte Concentration (mol L <sup>-1</sup> )	Double-Layer Thickness, 1/ $\kappa$ (nm)	Polymer Molecular Weight	Spatial Extension (nm)
10 <sup>-5</sup>	100	1,000,000	60
10 <sup>-4</sup>	30	100,000	20
10 <sup>-3</sup>	10	10,000	6
10 <sup>-2</sup>	3	1000	2
10 <sup>-1</sup>	1		

Source: Reprinted from Hunter, R.J., *Foundations of Colloid Science*, Vol. 1, 1987 by permission of Oxford University Press.

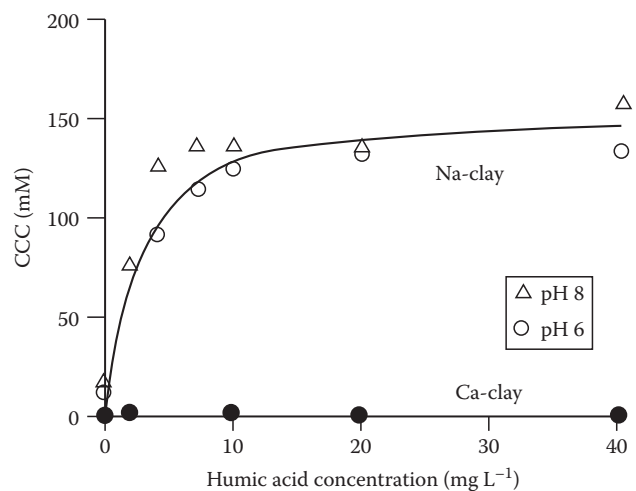


**FIGURE 15.14** Effect of the humic acid concentration on the CCC of a Na-clay and a Ca-clay. (After Tarchitzky, J., Y. Chen, and A. Banin. 1993. Humic substances and pH effects on sodium and calcium-montmorillonite flocculation and dispersion. *Soil Sci. Soc. Am. J.* 57:367–372.)

Tarchitzky et al. (1993) showed similar comparisons between Na- and Ca-montmorillonite suspensions with varying additions of humic and fulvic acids (Figure 15.14). The effect of organic matter on stability of soil colloids is a function of its size. Large organic materials such as polysaccharides and hyphae act to bind colloid particles together. Small organic molecules such as fulvic acid and organic acids increase dispersion of soil colloids through their effect on particle charge. A more detailed review of organic matter chemistry and its effect on soils is provided in Stevenson (1982) and Nelson and Oades (1998).

## 15.3.3 Measurement of Colloidal Stability

### 15.3.3.1 Flocculation Series Test

CCC are commonly determined using the flocculation series test. The experiment can be performed by taking a series of test tubes containing the same concentration of the colloid and adding varying amounts of the coagulating electrolyte. The tubes are then shaken and allowed to stand for a given time. If the electrolyte range has been properly chosen, the CCC is defined as the concentration above which the settling material leaves behind a perfectly clear supernatant solution. Below the CCC, the supernatant retains some of the uncoagulated colloid. The concentration of colloidal particles at which the flocculation test must be performed should not exceed 10 g L<sup>-1</sup>, thus avoiding interferences from different particle interactions such as gel formation.

### 15.3.3.2 Dispersion Indices

There are several methods (qualitative, semiquantitative, and quantitative) to determine the dispersion or flocculation status of soil colloids. Qualitative analyses of the dispersion state are those based on direct observation of small particles when the soil is immersed in water. This observation can be made with the optical microscope or with the naked eye, as is the case for

the test of Emerson (1967). Methods based on turbidity of a suspension of dispersed soil can be considered semiquantitative when comparative measurements are made. Normally, a standard curve is constructed using known amounts of dispersed clay. The soil under evaluation is assigned a dispersion value by comparison with the standard. The most commonly used quantitative method to determine soil flocculation state is the dispersion index. This index is the ratio of the amount of soil colloids in water to the amount of soil colloids in solution when the soil has been treated with a dispersant. This procedure is recommended by the Soil Conservation Service (Sherard et al., 1977). Different variations regarding particle size, dispersing agent, and manipulation of samples are found in the methods proposed by El-Swaify et al. (1970) and Dong et al. (1983), among others.

### 15.3.3.3 Bingham Yield Stress

Rheology is the study of the flow and deformation of colloidal systems under the influence of mechanical forces (van Olphen, 1977). A Newtonian liquid when confined between two parallel plates moves at a constant shear rate ( $\dot{\gamma}$ ) proportional to the applied shear stress ( $\tau$ ):

$$\tau = \eta \dot{\gamma} \quad (15.36)$$

Non-Newtonian fluids obey different relations between shear stress and shear rate. Plastic flow is flow that occurs only above a certain finite stress ( $\tau_0$ ) called the yield stress. Ideal plastic flow exhibits a linear relationship between shear rate and shear stress over all rates of shear. Many colloidal dispersions exhibit Bingham flow, which is characterized by the equation

$$\tau = \tau_B + \eta_{\Delta} \dot{\gamma} \quad (15.37)$$

where

$\tau_B$  is the Bingham yield stress found by extrapolating Equation 15.37 to zero shear rate

$\eta_{\Delta}$  is the differential or plastic viscosity

The differential viscosity is the derivative of shear stress with respect to shear rate at a given shear rate (van Olphen, 1977). Shear rate versus shear stress relationships for Newtonian flow, ideal plastic flow, and Bingham flow are presented in Figure 15.15.

Bingham yield stress is a measure of the degree of coagulation of a colloidal suspension and the mode of particle interaction. Bingham yield stress is a function of both the number of particle-particle linkages in the coagulated structure and the energy required to break these linkages (Rand and Melton, 1977). A stable clay dispersion exhibits ideal plastic flow, while flocculated suspensions exhibit Bingham flow as can be seen in Figure 15.16 for kaolinite. Differential viscosity can also be used to assess the extent of particle flocculation, but it is a much less sensitive parameter than Bingham yield stress (Heath and Tadros, 1983).

Rheological studies have been carried out on kaolinite (Flegman et al., 1969; Rand and Melton, 1977; Yong et al., 1979; Diz and Rand, 1989; Ma and Pierre, 1999), illite (Yong et al., 1979;

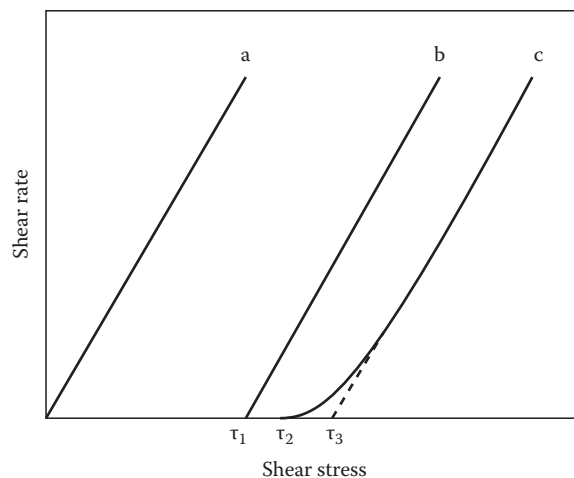


FIGURE 15.15 Shear rate versus shear stress relationships. Curve a represents Newtonian flow, curve b represents ideal plastic flow, and curve c represents Bingham flow. (Adapted from van Olphen, H. 1977. An introduction to clay colloid chemistry, 2nd Ed. John Wiley & Sons, New York.)

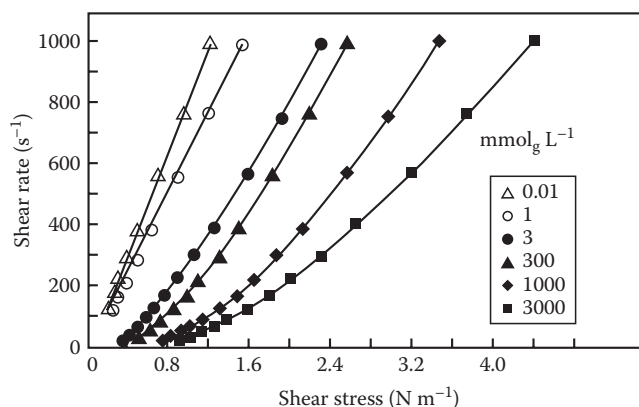


FIGURE 15.16 Shear rate versus shear stress for Na-kaolinite. The open symbols represent dispersed systems and ideal plastic flow. The closed symbols represent coagulated systems and Bingham flow. (Adapted from Yong, R.N., A.J. Sadh, H.P. Ludwig, and M.A. Jorgensen. 1979. Interparticle action and rheology of dispersive clays. *J. Geotech. Eng. Div.* 105:1193–1209.)

Ohtsubo et al., 1991; Hesterberg and Page, 1993), montmorillonite (Rand et al., 1980; Heath and Tadros, 1983; Keren, 1988, 1989a; Tombácz et al., 1989; Miano and Rabaioli, 1994; Benna et al., 1999; Duran et al., 2000), laponite (Laxton and Berg, 2006), clay mixtures (Yong et al., 1979; Keren, 1989b, 1991), soil clays (Zhao et al., 1991), and soils (Ghezzehei and Or, 2001; Markgraf et al., 2006). A series of curves of Bingham yield stress as a function of pH obtained at successively increasing electrolyte concentration should coincide at one point. This point is characteristic of the pH value of the edge p.z.c. of the mineral (Rand and Melton, 1977). Edge p.z.c. values have been determined in this manner for various kaolinites and range in value from pH 5.6 to 8.8 (Diz and Rand, 1989). Kaolinite particles occur in edge-face associations below the edge p.z.c. and in edge-edge associations around the edge p.z.c. (Rand and Melton, 1977).

Montmorillonite exhibits no edge–face associations over the pH range 4–11; coagulation produced by electrolyte additions is initially the result of edge–edge interactions with face–face interactions occurring at high-electrolyte concentrations (Rand et al., 1980). No edge p.z.c. could be determined on montmorillonite using this method. This is likely because the edge area is small and attraction between edges and faces is small compared to repulsion between faces (Rand et al., 1980). From yield stress and electrophoretic mobility measurements determined without electrolyte addition, Benna et al. (1999) suggested that the p.z.c. of three bentonites occurred in the pH range of 7.5–8.5.

In distilled water, Ca-montmorillonite exhibited Newtonian flow. With increasing exchangeable sodium percentage (ESP), differential viscosity, deviation from Newtonian flow, and Bingham yield stress of montmorillonite all increased (Keren, 1988). These increases are likely due to the increased number of particles in solution as tactoids break down. Differential viscosity and Bingham yield stress decreased with increasing electrostatic charge density of smectites (Keren, 1989a). This result is attributed to the reduced swelling of higher charge density smectites. Kaolinite exhibited Newtonian flow at all ESPs. The introduction of even 5% montmorillonite into the kaolinite systems resulted in deviations from Newtonian flow and increased differential viscosity (Keren, 1989b). Bingham yield stress and deviations from Newtonian flow of kaolinite–montmorillonite mixtures also increased with ESP (Keren, 1991). Bingham yield stress of kaolinite, Ca-montmorillonite, Na-montmorillonite, and two soils increased exponentially with decreasing water content (Ghezzehei and Or, 2001).

## 15.4 Colloid Transport

As previously discussed, colloidal materials found in soils include phyllosilicate clays, Al, Fe, and other metal oxides, carbonate minerals, microorganisms, and other biological debris, much of which falls into the “nanoparticle” size range (see Section 15.1.2). The fundamental processes involved in colloid migration in the soil environment include mobilization, transport, and deposition, representing primarily a balance between the two opposing processes of colloid mobilization and deposition. The study of colloid transport in the subsurface environment has received considerable attention in recent years because of concern that mobile colloids may enhance the mobility of strongly sorbing contaminants (i.e., facilitated transport) and alter the hydraulic properties of soil and aquifer materials. In addition, the migration of biocolloids such as bacteria and viruses has important implications to in situ bioremediation, the protection of drinking water supplies, and the spread of disease (Khilar and Fogler, 1984; McDowell-Boyer et al., 1986; Kia et al., 1987; Ryan and Elimelech, 1996; Kretzschmar et al., 1999; de Jonge et al., 2004b; McCarthy and McKay, 2004; Tufenkji, 2007). However, our ability to predict colloid movement and deposition is often confounded by the complexities of surface interactions in such heterogeneous natural systems. Understanding colloid

transport requires consideration not only of the chemical and biological processes and reactions but also of the physical principles of filtration and deposition in porous media.

Several mechanisms have been identified by which colloidal materials can be mobilized in the soil environment (Figure 15.17) including clay dispersion resulting from changes in pore-water chemistry that increase electrostatic repulsion between the colloid and collector surfaces, water film expansion and air–water interface scouring during episodic wetting events (imbibition), raindrop impact at the soil surface, and increased shear forces associated with transient hydrodynamic events (i.e., precipitation, groundwater pumping, subsurface recharge injection). Mobile colloids can also be formed in situ through precipitation reactions resulting from changes in pore-water chemistry. Clearly, colloid mobilization is associated with a physical and/or chemical perturbation sufficient to overcome the energy barrier limiting particle detachment (McCarthy and Degueldre, 1993; Ryan and Elimelech, 1996; DeNovio et al., 2004).

Compared to saturated aquifer systems, chemical and physical perturbations are common within the soil environment, with the presence of air providing an additional system interface for colloid partitioning (Wan and Wilson, 1994; Sirivithayapakorn and Keller, 2003). The presence of a dynamic air–water interface and fluctuating chemical and hydrological conditions complicate our understanding of colloid transport processes in the soil and vadose environments (Bradford and Torkzaban, 2008). Preferential flow paths can increase the mobility of colloidal material in close proximity to the pathway, while limiting the reactivity of colloidal sorbents isolated from the flow path (DeNovio et al., 2004; McCarthy and McKay, 2004).

The energy barrier limiting colloid detachment is the difference between the interaction minimum and the maximum energy potential described in Figure 15.12. In terms of chemical perturbations, soil colloid mobilization can result from changes in pore-water pH, ionic strength, and/or  $\text{Na}^+/\text{Ca}^{2+}$  ratios (McDowell-Boyer, 1992; Ryan and Gschwend, 1994; Gamedainger and Kaplan, 2001; Bunn et al., 2002; Khaleel et al., 2002; McCarthy et al., 2002; Grolimund and Borkovec, 2006), alteration of surface charge resulting from a chemical dispersing agent or dissolved organic matter (Ryan and Gschwend, 1994; Seaman and Bertsch, 2000; Johnson et al., 2001), or dissolution of carbonate or Fe cementing agents resulting in the release and transport of silicate clays (Gschwend et al., 1990; Ryan and Gschwend, 1990; Ronen et al., 1992; Swartz and Gschwend, 1998). Furthermore, potentially mobile colloids may precipitate in situ due to altered chemical gradients (Gschwend and Reynolds, 1987; Mashal et al., 2004). In many instances, more than one of the mechanisms may be operative in order to trigger significant colloid mobilization, such as a change in pore-water chemistry that reduces particle attraction combined with an increase in pore-water velocity and shear forces.

Under ideal laminar flow conditions, the hydrodynamic shear force acting on a spherical particle attached to a flat surface can be expressed as follows:

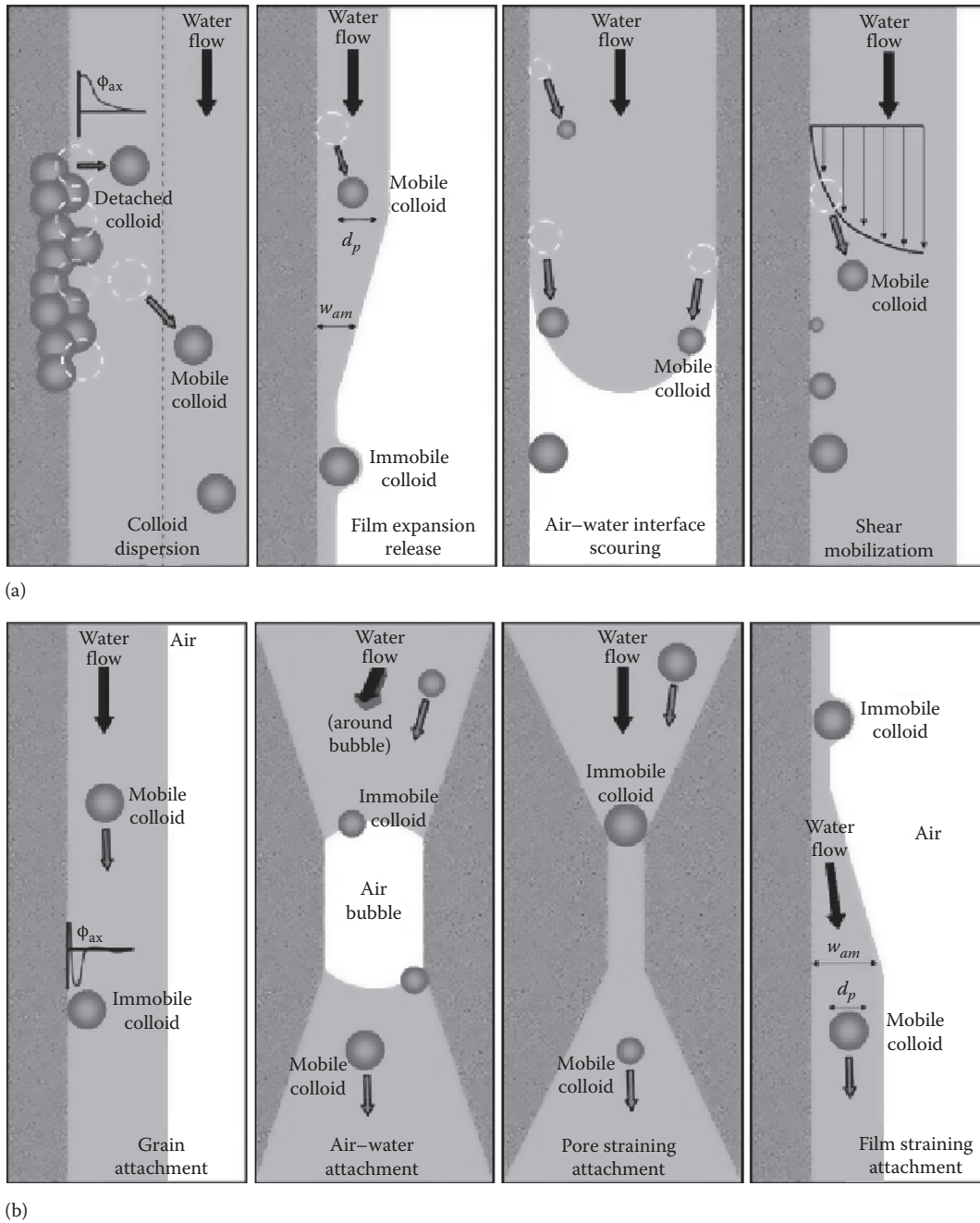


**FIGURE 15.17** Colloid mobilization (a) mechanisms include dispersion due to chemical perturbation, expansion of water film during imbibition, air–water interface scouring and shear mobilization. Colloid deposition (b) mechanisms include attachment associated with physicochemical filtration, attachment to the air–water interface, physical pore straining, and water film straining. (Adapted from DeNovio, N.M., J.E. Saiers, and J.N. Ryan. 2004. Colloid movement in unsaturated porous media: Recent advances and future directions. *Vadose Zone J.* 3:338–351.)

$$F_{shear} = (1.7)6\pi\mu rV \quad (15.38)$$

where

$V$  is the flow velocity at the center of the particle

$\mu$  is the fluid viscosity

$r$  is the particle radius (Sharma et al., 1992; Ryan and Elimelech, 1996; Ryan et al., 1998; DeNovio et al., 2004)

Adhesive forces that oppose shear stress are subject to changes in solution chemistry. The critical velocity for particle release decreases with increasing particle size, even though the required hydrodynamic force increases for non-Brownian particles, that is,  $>1 \mu\text{m}$  in diameter (Sharma et al., 1992). As one might expect, the amount of particles mobilized should generally increase with increasing flow velocity, but greater flow velocities are required to mobilize smaller particles that extend to a lesser degree into

the advective stream. However, many assumptions inherent in applying such a physical approach to soil and aquifer systems are likely in question. In more realistic systems, interrelated factors such as contact area, adhesion strength, and surface charge heterogeneity are important in countering shear forces (Sharma et al., 1992).

In addition to the chemical factors affecting colloid stability, transport of colloids is related to soil physical factors such as pore size distribution, geometry, and continuity (Torkzaban et al., 2008; Bradford et al., 2009). Coarse-textured soils have a larger distribution of pore sizes (with larger pores) than fine-textured soils, suggesting greater potential for colloid movement. This is not generalizable since some fine-textured materials experience cracking and formation of continuous structural macropores that provide a preferential pathway for colloid transport.

### 15.4.1 Colloid Transport Modeling

Physical and chemical processes affect the transport of soil colloids. Colloid transport can be represented by the physical processes of molecular diffusion (Brownian movement), advective flow, and gravitational forces. Molecular diffusion, the random motion of particles caused by thermal effects, is related to temperature and viscosity. Deposition is the process whereby moving particles are attached to stationary surfaces based on the balance of attractive and repulsive forces, that is, attractive van der Waals forces and the combined influence of attractive and repulsive electrostatic forces, as described by DLVO theory of colloid stability (see Sections 15.2.2, 15.2.3, and 15.3.1).

The attachment process involves two steps: transport to the collector surface and attachment that binds the two surfaces together. The transport step reflects a combination of diffusion, convection, and gravity, with electrostatic and van der Waals forces controlling colloid binding. Models used in describing colloid transport are typically extensions of the advection dispersion equation (ADE) for describing solute movement in a homogeneous saturated porous medium:

$$\frac{\partial C}{\partial t} + \frac{\rho_b}{\theta} \frac{\partial S}{\partial t} = D \frac{\partial^2 C}{\partial x^2} - v \frac{\partial C}{\partial x} \quad (15.39)$$

where

- $C$  is the aqueous phase concentration for the solute or suspended colloidal material of interest
- $x$  is distance
- $t$  is time
- $D$  is the hydrodynamic dispersion coefficient
- $v$  is the pore-water velocity
- $S$  is the sorbed concentration of colloids or solutes
- $\rho_b$  is the matrix bulk density
- $\theta$  is the volumetric water content (Grolimund and Borkovec, 2001; Bradford et al., 2003; Tufenkji, 2007)

Hydrodynamic dispersion and dispersivity appear to decrease with increasing particle size (Sinton et al., 2000; Auset and Keller, 2004). As the colloidal material moves through porous medium, it may be removed from solution by various physico-chemical filtration processes, with various expressions, such as the equilibrium partitioning ( $K_{eq}$ ), used to describe reversible colloid attachment processes in a manner analogous to the equilibrium partitioning of solutes. Using a numerical solution to the ADE, equilibrium partitioning can be modified to reflect any one of a variety of phenomenological equilibrium partitioning expressions, that is, Freundlich, Langmuir, etc.

In contrast to equilibrium partitioning, colloid attachment is more often viewed as a kinetically controlled process with terms accounting for both attachment ( $k_{att}$ ) and detachment ( $k_{det}$ ) rates:

$$\frac{\rho_b}{\theta} \frac{\partial S}{\partial t} = k_{att} C - \frac{\rho_b}{\theta} k_{det} S \quad (15.40)$$

yielding an expression that is mathematically equivalent to the reversible first-order kinetic equation for partitioning solutes. Ripening and blocking are terms that are used to describe an increase or decrease in colloid attachment efficiency (i.e.,  $k_{att}$  and  $k_{det}$ ) with time or distance.

Figure 15.18 illustrates colloid breakthrough behavior for irreversible (Figure 15.18a) and reversible (Figure 15.18b) attachment kinetics. Colloid attachment is commonly assumed to be irreversible (i.e.,  $k_{det} = 0$ ) as described by clean-bed colloid filtration theory (CFT) (O'Melia and Tiller, 1993; Bradford et al., 2003; Simunek et al., 2006; Tufenkji, 2007). For irreversible attachment (i.e., CFT), the kinetic rate coefficient determines the plateau level of colloid breakthrough, while more complex breakthrough behavior is observed when both attachment and detachment occur at differing rates. When  $k_{att} = k_{det}$ , colloid behavior becomes analogous to that of a conservative tracer, that is,  $R = 1$ . Colloid retention profiles for irreversible attachment (Figure 15.18c) remain unchanged after the inlet colloid source is removed and an exponential decrease in retained colloids is observed with transport distance. Again, a more complex colloid retention profile is observed for reversible attachment that depends on both the forward and reverse rate coefficients and the treatment duration (Figure 15.18d).

The irreversible colloid attachment/depositional rate constant for a clean-bed filter is

$$k_{att} = \frac{3(1-\theta)v}{2d_c} \eta_0 \alpha \quad (15.41)$$

where

- $d_c$  is the average grain size of the matrix
- $\eta_0$  is the collector contact efficiency for the three transport mechanisms (diffusion, gravity, convection)
- $\alpha$  is the attachment efficiency (Yao et al., 1971; Bradford et al., 2003; Li et al., 2004)

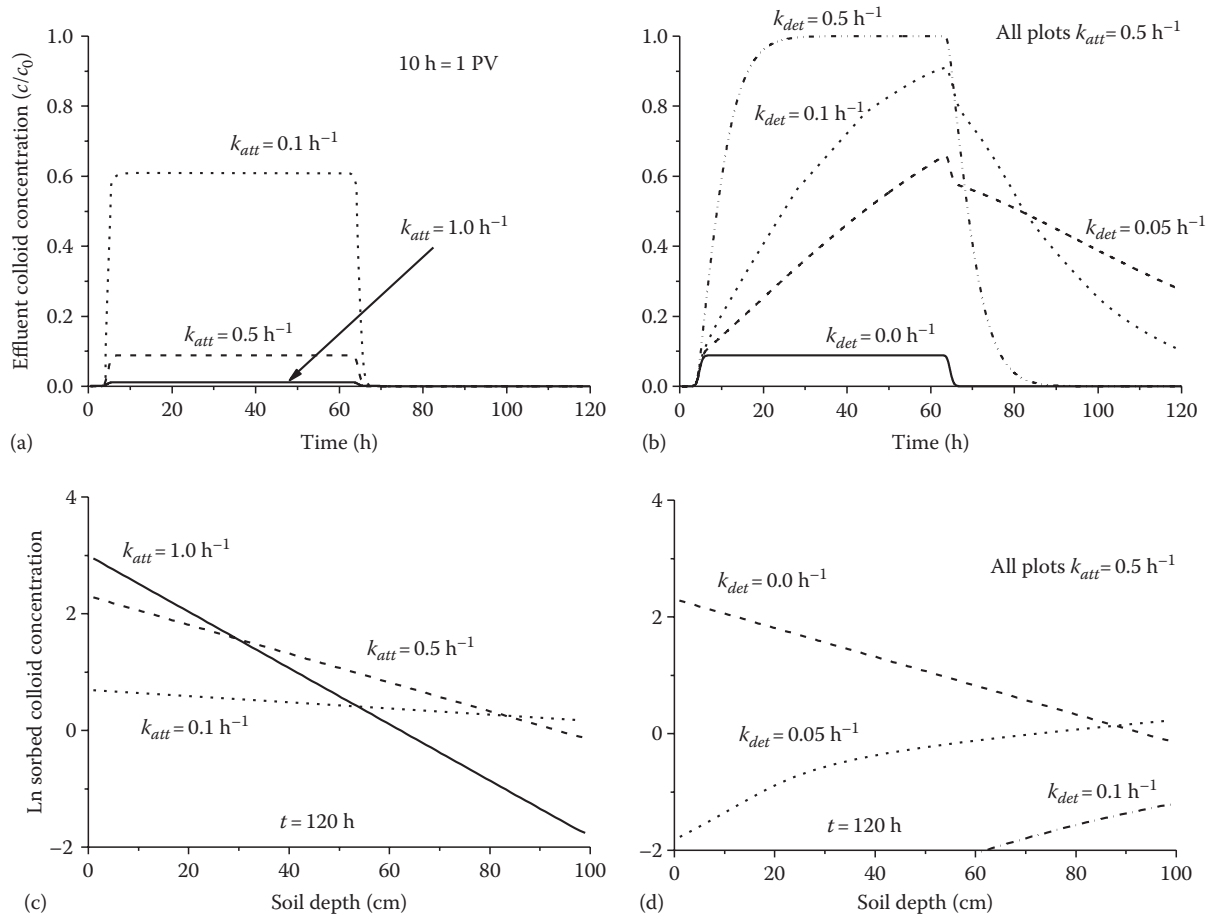


**FIGURE 15.18** Simulated colloid breakthrough for a 1 m column with a saturated flow velocity of  $2.4 \text{ m day}^{-1}$  ( $\theta = 0.5$ ,  $DL = 0.01 \text{ m}$ ) exposed to a 60 h colloid pulse with kinetically controlled attachment (a = clean-bed filtration theory), and kinetically controlled attachment and detachment (b). Retained colloid profile for irreversible (c), and reversible attachment (d) after 60 h colloid pulse followed by 60 h of colloid-free inlet solution.

The collector efficiency reflects the colloid collisions with the stationary matrix resulting from diffusion, advective flow, and gravitational forces, and can be calculated (Tufenkji and Elimelech, 2004a). The attachment efficiency term ( $\alpha$ ) is generally determined experimentally by fitting colloid breakthrough results to the CFT model based on  $k_{att}$  and the calculated  $\eta$  (O'Melia and Tiller, 1993; Elimelech et al., 2000; Bradford et al., 2004; Tufenkji and Elimelech, 2004a; Tufenkji, 2007). Additional mechanisms of material loss, such as cell motility, growth, and inactivation, must also be considered when evaluating the transport of microbes. Furthermore, research in the last decade has demonstrated the importance of surface biomolecules, which can vary in response to the local environment, and among microbial strains and species in controlling their adhesion properties (Bolster et al., 2000; Walker et al., 2004; Tufenkji, 2007).

Studies using model colloidal systems indicate that CFT is generally applicable under conditions favoring particle attachment, that is, no significant electrostatic repulsion. However, the CFT approach fails in describing experimental data under apparently unfavorable conditions when significant electrostatic repulsion exists between the mobile colloid and matrix

grain surface. For particles with the same charge, a deep primary attractive force exists at very short separation distances, known as the primary minimum (Figure 15.12). However, electrostatic repulsion supposedly limits particle approach in a manner similar to chemical activation energies. Such discrepancies in deposition studies, and in batch aggregation experiments, have been attributed to porous media heterogeneity that can be difficult to quantify experimentally (i.e., grain size, morphology, and surface charge) and a secondary energy minimum that favors colloid sorption without the necessity to overcome the full electrostatic repulsion required to enter the primary minimum (Figure 15.12), resulting in an apparent change in the attachment rate coefficient ( $k_{att}$ ) with transport distance (Roy and Dzombak, 1996; Elimelech et al., 2000; Chen et al., 2001; Bradford et al., 2002, 2003; Tufenkji et al., 2003; Hahn and O'Melia, 2004; Li et al., 2004; Redman et al., 2004; Tufenkji and Elimelech, 2005; Tufenkji, 2007). The secondary minimum reflects the exponential decay in electrostatic forces with separation distance, in contrast to van der Waals forces that decrease more slowly with distance. The inability to remobilize particles trapped within the "secondary" minimum by altering solution chemistry, that is, reducing ionic strength, further demonstrates the hydrodynamic



and physicochemical complexity of colloid retention mechanisms (Bradford and Torkzaban, 2008; Torkzaban et al., 2008; Bradford et al., 2009).

Verifying the spatial distribution of retained colloids based on the attachment parameter ( $\alpha_{BTC}$ ) derived from effluent breakthrough data is a good method for testing the validity of the CFT model. In many instances, the slope of the relationship is greater than CFT predictions, indicating higher initial colloid retention that decreases with increasing transport distance (Li et al., 2004; Tufenkji, 2007). Such discrepancies have been addressed through the use of multiple deposition rate constants, that is, a fast and a slow rate, or a defined statistical distribution of randomly assigned particle deposition rates that reflect the inherent variability in colloidal surface potentials (Li et al., 2004; Tufenkji and Elimelech, 2004b; Tufenkji, 2007). It is interesting to note that the statistical distribution in observed deposition rate coefficients appears to narrow as colloid deposition becomes more favorable, for example, reduced flow velocities and increased ionic strengths (Li et al., 2004).

Attachment kinetics are highly sensitive to colloid–collector interaction potentials. Moderate changes with respect to colloid surface potentials can result in relatively large changes in collision efficiency and attachment rate (Elimelech and O’Melia, 1990; Ryan and Elimelech, 1996; Elimelech et al., 2000; Li et al., 2004). Deviation from the breakthrough plateau with time is indicative of a change in the colloid deposition efficiency during the course of injection, that is, filter ripening or blocking. In addition, surface modifiers such as Fe oxides and soil organics, often present in relatively minor amounts, can alter the expression of electrostatic repulsion on soil mineral surfaces (Goldberg and Forster, 1990; Kretzschmar et al., 1993; Kaplan et al., 1993, 1997; Bertsch and Seaman, 1999; Franchi and O’Melia, 2003; Seaman et al., 1995, 2003).

Recent studies indicate that pore structure and particle straining may also be more significant than previously recognized for intermediate colloid and matrix grain sizes. Colloid straining, trapping colloids in pore regions that are too small to permit passage, is generally considered to be an irreversible process. Within a transport model, straining can be addressed by including an additional first-order expression to the deposition equation given above. In the absence of colloid detachment, the kinetic deposition model accounting for colloid straining becomes

$$\frac{\rho_b}{\theta} \frac{\partial S}{\partial t} = k_{att}C - k_{str}\psi_{str}C \quad (15.42)$$

where

$k_{str}$  is the straining rate constant

$\psi_{str}$  is the depth-dependent colloid straining function (Bradford et al., 2002, 2003, 2004)

In contrast to straining, traditionally considered a physical phenomenon insensitive to solution chemistry, recent hydrodynamic modeling efforts have verified particle capture within hydrodynamically disconnected regions of the porous matrix near two

collector particle surfaces where the magnitude of fluid velocity is quite small compared to the bulk solution, analogous to the “immobile” regions evident in solute transport behavior. Within the immobile regions, greater colloid/colloid and colloid/collector surface interactions lead to enhanced colloid immobilization in a manner that depends on both solution chemistry and pore geometry. Furthermore, particles weakly retained in the secondary minimum can be subsequently funneled to the immobile capture regions by hydrodynamic forces that are insufficient to induce full colloid detachment (Bradford and Torkzaban, 2008; Torkzaban et al., 2008; Bradford et al., 2009).

## 15.4.2 Colloid-Mediated Contaminant Transport

Numerous studies have established that organic and inorganic chemicals, which are highly sorbed onto soil nonetheless, are often transported in the subsurface to a greater degree than expected. Such anomalies have been attributed to kinetic effects associated with nonequilibrium sorption and bypass flow, as well as contaminant transport associated with a mobile colloidal fraction that enhances apparent migration beyond the levels controlled by thermodynamically based solubilities or partitioning reactions. Furthermore, colloidal materials may move at rates that are similar or faster than those of nonreactive solute tracers because of physical size or electrostatic exclusion from a fraction of the saturated pore space (Simunek et al., 2006). In general, colloid-facilitated transport is only significant when the contaminant is strongly sorbed to the mobile colloidal phase, approaching irreversible partitioning. Otherwise, the sorbed contaminant will desorb in response to the decrease in the aqueous phase contaminant concentration when the colloidal phase travels faster than the aqueous phase (Grolimund and Borkovec, 2005).

Models that include colloid-facilitated transport generally differ in the manner in which they account for the various colloid release and attachment processes described in Section 15.4.1 (i.e., reversible vs. irreversible attachment, kinetic vs. equilibrium) (Mills et al., 1991; Dunnivant et al., 1992; Corapcioglu and Jiang, 1993; Grolimund and Borkovec, 2005) with additional equilibrium or kinetic expressions used to account for contaminant–colloid interactions. Only recently have models been developed that address partially saturated conditions, colloid straining, and size exclusion (Simunek et al., 2006). The development of such a contaminant transport model, while requiring numerous simplifying assumptions (van de Weerd and Leijnse, 1997; Simunek et al., 2006), still results in a significant list of parameters required to account for both contaminant sorption and colloid attachment. For example, transport and mass balance expressions must account for the aqueous phase contaminant, contaminant sorbed to the immobile matrix, contaminant sorbed to the mobile colloids, and contaminant sorbed to colloids immobilized by various mechanisms, that is, stationary phase attachment, air–water interphase attachment, and straining. Additional expressions are required to account for colloid mass balance as well, illustrating the potential level of model

complexity. Simunek et al. (2006) recommend the use of sensitivity analysis to discern the relative importance of such variables in accurately describing contaminant fate and transport.

Although subject to numerous sampling artifacts, significant concentrations of mobile colloids have been observed in soil and groundwater systems (Ronen et al., 1992; McCarthy and Degueldre, 1993; DeNovio et al., 2004). However, contaminant transport models generally fail to account for the impact of mobile colloids in facilitating the transport of strongly sorbing contaminants. For example, colloid-facilitated transport has been implicated in the migration of organic contaminants (e.g., atrazine, prochloraz, and dichlorodiphenyltrichloroethane [DDT]) (Vinten et al., 1983; Seta and Karathanasis, 1996; Seta and Karathanasis, 1997; de Jonge et al., 1998; Roy and Dzombak, 1998), metals (e.g., Pb, Ni, Cu, and Zn) (Kaplan et al., 1994b, 1995; Grolimund et al., 1996; Roy and Dzombak, 1997; Karathanasis, 1999; Grolimund and Borkovec, 2005; Karathanasis et al., 2005), radionuclides (e.g.,  $^{137}\text{Cs}$ ) (Von Gunten et al., 1988; Kaplan et al., 1994a; Kersting et al., 1999; Flury et al., 2002), and sparingly soluble nutrients, such as phosphate (de Jonge et al., 2004b). Some of the general issues concerning contaminant migration via colloid-facilitated transport are discussed by McDowell-Boyer et al. (1986), McCarthy and Zachara (1989), Ryan and Elimelech (1996), and Kretzschmar et al. (1999).

### 15.4.3 Effect of Colloid Transport on Hydraulic Conductivity and Soil Formation

Some degree of colloid movement is generally considered a major factor in soil profile development. However, dispersion and transport of soil colloids have been linked to soil crust formation, reduced infiltration and hydraulic conductivity, and erosion (Shainberg et al., 1981; Miller and Baharuddin, 1986; Miller and Radcliffe, 1992). Reductions in hydraulic conductivity caused by colloid transport can be divided into two groups: formation of crusts and migration and deposition within the medium. Crust formation results when the colloids are not able to enter the soil media and form a compact layer above the soil. Alternatively, the particles may enter the medium, flow with the water in a suspension, and be deposited within the medium. This process may result from either mechanical filtration of large colloids or physicochemical processes of attraction/repulsion of small colloids as discussed above (see Section 15.4.1).

Research in soil science related to the effects of colloid transport on hydraulic conductivity has focused primarily on description of the chemical process affecting clay movement, rather than on mathematical expressions for prediction of flow rates. Conditions of low ionic strength, high exchangeable Na, and elevated pH were related to both dispersion of clays (Suarez et al., 1984; Goldberg and Forster, 1990; Miller et al., 1990) and subsequent migration and reduction in soil hydraulic conductivity (Suarez et al., 1984). In highly weathered acid soils where positively charged colloids are important, Seaman et al. (1995, 1997) determined that addition of  $\text{CaCl}_2$  initially enhanced colloid mobility, likely due to release of exchangeable Al and a decrease in pH.

Soil profile development is often affected by colloid movement. Among these processes are the formation of impermeable clay layers in the subsurface and movement of Fe and Al, most probably as organic metal complexes. Moderately to strongly developed soils are generally characterized by depleted clay contents in the A horizon and larger amounts of clay generally in the upper portion of the B horizon. A substantial portion of the argillic B horizon is related to migration of clays from the upper portion of the profile and subsequent deposition (Birkeland, 1974). Flocculation in the lower part of the profile is enhanced by increased electrolyte concentration relative to the surface horizons. Clay colloid migration is evident by the presence of clay films over ped surfaces and inside voids and presence of oriented clay particles. This process is also observed in aridisols where low organic matter and elevated exchangeable Na enhance colloid transport. Clay deposition is enhanced by increasing electrolyte concentration and removal of water by evapotranspiration. In general, formation of argillic horizons requires that the soil be at least partially dry during some part of the season.

Formation of Fe- and Al-rich layers by translocation (podzolization) is probably caused by transport of metal-fulvic acid complexes, rather than movement of the dissolved metals. The spodic B horizon marks the location at which these chelates either flocculate due to increases in electrolyte concentration or by decomposition of the organic matter (Birkeland, 1974).

## References

- Adamson, A.W. 1976. *Physical chemistry of surfaces*, 3rd Ed. John Wiley & Sons, New York.
- Appel, C., L.Q. Ma, R.D. Rhue, and E. Kennelley. 2003. Point of zero charge determination in soils and minerals via traditional methods and detection of electroacoustic mobility. *Geoderma* 113:77–93.
- Aringhieri, R., G. Pardini, M. Gispert, and A. Sole. 1992. Testing a simple methylene blue method for surface area estimation in soils. *Agrochimica* 36:224–232.
- Auset, M., and A.A. Keller. 2004. Pore-scale processes that control dispersion of colloids in saturated porous media. *Water Resour. Res.* 40:W03503, 1–11.
- Babcock, K.L. 1963. Theory of chemical properties of soil colloidal systems at equilibrium. *Hilgardia* 34:417–542.
- Babick, F., F. Hinze, and S. Ripperger. 2000. Dependence of ultrasonic attenuation on the material properties. *Colloids Surf. A* 172:33–46.
- Babick, F., and S. Ripperger. 2002. Information content of acoustic attenuation spectra. Part. Part. Syst. Charact. 19:176–185.
- Balnois, E., G. Papastavrou, and K.J. Wilkinson. 2007. Force microscopy and force measurements of environmental colloids, p. 405–467. *In* K.J. Wilkinson and J.R. Lead (eds.) *Environmental colloids and particles: Behavior, structure and characterization*. IUPAC series on analytical and physical chemistry of environmental systems. John Wiley & Sons, Chichester, U.K.

- Bar-on, P., I. Shainberg, and I. Michaeli. 1970. Electrophoretic mobility of montmorillonite particles saturated with Na/Ca ions. *J. Colloid Interface Sci.* 33:471–472.
- Baumann, T., and C.J. Werth. 2004. Visualization and modeling of polystyrol colloid transport in a silicon micromodel. *Vadose Zone J.* 3:434–443.
- Beckett, R. 1991. Field-flow fractionation-ICP-MS: A powerful new analytical tool for characterizing macromolecules and particles. *Atomic Spectrosc.* 12:215–246.
- Beckett, R., and B.T. Hart. 1993. Use of field-flow fractionation techniques to characterize aquatic particles, colloids and macromolecules, p. 165–205. *In* J. Buffle and H.P. van Leeuwen (eds.) *Environmental particles*, Vol. 2. Lewis Publishers, Ann Arbor, MI.
- Beckett, R., D. Murphy, S. Tadjiki, D.J. Chittleborough, J.C. Giddings. 1997. Determination of thickness, aspect ratio and size distribution for platey particles using sedimentation field-flow fractionation and electron microscopy. *Colloids Surf. A* 120:17–26.
- Benna, M., N. Kbir-Arighuib, A. Magnin, and F. Bergaya. 1999. Effect of pH on rheological properties of purified sodium bentonite suspensions. *J. Colloid Interface Sci.* 218:442–455.
- Bertsch, P.M., and J.C. Seaman. 1999. Characterization of complex minerals assemblages: Implications for contaminant transport and environmental remediation. *PNAS* 96:3350–3357.
- Bertuzzo, E., S. Azaele, A. Maritan, M. Gatto, I. Rodriguez-Iturbe, and A. Rinaldo. 2008. On the space-time evolution of a cholera epidemic. *Water Resour. Res.* W01424, doi: 10.1029/2007WR006211.
- Birkeland, P.W. 1974. *Pedology, weathering, and geomorphological research*. Oxford University Press, New York.
- Blo, G., C. Contado, F. Fagioli, M.H. Bollain-Rodriguez, and F. Dondi. 1995. Analysis of kaolin by sedimentation field-flow fractionation and electrothermal atomic absorption spectrometry detection. *Chromatographia* 41:715–721.
- Bohn, H.L., B.L. McNeal, and G.A. O'Connor. 1985. *Soil chemistry*. John Wiley & Sons, New York.
- Bolster, C.H., A.L. Mills, G. Hornberger, and J. Herman. 2000. Effect of intra-population variability on the long-distance transport of bacteria. *Ground Water* 38:370–375.
- Borchardt, G.A. 1977. Montmorillonite and other smectite minerals, p. 293–330. *In* J.B. Dixon and S.B. Weed (eds.) *Minerals in soil environments*. SSSA, Madison, WI.
- Borkovec, M., Q. Wu, G. Degovics, P. Laggner, and H. Sticher. 1993. Surface area and size distribution of soil particles. *Colloids Surf. A* 73:65–76.
- Bower, C.A., and J.O. Goertzen. 1959. Surface area of soils by an equilibrium ethylene glycol method. *Soil Sci.* 87:289–292.
- Bradford, S.A., M. Bettahar, J. Simunek, and M.T. van Genuchten. 2004. Straining and attachment of colloids in physically heterogeneous porous media. *Vadose Zone J.* 3:384–394.
- Bradford, S.A., J. Simunek, M. Bettahar, M.T. van Genuchten, and S.R. Yates. 2003. Modeling colloid attachment, straining, and exclusion in saturated porous media. *Environ. Sci. Technol.* 37:2242–2250.
- Bradford, S.A., and S. Torkzaban. 2008. Colloid transport and retention in unsaturated porous media: A review of interface-, collector-, and pore-scale processes and models. *Vadose Zone J.* 7:667–681.
- Bradford, S.A., S. Torkzaban, F. Leij, J. Simunek, and M.T. van Genuchten. 2009. Modeling the coupled effects of pore space geometry and velocity on colloid transport and retention. *Water Resour. Res.* 45:W02414, doi: 10.1029/2008WR007096.
- Bradford, S.A., S.R. Yates, M. Bettahar, and J. Simunek. 2002. Physical factors affecting the transport and fate of colloids in saturated porous media. *Water Resour. Res.* 38:63/1–63/12.
- Brown, G., A.C.D. Newman, J.H. Rayner, and A.H. Weir. 1978. The structure and chemistry of soil clay minerals, p. 29–178. *In* D.G. Greenland and M.H.B. Hayes (eds.) *The chemistry of soil constituents*. John Wiley & Sons, New York.
- Brunauer, S., P.H. Emmett, and E. Teller. 1938. Adsorption of gases in multimolecular layers. *J. Am. Chem. Soc.* 60:309–319.
- Buffle, J., and G.G. Leppard. 1995a. Characterization of aquatic colloids and macromolecules. 1. Structure and behavior of colloidal materials. *Environ. Sci. Technol.* 29:2169–2175.
- Buffle, J., and G.G. Leppard. 1995b. Characterization of aquatic colloids and macromolecules. 2. Key role of physical structures on analytical results. *Environ. Sci. Technol.* 29:2176–2184.
- Bunn, R.A., R.D. Magelky, J.N. Ryan, and M. Elimelech. 2002. Mobilization of natural colloids from an iron oxide-coated sand aquifer: Effect of pH and ionic strength. *Environ. Sci. Technol.* 36:314–322.
- Bunville, L.G. 1984. Commercial instrumentation for particle size analysis, p. 1–42. *In* H.G. Barth (ed.) *Modern methods of particle size analysis*. John Wiley & Sons, New York.
- Carter, D.L., M.M. Mortland, and W.D. Kemper. 1986. Specific surface, p. 413–423. *In* A. Klute (ed.) *Methods of soil analysis. Part 1—Physical and mineralogical methods*, 2nd Ed. SSSA Publ., Madison, WI.
- Chanudet, V., and M. Filella. 2006. A non-perturbing scheme for the mineralogical characterization and quantification of inorganic colloids in natural waters. *Environ. Sci. Technol.* 40:5045–5051.
- Chen, J.Y., C. Ko, S. Bhattacharjee, and M. Elimelech. 2001. Role of spatial distribution of porous medium surface charge heterogeneity in colloid transport. *Colloids Surf. A* 191:3–15.
- Chittleborough, D.J., S. Tadjiki, J.F. Ranville, F. Shanks, and R. Beckett. 2004. Soil colloid analysis by field-flow fractionation. *Super Soil 2004*, 3rd Australian N.Z. Soils Conf., December 5–9, 2004. University of Sydney, Sydney, Australia.
- Chorom, M., and P. Rengasamy. 1995. Dispersion and zeta potential of pure clays as related to net particle charge under varying pH, electrolyte concentration and cation type. *Eur. J. Soil Sci.* 46:657–665.
- Coll, H., and L.E. Oppenheimer. 1987. Improved techniques in disc centrifugation, p. 202–214. *In* T. Provder (ed.) *Particle size distribution. Assessment and characterization*. American Chemical Society, Washington, DC.

- Contado, C., G. Blo, F. Fagioli, F. Dondi, and R. Beckett. 1997. Characterisation of river Po particles by sedimentation field-flow fractionation coupled to GFAAS and ICP-MS. *Colloids Surf. A* 120:47–59.
- Corapcioglu, M.Y., and S.Y. Jiang. 1993. Colloid-facilitated groundwater contaminant transport. *Water Resour. Res.* 29:2215–2226.
- Cotton, A., and H. Mouton. 1907. Magneto-optical properties of colloids and heterogeneous liquids. *Ann. Chim. Phys.* 11:145–203, 289–339.
- Crist, J.T., J.F. McCarthy, Y. Zevi, P. Baveye, J.A. Throop, and T.S. Steenhuis. 2004. Pore-scale visualization of colloid transport and retention in partly saturated porous media. *Vadose Zone J.* 3:444–450.
- Davis, J.A., and D.B. Kent. 1990. Surface complexation modeling in aqueous geochemistry. *Rev. Mineral. Geochem.* 23:177–260.
- de Jong, E. 1999. Comparison of three methods of measuring surface area of soils. *Can. J. Soil Sci.* 79:345–351.
- de Jonge, H., O.H. Jacobsen, L.W. de Jonge, and P. Moldrup. 1998. Particle-facilitated transport of prochloraz in undisturbed sandy loam soil columns. *J. Environ. Qual.* 27:1495–1503.
- de Jonge, L.W., C. Kjaergaard, and P. Moldrup. 2004a. Colloids and colloid-facilitated transport of contaminants in soils: An introduction. *Vadose Zone J.* 3:321–325.
- de Jonge, L.W., P. Moldrup, G.H. Rubaek, K. Schelde, and J. Djurhuus. 2004b. Particle leaching and particle-facilitated transport of phosphorus at field scale. *Vadose Zone J.* 3:462–470.
- Delgado, A.V., S. Ahualli, F.J. Arroyo, and F. Carrique. 2005. Dynamic electrophoretic mobility of concentrated suspensions comparison between experimental data and theoretical predictions. *Colloids Surf. A* 267:95–102.
- DeNovio, N.M., J.E. Saiers, and J.N. Ryan. 2004. Colloid movement in unsaturated porous media: Recent advances and future directions. *Vadose Zone J.* 3:338–351.
- Dixon, J.B. 1977. Kaolinite and serpentine group minerals, p. 357–403. *In* J.B. Dixon and S.B. Weed (eds.) *Minerals in soil environments*. SSSA Inc., Madison, WI.
- Dixon, J.B., and S.B. Weed. 1989. *Minerals in soil environments*. SSSA Inc., Madison, WI.
- Diz, H.M.M., and B. Rand. 1989. The variable nature of the isoelectric point of the edge surface of kaolinite. *Br. Ceram. Trans.* 88:162–166.
- Dong, A., G. Chesters, and G.V. Simsiman. 1983. Soil dispersibility. *Soil Sci.* 136:208–212.
- Doucet, F.J., L. Maguire, and J.R. Lead. 2004. Size fractionation of aquatic colloids and particles by cross flow filtration: Analysis by scanning electron and atomic force microscopy. *Anal. Chim. Acta* 522:59–71.
- Douglas, L.A. 1977. Vermiculites, p. 259–292. *In* J.B. Dixon and S.B. Weed (eds.) *Minerals in soil environments*. SSSA Inc., Madison, WI.
- Ducker, W.A., and R.M. Pashley. 1992. Forces between mica surfaces in the presence of rod-shaped divalent counterions. *Langmuir* 8:109–112.
- Ducker, W.A., T.J. Senden, and R.M. Pashley. 1991. Direct measurement of colloidal forces using an atomic force microscope. *Nature* 353:239–241.
- Dukhin, A.S., and P.J. Goetz. 1996. Acoustic and electroacoustic spectroscopy. *Langmuir* 12:4336–4344.
- Dukhin, A.S., and P.J. Goetz. 1998. Characterization of aggregation phenomena by means of acoustic and electroacoustic spectroscopy. *Colloids Surf. A* 144:49–58.
- Dukhin, A.S., and P.J. Goetz. 2001. Acoustic and electroacoustic spectroscopy for characterizing concentrated dispersions and emulsions. *Adv. Colloid Interface Sci.* 92:71–132.
- Dukhin, A.S., and P.J. Goetz. 2002. *Ultrasound for characterizing colloids*. Elsevier, Amsterdam, the Netherlands.
- Dukhin, A.S., P.J. Goetz, and S. Truesdail. 2001. Titration of concentrated dispersions using electroacoustic potential probe. *Langmuir* 17:964–968.
- Dunnivant, F.M., P.M. Jardine, D.L. Taylor, and J.F. McCarthy. 1992. Transport of naturally occurring dissolved organic carbon in laboratory columns containing aquifer material. *Soil Sci. Soc. Am. J.* 56:437–444.
- Duchaufour, P. 1970. *Precis de pedologie*. Masson et Cie., Paris, France.
- Duran, J.D.G., M.M. Ramos-Tejeda, F.J. Arroyo, and F. Gonzalez-Caballero. 2000. Rheological and electrokinetic properties of sodium montmorillonite suspensions. I. Rheological properties and interparticle energy of interaction. *J. Colloid Interface Sci.* 219:107–117.
- Dyal, R.S., and S.B. Hendricks. 1950. Total surface of clays in polar liquids as a characteristic index. *Soil Sci.* 69:421–432.
- Edwards, D.G., A.M. Posner, and J.P. Quirk. 1965a. Repulsion of chloride ions by negatively charged clay surfaces. Part 1. Monovalent cation Fithian illites. *Trans. Faraday Soc.* 61:2808–2815.
- Edwards, D.G., A.M. Posner, and J.P. Quirk. 1965b. Repulsion of chloride ions by negatively charged clay surfaces. Part 2. Monovalent montmorillonites. *Trans. Faraday Soc.* 61:2816–2819.
- Elimelech, M., and C.R. O'Melia. 1990. Kinetics of deposition of colloidal particles in porous media. *Environ. Sci. Technol.* 24:1528–1536.
- Elimelech, M., M. Nagai, C. Ko, and J.N. Ryan. 2000. Relative insignificance of mineral grain zeta potential to colloid transport in geochemically heterogeneous porous media. *Environ. Sci. Technol.* 34:2143–2148.
- El-Swaify, S.A., S. Ahmed, L.D. Swindale. 1970. Effects of adsorbed cations on physical properties of tropical red and tropical black earths. II. Liquid limit, degree of dispersion, and moisture retention. *J. Soil Sci.* 21:188–198.
- Emerson, W.W. 1967. A classification of soil aggregates based on their coherence in water. *Aust. J. Soil Res.* 15:255–262.
- Fanning, D.S., and V.Z. Keramidas. 1977. Micas, p. 195–258. *In* J.B. Dixon and S.B. Weed (eds.) *Minerals in soil environments*. SSSA Inc., Madison, WI.
- Farmer, V.C. 1978. Water on particle surfaces, p. 405–448. *In* D.J. Greenland and M.H.B. Hayes (eds.) *The chemistry of soil constituents*. John Wiley & Sons, New York.

- Filella, M., and J. Buffle. 1993. Factors controlling the stability of submicron colloids in natural waters. *Colloids Surf. A* 73:255–273.
- Filella, M., J. Zhang, M.E. Newman, and J. Buffle. 1997. Analytical applications of photon correlation spectroscopy for size distribution measurements of natural colloidal suspensions: Capabilities and limitations. *Colloids Surf. A* 120:27–46.
- Finsy, R. 1994. Particle sizing by quasi-elastic light scattering. *Adv. Colloid Interface Sci.* 52:79–143.
- Flegman, A.W., J.W. Goodwin, and R.H. Ottewill. 1969. Rheological studies on kaolinite suspensions. *Proc. Br. Ceram. Soc.* 13:31–45.
- Flury, M., J.B. Mathison, and J.B. Harsh. 2002. In situ mobilization of colloids and transport of cesium in Hanford sediments. *Environ. Sci. Technol.* 36:5335–5341.
- Franchi, A., and C.R. O'Melia. 2003. Effects of natural organic matter and solution chemistry on the deposition and reentrainment of colloids in porous media. *Environ. Sci. Technol.* 37:1122–1129.
- Frenkel, H., G.J. Levy, and M.V. Fey. 1992. Clay dispersion and hydraulic conductivity of clay-sand mixtures as affected by the addition of various anions. *Clays Clay Miner.* 40:515–521.
- Freundlich, H. 1932. *Kapillarchemie II. Eine Darstellung der Chemie der Kolloide und verwandter Gebiete.* 4. Akademische Verlagsgesellschaft, Leipzig, Germany.
- Gamerding, A.P., and D.I. Kaplan. 2001. Colloid transport and deposition in water-saturated Yucca Mountain tuff as determined by ionic strength. *Environ. Sci. Technol.* 35:3326–3331.
- Ghezzehei, T.A., and D. Or. 2001. Rheological properties of wet soils and clays under steady and oscillatory stresses. *Soil Sci. Soc. Am. J.* 65:624–637.
- Giddings, J.C. 1993. Field-flow fractionation: Analysis of macromolecular, colloidal, and particulate materials. *Science* 260:1456–1465.
- Goldberg, S., and H.S. Forster. 1990. Flocculation of reference clays and arid-zone soil clays. *Soil Sci. Soc. Am. J.* 54:714–718.
- Goldberg, S., H.S. Forster, and C.L. Godfrey. 1996. Molybdenum adsorption on oxides, clay minerals, and soils. *Soil Sci. Soc. Am. J.* 60:425–432.
- Goldstein, J.I., D.E. Newbury, P. Echlin, D.C. Joy, A.D. Romig, C.E. Lyman, C. Fiori, and E. Lifshin. 1992. *Scanning electron microscopy and X-ray microanalysis*, 2nd Ed. Plenum Press, New York.
- Greathouse, J.A., S.E. Feller, and D.A. McQuarrie. 1994. The modified Gouy–Chapman theory: Comparisons between electrical double layer models of clay swelling. *Langmuir* 10:2125–2130.
- Greenwood, R. 2003. Review of the measurement of zeta potentials in concentrated aqueous suspensions using electroacoustics. *Adv. Colloid Interface Sci.* 106:55–81.
- Gregg, S.J., and K.S.W. Sing. 1982. *Adsorption, surface area and porosity.* Academic Press, New York.
- Grolimund, D., and M. Borkovec. 2001. Release and transport of colloidal particles in natural porous media: 1. Modeling. *Water Resour. Res.* 37:559–570.
- Grolimund, D., and M. Borkovec. 2005. Colloid-facilitated transport of strongly sorbing contaminants in natural porous media: Mathematical modeling and laboratory column experiments. *Environ. Sci. Technol.* 39:6378–6386.
- Grolimund, D., and M. Borkovec. 2006. Release of colloidal particles in natural porous media by monovalent and divalent cations. *J. Contam. Hydrol.* 87:155–175.
- Grolimund, D., M. Borkovec, K. Bartmettler, and H. Sticher. 1996. Colloid-facilitated transport of strongly sorbing contaminants in natural porous media: A laboratory column study. *Environ. Sci. Technol.* 30:3118–3123.
- Groves, M.J. 1984. The application of particle characterization methods to submicron dispersion and emulsions, p. 43–91. *In* H.G. Barth (ed.) *Modern methods of particle size analysis.* John Wiley & Sons, New York.
- Gschwend, P.M., D.A. Backhus, J.K. MacFarlane, and A.L. Page. 1990. Mobilization of colloids in groundwater due to infiltration of water at coal ash disposal site. *J. Contam. Hydrol.* 6:307–320.
- Gschwend, P.M., and M.D. Reynolds. 1987. Monodisperse ferrous phosphate colloids in an anoxic groundwater plume. *J. Contam. Hydrol.* 1:309–327.
- Gu, B., and H.E. Doner. 1993. Dispersion and aggregation of soils as influenced by organic and inorganic polymers. *Soil Sci. Soc. Am. J.* 57:709–716.
- Guerin, M., and J.C. Seaman. 2004. Characterizing clay mineral suspensions using acoustic and electroacoustic spectroscopy. *Clays Clay Miner.* 52:145–157.
- Guerin, M., J.C. Seaman, C. Lehmann, and A. Jurgenson. 2004. Acoustic and electroacoustic characterization of variable-charge mineral suspensions. *Clays Clay Miner.* 52:158–170.
- Gunnarsson, M., M. Rasmusson, S. Wall, E. Ahlberg, and J. Ennis. 2001. Electroacoustic and potentiometric studies of the hematite/water interface. *J. Colloid Interface Sci.* 240:448–458.
- Hahn, M.W., and C.R. O'Melia. 2004. Deposition and reentrainment of Brownian particles in porous media under unfavorable chemical conditions: Some concepts and applications. *Environ. Sci. Technol.* 38:210–220.
- Handy, R.D., F. von der Kammer, J.R. Lead, M. Hasselov, R. Owen, and M. Crane. 2008. The ecotoxicology and chemistry of manufactured nanoparticles. *Ecotoxicology* 17:287–314.
- Hang, P.T., and G.W. Brindley. 1970. Methylene blue adsorption by clay minerals: Determination of surface areas and cation exchange capacities. *Clays Clay Miner.* 18:203–212.
- Hasselov, M., J.W. Readman, J.F. Ranville, and K. Tiede. 2008. Nanoparticle analysis and characterization methodologies in environmental risk assessment of engineered nanoparticles. *Ecotoxicology* 17:344–361.
- Hasselov, M., F. von der Kammer, and R. Beckett. 2007. Characterisation of aquatic colloids and macromolecules by field-flow fractionation, p. 23–276. *In* K.J. Wilkinson

- and J.R. Lead (eds.) Environmental colloids and particles: Behavior, structure and characterization. IUPAC series on analytical and physical chemistry of environmental systems. John Wiley & Sons, Chichester, U.K.
- Heath, D., and Th.F. Tadros. 1983. Influence of pH, electrolyte and poly(vinyl alcohol) addition on the rheological characteristics of aqueous dispersions of sodium montmorillonite. *J. Colloid Interface Sci.* 93:307–319.
- Heil, D., and G. Sposito. 1993. Organic matter role in illitic soil colloids flocculation: II. Surface charge. *Soil Sci. Soc. Am. J.* 57:1246–1253.
- Heister, K., P.J. Kleingeld, T.J.S. Keijzer, and J.P.G. Loch. 2005. A new laboratory set-up for measurements of electrical, hydraulic, and osmotic fluxes in clays. *Eng. Geol.* 77:295–303.
- Hesterberg, D.L. 1988. Critical coagulation concentrations and rheological properties of illite. Ph.D. Thesis. University of California, Riverside, CA.
- Hesterberg, D., and A.L. Page. 1990a. Flocculation series test yielding time-invariant critical coagulation concentrations of sodium illite. *Soil Sci. Soc. Am. J.* 54:729–735.
- Hesterberg, D., and A.L. Page. 1990b. Critical coagulation concentration of sodium and potassium illite as affected by pH. *Soil Sci. Soc. Am. J.* 54:735–739.
- Hesterberg, D., and A.L. Page. 1993. Rheology of sodium and potassium illite suspensions in relation to colloidal stability. *Soil Sci. Soc. Am. J.* 57:697–704.
- Hiemenz, P.C. 1977. Principles of colloid and surface chemistry. Marcel Dekker Inc., New York.
- Hiemenz, P.C., and R. Rajagopalan. 1997. Principles of colloid and surface chemistry, 3rd Ed. Marcel Dekker, New York.
- Hochella, M.F. 2008. Nanogeoscience: From origins to cutting-edge applications. *Elements* 4:373–379.
- Holsworth, R.M., T. Provder, and J.J. Stansbrey. 1987. External-gradient-formation method for disc centrifuge photosedimentometric particle size distribution analysis, p. 191–201. *In* T. Provder (ed.) Particle size distribution. Assessment and characterization. American Chemical Society, Washington, DC.
- Hsu, P.H. 1977. Aluminum hydroxides and oxyhydroxides, p. 99–143. *In* J.B. Dixon and S.B. Weed (eds.) Minerals in soil environments. SSSA Inc., Madison, WI.
- Hsu, J.P. 1999. Interfacial forces and fields: Theory and applications. CRC Press, New York.
- Huang, C.P. 1981. The surface acidity of hydrous solids, p. 183–217. *In* M.A. Anderson and A.J. Rubin (eds.) Adsorption of inorganics at solid–liquid interfaces. Ann Arbor Science, Ann Arbor, MI.
- Hunter, R.J. 1981. Zeta potential in colloid science. Academic Press, London, U.K.
- Hunter, R.J. 1987. Foundations of colloid science, Vol. 1. Oxford University Press, New York.
- Hunter, R.J. 1989. Foundations of colloid science, Vol. 2. Oxford University Press, New York.
- Hutton, J.T. 1977. Titanium and zirconium minerals, p. 673–688. *In* J.B. Dixon and S.B. Weed (eds.) Minerals in soil environments. SSSA Inc., Madison, WI.
- Ise, N., and M.V. Smalley. 1994. Thermal compression of colloidal crystals: Paradox of repulsion-only assumption. *Phys. Rev. B Condens. Matter.* 50:16722–16725.
- Israelachvili, J.N. 1992. Intermolecular and surface forces, 2nd Ed. Academic Press, San Diego, CA.
- IUPAC. 2009. International Union of Pure and Applied Chemistry. <http://www.iupac.org>
- Johnson, C.R., L.A. Hellerich, N.P. Nikolaidis, and P.M. Gschwend. 2001. Colloid mobilization in the field using citrate to remediate chromium. *Ground Water* 39:895–903.
- Kaplan, D.I., P.M. Bertsch, and D.C. Adriano. 1995. Facilitated transport of contaminant metals through an acidified aquifer. *Ground Water* 33:708–717.
- Kaplan, D.I., P.M. Bertsch, and D.C. Adriano. 1997. Mineralogical and physicochemical differences between mobile and non-mobile colloidal phases in reconstructed pedons. *Soil Sci. Soc. Am. J.* 61:641–649.
- Kaplan, D.I., P.M. Bertsch, D.C. Adriano, and W.P. Miller. 1993. Soil-borne colloids as influenced by water flow and organic carbon. *Environ. Sci. Technol.* 27:1193–1200.
- Kaplan, D.I., P.M. Bertsch, D.C. Adriano, and K.A. Orlandini. 1994a. Actinide association with groundwater colloids in a coastal plain aquifer. *Radiochim. Acta* 66/67:181–187.
- Kaplan, D.I., D.B. Hunter, P.M. Bertsch, S. Bajt, and D.C. Adriano. 1994b. Application of synchrotron x-ray fluorescence spectroscopy and energy dispersive x-ray analysis to identify contaminant metals on groundwater colloids. *Environ. Sci. Technol.* 28:1186–1189.
- Karathanasis, A.D. 1999. Subsurface migration of copper and zinc mediated by soil colloids. *Soil Sci. Soc. Am. J.* 63:830–838.
- Karathanasis, A.D., D.M.C. Johnson, and C.J. Matocha. 2005. Biosolid colloid-mediated transport of copper, zinc, and lead in waste-amended soils. *J. Environ. Qual.* 34:1153–1164.
- Kavanaugh, M.C., and J.O. Leckie. 1980. Particulates in water. *Adv. Chem. Ser. No. 189.* American Chemical Society, Washington, DC.
- Kékicheff, P., S. Marcelja, T.J. Senden, and V.E. Shubin. 1993. Charge reversal seen in electrical double layer interaction of surfaces immersed in 2:1 calcium electrolyte. *J. Chem. Phys.* 99:6098–6113.
- Keren, R. 1988. Rheology of aqueous suspension of sodium/calcium montmorillonite. *Soil Sci. Soc. Am. J.* 52:924–928.
- Keren, R. 1989a. Effect of clay charge density and adsorbed ions on the rheology of montmorillonite suspension. *Soil Sci. Soc. Am. J.* 53:25–29.
- Keren, R. 1989b. Rheology of mixed kaolinite–montmorillonite suspensions. *Soil Sci. Soc. Am. J.* 53:725–730.
- Keren, R. 1991. Adsorbed sodium fraction's effect on rheology of montmorillonite–kaolinite suspensions. *Soil Sci. Soc. Am. J.* 55:376–379.

- Kersting, A.B., D.W. Efurud, D.L. Finnegan, D.J. Rokop, D.K. Smith, and J.L. Thompson. 1999. Migration of plutonium in ground-water at the Nevada Test Site. *Nature* 397:56–59.
- Khaleel, R., T.C.J. Yeh, and Z. Lu. 2002. Upscaled flow and transport properties for heterogeneous unsaturated media. *Water Resour. Res.* 38:11/1–11/12.
- Khilar, K.C., and H.S. Fogler. 1984. The existence of a critical salt concentration for particle release. *J. Colloid Interface Sci.* 101:214–224.
- Kia, S.F., H.S. Fogler, and M.G. Reed. 1987. Effect of pH on colloidal induced fines migration. *J. Colloid Interface Sci.* 118:158–168.
- Kim, S.-O., S.-H. Moon, and K.-W. Kim. 2001. Removal of heavy metals from soils using enhanced electrokinetic soil processing. *Water Air Soil Pollut.* 125:259–272.
- Kjellander, R., S. Marcelja, R.M. Pashley, and J.P. Quirk. 1990. A theoretical and experimental study of forces between charged mica surfaces in aqueous  $\text{CaCl}_2$  solutions. *J. Chem. Phys.* 92:4399–4407.
- Koehler, M.E., R.A. Zandler, T. Gill, T. Provder, and T.F. Niemann. 1987. An improved disc centrifuge photosedimentometer and data system for particle size distribution analysis, p. 180–190. *In* T. Provder (ed.) Particle size distribution. Assessment and characterization. American Chemical Society, Washington, DC.
- Kosmulski, M. 2002. Confirmation of the differentiating effect of small cations in the shift of the isoelectric point of oxides at high ionic strengths. *Langmuir* 18:785–787.
- Kosmulski, M., E. Maczka, E. Jartych, and J.B. Rosenholm. 2003. Synthesis and characterization of goethite and goethite-hematite composite: Experimental study and literature survey. *Adv. Colloid Interface Sci.* 103:57–76.
- Kosmulski, M., E. Maczka, and J.B. Rosenholm. 2002. Isoelectric points of metal oxides at high ionic strengths. *J. Phys. Chem. B* 106:2918–2921.
- Kretschmar, R., M. Borkovec, D. Grolimund, and M. Elimelech. 1999. Mobile subsurface colloids and their role in contaminant transport. *Adv. Agron.* 66:121–193.
- Kretschmar, R., D. Hesterberg, and H. Sticher. 1997. Effects of adsorbed humic acid on surface charge and flocculation of kaolinite. *Soil Sci. Soc. Am. J.* 61:101–108.
- Kretschmar, R., W.P. Robarge, and S.B. Weed. 1993. Flocculation of kaolinitic soil clays: Effects of humic substances and iron oxides. *Soil Sci. Soc. Am. J.* 57:1277–1283.
- Langmuir, I. 1918. The adsorption of gases on plane surfaces of glass, mica, and platinum. *J. Am. Chem. Soc.* 40:1361–1402.
- Laskin, A., and J.P. Cowin. 2001. Automated single-particle SEM/EDX analysis of submicrometer particles down to 0.1  $\mu\text{m}$ . *Anal. Chem.* 73:1023–1029.
- Laxton, P.B., and J.C. Berg. 2006. Relating clay yield stress to colloidal parameters. *J. Colloid Interface Sci.* 296:749–755.
- Lead, J.R., D. Muirhead, and C.T. Gibson. 2005. Characterization of freshwater natural aquatic colloids by atomic force microscopy (AFM). *Environ. Sci. Technol.* 39:6930–6936.
- Lead, J.R., and K.J. Wilkinson. 2007. Environmental colloids and particles: Current knowledge and future developments, p. 1–15. *In* K.J. Wilkinson and J.R. Lead (eds.) Environmental colloids and particles: Behavior, structure and characterization. IUPAC series on analytical and physical chemistry of environmental systems. John Wiley & Sons, Chichester, U.K.
- Lead, J.R., K.J. Wilkinson, E. Balnois, B. Cutak, C. Larive, S. Assemi, and R. Beckett. 2000. Diffusion coefficients and polydispersities of the Suwannee River fulvic acid: Comparison of fluorescence correlation spectroscopy, pulsed-field gradient nuclear magnetic resonance and flow field-flow fractionation. *Environ. Sci. Technol.* 34:3508–3513.
- Lebron, I., M.G. Schaap, and D.L. Suarez. 1999. Saturated hydraulic conductivity prediction from microscopic pore geometry measurements and neural network analysis. *Water Resour. Res.* 35:3149–3157.
- Lebron, I., and D.L. Suarez. 1992a. Electrophoretic mobility of illite and micaceous soil clays. *Soil Sci. Soc. Am. J.* 56:1106–1115.
- Lebron, I., and D.L. Suarez. 1992b. Variations in soil stability within and among soil types. *Soil Sci. Soc. Am. J.* 56:1412–1421.
- Lebron, I., D.L. Suarez, C. Amrhein, and J.E. Strong. 1993. Size of mica domains and distribution of the adsorbed Na–Ca ions. *Clays Clay Miner.* 41:380–388.
- Ledin, A., S. Karlsson, A. Duker, and B. Allard. 1993. Applicability of photon correlation spectroscopy for measurement of concentration and size distribution of colloids in natural waters. *Anal. Chim. Acta* 281:421–428.
- Ledin, A., S. Karlsson, A. Duker, and B. Allard. 1994. Measurements in-situ of concentration and size distribution of colloidal matter in deep groundwaters by photon-correlation spectroscopy. *Water Res.* 28:1539–1545.
- Li, X., T.D. Scheibe, and W.P. Johnson. 2004. Apparent decreases in colloid deposition rate coefficients with distance of transport under unfavorable deposition conditions: A general phenomenon. *Environ. Sci. Technol.* 38:5616–5625.
- Lowell, S. 1979. Introduction to powder surface area. John Wiley & Sons, New York.
- Ma, K., and A.C. Pierre. 1999. Clay sediment-structure formation in aqueous kaolinite suspensions. *Clays Clay Miner.* 47:522–526.
- Maes, A., and A. Cremers. 1977. Charge density effects in ion exchange. Part 1. Heterovalent exchange equilibria. *J. Chem. Soc. Faraday Trans. 1.* 73:1807–1814.
- Markgraf, W., R. Horn, and S. Peth. 2006. An approach to rheometry in soil mechanics—Structural changes in bentonite, clayey and silty soils. *Soil Till. Res.* 91:1–14.
- Mashal, K., J.B. Harsh, M. Flury, A.R. Felmy, and H. Zhao. 2004. Colloid formation in Hanford sediments reacted with simulated tank waste. *Environ. Sci. Technol.* 38:5750–5756.
- Mavrocordatos, D., D. Perret, and G.D. Leppard. 2007. Strategies and advances in the characterization of environmental colloids by electron microscopy, p. 345–404. *In* K.J. Wilkinson

- and J.R. Lead (eds.) Environmental colloids and particles: Behavior, structure and characterization. IUPAC series on analytical and physical chemistry of environmental systems. John Wiley & Sons, Chichester, U.K.
- McBride, M.B. 1989. Surface chemistry of soil minerals, p. 35–88. *In* J.B. Dixon and S.B. Weed (eds.) Minerals in soil environments, 2nd Ed. Soil Sci. Soc. Am. Book Ser. 1. SSSA, Madison, WI.
- McBride, M.B. 1994. Environmental chemistry of soils. Oxford University Press, New York.
- McBride, M.B., and P. Baveye. 2002. Diffuse double-layer models, long-range forces, and ordering in clay colloids. *Soil Sci. Soc. Am. J.* 66:1207–1217.
- McCarthy, J.F., and C. Degueldre. 1993. Sampling and characterization of colloids and particles in groundwater for studying their role in contaminant transport, p. 247–315. *In* J. Buffle and H.P. van Leeuwen (eds.) Environmental particles, Vol. 2. Lewis Publishers, Ann Arbor, MI.
- McCarthy, J.F., and L.D. McKay. 2004. Colloid transport in the subsurface: Past, present, and future challenges. *Vadose Zone J.* 3:326–337.
- McCarthy, J.F., L.D. McKay, and D.D. Bruner. 2002. Influence of ionic strength and cation charge on transport of colloidal particles in fractured shale saprolite. *Environ. Sci. Technol.* 36:3735–3743.
- McCarthy, J.E., and J.M. Zachara. 1989. Subsurface transport of contaminants. *Environ. Sci. Technol.* 23:496–502.
- McDowell-Boyer, L.M. 1992. Chemical mobilization of micron-sized particles in saturated porous media under steady flow conditions. *Environ. Sci. Technol.* 26:586–593.
- McDowell-Boyer, L.M., J.R. Hunt, and N. Sitar. 1986. Particle transport through porous media. *Water Resour. Res.* 22:1901–1921.
- McKenzie, R.M. 1989. Manganese oxides and hydroxides, p. 439–465. *In* J.B. Dixon and S.B. Weed (eds.) Minerals in soil environments, 2nd Ed. SSSA Inc., Madison, WI.
- Miano, F., and M.R. Rabaioli. 1994. Rheological scaling of montmorillonite suspensions: The effect of electrolytes and poly-electrolytes. *Colloids Surf. A* 84:229–237.
- Miller, W.P., and M.K. Baharuddin. 1986. Relationship of soil dispersibility to infiltration and erosion of southeastern soils. *Soil Sci. Soc. Am. J.* 54:346–351.
- Miller, W.P., H. Frenkel, and K.D. Newman. 1990. Flocculation concentration and sodium/calcium exchange of kaolinitic soil clays. *Soil Sci. Soc. Am. J.* 54:346–351.
- Miller, W.P., and D.E. Radcliffe. 1992. Soil crusting in the southeastern United States, p. 233–266. *In* M.E. Sumner and B.A. Stewart (eds.) Soil crusting: Chemical and physical processes. Lewis Publishers, Boca Raton, FL.
- Mills, W.B., S. Liu, and F.K. Fong. 1991. Literature review and model (comet) for colloid/metals transport in porous media. *Ground Water* 29:199–208.
- Murphy, D.M., J.R. Garbarino, H.W. Taylor, B.T. Hart, R. Beckett. 1993. Determination of size and element composition distributions of complex colloids by sedimentation field-flow fractionation-inductively coupled plasma mass spectrometry. *J. Chromatogr.* 642:459–467.
- Napper, D.H., and R.J. Hunter. 1974. Hydrosols, p. 161–213. *In* M. Kerker (ed.) M.T.P. Int. Rev. Sci. Phys. Chem. Ser. Butterworths, London, U.K.
- Nelson, P.N., and J.M. Oades. 1998. Organic matter, sodicity and soil structure. p. 51–75. *In* M.E. Sumner and R. Naidu (eds.) Sodic soils: Distribution, properties, management and environmental consequences. Oxford University Press, New York.
- Newman, A.C.D. 1983. The specific surface of soils determined by water sorption. *Soil Sci.* 34:23–32.
- Newman, M.E., M. Filella, Y.W. Chen, J.C. Negre, D. Perret, and J. Buffle. 1994. Submicron particles in the Rhine river. 2. Comparison of field observations and model predictions. *Water Res.* 28:107–118.
- Nishimura, S., M. Kodama, K. Yao, Y. Imai, and H. Tateyama. 2002b. Direct surface force measurement for synthetic smectites using the atomic force microscope. *Langmuir* 18:4681–4688.
- Nishimura, S., H. Tateyama, K. Tsunematsu, and K. Jinnai. 1992. Zeta potential measurement of muscovite mica basal plane-aqueous solution interface by means of plane interface technique. *J. Colloid Interface Sci.* 152:359–367.
- Nishimura, S., K. Yao, M. Kodama, Y. Imai, K. Ogino, and K. Mishima. 2002a. Electrokinetic study of synthetic smectites by flat plate streaming potential technique. *Langmuir* 18:188–193.
- Norrish, K., and J.A. Rausell-Colom. 1961. Low-angle X-ray diffraction studies of the swelling of montmorillonite and vermiculite. *Clays Clay Miner.* 10:123–149.
- Ohtsubo, M., A. Yoshimura, S.-I. Wada, and R.N. Yong. 1991. Particle interaction and rheology of illite-iron oxide complexes. *Clays Clay Miner.* 39:347–354.
- O’Melia, C.R., and C.L. Tiller. 1993. Physicochemical aggregation and deposition in aquatic environments, p. 353–385. *In* J. Buffle and H. van Leeuwen (eds.) Environmental particles, Vol. 2. Lewis Publishers, Boca Raton, FL.
- Overbeek, J.Th.G. 1952. Stability of hydrophobic colloids and emulsions. p. 302–341. *In* H.R. Kryt (ed.) *J. Colloid Sci.* Vol. 1, Elsevier, Amsterdam.
- Parker, J.C., L.W. Zelazny, S. Sampath, and W.G. Harris. 1979. A critical evaluation of the extension of zero point of charge (ZPC) theory to soil systems. *Soil Sci. Soc. Am. J.* 43:668–674.
- Pashley, R.M. 1981. DLVO and hydration forces between mica surfaces in Li<sup>+</sup>, Na<sup>+</sup>, K<sup>+</sup>, and Cs<sup>+</sup> electrolyte solutions: A correlation of double-layer and hydration forces with surface cation. *J. Colloid Interface Sci.* 83:531–546.
- Pashley, R.M., and J.P. Quirk. 1984. The effect of cation valency on DLVO and hydration forces between macroscopic sheets of muscovite mica in relation to clay swelling. *Colloids Surf.* 9:1–17.
- Pecora, R. 1983. Quasi-elastic light scattering of macromolecules and particles in solution and suspension, p. 3–30. *In* B.E. Dahneke (ed.) Measurement of suspended particles by quasi-elastic light scattering. John Wiley & Sons, New York.



- Perret, D., M.E. Newman, J.C. Negre, Y.W. Chen, and J. Buffle. 1994. Submicron particles in the Rhine river. 1. Physicochemical characterization. *Water Res.* 28:91-106.
- Pennell, K.D., S.A. Boyd, and L.M. Abriola. 1995. Surface area of soil organic matter reexamined. *Soil Sci. Soc. Am. J.* 59:1012-1018.
- Quirk, J.P. 1994. Interparticle forces: A basis for the interpretation of soil physical behavior. *Adv. Agron.* 53:121-183.
- Quirk, J.P., and L.A.G. Aylmore. 1971. Domain and quasi-crystalline regions in clay systems. *Proc. Soil Sci. Soc. Am.* 35:652-654.
- Quirk, J.P., and R.S. Murray. 1991. Towards a model for soil structural behavior. *Aust. J. Soil Res.* 29:829-867.
- Quirk, J.P., and R.K. Schofield. 1955. The effect of electrolyte concentration on soil permeability. *J. Soil Sci.* 6:163-178.
- Rand, B., and I.E. Melton. 1977. Particle interactions in aqueous kaolinite suspensions. I. Effect of pH and electrolyte upon the mode of particle interaction in homoionic sodium kaolinite suspensions. *J. Colloid Interface Sci.* 60:308-320.
- Rand, B., E. Pekenc, J.W. Goodwin, and R.W. Smith. 1980. Investigation into the existence of edge-face coagulated structures in Na-montmorillonite suspensions. *J. Chem. Soc. Faraday Trans. 1* 76:225-235.
- Ranville, J.F., D.J. Chittleborough, and R. Beckett. 2005. Particle-size and element distributions of soil colloids: Implications for colloid transport. *Soil Sci. Soc. Am. J.* 69:1173-1184.
- Ranville, J.F., D.J. Chittleborough, F. Sanks, R.J.S. Morrison, T. Harris, F. Doss, et al. 1999. Development of sedimentation field-flow fractionation-inductively coupled plasma mass-spectroscopy for the characterization of environmental colloids. *Anal. Chim. Acta* 381:315-329.
- Redman, J.A., S.L. Walker, and M. Elimelech. 2004. Bacterial adhesion and transport in porous media: Role of the secondary energy minimum. *Environ. Sci. Technol.* 38:1777-1785.
- Rees, L.B. 1990. A Monte-Carlo approach to x-ray attenuation corrections for proton-induced x-ray-emission from particulate samples. *Nucl. Instrum. Meth. Phys. Res. Sect. A* 299:614-617.
- Rockhold, M.L., R.R. Yarwood, and J.S. Selker. 2004. Coupled microbial and transport processes in soil. *Vadose Zone J.* 3:368-383.
- Ronen, D., M. Magaritz, U. Weber, A.J. Amiel, and E. Klein. 1992. Characterization of suspended particles collected in groundwater under natural gradient flow conditions. *Water Resour. Res.* 28:1279-1291.
- Ross, G. 1978. Relationships of specific surface area and clay content to shrink-swell potential of soils having different clay mineralogical compositions. *Can. J. Soil Sci.* 58:159-166.
- Roy, S.B., and D.A. Dzombak. 1996. Colloid release and transport processes in natural and model porous media. *Colloids Surf. A* 107:245-262.
- Roy, S.B., and D.A. Dzombak. 1997. Chemical factors influencing colloid-facilitated transport of contaminants in porous media. *Environ. Sci. Technol.* 37:656-664.
- Roy, S.B., and D.A. Dzombak. 1998. Sorption nonequilibrium effects on colloid-enhanced transport of hydrophobic compounds in porous media. *J. Contam. Hydrol.* 30:179-200.
- Ryan, J.N., and M. Elimelech. 1996. Colloid mobilization and transport in groundwater. *Colloids Surf. A* 107:1-56.
- Ryan, J.N., and P.M. Gschwend. 1990. Colloid mobilization in two Atlantic Coastal Plain aquifers: Field studies. *Water Resour. Res.* 26:307-322.
- Ryan, J.N., and P.M. Gschwend. 1994. Effect of solution chemistry on clay colloid release from an iron oxide-coated aquifer sand. *Environ. Sci. Technol.* 28:1717-1726.
- Ryan, J.N., T.H. Illangsekare, M.I. Litaor, and R. Shannon. 1998. Particle and plutonium mobilization in macroporous soils during rainfall simulations. *Environ. Sci. Technol.* 32:476-482.
- Scales, P.J., F. Grieser, and T.W. Healy. 1990. Electrokinetics of the muscovite mica-aqueous solution interface. *Langmuir* 6:582-589.
- Schofield, R.K. 1949. Calculation of surface areas of clays from measurements of negative adsorption. *Trans. Br. Ceram. Soc.* 48:207-213.
- Schofield, R.K., and H.R. Samson. 1954. Flocculation of kaolinite due to the attraction of oppositely charged crystal faces. *Discuss. Faraday Soc.* 18:135-145.
- Schramm, L.L., and J.C.T. Kwak. 1982a. Influence of exchangeable cation composition on the size and shape of montmorillonite particles in dilute suspensions. *Clays Clay Miner.* 30:40-48.
- Schramm, L.L., and J.C.T. Kwak. 1982b. Interactions in clay suspensions: The distribution of ions in suspension and the influence of tactoid formation. *Colloids Surf.* 3:43-60.
- Schulthess, C.P., and D.L. Sparks. 1986. Backtitration technique for proton isotherm modeling of oxide surfaces. *Soil Sci. Soc. Am. J.* 50:1406-1411.
- Schultz, D.S. 1997. Electroosmosis technology for soil remediation: Laboratory results, field trial, and economic modeling. *J. Hazard. Mater.* 55:81-91.
- Schulze, D.G. 2002. An introduction to soil mineralogy, p. 1-35. *In* J.B. Dixon and D.G. Schulze (eds.) *Soil mineralogy with environmental applications*. SSSA, Madison, WI.
- Schurtenberger, P., and M.E. Newman. 1993. Characterization of biological and environmental particles using static and dynamic light scattering, p. 37-115. *In* J. Buffle and H.P. van Leeuwen (eds.) *Environmental particles*, Vol. 2. Lewis Publishers, Ann Arbor, MI.
- Schwertmann, U., and R.M. Taylor. 1977. Iron oxides, p. 145-180. *In* J.B. Dixon and S.B. Weed (eds.) *Minerals in soil environments*. SSSA Inc., Madison, WI.
- Seaman, J.C. 2000. Thin-foil SEM analysis of soil and groundwater colloids: Reducing instrument and operator bias. *Environ. Sci. Technol.* 34:187-191.
- Seaman, J.C., and P.M. Bertsch. 2000. Selective colloid mobilization through surface-charge manipulation. *Environ. Sci. Technol.* 34:3749-3755.

- Seaman, J.C., P.M. Bertsch, and W.P. Miller. 1995. Chemical controls on colloid generation and transport in a sandy aquifer. *Environ. Sci. Technol.* 29:1808–1815.
- Seaman, J.C., P.M. Bertsch, and R.N. Strom. 1997. Characterization of colloids mobilized from southeastern coastal plain sediments. *Environ. Sci. Technol.* 31:2782–2790.
- Seaman, J.C., M. Guerin, B.P. Jackson, P.M. Bertsch, and J.F. Ranville. 2003. Analytical techniques for characterizing complex mineral assemblages: Mobile soil and groundwater colloids, p. 271–309. *In* H.M. Selim and W.L. Kingery (eds.) *Geochemical and hydrological reactivity of heavy metals in soils*. CRC Press, Washington, DC.
- Secor, R.B., and C.J. Radke. 1985. Spillover of the diffuse double layer on montmorillonite particles. *J. Colloid Interface Sci.* 103:237–244.
- Seta, A.K., and A.D. Karathanasis. 1996. Colloid-facilitated transport of metolachlor through intact soil columns. *J. Environ. Sci. Health B* 31:949–968.
- Seta, A.K., and A.D. Karathanasis. 1997. Atrazine adsorption by soil colloids and co-transport through subsurface environments. *Soil Sci. Soc. Am. J.* 61:612–617.
- Shainberg, I., and H. Otoh. 1968. Size and shape of montmorillonite particles saturated with Na/Ca ions (inferred from viscosity and optical measurements). *Isr. J. Chem.* 6:251–259.
- Shainberg, I., J.D. Rhoades, and R.J. Prather. 1981. Effect of low electrolyte concentration on clay dispersion and hydraulic conductivity of a sodic soil. *Soil Sci. Soc. Am. J.* 45:273–277.
- Shapiro, A.P., and R.F. Probst. 1993. Removal of contaminants from saturated clay by electroosmosis. *Environ. Sci. Technol.* 27:283–291.
- Sharma, M.M., H. Chamoun, D.H.S.S.R. Sarma, and R.S. Schecter. 1992. Factors controlling the hydrodynamic attachment of particles from surfaces. *J. Colloid Interface Sci.* 149:121–134.
- Sherard, J.L., L.P. Dunningan, and R.S. Decker. 1977. Identification and nature of dispersive soils. *J. Geotech. Eng. Am. Soc. Chem. Eng.* 4:287–301.
- Simunek, J., C. He, L. Pang, and S.A. Bradford. 2006. Colloid-facilitated solute transport in variably saturated porous media: Numerical model and experimental verification. *Vadose Zone J.* 5:1035–1047.
- Sinton, L.W., M.J. Noonan, R.K. Finlay, L. Pang, and M.E. Close. 2000. Transport and attenuation of bacteria and bacteriophages in an alluvial gravel aquifer. *N.Z. J. Mar. Freshwater Res.* 34:175–186.
- Sirivithayapakorn, S., and A. Keller. 2003. Transport of colloids in unsaturated porous media: A pore-scale observation of processes during the dissolution of air–water interface. *Water Resour. Res.* 39:SBH 6/1–6/10.
- Smalley, M.V. 1990. Electrostatic interaction in macro-ionic solutions and gels. *Mol. Phys.* 71:1251–1267.
- Sogami, I., and N. Ise. 1984. On the electrostatic interaction in macroionic solutions. *J. Chem. Phys.* 81:6320–6332.
- Sposito, G. 1984. *The surface chemistry of soils*. Oxford University Press, New York.
- Stevenson, F.J. 1982. *Humus chemistry. Genesis, composition, reactions*. John Wiley & Sons, New York.
- Suarez, D.L., J.D. Rhoades, R. Lavado, and C.M. Grieve. 1984. Effect of pH on saturated hydraulic conductivity and soil dispersion. *Soil Sci. Soc. Am. J.* 48:50–55.
- Sun, Y.-P., X.-Q. Li, J. Cao, W.-X. Zhang, and H.P. Wang. 2006. Characterization of zero-valent iron nanoparticles. *Adv. Colloid Interface Sci.* 120:47–56.
- Supak, J.R., A.R. Swoboda, and J.B. Dixon. 1978. Adsorption of aldicarb by clays and soil organo-clay complexes. *Soil Sci. Soc. Am. J.* 42:244–248.
- Swartz, C.H., and P.M. Gschwend. 1998. Mechanisms controlling release of colloids to groundwater in a southeastern coastal plain aquifer sand. *Environ. Sci. Technol.* 32:1779–1785.
- Taboada-Serrano, P., V. Vithayaveroj, S. Yiacoumi, and C. Tsouris. 2005. Surface charge heterogeneities measured by atomic force microscopy. *Environ. Sci. Technol.* 39:6352–6360.
- Tarchitzky, J., Y. Chen, and A. Banin. 1993. Humic substances and pH effects on sodium and calcium-montmorillonite flocculation and dispersion. *Soil Sci. Soc. Am. J.* 57:367–372.
- Theng, B.K., and G. Yuan. 2008. Nanoparticles in the soil environment. *Elements* 4:395–399.
- Tiller, K.G., and L.H. Smith. 1990. Limitations of EGME retention to estimate the surface area of soils. *Aust. J. Soil Res.* 28:1–26.
- Tombácz, E., J. Balázs, J. Lakatos, and F. Szántó. 1989. Influence of the exchangeable cations on stability and rheological properties of montmorillonite suspensions. *Colloid Polym. Sci.* 267:1016–1025.
- Torkzaban, S., S.S. Tazehkand, S.L. Walker, and S.A. Bradford. 2008. Transport and fate of bacteria in porous media: Coupled effects of chemical conditions and pore space geometry. *Water Resour. Res.* 44:W04403, doi: 10.1029/2007WR006541.
- Tufenkji, N. 2007. Modeling microbial transport in porous media: Traditional approaches and recent developments. *Adv. Water Resour.* 30:1455–1469.
- Tufenkji, N., and M. Elimelech. 2004a. Correlation equation for predicting single-collector efficiency in physicochemical filtration in saturated porous media. *Environ. Sci. Technol.* 38:529–536.
- Tufenkji, N., and M. Elimelech. 2004b. Deviation from the classical colloid filtration theory in the presence of repulsive DLVO interactions. *Langmuir* 20:10818–10828.
- Tufenkji, N., and M. Elimelech. 2005. Breakdown of colloid filtration theory: Role of the secondary energy minimum and surface charge heterogeneities. *Langmuir* 21:841–852.
- Tufenkji, N., J.A. Redman, and M. Elimelech. 2003. Interpreting deposition patterns of microbial particles in laboratory-scale column experiments. *Environ. Sci. Technol.* 37:616–623.
- van de Weerd, H., and A. Leijnse. 1997. Assessment of the effect of kinetics on colloid facilitated radionuclide transport in porous media. *J. Contam. Hydrol.* 26:245–256.
- van Olphen, H. 1977. *An introduction to clay colloid chemistry*, 2nd Ed. John Wiley & Sons, New York.

- Verwey, E.J.W., and J.Th.G. Overbeek. 1948. Theory of stability of lyophobic colloids. Elsevier, Amsterdam, the Netherlands.
- Vinten, A.J.A., B. Yaron, and P.H. Nye. 1983. Vertical transport of pesticides when adsorbed on suspended particles. *J. Agric. Food Chem.* 31:662–664.
- Von Gunten, H.R., U.E. Warber, and U. Krahenbuhl. 1988. The reactor accident at Chernobyl: A possibility to test colloid-controlled transport of radionuclides in a shallow aquifer. *J. Contam. Hydrol.* 2:237–247.
- von Smoluchowski, M. 1916. Three discourses on diffusion, Brownian movements, and the coagulation of colloid particles. *Phys. Z.* 17:557–571, 585–599.
- von Smoluchowski, M. 1917. Mathematical theory of the kinetics of the coagulation of colloidal suspensions. *Z. Phys. Chem.* 92:129–168.
- Walker, S.L., J.A. Redman, and M. Elimelech. 2004. Role of cell surface lipopolysaccharides in *Escherichia coli* K12 adhesion and transport. *Langmuir* 20:7736–7746.
- Wan, J., and J.L. Wilson. 1994. Visualization of the role of the gas–water interface on the fate and transport of colloids in porous media. *Water Resour. Res.* 30:11–23.
- Waychunas, G.A., and H. Zhang. 2008. Structure, chemistry, and properties of mineral nanoparticles. *Elements* 4:381–387.
- Wilding, L.P., N.E. Smeck, and L.R. Drees. 1977. Silica in soils: Quartz, cristobalite, tridymite, and opal, p. 471–552. In J.B. Dixon and S.B. Weed (eds.) *Minerals in soil environments*. SSSA Inc., Madison, WI.
- Wilkinson, K.J., and J.R. Lead. 2007. *Environmental colloids and particles: Behavior, structure and characterization*. IUPAC series on analytical and physical chemistry of environmental systems. John Wiley & Sons, Chichester, U.K.
- Yao, K.M., T. Habibian, and C.R. O’Melia. 1971. Water and waste water filtration, concepts and applications. *Environ. Sci. Technol.* 5:1105–1112.
- Yong, R.N., A.J. Sadh, H.P. Ludwig, and M.A. Jorgensen. 1979. Interparticle action and rheology of dispersive clays. *J. Geotech. Eng. Div.* 105:1193–1209.
- Zhao, H., S. Bhattacharjee, R. Chow, D. Wallace, J.H. Masliyah, and Z. Xu. 2008. Probing surface charge potentials of clay basal planes and edges by direct force measurements. *Langmuir* 24:12899–12910.
- Zhao, H., P.F. Low, and J.M. Bradford. 1991. Effects of pH and electrolyte concentration on particle interaction in three homoionic sodium soil clay suspensions. *Soil Sci.* 151:196–207.



# Ion Exchange Phenomena

16.1	Introduction .....	16-1
16.2	Surface Charge and Ion Exchange Capacities.....	16-2
16.3	Ion Exchange Thermodynamics.....	16-4
16.4	Trends in ${}^{\vee}K$ and ${}^{\text{ex}}K$ .....	16-5
	Smectites • Micaceous Minerals • Soils and Sediments	
16.5	Ion Exchange and Chemical Speciation Models.....	16-8
	Modeling Ion Exchange as a Surface Complexation Process • Modeling Ion Exchange as a Solid-Solution Process	
16.6	Micro- and Nanoscale Perspectives on Ion Exchange Selectivity .....	16-9
	Molecular-Scale Coordination and Dynamics of Exchangeable Ions • Coupling between Cation Exchange and Exchanger Structure	
	References.....	16-11

Ian C. Bourg

University of California

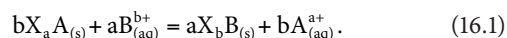
Garrison Sposito

University of California, Berkeley

## 16.1 Introduction

Ion exchange phenomena involve the population of *readily exchangeable ions*, the subset of adsorbed solutes that balance the intrinsic surface charge and can be readily replaced by major background electrolyte ions (Sposito, 2008). These phenomena have occupied a central place in soil chemistry research since Way (1850) first showed that potassium uptake by soils resulted in the release of an equal quantity of moles of charge of calcium and magnesium. Ion exchange phenomena are now routinely modeled in studies of soil formation (White et al., 2005), soil reclamation (Kopittke et al., 2006), soil fertilization (Agbenin and Yakubu, 2006), colloidal dispersion/flocculation (Charlet and Tournassat, 2005), the mechanics of argillaceous media (Gajo and Loret, 2007), aquitard pore water chemistry (Tournassat et al., 2008), and groundwater (Timms and Hendry, 2007; McNab et al., 2009) and contaminant hydrology (Chatterjee et al., 2008; van Oploo et al., 2008; Serrano et al., 2009).

The prototypical chemical reaction equation for the exchange of cations  $A^{a+}$  and  $B^{b+}$  can be written as follows if  $X^-$  represents a mole of negative charge carried by the solid exchanger:



Equation 16.1 can be modified in a straightforward manner to describe anion exchange reactions on positively charged surface sites. An example of Equation 16.1 of importance to sodicity

and the physical properties of soils is the heterovalent Na–Ca exchange reaction:

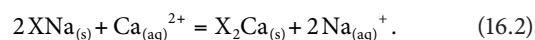
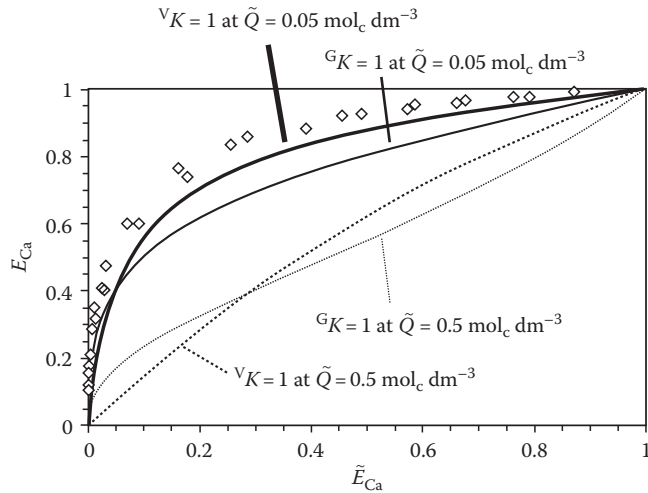


Figure 16.1 shows an experimental *ion exchange isotherm* for the binary Na–Ca exchange reaction on a montmorillonitic soil (Fletcher and Sposito, 1984a), plotted as the fractional contribution of  $Ca^{2+}$  to the total adsorbed charge of exchangeable cations ( $E_{Ca} = q_{Ca}/Q$ , where  $q_i = z_i n_i$  is the adsorbed charge of species  $i$  in  $\text{mol}_c \text{ kg}^{-1}$  of solid,  $z_i$  and  $n_i$  being the valence of  $i$  and the moles of adsorbed  $i$  per kilogram of solid, respectively, and  $Q = \sum_i q_i$ ) against its fractional contribution to the charge concentration of all cations in solution ( $\tilde{E}_{Ca} = z_{Ca} C_{Ca} / \tilde{Q}$ , where  $C_i$  is the molar concentration of species  $i$  [ $\text{mol dm}^{-3}$ ] and  $\tilde{Q} = \sum_i z_i C_i$ ). The convexity of the isotherm in Figure 16.1 is typical of the competitive adsorption of the higher-valence ion in heterovalent exchange reactions. As shown below, however, this convexity does not imply selectivity or thermodynamic preference of the solid exchanger for  $Ca^{2+}$  vs.  $Na^+$ .

For practical applications, ion exchange isotherms are fitted with a variety of empirical one- or two-parameter models. The most widely used one-parameter models are those introduced by Vanselow (1932), Gapon (1933), and Gaines and Thomas (1953):

$${}^{\vee}K_A^B = \frac{x_B^a (A^{a+})^b}{x_A^b (B^{b+})^a} \quad (\text{Vanselow}), \quad (16.3)$$



**FIGURE 16.1** Binary Na–Ca ion exchange isotherm on a montmorillonitic soil at  $\tilde{Q} = 0.05 \text{ mol}_c \text{ dm}^{-3}$  (diamonds, Fletcher et al. (1984b)) plotted as  $E_{Ca}$  vs.  $\tilde{E}_{Ca}$ . Nonselective isotherms were calculated for the Vanselow (thick lines) and Gapon conventions (thin lines) at  $\tilde{Q} = 0.05$  and  $0.5 \text{ mol dm}^{-3}$  (solid lines and dashed lines, respectively).

$${}^G K_A^B = \frac{E_B (A^{a+})^{1/a}}{E_A (B^{b+})^{1/b}} \quad (\text{Gapon}), \quad (16.4)$$

$${}^{GT} K_A^B = \frac{E_B^a (A^{a+})^b}{E_A^b (B^{b+})^a} \quad (\text{Gaines and Thomas}), \quad (16.5)$$

where

${}^V K$ ,  ${}^G K$ , and  ${}^{GT} K$  are the Vanselow, Gapon, and Gaines–Thomas *selectivity coefficients*, respectively

$(A^{a+})$  is the thermodynamic activity of  $A^{a+}$  in aqueous solution

$x_A$  is the fractional contribution of  $A^{a+}$  to the total number of moles of exchangeable cations ( $x_A = n_A / \sum_i n_i$ )

By definition, nonselective (or nonpreference) Na–Ca binary exchange isotherms are obtained if  ${}^V K = 1$ ,  ${}^G K = 1$ , or  ${}^{GT} K = 1$ ; examples are plotted in Figure 16.1 for  $\tilde{Q} = 0.05 \text{ mol dm}^{-3}$  (solid lines) and  $\tilde{Q} = 0.5 \text{ mol dm}^{-3}$  (dashed lines). Clearly, despite its name, nonselective exchange can differ among models and produce a strong,  $\tilde{Q}$ -dependent adsorption of the higher-valence ion; caution should therefore be used in assigning underlying mechanistic significance to isotherm shapes or selectivity coefficient values.

The most popular two-parameter model is the Rothmund–Kornfeld type model, in which the ratio of solute activities in Equations 16.3 through 16.5 is raised to a fitted power  $n$  (Bond, 1995). The Rothmund–Kornfeld model based on Equation 16.3, for example, is (Bond, 1995):

$${}^{VRK} K_A^B = \frac{x_B^a}{x_A^b} \left[ \frac{(A^{a+})^b}{(B^{b+})^a} \right]^n. \quad (16.6)$$

## 16.2 Surface Charge and Ion Exchange Capacities

As noted above, ion exchange phenomena involve adsorption reactions that balance the intrinsic surface charge of soil particles. The intrinsic surface charge density  $\sigma_{in}$  ( $\text{mol}_c \text{ kg}^{-1}$ ) is the sum of the net structural surface charge density  $\sigma_0$  ( $\text{mol kg}^{-1}$ ) and the net proton surface charge density  $\sigma_H$  ( $\text{mol kg}^{-1}$ ) (Sposito, 1998, 2008):

$$\sigma_{in} \equiv \sigma_0 + \sigma_H. \quad (16.7)$$

The net structural (“permanent”) surface charge density  $\sigma_0$  results from crystalline defects, such as isomorphous substitutions of Si(IV), Al(III), or Mg(II) by lower-valence cations in 2:1 phyllosilicates (smectites, vermiculites, illites, and micas; Figure 16.2a); for these 2:1 phyllosilicates,  $\sigma_0$  contributes dominantly to  $\sigma_{in}$  and is invariably negative. The net proton (“variable”) surface charge density  $\sigma_H$  (the difference between the moles of protons and the moles of hydroxide ions complexed by surface functional groups ( $\sigma_H = q_H - q_{OH}$ )) results from Brønsted acid surface groups with a pH-dependent charge, such as hydroxyl, carboxyl, or phenol groups (Figure 16.2b); it is predominant in natural organic matter, kaolinite, and oxide minerals and can be negative, zero, or positive depending on pH, ionic strength, and other conditions.

Charge balance at solid–water interfaces imposes that  $\Delta q$ , the sum of the adsorbed ion charge densities  $q_i$  of all species except surface-complexed  $H^+$  and  $OH^-$  ions, equals the opposite of the intrinsic surface charge density (Sposito, 1998, 2008):

$$\sigma_0 + \sigma_H + \Delta q = 0. \quad (16.8)$$

The net adsorbed ion charge  $\Delta q$  can be expressed as a sum of the net charge of ions adsorbed in the Stern layer ( $\sigma_s$ ) (ions immobile on timescales  $>10 \text{ ps}$  [Sposito et al., 1999]) or in the diffuse ion swarm ( $\sigma_d$ ). The Stern layer charge component can be further divided into the contributions of inner-sphere ( $\sigma_{is}$ ) and outer-sphere ( $\sigma_{os}$ ) surface complexes (formed by direct contact of surface functional groups or through one or more interposed water molecules, respectively) to yield the expression (Sposito, 1998, 2008):

$$\Delta q = \sigma_{is} + \sigma_{os} + \sigma_d. \quad (16.9)$$

The utility of Equation 16.9 depends on the extent to which the molecular-scale coordination of adsorbed ions can be determined. Equations 16.7 and 16.8 show that  $\sigma_{in}$  and  $\Delta q$  can vary significantly with pH, ionic strength, and other variables that influence  $\sigma_H$ , especially in soils with low permanent structural charge (i.e., soils poor in 2:1 phyllosilicates). Experimental data on  $\Delta q$  vs.  $\sigma_H$  for a kaolinitic tropical soil suspended in

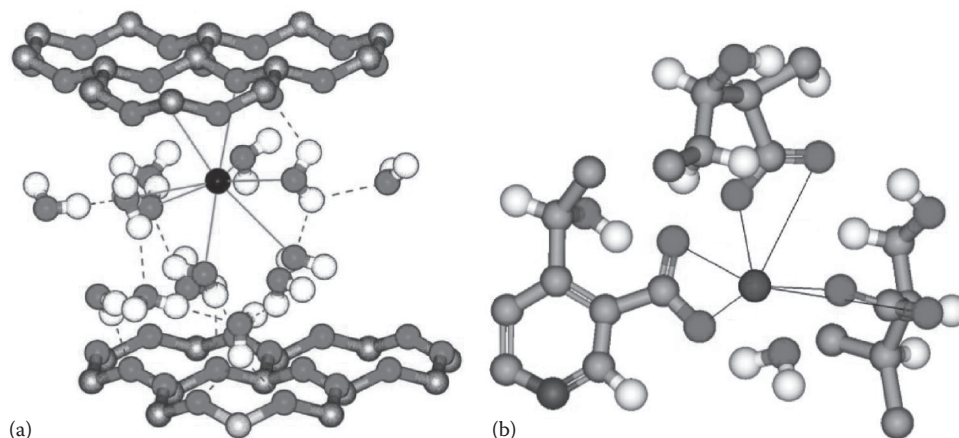


**FIGURE 16.2** Major types of ion exchange sites in natural materials: (a) clay siloxane surfaces located near a site of isomorphous substitution (shown only as the basal surface O atoms (matte gray) and tetrahedral sheet Si atoms (shiny gray) of two stacked smectite lamellae with a K<sup>+</sup> ion (black, forming an inner-sphere surface complex) and nearby water molecules in the interlayer space. (From Sposito, G., N.T. Skipper, R. Sutton, S.-H. Park, A.K. Soper, and J.A. Greathouse. 1999. Surface geochemistry of the clay minerals. Proc. Natl. Acad. Sci. U. S. A. 96:3358–3364. Copyright 1999 National Academy of Sciences, U.S.A.) (b) pH-dependent sites resulting from the deprotonation of Lewis acid groups on organic matter or mineral oxide surfaces (here three carboxyl groups of natural organic matter (with O atoms in matte gray) coordinating an almost completely desolvated Ca<sup>2+</sup> ion (central dark gray atom)). (From Sutton, R., G. Sposito, M.S. Diallo, and H.-R. Schulten. 2005. Molecular simulation of a model of dissolved organic matter. Environ. Toxicol. Chem. 24:1902–1911. Copyright Wiley-VCH Verlag GmbH & Co. KGaA. With permission.)

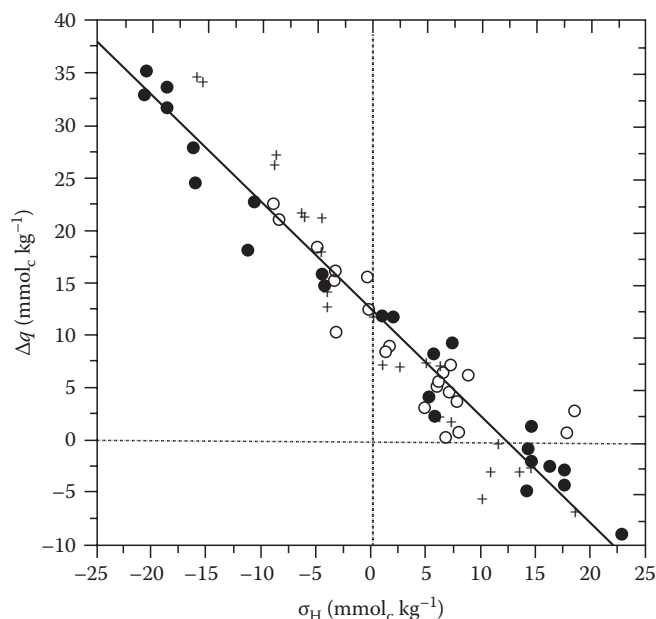


**FIGURE 16.3** “Chorover plot” (Chorover and Sposito, 1995) of the net adsorbed ion charge against the net proton surface charge density for a Brazilian oxisol (Manaus soil). The combined data, for ionic strengths of 0.001 (open circles), 0.005 (crosses), and 0.01 (filled circles) mol kg<sup>-1</sup>, can be fit to the regression equation (solid line):  $\Delta q = -1.01(\pm 0.07)\sigma_H + 12.5(\pm 0.8)$ , where  $\Delta q$  and  $\sigma_H$  are in mmol<sub>c</sub> kg<sup>-1</sup>. Charge balance is confirmed by the values of the slope and both intercepts ( $\sigma_0 = 12.5 \pm 0.4$  mmol<sub>c</sub> kg<sup>-1</sup> in direct measurement). (From *Geochim. Cosmochim. Acta*, 59, Chorover, J. and Sposito, G., Surface charge characteristics of kaolinitic tropical soils, 875–884, Copyright 1995, with permission from Elsevier.)

LiCl solutions of varying ionic strength and pH (Figure 16.3) confirm the inverse relationship between  $\Delta q$  and  $\sigma_H$  in Equation 16.8 and the strong dependence of intrinsic surface charge density on experimental conditions. Thus, measured ion exchange isotherms and Q values for such variable-charge soils may be highly sensitive to pH and other conditions that determine  $\sigma_H$ .

The pH dependence of surface charge is characterized by points of zero charge, pH values at which one or more of the surface charge components in Equations 16.8 and 16.9 vanishes at fixed temperature, applied pressure, and aqueous solution composition (Sposito, 1998, 2008). For example, the pH value at which  $\sigma_{in} = 0$  (where adsorbed cation and anion charge densities are equal according to Equations 16.7 and 16.8) is the point of zero net charge (p.z.n.c.). Nomenclature for these points of zero charge is listed in Table 16.1. Unfortunately, previous terminology for the points of zero charge has been highly erratic (e.g., both the p.z.s.e. and the p.z.n.c. have been termed points of zero charge, while the p.z.n.p.c. has been termed zero point of charge). Furthermore, the points of zero charge frequently have been indirectly determined from experimental data on electrophoretic mobility or particle flocculation (calculations sensitive

**TABLE 16.1** Points of Zero Charge

Symbol	Name	Definition
p.z.n.c.	Point of zero net charge	$\sigma_{in} = 0$
p.z.n.p.c.	Point of zero net proton charge	$\sigma_H = 0$
p.z.c.	Point of zero charge	$\sigma_p = 0^a$
p.z.s.e.	Point of zero salt effect	$\partial\sigma_H/\partial I = 0$

<sup>a</sup>  $\sigma_p$  ( $\equiv \sigma_0 + \sigma_H + \sigma_{IS} + \sigma_{OS}$ ) is the net particle surface charge density.

**TABLE 16.2** Typical Cation Exchange Capacities (CEC, in mol<sub>c</sub> kg<sup>-1</sup>) of Soils and Major Soil Constituents

Solid	CEC
Soils	0.01–1.4
Natural organic matter	0.8–10 <sup>a</sup>
Vermiculite	1.6–2.5
Smectite	0.7–1.7
Illite	0.2
Mica	0.1
Kaolinite	<0.05

<sup>a</sup> Increasing with pH and in the order peat < humic acid.

Source: Sposito, G. 2004. The surface chemistry of natural particles. Oxford University Press, Oxford, U.K.; Sposito, G. 2008. The surface chemistry of soils. 2nd edn. Oxford University Press, Oxford, U.K.

to the assumed distribution and mobility of ions in the electrical double layer [Fair and Anderson, 1989; Hunter, 1993]) or from acid–base titrations of solid suspensions (calculations that often use untested assumptions on the initial value of the net proton surface charge [Sposito, 1998; Bourg et al., 2007]).

If all adsorbed ions (except surface-complexed H<sup>+</sup> and OH<sup>-</sup>) are readily exchangeable, then  $\Delta q = \text{CEC} - \text{AEC}$ , where CEC is the cation exchange capacity (equal to  $Q$  plus the usually small positive equivalent adsorbed charge contributed by anion exclusion from the vicinity of X<sup>-</sup> surface sites [Sposito, 2008]) and AEC is the anion exchange capacity (defined equivalently for anion exchange on positively charged surface functional groups). Ranges of the CEC of soils and soil constituents are listed in Table 16.2. The AEC of soils is usually less than 0.05 mol<sub>c</sub> kg<sup>-1</sup> (Sposito, 2008). Major contributors to the CEC of soils are the widely studied smectite clay minerals (Sposito et al., 1999; Sposito, 2008) and the less well-characterized soil organic matter (Helling et al., 1964; Curtin et al., 1998; Sutton and Sposito, 2005; Sposito, 2008). Micaceous minerals (illite, mica) also play an important role in the uptake of small quantities of weakly solvated ions, such as K<sup>+</sup>, NH<sub>4</sub><sup>+</sup>, and Cs<sup>+</sup> (Maes and Cremers, 1986; Bradbury and Baeyens, 2000).

### 16.3 Ion Exchange Thermodynamics

If Equation 16.1 describes a true chemical equilibrium and the exchanger sites X<sup>-</sup> are all identical (or are taken to represent an average site), a thermodynamic equilibrium constant or exchange equilibrium coefficient <sup>ex</sup> $K$  can be defined with the relation (Sposito, 1994):

$${}^{\text{ex}}K_A^{\text{B}} = \frac{(X_b\text{B})^a (A^{a+})^b}{(X_a\text{A})^b (B^{b+})^a}, \quad (16.10)$$

where  $(i)$  represents the thermodynamic activity of species  $i$ . The equilibrium constant <sup>ex</sup> $K$  is directly related to the difference

between the standard-state chemical potentials  $\mu^0[\dots]$  of the products and reactants in Equation 16.1, termed the standard Gibbs energy change of the reaction:

$$\Delta_r G^0 = -RT \ln {}^{\text{ex}}K_A^{\text{B}} = a\mu^0[X_b\text{B}] + b\mu^0[A^{a+}] - b\mu^0[X_a\text{A}] - a\mu^0[B^{b+}],$$

where

$R$  is the molar gas constant

$T$  is the absolute temperature

The equilibrium chemical potentials  $\mu$  of reactants and products typically differ from their standard-state values  $\mu^0$ , and this difference must enter Equation 16.10 through the thermodynamic activities on its right side. For the aqueous species A<sup>a+</sup> and B<sup>b+</sup>, the activity is defined by setting

$$(i) \equiv \gamma_i C_i, \quad (16.11)$$

where  $\gamma_i$  is an activity coefficient (dm<sup>-3</sup> mol), commonly expressed relative to the infinite dilution reference state at  $T = 298.15$  K and  $P = 1$  atm with the semiempirical Davies equation (Sposito, 1994):

$$\ln \gamma_i = -0.512 z_i^2 \left\{ \frac{\sqrt{I}}{1 + \sqrt{I}} - 0.3I \right\} \quad (I < 0.5 \text{ mol dm}^{-3}) \quad (16.12)$$

where  $I$  is the ionic strength ( $I = 1/2 \sum_i z_i^2 C_i$ ). For adsorbed species, if the exchanger phase is pictured as analogous to a solid solution of two components X<sub>a</sub>A and X<sub>b</sub>B, an appropriate model of thermodynamic activity should be (Argersinger et al., 1950; Sposito, 1994)

$$(i) \equiv f_i x_i, \quad (16.13)$$

where the rational activity coefficient  $f_i$  (dimensionless) is equal to 1 in the conventionally chosen reference state  $x_i = 1$ ,  $I = 0$ ,  $T = 298.15$  K, and  $P = 1$  atm (Gaines and Thomas, 1953; Sposito, 1994). No model for  $f_i$  of similar applicability and simplicity to Equation 16.12 currently exists for  $f_i$ . However, Equations 16.3, 16.10, and 16.13, and the Gibbs–Duhem relation at fixed  $T$ ,  $P$  [ $x_A d \ln f_A + x_B d \ln f_B = 0$ ] yield closed-form expressions for calculating <sup>ex</sup> $K$  and  $f_i$  from experimental ion exchange isotherms at fixed  $\tilde{Q}$  (Argersinger et al., 1950; Sposito, 1994):

$$\ln {}^{\text{ex}}K_A^{\text{B}} = \int_0^1 \ln {}^{\text{V}}K_A^{\text{B}} dE_B, \quad (16.14)$$

$$b \ln f_A = E_B \ln {}^{\text{V}}K_A^{\text{B}} - \int_0^{E_B} \ln {}^{\text{V}}K_A^{\text{B}} dE_B. \quad (16.15)$$



In the context of the solid-solution picture, the A–B exchange is defined as *ideal* if  $f_A = f_B = 1$ , that is, if  ${}^V K_A^B = {}^{\text{ex}} K_A^B$ , and *nonpreference* if  ${}^{\text{ex}} K_A^B = 1$ . The Vanselow model in Equation 16.3 therefore describes ideal binary exchange and the nonselective isotherms with  ${}^V K = 1$  in Figure 16.1 are *ideal thermodynamic nonpreference isotherms*. Binary exchange  ${}^{\text{ex}} K$  values should obey the “triangle rule”:  $\text{clog } {}^{\text{ex}} K_A^B + \text{a log } {}^{\text{ex}} K_B^C + \text{b log } {}^{\text{ex}} K_C^A = 0$ , as has been verified within  $\pm 0.1$  log units for montmorillonite (Lewis and Thomas, 1963; Gast, 1969), vermiculite (Wild and Keay, 1964), and illite (Brouwer et al., 1983).

Since the reference state for surface species includes the ionic strength condition  $I = 0$ , Equations 16.14 and 16.15 are strictly valid only if applied to  ${}^V K_A^B$  vs.  $E_B$  data measured at several  $\bar{Q}$  values and then extrapolated to  $\bar{Q} = 0$  (Gaines and Thomas, 1953). In practice, this extrapolation is rarely done, but  ${}^V K$  values for exchange reactions on smectites and soils have been shown to have a rather small  $\bar{Q}$ -dependence ( $\leq 0.1$  log units) if  $\bar{Q} \leq 0.2 \text{ mol}_c \text{ dm}^{-3}$  (Laudelout et al., 1972; Jensen and Babcock, 1973). Furthermore, the rational activity coefficients  $f_i$  calculated with Equation 16.15 are strictly valid only for the binary systems in which they were measured; expressions for  $f_i$  in ternary or more complex exchange systems are much more complicated (Chu and Sposito, 1981; Sposito, 1994). However, several models of comparable accuracy have been proposed for estimating ternary-system activity coefficients from binary ion exchange isotherm data (Bond and Verburg, 1997).

## 16.4 Trends in ${}^V K$ and ${}^{\text{ex}} K$

Broad syntheses of ion exchange data for natural materials are scarce, despite the large number of reported experimental studies. This scarcity results in part from the complexity of soils. Even for smectite minerals (the most widely studied soil constituent), analyses of ion exchange data are complicated by the difficulty of isolating these clays (exchangeable cation homogenization and removal of carbonate, organic matter, and Al and Fe hydroxide impurities require a careful choice of sample pretreatment and storage procedures [Duc et al., 2005]) and of accurately calculating the selectivity coefficient ( ${}^V K$  calculated without measuring  $C_i$  and  $q_i$  for all competing ions may be highly imprecise [Pabalan and Bertetti, 1999]). In addition, the measured selectivity coefficients may vary with experimental conditions, such as  $\bar{Q}$ , pH, solid–liquid ratio  $m_s$ , or type of background anion because of poorly understood processes, such as ion-pair adsorption (Sposito et al., 1983a, 1983b; Griffioen and Appelo, 1993; Charlet and Tournassat, 2005), adsorption on variable-charge sites on the edge surfaces of smectite lamellae (Fletcher and Sposito, 1989; Chen and Hayes, 1999), or the influence of experimental conditions on exchanger structure (Laird and Shang, 1997).

In this section, we summarize current knowledge of the ion exchange selectivity of smectites, micaceous minerals, and soils based on reported  ${}^V K$  and  ${}^{\text{ex}} K$  values. In the case of smectites, we base our analysis as much as possible on studies that (1) used solid pretreatment practices known to produce pure, homoionic

materials (a series of several acid washes [pH  $\approx$  4], exchangeable cation homogenization [ $I \approx 1 \text{ M}$ ], and rinsing steps followed by storage in liquid water at low temperature [Duc et al., 2005; Bourg et al., 2007]), and (2) measured  $q_i$  and  $C_i$  for all competing ions (Table 16.3). For the sake of brevity, we focus on results obtained at  $T \approx 298 \text{ K}$  and do not discuss the temperature dependence of  ${}^V K$  or the estimation of enthalpic and entropic contributions to the Gibbs energy of exchange (Gast, 1972; Maes and Cremers, 1978; Morel et al., 2007).

### 16.4.1 Smectites

Ion exchange reactions on smectites that involve only strongly hydrated cations ( $\text{Li}^+$ ,  $\text{Na}^+$ , and divalent metal cations  $\text{M}^{2+}$ ) have  ${}^V K$  values that display no hysteresis (Verburg and Baveye, 1994) and are independent of  $E_i$  within 0.1 log units (Gast, 1969; Sposito et al., 1981, 1983a, 1983b, 1983c; Tang and Sparks, 1993; Zhang and Sparks, 1996), that is, they are *ideal* within experimental precision. (Erroneous reports of “nonideal” heterovalent exchange reactions have been based on plots of  ${}^{\text{GT}} K_A^B$  vs.  $E_B$  [Banin, 1968; Keren, 1979; McBride, 1980]; for example, the significant dependence of  ${}^{\text{GT}} K_{\text{Na}}^M$  on  $E_M$  [ $M = \text{Cu}, \text{Ni}, \text{or Zn}$ ] observed for montmorillonite is in fact consistent with an ideal exchange reaction since  ${}^V K_{\text{Na}}^M$  is independent of  $E_M$  [Sposito and Mattigod, 1979].) Exchange reactions between strongly hydrated cations are mildly selective (i.e., slightly favor the adsorption of cations of larger ionic radius or larger valence) and weakly affected by the type of smectite (Table 16.4). As expected from the near ideality and weak selectivity of cation exchange reactions on smectites in the absence of weakly hydrated ions, chemical speciation in such systems can be reasonably well described using  $\log K_v \approx 0$  for all ion exchange reactions, for example, the systems Na–H (Tournassat et al., 2004), Na–Cd, and Na– $\text{UO}_2$ – $\text{UO}_2(\text{OH})$ – $(\text{UO}_2)_3(\text{OH})_5$  (Zachara and McKinley, 1993).

Binary reactions that involve at least one weakly hydrated cation ( $\text{K}^+$ ,  $\text{NH}_4^+$ ,  $\text{Rb}^+$ ,  $\text{Cs}^+$ , large organic cations, and, to a smaller extent,  $\text{Ba}^{2+}$ ) are typically *nonideal*, and they frequently display hysteresis (Verburg and Baveye, 1994; Laird and Shang, 1997; Chatterjee et al., 2008) along with a strong dependence of  ${}^V K$  on  $E_i$  (Gast, 1969; Maes and Cremers, 1978; McBride, 1979; Shainberg et al., 1987; Amrhein and Suarez, 1991), especially if the exchanging cations have very different hydration energies. This nonideality may result in part (but not entirely [Maes and Cremers, 1978; Laird and Shang, 1997]) from the greater selectivity of *octahedral-charge sites* vs. *tetrahedral-charge sites* (i.e., sites resulting from isomorphic substitutions in the octahedral or tetrahedral sheet, respectively, of phyllosilicate minerals) for weakly hydrated cations (Xu and Harsh, 1992; Onodera et al., 1998). Among alkali metals and organic cations, the adsorption selectivity of weakly hydrated cations increases with ionic radius (Gast, 1972; Maes and Cremers, 1986; Teppen and Aggarwal, 2007) because larger, less strongly hydrated ions have lower affinity for the aqueous solution phase (Mizutani et al., 1995; Teppen and Miller, 2006; Teppen and Aggarwal, 2007). Selectivity also increases

**TABLE 16.3** Compilation of the Best Available Data Sets on Cation Exchange on Smectite Clay Minerals

Reference	Solid	Cations	Comments
Gast (1972)	Arizona montmorillonite	Na–Li, Na–K, Na–Rb, and Na–Cs	$\tilde{Q} = 1 \text{ mmol}_c \text{ dm}^{-3}$ (Cl <sup>-</sup> electrolyte); $T = 298 \text{ K}$ ; $m_s$ not specified; $q_i$ values not measured
Maes and Cremers (1977)	Otay and RCCB <sup>a</sup> montmorillonites	Na–Ca	$\tilde{Q} = 10 \text{ mmol}_c \text{ dm}^{-3}$ (Cl <sup>-</sup> electrolyte); $T = 298 \text{ K}$ ; $m_s \approx 10 \text{ g kg}^{-1}$ ; $q_i$ values not measured
Maes and Cremers (1978)	Otay and RCCB montmorillonites, hectorite	Na–Cs	$\tilde{Q} = 10 \text{ mmol dm}^{-3}$ (Cl <sup>-</sup> electrolyte); $T = 298 \text{ K}$ ; $m_s$ not specified; pH = 5.5–6; clay stored in freeze-dried form; $q_i$ values not measured
Sposito et al. (1981)	Wyoming montmorillonite	Na–Cu	$\tilde{Q} = 10 \text{ mmol}_c \text{ dm}^{-3}$ (Cl <sup>-</sup> or ClO <sub>4</sub> <sup>-</sup> electrolytes); $T = 298 \text{ K}$ ; $m_s = 13\text{--}21 \text{ g kg}^{-1}$ ; pH = 5–6 to avoid Cu adsorption on oxide-type edge surface sites
Sposito et al. (1983a, 1983b, 1983c)	Wyoming montmorillonite	Na–Ca, Na–Mg, Ca–Mg, and Na–Ca–Mg	$\tilde{Q} = 50 \text{ mmol}_c \text{ dm}^{-3}$ (Cl <sup>-</sup> or ClO <sub>4</sub> <sup>-</sup> electrolytes); $T = 298 \text{ K}$ ; $m_s = 20\text{--}30 \text{ g kg}^{-1}$ ; pH = 6.8–7.1
Xu and Harsh (1992)	Cameron montmorillonite	Na–Li, Na–K, Na–Rb, and Na–Cs	$\tilde{Q} = 10 \text{ mmol}_c \text{ dm}^{-3}$ (Cl <sup>-</sup> electrolyte); $T = 298 \text{ K}$ ; $m_s$ not specified; $C_i$ and $q_i$ values not reported; <sup>V</sup> K values reported only at $E_{\text{Na}} = 0.5$
Tang and Sparks (1993)	Wyoming montmorillonite	Na–Ca and K–Ca	$I = 10 \text{ mmol dm}^{-3}$ (Cl <sup>-</sup> electrolyte); $T = 296 \text{ K}$ ; $m_s = 10.2 \text{ g dm}^{-3}$ ; pH = 6.8; clay stored in freeze-dried form
Zhang and Sparks (1996)	Wyoming montmorillonite	Na–Cu	$\tilde{Q} = 20 \text{ mmol}_c \text{ dm}^{-3}$ (ClO <sub>4</sub> <sup>-</sup> , Cl <sup>-</sup> , NO <sub>3</sub> <sup>-</sup> , or SO <sub>4</sub> <sup>2-</sup> electrolyte); $T = 298 \text{ K}$ ; $m_s \approx 16\text{--}17 \text{ g dm}^{-3}$ ; pH = 5.2–6.5, decreasing with $q_{\text{Cu}}$ ; clay stored in freeze-dried form
Laird and Shang (1997)	Synthetic fluorohectorite	Mg–Ba	$\tilde{Q} = 20 \text{ mmol}_c \text{ dm}^{-3}$ (Cl <sup>-</sup> electrolyte); $T = \text{room temperature}$ ; $m_s = 10 \text{ g dm}^{-3}$ ; no acid wash, but the material (a synthetic magnesium silicate) should not contain Al or Fe hydroxides or organic impurities; clay stored in freeze-dried form
Charlet and Tournassat (2005)	Wyoming montmorillonite	Na–Fe(II), Ca–Fe(II), Na–Ca–Fe(II)	$\tilde{Q} = 50$ or $130 \text{ mmol}_c \text{ dm}^{-3}$ (Cl <sup>-</sup> electrolyte); $T$ not specified; $m_s = 4\text{--}8 \text{ g dm}^{-3}$ ; pH = 2.1–3.6 to avoid Fe adsorption on oxide-type edge surface sites; $q_{\text{Fe}}$ not measured (estimated by mass balance)

<sup>a</sup> RCCB montmorillonite: reduced-charge Camp-Berteau (Morocco) montmorillonite. Layer charge was reduced by 5%–41% using the Hofmann–Klemen effect (Maes and Cremers, 1977, 1978).

The studies by Gast (1972) and Maes and Cremers (1977, 1978) are tentatively included, despite the fact that they did not include measurements of  $q_i$  values, because of the good quality of their pretreatment methods. Studies that used smectites stored by freeze-drying also are tentatively included, although storage in liquid water at low temperature is preferred (Duc et al., 2005). Experimental procedures that may adversely affect the quality of experimental results are reported in italics in the last column.

with surface charge density (Gast, 1972; Maes and Cremers, 1978; Shainberg et al., 1987; Xu and Harsh, 1992) (Table 16.4) and perhaps especially with the charge density of octahedral-charge sites (Xu and Harsh, 1992).

Metal–ligand complexes also can adsorb by ion exchange, but this process has not been deeply studied. The strong adsorption of copper-ethylenediamine complexes Cu(en)<sub>2</sub><sup>2+</sup> (Maes and Cremers, 1986) and the complexation of nitroaromatic compound with exchangeable cations on smectite surfaces (Chatterjee et al., 2008) are consistent with the expectation that metal–organic complexes should have an affinity similar to large organic cations for smectite surfaces. Divalent metals are known to coadsorb with anions, such as Cl<sup>-</sup> (Sposito et al., 1983a, 1983b; Charlet and Tournassat, 2005) or HCO<sub>3</sub><sup>-</sup> (Griffoen and Appelo, 1993), but the mechanism of this coadsorption (ion-pair formation or diffuse layer process) and its dependence on experimental conditions are not well understood (Sposito, 1991).

### 16.4.2 Micaceous Minerals

Illites and micas have a lamellar morphology similar to that of smectites but with collapsed, K<sup>+</sup>-filled interlayers (Sposito, 2008).

The reactivity of external basal surfaces of illite and mica crystals is thought to be similar to that of smectites (Brouwer et al., 1983), but the crystals also carry a small population of sites (0.1%–10%) with a very high affinity for weakly hydrated cations (K<sup>+</sup>, NH<sub>4</sub><sup>+</sup>, Rb<sup>+</sup>, and Cs<sup>+</sup>) (Brouwer et al., 1983; Thellier and Sposito, 1989; Liu et al., 2004; Tournassat et al., 2007). These so-called *frayed-edge sites* occur at partially propped-open, K<sup>+</sup>-depleted edges of collapsed interlayers (Rajec et al., 1999; McKinley et al., 2004). Adsorption on frayed-edge sites may be determined to a certain extent by nonequilibrium processes, such as diffusion-controlled adsorption over timescales of weeks or more (Comans et al., 1991). Such processes can cause difficulties in defining and measuring ion exchange selectivity, since the population of “accessible” frayed-edge sites may vary with time, experimental conditions, the type of exchangeable cation, and the choice of agent used to extract adsorbed cations for measuring  $q_i$  (Brouwer et al., 1983; Comans et al., 1991; Baeyens and Bradbury, 2004; Tournassat et al., 2007). Nevertheless, the finding that frayed-edge sites obey the “triangle rule” (Brouwer et al., 1983) suggests that ion exchange on these sites can be reasonably well described on certain timescales as a thermodynamic process. If ion B = K, Rb, or Cs, experimental <sup>V</sup>K<sub>A</sub><sup>B</sup> values decrease sharply with  $E_B$

**TABLE 16.4** Recommended Values for  ${}^V K$  on Smectite Based on the Studies Listed in Table 16.3

Variable	$\log K$	References
<i>Exchanges of two strongly hydrated cations</i>		
${}^V K_{\text{Na}}^{\text{Li}}$	$-0.08 \pm 0.06$	Gast (1972), Xu and Harsh (1992)
${}^V K_{\text{Na}}^{\text{M(II)}}$	$0.11 \pm 0.11^a$ (M = Mg, Ca, and Cu)	Maes and Cremers (1977), Sposito et al. (1981, 1983a), Tang and Sparks (1993), Zhang and Sparks (1996)
${}^V K_{\text{Mg}}^{\text{Ca}}$	$0.01 \pm 0.02$ ( $E_{\text{Na}} = 0, 0.016, \text{ or } 0.036$ )	Sposito et al. (1983b, 1983c)
${}^V K_{\text{Fe(II)}}^{\text{Ca}}$	$\sim 0.01$	Charlet and Tournassat (2005) <sup>b</sup>
<i>Exchanges involving at least one weakly hydrated cation</i>		
${}^{\text{ex}} K_{\text{Na}}^{\text{K}}$	$0.58 \pm 0.14^c$	Gast (1972), Xu and Harsh (1992)
${}^{\text{ex}} K_{\text{Na}}^{\text{Rb}}$	$1.08 \pm 0.25^c$	Gast (1972), Xu and Harsh (1992)
${}^{\text{ex}} K_{\text{Na}}^{\text{Cs}}$	$1.23 \times \text{CEC} - 0.06^d$	Gast (1972), Maes and Cremers (1978), Xu and Harsh (1992)
${}^V K_{\text{Mg}}^{\text{Ba}}$	$\sim 0.5$ in the three-layer hydrate, increasing to $\sim 1.4$ in the two-layer hydrate	Laird and Shang (1997)

Confidence intervals calculated as  $\pm 2\sigma$  where several  ${}^V K$  values were available.

<sup>a</sup> Neglecting Na–Ca exchange data obtained with reduced-charge montmorillonites, which show  ${}^V K_{\text{Na}}^{\text{Ca}}$  values closer to 0 (Maes and Cremers, 1977).

<sup>b</sup> Charlet and Tournassat (2005) erroneously reported their  ${}^{\text{GT}} K$  values as  ${}^V K$  values, but for homoionic Ca–Fe(II) exchange  ${}^{\text{GT}} K = {}^V K$ .

<sup>c</sup>  $\log {}^{\text{ex}} K_{\text{Na}}^{\text{K}}$  and  $\log {}^{\text{ex}} K_{\text{Na}}^{\text{Rb}}$  are thought to increase with  $Q$  (Shainberg et al., 1987; Xu and Harsh, 1992).

<sup>d</sup> Linear regression with  $r^2 = 0.91$ ,  $p < 0.001$ ;  $\text{CEC} = 0.66\text{--}1.44 \text{ mol}_c \text{ kg}^{-1}$ , estimated from the number of octahedral and tetrahedral substitutions in the clay unit cell formula.

when the frayed-edge sites become B-saturated (Brouwer et al., 1983), a behavior that can be described with a two- or three-site model, that is, one or two types of highly selective frayed-edge site plus weakly selective basal surface sites (Maes and Cremers, 1986; Liu et al., 2004; Tournassat et al., 2007).

### 16.4.3 Soils and Sediments

For highly heterogeneous, multiphase media such as soils and sediments, Equations 16.14 and 16.15 have no clear thermodynamic meaning and any selectivity model may be suitable on a case-by-case basis. For example, the Gapon selectivity coefficient has been found to be less variable than  ${}^V K$  over broad ranges of exchanger phase composition for Na–Ca, Mg–K, and Ca–K exchange reactions in some soils (Naylor and Overstreet, 1969; Jensen and Babcock, 1973; Evangelou and Coale, 1987; Feigenbaum et al., 1991; Agbenin and Yakubu, 2006). Experimental data on  $\log {}^V K_{\text{Ca}}^{\text{M}}$  vs.  $E_{\text{M}}$  (M = Na, K, or Mg) obtained for a range of conditions of pH,  $\bar{Q}$ , and soil type illustrate the variability of the ion exchange selectivities of soils (Figure 16.4). The scatter of  $\log {}^V K_{\text{Ca}}^{\text{Na}}$  values at  $E_{\text{Na}} \leq 0.2$  in Figure 16.4b may reflect in part the high sensitivity of  ${}^V K$  at small  $E_i$  values to sources of error such as the dissolution of soil materials (Carlson and Buchanan, 1973; Sheta et al., 1981).

Despite the inherent complexity of soil and sediment ion exchange properties, these have been modeled conceptually with some success assuming their exchange properties result from their smectite constituent (Charlet and Tournassat, 2005) or from the sum of their smectite, organic matter (Curtin et al., 1998), and/or micaceous constituents (Bradbury and Baeyens, 2000).

The first type of approximation is exemplified by the ion exchange properties of Amazon river suspended matter in the system Na–K–Ca–Mg, which are essentially identical to those of montmorillonite, even though only half of the CEC of the suspended matter originates from its clay-size fraction (Charlet and Tournassat, 2005). The second type of approximation is well illustrated by the fact that the Mg–Ca exchange selectivity of soils is correlated with their ratio of organic carbon to clay content (Curtin et al., 1998). Curtin et al. (1998) successfully described the Mg–Ca selectivity of several soils with a two-site model where the soil organic matter and clay fractions were represented by  $\log {}^V K_{\text{Mg}}^{\text{Ca}} = 0.6$  and  $0.1$ , respectively. Similar additive behavior of soil smectites and soil organic matter has been used to interpret the ion exchange selectivity of montmorillonitic soils in the system Na–Ca–Mg (Fletcher et al., 1984a; Sposito and Fletcher, 1985) and may also explain the Ca–Sr selectivity of soils (Juo and Barber, 1969) and the Ca–Cd and Ca–Zn selectivity of acidic soils (Voegelin and Kretzschmar, 2003). Additive behavior of micaceous materials and other soil constituents may explain the strong adsorption of  $\text{K}^+$  and  $\text{Cs}^+$  at low  $E_{\text{K}}$  or  $E_{\text{Cs}}$  values in numerous soils and sediments (Feigenbaum et al., 1991; Bradbury and Baeyens, 2000; Sinanis et al., 2003; Liu et al., 2004; Agbenin and Yakubu, 2006). The concept that soil ion exchange selectivity is a sum of the selectivities of component phases evidently can be quite powerful (Sposito and Fletcher, 1985; Curtin et al., 1998; Bradbury and Baeyens, 2000; Charlet and Tournassat, 2005), although it neglects nonadditive behavior such as the enhanced (about 0.3 log unit greater) Na–Ca selectivity of smectites when their interlayers contain Al-hydroxide polymers (Keren, 1979; Janssen et al., 2003).

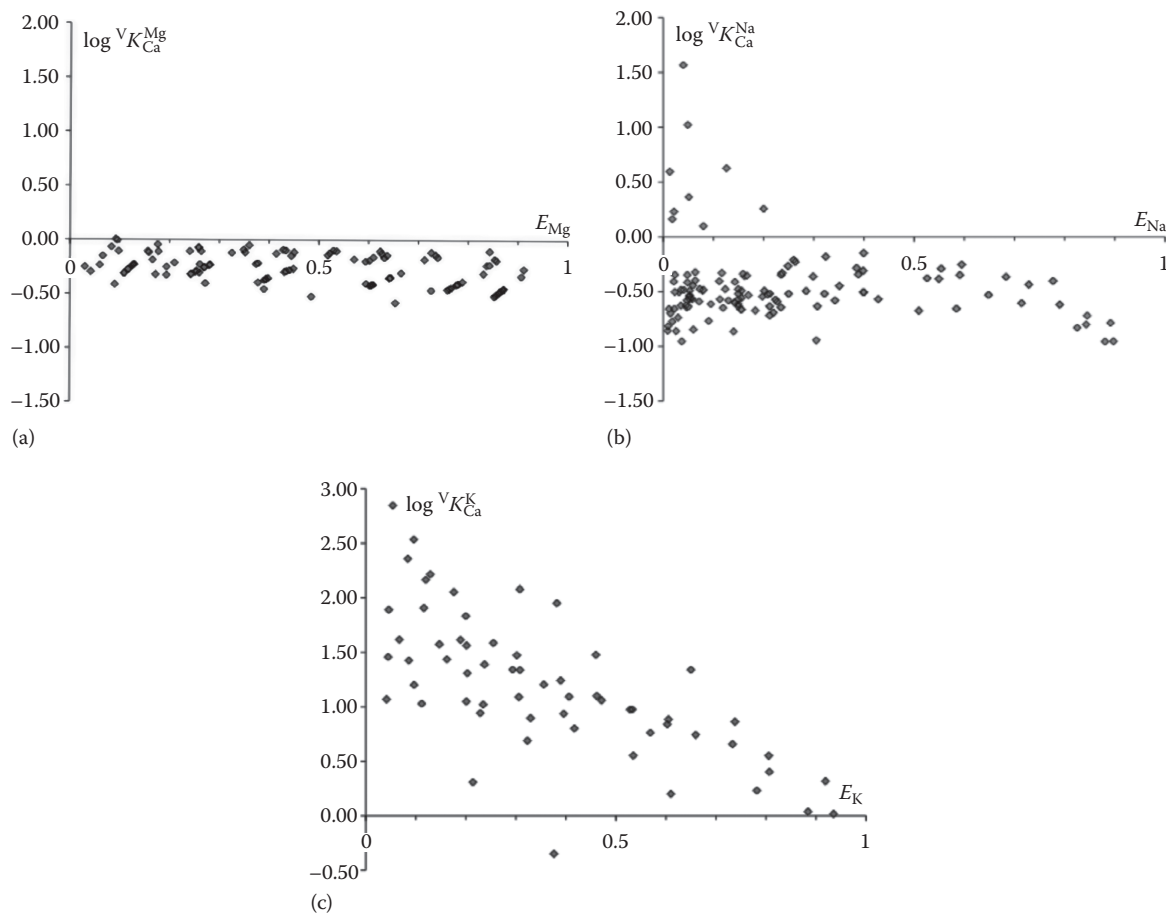
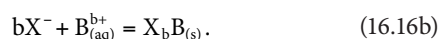
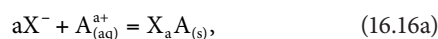


**FIGURE 16.4** Compilation of experimental data on  $\log {}^V K_{Ca}^M$  vs.  $E_M$  ( $M = Mg^{2+}$ ,  $Na^+$ , or  $K^+$ ) in soils if  $\bar{Q} \leq 0.2 \text{ mol dm}^{-3}$  and  $T = 298 \text{ K}$ ; (a)  $\log {}^V K_{Ca}^{Mg}$  data for a loam soil (Jensen and Babcock, 1973), calcareous clay soils (Van Bladel and Gheyi, 1980), smectitic soils with 27–96  $\text{g kg}^{-1}$  organic carbon (Curtin et al., 1998), and a montmorillonitic soil (DeSutter et al., 2006); (b)  $\log {}^V K_{Ca}^{Na}$  for a montmorillonitic soil (Fletcher et al., 1984b), kaolinitic soils (Levy et al., 1988), a kaolinitic sandy loam soil with 25.7  $\text{g kg}^{-1}$  organic carbon (Rhue and Mansell, 1988), a calcareous, smectitic clay soil (Amrhein and Suarez, 1991), and an illite–kaolinite clay soil (Bond, 1995); (c)  $\log {}^V K_{Ca}^K$  for a loam soil (Jensen and Babcock, 1973), kaolinitic soils (Levy et al., 1988), a kaolinitic sandy loam soil with 25.7  $\text{g kg}^{-1}$  organic carbon (Rhue and Mansell, 1988), an illite–kaolinite clay soil (Bond, 1995), and a tropical soil (Agbenin and Yakubu, 2006).

## 16.5 Ion Exchange and Chemical Speciation Models

Analytical solutions of thermodynamic equations to determine exchanger phase composition rapidly become intractable in systems that involve more than three exchangeable ions (Bond and Verburg, 1997). For such complex systems, a numerical solution can be implemented in chemical speciation models after dividing Equation 16.1 into two hypothetical half-reactions involving a fictitious anionic species  $X^-$  (Sposito and Mattigod, 1977; Shaviv and Mattigod, 1985; Fletcher and Sposito, 1989):



Equation 16.16 can be incorporated into conventional chemical speciation models using its analogy with surface complexation or solid-solution reactions, as described below.

### 16.5.1 Modeling Ion Exchange as a Surface Complexation Process

Most chemical speciation programs include a model of surface complexation reactions (similar in form to Equation 16.16) where the thermodynamic activities of uncharged surface species arbitrarily are set equal to their concentrations  $[X_i]$  (Sposito, 2004). On this model, the half-reaction selectivity coefficients associated with Equation 16.16 are the following (Fletcher and Sposito, 1989; Stadler and Schindler, 1993):

$$\text{half } K^A = \frac{[X_a A]}{(X^-)^a (A^{a+})}, \quad (16.17a)$$

$${}^{\text{half}}K^{\text{B}} = \frac{[X_{\text{b}}\text{B}]}{(X^-)^{\text{b}}(\text{B}^{\text{b}+})}. \quad (16.17\text{b})$$

Equation 16.17 can be incorporated into any program that models surface complexation reactions; typically,  ${}^{\text{half}}K$  is set to a very large value ( $10^{10}$ – $10^{20}$ ) for a reference cation, such that the wholly uncomplexed  $X^-$  sites contribute negligibly to the total mass balance on X, and the  ${}^{\text{half}}K$  values of other cations are chosen to fit experimental equilibrium constants (Flechter and Sposito, 1989; Stadler and Schindler, 1993). Certain chemical speciation programs include a specific model of ion exchange reactions based on Equation 16.17. For example, in the program PHREEQC2 (Appelo and Postma, 2005), the fictitious species  $X^-$  is excluded from the total mass balance on X and  $\text{Na}^+$  is chosen as a reference species with  $\log {}^{\text{half}}K^{\text{Na}} = 0$ . Suggested values of  ${}^{\text{half}}K$  for other cations on smectite are provided in the PREEQC2 database (Appelo and Postma, 2005). The use of Equation 16.17 with fixed  ${}^{\text{half}}K$  values corresponds to an implicit assumption that  ${}^{\text{GT}}K$  is equal to an equilibrium constant, since  ${}^{\text{GT}}K$  and  ${}^{\text{half}}K$  are related through

$${}^{\text{GT}}K_{\text{A}}^{\text{B}} = \left[ \frac{({}^{\text{half}}K^{\text{B}})^{\text{a}}}{({}^{\text{half}}K^{\text{A}})^{\text{b}}} \right] \left( \frac{\text{b}^{\text{a}}}{\text{a}^{\text{b}}} \right) Q^{(\text{b}-\text{a})}. \quad (16.18)$$

Equation 16.17 has been used to model ion exchange reactions involving protons, alkali metals, trace metals, and actinides on clay minerals (Stadler and Schindler, 1993; Zachara and McKinley, 1993; Poinssot et al., 1999; Bradbury and Baeyens 2000, 2005, 2009; Baeyens and Bradbury, 2004; Charlet and Tournassat, 2005; Heidmann et al., 2005; Bourg et al., 2007; Gu and Evans, 2008). Most of these studies (with the notable exception of Charlet and Tournassat, 2005) investigated systems where  ${}^{\text{half}}K$  should be constant if ion exchange is ideal, either because the main background electrolyte cation was  $\text{A}^{3+}$  and occupied most ion exchange sites, such that  ${}^{\text{GT}}K_{\text{A}}^{\text{B}} \oplus {}^{\text{V}}K_{\text{A}}^{\text{B}}(\text{b}/\text{a})^{\text{a}}$ , or because the system studied was homovalent, in which case  ${}^{\text{GT}}K_{\text{A}}^{\text{B}} = {}^{\text{V}}K_{\text{A}}^{\text{B}}$ .

### 16.5.2 Modeling Ion Exchange as a Solid-Solution Process

Some chemical speciation programs include a model of solid-solution formation, which is also similar in form to Equation 16.16. The “solubility coefficients” associated with Equation 16.16 are described as follows in the solid-solution formalism (Appelo and Postma, 2005):

$${}^{\text{solubility}}K^{\text{A}} = \frac{(X^-)^{\text{a}}(\text{A}^{\text{a}+})}{x_{\text{A}}f_{\text{A}}}, \quad (16.19\text{a})$$

$${}^{\text{solubility}}K^{\text{B}} = \frac{(X^-)^{\text{b}}(\text{B}^{\text{b}+})}{x_{\text{B}}f_{\text{B}}}. \quad (16.19\text{b})$$

where  $(X^-)$  is the activity of a fictitious dissolved species. In the program PHREEQC2, Equation 16.19 can be solved by defining  $X^-$ ,  $\text{A}^{\text{a}+}$ , and  $\text{B}^{\text{b}+}$  as dissolved species and  $X_{\text{a}}\text{A}$  and  $X_{\text{b}}\text{B}$  as solid phases and by setting  ${}^{\text{solubility}}K \ll 1$  for a chosen reference cation, such that  $X^-$  contributes negligibly to the mass balance on X. If  $f_{\text{A}} = f_{\text{B}} = 1$ , Equation 16.19 is identical to the Vanselow model with

$${}^{\text{V}}K_{\text{A}}^{\text{B}} = \left[ \frac{({}^{\text{solubility}}K^{\text{B}})^{\text{a}}}{({}^{\text{solubility}}K^{\text{A}})^{\text{b}}} \right]. \quad (16.20)$$

The ideality of ion exchange reactions between strongly hydrated cations on smectite (Table 16.4) suggests that Equation 16.19 may be more accurate than Equation 16.17 for multicomponent ion exchange reactions on smectite over broad ranges of exchanger phase composition. However, to our knowledge, Equation 16.19 has never been used for this purpose.

## 16.6 Micro- and Nanoscale Perspectives on Ion Exchange Selectivity

Micro- and nanoscale studies have yielded insight into the processes that determine  ${}^{\text{V}}K$  using theoretical estimates of long-range electrostatic forces (Barak, 1989; Rytwo et al., 1996), short-range interactions (Shainberg and Kemper, 1966; Eberl, 1980), or statistical mechanical quantities (Sposito, 1993; Benjamin, 2002). In the present chapter, we focus on two subfields illustrating micro- and nanoscale studies: (1) the molecular-scale coordination and dynamics of exchangeable ions and (2) the influence of exchanger microstructure on ion exchange selectivity.

### 16.6.1 Molecular-Scale Coordination and Dynamics of Exchangeable Ions

Spectroscopic and molecular simulation methods have been widely used to probe the coordination environment and dynamics of exchangeable cations in smectites (Sposito and Prost, 1982; Sposito, 2004; Skipper et al., 2006) and have been increasingly applied to other exchanger phases (Skipper et al., 1995; Kim and Kirkpatrick, 1998; Schlegel et al., 2006; Xu et al., 2006). Spectroscopic techniques can probe the molecular structure of the interface as a function of distance from a solid surface (by x-ray reflectivity [Schlegel et al., 2006; Park et al., 2008]), the dynamics of water H atoms (by quasielastic neutron scattering [QENS] [Marry et al., 2008]), the local coordination environment of certain atomic probes (such as water or Li by neutron diffraction with isotopic substitution [NDIS] [Skipper et al., 1995; Powell et al., 1998] or Co, Sr, Pb, Cu, Cs, and other atoms by x-ray absorption spectroscopy [XAS] [Papelis and Hayes, 1996; Chen and Hayes, 1999; Strawn and Sparks, 1999; Morton et al., 2001; Bostick et al., 2002]), the coordination environment and

rotational dynamics of paramagnetic atoms such as Cu (by electron spin resonance [ESR] or electron spin-echo modulation [ESEM] [McBride et al., 1975; Brown and Kevan, 1988]), and the local molecular environment (“chemical shielding”) of atoms with an odd number of nucleons or protons such as  $^{23}\text{Na}$ ,  $^{133}\text{Cs}$ ,  $^{113}\text{Cd}$ , or  $^{35}\text{Cl}$  (by nuclear magnetic resonance [NMR] [Weiss et al., 1990; Kim and Kirkpatrick, 1998; Xu et al., 2006]). Molecular simulation techniques, primarily Monte Carlo (MC) and molecular dynamics (MD), have been used for over a decade to complement spectroscopic results (Chang et al., 1995; Park and Sposito, 2002). Most spectroscopic and simulation studies have been used to probe homoionic exchangers, but a few studies have investigated the behavior of a “reporter” cation doped into a smectite that is almost homoionic in another cation (McBride et al., 1975; Brown and Kevan, 1988; Marry and Turq, 2003; Bourg and Sposito, 2010).

Spectroscopic and molecular simulation studies have shown that the aqueous phase in smectite interlayers is analogous to a concentrated ionic solution (Sposito and Prost, 1982; Powell et al., 1998); in the two- and three-layer hydrates and on external basal surfaces, it diffuses about 30%–40% as fast as bulk liquid water (Chang et al., 1997; Marry et al., 2008; Bourg and Sposito, 2010). Exchangeable cations in smectite one-layer hydrates form inner-sphere surface complexes (ISSC) for obvious steric reasons, and they diffuse very slowly (McBride et al., 1975; Chang et al., 1995, 1997; Bourg and Sposito, 2010); at higher hydration levels, they can be divided into three categories based on their interaction with smectite surfaces: divalent metal cations ( $\text{M}^{2+}$ ), strongly hydrated alkali metal cations ( $\text{Li}^+$ ,  $\text{Na}^+$ ), and weakly hydrated cations ( $\text{K}^+$ ,  $\text{Rb}^+$ ,  $\text{Cs}^+$ ). The divalent cations are adsorbed in fully solvated form as outer-sphere surface complexes (OSSC) or in the diffuse layer (DL) (McBride et al., 1975; Brown and Kevan, 1988; Papelis and Hayes, 1996; Chen and Hayes, 1999; Strawn and Sparks, 1999; Greathouse et al., 2000; Chávez-Páez et al., 2001; Morton et al., 2001; Whitley and Smith, 2004); they tumble and diffuse slowly, about 1%–10% as fast as in bulk liquid water (McBride et al., 1975; Brown and Kevan, 1988; Greathouse et al., 2000; Bourg and Sposito, 2010). The strongly hydrated monovalent cations ( $\text{Li}^+$ ,  $\text{Na}^+$ ) also adsorb as OSSC or DL species on octahedral-charge sites, but they form inner-sphere surface complexes (ISSC) on tetrahedral-charge sites (Chang et al., 1995, 1997; Leote de Carvalho and Skipper, 2001; Marry and Turq, 2003; Marry et al., 2003; Tambach et al., 2004, 2006; Greathouse and Cygan, 2005); they diffuse about 20%–60% as fast as in bulk water if adsorbed on octahedral-charge sites, but are essentially immobile (on subnanosecond timescales) on tetrahedral-charge sites (Chang et al., 1995, 1997; Leote de Carvalho and Skipper, 2001; Marry and Turq, 2003; Bourg and Sposito, 2010). Finally, the weakly hydrated cations form primarily ISSC on smectite surfaces along with small amounts of OSSC or DL species (Chang et al., 1998; Nakano et al., 2003; Whitley and Smith, 2004; Tambach et al., 2006; Liu et al., 2008); two populations of ISSC exist in Cs- and K-smectite interlayers that may correspond to cations located above ditrigonal cavities or “triads” of O atoms of the siloxane surface (Weiss et al., 1990; Onodera

et al., 1998; Park and Sposito, 2002; Nakano et al., 2003); the mobility of these cations along smectite basal surfaces is not well characterized (Kosakowski et al., 2008), but recent results suggest that they diffuse only 5%–8% as fast as in bulk liquid water (Bourg and Sposito, 2010). Clearly, the molecular-scale behavior of cations on smectites parallels their ion exchange selectivity: The strongly hydrated cations ( $\text{M}^{2+}$ ,  $\text{Li}^+$ ,  $\text{Na}^+$ ) adsorb mainly as fully solvated OSSC or DL species and display ideal, weakly selective ion exchange behavior, whereas the weakly hydrated ions adsorb mainly as ISSC and display nonideal, strongly selective ion exchange behavior. The ISSC formed by  $\text{Li}^+$  and  $\text{Na}^+$  on tetrahedral-charge sites do not fit this simple classification, suggesting that  $\text{Li}^+$  and  $\text{Na}^+$  may show nonideal exchange behavior on smectites with high tetrahedral charge. This point may not have been noticed previously because reference smectites typically carry  $80\% \pm 20\%$  octahedral-charge sites (Xu and Harsh, 1992).

Thanks to increases in computational capabilities, MD and MC simulations may soon be able to “bridge the gap” from the time and length scales (or number of MC simulation steps) required to probe molecular exchanger phase structure and dynamics ( $<1$  ns and  $\leq 1$  nm) to the time and length scales (tens of nanoseconds and nanometers) on which ion exchange equilibria become established (Greathouse and Cygan, 2005; Rotenberg et al., 2007). Molecular simulation methods could then be used to test Equation 16.13 directly or to predict  ${}^V K$  values (Greathouse and Cygan, 2005; Teppen and Miller, 2006). Teppen and Miller (2006) showed that the Gibbs energy difference between K-, Rb-, and Cs-montmorillonite (one component of the Gibbs energy of exchange) at fixed interlayer spacing and interlayer water content could be determined by MD simulation. Greathouse and Cygan (2005) found that ten 1 ns MD simulations of a 4 nm thick  $\text{Na}^+ - \text{UO}_2^{2+} - \text{CO}_3^{2-}$  aqueous solution on a montmorillonite basal surface were too short and small scale to determine  ${}^V K$  accurately, but were sufficient to identify important processes, such as the formation of  $[\text{Na}_2\text{UO}_2(\text{CO}_3)_3]^{2-}$  complexes.

### 16.6.2 Coupling between Cation Exchange and Exchanger Structure

As pointed out above, Equation 16.10 has strict thermodynamic meaning only if all exchanger sites  $\text{X}^-$  are identical. For smectites (Sposito, 1992; Laird and Shang, 1997) and natural organic matter (Sutton et al., 2005), however, the microstructure of the exchanger phase depends on experimental conditions and, therefore, the  $\text{X}^-$  may *not* be identical at different points along a binary exchange isotherm, or even in different regions of the exchanger phase within a single sample. In the case of smectite clay minerals, the stacking arrangement of smectite lamellae (number of layers per stack, interlayer spacing) is a dynamic, nonuniform property (several interlayer hydration levels may coexist [Tamura et al., 2000; Wilson et al., 2004; Ferrage et al., 2005]), which depends on the magnitude and location of clay structural charge (Slade et al., 1991; Tambach et al., 2004), the

population of adsorbed cations (Schramm and Kwak, 1982; Sposito, 1992; Laird and Shang, 1997; Ferrage et al., 2005; Table 16.5), the thermodynamic activity of water (Norrish, 1954; Slade et al., 1991; Laird et al., 1995), as well as the previous history of the clay (Verburg and Baveye, 1994; Laird et al., 1995; Chatterjee et al., 2008) and its degree of compaction (Kozaki et al., 1998). Molecular-scale simulations confirm that homoionic montmorillonites frequently exhibit several stable states of crystalline swelling separated by energy barriers (Whitley and Smith, 2004; Tambach et al., 2004, 2006; Smith et al., 2006). Transitions between these states are predominantly enthalpic (Whitley and Smith, 2004), driven by cationic solvation energy (Whitley and Smith, 2004)—as opposed to being determined by the hydrogen bond network of interlayer water (Tambach et al., 2006)—strongly hysteretic (Tambach et al., 2006), and in fact thermodynamically analogous to a phase transition (Laird and Shang, 1997; Whitley and Smith, 2004).

The stacking arrangement, in turn, determines the fraction of  $X^-$  sites located on external vs. internal basal surfaces, which may

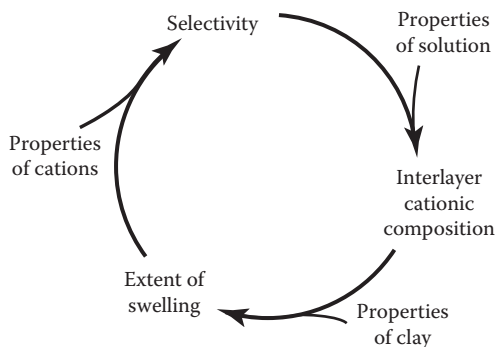


**FIGURE 16.5** Conceptual model of the feedback between the ion exchange selectivity ( $^{\vee}K$ ), population of exchangeable ions ( $E$ ), and arrangement of clay particles (interlayer spacing, number of layers per stack) in smectite clay minerals. (Reproduced from Laird, D.A., and C. Shang. 1997. Relationship between cation exchange selectivity and crystalline swelling in expanding 2:1 phyllosilicates. *Clays Clay Miner.* 45:681–689. With permission of The Clay Minerals Society, publisher of *Clays and Clay Minerals*.)

**TABLE 16.5** Interlayer Hydration Level (Norrish, 1954; Laird and Shang, 1997; Chatterjee et al., 2008) and Number of Lamellae per Stack (Sposito, 1992; Verburg and Baveye, 1994; Verburg et al., 1995) in Dilute Aqueous Suspensions of Homoionic Montmorillonite

Cation	Hydration Level <sup>a</sup>	Lamellae per Stack
Li <sup>+</sup>	>3	1.0
Na <sup>+</sup>	>3	1.0–1.7
K <sup>+</sup>	2	1.0–7.0
Cs <sup>+</sup>	1–2	1.4–4.0
Mg <sup>2+</sup>	3	2.7–14.0
Ca <sup>2+</sup>	3	3.0–20.0
Ba <sup>2+</sup>	2–3	2.7–7.0

<sup>a</sup> Number of statistical water monolayers in each smectite interlayer.

have unequal cation exchange selectivities (Keren, 1979; Sposito et al., 1983a), and the fraction of internal-surface  $X^-$  sites in contact with one-, two- or three-layer interlayer hydrates, which also may have unequal cation exchange selectivities (Barak, 1989; Laird and Shang, 1997; Van Loon and Glaus, 2008). Thus, cation exchange on swelling clay minerals involves a feedback loop among adsorption, exchanger structure, and selectivity (Laird and Shang, 1997; Figure 16.5) that is reminiscent of the behavior of certain ion-selective pores (Kuyucak et al., 2001). This feedback loop may explain the occurrence of exchangeable cation “de-mixing” (Shainberg and Otoh, 1968; Fink et al., 1971; Iwasaki and Watanabe, 1988), increased selectivity for the preferred cation at high surface loading of the same cation (Shainberg et al., 1980; Laird and Shang, 1997; Janssen et al., 2003), cation exchange hysteresis (Fripiat et al., 1965; Verburg et al., 1995), and increased selectivity for weakly hydrated ions as smectite charge density increases (Maes and Cremers, 1978; Shainberg et al., 1987). Smectite  $^{\vee}K$  values would then have thermodynamic meaning only if defined for a certain particle arrangement (Laird and Shang, 1997). Thus, the nonideality of cation exchange reactions that involve weakly hydrated cations may be related to the fact that these cations cause a sequential collapse of the interlayer from a three-layer hydrate or more (for Li<sup>+</sup>, Na<sup>+</sup>, and strongly hydrated divalent cations M<sup>2+</sup>) to a two-layer hydrate (for K<sup>+</sup> and Ba<sup>2+</sup>) to a one-layer hydrate (for Cs<sup>+</sup>; Table 16.5).

## References

- Agbenin, J.O., and S. Yakubu. 2006. Potassium-calcium and potassium-magnesium exchange equilibria in an acid savanna soil from northern Nigeria. *Geoderma* 136:542–554.
- Amrhein, C., and D.L. Suarez. 1991. Sodium-calcium exchange with anion exclusion and weathering corrections. *Soil Sci. Soc. Am. J.* 55:698–706.
- Appelo, C.A.J., and D. Postma. 2005. *Geochemistry, groundwater and pollution*. 2nd edn. Balkema Publications, New York.
- Argersinger, W.J., Jr., A.W. Davidson, and O.D. Bonner. 1950. Thermodynamics and ion exchange phenomena. *Trans. Kansas Acad. Sci.* 53:404–410.
- Baeyens, B., and M.H. Bradbury. 2004. Cation exchange capacity measurements on illite using the sodium and cesium isotope dilution technique: Effects of the index cation, electrolyte concentration and competition: Modeling. *Clays Clay Miner.* 52:421–431.
- Banin, A. 1968. Ion exchange isotherms of montmorillonite and structure factors affecting them. *Isr. J. Chem.* 6:27–36.
- Barak, P. 1989. Double layer theory prediction of Al–Ca exchange on clay and soil. *J. Colloid Interface Sci.* 133:479–490.
- Benjamin, M.M. 2002. Modeling the mass-action expression for bidentate adsorption. *Environ. Sci. Technol.* 36:307–313.
- Bond, W.J. 1995. On the Rothmund–Kornfeld description of cation exchange. *Soil Sci. Soc. Am. J.* 59:436–443.

- Bond, W.J., and K. Verburg. 1997. Comparison of methods for predicting ternary exchange from binary isotherms. *Soil Sci. Soc. Am. J.* 61:444–454.
- Bostick, B.C., M.A. Vairavamurthy, K.G. Karthikeyan, and J. Chorover. 2002. Cesium adsorption on clay minerals: An EXAFS spectroscopic investigation. *Environ. Sci. Technol.* 36:2670–2676.
- Bourg, I.C., and G. Sposito. 2010. Connecting the molecular scale to the continuum scale for diffusion processes in smectite-rich porous media. *Environ. Sci. Technol.* 44:2085–2091.
- Bourg, I.C., G. Sposito, and A.C.M. Bourg. 2007. Modeling the acid–base surface chemistry of montmorillonite. *J. Colloid Interface Sci.* 312:297–310.
- Bradbury, M.H., and B. Baeyens. 2000. A generalized sorption model for the concentration dependent uptake of caesium by argillaceous rocks. *J. Contam. Hydrol.* 42:141–163.
- Bradbury, M.H., and B. Baeyens. 2005. Modelling the sorption of Mn(II), Co(II), Ni(II), Zn(II), Cd(II), Eu(III), Am(III), Sn(IV), Th(IV), Np(V) and U(VI) on montmorillonite: Linear free energy relationships and estimates of surface binding constants for some selected heavy metals and actinides. *Geochim. Cosmochim. Acta* 69:875–892.
- Bradbury, M.H., and B. Baeyens. 2009. Sorption modelling on illite Part I: Titration measurements and the sorption of Ni, Co, Eu and Sn. *Geochim. Cosmochim. Acta* 73:990–1003.
- Brouwer, E., B. Baeyens, A. Maes, and A. Cremers. 1983. Cesium and rubidium ion equilibria in illite clay. *J. Phys. Chem.* 87:1213–1219.
- Brown, D.R., and L. Kevan. 1988. Aqueous coordination and location of exchangeable  $\text{Cu}^{2+}$  cations in montmorillonite clay studied by electron spin resonance and electron spin-echo modulation. *J. Am. Chem. Soc.* 110:2743–2748.
- Carlson, R.M., and J.R. Buchanan. 1973. Calcium-magnesium-potassium equilibria in some California soils. *Soil Sci. Soc. Am. Proc.* 37:851–855.
- Chang, F.-R.C., N.T. Skipper, and G. Sposito. 1995. Computer simulation of interlayer molecular structure in sodium montmorillonite hydrates. *Langmuir* 11:2734–2741.
- Chang, F.-R.C., N.T. Skipper, and G. Sposito. 1997. Monte Carlo and molecular dynamics simulations of interfacial structure in lithium-montmorillonite hydrates. *Langmuir* 13:2074–2082.
- Chang, F.-R.C., N.T. Skipper, and G. Sposito. 1998. Monte Carlo and molecular dynamics simulations of electrical double-layer structure in potassium montmorillonite hydrates. *Langmuir* 14:1201–1207.
- Charlet, L., and C. Tournassat. 2005. Fe(II)-Na(I)-Ca(II) cation exchange on montmorillonite in chloride medium: Evidence for preferential clay adsorption of chloride—Metal ion pairs in seawater. *Aquat. Geochem.* 11:115–137.
- Chatterjee, R., D.A. Laird, and M.L. Thompson. 2008. Interactions among  $\text{K}^+$ - $\text{Ca}^{2+}$  exchange, sorption of m-dinitrobenzene, and smectite quasicrystal dynamics. *Environ. Sci. Technol.* 42:9099–9103.
- Chávez-Páez, M., L. de Pablo, and J.J. de Pablo. 2001. Monte Carlo simulations of Ca-montmorillonite hydrates. *J. Chem. Phys.* 114:10948–10953.
- Chen, C.-C., and K.F. Hayes. 1999. X-ray absorption spectroscopy investigation of aqueous Co(II) and Sr(II) sorption at clay-water interfaces. *Geochim. Cosmochim. Acta* 63:3205–3215.
- Chorover, J., and G. Sposito. 1995. Surface charge characteristics of kaolinitic tropical soils. *Geochim. Cosmochim. Acta* 59:875–884.
- Chu, S.-Y., and G. Sposito. 1981. The thermodynamics of ternary cation exchange systems and the subregular model. *Soil Sci. Soc. Am. J.* 45:1084–1089.
- Comans, R.N.J., M. Haller, and P. de Preter. 1991. Sorption of cesium on illite: Non-equilibrium behaviour and reversibility. *Geochim. Cosmochim. Acta* 55:433–440.
- Curtin, D., F. Selles, and H. Steppuhn. 1998. Estimating calcium-magnesium selectivity in smectitic soils from organic matter and texture. *Soil Sci. Soc. Am. J.* 62:1280–1285.
- DeSutter, T.M., G.M. Pierzynski, and L.R. Baker. 2006. Flow-through and batch methods for determining calcium-magnesium and magnesium-calcium selectivity. *Soil Sci. Soc. Am. J.* 70:550–554.
- Duc, M., F. Gaboriaud, and F. Thomas. 2005. Sensitivity of the acid-base properties of clays to the methods of preparation and measurement. 1. Literature review. *J. Colloid Interface Sci.* 289:139–147.
- Eberl, D.D. 1980. Alkali cation selectivity and fixation by clay minerals. *Clays Clay Miner.* 28:161–172.
- Evangelou, V.P., and F.J. Coale. 1987. Dependence of the Gapon coefficient on exchangeable sodium for mineralogically different soils. *Soil Sci. Soc. Am. J.* 51:68–72.
- Fair, M.C., and J.L. Anderson. 1989. Electrophoresis of nonuniformly charged ellipsoidal particles. *J. Colloid Interface Sci.* 127:388–400.
- Feigenbaum, S., A. Bar-Tal, R. Portnoy, and D.L. Sparks. 1991. Binary and ternary exchange of potassium on calcareous montmorillonitic soils. *Soil Sci. Soc. Am. J.* 55:49–56.
- Ferrage, E., C. Tournassat, E. Rinnert, and B. Lanson. 2005. Influence of pH on the interlayer cationic composition and hydration state of Ca-montmorillonite: Analytical chemistry, chemical modelling and XRD profile modelling study. *Geochim. Cosmochim. Acta* 69:2797–2812.
- Fink, D.H., F.S. Nakayama, and B.L. McNeal. 1971. Demixing of exchangeable cations in free-swelling bentonite clay. *Soil Sci. Soc. Am. Proc.* 35:552–555.
- Fletcher, P., K.M. Holtzclaw, C. Jouany, G. Sposito, and C.S. LeVesque. 1984a. Sodium-calcium-magnesium exchange reactions on a montmorillonitic soil: II. Ternary exchange reactions. *Soil Sci. Soc. Am. J.* 48:1022–1025.
- Fletcher, P., and G. Sposito. 1989. The chemical modelling of clay/electrolyte interactions for montmorillonite. *Clay Miner.* 24:375–391.
- Fletcher, P., G. Sposito, and C.S. LeVesque. 1984b. Sodium-calcium-magnesium exchange reactions on a montmorillonitic soil: I. Binary exchange reactions. *Soil Sci. Soc. Am. J.* 48:1016–1021.



- Fripiat, J.J., P. Cloos, and A. Poncelet. 1965. Comparison entre les propriétés d'échange de la montmorillonite et d'une résine vis-à-vis des cations alcalins et alcalino-terreux. I. Réversibilité des processus. *Bull. Soc. Chim. Fr.* 1:208–215.
- Gaines, G.L., and H.C. Thomas. 1953. Adsorption studies on clay minerals. II. A formulation of the thermodynamics of exchange adsorption. *J. Chem. Phys.* 21:714–718.
- Gajo, A., and B. Loret. 2007. The mechanics of active clays circulated by salts, acids and bases. *J. Mech. Phys. Solids* 55:1762–1801.
- Gapon, Y.N. 1933. On the theory of exchange adsorption in soils. *J. Gen. Chem. USSR (Engl. Trans.)* 3:144–160, cited by Sposito and Mattigod (1977).
- Gast, R.G. 1969. Standard free energies of exchange for alkali metal cations on Wyoming bentonite. *Soil Sci. Soc. Am. Proc.* 33:37–41.
- Gast, R.G. 1972. Alkali metal cation exchange on Chambers montmorillonite. *Soil Sci. Soc. Am. Proc.* 36:14–19.
- Greathouse, J.A., and R.T. Cygan. 2005. Molecular dynamics simulation of uranyl(VI) adsorption equilibria onto an external montmorillonite surface. *Phys. Chem. Chem. Phys.* 7:3580–3586.
- Greathouse, J.A., K. Refson, and G. Sposito. 2000. Molecular dynamics simulation of water mobility in magnesium-smectite hydrates. *J. Am. Chem. Soc.* 122:11459–11464.
- Griffoen, J., and C.A.J. Appelo. 1993. Adsorption of calcium and its complexes by two sediments in calcium-hydrogen-chlorine-carbon dioxide systems. *Soil Sci. Soc. Am. J.* 57:716–722.
- Gu, X., and L.J. Evans. 2008. Surface complexation modelling of Cd(II), Cu(II), Ni(II), Pb(II) and Zn(II) adsorption onto kaolinite. *Geochim. Cosmochim. Acta* 72:267–276.
- Heidmann, I., I. Christl, C. Leu, and R. Kretzschmar. 2005. Competitive sorption of protons and metal cations onto kaolinite: Experiments and modeling. *J. Colloid Interface Sci.* 282:270–282.
- Helling, C.S., G. Chesters, and R.B. Corey. 1964. Contribution of organic matter and clay to soil cation-exchange capacity as affected by the pH of the saturating solution. *Soil Sci. Soc. Am. Proc.* 28:517–520.
- Hunter, R.J. 1993. *Introduction to modern colloid science*. Oxford University Press, Oxford, U.K.
- Iwasaki, T., and T. Watanabe. 1988. Distribution of Ca and Na ions in dioctahedral smectites and interstratified dioctahedral mica/smectites. *Clays Clay Miner.* 36:73–82.
- Janssen, R.P.T., M.G.M. Bruggenwert, and W.H. van Riemsdijk. 2003. Effect of Al hydroxide polymers on cation exchange of montmorillonite. *Eur. J. Soil Sci.* 54:335–345.
- Jensen, H.E., and K.L. Babcock. 1973. Cation-exchange equilibria on a Yolo loam. *Hilgardia* 41:475–487.
- Juo, A.S.R., and S.A. Barber. 1969. An explanation for the variability in Sr-Ca exchange selectivity of soils, clays and humic acid. *Soil Sci. Soc. Am. Proc.* 33:360–363.
- Keren, R. 1979. The effect of hydroxy-aluminum precipitation on the exchange properties of montmorillonite. *Clays Clay Miner.* 27:303–304.
- Kim, Y., and R.J. Kirkpatrick. 1998. NMR  $T_1$  relaxation study of  $^{133}\text{Cs}$  and  $^{23}\text{Na}$  adsorbed on illite. *Am. Mineral.* 83:661–665.
- Kopittke, P.M., H.B. So, and N.W. Menzies. 2006. Effect of ionic strength and clay mineralogy on Na–Ca exchange and the SAR-ESP relationship. *Eur. J. Soil Sci.* 57:626–633.
- Kosakowski, G., S.V. Churakov, and T. Thoenen. 2008. Diffusion of Na and Cs in montmorillonite. *Clays Clay Miner.* 56:190–206.
- Kozaki, T., A. Fujishima, S. Sato, and H. Ohashi. 1998. Self-diffusion of sodium ions in compacted sodium montmorillonite. *Nucl. Technol.* 121:63–69.
- Kuyucak, S., O.S. Andersen, and S.-H. Chung. 2001. Models of permeation in ion channels. *Rep. Prog. Phys.* 64:1427–1472.
- Laird, D.A., and C. Shang. 1997. Relationship between cation exchange selectivity and crystalline swelling in expanding 2:1 phyllosilicates. *Clays Clay Miner.* 45:681–689.
- Laird, D.A., C. Shang, and M.L. Thompson. 1995. Hysteresis in crystalline swelling of smectites. *J. Colloid Interface Sci.* 171:240–245.
- Laudelout, H., R. van Bladel, and J. Robeyns. 1972. Hydration of cations adsorbed on a clay surface from the effect of water activity on ion-exchange selectivity. *Soil Sci. Soc. Am. Proc.* 36:30–34.
- Leote de Carvalho, R.J.F., and N.T. Skipper. 2001. Atomistic computer simulation of the clay-fluid interface in colloidal laponite. *J. Chem. Phys.* 114:3727–3733.
- Levy, G.J., H.V.H. van der Watt, I. Shainberg, and H.M. du Plessis. 1988. Potassium-calcium and sodium-calcium exchange on kaolinite and kaolinitic soils. *Soil Sci. Soc. Am. J.* 52:1259–1264.
- Lewis, R.J., and H.C. Thomas. 1963. Adsorption studies on clay minerals. VIII. A consistency test of exchange sorption in the systems sodium-cesium-barium montmorillonite. *J. Phys. Chem.* 67:1781–1783.
- Liu, X., X. Lu, R. Wang, and H. Zhou. 2008. Effects of layer-charge distribution on the thermodynamic and microscopic properties of Cs-smectite. *Geochim. Cosmochim. Acta* 72:1837–1847.
- Liu, C., J.M. Zachara, and S.C. Smith. 2004. A cation exchange model to describe  $\text{Cs}^+$  sorption at high ionic strength in subsurface sediments at Hanford site, USA. *J. Contam. Hydrol.* 68:217–238.
- Maes, A., and A. Cremers. 1977. Charge density effects in ion exchange. Part 1. Heterovalent exchange equilibria. *J. Chem. Soc. Faraday Trans. I* 73:1807–1814.
- Maes, A., and A. Cremers. 1978. Charge density effects in ion exchange. Part 2. Homovalent exchange equilibria. *J. Chem. Soc. Faraday Trans. I* 74:1234–1241.
- Maes, A., and A. Cremers. 1986. Highly selective ion exchange in clay minerals and zeolites, p. 254–295. *In* J.A. Davis, and K.F. Hayes (eds.) *Geochemical processes at mineral surfaces*. American Chemical Society, Washington, DC.
- Marry, V., J.F. Dufreche, M. Jardat, G. Meriguet, P. Turq, and F. Grun. 2003. Dynamics and transport in charged porous media. *Colloids Surf. A* 222:147–153.

- Marry, V., N. Malikova, A. Cadène, E. Dubois, S. Durand-Vidal, P. Turq, J. Breu, S. Longeville, and J.-M. Zanotti. 2008. Water diffusion in a synthetic hectorite by neutron scattering—Beyond the isotropic translational model. *J. Phys. Condens. Matter* 20:104205.
- Marry, V., and P. Turq. 2003. Microscopic simulations of interlayer structure and dynamics in bihydrated heteroionic montmorillonites. *J. Phys. Chem. B* 107:1832–1839.
- McBride, M.B. 1979. An interpretation of cation selectivity variations in  $M^+ - M^+$  exchange on clays. *Clays Clay Miner.* 27:417–422.
- McBride, M.B. 1980. Interpretation of the variability of selectivity coefficients for exchange between ions of unequal charge on smectites. *Clays Clay Miner.* 28:255–261.
- McBride, M.B., T.J. Pinnavaia, and M.M. Mortland. 1975. Electron spin resonance studies of cation orientation in restricted water layers on phyllosilicate (smectite) surfaces. *J. Phys. Chem.* 79:2430–2435.
- McKinley, J.P., J.M. Zachara, S.M. Heald, A. Dohnalkova, M.G. Newville, and S.R. Sutton. 2004. Microscale distribution of cesium sorbed to biotite and muscovite. *Environ. Sci. Technol.* 38:1017–1023.
- McNab, W.W., Jr., M.J. Singleton, J.E. Moran, and B.K. Esser. 2009. Ion exchange and trace element surface complexation reactions associated with applied recharge of low-TDS water in the San Joaquin Valley, California. *Appl. Geochem.* 24:129–137.
- Mizutani, T., T. Takano, and H. Ogoshi. 1995. Selectivity of adsorption of organic ammonium ions onto smectite clays. *Langmuir* 11:880–884.
- Morel, J.-P., V. Marry, P. Turq, and N. Morel-Desrosiers. 2007. Effect of temperature on the retention of  $Cs^+$  by Na-montmorillonite: Microcalorimetric investigation. *J. Mater. Chem.* 17:2812–2817.
- Morton, J.D., J.D. Semrau, and K.F. Hayes. 2001. An x-ray absorption spectroscopy study of the structure and reversibility of copper adsorbed to montmorillonite clay. *Geochim. Cosmochim. Acta* 65:2709–2722.
- Nakano, M., K. Kawamura, and Y. Ichikawa. 2003. Local structural information of Cs in smectite hydrates by means of an EXAFS study and molecular dynamics simulations. *Appl. Clay Sci.* 23:15–23.
- Naylor, D.V., and R. Overstreet. 1969. Sodium-calcium exchange behavior in organic soils. *Soil Sci. Soc. Am. Proc.* 33:848–851.
- Norrish, K. 1954. Manner of swelling of montmorillonite. *Nature* 173:256–257.
- Onodera, Y., T. Iwasaki, T. Ebina, H. Hayashi, K. Torii, A. Chatterjee, and H. Mimura. 1998. Effect of layer charge on fixation of cesium ions in smectites. *J. Contam. Hydrol.* 35:131–140.
- Pabalan, R.T., and F.P. Bertetti. 1999. Experimental and modeling study of ion exchange between aqueous solutions and the zeolite mineral clinoptilolite. *J. Solution Chem.* 28:367–393.
- Papelis, C., and K.F. Hayes. 1996. Distinguishing between interlayer and external sorption sites of clay minerals using x-ray absorption spectroscopy. *Colloids Surf. A* 107:89–96.
- Park, C., P.A. Fenter, N.C. Sturchio, and K.L. Nagy. 2008. Thermodynamics, interfacial structure, and pH hysteresis of  $Rb^+$  and  $Sr^{2+}$  adsorption at the muscovite (001)-solution interface. *Langmuir* 24:13993–14004.
- Park, S.-H., and G. Sposito. 2002. Structure of water adsorbed on a mica surface. *Phys. Rev. Lett.* 89:085501.
- Poinssot, C., B. Baeyens, and M.H. Bradbury. 1999. Experimental and modelling studies of caesium sorption on illite. *Geochim. Cosmochim. Acta* 63:3217–3227.
- Powell, D.H., H.E. Fischer, and N.T. Skipper. 1998. The structure of interlayer water in Li-montmorillonite studied by neutron diffraction with isotopic substitution. *J. Phys. Chem. B* 102:10899–10905.
- Rajec, P., V. Šucha, D.D. Eberl, J. Šrodón, and F. Elsass. 1999. Effect of illite particle shape on cesium sorption. *Clays Clay Miner.* 47:755–760.
- Rhue, R.D., and R.S. Mansell. 1988. The effect of pH on sodium-calcium and potassium-calcium exchange selectivity for Cecil soil. *Soil Sci. Soc. Am. J.* 52:641–647.
- Rotenberg, B., V. Marry, R. Vuilleumier, N. Malikova, C. Simon, and P. Turq. 2007. Water and ions in clays: Unraveling the interlayer/micropore exchange using molecular dynamics. *Geochim. Cosmochim. Acta* 71:5089–5101.
- Rytwo, G., A. Banin, and S. Nir. 1996. Exchange reactions in the Ca-Mg-Na-montmorillonite system. *Clays Clay Miner.* 44:276–285.
- Schlegel, M.L., K.L. Nagy, P. Fenter, L. Cheng, N.C. Sturchio, and S.D. Jacobsen. 2006. Cation sorption on the muscovite (001) surface in chloride solutions using high-resolution x-ray reflectivity. *Geochim. Cosmochim. Acta* 70:3549–3565.
- Schramm, L.L., and J.C.T. Kwak. 1982. Influence of exchangeable cation composition on the size and shape of montmorillonite particles in dilute suspension. *Clays Clay Miner.* 30:40–48.
- Serrano, S., P.A. O'Day, D. Vlassopoulos, M.T. García-González, and F. Garrido. 2009. A surface complexation and ion exchange model of Pb and Cd competitive sorption on natural soils. *Geochim. Cosmochim. Acta* 73:543–558.
- Shainberg, I., N.I. Alperovitch, and R. Keren. 1987. Charge density and Na-K-Ca exchange on smectites. *Clays Clay Miner.* 35:68–73.
- Shainberg, I., and W.D. Kemper. 1966. Hydration status of adsorbed cations. *Soil Sci. Soc. Am. Proc.* 30:707–713.
- Shainberg, I., J.D. Oster, and J.D. Wood. 1980. Sodium/calcium exchange in montmorillonite and illite suspension. *Soil Sci. Soc. Am. J.* 44:960–964.
- Shainberg, I., and H. Otoh. 1968. Size and shape of montmorillonite particles saturated with Na/Ca ions (inferred from viscosity and optical measurements). *Isr. J. Chem.* 6:251–259.
- Shaviv, A., and S.V. Mattigod. 1985. Cation exchange equilibria in soils expressed as cation-ligand complex formation. *Soil Sci. Soc. Am. J.* 49:569–573.
- Sheta, T.H., G.R. Gobran, J.E. Dufey, and H. Laudelout. 1981. Sodium-calcium exchange in Nile delta soils: Single values for Vanselow and Gaines-Thomas selectivity coefficients. *Soil Sci. Soc. Am. J.* 45:749–753.

- Sinanis, C., V.Z. Keramidas, and S. Sakellariadis. 2003. Thermodynamics of potassium-magnesium exchange in two alfisols of northern Greece. *Commun. Soil Sci. Plant Anal.* 34:439–456.
- Skipper, N.T., P.A. Lock, J.O. Titiloye, J. Swenson, Z.A. Mirza, W.S. Howells, and F. Fernandez-Alonso. 2006. The structure and dynamics of 2-dimensional fluids in swelling clays. *Chem. Geol.* 230:182–196.
- Skipper, N.T., M.V. Smalley, G.D. Williams, A.K. Soper, and C.H. Thompson. 1995. Direct measurement of the electric double-layer structure in hydrated lithium vermiculite clays by neutron diffraction. *J. Phys. Chem.* 99:14201–14204.
- Slade, P.G., J.P. Quirk, and K. Norrish. 1991. Crystalline swelling of smectite samples in concentrated NaCl solutions in relation to layer charge. *Clays Clay Miner.* 39:234–238.
- Smith, D.E., Y. Wang, A. Chaturvedi, and H.D. Whitley. 2006. Molecular simulations of the pressure, temperature, and chemical potential dependencies of clay swelling. *J. Phys. Chem. B* 110:20046–20054.
- Sposito, G. 1991. Effect of chloride ions on sodium-calcium and sodium-magnesium exchange on montmorillonite. *Soil Sci. Soc. Am. J.* 55:965–967.
- Sposito, G. 1992. The diffuse-ion swarm near smectite particles suspended in 1:1 electrolyte solutions: Modified Gouy–Chapman theory and quasicrystal formation, p. 128–155. *In* N. Güven and R.M. Pollastro (eds.) *Clay–water interface and its rheological implications*. The Clay Minerals Society, Boulder, CO.
- Sposito, G. 1993. Surface complexation of metals by natural colloids, p. 211–236. *In* J.A. Marinsky and Y. Marcus (eds.) *Ion exchange and solvent extraction*. Vol. 2. Marcel Dekker, New York.
- Sposito, G. 1994. *Chemical equilibria and kinetics in soils*. Oxford University Press, Oxford, U.K.
- Sposito, G. 1998. On points of zero charge. *Environ. Sci. Technol.* 32:2815–2819.
- Sposito, G. 2004. *The surface chemistry of natural particles*. Oxford University Press, Oxford, U.K.
- Sposito, G. 2008. *The surface chemistry of soils*. 2nd edn. Oxford University Press, Oxford, U.K.
- Sposito, G., and P. Fletcher. 1985. Sodium-calcium-magnesium exchange reactions on a montmorillonitic soil: III. Calcium-magnesium exchange selectivity. *Soil Sci. Soc. Am. J.* 49:1160–1163.
- Sposito, G., K.M. Holtzclaw, L. Charlet, C. Jouany, and A.L. Page. 1983a. Sodium-calcium and sodium-magnesium exchange on Wyoming bentonite in perchlorate and chloride background ionic media. *Soil Sci. Soc. Am. J.* 47:51–56.
- Sposito, G., K.M. Holtzclaw, C.T. Johnston, and C.S. LeVesque-Madore. 1981. Thermodynamics of sodium-copper exchange on Wyoming bentonite at 298 K. *Soil Sci. Soc. Am. J.* 45:1079–1084.
- Sposito, G., K.M. Holtzclaw, C. Jouany, and L. Charlet. 1983b. Cation selectivity in sodium-calcium, sodium-magnesium and calcium-magnesium exchange on Wyoming bentonite at 298 K. *Soil Sci. Soc. Am. J.* 47:917–921.
- Sposito, G., C. Jouany, K.M. Holtzclaw, and C.S. LeVesque. 1983c. Calcium-magnesium exchange on Wyoming bentonite in the presence of adsorbed sodium. *Soil Sci. Soc. Am. J.* 47:1081–1085.
- Sposito, G., and S.V. Mattigod. 1977. On the chemical foundation of the sodium adsorption ratio. *Soil Sci. Soc. Am. J.* 41:323–329.
- Sposito, G., and S.V. Mattigod. 1979. Ideal behavior in Na<sup>+</sup>-trace metal cation exchange on Camp Berteau montmorillonite. *Clays Clay Miner.* 27:125–128.
- Sposito, G., and R. Prost. 1982. Structure of water adsorbed on smectites. *Chem. Rev.* 82:553–573.
- Sposito, G., N.T. Skipper, R. Sutton, S.-H. Park, A.K. Soper, and J.A. Greathouse. 1999. Surface geochemistry of the clay minerals. *Proc. Natl. Acad. Sci. U. S. A.* 96:3358–3364.
- Stadler, M., and P.W. Schindler. 1993. Modeling of H<sup>+</sup> and Cu<sup>2+</sup> adsorption on calcium-montmorillonite. *Clays Clay Miner.* 41:288–296.
- Strawn, D.G., and D.L. Sparks. 1999. The use of XAFS to distinguish between inner- and outer-sphere lead adsorption complexes on montmorillonite. *J. Colloid Interface Sci.* 216:257–269.
- Sutton, R., and G. Sposito. 2005. Molecular structure in soil humic substances: The new view. *Environ. Sci. Technol.* 39:9009–9015.
- Sutton, R., G. Sposito, M.S. Diallo, and H.-R. Schulten. 2005. Molecular simulation of a model of dissolved organic matter. *Environ. Toxicol. Chem.* 24:1902–1911.
- Tambach, T.J., P.G. Bolhuis, E.J.M. Hensen, and B. Smit. 2006. Hysteresis in clay swelling induced by hydrogen bonding: Accurate prediction of swelling states. *Langmuir* 22:1223–1234.
- Tambach, T.J., E.J.M. Hensen, and B.J. Smit. 2004. Molecular simulations of swelling clay minerals. *J. Phys. Chem. B* 108:7586–7596.
- Tamura, K., H. Yamada, and H. Nakazawa. 2000. Stepwise hydration of high-quality synthetic smectite with various cations. *Clays Clay Miner.* 48:400–404.
- Tang, L., and D.L. Sparks. 1993. Cation-exchange kinetics on montmorillonite using pressure-jump relaxation. *Soil Sci. Soc. Am. J.* 57:42–46.
- Teppen, B.J., and V. Aggarwal. 2007. Thermodynamics of organic cation exchange selectivity in smectites. *Clays Clay Miner.* 55:119–130.
- Teppen, B.J., and D.M. Miller. 2006. Hydration energy determines isoivalent cation exchange selectivity by clay minerals. *Soil Sci. Soc. Am. J.* 70:31–40.
- Thellier, C., and G. Sposito. 1989. Influence of electrolyte concentration on quaternary cation exchange by Silver Hill illite. *Soil Sci. Soc. Am. J.* 53:705–711.
- Timms, W.A., and M.J. Hendry. 2007. Quantifying the impact of cation exchange on long-term solute transport in a clay-rich aquitard. *J. Hydrol.* 332:110–122.
- Tournassat, C., E. Ferrage, C. Poinson, and L. Charlet. 2004. The titration of clay minerals. Part II. Structural-based model and implications for clay reactivity. *J. Colloid Interface Sci.* 273:234–246.

- Tournassat, C., H. Gailhanou, C. Crouzet, G. Braibant, A. Gautier, A. Lassin, P. Blanc, and E.C. Gaucher. 2007. Two cation exchange models for direct and inverse modelling of solution major cation composition in equilibrium with illite surfaces. *Geochim. Cosmochim. Acta* 71:1098–1114.
- Tournassat, C., C. Lerouge, P. Blanc, J. Brendlé, J.-M. Greneche, S. Touzelet, and E.C. Gaucher. 2008. Cation exchanged Fe(II) and Sr compared to other divalent cations (Ca, Mg) in the bure Callovian–Oxfordian formation: Implications for pore-water composition modelling. *Appl. Geochem.* 23:641–654.
- Van Bladel, R., and H.R. Gheyi. 1980. Thermodynamic study of calcium-sodium and calcium-magnesium exchange in calcareous soils. *Soil Sci. Soc. Am. J.* 44:938–942.
- Van Loon, L.R., and M.A. Glaus. 2008. Mechanical compaction of smectite clays increases ion exchange selectivity for cesium. *Environ. Sci. Technol.* 42:1600–1604.
- van Oploo, P., I. White, P. Ford, M.D. Melville, and B.C.T. Macdonald. 2008. Pore water chemistry of acid sulfate soils: Chemical flux and oxidation rates. *Geoderma* 146:32–39.
- Vanselow, A.P. 1932. Equilibria of the base-exchange reactions of bentonites, permutites, soil colloids, and zeolites. *Soil Sci.* 33:95–113.
- Verburg, K., and P. Baveye. 1994. Hysteresis in the binary exchange of cations on 2:1 clay minerals: A critical review. *Clays Clay Miner.* 42:207–220.
- Verburg, K., P. Baveye, and M.B. McBride. 1995. Cation-exchange hysteresis and dynamics of formation and breakdown of montmorillonite quasi-crystals. *Soil Sci. Soc. Am. J.* 59:1268–1273.
- Voegelin, A., and R. Kretschmar. 2003. Modelling sorption and mobility of cadmium and zinc in soils with scaled exchange coefficients. *Eur. J. Soil Sci.* 54:387–400.
- Way, J.T. 1850. On the power of soils to absorb manure. *J. R. Agric. Soc. Engl.* 11:313–379.
- Weiss, C.A., Jr., R.J. Kirkpatrick, and S.P. Altaner. 1990. The structural environments of cations adsorbed onto clays:  $^{133}\text{Cs}$  variable-temperature MAS NMR spectroscopic study of hectorite. *Geochim. Cosmochim. Acta* 54:1655–1669.
- White, A.F., M.S. Schulz, D.V. Vivit, A.E. Blum, D.A. Stonestrom, and J.W. Harden. 2005. Chemical weathering rates of a soil chronosequence on granitic alluvium: III. Hydrochemical evolution and contemporary solute fluxes and rates. *Geochim. Cosmochim. Acta* 69:1975–1996.
- Whitley, H.D., and D.E. Smith. 2004. Free energy, energy, and entropy of swelling in Cs-, Na-, and Sr-montmorillonite clays. *J. Chem. Phys.* 120:5387–5395.
- Wild, A., and J. Keay. 1964. Cation-exchange equilibria with vermiculite. *J. Soil Sci.* 15:135–144.
- Wilson, J., J. Cuadros, and G. Cressey. 2004. An in situ time-resolved XRD-PSD investigation into Na-montmorillonite interlayer and particle rearrangement during dehydration. *Clays Clay Miner.* 52:180–191.
- Xu, S., and J.B. Harsh. 1992. Alkali cation selectivity and surface charge of 2:1 clay minerals. *Clays Clay Miner.* 40:567–574.
- Xu, X., A.G. Kalinichev, and R.J. Kirkpatrick. 2006.  $^{133}\text{Cs}$  and  $^{35}\text{Cl}$  NMR spectroscopy and molecular dynamics modeling of  $\text{Cs}^+$  and  $\text{Cl}^-$  complexation with natural organic matter. *Geochim. Cosmochim. Acta* 70:4319–4331.
- Zachara, J.M., and J.P. McKinley. 1993. Influence of hydrolysis on the sorption of metal cations by smectites: Importance of edge coordination reactions. *Aquat. Sci.* 55:250–261.
- Zhang, Z.Z., and D.L. Sparks. 1996. Sodium-copper exchange on Wyoming montmorillonite in chloride, perchlorate, nitrate, and sulfate solutions. *Soil Sci. Soc. Am. J.* 60:1750–1757.

# Chemisorption and Precipitation Reactions

Robert G. Ford  
United States Environmental  
Protection Agency

17.1	Introduction .....	17-1
17.2	Conceptual Distinctions in Chemisorption and Precipitation .....	17-1
	Chemisorption • Precipitation and Coprecipitation	
17.3	Influence of Abiotic and Biotic Processes .....	17-6
17.4	Quantitative Descriptions of Chemisorption and Precipitation Reactions .....	17-8
17.5	Observations of Cation and Anion Solid-Phase Partitioning in Soils .....	17-9
	Nickel • Selenium	
	References.....	17-15

## 17.1 Introduction

The partitioning of dissolved components to a solid surface in soils is governed by the competition between sorption and desorption reactions. Chemisorption (or chemical adsorption) of a dissolved component (adsorbate) to a solid surface (adsorbent) has been defined as “adsorption that results from chemical bond formation (strong interaction) between the adsorbent and the adsorbate in a monolayer on the surface” (IUPAC, 1997). These partitioning reactions may be influenced by electrostatic forces between the adsorbate and adsorbent, similar to those controlling ion-exchange reactions (discussed in this volume). It has also been observed that sorption of solution species may result in more than monolayer coverage at the surface of solid surfaces. In these cases, the adsorbate may form polynuclear surface complexes or surface precipitates (e.g., Scheidegger and Sparks, 1996). Surface precipitation can be considered as a special form of homogeneous precipitation reaction where a solid component in the soil participates in the overall reaction process (Chapter 7 in Stumm and Morgan, 1996). In the following discussion, surface precipitation includes all processes that result in incorporation of the sorbate into a solid structure that could not form in the absence of the adsorbent. This includes (1) formation of a dilute solid solution with a structure that is distinct from or shared with the original adsorbent, (2) epitaxial growth of a new solid phase sharing a structural relationship with the adsorbent, and (3) nucleation of a new solid phase at the solid–water interface. Background information and discussion of the literature (dating up to 1998) addressing chemisorption and precipitation reactions in soils were provided by McBride (1999). The following discussion provides an update on the current understanding of these reactions in soil systems.

## 17.2 Conceptual Distinctions in Chemisorption and Precipitation

### 17.2.1 Chemisorption

Chemisorption reactions involving formation of mononuclear chemical bond between solutes in the solid solution and reactive surfaces in solid matrix are referred to as *surface complexation* reactions and are typically categorized by the relative binding strength of interaction between the adsorbate (species in solution) and the adsorbent (soil solid). One should note that the conceptual underpinning that guides our historical and contemporary understanding of chemisorption/surface complexation reactions is the notion that reactive surface sites can be viewed as a special type of ligand that coordinates to cations or exchanges with anions from solution (Schindler et al., 1976; Sigg and Stumm, 1981; Sposito, 1998, 1999). While our molecular-level understanding of the physicochemical forces that govern the characteristics of these surface reactions has improved over the years, the underlying conceptual basis remains technically sound. The driving force for molecules or ions in soil solution to form surface complexes with sites of adsorption in the soil solid matrix is governed by the physical and chemical properties of the adsorbate, sorption sites, and the soil solution (i.e., “solute,” “sorbent,” and “solvent” in the more general terminology in Stumm [1992]). As an example, the probability that a cation will form an inner-sphere versus an outer-sphere surface complex will, in part, be governed by the relative free-energy change between the cation maintaining a water molecule versus a surface hydroxyl site within its immediate coordination sphere. Cations for which coordination with a water molecule is more energetically favorable will tend to favor outer-sphere surface complexes.

However, the overall tendency for surface complex formation will be governed by other factors such as electrostatic forces between the adsorbate and sorption site. Therefore, projecting trends in surface complex formation must be predicated on knowledge of the physicochemical properties of the three primary components in the reaction (i.e., adsorbate, sorption sites, and solvent), in addition to how the surface complexation reaction(s) may be modified by interactions of any or all of these primary components with other solution or solid components in the reaction system.

There are several recent discussions that provide useful perspective on the fundamental chemical factors that govern the extent for and relative strength of surface complex bond formation (e.g., Sverjensky, 2006; Brown, 2009). It should be noted that current developments in our understanding of the physicochemical forces controlling chemisorption reactions have benefited from exploration of the molecular-level processes controlling ion partitioning onto soil solids, as reflected in discussions of bond formation by Sverjensky (2006) and Brown (2009). This emphasis is, to some extent, a departure from past efforts to relate apparent trends in ion partitioning based on periodic properties of the elements (i.e., adsorbate), for example, reference to apparent macroscopic trends with respect to qualitative concepts such as the “lyotropic” or “Hofmeister” series. However, as noted in several studies, deviations in observed ion partitioning trends from qualitative concepts specific to the sorbate support the need to further development of our molecular-level understanding of chemisorption reactions (e.g., Dove and Craven, 2005; Teppen and Miller, 2006; Rotenberg et al., 2009; Kowacz et al., 2010). (Another form of solid-solution partitioning, hydrophobic bonding, plays an important role in governing uptake of nonpolar organic compounds onto soil solids. This specific partitioning mechanism is not discussed further within this chapter, and the reader is referred to other comprehensive reviews [e.g., Karickhoff, 1981; Stumm, 1992; Schwarzenbach et al., 1993], along with recent developments in the concept of bonding mechanisms intermediate between nonspecific (hydrophobic) bonding and chemisorption reactions for organic molecules [e.g., Lambert, 2008; Keiluweit and Kleber, 2009].)

There is a range of binding strength for ion adsorption that depends on characteristics of the adsorbate, adsorbent, and chemistry of the soil solution. However, discussions of binding strength are generally couched in terms of “weak” or “strong” surface complexation reactions, albeit a common convention in chemistry would categorize both the covalent and electrostatic interactions involved in adsorption as “strong” intermolecular forces (Israelachvili, 1994). For description of surface complexation reactions, the microscopic distinction that the adsorbate possesses solvation properties is borrowed from the characterization of soluble ion pairs (Westall, 1986; Stumm, 1992). If solvating water molecules are interposed between the cation or anion and the surface, the surface complex is referred to as *outer sphere* and is considered to be “weak.” Conversely, if upon surface complexation, the adsorbate loses waters of hydration such that there are no water molecules interposed between the cation

or anion and the surface, the surface complex is referred to as *inner sphere* and is considered to be “strong” (Sposito, 1984). The propensity of a cation or anion to form either an inner-sphere or outer-sphere surface complex is a function of the adsorbate, the surface functional groups of the adsorbent, and the aqueous-phase chemistry (e.g., pH and ionic strength).

For inner-sphere complexation of ions onto solid surfaces, the molecular rationale for the reaction is formation of covalent bonding within an ion’s first coordination sphere. From this perspective, several authors have observed an apparent consistency between the approach to establish linear free-energy relationships (LFER) for aqueous coordination reactions and surface complexation reactions developed for the formation of surface complexes (e.g., Schindler et al., 1976; Sigg and Stumm, 1981; Tamura and Furuichi, 1997). The apparent systematic correlation captured in an LFER reflects the relationship between the free energies of complex formation and thermodynamic properties of ions. For surface complexation reactions, LFER plots of the stability constants of metal complexation with hydroxyl surface sites versus the hydrolysis constant for metals in aqueous solutions have been interpreted as providing a thermodynamic basis for the apparent selectivity trends for metal adsorption onto reference hydrous metal oxides. Recent compilations by Bradbury and Baeyens (2005, 2009) extend these relationships to metal adsorption onto the phyllosilicate minerals, montmorillonite, and illite. As stated by the authors, the utility of these relationships is their use as a tool to estimate surface complexation constants for ions in which no data or data of high uncertainty are available. In Figure 17.1, LFER plots of published data for cations and anions are provided to illustrate the correlations that one may observe with similarities in the energetics and molecular characteristics of homogeneous (aqueous) and heterogeneous (surface) coordination reactions. While these relationships are tied to our conceptual understanding of the molecular characteristics of surface-coordination reactions, their use to project surface complexation trends in soil systems should be limited to qualitative applications. The number of interacting components, both aqueous and solid, within a soil system necessitates a more comprehensive perspective.

Important adsorbent phases commonly found in the environment include phyllosilicate minerals, metal-oxohydroxide phases, sulfide phases, and natural organic matter (Dixon and Schulze, 2002). Many phyllosilicate minerals possess a permanent negative charge as a result of the substitution of lower-valence cations, that is, Mg(II), Fe(II), Li(I) for Al(III) in the octahedral layer and/or Al(III) for Si(IV) in the tetrahedral layer (referred to as isomorphic substitution). There are two main classes of phyllosilicate minerals based on layer structure. The 1:1 mineral layer type is comprised of one Si-tetrahedral layer and one Al-octahedral layer, which in soils is commonly represented by the mineral kaolinite having the general formula  $[\text{Si}_4\text{Al}_4\text{O}_{10}(\text{OH})_8 \cdot n\text{H}_2\text{O}]$ . Kaolinite and related minerals generally have insignificant degrees of cation substitution within their octahedral and tetrahedral layers, and, thus generally possess a very low permanent negative charge. The 2:1 mineral type is

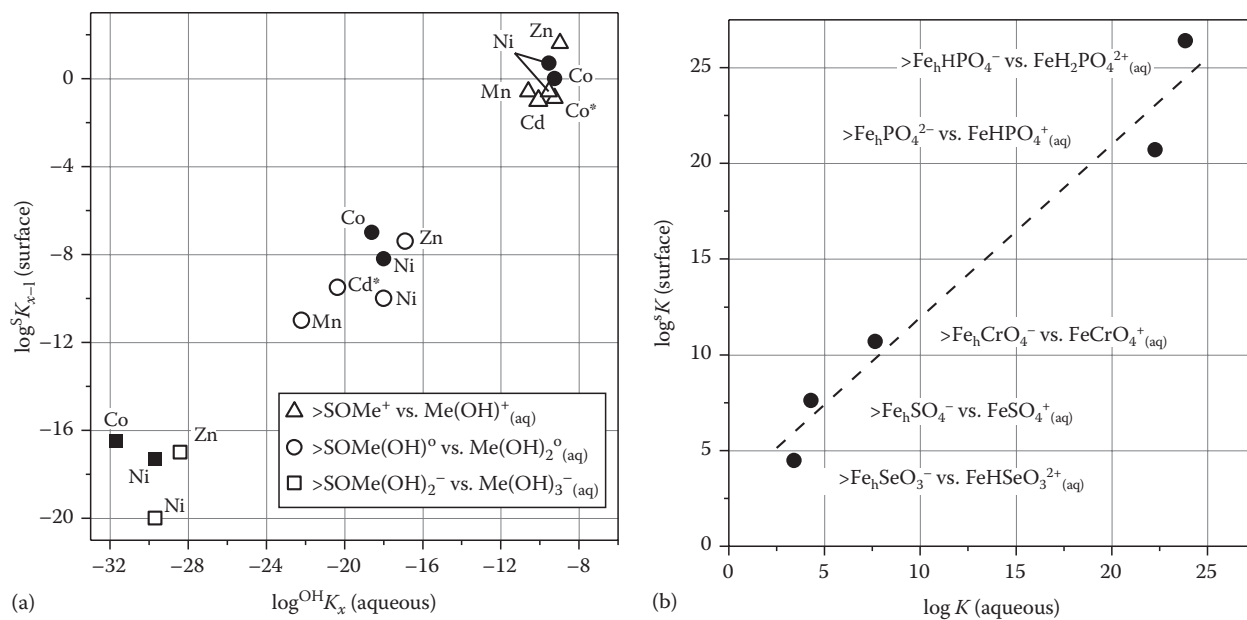


**FIGURE 17.1** Comparison of related formation constants for surface and aqueous complexes for coordination reactions between a selection of ions and aqueous or surface functional groups. (a) Relationship between the stability constant for cation complexation with surface hydroxyls of Na-exchanged montmorillonite/illite versus the metal hydrolysis species formation constant in solution (Bradbury and Baeyens, 2005, 2009). Species stoichiometry noted in legend; starred metal labels indicate surface stability constant is for Ca-exchanged montmorillonite. (b) Relationship between the formation constant for anion ligand exchange with surface hydroxyls on hydrous ferric oxide versus formation of aqueous complexes with  $Fe^{3+}$  (Visual MINTEQ, 2009). Species stoichiometry shown next to data point.

comprised of one Al-octahedral layer interposed between two Si-tetrahedral layers comparable to the mica structures. The 2:1 layer class is represented by a variety of minerals, which are classified based on the location (tetrahedral versus octahedral layer) and relative amount of isomorphous substitution. The three major mineral classes within the 2:1 layer type are illite ( $M_x[Si_{6.8}Al_{1.2}](Al_3Fe_{0.25}Mg_{0.75})O_{20}(OH)_4$ ), vermiculite ( $M_x[Si_7Al](Al_3Fe_{0.5}Mg_{0.5})O_{20}(OH)_4$ ), and smectite ( $M_x[Si_8]Al_{3.2}Fe_{0.2}Mg_{0.6}O_{20}(OH)_4$ ), which display different levels of cation substitution in their tetrahedral and octahedral layers. The permanent negative charge imparted to 2:1 clay minerals by isomorphous substitution is typically balanced through exchange reactions involving major cations in soil solution (e.g.,  $Na^+$ ,  $K^+$ ,  $Ca^{2+}$ , or  $Mg^{2+}$ ; represented by “ $M_x$ ” in the formulas listed above).

Chemisorption of ions to phyllosilicates may occur via electrostatic exchange reactions (on the basal plane or within clay particle interlayers) or surface complexation with surface functional groups, for example, terminal silanol or aluminol functional groups at the edges of clay particles, for example, montmorillonite (Bradbury and Baeyens, 2005) and illite (Bradbury and Baeyens, 2009). Due to differences in the levels of isomorphous substitution for the 1:1 and 2:1 clay-mineral classes, ion exchange is usually only significant for 2:1 phyllosilicates. In addition to siloxane oxygen atoms along the basal plane, phyllosilicates possess two types of terminal ionizable hydroxyl groups ( $>OH^o$ ), aluminol and silanol, protruding from the edge surface. These edge  $>OH^o$  groups can form both inner- and outer-sphere surface complexes with metal cations and oxyanions depending on

the pH of the bathing solution and on the specific chemical characteristics of the adsorbate.

The most important inorganic phases for surface reactions with ions in many soil systems are the metal-oxohydroxide phases. These phases are characterized by hexagonal or cubic close-packed O or OH anions with Fe(II)/Fe(III), Al(III), and/or Mn(III)/Mn(IV) occupying octahedral sites. These oxides are present as discrete phases and as complex mineral assemblages, being associated with phyllosilicates and primary minerals as coatings or with humic macromolecules. In soils, the crystallinity of these phases typically varies from poorly ordered to well-crystalline forms and grain size from the nanometer to micrometer scale. Among the most common Fe-oxohydroxide phases found in soils are the poorly ordered phase ferrihydrite ( $Fe_2O_3 \cdot nH_2O$ ), and the moderate to well-crystalline phases, goethite ( $\alpha$ - $FeOOH$ ), and hematite ( $\alpha$ - $Fe_2O_3$ ). The most common Al-oxohydroxide phase found in soils is gibbsite ( $\gamma$ - $Al(OH)_3$ ). Additionally, poorly ordered aluminosilicates can be important reactive phases in certain soils and these include the very poorly ordered allophanes (Si/Al ratios 1:2–1:1) and the paracrystalline phase, imogolite ( $SiO_2 \cdot Al_2O_3 \cdot 2H_2O$ ). While Mn oxohydroxides are less prevalent than Fe and Al oxohydroxides in soils, they are very important phases in terms of surface-mediated redox reactions and because of their propensity for high metal sorption. The mineralogy of Mn is complicated by the range in Mn–O bond lengths resulting from extensive substitution of Mn(II) and Mn(III) for Mn(IV). Thus, there exists a continuous series of stable and metastable compositions from

MnO to MnO<sub>2</sub> forming a large variety of minerals. Among the more common Mn oxohydroxides are pyrolusite ( $\beta$ -MnO<sub>2</sub>), the hollandite–cryptomelane family ( $\alpha$ -MnO<sub>2</sub>), todorokite, and birnessite ( $\delta$ -MnO<sub>2</sub>).

The reactive surface functional group for all of the metal-oxohydroxide phases is the inorganic  $>\text{OH}^\ominus$  moiety exposed on the outer periphery of these minerals. The reactivity of a specific metal oxohydroxide is dependent on the surface area ( $S_A$ ), surface-site density ( $N_S$ ), the degree of coordination of the  $>\text{OH}^\ominus$  group to the bulk structure, and the point of zero charge (PZC). The charge on the mineral surface may impose either attractive or repulsive contributions to the overall adsorption reaction, depending on the type of charge possessed by the adsorbate. The surface charge of oxohydroxide minerals and edge sites on phyllosilicates is derived from the protonation and ionization of exposed surface hydroxyl groups, represented by  $>\text{OH}^\ominus$ , where “>” represents the bond to structural elements within the solid (e.g., Fe, Al, Mn). As a function of pH, the surface functional groups can be generally described with the following idealized nomenclature:  $>\text{OH}_2^+$ ,  $>\text{OH}^\ominus$ , and  $>\text{O}^-$ , which illustrates the pH-dependent charging behavior in the absence of other potential-determining ions in solution. The exact charge associated with the various surface functional groups is difficult to measure, so the main purpose of employing this nomenclature is to illustrate that surface charge varies as a function of soil solution chemistry. Discussions of surface-charging behavior and surface-coordination reactions for a range of common soil minerals is provided elsewhere (e.g., Stumm, 1992; Sparks, 2003). The properties of the adsorbent that impact surface complexation are controlled by both the grain size and specific chemical structure of the solid phase.

While the surfaces of oxohydroxide minerals constitute a significant fraction of sites that participate in chemisorption reactions, they are not the only type of surface sites present. Depending on soil type and mineralogy, other sources of reactive surfaces may include carbonates, sulfides, and soil organic matter. For these solids, the same conceptual convention can be employed to identify the reactive chemical surface moiety for the purpose of describing chemisorption reactions based on chemical and electrostatic properties. There are several published examples that illustrate application of the surface complexation model (SCM) concept to describe ion chemisorption to the surface of carbonates (Villegas-Jimenez et al., 2009), sulfides (Wolthers et al., 2005), and components of soil organic matter (Westall et al., 1995; Cabaniss, 2008; Cabaniss, 2009). Summarized in Table 17.1 is a listing of the types of chemical nomenclature used to represent the reactive surface sites for these solid components.

Soil organic matter, or humus, is derived from the physical, chemical, and biological breakdown of vegetation and fauna originating from above and below the soil surface (e.g., Wershaw, 1994; Zech et al., 1997; Ponge, 2003; Sutton and Sposito, 2005). The recalcitrant soil organic matter thus produced is comprised of complex polymers called humic substances, which constitute another very important reactive phase in soil solids

**TABLE 17.1** Published Examples for Chemical Representations of Reactive Surface Sites Used in Development of Surface Complexation Models to Describe Protonation–Deprotonation Reactions for Variably Charged Solids

Chemical Representations of Reactive Surface Sites	
Chemical System	Protonation–Deprotonation Reactions
CaCO <sub>3</sub> (calcite)–H <sub>2</sub> O–CO <sub>2</sub> (Martin-Garin et al., 2003; Gaskova et al., 2009)	$>\text{CaOH}^\ominus + \text{H}^+ = >\text{CaOH}_2^+$ $>\text{CaOH}^\ominus = >\text{CaO}^- + \text{H}^+$ $>\text{CaOH}^\ominus + \text{CO}_3^{2-} + 2\text{H}^+ = >\text{CaHCO}_3^\ominus + \text{H}_2\text{O}$ $>\text{CaOH}^\ominus + \text{CO}_3^{2-} + \text{H}^+ = >\text{CaCO}_3^- + \text{H}_2\text{O}$ $>\text{CO}_3\text{H}^\ominus = >\text{CO}_3^- + \text{H}^+$ $>\text{CO}_3\text{H}^\ominus + \text{Ca}^{2+} = >\text{CO}_3\text{Ca}^+ + \text{H}^+$
FeS (mackinawite)–H <sub>2</sub> O (Wolthers et al., 2005)	$>\text{FeSH}^\ominus + \text{H}^+ = >\text{FeSH}_2^+$ $>\text{FeSH}^\ominus = >\text{FeS}^- + \text{H}^+$ $>\text{Fe}_3\text{SH}^\ominus + \text{H}^+ = >\text{Fe}_3\text{SH}_2^+$ $>\text{Fe}_3\text{SH}^\ominus = >\text{Fe}_3\text{S}^- + \text{H}^+$
Lignocellulosic substrate–H <sub>2</sub> O (Ravat et al., 2000)	$>\text{S}_1\text{OH} = >\text{S}_1\text{O}^- + \text{H}^+$ (carboxylic sites) $>\text{S}_2\text{OH} = >\text{S}_2\text{O}^- + \text{H}^+$ (phenolic sites)

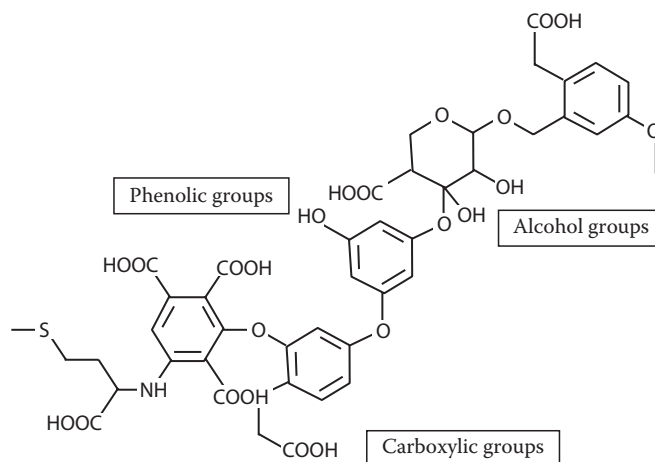


**FIGURE 17.2** Hypothetical structural model of a soil organic matter structural fragment illustrating types of reactive functional groups. Protonation–deprotonation reactions occurring during acid titration are generally attributed to carboxylic and phenolic moieties.

(e.g., Kelleher and Simpson, 2006; Simpson et al., 2007a, 2007b; Smejkalova and Piccolo, 2008). A variety of functional groups are present in humic substances, and, like  $>\text{OH}^\ominus$  functional groups of the inorganic metal oxohydroxides, these also are characterized by pH-dependent charging mechanisms. The primary functional groups associated with humic substances in terms of surface charge are typically represented as carboxyl and phenolic groups (Figure 17.2); however, less abundant amino, imidazole, sulfhydryl, or other potential structural groups may play an important role in protonation–deprotonation and chemisorption reactions of some ions when present at trace levels (e.g., Schaumann, 2006; Niederer et al., 2007; Matynia et al., 2010). Degradation of natural organic matter in soils leads to a change in the relative distribution of the chemical structures within the complex suite of macromolecular compounds that constitute



soil organic matter. As an example, Lorenz et al. (2007) illustrate a general scheme for the evolution of the chemical makeup of terrestrial biomass during weathering resulting in the depletion of oxygenated-alkyl carbon structures and the enhancement of alkyl carbon structures. As illustrated in the review by Chefetz and Xing (2009), changes in the relative proportion of structural components in soil organic matter may influence the reactivity of this adsorbent pool within soils, since these structural components comprise the reactive moieties in soil organic matter that are binding sites for dissolved inorganic and organic compounds in the soil solution.

As illustrated by the previous discussion, chemical bonding between solutes in the soil solution and the surfaces of soil solids will exert control over solute concentrations. Typically, these reactions dominate solid-water partitioning at low solute concentrations or in systems where there is minimal active precipitation of new soil minerals. However, some soil systems will be characterized by large fluxes of ions through the soil pore water either due to infiltration from external water sources or internal instability of the mineral matrix as a function of soil age (e.g., Huggett, 1998; Lilienfein et al., 2003) or microbial activity (e.g., Wiederhold et al., 2007). In these systems, active precipitation of new solid phases may dominate over chemisorption reactions to control solute concentrations in the soil solution.

## 17.2.2 Precipitation and Coprecipitation

Mineral-water reactions occur during movement of water through soil pores. These reactions may result in the release of structural components from soil solids due to mineral dissolution or result in the buildup to oversaturation and consequent precipitation of secondary minerals. As an outcome of mineral-water reactions along a flow path, fluid compositions and the mineralogical makeup of the soil matrix will continuously evolve toward a stable state or an equilibrium state. Mineral precipitation processes in soil systems may govern the concentrations of major and trace elements in the soil solution.

Full treatment of precipitation processes, including coverage of relevant thermodynamic and kinetic concepts, is outside the scope of this document. The reader is referred to numerous standard textbooks in geochemistry, soil science, and aquatic chemistry (e.g., Lindsay, 1979; Drever, 1982; Stumm, 1992; McBride, 1994; Stumm and Morgan, 1996; Langmuir, 1997; Lasaga, 1999; Sparks, 2003; Sposito, 2008). The purpose of this section is to introduce key concepts and issues regarding the potential impact precipitation reactions may exert on solute partitioning in soils. In general, mineral precipitation in relation to the solid-phase partitioning of soil solutes can be discussed in the context of four widely studied processes:

- *Precipitation from solution:* Nucleation and growth of a solid phase exhibiting a molecular unit that repeats itself in three dimensions. Homogeneous nucleation occurs from bulk solution and heterogeneous nucleation

occurs on the surfaces of organic or mineral particles. Heterogeneous nucleation is thought to be more important in natural systems that are rich in reactive inorganic and biological surfaces. Precipitation may result in the formation of sparingly soluble oxohydroxides, carbonates, and, in anoxic systems, sulfides. Many precipitation reactions have a strong dependence on pH.

- *Coprecipitation:* Incorporation of an element as a trace or minor constituent within a precipitating phase. In this case, the ion substitutes for a more concentrated component in the crystal lattice (isomorphous substitution). This process is distinct from adsorption due to incorporation of the ion within the bulk structure of the major mineral phase. Examples of coprecipitation include Cr(III) in hydrous ferric oxide, Cd(II) in calcium carbonate, and As(III) in iron sulfide.
- *Surface precipitation:* A precipitation process intermediate between surface complexation and precipitation from bulk solution. Surface precipitation represents the continuous growth of particles formed via heterogeneous nucleation. Macroscopic studies of adsorption of some solutes, particularly divalent and trivalent cations, suggest that precipitation occurs at surfaces under conditions where the solid is apparently undersaturated based on solution concentrations (Dzombak and Morel, 1990).
- *Mineral transformation:* Adsorbed ions can become incorporated into minerals that form as a result of recrystallization or mineral transformation processes in soils. Transformation reactions may be accelerated or retarded by the ion, and in some cases mineral transformation may result in the exclusion of the solute from the solid phase. Examples include incorporation of anions, such as As(V) and U(VI), into metastable hydrous ferric oxide (poorly crystalline ferrihydrite) and transformation to more crystalline Fe oxohydroxides (e.g., Ford, 2002; Nico et al., 2009), coprecipitation of metals with iron monosulfide and transformation to iron disulfide (e.g., Lowers et al., 2007), and incorporation of metals into layered double hydroxides (LDHs; typically with Al) as intermediates between adsorbed/surface precipitated metal ions like Ni and Zn and metal-ion-containing phyllosilicates.

The relative importance of these processes will be determined by solute characteristics as well as characteristics of soil solution and solids within a given system. These individual processes are discussed in more detail in the following sections.

### 17.2.2.1 Precipitation from Solution

Solution precipitation or crystallization can be divided into two main processes: nucleation and crystal growth. Nucleation occurs prior to growth of a mineral crystal. Both nucleation and growth processes require a system to be oversaturated in the new phase. The probability that nucleation will occur increases exponentially as a function of the degree of oversaturation. Nucleation of a new phase is often facilitated in the presence of

a surface (heterogeneous nucleation) rather than in bulk solution (homogeneous nucleation). Because nucleation and growth are processes that compete for dissolved solutes, at high degrees of oversaturation, the rate of nucleation may be so fast that all excess solute is partitioned into crystal nuclei. In contrast, lower levels of oversaturation can result in the growth of existing crystals without nucleation. Well-formed or euhedral crystals typically develop slowly via growth from solution at low degrees of oversaturation. During crystal growth, various chemical reactions can occur at the surface of the growing mineral, such as adsorption, ion exchange, diffusion, and formation of surface precipitates. In general, the rate of crystal growth is controlled either by transport of solutes to the growing surface (i.e., transport controlled), by reactions at the surface (i.e., surface controlled), or a combination of these factors.

For the most abundant cations present in soils, such as Al, Si, Fe, Mn, Ca, and Mg, precipitation of mineral forms is common and will in many cases control concentrations observed in solution (e.g., see Chapter 5 in Sposito, 2008). Concentrations of trace solutes are typically several orders of magnitude below the concentrations of the major ions in soil solutions. At low concentrations, adsorption, surface precipitation, or formation of a dilute solid solution (coprecipitation; e.g., Shao et al., 2009) may be the more probable removal processes for trace solutes (McBride, 1994).

### 17.2.2.2 Continuum from Surface Complexation to Precipitation

Experimental studies examining chemisorption at high solute concentrations have been used to illustrate that surface loadings can exceed monolayer coverages (Dzombak and Morel, 1990). Surface precipitation may result when adsorption leads to high sorbate coverage at the mineral–water interface. Surface precipitation can be thought of as an intermediate stage between surface complexation and bulk precipitation of the sorbing ion in solution (Farley et al., 1985; Katz and Hayes, 1995; Lützenkirchen and Behra, 1995). At low concentrations of the sorbing metal at the mineral surface, surface complexation is the dominant process. As the concentration of the sorbate increases, the surface complexation concentration increases to the point where nucleation and growth of a surface precipitate occurs. Surface precipitation can be viewed as a special case of coprecipitation, where the mineral interface is a mixing zone for ions incorporated into the surface precipitate and those from the underlying substrate (e.g., Thompson et al., 1999; Schlegel et al., 2001; Román-Ross et al., 2006; Schlegel and Manceau, 2006). It is generally believed that surface precipitation can occur from solutions that would appear to be undersaturated relative to precipitate formation based on considering solution saturation indices. The reasons for this may be due, in part, to incomplete consideration of all possible precipitate phases with lower solubility that could form under system conditions or to the way component activities at the mineral–water interface are modeled (Kulik, 2002a, 2002b; Sverjensky, 2003).

Characterization of metal partitioning in soils developed under a variety of conditions have confirmed the importance of the interfacial precipitation products identified in simple experimental systems (e.g., Manceau et al., 2000; Jacquat et al., 2008). However, it is unclear if these phases were formed via homogeneous or heterogeneous reactions in the observed soil systems. With improvements in the availability of solubility and thermochemical data for solids that were previously unidentified in soil systems, it may become apparent that their formation can be assumed as a more common feature of solute partitioning. It should be noted, however, that solid surfaces do play significant roles as collectors of solutes into a more confined reaction volume and they often serve as the primary source of soluble components that combine with solutes to form precipitation products.

## 17.3 Influence of Abiotic and Biotic Processes

The chemical characteristics of the soil solution and properties of soil mineral components are, in part, influenced by microbial reactions (e.g., Brown et al., 1999; Chadwick and Chorover, 2001; Birkham et al., 2007). Microbial activity within the soil system may also play a more direct role in controlling ion speciation and mobility via direct respiration of solutes in soil pore water or adsorbed to mineral surfaces (e.g., Lloyd et al., 2003). The influence of microbial reactions may be more pronounced in soils with large pools of degradable organic carbon and supporting nutrient fluxes. For microbially productive soil systems, soil-solution chemical parameters such as pH, alkalinity, and the concentrations of iron, manganese, and sulfur species may be regulated, in part, by microbial respiration. As an example, microbial respiration within the rhizosphere impacts the level of CO<sub>2</sub> in the soil solution, with resultant CO<sub>2</sub> partial pressure 10- to 100-fold higher than that of the atmosphere (Hinsinger et al., 2009). Ultimately, the soil solution chemistry will be governed by the dynamic interaction between these biotic processes and concurrent chemical weathering of solid components within the soil. In order to provide perspective on the potential influence of the subsurface microbiology, the following discussion provides an overview of general characteristics of subsurface microbiology and the influence of microbial activity on the redox state within soil pore water.

Since microorganisms chemically transform soil constituents such as dissolved oxygen, iron (aqueous and solid forms of Fe(III) and Fe(II)), and sulfur (aqueous species such as sulfate and dissolved sulfide), their metabolic reactions may exert significant influence on the redox chemistry within soil pore water. As previously discussed, redox conditions within the soil may govern precipitation–dissolution reactions that control precipitation or coprecipitation of solutes, as well as the types and concentration of soil solids that may serve as adsorbents. From this perspective, some knowledge about the microbial populations that a function within the soil system may be necessary

to understand the existing redox status and make projections about how it may evolve. For heterotrophic microorganisms, the electrons or reducing equivalents (hydrogen or electron-transferring molecules) produced during degradation of organic compounds must be transferred to a terminal electron acceptor (TEA). Observations of microbial systems have led to the development of a classification system that groups microorganisms into three categories, according to predominant TEAs (Chapelle et al., 2002; Salminen et al., 2006):

- *Aerobic bacteria*: Bacteria that can only utilize molecular oxygen as a TEA. Without molecular oxygen, these bacteria are not capable of degradation.
- *Facultative aerobes/anaerobes*: Bacteria that can utilize molecular oxygen or when oxygen concentrations are low or nonexistent, may switch to nitrate, manganese oxides, or iron oxides as electron acceptors.
- *Anaerobes*: Bacteria that cannot utilize oxygen as an electron acceptor and for which oxygen is toxic. Though members may utilize nitrate or other electron acceptors, it can be said that they generally utilize sulfate or carbon dioxide as electron acceptors.

In any environment in which microbial activity occurs, there is a progression from aerobic to anaerobic conditions (ultimately methanogenic) with an associated change in the redox status of the system. There is generally a definite sequence of electron acceptors used in this progression through distinctly different redox states. The rate, type of active microbial population, and level of activity under each of these environments are controlled by several factors. These include the concentration of the electron acceptors, substrates that can be utilized by the bacteria, and specific microbial populations active within the soil system. This results in a loss of organic carbon and various electron acceptors from the system as well as a progression in the types and physiological activity of the indigenous bacteria.

If microbial activity is high, the soil system would be expected to progress rapidly through these conditions. The following scenario outlines a general sequence of events in which aerobic metabolism of preferential carbon sources would occur first. The carbon source may be from anthropogenic organic sources or other more readily degradable forms of natural organic carbon, which has entered the system previously or simultaneously with surface infiltration.

- *Oxygen-reducing to nitrate-reducing conditions*: Once available oxygen is consumed, active aerobic populations begin to shift to nitrate respiration. Denitrification will continue until available nitrate is depleted or usable carbon sources become limiting.
- *Nitrate-reducing to manganese-reducing conditions*: Once nitrate is depleted, populations that reduce manganese may dominate. Bacterial metabolism of substrates utilized by manganese-reducing populations will continue until the concentration of manganese oxide becomes limiting.

- *Manganese-reducing to iron-reducing conditions*: When manganese oxide becomes limiting, iron reduction becomes the predominant reaction mechanism. Available evidence suggests that iron reduction does not occur until all Mn(IV) oxides are depleted. In addition, bacterial Mn(IV) respiration appears to be restricted to areas where sulfate is nearly or completely absent.
- *Iron-reducing to sulfate-reducing conditions*: Iron reduction continues until substrate or carbon limitations allow sulfate-reducing bacteria (SRB) to become active. SRB then dominate until usable carbon or sulfate limitations impede their activity.
- *Sulfate-reducing to methanogenic conditions*: Once usable carbon or sulfate limitations occur, methanogenic bacteria are able to dominate.

Ultimately, these processes may govern both the chemical speciation of solutes in soil solutions and the solid-phase partitioning reactions that control aqueous solute concentrations. For the latter, biotic controls on solution chemistry could potentially dictate the types of adsorbent surfaces or the saturation state of the soil solution relative to solute precipitation reactions.

As a unique example of the biogeochemical complexity of soil systems, it is worth examining the volume of soil immediately adjacent to living roots that project down from plants located at the soil surface. This zone within the soil system is referred to as the rhizosphere, which encompasses a unique setting relative to the fluxes of chemical constituents that are governed by interactions among plant physiological processes, soil microorganisms, soil mineral components, and the transport of soil water and gases (e.g., Belnap et al., 2003; Hinsinger et al., 2009). Within the rhizosphere, plants mediate the chemical composition of the soil solution via release of low-molecular-weight organic acids such as malate, citrate, and oxalate (Jones, 1998; Bais et al., 2006). These organic acids may form complexes with ions in solution, form surface complexes with soil minerals, or may be oxidized to forms of inorganic carbon via microbial degradation (along with new biomass). Depending on the relative concentration of these low-molecular-weight organic acids to ions and sorption sites, complexation reactions that occur in these ternary systems may lead to decreased (Kraemer et al., 1999; Neubauer et al., 2000) or increased (Neubauer et al., 2000) ion adsorption onto mineral surfaces. More complex organic molecules, such as siderophores and other hydroxamic acids that are secreted by plants and microorganisms (Kraemer et al., 2006; Crumbliss and Harrington, 2009), present a more specialized class of organic molecules that can form polydentate complexes with ions in solution. These organic molecules may possess specific functional roles such as increasing the availability of nutritional forms of iron (e.g., Crumbliss and Harrington, 2009) or detoxifying metal ions present in the soil solution (e.g., Gilis et al., 1998; Dimkpa et al., 2008). Interactions of ions with these organic molecules in the soil solution exert direct influence on the potential for chemisorption or precipitation reactions to occur.

## 17.4 Quantitative Descriptions of Chemisorption and Precipitation Reactions

Reviews of mathematical models for describing chemisorption reactions and their practical application for depicting solute complexation to solid surfaces in natural systems is provided in Zachara and Westall (1999) and Goldberg et al. (2007 and references therein). In general, these models can be grouped into two categories that project solute partitioning using semiempirical relationships or through the development of chemical reaction expressions that depict chemisorption as the formation of chemical bonds between the solute and surface sites representing the termination of the adsorbent structure. The second category of models is commonly referred to as SCMs. Their use for describing chemisorption reactions has become standard since they provide the following: (1) the means to rationalize observed patterns in solute binding to solid surfaces due to electrostatic and chemical properties of the reactants and (2) a mathematical framework consistent with thermodynamic descriptions of aqueous complexation and precipitation reactions. The utility and chemical sensibility of this modeling framework has resulted in the development of computer software applications and supporting data compilations of chemisorption reactions for cations and anions on soil mineral phases (e.g., Dzombak and Morel, 1990; Tonkin et al., 2004). Detailed descriptions of the chemical basis and development of SCMs is available in a number of sources (e.g., Sposito, 1984; Davis and Kent, 1990; Stumm and Morgan, 1996). Brown (2009) presents an alternative framework in which to evaluate thermodynamic properties of chemisorption reactions. In this approach, the bond valence model is invoked to assess constraints on the types of surface bonds that can form. A primary constraint that is applied in this framework is the valence sum rule, which states that the sum of bond valences around any atom should be equal to the atomic valence. In contrast to the common formalism within most SCMs of providing explicit descriptions and accounting of electrostatic interactions across the surface, the bond valence model incorporates all electrostatic effects into the bonds that are formed. The extent of adhesion between atoms in the solid and solution (i.e., surface complex formation) is evaluated by ensuring that the valence sum rule is obeyed around each atom in the system. Although the bond valence model provides a way to evaluate the chemical suitability of proposed bonding structures, this approach is not currently implemented in a mathematical framework that can be merged with existing thermodynamic formalisms for calculating solution complexation and precipitation reactions. Until this occurs, the formalisms employed for describing surface bond formation in current SCMs will likely continue to be employed.

Goldberg et al. (2007) and Goldberg and Criscenti (2008) have highlighted potential limitations for the application of SCMs to project chemisorption reactions in soil systems. Reaction expressions depicting chemisorption reactions presume knowledge of the types and availability of solid surfaces in the system being

modeled. The heterogeneity of soil systems hampers selection of appropriate reactive surfaces and adsorption site densities to be explicitly represented in an SCM. Two proposed modeling strategies to address this difficulty include the component additivity (CA) and general composite (GC) approaches. The CA approach is based on the summed contribution of individual adsorbent phases, and, thus, makes use of individual reaction expressions developed for each solute-adsorbent pair from model experimental systems. The predictive capability of the CA approach will be highly dependent on knowledge of the specific adsorbents active in solute chemisorption for a particular soil. The GC approach is based on the assumption that the assemblage of adsorbent phases within the soil can be represented by “generic” surface functional groups with reaction stoichiometries and formation constants derived from experimental adsorption data for individual soil samples. The utility of the GC approach over purely empirical partitioning coefficients is that the chemisorption model can be coupled to equilibrium models of aqueous solute speciation and solubility. Thus, chemisorption model projections will be sensitive to changes in aqueous solute speciation and/or solution saturation state relative to homogeneous precipitation of the solute. In addition, the GC approach allows for explicit accounting of electrostatic interactions across the surface (based on laboratory measurements of surface-charging behavior) or incorporation of these interactions implicitly within the optimized surface complexation constant determined for a given system.

Another limitation of SCMs has been the standard state used to express the activities of surface sites and surface species. Kulik (2002a, 2002b) and Sverjensky (2003) have illustrated that the hypothetical standard state employed in current model formulations results in equilibrium constants that are directly dependent on properties of the adsorbent such as the site density and surface area. Thus, surface protonation and stability constants for solute adsorption developed for a particular mineral specimen, for example, goethite, at a given solid:solution ratio may not be directly transferable to modeling adsorption of another goethite specimen with different specific surface area and/or solid:solution ratio. Both authors have proposed an alternative standard state that can be used to develop surface protonation and complex stability constants that are independent of individual adsorbent properties and experimental conditions. The new standard-state convention can be used to convert conditional stability constants derived using law-of-mass action (LMA) algorithms (Sverjensky, 2003) or the Gibbs energy minimization (GEM) approach (Kulik, 2002b). As illustrated by Kulik (2002a), surface complexation constants derived using the LMA convention can be converted to the GEM convention using the newly proposed standard state for surface species. In addition, Kulik (2002b) illustrates that the GEM approach also allows one to factor in which adsorbents are stable or metastable, and how the site types are distributed between the adsorbent surfaces. Given our understanding that the suite of mineral components, and their inherent solubility and surface complexation properties, undergoes dynamic transitions in soil systems

(e.g., Chadwick and Chorover, 2001), the GEM approach presents an attractive alternative for modeling low-temperature aqueous chemistry reactions.

A final issue of concern for modeling solute adsorption onto mineral surfaces is development of approaches to represent the transition from surface loadings less than to greater than monolayer coverage. As discussed previously, the formation of a mononuclear surface complex may represent an intermediate step to the development of a polynuclear species with 2D or 3D order, commonly referred to as surface precipitates. The composition of surface precipitates will be governed by the participating elements from the solution and the host mineral surface. Modeling strategies have been developed within the convention of the LMA-SCM (Farley et al., 1985; Katz and Hayes, 1995), and they have been employed to replicate sorption data for wide ranges of surface coverage assuming either the formation of a pure solid or solid solution incorporating the solute species (e.g., Charlet and Manceau, 1992; Román-Ross et al., 2006). For these applications, assumptions are made about the fraction of the adsorbent that participates in formation of binary or higher-order solid solutions, as well as the ideality of the modeled solid solutions relative to the endmember structures. Curti et al. (2005) and Kulik (2006) have proposed alternative strategies to represent and select the solid solutions that may realistically form based on GEM. Significant model development and testing remains before much confidence can be placed on projections of surface precipitation or surface solid-solution formation in soil systems.

## 17.5 Observations of Cation and Anion Solid-Phase Partitioning in Soils

The distribution of cations and anions between the solid-water interfaces present in soils is governed by chemical characteristics of the aqueous and solid species and the chemistry of the soil solution. The distribution between adsorbed and precipitated forms of these constituents will also be influenced by the total concentrations of reactive species, as well as the influence of biotic processes that govern the distributions of redox-sensitive reactants within the soil. As stated earlier, properties of the soil solution, adsorbate, and sorption sites will govern the types of chemisorption reactions that may take place. The solution speciation of cations/anions, as controlled by solution complexation reactions and the distribution of ion oxidation states will govern the saturation state of the soil solution with respect to potential precipitates. As one would anticipate, it is difficult to project what reactions may dominate solid-solution partitioning for ions without full knowledge of the solution chemistry and solid surface properties. For some ions, such as the alkali metals or halide anions, this task is simplified due to the predominance of a single oxidation state in natural systems and the high solubility of potential precipitate phases. However, this simplicity rapidly diminishes with departure from these bracketing groups within the periodic table of elements. Thus, the remaining discussion

will focus on illustrative examples of the types of chemical factors that influence chemisorption-precipitation versus an exhaustive review of the periodic properties of the elements. In order to illustrate the disparity in potential reaction paths for ions in soil solutions, the controls on solid-water partitioning for nickel (Ni) and selenium (Se) are reviewed in the following sections. These elements illustrate both the range of chemisorption-precipitation reactions that influence ion partitioning in soils and the degree of complexity inherent in monitoring and projecting these reactions in dynamic soil systems.

### 17.5.1 Nickel

Nickel is not commonly seen as a critical element in agricultural or environmental systems. However, as noted in a recent review by Hansch and Mendel (2009), it is considered to be an important micronutrient, and, for specific plant species, deficiencies in nickel availability may limit plant growth for agricultural (Bais et al., 2006) or phytoremediation applications (Wood et al., 2006). At higher concentrations in soil solutions, nickel may also exert a toxic effect on plant species (e.g., Khan et al., 2006). In ambient aqueous systems, nickel exists in the divalent oxidation state and is not subject to oxidation-state transformations under typical conditions. Nickel predominantly exists as a cationic species ( $\text{Ni}^{2+}$ ) or various hydrolysis species (e.g.,  $\text{NiOH}^+$ ) at near-neutral pH (Baes and Mesmer, 1986). However, nickel may also form dissolved complexes in the presence of high concentrations of inorganic ions such as carbonate/bicarbonate and sulfate (Hummel and Curti, 2003; Chen et al., 2005) or organic ligands such as natural/synthetic carboxylic acids and dissolved humic compounds (Bryce and Clark, 1996; Baeyens et al., 2003; Strathmann and Myneni, 2004). It is anticipated that nickel may form complexes with dissolved sulfide under sulfate-reducing conditions, although the current state of knowledge is insufficient to ascertain the relative importance of these species in aqueous systems (Thoenen, 1999). The formation of solution complexes, especially with organic ligands (e.g., Strobel, 2001; Fröberg et al., 2006), may limit sorption of nickel to mineral surfaces in soils (see Section 17.5.1.2).

The solid-solution partitioning of Ni is chosen as a point of reference for ions that are not subject to a change in valence state due to shifts in redox characteristics in the soil solution. However, redox chemistry may exert an indirect control on Ni partitioning by governing the distribution of solid surfaces that may influence chemisorption reactions, as well as the distribution and concentrations of solution species that limit the solubility of Ni-bearing precipitates that may form. Nickel also provides an example of an ion that demonstrates a wide range of solid-solution partitioning behavior including adsorption, surface precipitation, and homogeneous precipitation.

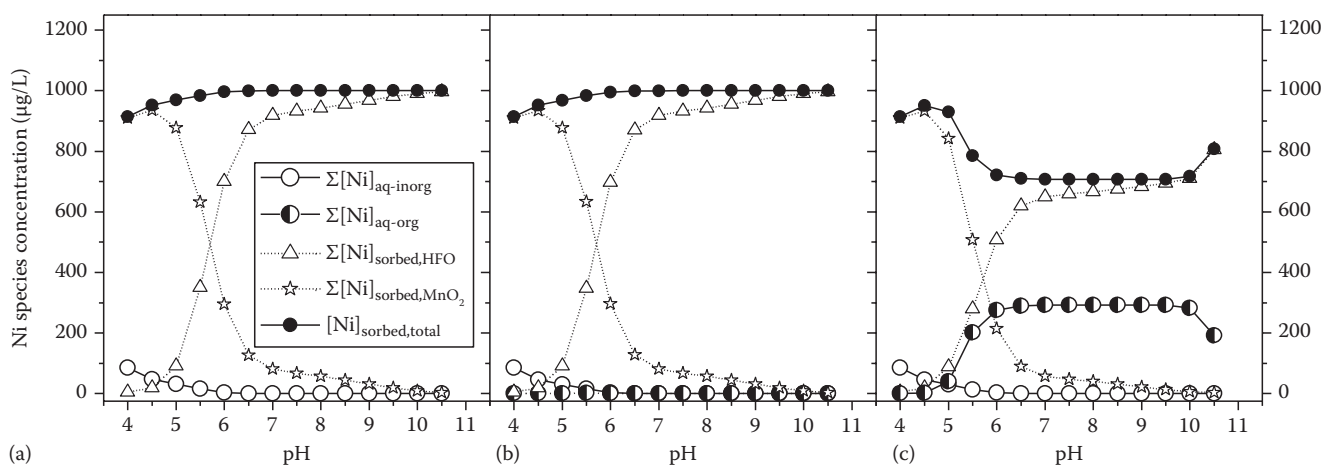
#### 17.5.1.1 Chemisorption

Nickel displays the commonly observed chemisorption behavior for cation adsorption onto soil minerals with uptake onto solid surface increasing with pH. Typically, the increase in

adsorption occurs over a narrow pH range, and the resultant plot of adsorption data has been given the name “adsorption edge” (e.g., Stumm, 1992; Sparks, 2003). Adsorption of nickel in soil environments is dependent on pH, temperature, and type of adsorbent (minerals or organic matter), as well as the concentration of aqueous complexing agents, competition from other adsorbing cations, and the ionic strength in the soil solution. Nickel has been shown to adsorb onto many solid components encountered in soils, including iron/manganese oxides, clay minerals (Dähn et al., 2003; Bradbury and Baeyens, 2005), and solid organic matter (Nachtegaal and Sparks, 2003). Sorption to iron/manganese oxides and clay minerals has been shown to be of particular importance for controlling nickel mobility in subsurface systems. The relative affinity of these individual minerals for nickel uptake will depend on the mass distribution of the adsorbent minerals as well as the predominant geochemical conditions (e.g., pH and Ni aqueous speciation). For example, the pH-dependent distribution of nickel between iron and manganese oxides (hydrrous ferric oxide [HFO] and a birnessite-like mineral [nominally  $\text{MnO}_2$ ]) for a representative soil solution composition is shown in Figure 17.3. Based on the available compilations for surface complexation constants onto these two solid phases (Dzombak and Morel, 1990; Tonkin et al., 2004), one would project the predominance of nickel sorption to  $\text{MnO}_2$  at more acidic pH and the predominance of HFO (or ferrihydrite) at more basic pH. With increasing mass of  $\text{MnO}_2$ , the solid-phase speciation of nickel will be progressively dominated by sorption to this phase. There are examples of the relative preference of nickel sorption to manganese oxides over iron oxides for natural systems (e.g., Manceau et al., 2002; Kjoller et al., 2004; Manceau et al., 2007). As shown in Figure 17.3b, the presence of

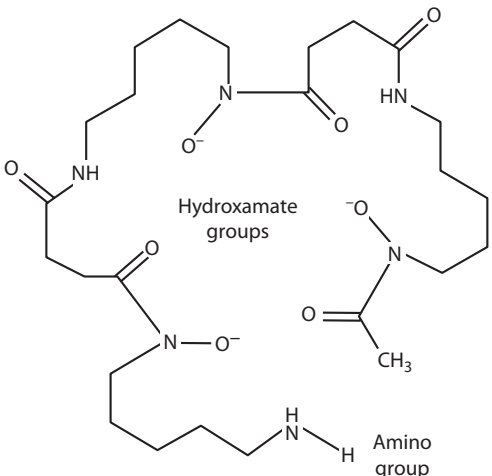
humic/fulvic compounds along with simple organic acids may not significantly influence the extent of nickel sorption to oxide surfaces. This behavior is predicated on the availability of sorption sites at concentrations significantly greater than competing ligands in solution.

In contrast, the presence of ligands that form highly stable or multidentate solution complexes may exert greater influence on the degree of nickel sorption to oxide surfaces. As shown in Figure 17.3c, nickel sorption may be inhibited (or nickel desorption enhanced) through the formation of solution complexes with some classes of organic ligands such as hydroxamate siderophores (Dimkpa et al., 2008). Published stability constants are available for a commonly occurring hydroxamate siderophore, desferrioxamine B (DFB; Farkas et al., 1999). In order to model the nickel speciation in Figure 17.3c, equilibrium expressions for the protonation of DFB and its complexation with nickel were derived from published conditional stability constants (Evers et al., 1989; Farkas et al., 1999; see Table 17.2). As discussed previously, the production of siderophores provides a mechanism for plants/organisms to overcome the low solubility of metals such as nickel in soil systems where the abundance of solid sorption sites is high. As shown in Figure 17.3, the stability of solution complexes with carboxylic acids (natural or synthetic) and the relative availability of sites for chemisorption affect that degree of competition. For the hypothetical conditions modeled in Figure 17.3, only strong complexation with DFB significantly inhibits Ni adsorption to surface of hydrous Fe/Mn oxides. This behavior is similar to that observed in experimental systems for the synthetic chelating agent, EDTA (e.g., Bryce and Clark, 1996; Nowack et al., 1997). The model calculations presented in Figure 17.3 do not include the possible formation of ternary surface



**FIGURE 17.3** (a) Nickel sorption as a function of pH in the presence of a hypothetical soil with iron and manganese oxides reflective of the crustal abundance of these elements (Schulze, 2002; assumed 30% porosity with  $185.0 \text{ g HFO L}^{-1}$  and  $1.66 \text{ g MnO}_2 \text{ L}^{-1}$ ); no organic ligands. (b) Same conditions as in (a) but with  $20 \text{ mg L}^{-1}$  dissolved organic carbon (DOC; humics and fulvics) and  $25 \mu\text{M}$  each of citrate, malonate, and oxalate. (c) Same conditions as in (a), but with  $5 \mu\text{M}$  DFB added as the sole organic ligand. Nominal water composition:  $0.005 \text{ mol L}^{-1}$  NaCl,  $0.001 \text{ mol L}^{-1}$   $\text{K}_2\text{SO}_4$ ,  $0.001 \text{ mol L}^{-1}$   $\text{MgNO}_3$ ,  $0.001 \text{ mol L}^{-1}$   $\text{CaCO}_3$ , and  $17 \mu\text{M}$  Ni ( $1 \text{ mg Ni L}^{-1}$ ). Model predictions using Visual MINTEQ (2009) Version 2.61 with available surface complexation parameters derived from Dzombak and Morel (1990) and Tonkin et al. (2004), and metal-DOC speciation using default settings in the DOC (SHM) module (Gustafsson, 2001); kaolinite set as an “infinite” solid for pH titration. This model does not make use of the alternate hypothetical reference states proposed by Kulik (2002a, 2002b) or Sverjensky (2003).

**TABLE 17.2** Complexation Reactions between Ni(II) and DFB, a Microbially Produced Trihydroxamate Siderophore in the Soil Rhizosphere

Acid-Base Reactions		Structure of DFB
Stoichiometry	Log K (25°C)	
$\text{H}_3\text{DFB} + \text{H}^+ = \text{H}_4\text{DFB}^+$	8.32	 <p>The diagram shows the chemical structure of Desferrioxamine B (DFB). It consists of a central carbon atom bonded to three nitrogen atoms, each part of a hydroxamate group (-N(OH)2). The hydroxamate groups are further substituted with various side chains: one with a long alkyl chain ending in a primary amino group (-NH2), another with a long alkyl chain ending in a secondary amine (-NH-), and the third with a long alkyl chain ending in a secondary amine (-NH-). The structure is labeled with 'Hydroxamate groups' and 'Amino group'.</p>
$\text{H}_3\text{DFB} - \text{H}^+ = \text{H}_2\text{DFB}^-$	-8.74	
$\text{H}_3\text{DFB} - 2\text{H}^+ = \text{HDFB}^{2-}$	-17.84	
$\text{H}_3\text{DFB} - 3\text{H}^+ = \text{DFB}^{3-}$	-27.95	
Complexation Reactions		
$\text{Ni}^{2+} + \text{H}_3\text{DFB} - 3\text{H}^+ = \text{NiDFB}^-$	-20.41	
$\text{Ni}^{2+} + \text{H}_3\text{DFB} - 2\text{H}^+ = \text{NiHDFB}$	-0.95	
$\text{Ni}^{2+} + \text{H}_3\text{DFB} - \text{H}^+ = \text{NiH}_2\text{DFB}^+$	-1.89	
$\text{Ni}^{2+} + \text{H}_3\text{DFB} = \text{NiH}_3\text{DFB}^{2+}$	3.90	

Equilibrium reaction expressions and associated constants for protonation and complexation with nickel were derived from Evers et al. (1989) and Farkas et al. (1999), respectively. All constants have been recalculated to zero ionic strength using the Davies equation for the estimation of single-ion activities (Stumm and Morgan, 1981, p. 135). Reaction expressions from the referenced sources were converted to the reaction format required within the Visual MINTEQ (2009) database using  $\text{H}^+$ ,  $\text{Ni}^{2+}$ , and  $\text{H}_3\text{DFB}$  as components (MINTEQA2/PRODEFA2, 1999).

complexes with DFB or other multidentate ligands that might serve as a bridging ligand between Ni and an oxyhydroxide surface (e.g., Nowack and Sigg, 1996; Nowack, 2002).

As previously noted, adsorption of nickel onto mineral surfaces may serve as a precursory step to the formation of trace precipitates that reduce the potential for desorption with changes in soil solution chemistry. This may be realized through the nucleation and growth of surface precipitates on clay mineral surfaces due to continued uptake of nickel. Three categories of surface precipitation have been identified in experimental systems: (1) heterogeneous nucleation of pure Ni-bearing phases such as hydroxides (e.g., Scheinost et al., 1999), (2) coherent growth of Ni-bearing solid phases that mimic the structure of the adsorbent (e.g., Dähn et al., 2002), and (3) nucleation of mixed-metal precipitates within the solid-water interface (e.g., Scheckel and Sparks, 2000, 2001; Scheckel et al., 2000; Dähn et al., 2006). This type of process may compete with other adsorption processes, such as ion exchange, depending on the prevailing soil solution chemistry and characteristics of the clay mineral (e.g., Elzinga and Sparks, 2001).

### 17.5.1.2 Precipitation

Nickel may be immobilized within soils through formation of pure nickel precipitates such as hydroxides, silicates, or sulfides (Merlen et al., 1995; Mattigod et al., 1997; Scheidegger et al., 1998; Thoenen, 1999; Scheinost and Sparks, 2000; Peltier et al., 2006) or through coprecipitation with other soil-forming minerals such as silicates, iron oxides/sulfides, or carbonates (Manceau et al., 1985; Manceau and Calas, 1986; Huerta-Diaz

and Morse, 1992; Ford et al., 1999a; Hoffmann and Stipp, 2001). Predicted nickel concentrations in the presence of sulfide for several potential pure nickel precipitates are shown in Figure 17.4a. These data suggest that phyllosilicate and LDH precipitates (incorporating aluminum) may limit Ni solubility in soils. These data also point to the limited capability of pure nickel carbonates and hydroxides in controlling dissolved nickel concentrations to sufficiently low values except under very alkaline conditions. For LDH precipitates, calorimetric measurements have demonstrated that the interlayer anion exerts significant influence on the precipitate stability (Peltier et al., 2006). In the presence of dissolved sulfide, the precipitation of a nickel sulfide may plausibly control the concentration of dissolved nickel. The influence of dissolved silicate on the stability of Ni-bearing precipitates is shown in Figure 17.4b. According to these data, nickel-bearing phyllosilicate and/or LDH precipitates possess large stability fields indicating their relative importance to controlling nickel solubility under a range of conditions. These calculations point to the importance of dissolved aluminum and silicon concentrations in the soil solution relative to the potential sequestration of nickel via precipitation (Ford et al., 1999b; Scheinost et al., 1999). As discussed in Section 17.5.1.1, the formation of these nickel-bearing precipitates may be facilitated through initial adsorption onto clay minerals within the soil.

Attenuation of nickel may also occur via coprecipitation during the formation of (hydr)oxides or sulfides of iron. These minerals have been observed to form at the boundaries between oxidizing and reducing zones within soil systems. There are numerous laboratory and field observations that demonstrate

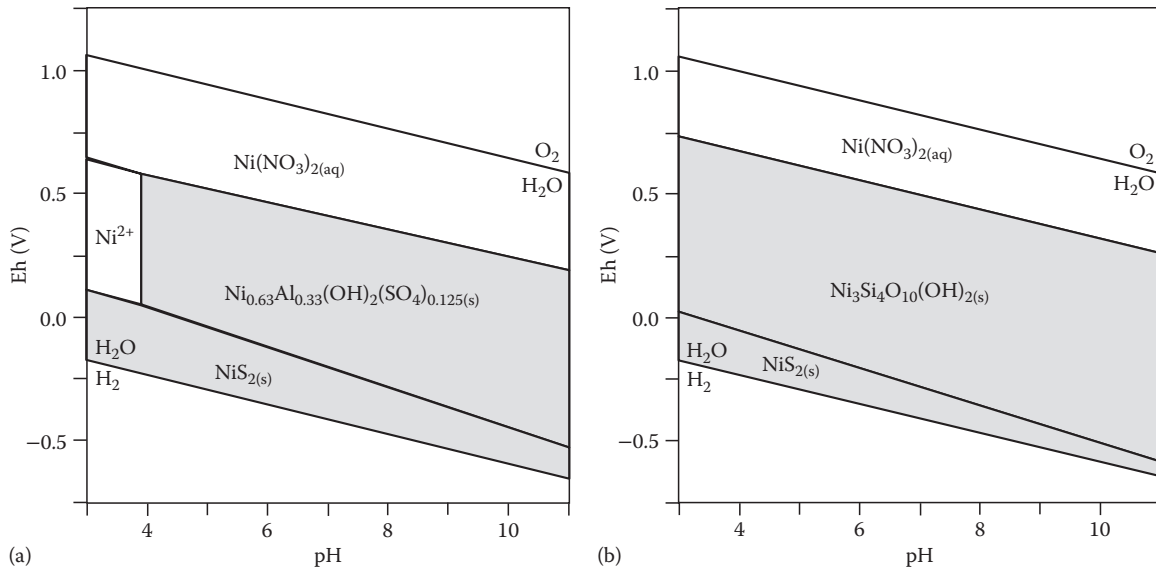


**FIGURE 17.4** Eh–pH diagrams for nickel at 25°C. (a) System Ni–H<sub>2</sub>O–Ca–Al–NO<sub>3</sub>–HCO<sub>3</sub>–SO<sub>4</sub> (2 mg Ni L<sup>-1</sup>; 40 mg Ca L<sup>-1</sup>; 3 mg Al L<sup>-1</sup>; 6 mg NO<sub>3</sub> L<sup>-1</sup>; 60 mg HCO<sub>3</sub> L<sup>-1</sup>; 100 mg SO<sub>4</sub> L<sup>-1</sup>). Stability fields for solids are shaded gray (Vaesite = NiS<sub>2</sub>). (b) Same system plus 3 mg Si L<sup>-1</sup>. Thermodynamic data for Ni<sub>3</sub>Si<sub>4</sub>O<sub>10</sub>(OH)<sub>2</sub> and Ni<sub>0.63</sub>Al<sub>0.33</sub>(OH)<sub>2</sub>(SO<sub>4</sub>)<sub>0.125</sub> are from Peltier et al. (2006). (Note that the solubility of the Ni–Al–SO<sub>4</sub> LDH was adjusted to correct for charge imbalance for the chemical structure published in Peltier et al. [2006].)

the capacity of these precipitates for nickel uptake (Schultz et al., 1987; Huerta-Diaz and Morse, 1992; Coughlin and Stone, 1995; Ford et al., 1997, 1999a). Under these circumstances, the solubility of nickel will depend on the stability of the host precipitate phase. For example, iron oxide precipitates may alternatively transform to more stable forms (Ford et al., 1997), stabilizing coprecipitated nickel over the long term, or these precipitates may dissolve concurrently with changes in soil solution redox chemistry (e.g., Zachara et al., 2001).

### 17.5.2 Selenium

Selenium provides an example of an element that is subject to significant changes in solution and solid speciation as influenced by changes in system redox. Selenium is a metalloid exhibiting physical and chemical properties between that of metals and nonmetals. It chemically resembles sulfur and exists in organic and inorganic chemical forms. Inorganic species include selenide [Se(–II)], elemental selenium [Se(0)], selenite [Se(IV)], and selenate [Se(VI)] (e.g., Fernandez-Martínez and Charlet, 2009). Organic species include methylated compounds, selenoamino acids, and selenoproteins and their derivatives. The speciation of selenium is greatly influenced by the pH and redox conditions of the environment (Figure 17.5). For example, Se(–II) exists in a reducing environment as hydrogen selenide (H<sub>2</sub>Se) and as metal selenides. Reduction of selenate to selenite and Se(0) has been shown to decrease its mobility in saline, mildly alkaline water (White et al., 1991). When dissolved in water, H<sub>2</sub>Se can oxidize to elemental selenium. Elemental selenium is stable in a reduced environment, but it can be oxidized to selenite and to selenate by a variety of microorganisms (Sarithchandra and Watkinson, 1981; Dowdle and Oremland, 1998).

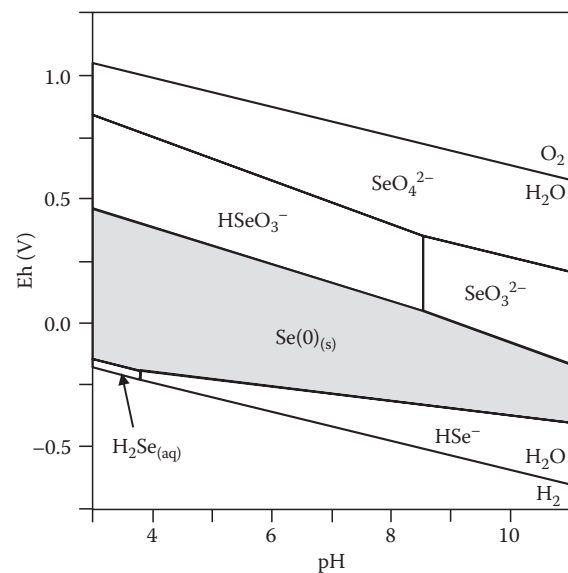


**FIGURE 17.5** Eh–pH diagram for selenium at 25°C using thermodynamic data from Seby et al. (2001).  $\Sigma\text{Se} = 10^{-5}$  M (790  $\mu\text{g L}^{-1}$ ). Solid stability field for elemental selenium is shaded gray.

Various strains of bacteria have been identified to facilitate selenate reduction in soil systems. Two microbial processes, namely, methylation of selenium and reduction of both selenate and selenite to Se(0), have a major influence on the fate and mobility of this element in the environment (Dungan and Frankenberger, 1999; Dungan et al., 2003). Methylation of selenium, and subsequent selenium volatilization, leads to dissipation of soil selenium to the atmosphere. Environmental factors such as the existing microbial community, pH,



temperature, moisture, and organic amendments control the rate of selenium volatilization from seleniferous soils (Frankenberger and Karlson, 1989; Zhang and Frankenburger, 1999). Under flooding conditions, part of the methylated selenium may be transported in water, thus decreasing selenium volatilization to the atmosphere (Zhang and Frankenburger, 1999). The addition of organic amendments to soils has been reported to stimulate indigenous microbes to methylate selenium (Abu-Erreish et al., 1968; Frankenberger and Karlson, 1989); whereas, organic substrates added to ponded sediments (submerged soils) have been found to accelerate the reduction of selenate and selenite to Se(0) (Tokunaga et al., 1996) and similar effects were reported in laboratory batch experiments (Zhang et al., 2003).

Mechanisms for selenium reduction by microbes are complex as it occurs under both aerobic (Lortie et al., 1992) and anaerobic conditions (Oremland et al., 1989, 1990; Tomei et al., 1992). Both dissimilatory and detoxification mechanisms are possible (Oremland, 1994). The occurrence of sequential reduction of selenate to selenite and then to Se(0) is suggested after amendment of contaminated soils with barley straw under field capacity moisture conditions (Camps Arbertain, 1998). The rate of selenate to selenite reduction in wastewaters is proportional to their respective concentrations in solution and also to the amount of the microbial biomass (Rege et al., 1999). A recent study has documented the occurrence of both intracellular and extracellular Se(0) granules in three phylogenetically and physiologically distinct bacteria that are able to respire selenium oxyanions, suggesting that this phenomenon appears to be widespread among such bacteria (Oremland et al., 2004). The metal sites of selenate reductase from *Thauera selenatis* have been characterized (Maher et al., 2004); the enzyme was found to contain Se in a reduced form (probably organic) and the Se is coordinated to both a metal (probably Fe) and carbon. Assessment of Se(IV) and Se(0) reduction in anaerobic microcosms demonstrated the sequential formation of Se(0) and ultimately Se(-II) during incubation with elemental selenium and/or lactate as electron donors for microbial reduction (Herbel et al., 2003). Dissolved Se(-II) did not accumulate in pore water during incubation due to precipitation with ferrous iron to form FeSe(s), which was determined via solid-phase characterization using x-ray absorption spectroscopy.

### 17.5.2.1 Chemisorption

As noted above, the most common species of selenium in soil solution are in the form of oxyanions. Thus, selenium adsorption onto soil minerals tends to be greatest under acidic pH with a gradual decrease as pH increases. In contrast to cation adsorption, the decrease in anion adsorption with increasing pH is more gradual, and the resultant plot of these adsorption data has been given the name "adsorption envelope" (e.g., Stumm, 1992; Sparks, 2003). Selenate and selenite adsorption behavior on individual soil minerals (Fe, Al, and Mn oxides, kaolinite, and calcite) and whole soils throughout the United

States has been documented (Neal et al., 1987; Neal and Sposito, 1989; Zachara et al., 1994). This research demonstrated the importance of Fe- and Al-oxide surfaces for selenium adsorption onto soils and highlighted the dependence of the extent of adsorption on the pH of soil solution and the presence of anions that compete for adsorption sites. Additional review of the published literature is provided in the following.

Selenate has been shown to behave like sulfate with minimal adsorption and high mobility (Goldberg and Glaubig, 1988; Neal and Sposito, 1989); whereas, selenite behaves analogously to phosphate, with greater adsorption than selenate (Neal et al., 1987; Barrow and Whelan, 1989a; Zhang and Sparks, 1990). Strawn et al. (2002) have observed selenite and selenate associated with iron-bearing minerals in acid-sulfate soils. In these soils, selenite was predominantly associated with iron oxyhydroxides and selenate was associated with jarosite, presumably in a coprecipitated form. Adsorption of selenite on goethite decreases with increasing pH, with decreasing selenite concentration, and with competing anions such as phosphate, silicate, citrate, molybdate, carbonate, oxalate, and fluoride (Balistrieri and Chao, 1987). More selenite is adsorbed onto montmorillonite than on kaolinite (Frost and Griffin, 1977). Selenite adsorption in seleniferous soils is decreased in the presence of sulfate, nitrate, and phosphate (Pareek et al., 2000). Selenite adsorption by aluminum hydroxides is adversely affected by organic acids (Dynes and Huang, 1997). Desorption of selenate is faster and more nearly complete than selenite after adsorption and incubation in soil (Barrow and Whelan, 1989b). Differences in the stability of selenate and selenite chemisorption to ferrihydrite are illustrated in Figure 17.6. Selenite adsorption predominates for most of the modeled pH range, but there is a small stability field for selenate adsorption in the pH range  $7 < \text{pH} < 9$ , in part, due to the pH-dependent distribution of selenium oxyanion oxidation state. As shown, model predictions indicate limited competition from competing oxyanions common to soil solutions (e.g., carbonate, silicate, and sulfate) when available surface-site densities are far from saturation.

Selenite selectively adsorbs at the carbonate ( $\text{CO}_3^{2-}$ ) site on calcite ( $\text{CaCO}_3$ ) via ionic exchange, forming a two-dimensional solid solution of the form  $\text{Ca}(\text{SeO}_3)_x(\text{CO}_3)_{1-x}$  at the interface; under identical chemical conditions, selenate adsorption is inhibited (Cheng et al., 1997). An earlier study showed selenate substitution in calcite may also be supported under appropriate conditions (Reeder et al., 1994).

Mechanisms of selenium adsorption have been studied from both macroscale batch and microscale spectroscopic approaches. The presence of either selenate or selenite lowers the electrophoretic mobility and decreases the PZC of ferrihydrite and goethite, suggesting inner-sphere complexation for both selenate and selenite species (Su and Suarez, 2000). Both in situ attenuated total reflectance-Fourier transform infrared (ATR-FTIR) and diffuse reflectance infrared Fourier transform (DRIFT) spectra indicated formation of bidentate complexes of selenate with ferrihydrite, and the DRIFT spectra of selenite on goethite indicated formation of bridging bidentate complex of selenite.

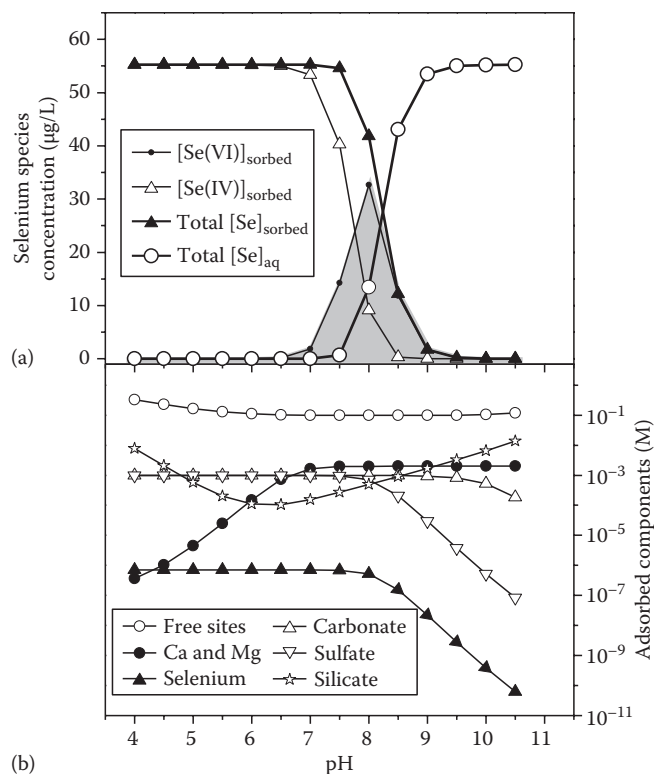


**FIGURE 17.6** (a) Selenium species adsorption as a function of pH in the presence of a hypothetical soil with iron oxide content reflective of the crustal abundance (Schulze, 2002; assumed 30% porosity with 185.0 g HFO L<sup>-1</sup>). (b) Total component adsorption for modeled water composition. Nominal water composition: 0.005 M NaCl, 0.001 M K<sub>2</sub>SO<sub>4</sub>, 0.001 M MgNO<sub>3</sub>, 0.001 M CaCO<sub>3</sub>, and 0.7 µM Se (55.2 µg Se L<sup>-1</sup>). Model predictions using Visual MINTEQ (2009) Version 2.61 with available surface complexation parameters derived from Dzombak and Morel (1990) at a fixed Eh = 500 mV; kaolinite set as an “infinite” solid for pH titration. This model does not make use of the alternate hypothetical reference states proposed by Kulik (2002a, 2002b) or Sverjensky (2003).

These results are consistent with an earlier in situ extended x-ray absorption fine structure (EXAFS) spectroscopic study (Manceau and Charlet, 1994) that shows that selenate forms an inner-sphere binuclear bridging surface complex on hydrous ferric oxide and goethite. On the contrary, an earlier EXAFS study (Hayes et al., 1987) concluded that selenate forms an outer-sphere surface complex on goethite. A recent combined data set of Raman and ATR-FTIR spectra indicate that both inner- and outer-sphere surface complexes of selenate occur on goethite, as predominantly monodentate inner-sphere surface complexes at pH < 6, and as predominantly outer-sphere surface complexes at pH > 6 (Wijnja and Schulthess, 2000).

### 17.5.2.2 Precipitation

Selenium has the potential of forming precipitates for all of its oxidation states (Seby et al., 2001; see Figure 17.7). For selenate and selenite, this includes precipitates with common major cations in soil solutions (Ca, Mg) as well as transition metals (Fe, Mn) or heavy metals that may be anticipated in contaminated

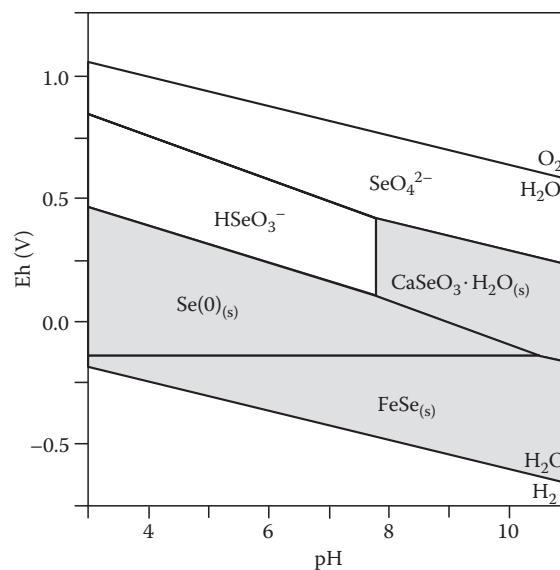
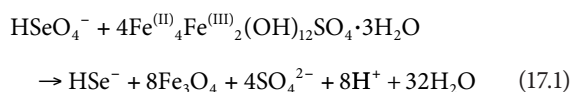


**FIGURE 17.7** Eh-pH diagram for selenium at 25°C using thermodynamic data from Seby et al. (2001). System Se-H<sub>2</sub>O-Fe-Ca, with  $\Sigma\text{Se} = 10^{-5}$  M (790 µg L<sup>-1</sup>),  $\Sigma\text{Fe} = 10^{-4}$  M (5.6 mg L<sup>-1</sup>), and  $\Sigma\text{Ca} = 10^{-2}$  M (400 mg L<sup>-1</sup>). Solid stability fields for elemental selenium, hydrous calcium selenite, and ferrous selenide are shaded gray. FeSe<sub>2</sub> was suppressed (data not available in the Seby et al., 2001); however, the stability field of the diselenide would be intermediate between elemental selenium and FeSe.

soils (Rai et al., 1995; Sharmasarkar et al., 1996). These phases are anticipated to primarily be significant in situations where selenium concentrations are highly elevated. Reduction to form elemental selenium [Se(0)] can result in very low concentrations of dissolved selenium. In general, it has been observed that selenium reduction to insoluble Se(0) results in immobilization and stabilization of this element in the soil matrix, since the reoxidation reaction of Se(0) to soluble selenate and selenite is relatively slow (Tokunaga et al., 1994; Zawislanski and Zavarin, 1996; Dowdle and Oremland, 1998; Losi and Frankenberger, 1998). Abiotic reduction of selenite to Se(0) was also suggested in SRB biofilms (Hockin and Gadd, 2003). Further reduction to selenide [Se(-II)] can lead to precipitation of metal selenides, including ferrous iron and manganese selenides, similar to the formation of metal sulfides under sulfate-reducing conditions. As demonstrated by Scheinost and Charlet (2008a) and Scheinost et al. (2008b), selenite may be reduced and precipitated via abiotic reactions with Fe(II)-bearing minerals in soils. The propensity to form elemental selenium versus ferrous-selenide precipitates will likely be governed by pH, major ion composition of the soil solution, and the solubility of ferrous iron.

While not commonly observed, it is anticipated that many suboxic soil environments (e.g., redoximorphic soils) contain green rust, which is a mixed ferrous, ferric hydroxide that also contains interlayer anions such as sulfate and carbonate in its structure (Feder et al., 2005). Identification of green rusts in soils

is hampered by the rapid oxidation of green rusts by atmospheric oxygen, and for this reason, they have not been commonly reported. However, recent thermodynamic and spectroscopic studies give direct evidence for the existence of green rusts in soils (Hansen et al., 1994; Trolard et al., 1997, 2007; Feder et al., 2005). Due to high reactivity, green rust minerals are envisioned as potential reducing agents of a number of anions such as nitrate, chromate, and selenate (Johnson and Bullen, 2003). Direct evidence for the formation of reduced selenium species under anoxic conditions via abiotic redox reactions with sulfate green rust was provided using x-ray absorption near-edge spectroscopy (XANES) and Fourier transform EXAFS spectroscopy (Myneni et al., 1997). The mechanism of selenate reduction was described by the following equation:



in which sulfate green rust was oxidized to form magnetite, whereas selenate was reduced to Se(0) and subsequently to selenide. In addition, a laboratory study has demonstrated that a significant fraction of dissolved selenate can be coprecipitated with Fe(II) and Fe(III) ions to form Fe(II)–Fe(III) hydroxy-selenate green rust with simultaneous reduction of an equal amount of selenate anions to selenite anions (Refait et al., 2000; similar to partitioning to LDH phases, You et al., 2001). In the subsurface environment, selenate reduction by coprecipitation and adsorption pathways can occur when reducing conditions develop (Pickering et al., 1995). In the coprecipitation–reduction pathway, reductive dissolution of Fe(III) oxides precipitates green rust with selenate followed by selenate reduction to Se(0) and selenide. Reduction of selenium oxyanions to Se(0) has also been observed in the presence of iron sulfides (Bruggeman et al., 2005) and ferrous hydroxide (Zingaro et al., 1997).

In summary, the chemical behavior of nickel and selenium point to the importance of identifying aqueous and solid speciation in confirming the processes controlling element partitioning for a given soil system. Chemical equilibrium models provide a tool for assessing potential endpoints for these partitioning reactions, but the accuracy of these projections will depend on the adequacy of the supporting thermochemical database for relevant solution and solid species. Advances have been made in modeling chemisorption and precipitation reactions, in part, due to developments in analytical approaches to identify aqueous and solid speciation for trace elements in soils. For trace-element partitioning, it is increasingly understood that the initial form of the chemisorbed solute may represent a metastable state relative to its long-term mobility. Due to the internal influence of biotic respiration in concert with external fluxes of aqueous and gaseous components physically transported through the soil matrix, the composition of the soil solution and associated solids will change in time. Ultimately, knowledge of the rates and extents of these aqueous and mineralogic changes will prove critical for understanding the dynamics of solute partitioning for soil systems.

## References

- Abu-Erreish, G.M., E.I. Whitehead, and O.E. Olson. 1968. Evolution of volatile selenium from soils. *Soil Sci.* 106:415–420.
- Baes, C.F., and R.E. Mesmer. 1986. *The hydrolysis of cations.* Krieger Publishing Company, Malabar, FL.
- Baeyens, B., M.H. Bradbury, and W. Hummel. 2003. Determination of aqueous nickel-carbonate and nickel-oxalate complexation constants. *J. Solution Chem.* 32:319–339.
- Bais, H.P., T.L. Weir, L.G. Perry, S. Gilroy, and J.M. Vivanco. 2006. The role of root exudates in rhizosphere interactions with plants and other organisms. *Annu. Rev. Plant Biol.* 57:233–266.
- Balistrieri, L.S., and T.T. Chao. 1987. Selenium adsorption by goethite. *Soil Sci. Soc. Am. J.* 51:1145–1151.
- Barrow, N.J., and B.R. Whelan. 1989a. Testing a mechanistic model. VII. The effects of pH and of electrolyte on the reaction of selenite and selenate with a soil. *J. Soil Sci.* 40:17–28.
- Barrow, N.J., and B.R. Whelan. 1989b. Testing a mechanistic model. VIII. The effects of time and temperature of incubation on the sorption and subsequent desorption of selenite and selenate by a soil. *J. Soil Sci.* 40:29–37.
- Belnap, J., C.V. Hawkes, and M.K. Firestone. 2003. Boundaries in miniature: Two examples from soil. *Bioscience* 53:739–749.
- Birkham, T.K., M.J. Hendry, L.I. Wassenaar, and C.A. Mendoza. 2007. A transient model of vadose zone reaction rates using oxygen isotopes and carbon dioxide. *Vadose Zone J.* 6:67–76.
- Bradbury, M.H., and B. Baeyens. 2005. Modelling the sorption of MnII, CoII, NiII, ZnII, CdII, EuIII, AmIII, SnIV, ThIV, NpV and UVI on montmorillonite: Linear free energy relationships and estimates of surface binding constants for some selected heavy metals and actinides. *Geochim. Cosmochim. Acta* 69:875–892.
- Bradbury, M.H., and B. Baeyens. 2009. Sorption modelling on illite. Part II: Actinide sorption and linear free energy relationships. *Geochim. Cosmochim. Acta* 73:1004–1013.
- Brown, I.D. 2009. Recent developments in the methods and applications of the bond valence model. *Chem. Rev.* 109:6858–6919.
- Brown, G.E., V.E. Henrich, W.H. Casey, D.L. Clark, C. Eggleston, A. Felmy, W. Goodman, M. Grätzel, G. Maciel, M.I. McCarthy, K.H. Nealson, D.A. Sverjensky, M.F. Toney, and J.M. Zachara. 1999. Metal oxide surfaces and their interactions with aqueous solutions and microbial organisms. *Chem. Rev.* 99:77–174.
- Bruggeman, C., A. Maes, J. Vancluyse, and P. Vandemussele. 2005. Selenite reduction in Boom clay: Effect of FeS<sub>2</sub>, clay minerals and dissolved organic matter. *Environ. Pollut.* 137:209–221.
- Bryce, A.L., and S.B. Clark. 1996. Nickel desorption kinetics from hydrous ferric oxide in the presence of EDTA. *Colloids Surf. A* 107:123–130.

- Cabaniss, S.E. 2008. Quantitative structure-property relationships for predicting metal binding by organic ligands. *Environ. Sci. Technol.* 42:5210–5216.
- Cabaniss, S.E. 2009. Forward modeling of metal complexation by NOM: I. A priori prediction of conditional constants and speciation. *Environ. Sci. Technol.* 43:2838–2844.
- Camps Arbostain, M. 1998. Effect of straw amendment and plant growth on selenium transfer in a laboratory soil-plant system. *Can. J. Soil Sci.* 78:187–195.
- Chadwick, O.A., and J. Chorover. 2001. The Chemistry of pedogenic thresholds. *Geoderma* 100:321–353.
- Chapelle, F.H., P.M. Bradley, D.R. Lovley, K. O'Neill, and J.E. Landmeyer. 2002. Rapid evolution of redox processes in a petroleum hydrocarbon-contaminated aquifer. *Ground Water* 40:353–360.
- Charlet, L., and A. Manceau. 1992. X-ray absorption spectroscopic study of the sorption of Cr(III) at the oxide-water interface. II. Adsorption, coprecipitation, and surface precipitation on hydrous ferric oxide. *J. Colloid Interface Sci.* 148:443–458.
- Chefetz, B., and B.S. Xing. 2009. Relative role of aliphatic and aromatic moieties as sorption domains for organic compounds: A review. *Environ. Sci. Technol.* 43:1680–1688.
- Chen, T., G. Hefter, and R. Buchner. 2005. Ion association and hydration in aqueous solutions of nickel(II) and cobalt(II) sulfate. *J. Solution Chem.* 34:1045–1066.
- Cheng, L., P.F. Lyman, N.C. Sturchio, and M.J. Bedzyk. 1997. X-ray standing wave investigation of the surface structure of selenite anions adsorbed on calcite. *Surf. Sci.* 382:L690–L695.
- Coughlin, B.R., and A.T. Stone. 1995. Nonreversible adsorption of divalent ions Mn(II), Co(II), Ni(II), Cu(II), and Pb(II) onto goethite: Effects of acidification, Fe(II) addition and picolinic acid addition. *Environ. Sci. Technol.* 29:2445–2455.
- Crumbliss, A.L., and J.M. Harrington. 2009. Iron sequestration by small molecules: Thermodynamic and kinetic studies of natural siderophores and synthetic model compounds. *Adv. Inorg. Chem.* 61:179–250.
- Curti, E., D.A. Kulik, and J. Tits. 2005. Solid solutions of trace Eu(III) in calcite: Thermodynamic evaluation of experimental data over a wide range of pH and pCO<sub>2</sub>. *Geochim. Cosmochim. Acta* 69:1721–1737.
- Dähn, R., M. Jullien, A.M. Scheidegger, C. Poinssot, B. Baeyens, and M.H. Bradbury. 2006. Identification of neoformed Ni-phylosilicates upon Ni uptake in montmorillonite: A transmission electron microscopy and extended X-ray absorption fine structure study. *Clay. Clay Miner.* 54:209–219.
- Dähn, R., A.M. Scheidegger, A. Manceau, M.L. Schlegel, B. Baeyens, M.H. Bradbury et al. 2003. Structural evidence for the sorption of Ni(II) atoms on the edges of montmorillonite clay minerals: A polarized X-ray absorption fine structure study. *Geochim. Cosmochim. Acta* 67:1–15.
- Dähn, R., A.M. Scheidegger, A. Manceau, M.L. Schlegel, B. Baeyens, M.H. Bradbury et al. 2002. Neoformation of Ni phyllosilicate upon Ni uptake on montmorillonite: A kinetics study by powder and polarized extended X-ray absorption fine structure spectroscopy. *Geochim. Cosmochim. Acta* 66:2335–2347.
- Davis, J.A., and D.B. Kent. 1990. Surface complexation modeling in aqueous geochemistry. *Rev. Mineral. Geochem.* 23:177–260.
- Dimkpa, C., A. Svatoš, D. Merten, G. Büchel, and E. Kothe. 2008. Hydroxamate siderophores produced by *Streptomyces acidiscabies* E13 bind nickel and promote growth in cowpea *Vigna unguiculata* L. under nickel stress. *Can. J. Microbiol.* 54:163–172.
- Dixon, J.B., and D.G. Schulze (eds.). 2002. Soil mineralogy with environmental applications. SSSA, Madison, WI.
- Dove, P.M., and C.M. Craven. 2005. Surface charge density on silica in alkali and alkaline earth chloride electrolyte solutions. *Geochim. Cosmochim. Acta* 69:4963–4970.
- Dowdle, P.R., and R.S. Oremland. 1998. Microbial oxidation of elemental selenium in soil slurries and bacterial cultures. *Environ. Sci. Technol.* 32:3749–3755.
- Drever, J.I. 1982. The geochemistry of natural waters. Prentice-Hall, Englewood Cliffs, NJ.
- Dungan, R.S., and W.T. Frankenberger Jr. 1999. Microbial transformations of selenium and the bioremediation of seleniferous environments. *Biorem. J.* 3:171–188.
- Dungan, R.S., S.R. Yates, and W.T. Frankenberger Jr. 2003. Transformations of selenate and selenite by *Stenotrophomonas maltophilia* isolated from a seleniferous agricultural drainage pond sediment. *Environ. Microbiol.* 5:287–295.
- Dynes, J.J., and P.M. Huang. 1997. Influence of organic acids on selenite sorption by poorly ordered aluminum hydroxides. *Soil Sci. Soc. Am. J.* 61:772–783.
- Dzombak, D.A., and F.M.M. Morel. 1990. Surface complexation modeling: Hydrous ferric oxide. John Wiley & Sons, New York.
- Elzinga, E.J., and D.L. Sparks. 2001. Reaction condition effects on nickel sorption mechanisms in illite-water suspensions. *Soil Sci. Soc. Am. J.* 65:94–101.
- Evers, A., R.D. Hancock, A.E. Martell, and R.J. Motekaitis. 1989. Metal ion recognition in ligands with negatively charged oxygen donor groups. Complexation of Fe(III), Ga(III), In(III), and other highly charged metal ions. *Inorg. Chem.* 28:2189–2195.
- Farkas, E., E.A. Enyedy, and H. Csoka. 1999. A comparison between the chelating properties of some dihydroxamic acids, desferrioxamine B and acetohydroxamic acid. *Polyhedron* 18:2391–2398.
- Farley, K.J., D.A. Dzombak, and F.M.M. Morel. 1985. A surface precipitation model for the sorption of cations on metal oxides. *J. Colloid Interface Sci.* 106:226–242.
- Feder, F., F. Trolard, G. Klingelhofer, and G. Bourrie. 2005. In situ Mossbauer spectroscopy: Evidence for green rust fougerite in a gleysol and its mineralogical transformations with time and depth. *Geochim. Cosmochim. Acta* 69:4463–4483.
- Fernandez-Martinez, A., and L. Charlet. 2009. Selenium environmental cycling and bioavailability: A structural chemist point of view. *Rev. Environ. Sci. Biotechnol.* 8:81–110.
- Ford, R.G. 2002. Rates of hydrous ferric oxide crystallization and the influence on coprecipitated arsenate. *Environ. Sci. Technol.* 36:2459–2463.

- Ford, R.G., P.M. Bertsch, and K.J. Farley. 1997. Changes in transition and heavy metal partitioning during hydrous iron oxide aging. *Environ. Sci. Technol.* 31:2028–2033.
- Ford, R.G., K.M. Kemner, and P.M. Bertsch. 1999a. Influence of sorbate-sorbent interactions on the crystallization kinetics of nickel- and lead-ferrihydrite coprecipitates. *Geochim. Cosmochim. Acta* 63:39–48.
- Ford, R.G., A.C. Scheinost, K.G. Scheckel, and D.L. Sparks. 1999b. The link between clay mineral weathering and the stabilization of Ni surface precipitates. *Environ. Sci. Technol.* 33:3140–3144.
- Frankenberger, W.T. Jr., and U. Karlson. 1989. Environmental factors affecting microbial production of dimethylselenide in a selenium-contaminated sediment. *Soil Sci. Soc. Am. J.* 53:1435–1442.
- Fröberg, M., D. Berggren, B. Bergkvist, C. Bryant, and J. Mulder. 2006. Concentration and fluxes of dissolved organic carbon DOC in three Norway spruce stands along a climatic gradient in Sweden. *Biogeochemistry* 77:1–23.
- Frost, R.R., and R.A. Griffin. 1977. Effect of pH on adsorption of arsenic and selenium from landfill leachate by clay minerals. *Soil Sci. Soc. Am. J.* 41:53–56.
- Gaskova, O.L., M.B. Bukaty, G.P. Shironosova, and V.G. Kabannik. 2009. Thermodynamic model for sorption of bivalent heavy metals on calcite in natural-technogenic environments. *Russ. Geol. Geophys.* 50:87–95.
- Gilis, A., P. Corbisier, W. Baeyens, S. Taghavi, M. Mergeay, and D. van der Lelie. 1998. Effect of the siderophore alcaligin E on the bioavailability of Cd to *Alcaligenes eutrophus* CH34. *J. Ind. Microbiol. Biotechnol.* 20:61–68.
- Goldberg, S., and L.J. Criscenti. 2008. Modeling adsorption of metals and metalloids by soil components, p. 215–264. *In* A. Violante, P.M. Huang, and G.M. Gadd (eds.) *Biophysicochemical processes of heavy metals and metalloids in soil environments*. Wiley-Interscience, Hoboken, NJ.
- Goldberg, S., L.J. Criscenti, D.R. Turner, J.A. Davis, and K.J. Cantrell. 2007. Adsorption–desorption processes in subsurface reactive transport modeling. *Vadose Zone J.* 6:407–435.
- Goldberg, S., and R.A. Glaubig. 1988. Anion sorption on a calcareous, montmorillonitic soil-selenium. *Soil Sci. Soc. Am. J.* 52:954–958.
- Gustafsson, J.P. 2001. Modeling the acid–base properties and metal complexation of humic substances with the Stockholm Humic Model. *J. Colloid Interface Sci.* 244:102–112.
- Hansch, R., and R.R. Mendel. 2009. Physiological functions of mineral micronutrients Cu, Zn, Mn, Fe, Ni, Mo, B, Cl. *Curr. Opin. Plant Biol.* 12:259–266.
- Hansen, H.C.B., O.K. Borggaard, and J. Sorensen. 1994. Evaluation of the free energy of formation of FeII-FeIII hydroxide-sulphate green rust and its reduction of nitrite. *Geochim. Cosmochim. Acta* 58:2599–2608.
- Hayes, K.F., A.L. Roe, G.E. Brown Jr., K.O. Hodgson, J.O. Leckie, and G.A. Parks. 1987. In situ X-ray absorption study of surface complexes: Selenium oxyanions on  $\alpha$ -FeOOH. *Science* 238:783–786.
- Herbel, M.J., J.S. Blum, R.S. Oremland, and S.E. Borglin. 2003. Reduction of elemental selenium to selenide: Experiments with anoxic sediments and bacteria that respire Se-oxyanions. *Geomicrobiol. J.* 20:587–602.
- Hinsinger, P., A.G. Bengough, D. Vetterlein, and I.M. Young. 2009. Rhizosphere: Biophysics, biogeochemistry and ecological relevance. *Plant Soil* 321:117–152.
- Hockin, S.L., and G.M. Gadd. 2003. Linked redox precipitation of sulfur and selenium under anaerobic conditions by sulfate-reducing bacterial biofilms. *Appl. Environ. Microb.* 69:7063–7072.
- Hoffmann, U., and S.L.S. Stipp. 2001. The behavior of  $\text{Ni}^{2+}$  on calcite surfaces. *Geochim. Cosmochim. Acta* 65:4131–4139.
- Huerta-Diaz, M.A., and J.W. Morse. 1992. Pyritization of trace metals in anoxic marine sediments. *Geochim. Cosmochim. Acta* 56:2681–2702.
- Huggett, R.J. 1998. Soil chronosequences, soil development, and soil evolution: A critical review. *Catena* 32:155–172.
- Hummel, W., and E. Curti. 2003. Nickel aqueous speciation and solubility at ambient conditions: A thermodynamic elegy. *Monatsh. Chem. Chem. Mon.* 134:941–973.
- Israelachvili, J.N. 1994. *Intermolecular and surface forces*. Academic Press Inc., San Diego, CA.
- IUPAC. 1997. *Compendium of chemical terminology*, 2nd Ed. The “gold book”. Compiled by A.D. McNaught and A. Wilkinson. Blackwell Scientific Publications, Oxford, UK. XML online corrected version: <http://goldbook.iupac.org> 2006—created by M. Nic, J. Jirat, B. Kosata; updates compiled by A. Jenkins. ISBN 0-9678550-9-8.
- Jacquat, O., A. Voegelin, A. Villard, M.A. Marcus, R. Kretzschmar. 2008. Formation of Zn-rich phyllosilicate, Zn-layered double hydroxide and hydrozincite in contaminated calcareous soils. *Geochim. Cosmochim. Acta* 72:5037–5054.
- Johnson, T.M., and T.D. Bullen. 2003. Selenium isotope fractionation during reduction by FeII-FeIII hydroxide-sulfate green rust. *Geochim. Cosmochim. Acta* 67:413–419.
- Jones, D.L. 1998. Organic acids in the rhizosphere—A critical review. *Plant Soil* 205:25–44.
- Karickhoff, S.W. 1981. Semi-empirical estimation of sorption of hydrophobic pollutants on natural sediments and soils. *Chemosphere* 108:833–846.
- Katz, L.E., and K.F. Hayes. 1995. Surface complexation modeling. 2. Strategy for modeling polymer and precipitation reactions at high surface coverage. *J. Colloid Interface Sci.* 170:491–501.
- Keiluweit, M., and M. Kleber. 2009. Molecular-level interactions in soils and sediments: The role of aromatic  $\pi$ -systems. *Environ. Sci. Technol.* 43:3421–3429.
- Kelleher, B.P., and A.J. Simpson. 2006. Humic substances in soils: Are they really chemically distinct? *Environ. Sci. Technol.* 40:4605–4611.
- Khan, M.R., S.M. Khan, F.A. Mohiddin, and T.H. Askary. 2006. Effects of high nickel soil on root-knot Nematode disease of tomato. *Nematropica* 36:79–87.

- Kjoller, C., D. Postma, and F. Larsen. 2004. Groundwater acidification and the mobilization of trace metals in a sandy aquifer. *Environ. Sci. Technol.* 38:2829–2835.
- Kowacz, M., M. Prieto, and A. Putnis. 2010. Kinetics of crystal nucleation in ionic solutions: Electrostatics and hydration forces. *Geochim. Cosmochim. Acta* 74:469–481.
- Kraemer, S.M., S.-F. Cheah, R. Zapf, J. Xu, K.N. Raymond, and G. Sposito. 1999. Effect of hydroxamate siderophores on Fe release and PbII adsorption by goethite. *Geochim. Cosmochim. Acta* 63:3003–3008.
- Kraemer, S.M., D.E. Crowley, and R. Kretschmar. 2006. Geochemical aspects of phytosiderophore-promoted iron acquisition by plants. *Adv. Agron.* 91:1–46.
- Kulik, D.A. 2002a. Sorption modelling by Gibbs energy minimisation: Towards a uniform thermodynamic database for surface complexes of radionuclides. *Radiochim. Acta* 90:815–832.
- Kulik, D.A. 2002b. Gibbs energy minimization approach to modeling sorption equilibria at the mineral–water interface: Thermodynamic relations for multi-site-surface complexation. *Am. J. Sci.* 302:227–279.
- Kulik, D.A. 2006. Dual-thermodynamic estimation of stoichiometry and stability of solid solution end members in aqueous–solid solution systems. *Chem. Geol.* 225:189–212.
- Lambert, J.-L. 2008. Adsorption and polymerization of amino acids on mineral surfaces: A review. *Orig. Life Evol. Biosph.* 38:211–242.
- Langmuir, D. 1997. *Aqueous environmental geochemistry*. Prentice-Hall, Upper Saddle River, NJ.
- Lasaga, A.C. 1999. *Kinetic theory in earth sciences*. Princeton University Press, Princeton, NJ.
- Lilienfein, J., R.G. Qualls, S.M. Uselman, and S.D. Bridgham. 2003. Soil formation and organic matter accretion in a young andesitic chronosequence at Mt. Shasta, California. *Geoderma* 116:249–264.
- Lindsay, W.L. 1979. *Chemical equilibria in soils*. John Wiley & Sons, New York.
- Lloyd, J.R., D.R. Lovley, and L.E. Macaskie. 2003. Biotechnological application of metal-reducing microorganisms. *Adv. Appl. Microbiol.* 53:85–128.
- Lorenz, K., R. Lal, C.M. Preston, and K.G.J. Nierop. 2007. Strengthening the soil organic carbon pool by increasing contributions from recalcitrant aliphatic biomacromolecules. *Geoderma* 142:1–10.
- Lortie, L., W.D. Gould, S. Rajan, R.G.L. McCreedy, and K.J. Cheng. 1992. Reduction of selenate and selenite to elemental selenium by a *Pseudomonas stutzeri* isolate. *Appl. Environ. Microbiol.* 58:4042–4044.
- Losi, M.E., and W.T. Frankenberger. 1998. Microbial oxidation and solubilization of precipitated elemental selenium in soil. *J. Environ. Qual.* 27:836–843.
- Lowers, H.A., G.N. Breit, A.L. Foster, J. Whitney, J. Yount, Md. N. Uddin, and Ad. A. Muneem. 2007. Arsenic incorporation into authigenic pyrite, Bengal Basin sediment, Bangladesh. *Geochim. Cosmochim. Acta* 71:2699–2717.
- Lützenkirchen, J., and P.H. Behra. 1995. On the surface precipitation model for cation sorption at the hydroxide water interface. *Aquat. Geochem.* 1:375–397.
- Maher, M.J., J. Santini, I.J. Pickering, R.C. Prince, J.M. Macy, and G.N. George. 2004. X-ray absorption spectroscopy of selenate reductase. *Inorg. Chem.* 43:402–404.
- Manceau, G., and G. Calas. 1986. Nickel-bearing clay minerals: II. Intracrystalline distribution of nickel: An X-ray absorption study. *Clay Miner.* 21:341–360.
- Manceau, G., G. Calas, and A. Decarreau. 1985. Nickel-bearing clay minerals: I. Optical spectroscopic study of nickel crystal chemistry. *Clay Miner.* 20:367–387.
- Manceau, A., and L. Charlet. 1994. The mechanism of selenate adsorption on goethite and hydrous ferric oxide. *J. Colloid Interface Sci.* 168:87–93.
- Manceau, A., M. Lanson, and N. Geoffroy. 2007. Natural speciation of Ni, Zn, Ba, and As in ferromanganese coatings on quartz using X-ray fluorescence, absorption, and diffraction. *Geochim. Cosmochim. Acta* 71:95–128.
- Manceau, A., B. Lanson, M.L. Schlegel, J.C. Hargé, M. Musso, L. Eybert-Bérard, J.-L. Hazemann, D. Chateigner, and G.M. Lambelle. 2000. Quantitative Zn speciation in smelter-contaminated soils by EXAFS spectroscopy. *Am. J. Sci.* 300:289–343.
- Manceau, A., N. Tamura, M.A. Marcus, A.A. MacDowell, R.S. Celestre, R.E. Sublett, G. Sposito, and H.A. Padmore. 2002. Deciphering Ni sequestration in soil ferromanganese nodules by combining X-ray fluorescence, absorption, and diffraction at micrometer scales of resolution. *Am. Mineral.* 87:1494–1499.
- Martin-Garin, A., P. Van Cappellen, and L. Charlet. 2003. Aqueous cadmium uptake by calcite: A stirred flow-through reactor study. *Geochim. Cosmochim. Acta* 67:2763–2774.
- Mattigod, S.V., D. Rai, A.R. Felmy, and L. Rao. 1997. Solubility and solubility product of crystalline NiOH<sub>2</sub>. *J. Solution Chem.* 26:391–403.
- Matynia, A., T. Lenoir, B. Causse, L. Spadini, T. Jacquet, and A. Manceau. 2010. Semi-empirical proton binding constants for natural organic matter. *Geochim. Cosmochim. Acta* 74:1836–1851.
- McBride, M.B. 1994. *Environmental chemistry of soils*. Oxford University Press, New York.
- McBride, M.B. 1999. Chemisorption and precipitation reactions, p. B265–B302. *In* M.E. Sumner (ed.) *Handbook of soil science*. CRC Press, Boca Raton, FL.
- Merlen, E., P. Guérault, J.-B. d’Espinoise de la Caillerie, B. Rebours, C. Bobin, and O. Clause. 1995. Hydrotalcite formation at the alumina/water interface during impregnation with Ni II aqueous solutions at neutral pH. *Appl. Clay Sci.* 10:45–56.
- MINTEQA2/PRODEFA2. 1999. A geochemical assessment model for environmental systems: User manual supplement for version 4.0. USEPA, Washington, DC. Available at <http://www.epa.gov/ceampubl/mmedia/minteq/SUPPLE1.PDF> (accessed on March 17, 2010)
- Myneni, S.C.B., T.K. Tokunaga, and G.E. Brown Jr. 1997. Abiotic selenium redox transformations in the presence of Fe(II,III) oxides. *Science* 278:1106–1109.

- Nachtegaal, M., and D.L. Sparks. 2003. Nickel sequestration in a kaolinite-humic acid complex. *Environ. Sci. Technol.* 37:529–534.
- Neal, R.H., and G. Sposito. 1989. Selenate adsorption on alluvial soils. *Soil Sci. Soc. Am. J.* 53:70–74.
- Neal, R.H., G. Sposito, K.M. Holtzclaw, and S.J. Traina. 1987. Selenite adsorption on alluvial soils: I. Soil composition and pH effects. *Soil Sci. Soc. Am. J.* 51:1161–1165.
- Neubauer, U., B. Nowack, G. Furrer, and R. Schulin. 2000. Heavy metal sorption on clay minerals affected by the siderophore Desferrioxamine B. *Environ. Sci. Technol.* 34:2749–2755.
- Nico, P.S., B.D. Stewart, and S. Fendorf. 2009. Incorporation of oxidized uranium into Fe hydroxides during FeII catalyzed remineralization. *Environ. Sci. Technol.* 43:7391–7396.
- Niederer, C., R.P. Schwarzenbach, and K.-U. Goss. 2007. Elucidating differences in the sorption properties of 10 humic and fulvic acids for polar and nonpolar organic chemicals. *Environ. Sci. Technol.* 41:6711–6717.
- Nowack, B. 2002. Environmental chemistry of aminopolycarboxylate chelating agents. *Environ. Sci. Technol.* 36:4009–4016.
- Nowack, B., and L.J. Sigg. 1996. Adsorption of EDTA and metal-EDTA complexes onto goethite. *J. Colloid Interface Sci.* 177:106–121.
- Nowack, B., H. Xue, and L. Sigg. 1997. Influence of natural and anthropogenic ligands on metal transport during infiltration of river water to groundwater. *Environ. Sci. Technol.* 31:866–872.
- Oremland, R.S. 1994. Biogeochemical transformations of selenium in anoxic environments, p. 389–419. *In* W.T. Frankenberger Jr. and S. Benson (eds.) *Selenium in the environment*. Marcel Dekker, New York.
- Oremland, R.S., M.J. Herbel, J.S. Blum, S. Langley, T.J. Beveridge, P.M. Ajayan et al. 2004. Structural and spectral features of selenium nanospheres produced by Se-respiring bacteria. *Appl. Environ. Microbiol.* 70:52–60.
- Oremland, R.S., J.T. Hollibaugh, A.S. Maest, T.S. Presser, L.G. Miller, and W.C. Culbertson. 1989. Selenate reduction to elemental selenium by anaerobic bacteria in sediments and culture: Biogeochemical significance of a novel, sulfate-independent respiration. *Appl. Environ. Microbiol.* 55:2333–2343.
- Oremland, R.S., N.A. Steinberg, A.S. Maest, L.G. Miller, and J.T. Hollibaugh. 1990. Measurement of in situ rates of selenate removal by dissimilatory bacteria reduction in sediments. *Environ. Sci. Technol.* 24:1157–1163.
- Pareek, N., K.S. Dhillon, and S.K. Dhillon. 2000. Effect of sulphate, nitrate and phosphate ions on adsorption of selenium in seleniferous soils of Punjab. *J. Nucl. Agric. Biol.* 29:167–174.
- Peltier, E., R. Allada, A. Navrotsky, and D.L. Sparks. 2006. Nickel solubility and precipitation in soils: A thermodynamic study. *Clay. Clay Miner.* 54:153–164.
- Pickering, I.J., G.E. Brown Jr., and T.K. Tokunaga. 1995. Quantitative speciation of selenium in soils using X-ray absorption spectroscopy. *Environ. Sci. Technol.* 29:2456–2459.
- Ponge, J.-F. 2003. Humus forms in terrestrial ecosystems: A framework to biodiversity. *Soil Biol. Biochem.* 35:935–945.
- Rai, D., A.R. Felmy, and D.A. Moore. 1995. The solubility product of crystalline ferric selenite hexahydrate and the complexation constant of  $\text{FeSeO}_3^+$ . *J. Solution Chem.* 24:735–752.
- Ravat, C., J. Dumonceau, and F. Monteil-Rivera. 2000. Acid/base and CuII binding properties of natural organic matter extracted from wheat bran: Modeling by the surface complexation model. *Water Res.* 34:1327–1339.
- Reeder, R.J., G.M. Lamble, J.F. Lee, and W.J. Staudt. 1994. Mechanism of  $\text{SeO}_4^{2-}$  substitution in calcite: An XAFS study. *Geochim. Cosmochim. Acta* 58:5639–5646.
- Refaat, P.H., L. Simon, C. Louis, and J.M.R. Genin. 2000. Reduction of  $\text{SeO}_4^{2-}$  anions and anoxic formation of ironII–ironIII hydroxy-selenate green rust. *Environ. Sci. Technol.* 34:819–825.
- Rege, M.A., D.R. Yonge, D.P. Mendoza, J.N. Petersen, Y. Bered-Samuel, D.L. Johnstone, W.A. Apel, and J.M. Barnes. 1999. Selenium reduction by a denitrifying consortium. *Biotechnol. Bioeng.* 62:479–484.
- Román-Ross, G., G.J. Cuello, X. Turrillas, A. Fernández-Martínez, and L. Charlet. 2006. Arsenite sorption and co-precipitation with calcite. *Chem. Geol.* 233:328–336.
- Rotenberg, B., J.-P. Morel, V. Marry, P. Turq, and N. Morel-Desrosiers. 2009. On the driving force of cation exchange in clays: Insights from combined microcalorimetry experiments and molecular simulation. *Geochim. Cosmochim. Acta* 73:4034–4044.
- Salminen, J.M., P.J. Hanninen, J. Leveinen, P.T.J. Lintinen, and K.S. Jørgensen. 2006. Occurrence and rates of terminal electron-accepting processes and recharge processes in petroleum hydrocarbon-contaminated subsurface. *J. Environ. Qual.* 35:2273–2282.
- Schaumann, G.E. 2006. Soil organic matter beyond molecular structure Part I: Macromolecular and supramolecular characteristics. *J. Plant Nutr. Soil Sci.* 169:145–156.
- Scheckel, K.G., A.C. Scheinost, R.G. Ford, and D.L. Sparks. 2000. Stability of layered Ni hydroxide surface precipitates—A dissolution kinetics study. *Geochim. Cosmochim. Acta* 64:2727–2735.
- Scheckel, K.G., and D.L. Sparks. 2000. Kinetics of the formation and dissolution of Ni precipitates in a gibbsite/amorphous silica mixture. *J. Colloid Interface Sci.* 229:222–229.
- Scheckel, K.G., and D.L. Sparks. 2001. Temperature effects on nickel sorption kinetics at the mineral–water interface. *Soil Sci. Soc. Am. J.* 65:719–728.
- Scheidegger, A.M., and D.L. Sparks. 1996. A critical assessment of sorption-desorption mechanisms at the soil mineral/water interface. *Soil Sci.* 161:813–831.
- Scheidegger, A.M., D.G. Strawn, G.M. Lamble, and D.L. Sparks. 1998. The kinetics of mixed Ni–Al hydroxide formation on clays and aluminum oxides: A time-resolved XAFS study. *Geochim. Cosmochim. Acta* 62:2233–2245.
- Scheinost, A.C., and L. Charlet. 2008a. Selenite reduction by mackinawite, magnetite and siderite: XAS characterization of nanosized redox products. *Environ. Sci. Technol.* 42:1984–1989.

- Scheinost, A.C., R.G. Ford, and D.L. Sparks. 1999. The role of Al in the formation of secondary Ni precipitates on pyrophyllite, gibbsite, talc, and amorphous silica: A DRS study. *Geochim. Cosmochim. Acta* 63:3193–3203.
- Scheinost, A.C., R. Kirsch, D. Banerjee, A. Fernandez-Martinez, H. Zaenker, H. Funke, and L. Charlet. 2008b. X-ray absorption and photoelectron spectroscopy investigation of selenite reduction by Fe<sup>II</sup>-bearing minerals. *J. Contam. Hydrol.* 102:228–245.
- Scheinost, A.C., and D.L. Sparks. 2000. Formation of layered single and double metal hydroxide precipitates at the mineral/water interface: A multiple-scattering XAFS analysis. *J. Colloid Interface Sci.* 223:167–178.
- Schindler, P.W., B. Furst, R. Dick, and P.U. Wolf. 1976. Ligand properties of surface silanol groups. I. Surface complex formation with Fe<sup>3+</sup>, Cu<sup>2+</sup>, Cd<sup>2+</sup> and Pb<sup>2+</sup>. *J. Colloid Interface Sci.* 55:469–475.
- Schlegel, M.L., and A. Manceau. 2006. Evidence for the nucleation and epitaxial growth of Zn phyllosilicate on montmorillonite. *Geochim. Cosmochim. Acta* 70:901–917.
- Schlegel, M.L., A. Manceau, L. Charlet, D. Chateigner, and J.-L. Hazemann. 2001. Sorption of metal ions on clay minerals. III. Nucleation and epitaxial growth of Zn phyllosilicate on the edges of hectorite. *Geochim. Cosmochim. Acta* 65:4155–4170.
- Schultz, M.F., M.M. Benjamin, and J.F. Ferguson. 1987. Adsorption and desorption of metals on ferrihydrite: Reversibility of the reaction and sorption properties of the regenerated solid. *Environ. Sci. Technol.* 21:863–869.
- Schulze, D.G. 2002. An introduction to soil mineralogy, p. 1–35. *In* J.B. Dixon and D.G. Schulze (eds.) *Soil mineralogy with environmental applications*. SSSA, Madison, WI.
- Schwarzenbach, R.P., P.M. Gschwend, and D.M. Imboden. 1993. *Environmental organic chemistry*, 1st Ed. Wiley-Interscience, New York.
- Seby, F., M. Potin-Gautier, E. Giffaut, G. Borge, and O.F.X. Donard. 2001. A critical review of thermodynamic data for selenium species at 25°C. *Chem. Geol.* 171:173–194.
- Shao, H., S.V. Dmytrieva, O. Kolditz, D.A. Kulik, W. Pfingsten, and G. Kosakowski. 2009. Modeling reactive transport in non-ideal aqueous–solid solution system. *Appl. Geochem.* 24:1287–1300.
- Sharmasarkar, S., K.J. Reddy, and G.F. Vance. 1996. Preliminary quantification of metal selenite solubility in aqueous solutions. *Chem. Geol.* 132:165–170.
- Sigg, L., and W. Stumm. 1981. The interactions of anions and weak acids with the hydrous goethite  $\alpha$ -FeOOH surface. *Colloids Surf.* 2:101–117.
- Simpson, A.J., M.J. Simpson, E. Smith, and B.P. Kelleher. 2007a. Microbially derived inputs to soil organic matter: Are current estimates too low? *Environ. Sci. Technol.* 41:8070–8076.
- Simpson, A.J., G. Song, E. Smith, B. Lam, E. Novotny, and M.H.B. Hayes. 2007b. Unraveling the structural components of soil humin by use of solution-state nuclear magnetic resonance spectroscopy. *Environ. Sci. Technol.* 41:876–883.
- Smejkalova, D., and A. Piccolo. 2008. Aggregation and disaggregation of humic supramolecular assemblies by NMR diffusion ordered spectroscopy DOSY-NMR. *Environ. Sci. Technol.* 42:699–706.
- Sparks, D.L. 2003. *Environmental soil chemistry*, 2nd Ed. Academic Press, New York.
- Sposito, G. 1984. *The surface chemistry of soils*. Oxford University Press, New York.
- Sposito, G. 1998. On points of zero charge. *Environ. Sci. Technol.* 32:2815–2819.
- Sposito, G. 1999. On points of zero charge. *Environ. Sci. Technol.* 33:208–208.
- Sposito, G. 2008. *The chemistry of soils*, 2nd Ed. Oxford University Press, New York.
- Strathmann, T.J., and S.C.B. Myneni. 2004. Speciation of aqueous NiII-carboxylate and NiII-fulvic acid solutions: Combined ATR-FTIR and XAFS analysis. *Geochim. Cosmochim. Acta* 68:3441–3458.
- Strawn, D., H. Doner, M. Zavarin, and S. McHugo. 2002. Microscale investigation into the geochemistry of arsenic, selenium, and iron in soil developed in pyritic shale materials. *Geoderma* 108:237–257.
- Strobel, B.W. 2001. Influence of vegetation on low-molecular-weight carboxylic acids in soil solution—A review. *Geoderma* 99:169–198.
- Stumm, W. 1992. *Chemistry of the solid-water interface*. John Wiley & Sons, New York.
- Stumm, W., and J.J. Morgan. 1981. *Aquatic chemistry: An introduction emphasizing chemical equilibria in natural waters*, 2nd Ed. John Wiley & Sons, New York.
- Stumm, W., and J.J. Morgan. 1996. *Aquatic chemistry: Chemical equilibria and rates in natural waters*, 3rd Ed. John Wiley & Sons, New York.
- Su, C., and D.L. Suarez. 2000. Selenate and selenite sorption on iron oxides: An infrared and electrophoretic study. *Soil Sci. Soc. Am. J.* 64:101–111.
- Sutton, R., and G. Sposito. 2005. Molecular structure in soil humic substances: The new view. *Environ. Sci. Technol.* 39:9009–9015.
- Sverjensky, D.A. 2003. Standard states for the activities of mineral surface sites and species. *Geochim. Cosmochim. Acta* 67:17–28.
- Sverjensky, D.A. 2006. Prediction of the speciation of alkaline earths adsorbed on mineral surfaces in salt solutions. *Geochim. Cosmochim. Acta* 70:2427–2453.
- Tamura, H., and R. Furuichi. 1997. Adsorption affinity of divalent heavy metal ions for metal oxides evaluated by modeling with the Frumkin isotherm. *J. Colloid Interface Sci.* 195:241–249.
- Teppen, B.J., and D.M. Miller. 2006. Hydration energy determines isoivalent cation exchange selectivity by clay minerals. *Soil Sci. Soc. Am. J.* 70:31–40.
- Thoenen, T. 1999. Pitfalls in the use of solubility limits for radioactive waste disposal: The case of nickel in sulfidic groundwaters. *Nucl. Technol.* 126:75–87.



- Thompson, H.A., G.A. Parks, and G.E. Brown. 1999. Dynamic interactions of dissolution, surface adsorption, and precipitation in an aging cobaltII-clay-water system. *Geochim. Cosmochim. Acta* 63:1767–1779.
- Tokunaga, T.K., I.J. Pickering, and G.E. Brown Jr. 1996. Selenium transformation in ponded sediments. *Soil Sci. Soc. Am. J.* 60:781–790.
- Tokunaga, T.K., S.R. Sutton, and S. Bajt. 1994. Mapping of selenium concentrations in soil aggregates with synchrotron X-ray fluorescence microprobe. *Soil Sci.* 158:421–434.
- Tomei, F.A., L.L. Barton, C.L. Lemanski, and T.G. Zocco. 1992. Reduction of selenate and selenite to elemental selenium by *Wolinella succinogenes*. *Can. J. Microbiol.* 38:1328–1333.
- Tonkin, J.W., L.S. Balistrieri, and J.W. Murray. 2004. Modeling sorption of divalent metal cations on hydrous manganese oxide using the diffuse double layer model. *Appl. Geochem.* 19:29–53.
- Trolard, F., G. Bourrie, M. Abdelmoula, P. Refait, and F. Feder. 2007. Fougérite, a new mineral of the pyroaurite-iowaite group: Description and crystal structure. *Clay. Clay Miner.* 55:323–334.
- Trolard, F., J.M.R. Genin, M. Abdelmoula, G. Bourrie, B. Humbert, and A. Herbillon. 1997. Identification of a green rust mineral in a reductomorphic soil by Mossbauer and Raman spectroscopies. *Geochim. Cosmochim. Acta* 61:1107–1111.
- Villegas-Jimenez, A., A. Mucci, O.S. Pokrovsky, and J. Schott. 2009. Defining reactive sites on hydrated mineral surfaces: Rhombohedral carbonate minerals. *Geochim. Cosmochim. Acta* 73:4326–4345.
- Visual MINTEQ. 2009. Version 2.61. Stockholm, Sweden. Available online at <http://www.lwr.kth.se/English/OurSoftware/vminteq/> (accessed on March 17, 2010)
- Wershaw, R.L. 1994. Membrane-micelle model for humus in soils and sediments and its relation to humification. *Water-Supply Paper 2410*. U.S. Geological Survey, Denver, CO.
- Westall, J. 1986. Reactions at the oxide-solution interface: Chemical and electrostatic models, p. 54–78. *In* J.A. Davis and K.F. Hayes (eds.) *Geochemical processes and mineral surfaces*. ACS Symp. Ser. 323. American Chemical Society, Washington, DC.
- Westall, J.C., J.D. Jones, G.D. Turner, and J.M. Zachara. 1995. Models for association of metal ions with heterogeneous environmental sorbents. 1. Complexation of CoII by Leonardite humic acid as a function of pH and NaClO<sub>4</sub> concentration. *Environ. Sci. Technol.* 29:951–959.
- White, A.F., S.M. Benson, A.W. Yee, H.A. Wollenberg, and S. Flexer. 1991. Groundwater contamination at the Kesterson reservoir, California, 2. Geochemical parameters influencing selenium mobility. *Water Resour. Res.* 27:1085–1098.
- Wiederhold, J.G., N. Teutsch, S.M. Kraemer, A.N. Halliday, and R. Kretzschmar. 2007. Iron isotope fractionation during pedogenesis in redoximorphic soils. *Soil Sci. Soc. Am. J.* 71:1840–1850.
- Wijnja, H., and C.P. Schulthess. 2000. Vibrational spectroscopy study of selenate and sulfate adsorption mechanisms on Fe and Al hydroxide surfaces. *J. Colloid Interface Sci.* 229:286–297.
- Wolthers, M., L. Charlet, P.R. van Der Linde, D. Rickard, and C.H. van Der Weijden. 2005. Surface chemistry of disordered mackinawite FeS. *Geochim. Cosmochim. Acta* 69:3469–3481.
- Wood, B.W., R. Chaney, and M. Crawford. 2006. Correcting micronutrient deficiency using metal hyperaccumulators: Alyssum biomass as a natural product for nickel deficiency correction. *Hortscience* 41:1231–1234.
- You, Y., G.F. Vance, and H. Zhao. 2001. Selenium adsorption on Mg-Al and Zn-Al layered double hydroxides. *Appl. Clay Sci.* 20:13–25.
- Zachara, J.M., J.K. Fredrickson, S.C. Smith, and P.L. Gassman. 2001. Solubilization of FeIII oxide-bound trace metals by a dissimilatory FeIII reducing bacterium. *Geochim. Cosmochim. Acta* 65:75–93.
- Zachara, J.M., D. Rai, D.A. Moore, G.D. Turner, and A.R. Felmy. 1994. Chemical attenuation reactions of selenium. TR-103535. Electric Power Research Institute, Palo Alto, CA.
- Zachara, J.M., and J.C. Westall. 1999. Chemical modeling of ion adsorption in soils, p. 47–96. *In* D.L. Sparks (ed.) *Soil physical chemistry*, 2nd Ed. CRC Press, Boca Raton, FL.
- Zawislanski, P.T., and M. Zavarin. 1996. Nature and rates of selenium transformations: A laboratory study of Kesterson Reservoir soils. *Soil Sci. Soc. Am. J.* 60:791–800.
- Zech, W., N. Senesi, G. Guggenberger, K. Kaiser, J. Lehmann, T.M. Miano, A. Miltner, and G. Schroth. 1997. Factors controlling humification and mineralization of soil organic matter in the tropics. *Geoderma* 79:117–161.
- Zhang, Y.Q., and W.T. Frankenburger Jr. 1999. Effects of soil moisture, depth, and organic amendments on selenium volatilization. *J. Environ. Qual.* 28:1321–1326.
- Zhang, P.C., and D.L. Sparks. 1990. Kinetics of selenate and selenite adsorption/desorption at the goethite/water interface. *Environ. Sci. Technol.* 24:1848–1856.
- Zhang, Y.Q., Z.A. Zahir, and W.T. Frankenburger Jr. 2003. Factors affecting reduction of selenate to elemental selenium in agricultural drainage water by *Enterobacter taylorae*. *J. Agr. Food Chem.* 51:7073–7078.
- Zingaro, R.A., D.C. Dufner, A.P. Murphy, and C.D. Moody. 1997. Reduction of oxoselenium anions by ironII hydroxide. *Environ. Int.* 23:299–304.



# Role of Abiotic Catalysis in the Transformation of Organics, Metals, Metalloids, and Other Inorganics

18.1	Introduction .....	18-1
18.2	Fundamentals of Catalysis .....	18-2
	Definition of Catalysis • Homogeneous and Heterogeneous Catalysis • Proton and Electron Transfer Catalysis	
18.3	Abiotic Catalysis of Natural and Anthropogenic Organic Compounds .....	18-3
	Oxidative Transformation of Phenolic and Other Organic Compounds • Polycondensation of Phenolic Compounds and Amino Acids • The Maillard Reaction and Integrated Polyphenol–Maillard Reactions • Surface Brønsted and Lewis Acidity and Hydrolysis of Organic Compounds • Reductive Transformation of Organic Compounds • Genotoxicity and Bioavailability of Xenobiotics as Influenced by Mineral Catalysis	
18.4	Abiotic Catalysis in the Transformation of Metals, Metalloids, and Other Inorganics .....	18-19
	Transformation of Metals and Metalloids • Transformation of Other Inorganics	
18.5	Role of Nanoparticles in Abiotic Catalysis .....	18-27
18.6	Conclusions.....	18-28
	Acknowledgment.....	18-29
	References.....	18-29

Pan Ming Huang  
(Deceased)  
*University of Saskatchewan*

A.G. Hardie  
*Stellenbosch University*

## 18.1 Introduction

Abiotic catalysis plays a vital role in many physicochemical processes in soil and related environments. Clay minerals, metal (oxy)hydroxides and oxides, and dissolved metals often demonstrate their ability to catalyze the transformations of natural organic and anthropogenic organic compounds, metals, metalloids, and other inorganics.

Metal (oxy)hydroxides and oxides and clay minerals have the ability to catalyze the transformation of biomolecules and the resultant formation of humic substances (Huang and Hardie, 2009). Iron (oxy)hydroxides and oxides (Scheffer et al., 1959; Shindo and Huang, 1984a; Wang and Huang, 2000a, 2000b; Gonzalez and Laird, 2004) and especially Mn oxides (Shindo and Huang, 1982, 1984a, 1984b; Kung and McBride, 1988; Wang and Huang, 1992, 2000a,b; Jokic et al., 2001a, 2001b, 2004a, 2004b; Hardie et al., 2007) are most reactive in mediating the transformations of phenolic compounds, amino acids, and sugars. Other organic compounds such as aromatic amines and organic acids can also be oxidatively transformed by abiotic

catalysis (Furukawa and Brindley, 1973; McBride, 1979; Jauregui and Reisenauer, 1982; Stone and Morgan, 1984b).

Abiotic catalytic reactions are also important in the transformations of anthropogenic organic compounds such as pesticides, antibiotics, explosives, and dyes (Theng, 1974, 1979; Cheng, 1991; Stone and Torrents, 1995; Smolen and Stone, 1998; Wang and Arnold, 2003; Szecsody et al., 2004; Barrett and McBride, 2005; Baldrian et al., 2006; Hofstetter et al., 2006; Kang et al., 2006; Rubert and Pedersen, 2006; Fimmen et al., 2007; Cheng et al., 2008; Zhang et al., 2008). Soils and sediments contain a series of solid surfaces and dissolved constituents. These components can catalyze the transformation reactions through Brønsted and Lewis acidity, hydrolysis, and oxidative or reductive processes, which can result in the alteration of transformation pathways and kinetics, thereby influencing the toxicity and environmental fate of these organic compounds.

Manganese oxides and Fe-bearing minerals have the ability to catalyze the transformations of metals, metalloids, and/or other inorganics. Manganese oxides are effective catalysts in promoting many reactions such as the transformation of As(III)

to As(V) (Oscarson et al., 1981a; Chiu and Hering, 2000; Power et al., 2005; Feng et al., 2006b), Fe(II) to Fe(III) (Krishnamurti and Huang, 1987, 1988), Pu(III/IV) (Cleveland, 1970; Amacher and Baker, 1982; Morgenstern and Choppin, 2002) and Pu(V) (Keeneykennicutt and Morse, 1985; Duff et al., 1999) to Pu(VI), as well as Cr(III) to the more toxic and mobile Cr(VI) (Bartlett and James, 1979; Amacher and Baker, 1982; Stepniewska et al., 2004; Negra et al., 2005; Feng et al., 2007). Manganese(IV) oxides also catalyze the oxidation of nitrite to nitrate (Bartlett, 1981; Luther and Popp, 2002), and  $\text{NH}_3$  and organic N to  $\text{N}_2$  (Luther et al., 1997). Heterogeneous oxidation/reduction reactions involving electron transfer between metals/metalloids and Fe-bearing minerals have been demonstrated (Wehrli and Stumm, 1989; Ilton and Veblen, 1994; Peterson et al., 1996; White and Peterson, 1996; Myneni et al., 1997; Powell et al., 2004; Jeon et al., 2005; Jung et al., 2007; Jang and Dempsey, 2008; Scheinost and Charlet, 2008; Su and Puls, 2008). Further, it has been suggested that reduced Fe and Mn minerals are responsible for catalyzing nitrate immobilization into dissolved and humic N fractions in soils and sediments (Davidson et al., 2003; Huygens et al., 2008).

Therefore, abiotic catalysis plays an important role in the transformation of organics, metals, metalloids, and other inorganics in soil and related environments. The impact of abiotic catalysis on environmental quality and ecosystem integrity deserves increasing attention.

## 18.2 Fundamentals of Catalysis

### 18.2.1 Definition of Catalysis

The process of changing the rate of a chemical reaction by the use of a catalyst is termed catalysis, coined by Berzelius in 1836 to describe some enhanced chemical reactions (Williams, 1965). The accepted definition of a catalyst, due to Oswald, is that it is a substance that changes the speed of a chemical reaction without itself undergoing any permanent chemical change. Since a reactant or a product may also be a catalyst, Bell (1941) suggests the definition, "A catalyst is a substance which appears in the rate expression to a power higher than that to which it appears in the stoichiometric equation." Actually many substances classified as catalysts are destroyed either as a result of the process that gives them their catalytic activity or because of subsequent combination with the products (Moore and Pearson, 1981). From a practical point of view, a catalyst is a substance that changes the rate of a desired reaction, regardless of the fate of the catalyst itself.

An important criterion of a catalyst is that it changes the mechanism of the parent reaction (Moore and Pearson, 1981). Without this change in mechanism, the observed change in rate could not occur. Since catalysts increase the rate of reaction, the mechanism must change to one that is easier for the system to follow, involving, in general, a lower energy barrier. Therefore, the catalyst provides an alternative pathway by which the reaction comes to equilibrium, although it does not alter the position of the equilibrium (Daintith, 1990). The catalyst itself takes part

in the reaction. In certain circumstances, very small quantities of catalyst can speed up very large reactions. Some catalysts are also highly specific in the type of reaction they catalyze, particularly in biochemical reactions.

### 18.2.2 Homogeneous and Heterogeneous Catalysis

The process of changing the rate of a chemical reaction by the use of a catalyst that has the same phase as the reactant is homogeneous catalysis (e.g., dissolved metals in catalyzing organic reactions or enzymes in biochemical reactions) (Daintith, 1990). A process driven by a catalyst that has a phase different from the reactant is heterogeneous catalysis (e.g., metal oxides in catalyzing organic and inorganic reactions). In heterogeneous catalysis, the catalyzed reaction steps take place at or very close to the solid surface. These steps may be between molecules adsorbed on the catalyst surface or may involve the topmost atomic layers of the catalysts (Twigg, 1989). The sequence of stages for a heterogeneous catalytic reaction is shown in Table 18.1. Any of these stages, if slow, may limit the overall rate of a catalytic reaction. Distinctions are often drawn between catalysts that are film-diffusion controlled (i.e., limited by stages 1 and/or 7), pore-diffusion controlled (i.e., limited by stages 2 and/or 6), and reaction controlled (i.e., limited by stages 3, 4, and/or 5). There is a complex interaction between the relative importance of these different stages and the resulting catalytic effect on organic and inorganic reactions.

Advances in surface science and catalysis are presented in a treatise edited by Hightower et al. (1996). Both homogeneous and heterogeneous catalytic reactions are significant in soil and environmental sciences (Bartlett, 1986; Huang, 1990, 1991b; Stumm, 1992; Stone and Torrents, 1995; Smolen and Stone, 1998; Davidson et al., 2003; Livens et al., 2004; Stepniewska et al., 2004; Barrett and McBride, 2005; Hofstetter et al., 2006; Cheng et al., 2008; Scheinost and Charlet, 2008; Zhang et al., 2008).

**TABLE 18.1** Sequence of Stages in the Catalysis of a Reaction by a Heterogeneous Catalyst<sup>a</sup>

1. Transport of reactants through the liquid or gas phase to the exterior of the catalyst
2. Transport of reactants through the pore system of the catalyst to a catalytically active site
3. Adsorption of reactants at the catalytically active site
4. Chemical reactions between reactants at the catalytically active site (frequently several steps)
5. Desorption of products from the catalytically active site
6. Transport of products through the catalyst pore system from the catalytically active site to the exterior of the catalyst
7. Transport of products into the liquid or gas phase from the exterior of the catalyst

*Source:* Modified from Twigg, M.V. 1989. Catalyst handbook. Wolfe Publishing Ltd., London, U.K. Copyright Wolfe Publishing Ltd., with permission.

<sup>a</sup> Several different catalytically active sites may be involved. Adsorption, possibly followed by reaction, may occur at one site, followed by transport of an intermediate product to a different site for further reactions.

### 18.2.3 Proton and Electron Transfer Catalysis

Brønsted acid–base catalysis is effective because proton transfers are generally rapid compared with the making and breaking of other chemical bonds. Therefore, reactions involving proton transfer in a typical acid or base catalysis are rapid compared with similar reactions of comparable free energy. The rate of a chemical reaction is related to the steric hindrance involved. Steric hindrance, which is the repulsion of nonbonded atoms in an activated complex, is the most important factor in determining the activation energy of a reaction (Moore and Pearson, 1981). Since a proton lacks the filled inner electron shells usually responsible for repulsion and is not surrounded by other groups, it is quite free from steric hindrance effects. Proton transfers involving oxygen–hydrogen bonds are generally rapid but they are not instantaneous. For instance, in the ionization of water, the activation energy is at least  $57 \text{ kJ mol}^{-1}$  (the heat of the reverse reaction) and the entropy of activation is negative; therefore, the rate constant ( $5 \times 10^{-7} \text{ mol L}^{-1} \text{ s}^{-1}$ ) is small (Moore and Pearson, 1981). This example demonstrates that an unfavorable equilibrium constant must necessarily make a reaction slow, even if other factors are quite favorable. Given a favorable equilibrium, proton transfers involving O and N bonds to H are almost always very fast, approaching diffusion control in many cases. Exceptions can occur if the proton is in a well-shielded position (Kresge, 1975).

Catalysis by proton transfer is by far the most common in homogeneous reactions. For those reactions that are subject to proton transfer catalysis, an expected relationship exists between the strength of the acid or base, as determined by its ionization constant, and its efficiency as a catalyst, determined by the observed rate constant. This relationship is best shown by the Brønsted catalysis law (Brønsted, 1928):

$$k_a = C_A K_a^\alpha \quad k_b = C_B K_b^\beta, \quad (18.1)$$

where

$k_a$  and  $k_b$  are the rate constants (also termed the catalytic constants) for acid and base catalytic reactions, respectively  
 $K_a$  and  $K_b$  are the acid and base ionization constants  
 $C_A$ ,  $C_B$ ,  $\alpha$ , and  $\beta$  are constants characteristic of the reaction, the solvent, and the temperature

Normally,  $\alpha$  and  $\beta$  are positive and have values between 0 and 1. In the Brønsted equation, a low value of  $\alpha$  and  $\beta$  signifies a low sensitivity of the catalytic constant to the strength of the catalyzing acid or base, and vice versa. Proton transfer catalysis is of significance in soils and associated environments (Theng, 1974, 1979; Cheng, 1991; Nannipieri and Gianfreda, 1998) as discussed later.

In acid catalysis of reactions involving negatively charged organic molecules, adsorption of a proton reduces their negative charge and, thus, facilitates the transfer of electrons (Steinberger and Westheimer, 1949, 1951). In agreement with this explanation, a number of multiply charged cations act as catalysts in the transformation of organic compounds (Stone and Torrents, 1995).

Presumably a metal–organic complex is formed that reduces the negative charge and increases the electron transfer. The catalytic efficiency of a metal ion depends both on its positive charge and on its ability to form a stable complex and chelate the reactant. In such reactions, the metal ions are acting as generalized acids. However, metal ions have some significant advantages over protons. They can have greater charges, which lead to greater polarization of the reactant molecules. Unlike the proton, metal ions can be stabilized by other ligands and, thus, can exist in neutral or even basic solutions. The high coordination numbers of metal ions permit the binding of a substrate at more than one site. This advantage helps to make metal ions very efficient catalysts for the hydrolysis of many organic compounds (Kroll, 1952). Further, some metal ions have the ability to simultaneously bind both a substrate and a reagent. This can have the effect of a template, in which the two reactants are assembled (brought into close proximity) prior to combination (Basolo and Pearson, 1968).

Many metal ions, especially of the transition series, have several stable oxidation states, which enables them to act as catalysts in certain redox reactions. Transition metals are the best catalysts, in most cases, for catalyzing reactions that are slow for symmetry reasons (Pearson, 1976). In addition to the slow three-body reactions, a second class of slow reactions is forbidden by orbital symmetry (Moore and Pearson, 1981). Even when the reaction is thermodynamically favorable, a large energy barrier can exist. Such reactions are prime candidates for catalysis. The reason why transition metals are often the best catalysts is due to their partly filled d orbitals, which have symmetry properties that are different from those of s and p orbitals. Because of the special properties of metal ions, particularly transition metal ions, they can catalyze a wide variety of organic and inorganic reactions in soil and related ecosystems.

## 18.3 Abiotic Catalysis of Natural and Anthropogenic Organic Compounds

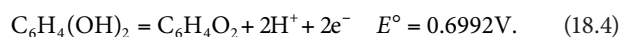
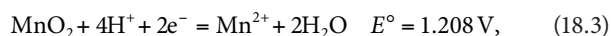
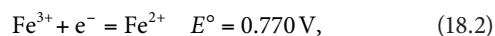
### 18.3.1 Oxidative Transformation of Phenolic and Other Organic Compounds

#### 18.3.1.1 Phenolics

Phenolics are the most widely distributed class of plant secondary metabolites and play an important role in regulating nutrient cycling in the terrestrial environment (Hättenschwiler and Vitousek, 2000). Phenolics may be released from natural sources, industrial activities, or agricultural practices; and they can harm the environment, especially in the form of pesticides (e.g., chlorophenols), nitrophenols, hormones, and azo dyes (Gianfreda et al., 2006). The oxidative transformation of phenolics can be accelerated enzymatically and nonenzymatically (Huang, 1990; Bollag et al., 1995; Naidja et al., 2000; Gianfreda et al., 2006). Soil minerals, in particular (SRO) Fe(III) and Mn(IV) oxides, play an important role in catalyzing the abiotic oxidative polymerization of phenolic compounds and the subsequent formation of humic

substances (Wang et al., 1986; Pal et al., 1994; Bollag et al., 1998; Huang, 2004; Huang et al., 2005). The surfaces of soil mineral colloids promote oxidative polymerization reactions by acting as electron acceptors. The rate-determining step in the formation of humic acids (HAs) from polyphenols is apparently the formation of a semiquinone-free radical involving a single electron transfer reaction (Schnitzer, 1982). Semiquinones couple with each other to form a stable HA polymer. The coupling of free radicals requires little activation energy, in contrast to electron transfer reactions (Chang and Allen, 1971). Therefore, coupling of semiquinones rather than the formation of quinones should be kinetically the preferred reaction pathway in the transformation of polyphenols to humic macromolecules.

Manganese(IV) oxides, such as birnessite ( $\delta$ -MnO<sub>2</sub>), cryptomelane ( $\alpha$ -MnO<sub>2</sub>), and pyrolusite ( $\beta$ -MnO<sub>2</sub>), which commonly occur in soils and sediments (McKenzie, 1989), are powerful catalysts of the abiotic oxidation of polyphenols, such as catechol (1,2-dihydroxybenzene), compared with Fe, Al, and Si oxides (Shindo and Huang, 1982, 1984a; Shindo, 1992; Liu and Huang, 2001; Colarieti et al., 2006). This is partially attributable to the lower electronegativity of Mn (Liu and Huang, 2001). The electronegativity values of Mn, Fe, Al, Si, H, and O are, respectively, 1.55, 1.83, 1.61, 1.90, 2.20, and 3.44 (Porterfield, 1983). Catechol acts as a hard Lewis base, and Mn, Fe, Al, and Si are hard Lewis acids. When Mn, Fe, Al, or Si replace H in catechol to form metal-catechol complexes, the electron cloud delocalizes from the phenolic oxygen into the  $\pi$ -orbital formed from overlap of the 2p orbitals of the aromatic C atoms, thus accelerating the formation of semiquinone-free radicals and their polymerization. The electron cloud around the Mn-O bond in the Mn oxide-phenolic complex should be more delocalized than that around the Al-O bond in the Al-catechol complex and especially the Si-O or Fe-O bond in the Si or Fe oxide-phenolic complex due to the lower electronegativity of Mn than those of Al, Fe, and Si. This provides a partial explanation for the greater accelerating effect of Mn oxide on the humification of catechol than Fe, Al, or Si oxides. Naturally, redox reactions also play an important role in many abiotic catalytic reactions. Aluminum and silicon oxides are not subject to redox reaction. The standard electrode potential ( $E^\circ$ ) values of the overall redox reaction of the Fe(III) oxide-catechol and Mn(IV) oxide-catechol systems are +0.071 V and +0.509 V, respectively, as indicated by the following reactions (Shindo and Huang, 1984a):



The positive  $E^\circ$  values of the overall redox reactions indicate that the reactions are thermodynamically feasible, and catechol oxidation can thus be accelerated by Fe oxide and especially Mn

oxide. This also explains the stronger catalytic ability of the Mn oxide than Fe, Al, and Si oxides in accelerating catechol oxidation. In addition, the lower point of zero salt effect (PZSE) and more negative charges of the Mn oxide than the Fe and Al oxides could also enhance the oxidation of catechol (Liu and Huang, 2001). A more negatively charged mineral surface may favor the binding of protons released from catechol and subsequently increase the catalytic reaction rate. Therefore, the catalytic ability of a metal oxide in polyphenol transformation depends on the  $E^\circ$  value of the overall redox reaction and the ability of the metal ions to complex with ligands, to shift electron density and molecular confrontation in the way conducive to the reaction, and to favor the binding of protons to the metal oxide.

Birnessite strongly promotes the formation of humic macromolecules from pyrogallol (1,2,3-trihydroxybenzene) under environmentally relevant conditions; total yields of humic substances were 10.5-fold higher than in pyrogallol reacted in the absence of birnessite (Wang and Huang, 1992). Manganese(IV) oxide has also been effectively used to treat polyphenol-polluted olive mill wastewater by enhancing humification (polymerization) (Brunetti et al., 2007). The Mn oxide-treated wastewater was found to enhance the humified C content of amended soils and increased the overall fertility of the soil (Brunetti et al., 2007).

During the abiotic catalytic transformation of pyrogallol to HA, Mn(IV), Fe(III), Al, and Si oxides also promote the abiotic generation of CO<sub>2</sub> through their ability to cleave the ring structure of pyrogallol (Wang and Huang, 1992, 2000b). The order of CO<sub>2</sub> release from the oxide-catalyzed pyrogallol reaction systems was Mn(IV) oxide >>> Fe(III) oxide > Al oxide > Si oxide (Wang and Huang, 2000b). The release of CO<sub>2</sub> was related to the development of carboxylic group contents in the HA fraction. Wang and Huang (2000a) showed that the infrared spectrum of the fulvic acid (FA) fraction from the Mn oxide-pyrogallol system closely resembles that of the FA fraction extracted from a natural Borosaprist soil. The abiotic ring cleavage of polyphenols by soil inorganic components may partially account for the findings of the high aliphaticity of natural humic substances (Wilson and Goh, 1977; Hatcher et al., 1981). Lee and Huang (1995) showed that the abiotic release of CO<sub>2</sub> in the birnessite-polyphenol and polyphenol systems increases with light intensity, a consequence of a photofragmentation of polyphenolics catalyzed by birnessite. These findings imply that the pathways of C turnover in the photic zones of soils and aquatic environments may differ from those in their subsurface and submerged layers.

Shindo and Huang (1992) compared the catalytic effects of Mn oxide and the oxidoreductase enzyme, tyrosinase, on the oxidative polymerization of diphenols over the pH range common in soil environments. Manganese oxide influences the oxidative polymerization of hydroquinone and resorcinol to a larger extent than does tyrosinase, whereas the reverse is true for catechol. The yields of HAs are significantly influenced by the kind of catalyst and polyphenol. In the Mn oxide system, the yield of HAs is in the order hydroquinone > catechol > resorcinol. In the tyrosinase system, catechol produces the highest yield of HA, followed by hydroquinone and resorcinol. These findings indicate that the

relative catalytic effects of Mn(IV) oxides and enzymes such as tyrosinase would vary with the type of polyphenols in soils. HAs formed by mineral catalysis have a better defined chemical structure than those formed by enzymatic oxidative polymerization, favoring the formation of components with lower degrees of aromatic ring condensation and lower molecular weights compared with those generated in the presence of tyrosinase (Naidja et al., 1998). Ahn et al. (2006) showed that the presence of the abiotic catalyst birnessite actually inhibits the catechol oxidative polymerization activity of the enzyme laccase, which was attributed to the  $Mn^{2+}$  released during the reduction of birnessite by catechol, which binds to the enzyme and alters its active site.

Phenolic acids have been shown to be oxidized rapidly in the presence of  $MnO_2$  to form a number of soluble products (Lehmann and Cheng, 1988). Mass spectrometric data show that some of the soluble products of the reaction have somewhat higher molecular weights than the parent compounds. However, the soluble products of the reaction of ferulic acid and  $MnO_2$  do not contain any ferulic acid hexamers (Liu et al., 1981; Bollag et al., 1982). The oxidized products of ferulic acids are apparently rapidly sorbed on the surfaces of  $MnO_2$ . Polyhydroxyphenolic acids with *p*- and *o*-OH groups are rapidly oxidized by Mn oxides (Pohlman and McColl, 1989) (Table 18.2) to polymeric humic products in both soil and Mn suspensions. On the other hand, *m*-polyhydroxyphenolic acids are not readily oxidized.

Monophenolic compounds, such as phenol (Jung et al., 2008b), and particularly those containing electron-donating substituent groups on the aromatic ring, can be oxidatively transformed by Mn(IV) oxides (Lehmann et al., 1987; Stone, 1987; Ulrich and Stone, 1989; Zhao et al., 2006). Manganese(IV) oxide has been found to be an effective abiotic catalyst of the oxidative transformation of highly toxic and recalcitrant compound, pentachlorophenol (PCP), under aquifer (Petrie et al., 2002) and near-dry

conditions (Pizzigallo et al., 2004). Pyrolusite is able to oxidatively degrade the carcinogenic pesticide and antiseptic agent TCP (2,4,6-trichlorophenol) under near-dry conditions; however, the transformation products may actually be more toxic and persistent than the parent compound (Smith et al., 2006). Methoxylyated phenols have been used to mediate the oxidative polymerization of the nonphenolic fungicide, cyprodinil (4-cyclopropyl-6-methyl-*N*-phenyl-2-pyrimidinamine), in the presence of birnessite (Kang et al., 2004). Birnessite-induced oxidative coupling also results in the decarboxylation, demethoxylation, and dehalogenation of substituted phenolic substrates (Dec et al., 2001, 2003). Electron-withdrawing substituents, such as  $-COOH$  and  $-Cl$ , are more susceptible to release than electron-donating ones, such as  $-OCH_3$  and  $-CH_3$  (Dec et al., 2003).

The catalytic ability of Fe oxides in the rapid oxidative polymerization of polyphenols (Scheffer et al., 1959) increases in the following order: ferrihydrite > goethite > maghemite > lepidocrocite > hematite. Ferrihydrite, which is SRO Fe oxide with high surface area, is most reactive in catalyzing the oxidative polymerization reaction. Besides the nature of Fe oxides, the catalytic ability of Fe is related to structure and functionality of phenolic compounds (Shindo and Huang, 1984a; Shindo, 1992; Pracht et al., 2001).

The oxidative polymerization of polyphenols is substantially influenced by the catalysis of Al hydroxides (Wang et al., 1983). Soluble silicic acid in aqueous solution and precipitated short-range order silica can catalyze the oxidation of polyphenols (Ziechmann, 1959). Liu and Huang (2000) reported that silicic acid and especially hydroxyl Al ions substantially enhance oxidative polymerization of catechol. Liu and Huang (2002) showed that hydroxy-aluminosilicate ions, which are precursors to noncrystalline aluminosilicates, are also effective in promoting the oxidative polymerization of catechol. The surface of ground quartz has a disturbed layer, which is SRO in nature (Iler, 1979). Similar disturbed surface layers are present on quartz grains in soils (Ribault, 1971). Oxidative polymerization of polyphenols may be catalyzed by the disturbed surface of quartz in soils.

Besides metal oxides, clay size layer silicates have the ability to catalyze the oxidative transformation of polyphenols. Before the pioneering work on the catalytic role of clay size layer silicates in oxidative polymerization of phenolic compounds and the subsequent formation of humic substances (Kumada and Kato, 1970; Filip et al., 1977; Wang and Li, 1977), the conversion of many aromatic amines into their color derivatives by clay minerals and clays had been investigated (Faust, 1940; Hauser and Legget, 1940). Solomon (1968) reported that, except for talc, a large number of representative minerals produce a blue color of varying intensity when brought into contact with a saturated solution of benzidine hydrochloride. The active sites for the oxidation of benzidine are located on the crystal edges and on transition metal atoms in the higher oxidation state that occupy octahedral sites in the silicate layers. Thompson and Moll (1973) measured the oxidative power of smectites by oxidation of hydroquinone to *p*-benzoquinone in a clay slurry. Oxidation occurs

**TABLE 18.2** Kinetic Constants for Polyhydroxyphenolic Acid Oxidation by Soil and Manganese Oxide Suspension<sup>a</sup>

Compound	Rate Constants ( $L \text{ mol}^{-1} \text{ s}^{-1}$ )	
	Challenge A Horizon	$MnO_2$
2,3-Dihydroxybenzoic acid	ND <sup>b</sup>	0.03
2,5-Dihydroxybenzoic acid	0.06	0.04
2,6-Dihydroxybenzoic acid	0.00 <sup>c</sup>	ND
3,4-Dihydroxybenzoic acid	0.10	0.04
3,5-Dihydroxybenzoic acid	0.00	0.00
Gallic acid	0.25	0.05
Syringic acid	ND	0.01
Vanillic acid	ND	0.00

Source: From Pohlman, A.A., and J.G. McColl. 1989. Organic oxidation and manganese and aluminum mobilization in forest soils. Soil Sci. Soc. Am. J. 53:686–690. With permission of the Soil Science Society of America.

<sup>a</sup> Oxidations were run using  $10 \text{ g L}^{-1}$  soil and  $2.5 \times 10^{-4} \text{ mol L}^{-1}$  phenolic acid or  $0.19 \text{ g L}^{-1} MnO_2$  and  $5.0 \times 10^{-4} \text{ mol L}^{-1}$  phenolic acid at pH 4.5 and  $30^\circ\text{C}$ .

<sup>b</sup> ND, not determined.

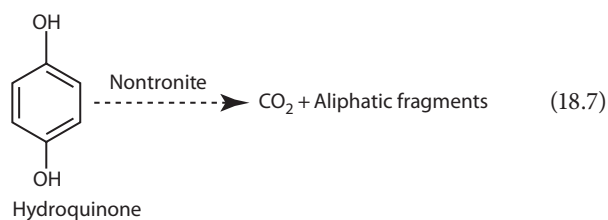
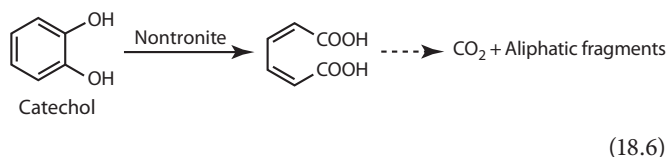
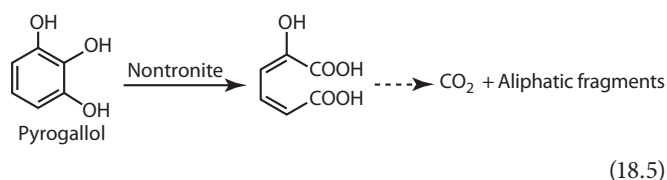
<sup>c</sup> No oxidation of phenolic acid within 120 min of reaction.

in the presence of O<sub>2</sub> (air), but not N<sub>2</sub> unless Fe<sup>3+</sup> or Cu<sup>2+</sup> are the exchangeable cations. Adsorbed O<sub>2</sub> molecules or radicals on the clay surface are apparently partially responsible for the oxidation.

Pinnavaia et al. (1974) reported aromatic radical cation formation on the intracrystal surfaces of transition metal-saturated layer silicates. Aromatic molecules, when reacted under very moderated conditions with Cu(II) or Fe(II) ions, may donate electrons to the metal cations, leading to the formation of polymers (Mortland and Halloran, 1976). Montmorillonite, vermiculite, illite, and kaolinite accelerate the formation of HAs to varying degrees (Shindo and Huang, 1985a). The promoting effect of 2:1 layer silicates is higher than that of 1:1 layer silicates because of the larger specific surface and lattice imperfections, which favor adsorption of O<sub>2</sub> molecules or radicals.

One of the well-identified precursors (Flaig et al., 1975; Hayes and Swift, 1978) for the formation of humic substances, hydroquinone, can be transformed in aqueous solution at near-neutral pH (6.5) to humic macromolecules and deposited in the interlayers of nontronite saturated with Ca, which is the most common and most abundant exchangeable cation in soils and sediments (Wang and Huang, 1986). Most of the interlayer humic macromolecules are highly resistant to alkali extraction and may, thus, be humin-type materials. Therefore, besides Al interlayers in 2:1 expansible layer silicates, the formation of humic substance interlayers in 2:1 expansible layer silicates, through polymerization of phenol monomers and the associated reactions in soils and sediments, deserves close attention.

The ability of nontronite to promote the oxidation of polyphenols is related to the structure and functionality of the polyphenols, and part of the reaction process may proceed as shown below (Wang and Huang, 1994):



Catechol with two *o*-OHs is evidently more easily cleaved than hydroquinone with two *p*-OHs while pyrogallol with three hydroxyls in adjacent positions is even more easily cleaved than

catechol. The resultant carboxyl group-containing intermediates are further oxidized to form CO<sub>2</sub> and aliphatic fragments. In the reaction systems, intermediate products and aliphatic fragments may form polycondensates. The structure and functionality of polyphenols thus have an important role in influencing the extent of catalytic transformations by nontronite.

Primary minerals, which are commonly present in soil environments (Dixon and Weed, 1989), can catalyze the oxidative polymerization of polyphenols (Shindo and Huang, 1985b). The degree of acceleration of the oxidative polymerization of hydroquinone is greatest in the tephroite system, which increases the total HA yields more than ninefold because (1) tephroite (ideal chemical formula, MnSiO<sub>4</sub>) is a Mn-bearing silicate, (2) part of the Mn in tephroite is present in the higher valence states, and (3) the oxidation of diphenols [C<sub>6</sub>H<sub>4</sub>(OH)<sub>2</sub>] by Mn(III) and Mn(IV) is thermodynamically favorable (Lide, 2008).

The hydroquinone-derived polymers with molecular weights of approximately 3500 and higher formed in the presence of the tephroite system (Shindo and Huang, 1985b) have similar IR absorption bands to those of humic substances (Schnitzer, 1978). The surface features of these polymers (Figure 18.1) are similar to those of soil HA and FA (Stevenson and Schnitzer, 1982) with the smallest discrete particles being spheroids with diameters of 0.1–0.2 μm (Figure 18.1a) and some aggregation of individual spheroids (Figure 18.1b and c). Small aggregates (Figure 18.1c) resemble moss while the large aggregates are nodule like (1–5 μm diameter) and doughnut like (6–8 μm diameter) (Figure 18.1a and b). The polymers do not appear to be associated with the surfaces of tephroite particles (Figure 18.1d). Consequently, the role of primary minerals in the oxidative polymerization of polyphenols and the subsequent formation of humic substances in soils should not be overlooked (Shindo and Huang, 1985b).

SRO aluminosilicates, such as allophane, are known to act as catalysts in the oxidative degradation of polyphenols (Kyuma and Kawaguchi, 1964; Kumada and Kato, 1970). Hydroxyaluminosilicate ions (proto-imogolite sol) also have the ability to catalyze polyphenol humification (Liu and Huang, 2002). However, the role of other SRO aluminosilicates remains obscure. On the other hand, the formation of SRO aluminosilicates is significantly affected by inorganic ligands, low-molecular-weight organic acids, humic substances, metallic cations, and expansible layer silicates (Huang, 1991a), resulting in the formation of ill-defined aluminosilicate complexes and hydroxyaluminosilicate-intercalated layer silicates. The catalytic ability of these SRO mineral colloids in the transformation of polyphenols and other organic compounds in soils has yet to be investigated.

### 18.3.1.2 Other Organic Compounds

Many naturally occurring organic acids, including salicylic, pyruvic, oxalic, and malic acids, are degraded by mineral colloids such as Mn oxides by electron transfer reactions (Stone and Morgan, 1984a, 1984b). A wide range of nonphenolic xenobiotic compounds, including pesticides, antibiotics, dyes, and



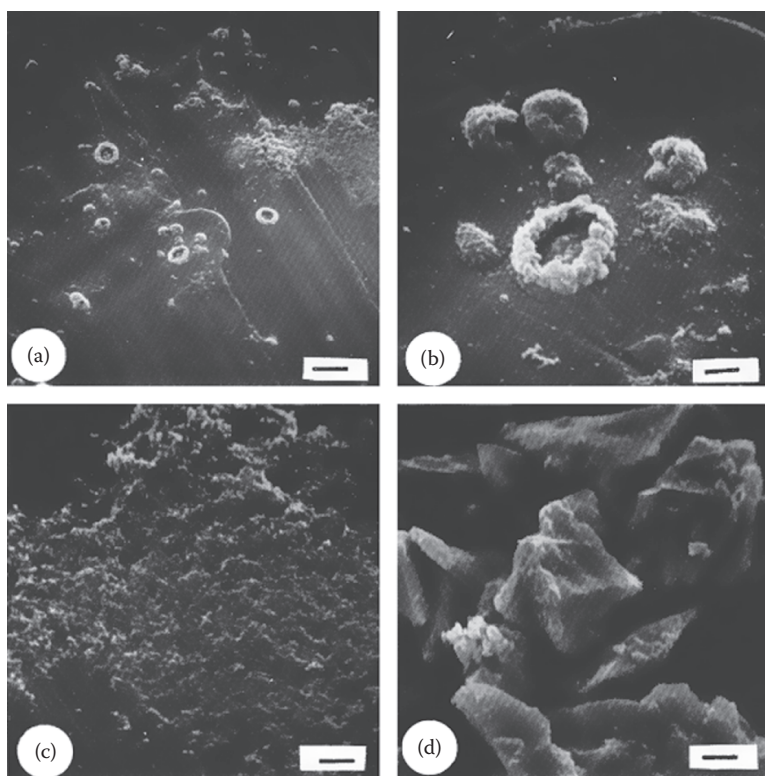


**FIGURE 18.1** SEM micrographs of hydroquinone polymers in the supernatant and mineral particles settled in the tephroite system at the ratio of mineral to hydroquinone solution of 0.01 at the initial pH of 6.0 at the end of 7 days. (a, b, c) Hydroquinone polymers; (d) tephroite particles after reaction with hydroquinone. Bar in (a) equals 10  $\mu\text{m}$ ; bars in (b)–(d) equals 2  $\mu\text{m}$ . (Reprinted from Shindo, H., and P.M. Huang. 1985b. Catalytic polymerization of hydroquinone by primary minerals. *Soil Sci.* 139:505–511.)

explosives, are subject to abiotic soil mineral-catalyzed oxidative transformation. Abiotic degradation pathways of biocides (pesticides and antibiotics) are particularly important in the environment as the toxicity of these substances can limit their biotic degradation.

#### 18.3.1.2.1 Pesticides

Manganese(IV) oxides are able to catalyze the oxidative polymerization of toxic anilines, chloroanilines, and other aromatic amines, which originate from pesticides, as well as from chemical manufacturing residues (Laha and Luthy, 1990; Pizzigallo et al., 1998; Li et al., 2003). Birnessite is an effective solid-state catalyst of the breakdown of organic pollutants such as the herbicide 2,4-D (2,4-dichlorophenoxyacetic acid) and diethyl ether, which are adsorbed on birnessite and rapidly oxidized (Cheney et al., 1996), both producing  $\text{CO}_2$  as a major product, but by somewhat different mechanisms. Nasser et al. (2000) demonstrated a dry mechanochemical technique for quickly and completely degrading 2,4-D by lightly grinding it with birnessite, thus eliminating the need for organic solvents such as diethyl ether. The widely used herbicide atrazine (2-chloro-4-ethylamino-6-isopropylamino-*s*-triazine) is also partially degraded by mechanochemical contact with Mn(IV) oxides (birnessite, cryptomelane, and pyrolusite) via N-dealkylation and subsequent

decarboxylation mechanisms (Shin et al., 2000). The removal of 4-chloroaniline and PCP by a mechanochemical procedure was far more effective than by batch contact (solution) in the presence of birnessite and ferrihydrite (Pizzigallo et al., 2004). The mechanochemical contact of polychlorinated biphenyls (PCBs) and birnessite produced a removal of pollutant that was a function of the number of chlorine atoms, that is, the more the chlorine atoms the less effective the oxidative degradation (Pizzigallo et al., 2004). Possible contributions of solid-state degradation to herbicide breakdown by abiotic catalysis should be considered in modeling herbicide breakdown or when designing experiments for soil remediation.

Birnessite is able to oxidatively degrade glyphosphate (*N*-phosphonomethyl-glycine), which is the most commonly used pesticide worldwide (Barrett and McBride, 2005). The abiotic degradation mechanism involves C–P and C–N bond cleavage of glyphosphate and its degradation product, sarcosine, due to electron transfer reactions at the Mn oxide surface (Figure 18.2; Barrett and McBride, 2005). Pyrolusite is able to effectively oxidatively degrade the widely found organic pollutant 2-mercaptobenzothiazole (a biocide and compound used in manufacture of rubber) into  $\text{SO}_4^{2-}$  and  $\text{NO}_3^-$ ; however, the presence of organic acids, carboxylic acids (oxalic, citric, tartaric, and malic acids), or metal ions ( $\text{Ni}^{2+}$ ,  $\text{Ca}^{2+}$ ,  $\text{Mn}^{2+}$ , and  $\text{Cr}^{3+}$ ) has an inhibiting effect on the rate of degradation (Li et al., 2008).

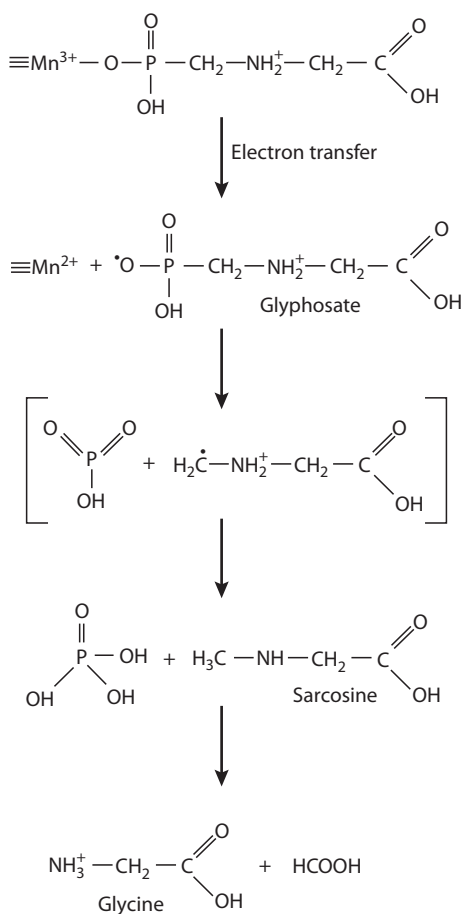


**FIGURE 18.2** A possible degradation reaction scheme for glyphosate adsorbed on Mn oxide. (Reprinted with permission from Barrett, K.A., and M.B. McBride. 2005. Oxidative degradation of glyphosate and aminomethylphosphonate by manganese oxide. *Environ. Sci. Technol.* 39:9223–9228. Copyright 2005 American Chemical Society.)

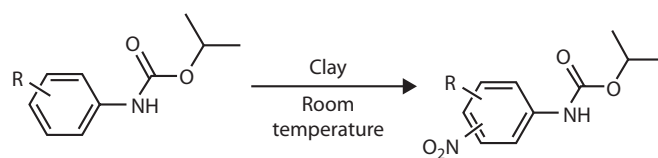


**FIGURE 18.3** Chemical structure of carbamates and their nitro derivatives in clay-catalyzed nitration. (Reprinted with permission from Kodaka, R., T. Sugano, T. Katagi, and Y. Takimoto. 2003. Clay-catalyzed nitration of a carbamate fungicide diethofencarb. *J. Agric. Food Chem.* 51:7730–7737. Copyright 2003 American Chemical Society.)

Clay minerals, kaolinite and montmorillonite, are able to catalyze the nitration of the carbamate fungicide, diethofencarb (isopropyl 3,4-diethoxycarbanilate), which most likely proceeds through the formation of  $\text{NO}_2^\bullet$  radicals on the surface of the clay (Figure 18.3). The similar nitration of the phenyl ring of the pesticide, famoxadone (3-anilino-5-methyl-5-(4-phenoxyphenyl)-1,3-oxazolidine-2,4-dione), has been reported (Jernberg and Philip, 1999). Nitration of pesticides is only known as a clay-catalyzed reaction (Nikalje et al., 2000).

### 18.3.1.2.2 Antibiotics

Manganese(IV) oxides are able to oxidatively degrade many of the leading groups of antibacterial agents used in the treatment of humans and animals, in livestock feed additives, or in active ingredients in personal care products (Zhang et al., 2008).

Manganese(IV) oxide is able to catalyze the oxidative degradation of the popular and potent fluoroquinolone (FQ) antibiotic agents under environmental conditions (Zhang and Huang, 2005a). The oxidative degradation mechanism (Figure 18.4) involves a surface reaction mechanism that likely begins with the formation of a surface complex between FQ and the surface-bound Mn(IV), followed by oxidation at the aromatic N1 atom of FQ's piperazine moiety to generate an aniliny radical intermediate. The radical intermediates subsequently undergo N-dealkylation, C-hydroxylation, and possibly coupling to yield a range of products. The  $\delta$ - $\text{MnO}_2$  exhibited reactivity to the FQ antibiotics in the order of ciprofloxacin  $\approx$  enrofloxacin  $\approx$  norfloxacin  $\approx$  ofloxacin  $>$  lomefloxacin  $>$  pipemidic acid  $\gg$  flumequine (Zhang and Huang, 2005a). The veterinary N-oxide antibiotics, carbadox, olaquinox, quinoline N-oxide, and quindoxin also exhibit high oxidation reactivity toward  $\text{MnO}_2$  (Zhang and Huang, 2005b). The transformation mechanism involves the formation of an N-oxide radical intermediate and the generation of Mn(II) (Zhang and Huang, 2005b).

Manganese(IV) oxides are also able to promote the appreciable degradation of tetracycline antibiotics (Rubert and Pedersen, 2006). Reactivity of tetracycline antibiotics toward  $\text{MnO}_2$  increases in the following order: rolitetracycline  $\approx$  oxytetracycline  $\leq$  tetracycline  $\approx$  mecloxycycline  $<$  chlortetracycline. Abiotic degradation of the veterinary ionophore and macrocyclic antibiotics, monensin and tylosin, does take place in soil, however at a much slower rate than by microbial degradation in soil (Sassman and Lee, 2007; Sassman et al., 2007).

### 18.3.1.2.3 Explosives and Dyes

The explosive CL-20 (hexanitrohexaazaisowurtzitane) was found to be quickly (in minutes) abiotically, and oxidatively degraded in the presence of 2:1 layer silicates (montmorillonite, hectorite, and nontronite), micas (biotite and illite), and birnessite (Szecsody et al., 2004). The exact mechanism remains unclear, but it is known that the cage structure of CL-20 is broken and that cleavage of C–C and C–N bonds occurs due to the formation of nitrite and formate anions (Szecsody et al., 2004). Birnessite has also been found to effectively catalyze the complete abiotic transformation of the  $\text{Fe}^0$ -induced reduction products of the explosive 2,4,6-trinitrotoluene (TNT) via oxidative-coupling reactions (Kang et al., 2006).

Magnetite and other mixed metal (Co, Cu, and Mn)-ferrite oxides are able to efficiently catalyze the oxidative degradation and decolorization of various dyes (bromophenol blue, Chicago sky blue, Cu-phthalocyanine, eosin yellowish, Evans blue, naphthol blue black, phenol red, poly B-411, and reactive orange 16) in the presence of hydrogen peroxide by generating hydroxyl-free radicals (Baldrian et al., 2006). The metal oxide catalysts are

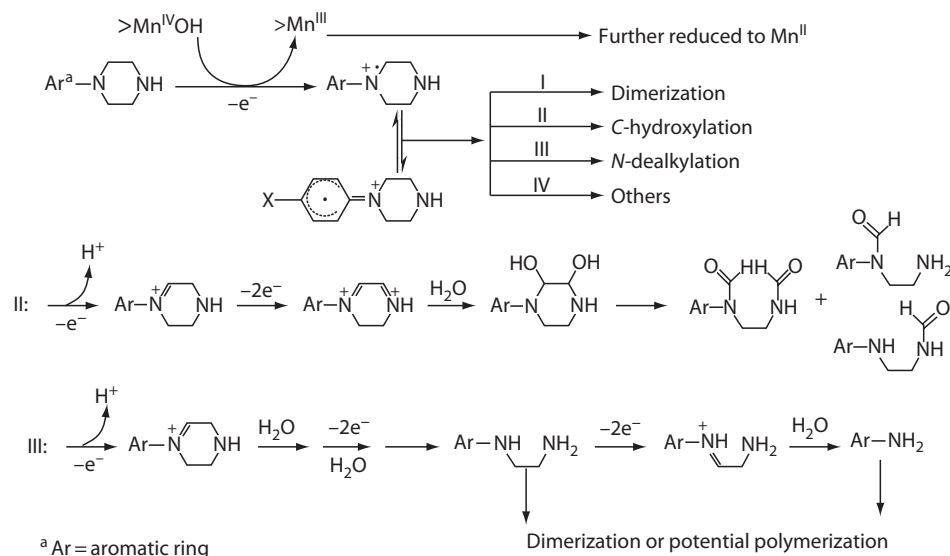


**FIGURE 18.4** Proposed reaction scheme for oxidation of fluoroquinolone antibiotics by  $\delta$ - $\text{MnO}_2$ . (Reprinted with permission from Zhang, H.C., and C.H. Huang, 2005a. Oxidative transformation of fluoroquinolone antibacterial agents and structurally related amines by manganese oxide. *Environ. Sci. Technol.* 39:4474–4483. Copyright 2005 American Chemical Society.)

able to retain their activity even after repeated catalytic cycles and over a broad pH range unlike enzymatic catalysts such as laccase (Baldrian et al., 2006). The ferric iron species in layer silicate clays are also able to catalyze the oxidative degradation of the organic dye, malachite green, in the presence of hydrogen peroxide (Cheng et al., 2008). The exchangeable interlayer Fe(III) ions exhibit a much higher reactivity than structural Fe(III) in the octahedral sheet. The Fe-containing clays are chemically and mechanically stable, and no loss of activity was observed after 14 recycles (Cheng et al., 2008).

### 18.3.2 Polycondensation of Phenolic Compounds and Amino Acids

The transformation of colorless amino acids and polyphenols by quinone–amino acid polycondensation reactions into darkly colored polymers is a significant browning reaction in nature (Bittner, 2006). Birnessite efficiently catalyzes the polycondensation of phenolic compounds and amino acids such as in hydroquinone–glycine systems in the common pH range (4–8) of soils

with the formation of  $\text{NH}_3$ -N and nitrogenous polymers (Table 18.3). The proposed processes are as follows: (1) the Mn oxide acts as Lewis acid by accepting electrons from hydroquinone, which is thus oxidized and subsequently polymerized; (2) the products of the reaction of glycine with hydroquinone polymerize to form nitrogenous polymers, thereby incorporating glycine into the polymers during the oxidative polymerization of hydroquinone; and (3) a partial deamination of glycine occurs during the second process.

Birnessite also catalyzes the polycondensation of glycine and pyrogallol and deamination and decarboxylation of glycine especially in the presence of pyrogallol (Wang and Huang, 1987). The formation of HA and FA is not evident in the presence of glycine alone. In a  $\text{N}_2$  atmosphere,  $\text{CO}_2$  release in the birnessite–glycine–pyrogallol system is drastically reduced. Birnessite also greatly enhances the formation of N-containing humic polymers. Most of the released  $\text{NH}_3$  can be attributed to the deamination of glycine by pyrogallol-derived free radicals as catalyzed by birnessite but an appreciable amount can also be directly derived from the deamination of glycine by birnessite.

**TABLE 18.3** Formation of  $\text{NH}_3$ -N and Polymer-N (in  $\text{mg kg}^{-1}$ ) in the Hydroquinone–Glycine System Both in the Absence and Presence of Mn Oxide at Different pH Values at the End of 24 h

	Initial pH of 4.0				Initial pH of 6.0				Initial pH of 7.3			
	Final pH	$\text{NH}_3$ -N	Polymer-N	Sum-N	Final pH	$\text{NH}_3$ -N	Polymer-N	Sum-N	Final pH	$\text{NH}_3$ -N	Polymer-N	Sum-N
Hydroquinone–glycine	4.1	4.4	3.0	7.4	6.1	6.0	2.0	8.0	6.9	11.7	3.4	15.1
Mn oxide hydroquinone–glycine	4.1	30.5	12.6	43.1	7.6	30.2	40.1	70.3	7.9	34.1	41.2	75.3

Source: Shindo, H., and P.M. Huang, 1984b. Significance of Mn(IV) oxide in abiotic formation of organic nitrogen complexes in natural environments. *Nature* 308:57–58. With permission of Macmillan, London.

Carbon-14 labeling of glycine was used to measure the extent of incorporation of carboxyl C and alkyl C into the polycondensates of pyrogallol and glycine (Wang and Huang, 1997). Birnessite promotes the incorporation of carboxyl and especially alkyl C of glycine into the polycondensates formed in the presence of pyrogallol (Wang and Huang, 1997, 2005). The results indicate that the formation of the C–C bond is more prevalent than that of the C–O bond in the polycondensation of glycine and pyrogallol catalyzed by birnessite.

Besides birnessite, clay size layer silicates also have the ability to catalyze the polycondensation of phenolic compounds and amino acids. Wang et al. (1985) show the catalytic effect of Ca-illite on the formation of N-containing HAs in the systems containing phenolic compounds and amino acids at neutral pH. The yields and N contents of the synthesized HAs depend on the nature of amino acids.

Nontronite in which structural Fe(III) acts as an electron acceptor analogous to Mn(IV) in MnO<sub>2</sub> (Solomon, 1968; Theng, 1974) also catalyzes the polycondensation of glycine and pyrogallol (Wang and Huang, 1991). The IR and electron spin resonance (ESR) spectra of the HA and FA formed, which show the presence of a stabilized organic free radical (semiquinone), are similar to those of natural soil HA and FA (Schnitzer, 1977; Senesi and Schnitzer, 1977; Schnitzer and Levesque, 1979; Hatcher et al., 1980; Schnitzer and Ghosh, 1982). The formation of semiquinone-free radicals appears to proceed through electron transfer from pyrogallol to Fe(III) or other variable-valence transition metal ions on the edges or in the nontronite structure (Solomon, 1968). Electrons diffuse or tunnel to octahedral sites from layer edges or basal surfaces (Tennakoon et al., 1974). The strong oxidation power of chemisorbed O<sub>2</sub> on silicates (Solomon and Hawthorne, 1983) such as nontronite seems to cause the ring cleavage of pyrogallol and the decarboxylation and deamination of glycine (Wang and Huang, 1991). Semiquinone-free radicals, aliphatic fragments, and glycine apparently undergo polycondensation to form humic polymers.

Natural soil clays, from temperate and tropical environments, have been shown to catalyze the polycondensation of pyrogallol and glycine, the ring cleavage of pyrogallol, its polymerization, and the deamination of glycine (Wang and Huang, 2003). The reactivity of the mollisol and oxisol clays was attributed to the catalysis of the layer silicates and oxides of Fe, Al, and Mn present in the natural soil clays (Wang and Huang, 2003).

### 18.3.3 The Maillard Reaction and Integrated Polyphenol–Maillard Reactions

The Maillard reaction (Maillard, 1913), involving condensation reactions between reducing sugars and amino acids, is considered to be an important pathway in natural humification (Ikan et al., 1996). Sugars and amino acids are among the most abundant constituents of terrestrial and aquatic environments (Anderson et al., 1989). The Maillard reaction involves numerous reactions between the degradation products of the precursor

sugars and amino acids, and reaction intermediates, known as Amadori and Heyns compounds (Yaylayan, 1997).

The initial reaction in the Maillard reaction involves condensation between the  $\alpha$ -hydroxy carbonyl group of a reducing sugar and the amino group from an amino acid with the formation of a Schiff base, which rearranges to form either Amadori or Heyns compounds. Aldohexoses generate Amadori compounds while ketohexoses generate Heyns products (Yaylayan, 1997). These compounds can undergo retroaldolization reactions forming  $\alpha$ -dicarbonyl and  $\alpha$ -hydroxyketone compounds. All these compounds are highly reactive and readily polymerize in the presence of amino compounds to form brown-colored melanoidins. Amino acids can react with the  $\alpha$ -dicarbonyl compounds, undergoing the Strecker degradation and then forming  $\alpha$ -amino ketones. The  $\alpha$ -amino ketones may then condense resulting in the formation of pyrazines (Ho, 1996; Yaylayan, 1997). In addition, the Maillard reaction can result in the formation of polyphenols, such as catechol, resorcinol, hydroquinone, and pyrogallol, which can enhance the degree of browning during the Maillard reaction by affecting the redox potential of the system (Haffenden and Yaylayan, 2005) and undergoing polymerization and polycondensation (Wang and Huang, 2005).

Commonly found soil metal oxides, birnessite (Jokic et al., 2001b), goethite (Gonzalez and Laird, 2004), and smectite clays (Gonzalez and Laird, 2004), have been shown to catalyze the Maillard reaction under typical pH and temperature ranges found in the natural environment. Jokic et al. (2001b) were the first to report that birnessite catalyzes the Maillard reaction between glucose and glycine. Their data showed that the presence of a redox-reactive mineral, namely, birnessite, significantly accelerates the reaction by one to two orders of magnitude under environmentally relevant temperatures (25°C and 45°C) and a neutral pH (7.00). This reaction is kinetically sluggish under ambient temperatures (Jokic et al., 2001c) but the presence of birnessite significantly catalyzes the reaction by decreasing the activation energy required. Other groups (Bosetto et al., 1995, 1997; Arafaioli et al., 1997, 1999) have also investigated the clay mineral catalysis of the Maillard reaction between various amino acids and glucose at relatively high temperatures (at 70°C).

Light enhances birnessite catalysis of the Maillard reaction, but the reaction still proceeds in the absence of light (Jokic et al., 2001a). This means that the reaction could readily occur in the subsoil in the presence of a mineral catalyst such as birnessite. The Maillard reaction between glucose and glycine as catalyzed by birnessite results in the formation of humic substances that contain significant amounts of (1) amides, which are the dominant N types in humic substances, soils, and sediments, and (2) heterocyclic N compounds, which are often referred to as *unknown* N (Jokic et al., 2004a) (Figure 18.5). The mineral-catalyzed Maillard reaction provides a possible explanation for one of the pathways for the formation of heterocyclic and amide N found in humic substances in the environment (Jokic et al., 2004a). The action of birnessite on glucose should promote the autoxidation of glucose, which results in the

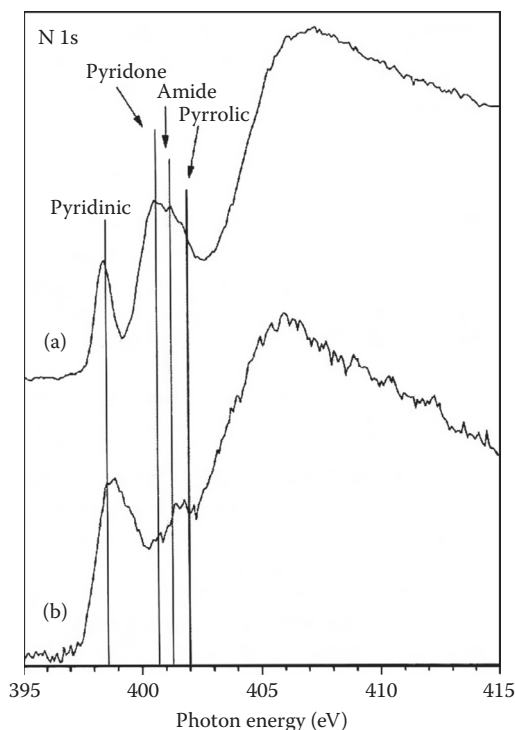
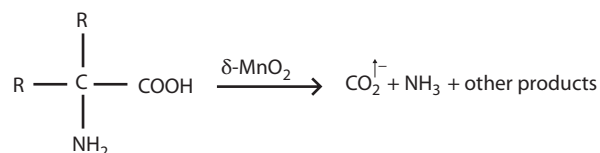


**FIGURE 18.5** N 1s XANES spectra of (a) fulvic acid isolated from a glucose-glycine- $\delta$ -MnO<sub>2</sub> system and (b) the lyophilized solid phase. The peaks are assigned to pyridinic (398.6 eV), pyridone (400.7 eV), amide (401.3 eV), and pyrrolic (402.0 eV) moieties. (Reprinted from Jokic, A., H.-R. Schulten, J.N. Cutler, M. Schnitzer, and P.M. Huang, 2004a. A significant abiotic pathway for the formation of *unknown* nitrogen in nature. *Geophys. Res. Lett.* 31:L05502. With permission of the American Geophysical Union.)

generation of reactive dicarbonyl compounds, hydrogen peroxide, and hydroxylating agents (Wolff, 1996). These reactive dicarbonyl compounds would then react with ammonia formed by the known deamination of glycine catalyzed by birnessite (Wang and Huang, 1987), as proposed by Vairavamurthy and Wang (2002) or with glycine (undergoing the Strecker degradation), resulting in either case in the formation of heterocyclic N compounds (Wong and Shibamoto, 1996). Ammonium ions are known to react with compounds containing reactive carboxyl groups to form pyridinic structures (Steelink, 1994). Carboxylic acids are produced during the Strecker degradation of amino acids (Wong and Shibamoto, 1996) or by the action of manganese dioxides on simple carbohydrates (Bose et al., 1959; Gonzalez and Laird, 2006). When heated, carboxylic acids react with ammonia to form amides (Smith and March, 2001). The scheme for possible amide formation is shown in Figure 18.6.

Gonzalez and Laird (2004) showed that four different smectites saturated with various metal cations (Ca, Na, Cu(II), and Al) could catalyze the Maillard reaction between arginine and glucose at an environmentally relevant temperature (37°C). They found that only saturation with Cu(II) significantly altered the amount of humic substances produced. They also observed that some of the adsorbed humic substances were intercalated into the smectites.

1. Oxidation of carbohydrate or Strecker aldehyde by  $\delta$ -MnO<sub>2</sub> to form carboxylic acid, or formation of carboxylic acid during Strecker degradation
2. Deamination of amino acid by  $\delta$ -MnO<sub>2</sub>



3. Amide formation



**FIGURE 18.6** Possible amide formation pathway including the key role of MnO<sub>2</sub>. (Reprinted from Jokic, A., H.-R. Schulten, J.N. Cutler, M. Schnitzer, and P.M. Huang, 2005. Catalysis of the Maillard reaction by  $\delta$ -MnO<sub>2</sub>: A significant abiotic sorptive condensation pathway for the formation of refractory N-containing biogeomacromolecules in nature, p. 127–152. In P.M. Huang, A. Violante, J.-M. Bollag, and P. Vityakon (eds.) *Soil abiotic and biotic interactions and impact on the ecosystem and human welfare*. Science Publishers Inc., Enfield, NH. Copyright Science Publishers Inc. With permission.)

Jokic et al. (2004b) were the first to study an integrated Maillard reaction and polyphenol (glucose, glycine, and catechol) pathway of humification, using birnessite as catalyst. Their data showed that birnessite significantly accelerates humification processes in an integrated polyphenol-Maillard reaction system under ambient conditions (25°C and 45°C). In nature, it is likely that the Maillard reaction and polyphenol pathways interact closely, since sugars, amino acids, and polyphenols coexist in soil solutions and natural waters. Jokic et al. (2004b) also showed that the integrated polyphenol-Maillard reaction system is more effective in generating humic polymers than the Maillard reaction alone. The type of polyphenol and the molar ratio of polyphenol to Maillard reagents in the polyphenol-Maillard reaction system significantly affect not only the humification processes but also the biomolecule-induced formation of inorganic C, namely, rhodochrosite (MnCO<sub>3</sub>) (Hardie et al., 2009). Increasing the molar ratio of polyphenols to Maillard reagents results in a significant enhancement of humification in the polyphenol-Maillard reaction in the presence of birnessite. Polyphenols with *ortho*-OH groups (pyrogallol) participate in direct electron transfer reactions with birnessite more readily than polyphenols with *meta*-OH groups (resorcinol), and subsequently undergo oxidative polymerization and ring-cleavage reactions to a greater extent. Thus, the humic polymers formed in the pyrogallol-Maillard system are significantly more aliphatic in character than those formed in the resorcinol-Maillard system. Furthermore, the greater extent of polymerization reactions in the birnessite-catalyzed pyrogallol-Maillard system results in the suppression of MnCO<sub>3</sub> formation. Hardie et al. (2007) also compared the HA fraction formed in the presence of birnessite from the Maillard reaction and two

polyphenol–Maillard reaction systems with natural soil and peat HA using C K-edge NEXAFS and found that these HAs are basically similar, especially the HA from the Maillard reaction and pyrogallol–Maillard systems.

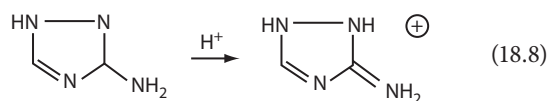
### 18.3.4 Surface Brønsted and Lewis Acidity and Hydrolysis of Organic Compounds

Mineral colloids may detoxify adsorbed pesticides by catalyzing their decompositions through the ability of mineral colloids to behave as Brønsted acids and donate protons or to act as Lewis acids and accept electron pairs. Brønsted acidity derives essentially from the dissociation of water molecules coordinated to surface-bound cations, resulting in the formation of active protons. This acidity is, thus, strongly influenced by the hydration status and polarizing power of surface-bound and structural cations on mineral colloids (Mortland, 1970, 1986). Low water contents and highly polarizing cations (small, high charge) promote Brønsted acidity. Lewis acidity arises from constituent ions such as Al and Fe ions exposed at the edges of mineral colloids (Sposito, 1984; McBride, 1994).

Many uncharged organic molecules that require extremely acid conditions to accept a  $H^+$  ion in solution can be protonated on the surface of mineral colloids (Huang, 1990; McBride, 1994). The Brønsted acid strength and the degree of protonation are related to the electronegativity and polarizing power of the exchangeable and structural metal cations in the following order (McBride, 1994):  $H^+ > Al^{3+}, Fe^{3+} > Mg^{2+} > Ca^{2+} > Na^+ > K^+$ . As clay surfaces become drier, the Brønsted acidity increases and protons are concentrated in a smaller volume of water resulting in more extreme surface acidity. Even very weak bases, that is, poor proton acceptors can be protonated on the surfaces of such mineral colloids.

The degradation of certain pesticides is catalyzed as the result of their adsorption on mineral colloids, which was first observed by formulation chemists who used clays as carriers and diluents (Fowkes et al., 1960). Surface-catalyzed degradation of pesticides on clays was later demonstrated for several organophosphate and *s*-triazine pesticides and has been attributed to the surface acidity of clay minerals (Brown and White, 1969; Saltzman et al., 1974; Minglegrin et al., 1977). Minglegrin and Saltzman (1979) demonstrated that the nature of the clay, its saturating cation, and hydration status determine the rate and mechanism of degradation of parathion. The adsorption-catalyzed degradation of parathion is a hydrolysis reaction that proceeds either directly or through a rearrangement step.

Magnesium-saturated montmorillonite converts the amino form of 3-aminotriazole to the imino form (Russell et al., 1968a) as shown below:



Triazine compounds can also be protonated on dry mineral colloids. Armstrong et al. (1967) showed that the addition of

sterilized soil to atrazine solution increased the hydrolysis rate of atrazine 10-fold. Soil catalytic degradation of atrazine through hydrolysis is an important pathway. Mineral surface acidity also catalyzes hydrolysis of the chloro-*s*-triazine herbicides to the nonphytotoxic 2-hydroxy-*s*-triazines (Russell et al., 1968b) and may be of significance in a wide range of other organic compounds (McBride, 1994).

Besides the Brønsted acid, the Lewis acid properties of metals appear to be of significance in mineral-catalyzed hydrolysis reactions. The oxides of Fe and Al in water, and especially in the dry state, have some catalytic function in organic hydrolysis reactions, at least for those that are known to be hydroxyl ion catalyzed (Hoffmann, 1990). Those hydrolyzable organics that have a suitable structure to chelate with the surface metal cations are, in general, the most susceptible to mineral-catalyzed degradation.

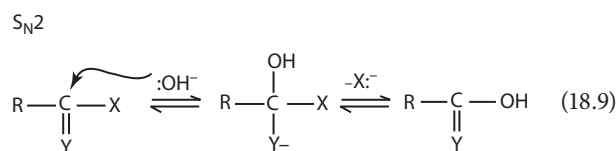
Dissolved metals and metal-containing surfaces play an important role in catalyzing the hydrolysis of organic pollutants. The catalytic effectiveness of a metal ion depends on its ability to complex reactant molecules (e.g., ester linkage, leaving group, and attacking nucleophile) and shift electron density and conformation in ways favorable to reaction (Hoffmann, 1980). Metals vary in their complex formation constants, which reflect difference in metal–ligand bond strengths and solvation forces. The following rules can explain the general features: (1) complex formation constants generally increase as the charge to radius ratio of the metal ion is increased, because the electrostatic contribution to bond formation is increased; (2) polarizable metals and ligands gain additional complex stability through covalent bond formation; and (3) as complex formation constants increase, competition for the metal among available ligands (including  $OH^-$  and other inorganic constituents) becomes more pronounced. Trivalent metals such as Al and Fe(III) and tetravalent metals such as Ti(IV) are classic hard metals, which form strong complexes with classic hard ligands (Pearson, 1966). Organic compounds possessing O and N donor atoms are classified as hard ligands, whereas those possessing S donor atoms are classified as soft ligands. Oxygen donor organic ligands form strong complexes with metals such as Al, Fe(III), and Ti(IV). However, they compete with hydroxo ( $OH^-$ ) and oxo ( $O^{2-}$ ) species that limit metal solubility near-neutral pH values. Although  $Ca^{2+}$  and  $Mg^{2+}$  are also classified as “hard” metals, their *s* and *p* orbitals form bonds that are primarily ionic in nature (Stone and Torrents, 1995).

Complex formation constants of metals with a ligand primarily vary with the ionic radius of metals, although increases in polarizability with increasing atomic number are also important (Houghton, 1979). Even if differences in metal–ligand complex formation constants are taken into consideration, differences in electronic structure cause some metals to emerge as particularly effective catalysts.

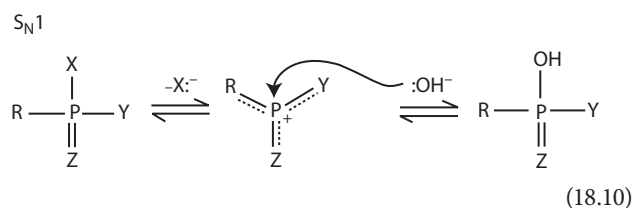
Metals can form a series of metal hydroxo complexes (Bases and Mesmer, 1986). Although metal hydroxo complexes are less reactive nucleophiles than hydroxide ions, their concentrations can be substantially higher, especially in the neutral to acidic

pH range. Because the  $pK_1$  values for strong Lewis acid metals are low, they generate hydroxo species across a wider pH range. The nucleophiles of various metal hydroxo complexes are governed by  $pK_1$  and the polarizability of the metal (Stone and Torrents, 1995).

The reactivity of hydrolyzable organic pollutants arises from the presence of electrophilic (electron deficient) sites within the molecules (Stone and Torrents, 1995). The  $S_N2$  mechanism (nucleophilic substitution) involves attack of the electrophilic sites by  $OH^-$  or  $H_2O$ , generation of a higher coordination number intermediate, subsequent elimination of the leaving group, and the formation of a hydrolysis product:



In the case of the  $S_N1$  mechanism (nucleophilic substitution monomolecular), the reaction proceeds with the loss of the leaving group to generate a lower coordination number intermediate and then followed by generation of the hydrolysis product by nucleophilic addition as shown below:



It is generally accepted that metal ions can catalyze hydrolysis in a way similar to acid catalysis. Metal ions and protons coordinate to the pollutants so that electron density is shifted away from the site of nucleophilic attack to facilitate the reaction. Because protons have an extremely high charge density and great polarizing power, metal catalysis is insignificant in acidic solutions. However, metal ions can readily coordinate two or more ligand donor sites on a molecule and can greatly outnumber protons in neutral and alkaline conditions (Plastourgou and Hoffmann, 1984). A list of metal catalysis mechanisms is given in Table 18.4.

The hydrolysis of compounds possessing good leaving groups is limited by the rate of nucleophilic attack. These compounds are susceptible to types 1, 3, 4, 6, and possibly 5 of metal catalysis. The hydrolysis of compounds possessing poor leaving groups is limited by the breakdown of the tetragonal intermediate; therefore, types 2, 7, and possibly 5 are important. A number of pesticides and other pollutants are in the intermediate region, where metal catalysis may shift the rate-limiting step from nucleophilic attack to breakdown of the tetrahedral intermediate or vice versa.

Many organic compounds are susceptible to metal ion catalysis. These include carboxylic acid esters, amides, anilides, phosphate-containing esters, and other hydrolyzable compounds

**TABLE 18.4** Mechanisms of Metal Catalysis

Type 1	The metal coordinates the electrophile, shifting the electronic distribution in the molecule in a way that enhances its reactivity
Type 2	The metal coordinates to the leaving group, increasing its leaving ability
Type 3	The metal acts as a center for simultaneous attachment of both the electrophile and attacking nucleophile (template effect)
Type 4	The metal coordinates the nucleophile and induces deprotonation (which increases the reactivity of the nucleophile)
Type 5	Coordination of the substrate with the metal induces conformation changes that facilitate reaction
Type 6	Coordination of the substrate with the metal makes the molecule more positive, lessening unfavorable electrostatic interaction with the nucleophile
Type 7	Coordination with the metal blocks inhibitory reverse reaction paths, such as (1) loss of $OH^-$ from a tetrahedral intermediate instead of loss of the leaving group $X^-$ or (2) nucleophilic attack by $X^-$

Source: From Stone, A.T., and A. Torrents. 1995. The role of dissolved metals and metal-containing surfaces in catalyzing the hydrolysis of organic pollutants, p. 275-298. In P.M. Huang, J. Berthelin, J.-M. Bollag, W.B. McGill, and A.L. Page (eds.) Environmental impact of soil component interactions, Vol. 1. Natural and anthropogenic organics. CRC Press/Lewis Publishers, Boca Raton, FL. With permission.

(Stone and Torrents, 1995). In the mid-1950s, the catalytic ability of metals in hydrolysis of thionophosphate pesticides such as parathion and EPN (thionobenzene phosphoric acid *O*-ethyl-*O*-*p*-nitrophenyl ester) was recognized (Ketelaar et al., 1956). Rate enhancements arising from the addition of  $1.0 \times 10^{-4}$  mol  $L^{-1}$   $Cu^{2+}$  are as high as 20-fold for parathion at pH 8.5 and 48-fold for EPN at pH 8.2. Coordination of the S donor group by  $Cu^{2+}$  activates the P center to nucleophilic attack (type 1 catalysis). Chlorpyrifos, a phosphorothionate pesticide, contains a pyridyl N capable of forming a six-membered chelate ring with the  $Cu^{2+}$  ion (Blanchet and St.-George, 1982).

Metal ion catalysis arises from the increased electrophilicity of the P atoms in the chelate ring (type 1 catalysis) (Blanchet and St.-George, 1982) and from possible leaving group effects (type 2 catalysis). Copper(II) is by far the most reactive catalyst among a number of metals [including Mg(II) and Al(III)], which have been observed to catalyze chlorpyrifos hydrolysis. However,  $Cu^{2+}$  concentration would have to exceed  $10^{-5}$  mol  $L^{-1}$ , which seldom occurs in soil solutions and other natural waters, in order for the metal-catalyzed pathway to surpass the rate of the uncatalyzed hydrolysis pathway (Mill and Mabey, 1988).

Many metals, which are potentially catalytic, form low-solubility inorganic solids within the pH domain of soils and associated environments. Therefore, surface-bound metals must be accessible to reactants in order for a metal-catalyzed effect to be observed. Since the mid-1950s, research has established that metal oxide/hydroxide precipitates act as hydrolysis catalysts for phosphate esters (Butcher and Westheimer, 1955; Wilkins, 1991). Much has been subsequently learned about the chemical properties and reactivities of naturally occurring solids such as oxides, carbonates, sulfides, and aluminosilicates (Stone and Torrents, 1995; Smolen and Stone, 1998).

Complex formation equilibria among dissolved and surface-bound metal species are similar in many aspects. Surface complex formation constants for the metal ions and organic ligands increase in magnitude as the formation constants of analogous complexes in solution are increased (Kummert and Stumm, 1980; Stumm et al., 1980; Davis and Hayes, 1986). Attempts have been made to compare reactivities of dissolved and surface-bound metal species (Wehrli, 1990; Wehrli et al., 1990). To compare the catalytic reactivity of dissolved and surface-bound metals, any unusual or unique characteristic of the mineral/water interface must be investigated. The high Lewis and Brønsted acidity of unoccupied coordinative sites is responsible for the well-known hydrolytic reactivity of dehydrated and partially dehydrated mineral surfaces (Theng, 1982; Voudrias and Reinhard, 1986). Although the catalysis by surface-bound metals is influenced by hydration, dramatic effects of solid surfaces on hydrolysis rates in aqueous suspensions have been demonstrated (Sanchez-Camazano and Sanchez-Martin, 1983).

The catalysis by surface-bound metals is observed when all participating reactants are adsorbed to a significant extent and when rate constants for the reactions at the mineral-water surface are comparable to or exceed rate constants for the reaction in homogeneous solution. Although adsorption phenomena have accounted for catalysis, relatively little is known about the conformation and stoichiometry of adsorbed species. This hampers our understanding of surface catalysis on a fundamental level. However, based on the existing literature, two generalities can be made: (1) auxiliary donor groups that facilitate metal catalysis by metal ions in solution should also facilitate surface catalysis and (2) phenomena of only secondary importance in reactions of dissolved complexes, for example, electrostatic and hydrophobic interactions may play a much greater role in surface catalysis (Stone and Torrents, 1995). The nature and potential significance of surface catalysis are summarized later.

The hydrolysis of phenyl picolinate (PHP) is catalyzed by both surface-bound and homogeneous solution metal ions (type 1 catalysis; Fife and Przystas, 1985; Torrents and Stone, 1991). Appropriate metal ions chelate the heterocyclic N and carbonyl O of PHP and increase the partial positive charge at the carbonyl C, thus facilitating nucleophilic attack and increasing its susceptibility to hydrolysis. Suspensions containing FeOOH or TiO<sub>2</sub> dramatically accelerate PHP hydrolysis rate, while in particle-free solution and suspensions containing Al<sub>2</sub>O<sub>3</sub> or SiO<sub>2</sub>, hydrolysis is negligible (Figure 18.7). Similar results are obtained with methyl picolinate (MEP; Stone and Torrents, 1995). Catalysis arises from reaction at the oxide surface and not from release of soluble metals, since removal of particles by filtration causes an immediate halt to any catalytic activity.

The susceptibility of hydrolyzable compounds to metal catalysis depends on the nature of the auxiliary donor group. The pyridyl N of PHP and MEP encourages chelate formation with Ti(IV) and Fe(III) in preference to less polarizable Al. Therefore, TiO<sub>2</sub> and FeOOH are effective hydrolysis catalysts and Al<sub>2</sub>O<sub>3</sub> is not. In contrast, O donor groups, such as the phenolic group in phenyl salicylate and the O heteroatom of methyl furanoate, are harder and thus more favorable to Al chelate formation (Stone and Torrents, 1995). Hydrolysis of PHP in the presence of TiO<sub>2</sub> is virtually pH independent and in the presence of FeOOH exhibits only a slight pH dependence. In particle-free solution, PHP exhibits classic base-catalyzed hydrolysis behavior; the reaction rate of the hydrolysis increases by an order of magnitude for every unit increase in pH. Activation of the ester linkage through chelate formation with a surface-bound metal ion is apparently strong enough to react with the weak nucleophile H<sub>2</sub>O, which dominates over the pH-dependent reaction with OH<sup>-</sup>.

Positively charged surfaces such as Al<sub>2</sub>O<sub>3</sub> (below pH 8.6) and TiO<sub>2</sub> (below pH 6.4) accelerate the hydrolysis of monophenyl terephthalate (MPT) by an order of magnitude or more (Stone and Torrents, 1995). Hydrolysis of MPT catalyzed by Al<sub>2</sub>O<sub>3</sub>

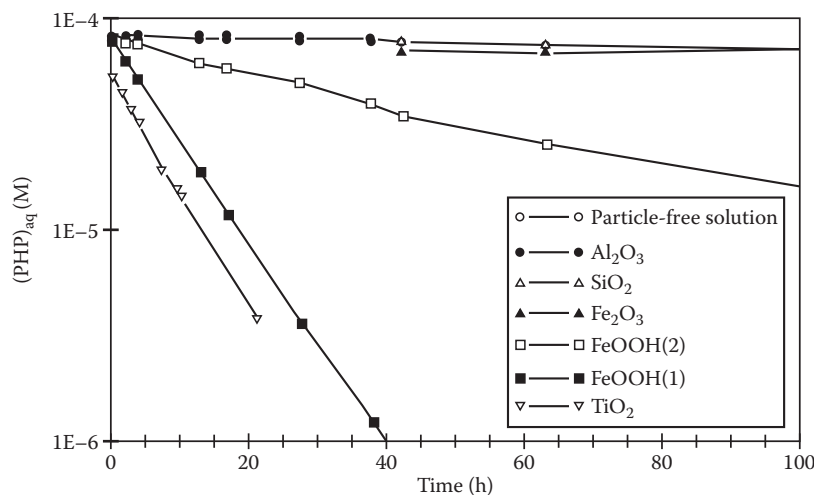


**FIGURE 18.7** Effect of various metal oxides on the loss of phenyl picolinate (PHP) from solution via hydrolysis. All suspensions contained 10 g L<sup>-1</sup> oxide, 1.0 mol L<sup>-1</sup> acetate buffer (pH 5.0), and 50 mM NaCl. (Reprinted with permission from Torrents, A., and A.T. Stone. 1991. Hydrolysis of phenyl picolinate at the mineral/water interface. *Environ. Sci. Technol.* 25:143–149. Copyright 1991 American Chemical Society.)



and  $\text{TiO}_2$  exhibits elements of both type 3 and type 6 catalyses. Positive oxide surfaces serve as the template to accumulate both anionic reactants,  $\text{OH}^-$  and  $\text{MPT}^-$  ions, increasing their encounter frequency. Type 6 catalysis (electrostatic interactions favoring encounter between like-charge species) is more important for surface chemical reactions than for solution reactions due to the additive electrostatic effect arising from neighboring charged groups. Type 3 catalysis (simultaneous attachment of substrate and nucleophile) is also typical of surface chemical reactions.

Many pesticides are susceptible to surface-catalyzed hydrolysis (Torrents, 1992). For example, catalysis of chlorpyrifos hydrolysis by  $\text{TiO}_2$ ,  $\text{FeOOH}$ , and  $\text{Al}_2\text{O}_3$  apparently involves chelate formation between the surface-bound metal ion, the thionate S, and pyridinyl N.

A surface-catalyzed reaction following type 4 catalysis has been postulated for the degradation of the fungicide oxycarboxin stored in borosilicate glass (Stanton, 1987). Because of low hydroxide ion concentration in neutral and acidic pH, hydrolytic ring cleavage is not observed in the absence of a catalyst. The glass exerts its catalytic effect by providing sufficiently strong nucleophiles (surface-bound  $\text{OH}^-$  and  $\text{O}_2^{2-}$ ) for attacking the oxathiin ring. Quartz and aluminosilicate surfaces present in soils and associated environments could also catalyze oxycarboxin hydrolysis. It has been reported that metal oxides catalyze the hydrolysis of *p*-nitrophenyl acetate by this mechanism (Hoffmann, 1990). However, in surface-catalyzed

hydrolysis reactions, the nature and relative significance of type 4 catalysis are poorly understood and, thus, merit closer attention.

Among the clay minerals, montmorillonite, beidellite, illite, and vermiculite, only montmorillonite is able to enhance the hydrolysis of the carbamate pesticides, carbosulfan, and aldicarb, probably due to its stronger surface acidity and chelating ability compared to the other clay minerals (Wei et al., 2001). Suspensions of sea sand,  $\text{TiO}_2$ ,  $\alpha\text{-Fe}_2\text{O}_3$ ,  $\alpha\text{-FeO(OH)}$ , laponite (smectite clay), and  $\text{SiO}_2$  are able to catalyze the hydrolysis of the cyclodiene pesticide, endosulfan to the less toxic endosulfan diol (Walse et al., 2002). The rates of endosulfan hydrolysis over the different surfaces correspond to their tritium-exchange site-density and suggest a mechanism involving surface coordination prior to nucleophilic attack (Walse et al., 2002).

Birnessite is able to catalyze the hydrolysis of the herbicide atrazine (2-chloro-4-(ethylamino)-6-(isopropylamino)-1,3,5-triazine) by acting as a Lewis acid activator and a source of metal-bound hydroxide as a nucleophile (Figure 18.8) (Shin and Cheney, 2004, 2005). Furthermore, birnessite is also able to catalyze the N-dealkylation of atrazine via a nonoxidative mechanism involving proton transfer to Mn(IV)-stabilized oxo and imido bonds (Wang et al., 1999; Shin and Cheney, 2005).

Recently, it has been shown that dissolved HAs are able to catalyze the abiotic hydrolysis of phenylurea herbicides by acting as bifunctional buffers, similar to  $\text{HCO}_3^-/\text{CO}_3^{2-}$  or  $\text{H}_2\text{PO}_4^-/\text{HPO}_4^{2-}$ . The hydrolysis reaction rate increases with the carboxyl group

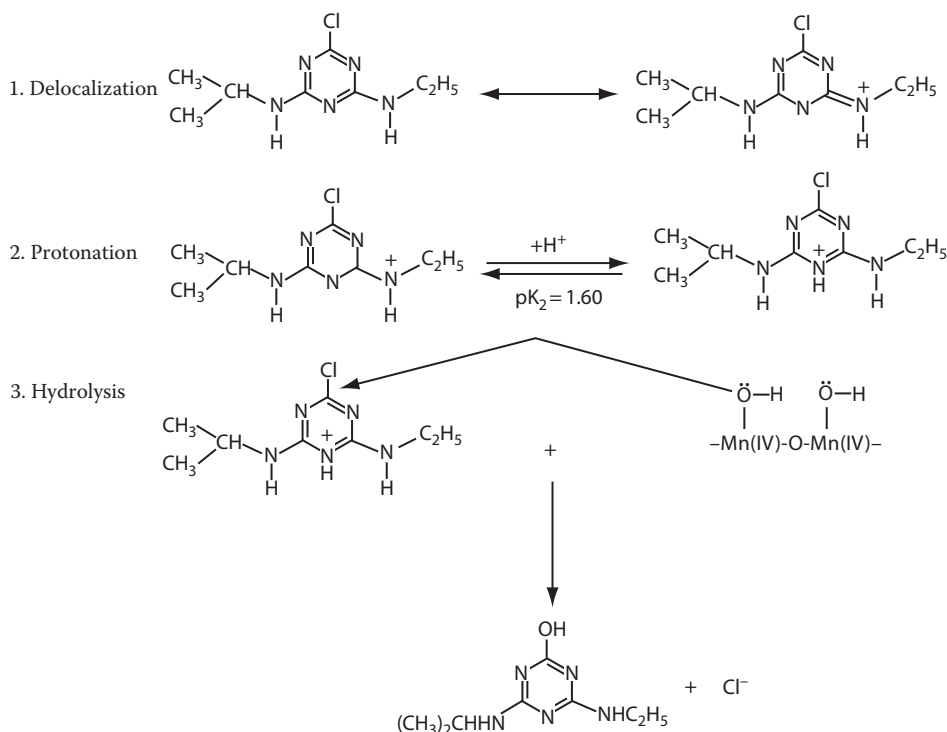


**FIGURE 18.8** Hypothesized hydroxyatrazine formation pathway from the reaction of atrazine with birnessite ( $\delta\text{-MnO}_2$ ) at pH 4.3 and 20°C. (From Shin, J.Y., and M.A. Cheney. 2005. Abiotic dealkylation and hydrolysis of atrazine by birnessite. *Environ. Toxicol. Chem.* 24:1353–1360. Copyright Wiley-VCH Verlag GmbH & Co. KGaA. Reproduced with permission.)

content of the HAs, indicating that the carboxyl groups are responsible for the catalysis (Salvestrini et al., 2008).

### 18.3.5 Reductive Transformation of Organic Compounds

In anoxic groundwater and surficial water, biogeochemical processes provide a variety of potential reductants for abiotic contaminant transformation. Persistent xenobiotics, such as polyhalogenated alkanes and alkenes, aromatic nitro and azo compounds, may be transformed to reaction products that can be further microbially degraded or to products that can be more toxic than the parent compounds (Hofstetter et al., 2006).

#### 18.3.5.1 Ferrous Iron as Catalyst

Soluble Fe(II) is an important reductant in anaerobic aqueous environments; however, its availability is limited in neutral and alkaline pH ranges by the precipitation of FeS,  $\text{Fe}_3(\text{PO}_4)_2$ ,  $\text{FeCO}_3$ , and other Fe(II)-rich minerals (Charlet et al., 1998). Ferrous iron present within or sorbed on iron oxide mineral particles is highly reactive even at high pH conditions (Charlet et al., 1998). Reduction of nitrite ions to  $\text{N}_2\text{O}$  by Fe(II) sorbed on lepidocrocite at a pH range of 6.0–8.5 was demonstrated by Sorensen and Thorling (1991). Above pH 5.5,  $\text{Fe}^{2+}$  starts to be adsorbed onto particles, and this adsorption is completed on most mineral phases around pH 7.5, that is, before the onset of precipitation. Above pH 6.5, a significant part of sorbed Fe(II) is present as a highly reactive hydroxylated surface complex,  $=\text{Fe}(\text{III})-\text{O}-\text{Fe}(\text{II})-\text{OH}$  (Charlet et al., 1998). This hydrolyzed surface species is a very effective reductant toward many persistent xenobiotics, such as 4-chloronitrobenzene (Charlet et al., 1998).

Mossbauer spectra of Fe(II) adsorbed to rutile ( $\text{TiO}_2$ ) and aluminum oxide ( $\text{Al}_2\text{O}_3$ ) show only Fe(II) species, whereas spectra of Fe(II) reacted with the iron oxides, goethite, hematite, and ferrihydrite demonstrate electron transfer between the adsorbed Fe(II) and the underlying iron(III) oxide (Williams and Scherer, 2004). The electron transfer reactions that occur during the reduction of nitrobenzene induce growth of an Fe(III) layer on the oxide surface that is similar to the bulk oxide (Williams and Scherer, 2004). Similarly, it has been shown that the reductive degradation of 4-chloronitrobenzene and trichloronitromethane in the presence of Fe(II) and goethite results in the growth of goethite in the *c*-direction; however, the newly formed goethite is progressively less reactive than the original goethite (Chun et al., 2006).

Ferrous iron in the presence of goethite can catalyze the abiotic reductive degradation of the widely used dinitroaniline herbicides (trifluralin, pendimethalin, nitralin, and isopropalin) at neutral solution pH (Klupinski and Chin, 2003; Wang and Arnold, 2003). Increasing the solution pH results in increased rate constants due to the increase in Fe(II) sorbed and creation of highly reactive species on the surface of the goethite (Figure 18.9) (Wang and Arnold, 2003). Nitrobenzenes and *N*-hydroxylanilines are reaction intermediates of the reduction of nitroaromatics. Nitrobenzenes, the first intermediates,

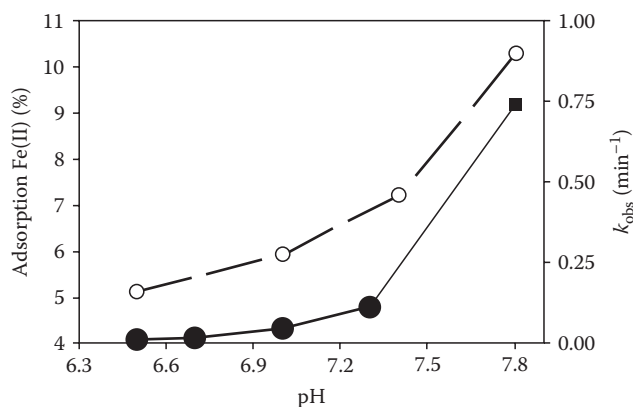


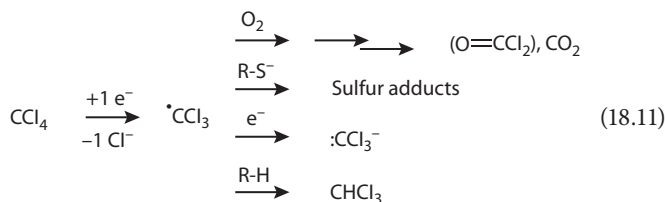
**FIGURE 18.9** Role of pH on the sorbed Fe(II) (○) and observed pseudo-first-order rate constants (●) for the reduction of trifluralin with  $1 \text{ mmol L}^{-1}$  Fe(II) in a suspension of  $7.2 \text{ m}^2 \text{ L}^{-1}$  ( $0.65 \text{ mg mL}^{-1}$ ) goethite. The  $k_{\text{obs}}$  value (■) at pH 7.8 was extrapolated from a regression of  $\log k_{\text{obs}}$  versus pH. (Reprinted from Wang, S., and W.A. Arnold. 2003. Abiotic reduction of dinitroaniline herbicides. *Water Res.* 37:4191–4201. Copyright 2003, With permission from Elsevier.)

are readily reduced by soluble Fe(II) and Fe(II)-treated goethite suspensions, especially if there are electron-withdrawing substituents in the *para* position (Colon et al., 2006b). However, *N*-hydroxylanilines, the second intermediates, are only reduced in the presence of Fe(II)-treated goethite suspensions, and in contrast to nitrobenzenes, electron-withdrawing substituents in the *para* position decrease the rate of reduction (Colon et al., 2006b). The rate of reduction of *p*-cyano-*N*-hydroxylaniline showed a linear relationship against the concentration of mineral surface-associated Fe(II) in hematite, goethite, and lepidocrocite suspensions (Colon et al., 2006b). The reactivity of mineral surface-associated Fe(II) toward the reduction of *p*-cyano-nitrobenzene decreases in the order hematite > goethite > lepidocrocite > ferrihydrite, and interestingly, the surface density of surface-bound Fe(II) does not play a major role in determining the observed reactivity trend (Colon et al., 2006a).

Ferrous iron in the presence of goethite and magnetite abiotically catalyzes the degradation of trichloronitromethane via reduction, while trichloroacetone, 1,1,1-trichloropropane, and trichloroacetaldehyde hydrate are transformed via both hydrolysis and reduction reactions (Chun et al., 2005). The Fe(II) bound to the iron minerals has a greater reactivity than either aqueous Fe(II) or structural Fe(II) present in magnetite (Chun et al., 2005). Ferrous iron bound to magnetite is an effective catalyst for the degradation of the high-energy explosive RDX (hexahydro-1,3,5-trinitro-1,3,5-triazine), ultimately breaking it down into  $\text{NH}_4^+$ ,  $\text{N}_2\text{O}$ , and formaldehyde (Gregory et al., 2004).

Ferrous iron sorbed on the surface of goethite is able to catalyze the abiotic reductive dehalogenation of carbon tetrachloride ( $\text{CCl}_4$ ) to form the even more toxic compound, chloroform ( $\text{CHCl}_3$ ) (Amonette et al., 2000). The reductive dehalogenation of carbon tetrachloride did not occur in the presence of soluble Fe(II) without goethite (Amonette et al., 2000). Reduction of  $\text{CCl}_4$  by surface-associated Fe(II) on goethite occurs in a single

electron transfer reaction and results in the cleavage of one C–Cl bond and the generation of unstable trichloromethyl radicals, as shown below (Elsner et al., 2004a):



The presence of oxygen and sulfur species can thus lead to completely dehalogenated reaction products in radical reactions. However, the presence of H radical donors, such as trace amounts of natural organic matter, promotes the formation of toxic chloroform (Elsner et al., 2004a). Ferrous iron bound to the surface of iron oxides (goethite, hematite, lepidocrocite, and magnetite) is capable of reducing a variety of other polyhalogenated methanes under aquifer conditions, and the pseudo-first-order reaction rate constants,  $k_{\text{obs}}$ , of the polyhalogenated methanes increased in the order  $\text{CHBrCl}_2 < \text{CHBr}_2\text{Cl} < \text{CHBr}_3 < \text{CCl}_4 < \text{CFBr}_3 < \text{CBrCl}_3 < \text{CBr}_2\text{Cl}_2$  (Pecher et al., 2002).

Reactive Fe(II) does form not only on the surface of oxides but also on the surfaces of other iron minerals such as iron sulfide (FeS), pyrite (FeS<sub>2</sub>), and siderite (FeCO<sub>3</sub>) (Elsner et al., 2004b). Elsner et al. (2004b) compared the 4-chloronitrobenzene, 4-chlorophenyl hydroxylamine, and hexachloroethane-reducing reactivity of Fe(II) aqueous suspensions in the presence of siderite, hematite, lepidocrocite, goethite, magnetite, sulfate green rust, pyrite, and mackinawite. The surface area-normalized reaction rates generally increase in the order Fe(II) + siderite < Fe(II) + iron oxides < Fe(II) + iron sulfides (Elsner et al., 2004b).

Ferrous iron-bearing minerals are also important environmental abiotic reductants. Magnetite, pyrite, and green rust are able to catalyze the abiotic reductive dechlorination of chlorinated ethylenes (Kriegman-King and Reinhard, 1994; Butler and Hayes, 1998; Lee and Batchelor, 2002a, 2002b). Surface area-normalized pseudo-first-order initial rate constants for the reduction of chlorinated ethylenes (tetrachloroethylene, trichloroethylene, *cis*-dichloroethylene, and vinyl chloride) by green rust were found to be 3.4–8.2 times greater than those by pyrite (Lee and Batchelor, 2002b), and the rate constants by pyrite were found to be 23.5–40.3 times greater than those by magnetite (Lee and Batchelor, 2002a).

In clay minerals, Fe(II) may be present as (1) structural Fe(II), (2) Fe(II) complexed by surface hydroxyl groups, and (3) Fe(II) bound by ion exchange. Hofstetter et al. (2003) investigated the accessibility and reactivity of these three types of Fe(II) species in suspensions of ferrous iron-bearing nontronite or iron-free hectorite. They found that both structural Fe(II) and Fe(II) complexed by surface hydroxyl groups of nontronite reduced the nitroaromatic compounds to anilines. Fe(II) bound by ion exchange did not contribute to the observed reduction of the nitroaromatic compounds. The abiotic reductive reactivity of

biotite, vermiculite, and montmorillonite on chlorinated ethylenes (tetrachloroethylene, trichloroethylene, *cis*-dichloroethylene, and vinyl chloride) with or without the addition of Fe(II) was investigated by Lee and Batchelor (2004). Biotite had the greatest rate constant among the phyllosilicates, both with and without Fe(II) addition (Figure 18.10), which is attributed to the higher content of Fe(II) sites on biotite. The Fe(II) content of biotite is 8 and 97.5 times higher than that of vermiculite and montmorillonite, respectively (Lee and Batchelor, 2003). The addition of Fe(II) to the mineral suspensions increased the rate constants of the dechlorination reactions, which is attributed to the regeneration of active sites on the phyllosilicates resulting from redox reaction with Fe(II) or due to the reactivity of Fe(II) that binds to the phyllosilicate surfaces (Lee and Batchelor, 2004).

Ferruginous smectite, chemically reduced with dithionite is able to reduce and dechlorinate trichloroacetonitrile and chloropicrin (Cervini-Silva et al., 2001). Similarly, chemically reduced montmorillonite and ferruginous smectite are able to catalyze the abiotic reduction of nitrobenzene to aniline, and as much as 40% of the structural Fe(II) in the reduced smectite was oxidized to Fe(III) during the reaction (Yan and Bailey, 2001). Hofstetter et al. (2006) investigated the reactivity of Fe(II) species in suspensions of chemically reduced montmorillonite, with a low structural iron content, and reduced iron-rich nontronite

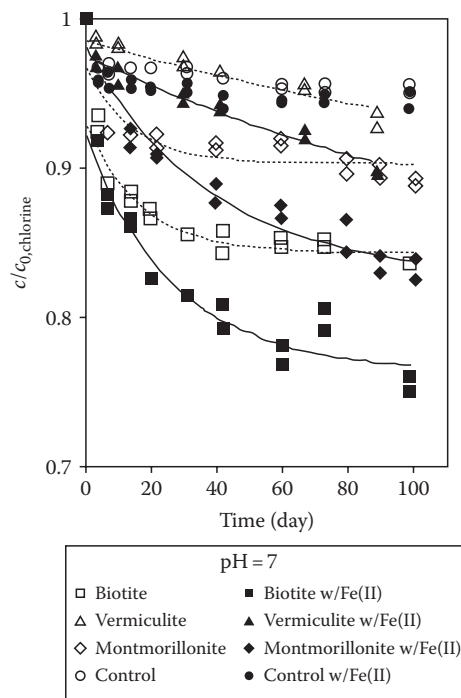


**FIGURE 18.10** Reductive dechlorination of chlorinated ethylenes (0.19 mM) in iron-bearing phyllosilicate suspensions (0.085 g g<sup>-1</sup>) with and without Fe(II) addition (4.28 mM). (Reprinted from Lee, W.J., and B. Batchelor, 2004. Abiotic reductive dechlorination of chlorinated ethylenes by iron-bearing phyllosilicates. *Chemosphere* 56:999–1009. Copyright 2004, with permission from Elsevier.) C<sub>0</sub> and C stand for the concentration (mM) of the organic chlorine compound at time 0 and the sampling time.

using acetylnitrobenzene compounds. Their results indicate that Fe(II) bound in the octahedral sheet of reduced smectites is the predominant reductant, and that electron transfer presumably occurs via basal siloxane planes. Nonreactive electron donor–acceptor complexation of the nitroaromatic compounds occurred at the basal smectite surfaces of the reduced montmorillonite but was not observed in suspensions of reduced iron-rich nontronite.

Reduced aquifer sediments from the perched Pantex aquifer (Amarillo, TX) were found to efficiently, abiotically degrade the explosives RDX, HMX (octahydro-1,3,5,7-tetranitro-1,3,5,7-tetrazocine), and TNT (Boparai et al., 2008). When Fe(II) was partially removed from the reduced sediments by washing (citrate-bicarbonate buffer), RDX degradation was suppressed, but the addition of Fe(II) restored the degradation efficiency of the sediment (Boparai et al., 2008).

### 18.3.5.2 Natural Organic Matter as Catalyst and Redox Mediator/Inhibitor

Humus plays a significant role in the anaerobic degradation of xenobiotics by shuttling electrons. Humic functional groups, in particular quinones, can act as redox mediators and electron donors for accelerating abiotic reductive transformation processes (Field et al., 2000; Doong and Chiang, 2005; Fimmen et al., 2007; Ratasuk and Nanny, 2007). Electrochemically reduced soil and aquatic HAs are able to reduce hexachloroethane at appreciable rates, which indicates that HA could play an important role in the reductive transformation of xenobiotics in anoxic environments (Kappler and Haderlein, 2003).

Natural organic matter can act as an electron transfer mediator in the presence of a bulk electron donor such as Fe(II) or HS<sup>-</sup> and thus significantly enhances the rate of reduction of halogenated hydrocarbons, such as carbon tetrachloride or bromoform (Curtis and Reinhard, 1994) or substituted nitrobenzenes (Dunnivant et al., 1992). Strathmann and Stone (2002) demonstrated that natural organic matter from the Great Dismal Swamp facilitates oxime carbamate pesticide reduction by Fe(II) in the same manner as individual organic ligands, carboxylate, and aminocarboxylate.

Complexation of Fe(II) by catechol and organothiol ligands, which are similar to the functional groups found in natural humic substances, leads to the formation of highly reactive aqueous species that are capable of reducing substituted nitroaromatic compounds (Naka et al., 2006, 2008). The nitroaromatic compounds are not reduced in Fe(II)-only or ligand-only solutions (Naka et al., 2006, 2008). The high reactivity of these Fe(II)–organic ligand complexes is attributed to a lowering of standard one-electron reduction potential of the Fe(III)/Fe(II) redox couple on complexation by the ligands. The organothiol ligands are also able to re-reduce the Fe(III) that forms when Fe(II) complexes are oxidized by reactions with the nitroaromatic compounds (Naka et al., 2008). Ferrous iron–catechol and ferrous iron–organothiol complexes are also able to completely reductively degrade the explosive RDX (Kim and Strathmann, 2007) and to catalyze the reductive degradation of polyhalogenated alkanes

(Bussan and Strathmann, 2007). Iron(II)–tiron complexes are able to quantitatively reduce trichloroethane to acetaldehyde, a product previously only reported for reactions with Cr(II), but not with Fe-based reductants (Bussan and Strathmann, 2007).

The explosive RDX is rapidly reductively degraded in the presence of black carbon (BC) and sulfide to low-molecular-weight ring-cleavage products (Kemper et al., 2008). RDX was not degraded in the presence of BC-only or sulfide-only suspensions. Due to the heterogeneous nature of BC, it remains unclear whether the quinone material in the BC or the ability of BC to sorb the hydrophobic RDX facilitated the reductive degradation (Kemper et al., 2008).

On the other hand, natural organic matter can decrease the reductive potential of Fe(II) by competing for reactive sites on Fe(II)-mineral surfaces. Hakala et al. (2007) found that dissolved organic matter only enhances the reductive capacity of Fe(II) toward nitroaromatic compounds in the absence of iron oxide colloids. Colon et al. (2008) found that Suwannee River HA decreases the reduction capacity of Fe(II)-treated goethite toward nitrobenzene, by complexing the surface-associated Fe(II) species or hindering access of nitrobenzenes to the Fe(II) sites.

### 18.3.6 Genotoxicity and Bioavailability of Xenobiotics as Influenced by Mineral Catalysis

Much is known about the toxicity of xenobiotic parent compounds, whereas, relatively little work has been carried out on investigating the toxicity of the degradation products of xenobiotics (Sinclair and Boxall, 2003). In some cases, the transformation products of xenobiotics, such as commonly used pesticides and herbicides, can be even more toxic than the parent compound (Osano et al., 2002; Sinclair and Boxall, 2003). To date, very little research has been carried out on investigating the bioavailability and toxicity of xenobiotics after reaction with abiotic catalysts, such as metal oxides or clay minerals.

The oxidative coupling of the polycyclic aromatic hydrocarbon, phenanthrene, with catechol as catalyzed by birnessite significantly reduces the bioavailability of phenanthrene to microorganisms (Russo et al., 2005). The oxidative coupling of phenol induced by birnessite or soil significantly decreases the toxicity of the compound as determined with a Microtox System (Jung et al., 2008b).

The pesticides, oxamyl (carbamate family) and alachlor (chloroacetanilide family), reacted with reduced nontronite clay (ferrous smectite) show a significant decrease in their overall mammalian cell cytotoxic (toxicity to cells) potential, whereas the pesticide 2,4-D (phenoxy family) shows no difference in toxicity after treatment with the reduced clay (Sorensen et al., 2004). The pesticide, dicamba (benzoic acid family), reacted with reduced nontronite clay actually generates products, which are more cytotoxic than the parent compound (Sorensen et al., 2004). Oxidized nontronite had no effect on the cytotoxicity of any of the aforementioned pesticides, which indicates reduced

Fe in smectites plays an important role in altering the cytotoxicity of pesticides and should thus be taken into account in pesticide management programs (Sorensen et al., 2004).

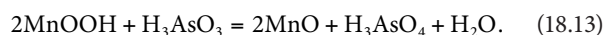
The genotoxic potency (potential damaging effect on DNA) of most pesticides in mammalian cells is unknown, let alone their abiotic transformation products. Sorensen et al. (2005) were the first group to investigate the effect of reduced ferruginous smectite on the genotoxicity of the pesticides 2,4-D, dicamba and oxamyl. Neither 2,4-D alone nor its transformation products after reaction with the reduced clay were found to be genotoxic. The genotoxicity of oxamyl actually decreased after reaction with the reduced clay. Dicamba alone was not genotoxic but became genotoxic after reaction with the reduced clay.

## 18.4 Abiotic Catalysis in the Transformation of Metals, Metalloids, and Other Inorganics

### 18.4.1 Transformation of Metals and Metalloids

#### 18.4.1.1 Arsenic

Arsenic bioavailability and toxicology depend on its chemical state (Huang and Fujii, 1996) with As(III) (arsenite) being much more toxic than As(V) (arsenate). Manganese(IV) oxides, such as birnessite (Table 18.5), are very effective oxidants of As(III) (Oscarson et al., 1981a, 1981c, 1983b; Feng et al., 2006b). In the control experiment, no detectable As(III) is oxidized in the absence of Mn(IV) oxide (Table 18.5). Arsenic(III) oxidation by birnessite proceeds through two single electron transfer steps with the formation of Mn(III) as intermediate (MnOOH), as follows (Nesbitt et al., 1998; Tournassat et al., 2002):



Poorly crystalline Fe(III) oxyhydroxides (Devitre et al., 1991; Nicholas et al., 2003; Jang and Dempsey, 2008) and the surfaces

**TABLE 18.5** Oxidation of As(III) and Sorption of As by Mn(IV) Oxide (in  $\mu\text{g mL}^{-1}$  in Solution)

As(III) or As(V) Added ( $\mu\text{g mL}^{-1}$ )	As(III)	As(V)	Mn	Final pH
100 As(III)	ND <sup>a</sup>	$83.5 \pm 1.4^b$	$0.41 \pm 0.12$	7.1
300 As(III)	$63.2 \pm 7.0$	$186 \pm 5$	$8.08 \pm 0.36$	7.1
500 As(III)	$213 \pm 4$	$205 \pm 1$	$6.06 \pm 0.60$	7.3
1000 As(III)	$665 \pm 5$	$216 \pm 4$	$4.16 \pm 0.86$	7.5
300 As(V)	ND	$298 \pm 1$	$0.06 \pm 0.02$	7.5

Source: Oscarson, D.W., P.M. Huang, C. Defosse, and A. Herbillon. 1981a. Oxidative power of Mn(IV) and Fe(III) oxides with respect to As(III) in terrestrial and aquatic environments. *Nature* 291:50–51. With permission of Macmillan, London.

<sup>a</sup> ND, not detectable.

<sup>b</sup> Mean  $\pm$  SD;  $n = 3$ .

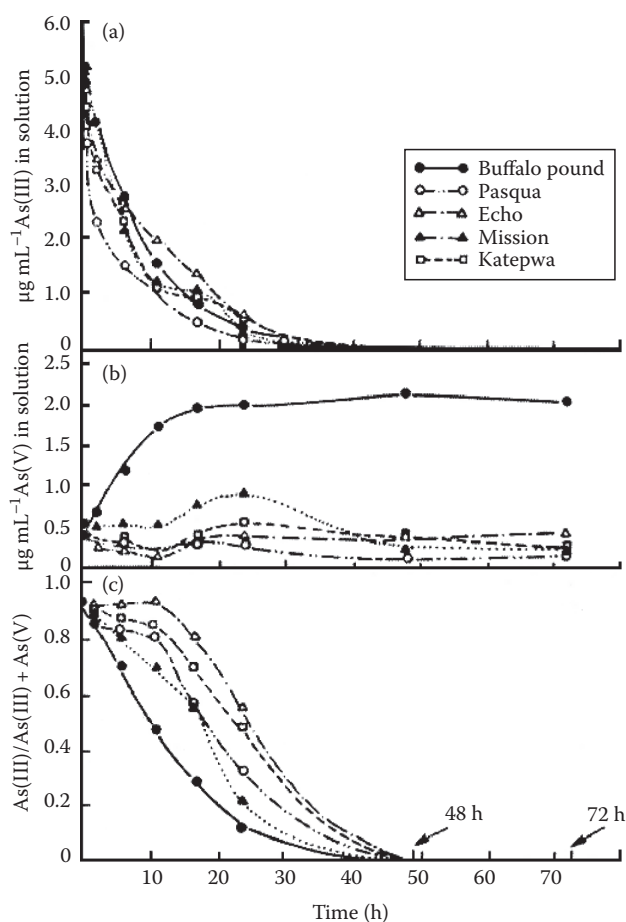


**FIGURE 18.11** Oxidation of As(III) to As(V) and the sorption of As by lake sediments as a function of time. (a) Concentration of As(III) in solution, (b) concentration of As(V) in solution, and (c) As(III)/As(III) + As(V). Ten  $\mu\text{g mL}^{-1}$  of As(III) were added initially. During the reaction period, the pH of the As-sediment suspension ranged from 8.0 to 8.2 for the Buffalo Pound sediment and from 7.3 to 7.6 for the other four sediments. (Reprinted from Oscarson, D.W., P.M. Huang, and W.K. Liaw. 1980. The oxidation of arsenite by aquatic sediments. *J. Environ. Qual.* 9:700–703. With permission of the American Society of Agronomy.)

of the clay minerals illite and kaolinite (Manning and Goldberg, 1997) are also able to catalyze the oxidation of As(III).

Although As(V) is a thermodynamically stable species in oxygenated water at common pH values (Penrose, 1974), the kinetics of oxidation of As(III) with  $\text{O}_2$  is very slow at near-neutral pH values (Kolthoff, 1921). Lake sediments from Saskatchewan, Canada, can oxidize As(III) ( $700 \mu\text{g As}$ ) to As(V) within 48 h (Figure 18.11). The oxidation of As(III) is not detectable within 72 h in the absence of sediment. The oxidation of As(III) to As(V) is not affected by flushing  $\text{N}_2$  or air through the sediment suspensions, nor does the addition of  $\text{HgCl}_2$  to the system eliminate the conversion of As(III) to As(V). This indicates that the oxidation of As(III) to As(V) is an abiotic process.

When the lake sediments are treated with hydroxylamine hydrochloride or sodium acetate, which are effective extractants for Mn, the oxidation of As(III) to As(V) by the treated sediments is greatly decreased relative to the untreated sediments

(Oscarson et al., 1981c). Hydroxylamine hydrochloride treatment also removes Fe oxide; however, the evidence obtained from colorimetry and x-ray photoelectron spectroscopy shows that a redox reaction between Fe oxide and As(III) does not occur within 72 h, indicating that the redox reaction between As(III) and Fe(III) is kinetically slow (Oscarson et al., 1981a). This supports the evidence that Mn oxide is the primary component responsible for catalyzing the conversion of As(III) to As(V). The rate constant increases with increasing temperature from 278 to 298 K; the heat of activation for the process varies from 13.8 to 35.6 kJ mol<sup>-1</sup>, indicating that the depletion of As(III) is predominantly a diffusion-controlled process (Oscarson et al., 1981b). Other recent studies have also suggested that Mn oxides are largely responsible for the oxidation of As(III) in aquifer sediments from Maine, USA (Amirbahman et al., 2006) and Dhaka, Bangladesh (Stollenwerk et al., 2007).

The ability of Mn oxides to deplete As(III) from solution (oxidation plus sorption) varies with their crystallinity and specific surface (Oscarson et al., 1983b). The depletion of As(III) by Mn oxides follows the first-order kinetics. Pyrolusite is highly ordered and has a low specific surface; conversely, birnessite and cryptomelane are poorly crystalline and have relatively high specific surfaces (Table 18.6). Because birnessite and cryptomelane have relatively high specific surface areas due to their porous nature (Huang, 1991b), their rate constants for the depletion of As(III) are much higher than those for pyrolusite (Table 18.6). On the other hand, the rate constants for the depletion of As(III) by birnessite are significantly greater than those for cryptomelane, despite its higher specific surface. Birnessite has a greater negative charge density than cryptomelane at pH 7 (McKenzie, 1981). Because As(V) is also negatively charged at pH 7, the repulsive interaction energy would be greater between birnessite than cryptomelane and As(V), which is why birnessite does not sorb a detectable amount of As(V) relative to cryptomelane (Oscarson et al., 1983b). Differences in the point of zero charge (p.z.c.) of birnessite and cryptomelane and their ability to sorb As(V) explain the greater As(III) depletion by birnessite than by cryptomelane even though cryptomelane has the greater surface area. Little As(V) is sorbed from solution by birnessite upon oxidation of As(III), and less total As is sorbed by birnessite than by cryptomelane; the electron-accepting sites on the surface of birnessite are, thus, blocked to a lesser extent than those on the surface

of cryptomelane. Consequently, the rate of depletion of As(III) from solution is greater for birnessite than for cryptomelane.

The structure and composition of Mn oxides, as well as the solution pH, ionic strength, and presence of organic ligands all affect the rate of As(III) oxidation by Mn oxides. Tunnel-structured cryptomelane has the strongest As(III) oxidation ability (842.2 mmol kg<sup>-1</sup>), compared with layered-structured birnessite (480.4 mmol kg<sup>-1</sup>), and Mn(II/III)-bearing hausmannite (117.9 mmol kg<sup>-1</sup>) (Feng et al., 2006b). Increasing the reaction system pH from 3.0 to 6.5 results in a significant increase in the rate of oxidation of As(III) by the three Mn oxides, whereas increasing the ionic strength results in a decrease in the oxidation of As(III) by birnessite and cryptomelane, while hausmannite is unaffected (Feng et al., 2006b). The presence of tartaric acid at a concentration below 4 mol L<sup>-1</sup> promotes oxidation of As(III) by birnessite, cryptomelane, and hausmannite, whereas it decreases As(III) oxidation by cryptomelane and hausmannite when the concentration is increased above 4 mol L<sup>-1</sup> (Feng et al., 2006b). The oxidation of As(III) by the Mn oxyhydroxide, manganite [MnO(OH)], occurs on the time scale of hours. The presence of competing anions such as phosphate decreases the oxidation rate of As(III) to As(V) by manganite (Chiu and Hering, 2000). The presence of a divalent cation, Zn<sup>2+</sup>, significantly suppresses the oxidation of As(III) by birnessite, and this suppression is more pronounced when the Zn<sup>2+</sup> is presorbed on the birnessite (Power et al., 2005).

The surfaces of many soil Mn oxides are coated with various chemical species (McKenzie, 1989). The rate constants for the depletion (oxidation plus sorption) of As(III) are generally substantially smaller for the Mn oxides with higher levels of coatings of Fe and Al oxides and CaCO<sub>3</sub> than those for the untreated MnO<sub>2</sub> or MnO<sub>2</sub> with lower levels of coatings (Oscarson et al., 1983a). HA coatings on natural Mn nodules also significantly reduce the As(III) depletion capacity of the nodules (Chen et al., 2006). The electron-accepting sites on MnO<sub>2</sub> are partially masked by the oxides, CaCO<sub>3</sub>, and organic matter. There is evidence that shows that Fe(III) and Al oxides and CaCO<sub>3</sub> do not oxidize As(III) to As(V) (Oscarson et al., 1981a, 1983a), and thus, the oxidation of As(III) to As(V) on the coated MnO<sub>2</sub> is solely attributed to MnO<sub>2</sub> in this case.

However, some studies have shown that Fe oxides and oxyhydroxides can catalyze the oxidation of As(III) to As(IV). Devitre et al. (1991) showed that As(III) is rapidly oxidized by diagenetic

**TABLE 18.6** Specific Surface and Point of Zero Charge (p.z.c.) of the Mn Dioxides and Rate Constants and Energies of Activation for the Depletion of As(III) by the Mn Dioxides

Mineral	Specific Surface (m <sup>2</sup> g <sup>-1</sup> )	p.z.c.	Rate Constant × 10 <sup>-3</sup> (h <sup>-1</sup> )			Energies of Activation (kJ mol <sup>-1</sup> )
			278 K	298 K	318 K	
Birnessite	277 ± 5 <sup>a</sup>	2.3 ± 0.1	126 ± 13	267 ± 6	533 ± 38	26.0 ± 0.2
Cryptomelane	346 ± 4	2.8 ± 0.1	54 ± 10	189 ± 8	318 ± 22	32.3 ± 6.7
Pyrolusite	8 ± 1	6.4 ± 0.3	0.12 ± 0.02	0.44 ± 0.03	0.58 ± 0.05	29.0 ± 9.8

Source: Oscarson, D.W., P.M. Huang, W.K. Liaw, and U.T. Hammer. 1983b. Kinetics of oxidation of arsenite by various manganese dioxides. *Soil Sci. Soc. Am. J.* 47:644–648. With permission of the Soil Science Society of America.

<sup>a</sup> Mean ± SE.

amorphous Fe(III) oxyhydroxides. The rapid oxidation of As(III) is observed on the Fe oxyhydroxide, ferrihydrite, in the presence of hydrogen peroxide (Nicholas et al., 2003). Jang and Dempsey (2008) found that the oxidation of As(III) by Fe oxyhydroxides is significant only in the presence of As(V). Magnetite (Fe<sub>3</sub>O<sub>4</sub>) is able to catalyze the oxidation of As(III), which is attributed to the presence of structural Fe(III) and possible Mn impurities in the magnetite (Su and Puls, 2008).

The oxidation of As(III) by the Mn oxides, birnessite, todorokite, and hausmannite, increases significantly in the presence of the Fe(III) oxide, goethite (Feng et al., 2006a). Goethite promotes As(III) oxidation on the Mn oxide minerals by adsorption of the As(V) produced during the reaction, thus decreasing the As(V) concentration in solution. Therefore, the combined effects of the Mn and Fe oxide minerals can lead to the rapid oxidation and immobilization of As in soils (Deschamps et al., 2003; Feng et al., 2006a).

The conversion of As(III) to As(V) by uncoated and coated Mn oxides has important implications for the transport, fate, and toxicity of As in terrestrial and associated environments. In some environments that have been contaminated with As(III), the addition of reactive Mn oxides may alleviate the toxicity of As(III) through their catalytic reactions.

#### 18.4.1.2 Selenium

Selenium is an essential trace element in the human and animal nutrition; however, there is a very narrow optimal concentration range between deficiency and toxicity (selenosis). The mobility and availability of Se are largely controlled by its redox state, which affects its sorption to mineral and organic matter surfaces (Masscheleyn et al., 1990; Charlet et al., 2007). Selenium(VI) is the stable valence state in oxic environments and exists as the selenate (SeO<sub>4</sub><sup>2-</sup>) oxyanion. Selenium(IV) is the stable valence state under mildly reducing or anoxic conditions and exists as the selenite (SeO<sub>3</sub><sup>2-</sup>) oxyanion. Selenate is weakly sorbed by minerals and is more soluble and bioavailable than selenite, which binds strongly to the surfaces of metal oxides by inner-sphere complexes. In reducing sediments, Se(VI) and Se(IV) can be reduced to Se(0) and other reduced species (oxidation states of -1 and -2), such as Se-pyrite or ferroselite. The formation of elemental and pyritic Se is regarded as an important mechanism for controlling the availability of Se in the environment (Belzile et al., 2000). The reduction of Se(VI) and Se(IV) may be facilitated by sorption of these species on the surfaces of Fe-Mn oxyhydroxides or Fe(II)-bearing minerals or by the involvement of HS<sup>-</sup>, pyrite, and organic matter (Myneni et al., 1997; Belzile et al., 2000; Bruggeman et al., 2005; Charlet et al., 2007; Scheinost and Charlet, 2008). Previously it was thought that these reactions are principally mediated by microorganisms (Myneni et al., 1997).

The abiotic reduction of Se(VI) and Se(IV) to Se(0) can be catalyzed by Fe(II) either sorbed on the surfaces of clays or structurally present in Fe-bearing minerals. Green rust, an Fe(II/III) oxide commonly present in reduced sediments and soils, is able to reduce Se(VI) to Se(IV) and Se(0) by adsorption

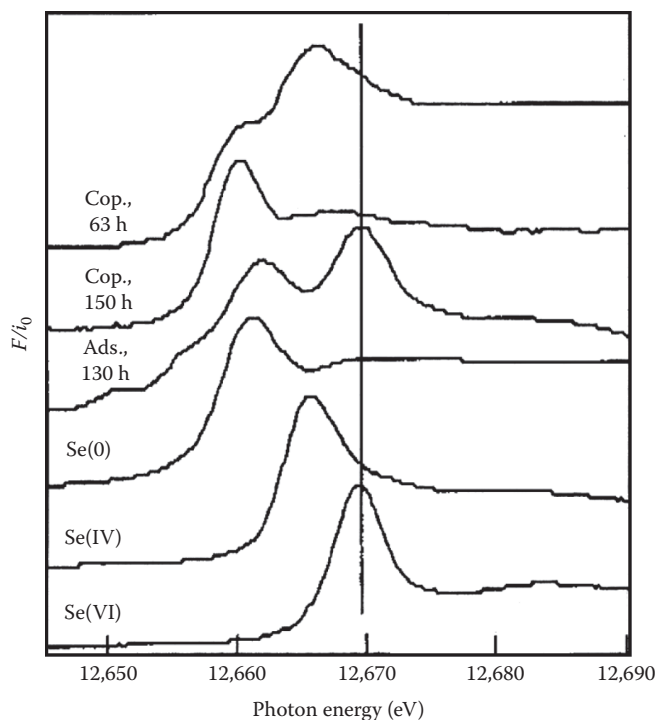
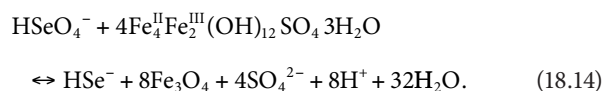


**FIGURE 18.12** In situ XANES spectra of Se(VI) reaction with green rust as a function of sorption mechanisms (coprecipitation [Cop.] and adsorption [Ads]). The XANES spectra of Se models in different oxidation states are shown for comparison. The vertical line in the center shows the position of Se(VI). (Reprinted from Myneni, S.C.B., T.K. Tokunaga, and G.E. Brown. 1997. Abiotic selenium redox transformations in the presence of Fe(II,III) oxides. *Science* 278:1106–1109. With permission of the American Association for the Advancement of Science.)

and coprecipitation mechanisms (Figure 18.12) (Myneni et al., 1997). The reaction proceeds as follows; magnetite is produced during the oxidation of the green rust:



Similarly, zero-valent iron reacted with Se(VI) catalyzes the formation of Se(0) and produces a green rust layer on the exposed surfaces of the iron(0) (Scheidegger et al., 2003).

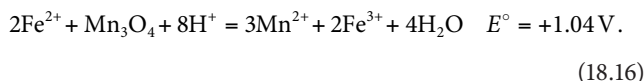
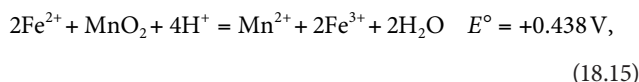
The reduction of selenite [Se(IV)] to solid Se(0) can be catalyzed by Fe(II)-bearing mineral, pyrite (FeS<sub>2</sub>), via the process of adsorption on the surface of pyrite (Bruggeman et al., 2005; Breynaert et al., 2008). The presence of illite-rich Boom clay sediments (Belgium) and natural humic substances decreases the rate of selenite reduction by pyrite due to the competitive adsorption (Bruggeman et al., 2005). Troilite (FeS) is also able to catalyze the reduction of selenite, however, through a different mechanism that involves reduction by dissolved sulfide and the formation of Se(0) as an intermediate (Breynaert et al., 2008). The Se(0) is then further reduced to FeSe<sub>2</sub> species, which precipitate on the surface of the troilite. Nanoparticulate Fe(II)-bearing

minerals mackinawite  $[(\text{Fe}, \text{Ni})_{1+x}\text{S}_x]$  and magnetite ( $\text{Fe}_3\text{O}_4$ ), and micrometer-sized siderite ( $\text{FeCO}_3$ ) are able to rapidly reduce selenite (Scheinost and Charlet, 2008). Mackinawite reduces selenite to  $\text{Se}(0)$  at pH 6.3 and  $\text{FeSe}$  at pH 4, whereas magnetite reduces selenite to  $\text{FeSe}$  and  $\text{Fe}_7\text{Se}_8$  species at pH 5. Siderite is weakest catalyst of three minerals and only partially reduces selenite to  $\text{Se}(0)$  (Scheinost and Charlet, 2008).

Montmorillonite equilibrated with  $\text{Fe}^{2+}$  is able to catalyze the slow reduction of selenite [ $\text{Se(IV)}$ ] to nanoparticulate  $\text{Se}(0)$  (Charlet et al., 2007). Mossbauer and XAS spectroscopy suggest that the Se and Fe redox reactions are not directly coupled, but rather that a small amount of  $\text{Fe(II)}$  that is presorbed on the montmorillonite is oxidized to  $\text{Fe(III)}$ , and the electrons that are produced during this reaction are stored by the formation of surface  $\text{H}_2$  species, which then later are able to reduce selenite (Charlet et al., 2007).

#### 18.4.1.3 Iron

Manganese oxides, which have different structural and surface properties, vary in their ability to catalyze the conversion of  $\text{Fe(II)}$  to  $\text{Fe(III)}$  and the subsequent formation of Fe oxides and oxyhydroxides (Krishnamurti and Huang, 1987, 1988). The standard electrode potential ( $E^\circ$ ) of the redox pairs  $\text{Fe}^{2+}$ - $\text{MnO}_2$  and  $\text{Fe}^{2+}$ - $\text{Mn}_3\text{O}_4$  can be described by the following equations (Bricker, 1965):



These  $E^\circ$  values indicate that oxidation of  $\text{Fe}^{2+}$  by Mn oxides is thermodynamically feasible. The Eh–pH diagram (Figure 18.13) indicates the feasibility of the conversion of  $\text{Mn}^{4+}$  and  $\text{Mn}^{3+}$  to  $\text{Mn}^{2+}$  in the Mn oxides in the Eh–pH ranges of the formation of Fe oxides and oxyhydroxides. Further, the ESR spectra of the filtrates after the reaction of  $\text{Fe}^{2+}$  with Mn oxides show the presence of a significant amount of  $\text{Mn}^{2+}$ , demonstrating the reduction of  $\text{Mn(IV)}$  and  $\text{Mn(III)}$  oxides to  $\text{Mn}^{2+}$  in the presence of  $\text{Fe}^{2+}$  in solution. Simultaneously, the oxidation of  $\text{Fe}^{2+}$  to  $\text{Fe}^{3+}$  by Mn oxides leads to subsequent hydrolysis of  $\text{Fe}^{3+}$  to form a series of the precipitation products including lepidocrocite, akaganeite, ferroxhyte, and magnetite. Because various Mn oxides differ in their ability to catalyze the formation of Fe oxides and oxyhydroxides, their role in the transformation of Fe deserves attention.

At neutral pH conditions, structural  $\text{Fe(III)}$  in hematite is able to catalyze the oxidation of sorbed  $\text{Fe(II)}$  to amorphous ferric oxide on the surface of hematite (Jeon et al., 2003). Solid-phase contact among hematite, amorphous ferric oxide, and structural  $\text{Fe(II)}$  eventually produces magnetite ( $\text{Fe}_3\text{O}_4$ ) (Jeon et al., 2003). Hydrous ferric oxide is able to catalyze the abiotic oxidation of

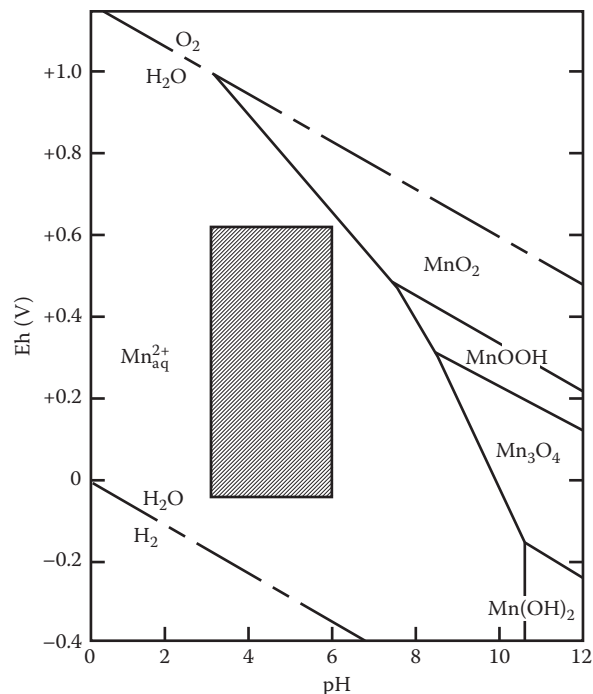


**FIGURE 18.13** Stability relations of different species of Mn at 25°C, 0.101 MPa, and  $a_{\text{Mn}^{2+}} = 10^{-6}$  (Bricker 1965). The Eh and pH ranges of the systems during the formation of iron oxide precipitates in the presence of Mn oxides in the present study are shown as shaded region. (Reprinted from Krishnamurti, G.S.R., and P.M. Huang, 1988. Influence of manganese oxide minerals on the formation of iron oxides. *Clay. Clay Miner.* 36:467–475. With permission of the Clay Minerals Society.)

$\text{Fe}^{2+}$  under anoxic conditions at neutral pH (Park and Dempsey, 2005). During this reaction, the hydrous ferric oxide is partially converted to goethite. The reaction mechanism involves an anode/cathode mechanism with  $\text{O}_2$  reduced at electron deficient sites with  $\text{Fe(II)}$  strongly sorbed, and  $\text{Fe(II)}$  is oxidized at electron-rich sites without sorbed  $\text{Fe(II)}$ . Iron(III) has been found to play a dominant role in pyrite ( $\text{FeS}_2$ ) oxidation in comparison with dissolved oxygen under acidic conditions (Mazumdar et al., 2008).

#### 18.4.1.4 Manganese

Although oxidation of Mn in soils by atmospheric  $\text{O}_2$  is a thermodynamic possibility throughout the pe and pH range common in well-aerated soils, Mn is not readily oxidized in solutions unless the pH is raised above pH 8.5 (Ross and Bartlett, 1981). A catalytic mechanism of some sort is apparently necessary. Oxidation of Mn in soil environments is generally assumed to be microbially mediated (Tebo et al., 2005; Thompson et al., 2005).

Oxidation of  $\text{Mn(II)}$  by soils has been shown to be proportional to the level of existing reactive Mn oxides (Ross and Bartlett, 1981). Arrhenius plots of rates of the oxidation between 1°C and 35°C show that the oxidation of  $\text{Mn(II)}$  by soils has nonbiological characteristics. Generally, oxidation of  $\text{Mn(II)}$  is initially rapid with no lag period and may be related to the mechanism proposed for the accumulation of Co and Zn on Mn oxide surfaces (Loganathan et al., 1977). The adsorption on



the oxide surfaces is specific and not a simple function of surface charge. Above pH 5–6, this adsorption reverses the surface charge of the Mn oxides from negative to positive, as measured by electrophoretic mobility. A positively charged surface should result in a higher  $\text{OH}^-$  concentration near the surface, which could enable oxidation of adsorbed Mn(II) by atmospheric  $\text{O}_2$ . The mechanism of specific adsorption is not fully understood, but the preferential adsorption of transition metals by Mn oxides is well documented (Jenne, 1977). The oxidation of Mn(II) by Mn oxides is theorized to be autocatalytic, involving specific adsorption of Mn(II) on existing Mn oxide surfaces (Ross and Bartlett, 1981).

The Fe(III) oxyhydroxide, akaganeite, promotes the formation of birnessite ( $\delta\text{-MnO}_2$ ) by catalyzing the air oxidation of surface adsorbed Mn(II) (Cornell and Giovanoli, 1991). Hematite, especially at a particle size below 4 nm, is able to promote the oxidation Mn(II) in the presence of  $\text{O}_2$  by donating electron density to adsorbed  $\text{Mn}^{2+}$ , which promotes reaction with  $\text{O}_2$  (Madden and Hochella, 2005).

#### 18.4.1.5 Radionuclides

Radionuclides are unstable isotopes of elements that are radioactive. Most elements with an atomic number greater than 83 have an unstable nucleus and are thus radioactive, and therefore, all of their isotopes are radionuclides. Many radionuclides are man-made, for example, plutonium and technetium, and are released into the environment as a result of nuclear waste, airborne emissions from nuclear reactors, nuclear weapons testing and processing, and infrequently due to incorrect disposal of medical or industrial radiation sources (Salbu et al., 2004; USEPA, 2009). Most of the commonly encountered polluting radionuclides have multiple oxidation states, and thus, redox chemistry plays a dominant role in their environmental mobility and availability.

Plutonium and neptunium are the chief radionuclides of concern for long-term storage of nuclear waste due to their long half-lives ( $t_{1/2} = 2.14 \times 10^6$  years for  $^{237}\text{Np}$  and  $2.41 \times 10^4$  years for  $^{239}\text{Pu}$ ), radiotoxicity, and chemotoxicity (Runde et al., 2002). Plutonium exists in the III–VI oxidation states as  $\text{Pu}^{3+}$ ,  $\text{Pu}^{4+}$ ,  $\text{PuO}_2^+$ , and  $\text{PuO}_2^{2+}$  in strong acid conditions. Plutonium(III/IV) cations are sorbed by soil constituents, and therefore, immobile in most aqueous and soil environments, whereas,  $\text{Pu(VI)}$  cations are not sorbed by temperate soils and thus quite mobile and bioavailable.  $\text{Pu(V)O}_2^+$  can be sorbed onto soil surfaces from dilute solutions or seawater (Keeneykennicutt and Morse, 1985). Neptunium tends to occur as highly mobile  $\text{Np(V)O}_2^+$  oxidation state under a wide range of environmental conditions (Wilk et al., 2005).

Manganese(III/IV) oxides and oxyhydroxides can oxidize  $\text{Pu(III/IV)}$  (Cleveland, 1970; Amacher and Baker, 1982; Morgenstern and Choppin, 2002) and  $\text{Pu(V)}$  (Keeneykennicutt and Morse, 1985; Duff et al., 1999) to the more mobile and toxic  $\text{Pu(VI)}$ . Conversely, Mn(II)-bearing oxides, hausmannite and manganite, can reduce  $\text{Pu(VI)}$  to  $\text{Pu(IV)}$ , which then forms strong inner-sphere complexes with the surface of the mineral

(Shaughnessy et al., 2003). Surprisingly, it has also been shown that pyrolusite ( $\alpha\text{-MnO}_2$ ), a Mn(IV)-bearing oxide, can promote the reduction of  $\text{Pu(VI)}$  (Kersting et al., 1999; Powell et al., 2006). Powell et al. (2006) attributed this to the observation that pyrolusite can initially oxidize  $\text{Pu(IV)}$  to  $\text{Pu(VI)}$ ; however, if the oxidized species remains associated with the solid phase, the initial oxidation step is followed by reduction to a stable hydrolyzed  $\text{Pu(IV)}$  species, which is not affected by the oxidizing surface, and over time becomes the predominant solid-phase  $\text{Pu}$  species. These findings are important when assessing the risk of the geological burying of nuclear waste in areas containing Mn(IV)-bearing minerals, such as Yucca Mountain or the Hanford sites (Powell et al., 2006).

Iron(II)-bearing minerals can reduce highly mobile  $\text{Np(V)}$  and  $\text{Pu(V/VI)}$  species, as well as, many other mobile higher valency species of radionuclides such as uranium and technetium. Natural uranium is mildly radioactive and occurs in trace amounts in most rocks, soils, and water. The more strongly radioactive isotope, U-235, is selectively enriched and used for nuclear weapons and for fuel for nuclear reactors. The U-235-depleted uranium is used for making weapons and armor, and has been used for counter weights in aircraft tails. All the above-mentioned uses result in the release of U into the environment. Similar to  $\text{Pu}$  and  $\text{Np}$ , U has a variety of oxidation states with uranyl  $\text{U(VI)O}_2^{2+}$  species being the most mobile. Technetium is an artificial element produced during nuclear fission and is commonly found in groundwater at sites where nuclear waste has been processed or stored. It has a similar chemistry to Mn and has several oxidation states. Under oxic conditions, it occurs as a pertechnetate anion,  $\text{Tc(VII)O}_4^-$ , which is poorly sorbed across the environmental pH range. The lower valency  $\text{Tc(IV)}$  readily precipitates as insoluble hydrous oxides or is sorbed on mineral surfaces.

Magnetite ( $\text{Fe}_3\text{O}_4$ ) can reduce  $\text{Pu(V)}$  to strongly sorbed  $\text{Pu(IV)}$  over a wide pH range (pH 3–8; Powell et al., 2004). Similarly, magnetite can reduce  $\text{Tc(VII)}$  to  $\text{Tc(IV)}$  (Cui and Eriksen, 1996),  $\text{Np(V)}$  to  $\text{Np(IV)}$  (Nakata et al., 2004), and  $\text{U(VI)}$  to  $\text{U(IV)}$  (Scott et al., 2005; El Aamrani et al., 2007). Biotite, which contains significant amounts of Fe(II), is also able to reduce  $\text{U(VI)}$  on exposed edge sites over a broad pH range (Ilton et al., 2004).

Green rusts, which are mixed Fe(II/III) hydrous oxides, are potent reducing agents in suboxic environments and can readily reduce  $\text{U(VI)}$  to  $\text{U(IV)}$  to precipitate nanoparticulate  $\text{UO}_2$  (O'Loughlin et al., 2003a) and reduce  $\text{Tc(VII)}$  pertechnetate anions to strongly surface-complexed  $\text{Tc(IV)}$  (Pepper et al., 2003). Likewise, amorphous  $\text{FeS}$  can reduce  $\text{U(VI)}$  to  $\text{U(V)}$  and  $\text{U(IV)}$  oxides (Hua and Deng, 2008). Mackinawite ( $\text{FeS}$ ) is able to reduce  $\text{Tc(VII)}$  to form  $\text{Tc(IV)S}_2$ ,  $\text{U(VI)}$  to  $\text{U(V/IV)}$  oxide phases, and  $\text{Np(V)}$  to  $\text{Np(IV)}$  surface complexes (Livens et al., 2004).

Fe(II) sorbed to the surface of Fe(III)-containing oxides, forming the reactive surface species  $\equiv\text{Fe}^{\text{III}}\text{O}-\text{Fe}^{\text{II}}\text{OH}^0$ , is also a potent reducing agent of radionuclides. In contrast to the abiotic reduction of organics (e.g., nitrobenzenes) by Fe(II) sorbed to hematite or magnetite, which is an outer-sphere mechanism, the

reduction of inorganics such as U(VI) involves an inner-sphere electron transfer mechanism (Charlet et al., 1998; Liger et al., 1999). The first step is the adsorption of U(VI) ion by the reactive surface species and the formation of an inner-sphere complex, followed by two reductive steps, which lead to the formation of a mixed U(IV)O<sub>2</sub>/Fe(OH)<sub>3</sub> solid phase (Charlet et al., 1998; Liger et al., 1999). The reduction of U(VI) by Fe(II) sorbed to synthetic Fe oxides (magnetite, goethite, and hematite) and natural Fe(III) oxide-containing sediments has been demonstrated, and the natural sediments are less efficient than the pure oxides due to their lower Fe(II) sorption capacity (Jeon et al., 2005). Iron(II) sorbed to hematite and goethite is much more efficient Tc(VII)-reducing agent than Fe(II) sorbed to phyllosilicates (vermiculite, illite, and muscovite) or structural Fe(II) in the phyllosilicates (Peretyazhko et al., 2008a). Iron(II) sorbed to Al oxyhydroxide, diaspore, and Al oxide, corundum, is also able to reduce Tc(VII) to insoluble Tc(IV) (Peretyazhko et al., 2008b).

Natural humic substances and quinoid-enriched humic substances are able to catalyze the abiotic reduction of Pu(V) to insoluble Pu(IV) over a wide pH range and under oxic and anoxic conditions (Andre and Choppin, 2000; Shcherbina et al., 2007a). Humic substances are only able to reduce Np(V) to Np(IV) under acidic, anoxic conditions (Shcherbina et al., 2007a, 2007b).

#### 18.4.1.6 Other Trace Metals

In addition to oxidation of metalloids such as As(III) and metals such as Fe(II), Mn(II), Mn oxides, and oxyhydroxides can catalyze the oxidation of trace metals by disproportionation of Mn<sup>2+</sup> and MnO<sub>2</sub>. The disproportionation facilitates electron transfer processes that can either greatly decrease or increase the equilibrium solubility of certain metals (Hem, 1978).

Chromium and Pu are similar in chemical behavior in aqueous environments (Rai and Serne, 1977; Bartlett and James, 1979). Chromium occurs in the II, III, and VI oxidation states in water. Chromium(II) is unstable. Chromium(III) has broad stability and exists as the cation Cr<sup>3+</sup> and its hydrolysis products or as the anion CrO<sub>2</sub><sup>-</sup>. Chromium(VI) exists under strongly oxidizing conditions, occurs as dichromate Cr<sub>2</sub>O<sub>7</sub><sup>2-</sup>, or chromate HCrO<sub>4</sub><sup>-</sup> and CrO<sub>4</sub><sup>2-</sup> anions. Chromium(III) cations are readily sorbed to soil constituents, and therefore, immobile in most aqueous and soil environments; however, Cr(VI) is not sorbed by temperate soils to any extent and is thus quite mobile in soils and associated aqueous environments. Therefore, hexavalent Cr is readily bioavailable and extremely toxic (Amacher and Baker, 1982) and, thus, of concern in food-chain contamination and ecosystem health. Manganese(III/IV) oxides can oxidize Cr(III) and are the only known oxidizers of Cr(III) in the soil environment (Stepniewska et al., 2004; Negra et al., 2005).

The kinetics of Cr(III) oxidation by Mn oxide is very rapid with most of the conversion of Cr(III) to Cr(VI) occurring during the first hour (Amacher and Baker, 1982). The oxidation of Cr(III) increases with increasing temperature. Manganite ( $\gamma$ -MnOOH) is also able to catalyze the oxidation of Cr(III), and the reaction rate increases under acidic conditions (Weaver et al., 2002). At higher

pH, Cr(III) hydroxy hydrate precipitates on the manganite surface, and the oxidation reactions are minimized (Weaver et al., 2002). Feng et al. (2007) compared the Cr(III) oxidative power of four different Mn oxides and found that order of reactivity was as follows (mmol Cr(III) kg<sup>-1</sup> oxide): birnessite (1330.0) > cryptomelane (422.6) > todorokite (59.7) > hausmannite (36.6). The Cr(III) oxidative ability of the Mn oxides depends on the crystallinity, structure, composition, and surface properties of the minerals (Feng et al., 2007).

The kinetics of Cr(III) oxidation on Mn(III/IV) oxides shows a trend similar to that observed for soils (Amacher and Baker, 1982). Negra et al. (2005) demonstrated that greater Mn(IV) oxide abundance in soils enhances the Cr(III) oxidation potential. It has also been shown that the oxidation state of Cr in soils in the long-term depends on balances between organic carbon availability (enhances Cr reduction) and the Mn redox status [Mn(III)/(IV) oxides enhance oxidation] (Stepniewska et al., 2004; Tokunaga et al., 2007). Nonliving biomaterials, such as seaweed, dead fungi, sawdust and pine bark, and needles, are able to abiotically (nonenzymatically) catalyze the adsorption-coupled reduction of Cr(VI) to Cr(III) (Park et al., 2004, 2007, 2008b). The Cr(VI)-reducing capacity of pine bark is 8.7 times higher than that of a common chemical Cr(VI) reductant, FeSO<sub>4</sub>·7H<sub>2</sub>O. When Cr(VI) comes in contact with biomaterials, there are two possible reduction mechanisms (Figure 18.14) (Park et al., 2005, 2007). Mechanism I, the direct reduction mechanism, involves the direct reduction of Cr(VI) to Cr(III) by contact with electron-donor groups of the biomaterial, such as amino and carboxyl groups (Figure 18.14). Mechanism II, the indirect reduction mechanism, involves three steps: (1) the binding of anionic Cr(VI) to the positively charged groups present on the biomaterial surface, (2) the reduction of Cr(VI) to Cr(III) by adjacent electron-donor groups, and (3) the release of the reduced Cr(III) into the aqueous phase due to electronic repulsion between the positively charged groups and the Cr(III), or the complexation of the reduced Cr(III) with adjacent groups (Figure 18.14). A lower pH makes the biosurface more positively charged and accelerates redox reactions, which enhances Cr(VI) removal (Park et al., 2007). The addition of soil slurry to nonliving biomaterials, such as pine bark, significantly enhances the Cr(VI)-reducing capability of the pine bark, by sorbing Cr(III) from solution (Park et al., 2008a). Therefore, although Mn oxides can enhance the mobility and toxicity of Cr in soils and related environments, the presence of organic matter decreases its oxidation potential.

Manganese oxides and oxyhydroxides can also catalyze the oxidation of other trace metals such as Co, Pb, Ni, Cu (Hem, 1978), and Sb (Belzile et al., 2001). The catalytic transformation of these metal ions may be directly influenced by redox processes coupled to disproportionation of Mn mixed valence oxide, to catalyzed oxidation by aqueous O<sub>2</sub>, or to other redox reactions involving changes from one Mn oxide species to another. When the oxidized form of the element has a lower solubility than the reduced form, this effect can be of major significance.

X-ray photoelectron spectroscopy measurements of Co adsorbed on MnO<sub>2</sub> reveal strong evidence that Co(II) is oxidized

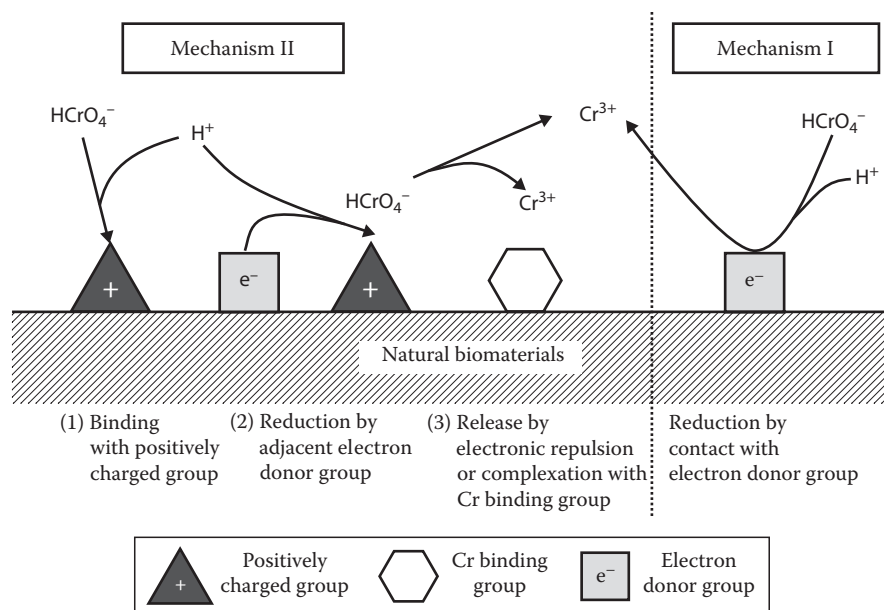


**FIGURE 18.14** Proposed direct and indirect mechanisms for Cr(VI) biosorption and reduction by natural biomaterials. (Reprinted from Park, D., Y.S. Yun, and J.M. Park. 2005. Studies on hexavalent chromium biosorption by chemically-treated biomass of *Ecklonia* sp. *Chemosphere* 60:1356–1364. Copyright 2005, with permission from Elsevier.)

to Co(III) in the presence of the strong electric field at the  $\text{MnO}_2$ -solution interface (Murray and Dillard, 1979). Nickel(II), however, cannot be oxidized at the interface except at very high concentrations. Strong experimental evidence for the oxidation of other trace metals catalyzed by Mn oxides still remains to be attained. Further, more information on the kinetics and mechanisms of redox reactions of these trace metals on the surfaces of Mn oxides is needed.

Other than Mn oxides, heterogeneous oxidation/reduction reactions involving electron transfer between transition metals and Fe-containing minerals have been investigated in numerous studies. Vanadium(II) and V(IV) can be oxidized by Fe(III) oxyhydroxides (Wehrli and Stumm, 1989). Amorphous Fe(III) oxyhydroxides present in natural waters and sediments can also oxidize the more toxic Sb(III) into Sb(V) (Belzile et al., 2001). The oxidation pseudo-first-order rate of Sb(III) by natural Fe oxyhydroxides is slower compared to synthetic Fe oxyhydroxides. This is attributed to the slight crystallinity of the natural oxides (compared to amorphous synthetic compounds) and to their more complex chemical composition, which can include adsorbed ions and organic matter (Belzile et al., 2001). Goethite has also been shown to catalyze the oxidation of Sb(III) to Sb(V) (Leuz et al., 2006).

Iron(II)-bearing minerals are able to reduce a variety of trace metals. Reduction of Cr(VI) by biotite has been shown by Eary and Rai (1989) and Ilton and Veblen (1994). Magnetite and ilmenite are the most common Fe(II)-containing oxide minerals in the earth's crust and potentially important in controlling heterogeneous redox reactions involving aqueous transition metals in soil environments. Direct evidence of Cr(VI) reduction on magnetite surfaces has been documented by Peterson et al. (1996) using x-ray adsorption fine structure (EXAFS)

spectroscopy. Structural Fe(II) in magnetite and ilmenite heterogeneously reduces aqueous Cu(II), V(IV), and Cr(VI) ions at the oxide surfaces over a pH range of 1–7 at 25°C (White and Peterson, 1996). Calcium carbonate coatings on the surface of magnetite reduce or eliminate its ability to reduce Cr(VI) (Doyle et al., 2004). Siderite ( $\text{FeCO}_3$ ) is also able to reduce aqueous Cr(VI), and its reactivity increases with addition of acid and with increasing temperature (Erdem et al., 2004). Pyrite is also an effective reductant of Cr(VI), and the reaction is about 100 times faster than reduction by biotite, which is related to the relative amount and dissolution rate of Fe(II) from the minerals (Chon et al., 2006). Similarly, Lin and Huang (2008) investigated the kinetics and effect of solution characteristics on Cr(VI) reduction by pyrite under dark and anaerobic conditions and found that the reduction is highly dependent on the solution pH, which influences the dissolution of Fe(II) and sulfide ions from pyrite, which are responsible for the reduction of Cr(VI). Magnetite (within days) and mackinawite (within minutes) are able to reduce Sb(V) to the more toxic Sb(III) form (Kirsch et al., 2008). The Sb(V) reduction by mackinawite proceeds solely by oxidation of surface Fe(II), while the oxidation state of sulfide is conserved, with the formation of amorphous or nanoparticulate  $\text{SbS}_3$ -like solids (Kirsch et al., 2008).

The Fe(II)-rich chlorite and corrensite clays are able to reduce Cr(VI) under acidic conditions, and during the reaction, structural Fe(II) is oxidized to Fe(III) (Brigatti et al., 2000). Mixed Fe(II)/Fe(III) hydroxides, known as green rusts, commonly found in suboxic environments are able to readily reduce a variety of trace metals, such as Ag(I), Au(III), Cu(II), and Hg(II) to Ag(0), Au(0), Cu(0), and Hg(0) (O'Loughlin et al., 2003b). Sulfate green rusts are able to effectively reduce Cr(VI) to Cr(III), which

initially involves chromate anions replacing sulfate in the inter-layer of the green rust, and then the chromate is reduced by Fe(II) (Skovbjerg et al., 2006). Even though the formation of sparingly soluble Cr(III) blocks further chromate entry, Cr(VI) reduction continues at the green rust solid/solution interface due to electron transfer from the center of the green rust crystals. During this process, Cr-substituted goethite is formed, which is sparingly soluble and thus essentially locks away the Cr, which has important implications for environmental remediation (Skovbjerg et al., 2006). Sulfate green rust is also able to reduce the highly stable Sb(V) to the more toxic Sb(III) (Mitsunobu et al., 2008).

Iron(II) sorbed to the surface of Fe oxides and clay minerals are also able to catalyze the reduction of Cr(VI) to Cr(III). Buerge and Hug (1999) compared the Cr(VI) reduction reactivity of Fe(II) in the presence of aluminum oxide, silicon dioxide, goethite, lepidocrocite, montmorillonite, and kaolinite and found that only  $\text{Al}_2\text{O}_3$  did not accelerate the reduction reaction in the presence of Fe(II). The order of reactivity was as follows (Buerge and Hug, 1999): goethite  $\approx$  lepidocrocite  $\gg$  montmorillonite  $>$  kaolinite  $\approx$   $\text{SiO}_2 \gg \text{Al}_2\text{O}_3$ . Similarly, Fe(II) added to magnetite significantly improves the Cr(VI) reductive ability of magnetite (Jung et al., 2007).

Organic complexes of Fe(II) also strongly affect the reduction of Cr(VI) to Cr(III) (Buerge and Hug, 1998). Fe(III)-stabilizing ligands such as bi- and multidentate carboxylates and phenolates generally accelerate the reduction reaction, whereas Fe(II)-stabilizing ligands such as phenanthroline essentially stop the reaction. Natural dissolved organic matter from a forest soil shows quantitatively the same accelerating behavior as the investigated Fe(II)-carboxylate complexes (Buerge and Hug, 1998).

### 18.4.2 Transformation of Other Inorganics

Nitrate formation in soils from  $\text{NO}_2^-$  is related to soil level of reactive Mn oxides, which catalyze the oxidation (Bartlett, 1981). Nitrite oxidation,  $\text{NO}_3^-$  formation, and  $\text{MnO}_2$  reduction are stoichiometrically related reactions both in the presence and the absence of atmospheric  $\text{O}_2$ . The relationship shown in Figure 18.15 suggests that at high ratios of  $\text{MnO}_2/\text{NO}_2^-$ , most of the Mn(IV) is reduced only to nonexchangeable solid Mn(III) oxide rather than to exchangeable Mn(II) ions. When the  $\text{MnO}_2/\text{NO}_2^-$  ratio is high, little Mn(II) becomes exchangeable relative to the  $\text{NO}_3^-$  formed, as indicated by high values of  $\text{NO}_3^-/\text{Mn(II)}$ . At low  $\text{MnO}_2/\text{NO}_2^-$  ratios, more exchangeable Mn(II) relative to  $\text{NO}_3^-$  is formed. Therefore, the more  $\text{MnO}_2$  relative to  $\text{NO}_2^-$ , the greater is the efficiency of the  $\text{NO}_2^-$  to  $\text{NO}_3^-$  transformation and the less exchangeable Mn(II) formed relative to  $\text{NO}_3^-$ . High  $\text{MnO}_2/\text{NO}_2^-$  ratios likely prevail in many soils. Equation 18.17, which does not involve a pH change, may describe the  $\text{NO}_2^-$  to  $\text{NO}_3^-$  transformation in high Mn oxide soils better than Equation 18.18:

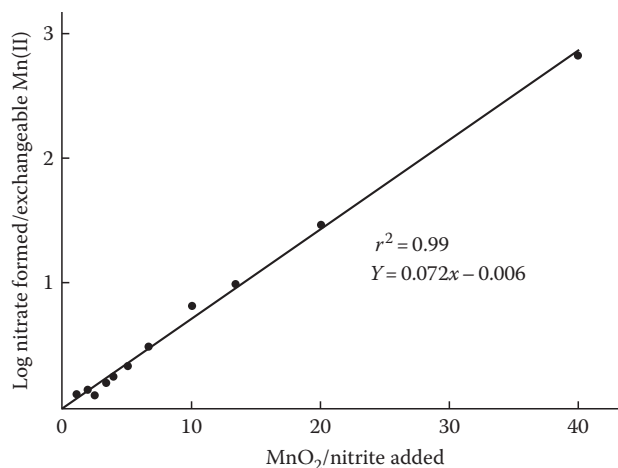
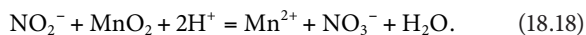
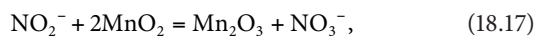


**FIGURE 18.15** The logs of the ratios of nitrate formed from nitrite over Mn reduced to the exchangeable form plotted against the  $\text{MnO}_2/\text{nitrite}$  ratios in the original suspensions. (Reprinted from Bartlett, R.J. 1981. Nonmicrobial nitrite-to-nitrate transformation in soils. *Soil Sci. Soc. Am. J.* 45:1054–1058. With permission of the Soil Science Society of America.)

Such a process of substantial reduction of Mn in the solid phase relative to the release of exchangeable Mn(II) might be described better as the insertion of electrons into the overlapping electronic orbitals of the solid, such that the electron excess is delocalized over the solid, rather than the reduction of one  $\text{Mn}^{4+}$  atom to  $\text{Mn}^{2+}$  at a particular surface site. The overlapping atomic orbitals form bands of many energy levels rather than a single energy level.

Luther and Popp (2002) studied the kinetics of nitrite oxidation by polymeric Mn(IV) oxides, which are highly reactive Mn oxide phases. The energy of activation and the entropy of activation show the oxidation reaction to be associative and diffusion controlled, occurring via an inner-sphere mechanism, likely with O atom transfer from  $\text{MnO}_2$  to  $\text{HNO}_2$ . The reaction requires protons and slows down at a pH above 5.5, where  $\text{NO}_2^-$  and  $\text{MnO}_2$  (negatively charged) become the dominant species (Luther and Popp, 2002).

Manganese(IV) oxide is also able to catalyze the oxidation of  $\text{NH}_3$  and organic N to  $\text{N}_2$ , which has traditionally been assumed to be a microbially mediated process in sediments (Luther et al., 1997). The  $\text{MnO}_2$ -catalyzed formation of  $\text{NO}_3^{2-}$  from  $\text{NH}_3$  can also occur, but the formation of  $\text{N}_2$  from  $\text{NH}_3$  is more favorable (Luther et al., 1997). Luther et al. also observed the reduction  $\text{NO}_3^{2-}$  to  $\text{N}_2$  by dissolved  $\text{Mn}^{2+}$ . These oxidation and reduction reactions can occur in the presence or absence of  $\text{O}_2$ . Hulth et al. (1999) found that introduction of Mn oxides from oxidized surface sediments into anoxic sediments results in anoxic nitrification and the net production of  $\text{NO}_3^-$  and  $\text{NO}_2^-$ . They found that the anoxic nitrification rates were directly related to the Mn oxide content of the sediment.

Iron(II)-bearing minerals can catalyze the abiotic reduction of nitrate and nitrite. Some field studies have suggested that structural Fe(II) in clay minerals catalyzes the reduction of  $\text{NO}_3^-$  to  $\text{NO}_2^-$ , as indicated by significant negative correlations in the

$\text{NO}_3^-$  and Fe(II) content in minerals in clayey till and catchment sediments (Ernstsen and Morup, 1992; Ernstsen, 1996). Chloride and sulfate intercalated green rusts (mixed Fe(II/III) hydrous oxides), which commonly occurs in anaerobic soils and sediments, are able to rapidly reduce  $\text{NO}_3^-$  to  $\text{NH}_4^+$   $\text{NH}_4^+$ , with the formation of magnetite ( $\text{Fe}_3\text{O}_4$ ) (Hansen et al., 1996; Hansen and Koch, 1998; Hansen et al., 2001). Wustite (FeO) is able to catalyze the rapid reduction of  $\text{NO}_3^{2-}$  to  $\text{NO}_2^-$  and ultimately  $\text{NH}_4^+$  (Rakshit et al., 2005). During this reaction, an Fe(II/III) oxide, magnetite ( $\text{Fe}_3\text{O}_4$ ), is formed. Siderite ( $\text{FeCO}_3$ ) is able to catalyze the abiotic reduction of  $\text{NO}_2^-$  to  $\text{N}_2\text{O}$ , during which siderite is transformed to lepidocrocite ( $\gamma\text{-FeOOH}$ ) (Rakshit et al., 2008).

Nitrate immobilization into dissolved and humic organic N fractions can be abiotically catalyzed in soils and sediments (Dail et al., 2001; Davidson et al., 2003; Huygens et al., 2008; Torres-Canabate et al., 2008). It has been suggested that anaerobic microsites in soils that contain reduced Fe and Mn minerals are responsible for catalyzing the reactions (Davidson et al., 2003; Torres-Canabate et al., 2008). The mechanism is thought to involve the abiotic reduction of  $\text{NO}_3^{2-}$  by Fe(II) (present in anaerobic microsites) to  $\text{NO}_2^-$ , which then rapidly abiotically reacts with existing organic matter via nitrosation (Thorn and Mikita, 2000) and thus is incorporated into the organic N fraction (Davidson et al., 2003). Further research is required to elucidate the exact mechanism of abiotic nitrate immobilization into organic N.

Manganese oxides also catalyze the oxidation of gaseous CO (Klier and Kuchynka, 1966). This reaction occurs by consumption of the structural  $\text{O}_2^{2-}$  of  $\text{MnO}_2$ . The catalyst must then be regenerated by chemisorption of  $\text{O}_2$ . Whether or not a similar cycle of Mn oxide reduction and  $\text{O}_2$  consumption occurs in soil environments, where adsorbed molecules such as  $\text{CO}_2$  and  $\text{H}_2\text{O}$  can poison the catalyst surface, remains unanswered.

Soil clay minerals and metal oxides, such as montmorillonite and goethite, can catalyze the abiotic hydrolytic degradation of high- and low-molecular-weight silicones, such as polydimethylsiloxane, by cleaving siloxane (Si-O-Si) bonds (Graiver et al., 2003). The resultant low-molecular-weight silanol units are volatile and thus evaporate into the atmosphere where they are degraded to silica, water, and  $\text{CO}_2$  by hydroxyl-free radicals in the atmosphere (Graiver et al., 2003).

## 18.5 Role of Nanoparticles in Abiotic Catalysis

Mineral nanoparticles are important constituents of natural terrestrial and aquatic environments (Gilbert and Banfield, 2005; Waychunas et al., 2005; Wigginton et al., 2007; Hochella et al., 2008; Wilson et al., 2008). Iron oxides, oxyhydroxides, and sulfides commonly occur as nanoparticles in nature; and various studies have investigated the abiotic transformation of organics (Klupinski et al., 2004; McCormick and Adriaens, 2004; Chun et al., 2006; Cwiertny et al., 2008) and inorganics, such as Sb (Kirsch et al., 2008) and Se (Loyo et al., 2008; Scheinost and Charlet, 2008) by nanoparticulate Fe-bearing minerals.

Mineral nanoparticles exhibit considerably different chemical and physical properties than their larger counterparts, due to the fact that a large percentage of their atoms are on the surface (e.g., for a particle with a diameter of 4 nm approximately 50% of its atoms are on the surface) (Grassian, 2008; Hochella et al., 2008). This can result in surface strain or reconstruction (relaxation), structural disorder, and variations in surface topography and crystallographic structure that is exposed. Although nanoparticles are highly reactive, which is attributable to their very high specific surface area, it has become clear that their increased reactivity cannot be solely attributed to this characteristic. Surface area-normalized studies have reported enhanced nanoparticle reactivity such as cation adsorption and redox reactions, which could only be attributed to a greater density of reactive sites per surface area unit or a greater inherent reactivity of nanoparticle surface sites (Waychunas et al., 2005; Grassian, 2008; Hochella et al., 2008).

Several studies have shown that the reactivity of Fe oxides and oxyhydroxides, which commonly occur as nanoparticles (3–10 nm range), is strongly dependent on particle size. The surface area-normalized reductive dissolution of 4 nm particles of ferrihydrite by hydroquinone is 20 times faster than that of 6 nm particles (Anschutz and Penn, 2005). Similarly, Erbs et al. (2008) investigated the effect of particle size on reductive dissolution of nanoparticulate ferrihydrite by hydroquinone, and they attributed the increased reactivity to increased reagent-surface encounters as indicated by a sixfold increase in the pre-exponential factor when comparing 3.9 nm particles to 5.9 nm particles. They hypothesized that the rate of diffusion of the reagent to the nanoparticle surface is size dependent, as the structure of the water is affected by the size of the nanoparticle.

Nanoparticulate hematite oxidation of soluble  $\text{Mn}^{2+}$  in the presence of  $\text{O}_2$  is dependent on the size of the nanoparticles as related to surface structure and topography (Madden and Hochella, 2005). The surface area-normalized oxidation rate of hematite particles with an average diameter of 7.3 nm is at least one order of magnitude higher than those with an average diameter of 37 nm. The oxidation reaction proceeds most readily at topographic features that distort the octahedral  $\text{Mn}^{2+}$  coordination environment. These distorting surface features increase as the particle size of hematite decreases. This has the effect of lowering the reorganization energy, which effectively controls the magnitude of the transition state barrier (Madden and Hochella, 2005).

Particle diameter of nanoparticulate magnetite strongly affects its reactivity toward the reductive degradation of carbon tetrachloride (Vikesland et al., 2007). Magnetite with a 9 nm diameter is far more reactive than 80 nm diameter magnetite on both a mass and surface area-normalized basis. The aggregation state of the 9 nm magnetite significantly affects its reactivity, and an increase in ionic strength leads to a decrease in reactivity due to increased aggregation of the nanoparticles. Jung et al. (2008a) compared the reactivity of biogenic and commercial nanoparticulate magnetite toward catalyzing the ozonation of parachlorobenzoic acid. Biogenic magnetite was found to be a less

efficient catalyst due to its tendency to form larger aggregates than the commercial magnetite (Jung et al., 2008a). While investigating the abiotic reductive transformation of nitrobenzene by Fe(II)-sorbed on goethite nanoparticles, Cwiertny et al. (2008) found that aggregation of the goethite nanoparticles resulted in the decreased BET-specific surface area-normalized rate constants, implying that they are less reactive than larger particles. They concluded that new methods are needed to quantify the amount of surface area accessible for reaction in wet nanoparticle suspensions rather than assuming the specific surface area of the dry nanoparticles is relevant.

In view of the high specific surface area and the density and nature of reactive sites of nanoparticles, their role in the catalytic reactions in soil and related environments merits increasing attention for years to come.

## 18.6 Conclusions

The significance of abiotic catalysis in the transformation of natural organic, anthropogenic organic compounds, metals, metalloids, and other inorganics is far greater than had previously been perceived. Mineral colloids are abundant in nature. Abiotic catalysts include metal (oxy)hydroxides and oxides, SRO aluminosilicates, layer silicates, and primary minerals. The ability of these catalysts to promote the transformation of vital elements and environmental pollutants varies significantly with their atomic bonding and structural configuration and surface chemistry and the structure and functionality of the substrates.

The transformation of biomolecules to humic substances is substantially promoted by abiotic catalysis. Phenolics are the most widely distributed class of plant secondary metabolites and play an important role in regulating nutrient cycling in the terrestrial environment. Abiotic catalysis promotes the formation of humic substances from the phenolic compounds especially in the presence of the amino acids through oxidative polymerization, polycondensation, ring cleavage, decarboxylation, dealkylation, and/or deamination. Sugars and amino acids are among the most abundant constituents of the terrestrial ecosystem. The Maillard reaction, involving condensation reactions between reducing sugars and amino acids, is substantially promoted by abiotic catalysis. In nature, the Maillard reaction and polyphenol pathways should interact closely, since sugars, amino acids, and polyphenols coexist in soil solutions and natural waters. The integrated polyphenol–Maillard reaction system under abiotic catalysis is more effective in generating humic polymers than the Maillard reaction or the polyphenol pathway alone. A series of mineral colloids promotes such catalytic reactions. Among abiotic catalysts, Mn oxides are most reactive in the transformation of these biomolecules.

Mineral colloids can catalyze the hydrolysis of many xenobiotics through the ability of their metal-containing surfaces to behave as Brønsted acids and donate protons or to act as Lewis acids and accept electron pairs. The catalytic effectiveness of a metal ion depends on its ability to complex reactant molecules

and shift electron density and conformation in ways favorable to the reactions. A wide range of xenobiotics such as pesticides, antibiotics, dyes, and explosives are subject to abiotic soil mineral-catalyzed oxidative transformation. In anoxic groundwater and surficial waters, biogeochemical processes provide a variety of potential reductants to catalyze abiotic transformation of persistent xenobiotics. Abiotic degradation pathways of biocides (pesticides and antibiotics) are particularly important in the environment as the toxicity of these substances can limit their biotic degradation. Much is known about the toxicity of xenobiotic parent compounds. To date, relatively little is known about the bioavailability and toxicity of xenobiotics after reaction with abiotic catalysts, such as metal (oxy)hydroxides and oxides and clay minerals.

The transformations of metals and metalloids are substantially influenced by Mn oxides and Fe-bearing minerals. Manganese(IV) oxides have the ability to catalyze many reactions such as the oxidation of As(III) to As(V), Fe(II) to Fe(III), Pu(III, IV, V) to Pu(VI), and Cr(III) to Cr(IV). The ability of Mn(IV) oxides to catalyze these transformation reactions varies with their structure and surface properties and can also be influenced by the kinds and levels of surface coatings. Iron(III)-bearing minerals also have the ability to catalyze the oxidation of some transition metals such as the transformation of V(II) to V(IV) and Sb(III) to Sb(V). On the other hand, the ability of Fe(II)-bearing minerals to catalyze the reduction reactions of a variety of trace metals and metalloids (e.g., Cr, Sb, V, Hg, U, Tc, Pu, Np, and Se) has been demonstrated. Besides Fe(II)-bearing minerals, nonliving biomaterials are able to abiotically catalyze the adsorption-coupled reduction of Cr(VI) to Cr(III). The solubility, mobility, toxicity, and food-chain contamination of metals and metalloids can be significantly influenced by abiotic catalysis.

Manganese(IV) oxides have been shown to catalyze the conversion of  $\text{NO}_2^-$  to  $\text{NO}_3^-$ . The reaction is theorized as mainly the insertion of electrons from  $\text{NO}_2^-$  into the overlapping electron orbitals of the Mn oxides. Manganese(IV) oxides also catalyze the oxidation of gaseous CO through consumption of structural  $\text{O}_2^-$ . Furthermore, nitrate immobilization into dissolved and humic organic N fractions can be abiotically catalyzed by reduced Fe and Mn (present in anaerobic microsites) in soils and sediments. Further research is required to elucidate the exact mechanism of nitrate immobilization into organic N.

Nanoparticles are important environmental particles, which influence the pedosphere, hydrosphere, biosphere, and atmosphere. Mineral nanoparticles exhibit considerably different chemical and physical properties, compared with their larger counterparts. This is ascribed to the exposure of a large percentage of atoms on the surface of nanoparticles and the resultant high specific surface area and the increase in density and reactivity of reactive sites of nanoparticles. The catalytic role of mineral nanoparticles in the transformation of organics and inorganics has been demonstrated. More in-depth research on the abiotic catalysis of environmental nanoparticles and on the biogeochemical and ecological impacts is warranted.

Therefore, abiotic catalysis deserves close attention in sustaining environmental quality and ecosystem health. Furthermore, abiotic and biotic catalysts coexist in soil and associated environments. Abiotic catalysts can influence microbial formation of enzymes (biotic catalysts) and enzymatic activity. The interactions and relative importance of abiotic and biotic catalysts and the impact on terrestrial ecosystem integrity should, thus, be an important and exciting issue for years to come.

## Acknowledgment

This study is supported by Discovery Grant GP 2383-2008 of the Natural Sciences and Engineering Research Council of Canada.

## References

- Ahn, M.-Y., C.E. Martínez, D.D. Archibald, A.R. Zimmerman, J.-M. Bollag, and J. Dec. 2006. Transformation of catechol in the presence of a laccase and birnessite. *Soil Biol. Biochem.* 38:1015–1020.
- Amacher, M.L., and D.E. Baker. 1982. Redox reactions involving chromium, plutonium, and manganese in soils. *DOE/DP/04515-1*. Pennsylvania State University, University Park, PA.
- Amirbahman, A., D.B. Kent, G.P. Curtis, and J.A. Davis. 2006. Kinetics of sorption and abiotic oxidation of arsenic(III) by aquifer materials. *Geochim. Cosmochim. Acta* 70:533–547.
- Amonette, J.E., D.J. Workman, D.W. Kennedy, J.S. Fruchter, and Y.A. Gorby. 2000. Dechlorination of carbon tetrachloride by Fe(II) associated with goethite. *Environ. Sci. Technol.* 34:4606–4613.
- Anderson, H.A., W. Bick, A. Hepburn, and M. Stewart. 1989. Nitrogen in humic substances, p. 223–253. *In* M.H.B. Hayes, P. MacCarthy, R.L. Malcolm, and R.S. Swift (eds.) *Humic substances II. In search of structure*. Wiley-Interscience, Chichester, U.K.
- Andre, C., and G.R. Choppin. 2000. Reduction of Pu(V) by humic acid. *Radiochim. Acta* 88:613–616.
- Anschutz, A.J., and R.L. Penn. 2005. Reduction of crystalline iron(III) oxyhydroxides using hydroquinone: Influence of phase and particle size. *Geochem. Trans.* 6:60–66.
- Arafaoli, P., O.L. Pantani, M. Bosetto, and G.G. Ristori. 1999. Influence of clay minerals and exchangeable cations on the formation of humic-like substances (melanoidins) from D-glucose and L-tyrosine. *Clay Miner.* 34:487–497.
- Arafaoli, P., G.G. Ristori, M. Bosetto, and P. Fusi. 1997. Humic-like compounds formed from L-tryptophan and D-glucose in the presence of Cu(II). *Chemosphere* 35:575–584.
- Armstrong, D.E., G. Chesters, and R.F. Harris. 1967. Atrazine hydrolysis in soils. *Soil Sci. Soc. Am. Proc.* 31:61–66.
- Baldrian, P., V. Merhautová, J. Gabriel et al. 2006. Decolorization of synthetic dyes by hydrogen peroxide with heterogeneous catalysis by mixed iron oxides. *Appl. Catal. B* 66:258–264.
- Barrett, K.A., and M.B. McBride. 2005. Oxidative degradation of glyphosate and aminomethylphosphonate by manganese oxide. *Environ. Sci. Technol.* 39:9223–9228.
- Bartlett, R.J. 1981. Nonmicrobial nitrite-to-nitrate transformation in soils. *Soil Sci. Soc. Am. J.* 45:1054–1058.
- Bartlett, R.J. 1986. Soil redox behavior, p. 179–207. *In* D.L. Sparks (ed.) *Soil physical chemistry*. CRC Press, Boca Raton, FL.
- Bartlett, R.J., and B. James. 1979. Behavior of chromium in soils. III. Oxidation. *J. Environ. Qual.* 8:31–35.
- Bases, C.F., and R.E. Mesmer. 1986. *The hydrolysis of cations*. Krieger Publishing Company, Malabar, FL.
- Basolo, F., and R.G. Pearson. 1968. *Mechanisms of inorganic reactions*, 2nd Ed. John Wiley & Sons, New York.
- Bell, R.P. 1941. *Acid–base catalysis*. Oxford University Press, Oxford, U.K.
- Belzile, N., Y.W. Chen, and Z.J. Wang. 2001. Oxidation of antimony (III) by amorphous iron and manganese oxyhydroxides. *Chem. Geol.* 174:379–387.
- Belzile, N., Y.W. Chen, and R.R. Xu. 2000. Early diagenetic behaviour of selenium in freshwater sediments. *Appl. Geochem.* 15:1439–1454.
- Bittner, S. 2006. When quinones meet amino acids: Chemical, physical and biological consequences. *Amino Acids* 30:205–224.
- Blanchet, P.-F., and A. St.-George. 1982. Kinetics of chemical degradation of organophosphorus pesticides: Hydrolysis of chlorpyrifos and chlorpyrifos-methyl in the presence of copper (II). *Pestic. Sci.* 13:85–91.
- Bollag, J.-M., J. Dec, and P.M. Huang. 1998. Formation mechanisms of complex organic structures in soil habitats. *Adv. Agron.* 63:237–266.
- Bollag, J.-M., S.-Y. Liu, and R.D. Minard. 1982. Enzymatic oligomerization of vanillic acid. *Soil Biol. Biochem.* 14:157–163.
- Bollag, J.-M., C. Myers, S. Pal, and P.M. Huang. 1995. The role of abiotic and biotic catalysts in the transformation of phenolic compounds, p. 299–310. *In* P.M. Huang, J. Berthelin, J.-M. Bollag, W.B. McGill, and A.L. Page (eds.) *Environmental impact of soil component interactions*, Vol. 1. Natural and anthropogenic organics. Lewis Publishers, Boca Raton, FL.
- Boparai, H.K., S.D. Comfort, P.J. Shea, and J.E. Szecsody. 2008. Remediating explosive-contaminated groundwater by in situ redox manipulation (ISRM) of aquifer sediments. *Chemosphere* 71:933–941.
- Bose, J.L., A.B. Foster, M. Stacey, and J.M. Webber. 1959. Action of manganese dioxide on simple carbohydrates. *Nature* 184:1301–1302.
- Bosetto, M., P. Arafaoli, O.L. Pantani, and G.G. Ristori. 1997. Study of the humic-like compounds formed from L-tyrosine on homoionic clays. *Clay Miner.* 32:341–349.
- Bosetto, M., P. Arafaoli, G.G. Ristori, and P. Fusi. 1995. Formation of melanin-type compounds from L-tryptophan on Ca-saturated and Al-saturated clays. *Fresenius Environ. Bull.* 4:369–374.

- Breynaert, E., C. Bruggeman, and A. Maes. 2008. XANES-EXAFS analysis of Se solid-phase reaction products formed upon contacting Se(IV) with FeS<sub>2</sub> and FeS. *Environ. Sci. Technol.* 42:3595–3601.
- Bricker, O. 1965. Some stability relations in the system Mn–O<sub>2</sub>–H<sub>2</sub>O at 25°C and one atmosphere total pressure. *Am. Mineral.* 50:1296–1354.
- Brigatti, M.F., C. Lugli, G. Cibin et al. 2000. Reduction and sorption of chromium by Fe(II)-bearing phyllosilicates: Chemical treatments and X-ray absorption spectroscopy (XAS) studies. *Clay. Clay Miner.* 48:272–281.
- Brønsted, J.N. 1928. Acid and base catalysis. *Chem. Rev.* 5:231–338.
- Brown, C.B., and J.L. White. 1969. Reactions of 12 *s*-triazines with soil clays. *Soil Sci. Soc. Am. J. Proc.* 33:863–867.
- Bruggeman, C., A. Maes, J. Vancluysen, and P. Vandermussele. 2005. Selenite reduction in Boom clay: Effect of FeS<sub>2</sub>, clay minerals and dissolved organic matter. *Environ. Pollut.* 137:209–221.
- Brunetti, G., N. Senesi, and C. Plaza. 2007. Effects of amendment with treated and untreated olive oil mill wastewaters on soil properties, soil humic substances and wheat yield. *Geoderma* 138:144–152.
- Buerge, I.J., and S.J. Hug. 1998. Influence of organic ligands on chromium(VI) reduction by iron(II). *Environ. Sci. Technol.* 32:2092–2099.
- Buerge, I.J., and S.J. Hug. 1999. Influence of mineral surfaces on chromium(VI) reduction by Iron(II). *Environ. Sci. Technol.* 33:4285–4291.
- Bussan, A.L., and T.J. Strathmann. 2007. Influence of organic ligands on the reduction of polyhalogenated alkanes by iron(II). *Environ. Sci. Technol.* 41:6740–6747.
- Butcher, W.W., and F.H. Westheimer. 1955. The lanthanum hydroxide gel promoted hydrolysis of phosphate esters. *J. Am. Chem. Soc.* 77:2420–2424.
- Butler, E.C., and K.F. Hayes. 1998. Effects of solution composition and pH on the reductive dechlorination of hexachloroethane by iron sulfide. *Environ. Sci. Technol.* 32:1276–1284.
- Cervini-Silva, J., R.A. Larson, J. Wu, and J.W. Stucki. 2001. Transformation of chlorinated aliphatic compounds by ferrous smectite. *Environ. Sci. Technol.* 35:805–809.
- Chang, H.M., and G.G. Allen. 1971. Oxidation, p. 433–485. *In* K.V. Sarkanene and C.H. Ludwig (eds.) *Lignins*. Wiley-Interscience, New York.
- Charlet, L., A.C. Scheinost, C. Tournassat et al. 2007. Electron transfer at the mineral/water interface: Selenium reduction by ferrous iron sorbed on clay. *Geochim. Cosmochim. Acta* 71:5731–5749.
- Charlet, L., E. Silvester, and E. Liger. 1998. N-compound reduction and actinide immobilisation in surficial fluids by Fe(II): The surface Fe(III)OFe(II)OH degrees species, as major reductant. *Chem. Geol.* 151:85–93.
- Chen, Z., K.W. Kim, Y.G. Zhu, R. McLaren, F. Liu, and J.Z. He. 2006. Adsorption (As-III, As-V) and oxidation (As-III) of arsenic by pedogenic Fe–Mn nodules. *Geoderma* 136:566–572.
- Cheney, M.A., G. Sposito, A.E. McGrath, and R.S. Criddle. 1996. Abiotic degradation of 2,4-D (dichlorophenoxyacetic acid) on synthetic birnessite: A calorimetric method. *Colloids Surf. A* 107:131–140.
- Cheng, H.H. 1991. Pesticides in the soil environment: Processes, impacts, and modeling. SSSA, Madison, WI.
- Cheng, M.M., W.J. Song, W.H. Ma et al. 2008. Catalytic activity of iron species in layered clays for photodegradation of organic dyes under visible irradiation. *Appl. Catal. B* 77:355–363.
- Chiu, V.Q., and J.G. Hering. 2000. Arsenic adsorption and oxidation at manganite surfaces. 1. Method for simultaneous determination of adsorbed and dissolved arsenic species. *Environ. Sci. Technol.* 34:2029–2034.
- Chon, C.M., J.G. Kim, and H.S. Moon. 2006. Kinetics of chromate reduction by pyrite and biotite under acidic conditions. *Appl. Geochem.* 21:1469–1481.
- Chun, C.L., R.M. Hozalski, and T.A. Arnold. 2005. Degradation of drinking water disinfection byproducts by synthetic goethite and magnetite. *Environ. Sci. Technol.* 39:8525–8532.
- Chun, C.L., R.L. Penn, and W.A. Arnold. 2006. Kinetic and microscopic studies of reductive transformations of organic contaminants on goethite. *Environ. Sci. Technol.* 40:3299–3304.
- Cleveland, J.M. 1970. The chemistry of plutonium. Gordon and Breach, New York.
- Colarieti, M.L., G. Toscano, M.R. Ardi, and G. Greco. 2006. Abiotic oxidation of catechol by soil metal oxides. *J. Hazard. Mater.* 134:161–168.
- Colon, D., E.J. Weber, and J.L. Anderson. 2006a. QSAR study of the reduction of nitroaromatics by Fe(II) species. *Environ. Sci. Technol.* 40:4976–4982.
- Colon, D., E.J. Weber, and J.L. Anderson. 2008. Effect of natural organic matter on the reduction of nitroaromatics by Fe(II) species. *Environ. Sci. Technol.* 42:6538–6543.
- Colon, D., E.J. Weber, J.L. Anderson, P. Winget, and L.A. Suarez. 2006b. Reduction of nitrosobenzenes and *N*-hydroxylanilines by Fe(II) species: Elucidation of the reaction mechanism. *Environ. Sci. Technol.* 40:4449–4454.
- Cornell, R.M., and R. Giovanoli. 1991. Transformation of akaganite into goethite and hematite in the presence of Mn. *Clay. Clay Miner.* 39:144–150.
- Cui, D.Q., and T.E. Eriksen. 1996. Reduction of pertechnetate by ferrous iron in solution: Influence of sorbed and precipitated Fe(II). *Environ. Sci. Technol.* 30:2259–2262.
- Curtis, G.P., and M. Reinhard. 1994. Reductive dehalogenation of hexachloroethane, carbon-tetrachloride, and bromoform by anthrahydroquinone disulfonate and humic-acid. *Environ. Sci. Technol.* 28:2393–2401.
- Cwiertny, D.M., R.M. Handler, M.V. Schaefer, V.H. Grassian, and M.M. Scherer. 2008. Interpreting nanoscale size-effects in aggregated Fe-oxide suspensions: Reaction of Fe(II) with goethite. *Geochim. Cosmochim. Acta* 72:1365–1380.
- Dail, D.B., E.A. Davidson, and J. Chorover. 2001. Rapid abiotic transformation of nitrate in an acid forest soil. *Biogeochemistry* 54:131–146.



- Daintith, J. 1990. A concise dictionary of chemistry. Oxford University Press, Oxford, U.K.
- Davidson, E.A., J. Chorover, and D.B. Dail. 2003. A mechanism of abiotic immobilization of nitrate in forest ecosystems: The ferrous wheel hypothesis. *Global Change Biol.* 9:228–236.
- Davis, J.A., and K.F. Hayes. 1986. Geochemical processes at mineral surfaces. American Chemical Society, Washington, DC.
- Dec, J., K. Haider, and J.-M. Bollag. 2001. Decarboxylation and demethoxylation of naturally occurring phenols during coupling reactions and polymerization. *Soil Sci.* 166:660–671.
- Dec, J., K. Haider, and J.-M. Bollag. 2003. Release of substituents from phenolic compounds during oxidative coupling reactions. *Chemosphere* 52:549–556.
- Deschamps, E., V.S.T. Ciminelli, P.G. Weidler, and A.Y. Ramos. 2003. Arsenic sorption onto soils enriched in Mn and Fe minerals. *Clay. Clay Miner.* 51:197–204.
- Devitre, R., N. Belzile, and A. Tessier. 1991. Speciation and adsorption of arsenic on diagenetic iron oxyhydroxides. *Limnol. Oceanogr.* 36:1480–1485.
- Dixon, J.B., and S.B. Weed. 1989. Minerals in soil environments. SSSA, Madison, WI.
- Doong, R.A., and H.C. Chiang. 2005. Transformation of carbon tetrachloride by thiol reductants in the presence of quinone compounds. *Environ. Sci. Technol.* 39:7460–7468.
- Doyle, C.S., T. Kendelewicz, and G.E. Brown. 2004. Inhibition of the reduction of Cr(VI) at the magnetite–water interface by calcium carbonate coatings. *Appl. Surf. Sci.* 230:260–271.
- Duff, M.C., D.B. Hunter, I.R. Triay et al. 1999. Mineral associations and average oxidation states of sorbed Pu on tuff. *Environ. Sci. Technol.* 33:2163–2169.
- Dunnivant, F.M., R.P. Schwarzenbach, and D.L. Macalady. 1992. Reduction of substituted nitrobenzenes in aqueous solutions containing natural organic matter. *Environ. Sci. Technol.* 26:2133–2141.
- Eary, L.E., and D. Rai. 1989. Kinetics of chromate reduction by ferrous ions derived from hematite and biotite at 25°C. *Am. J. Sci.* 289:180–213.
- El Aamrani, S., J. Gimenez, M. Rovira et al. 2007. A spectroscopic study of uranium(VI) interaction with magnetite. *Appl. Surf. Sci.* 253:8794–8797.
- Elsner, M., S.B. Haderlein, T. Kellerhals et al. 2004a. Mechanisms and products of surface-mediated reductive dehalogenation of carbon tetrachloride by Fe(II) on goethite. *Environ. Sci. Technol.* 38:2058–2066.
- Elsner, M., R.P. Schwarzenbach, and S.B. Haderlein. 2004b. Reactivity of Fe(II)-bearing minerals toward reductive transformation of organic contaminants. *Environ. Sci. Technol.* 38:799–807.
- Erbs, J.J., B. Gilbert, and R.L. Penn. 2008. Influence of size on reductive dissolution of six-line ferrihydrite. *J. Phys. Chem. C* 112:12127–12133.
- Erdem, M., F. Gur, and F. Tumen. 2004. Cr(VI) reduction in aqueous solutions by siderite. *J. Hazard. Mater.* 113:219–224.
- Ernstsen, V. 1996. Reduction of nitrate by Fe<sup>2+</sup> in clay minerals. *Clay. Clay Miner.* 44:599–608.
- Ernstsen, V., and S. Morup. 1992. Nitrate reduction in clayey till by Fe(II) in clay-minerals. *Hyperfine Interact.* 70:1001–1004.
- Faust, G.T. 1940. Staining of clay minerals as a rapid means of identification in natural and beneficiation products. Report of Investigation 3522. Bureau of Mines, Washington, DC.
- Feng, X.H., W.F. Tan, F. Liu, H.D. Ruan, and J.Z. He. 2006a. Oxidation of As-III by several manganese oxide minerals in absence and presence of goethite. *Acta Geol. Sin.* 80:249–256.
- Feng, X.H., L.M. Zhai, W.F. Tan, F. Liu, and J.Z. He. 2007. Adsorption and redox reactions of heavy metals on synthesized Mn oxide minerals. *Environ. Pollut.* 147:366–373.
- Feng, X.H., Y.Q. Zu, W.F. Tan, and F. Liu. 2006b. Arsenite oxidation by three types of manganese oxides. *J. Environ. Sci.* 18:292–298.
- Field, J.A., F.J. Cervantes, F.P. van der Zee, and G. Lettinga. 2000. Role of quinones in the biodegradation of priority pollutants: A review. *Water Res.* 42:215–222.
- Fife, T.H., and T.J. Przystas. 1985. Divalent metal ion catalysis in the hydrolysis of ester of picolinic acid. Metal ion promoted hydroxide ion and water catalyzed reactions. *J. Am. Chem. Soc.* 107:1041–1047.
- Filip, Z., W. Flaig, and E. Ritz. 1977. Oxidation of some phenolic substances as influenced by clay minerals. *Soil Org. Matter Stud. Proc. Symp.* 2:91–96.
- Fimmen, R.L., R.M. Cory, Y.P. Chin, T.D. Trouts, and D.M. McKnight. 2007. Probing the oxidation–reduction properties of terrestrially and microbially derived dissolved organic matter. *Geochim. Cosmochim. Acta* 71:3003–3015.
- Flaig, W., H. Beutelspacher, and E. Rietz. 1975. Chemical composition and physical properties of humic substances, p. 1–211. In J.E. Gieseking (ed.) *Soil components*, Vol. 1. Organic components. Springer-Verlag, New York.
- Fowkes, F.M., H.A. Benesi, R.B. Ryland et al. 1960. Clay catalyzed decomposition of insecticides. *J. Agric. Food Chem.* 8:203–210.
- Furukawa, T., and G.W. Brindley. 1973. Adsorption and oxidation of benzidine and aniline by montmorillonite and hectorite. *Clay. Clay Miner.* 21:279–288.
- Gianfreda, L., G. Iamarino, R. Scelza, and M.A. Rao. 2006. Oxidative catalysts for the transformation of phenolic pollutants: A brief review. *Biocatal. Biotransform.* 24:177–187.
- Gilbert, B., and J.F. Banfield. 2005. Molecular-scale processes involving nanoparticulate minerals in biogeochemical systems. *Rev. Mineral. Geochem.* 59:109–155.
- Gonzalez, J.M., and D.A. Laird. 2004. Role of smectites and Al-substituted goethites in the catalytic condensation of arginine and glucose. *Clay. Clay Miner.* 52:443–450.
- Gonzalez, J.M., and D.A. Laird. 2006. Smectite-catalyzed dehydration of glucose. *Clay. Clay Miner.* 54:38–44.
- Graiver, D., K.W. Farminer, and R. Narayan. 2003. A review of the fate and effects of silicones in the environment. *J. Polym. Environ.* 11:129–136.

- Grassian, V.H. 2008. When size really matters: Size-dependent properties and surface chemistry of metal and metal oxide nanoparticles in gas and liquid phase environments. *J. Phys. Chem. C* 112:18303–18313.
- Gregory, K.B., P. Larese-Casanova, G.F. Parkin, and M.M. Scherer. 2004. Abiotic transformation of hexahydro-1,3,5-trinitro-1,3,5-triazine by Fe<sup>II</sup> bound to magnetite. *Environ. Sci. Technol.* 38:1408–1414.
- Haffenden, L.J.W., and V.A. Yaylayan. 2005. Mechanism of formation of redox-reactive hydroxylated benzenes and pyrazine in <sup>13</sup>C-labelled glycine/D-glucose model systems. *J. Agric. Food Chem.* 53:9742–9746.
- Hakala, J.A., Y.P. Chin, and E.J. Weber. 2007. Influence of dissolved organic matter and Fe(II) on the abiotic reduction of pentachloronitrobenzene. *Environ. Sci. Technol.* 41:7337–7342.
- Hansen, H.C.B., S. Guldberg, M. Erbs, and C.B. Koch. 2001. Kinetics of nitrate reduction by green rusts—Effects of interlayer anion and Fe(II): Fe(III) ratio. *Appl. Clay Sci.* 18:81–91.
- Hansen, H.C.B., and C.B. Koch. 1998. Reduction of nitrate to ammonium by sulfate green rust: Activation energy and reaction mechanism. *Clay Miner.* 33:87–101.
- Hansen, H.C.B., C.B. Koch, H. NanckeKrogh, O.K. Borggaard, and J. Sorensen. 1996. Abiotic nitrate reduction to ammonium: Key role of green rust. *Environ. Sci. Technol.* 30:2053–2056.
- Hardie, A.G., J.J. Dynes, L.M. Kozak, and P.M. Huang. 2007. Influence of polyphenols on the integrated polyphenol–Maillard reaction humification pathway as catalyzed by birnessite. *Ann. Environ. Sci.* 1:91–110.
- Hardie, A.G., J.J. Dynes, L.M. Kozak, and P.M. Huang. 2009. Biomolecule-induced carbonate genesis in abiotic formation of humic substances in nature. *Can. J. Soil Sci.* 89:445–453.
- Hatcher, P.G., I.A. Breger, and M.A. Mattingly. 1980. Structural characteristics of fulvic acids from continental shelf sediments. *Nature* 285:560–562.
- Hatcher, P.G., M. Schnitzer, L.W. Dennis, and G.E. Maciel. 1981. Aromaticity of humic substances in soils. *Soil Sci. Soc. Am. J.* 45:1089–1094.
- Hättenschwiler, S., and P.M. Vitousek. 2000. The role of polyphenols in terrestrial ecosystem nutrient cycling. *Trends Ecol. Evol.* 15:238–243.
- Hauser, E.A., and M.B. Legget. 1940. Color reactions between clays and amines. *J. Am. Chem. Soc.* 62:1811–1814.
- Hayes, M.H.B., and R.S. Swift. 1978. The chemistry of soil organic colloids, p. 179–319. *In* D.J. Greenland and M.H.B. Hayes (eds.) *The chemistry of soil constituents*. John Wiley & Sons, New York.
- Hem, J.D. 1978. Redox processes at surfaces of manganese oxide and their effects on aqueous metal ions. *Chem. Geol.* 21:199–218.
- Hightower, J.W., W.N. Delgass, E. Iglesia, and A.T. Bell. 1996. *Studies in surface science and catalysis*. Elsevier, Amsterdam, the Netherlands.
- Ho, C.-T. 1996. Thermal generation of Maillard aromas, p. 27–35. *In* R. Ikan (ed.) *The Maillard reaction. Consequences for the chemical and life sciences*. John Wiley & Sons, Chichester, U.K.
- Hochella, M.F., S.K. Lower, P.A. Maurice, R.L. Penn, M. Sahai, D.L. Sparks, and B.S. Twining. 2008. Nanominerals, mineral nanoparticles, and earth systems. *Science* 319:1631–1635.
- Hoffmann, M.R. 1980. Trace metal catalysis in aquatic environments. *Environ. Sci. Technol.* 14:1061–1066.
- Hoffmann, M.R. 1990. Catalysis in aquatic environments, p. 71–111. *In* W. Stumm (ed.) *Aquatic chemical kinetics*. John Wiley & Sons, New York.
- Hofstetter, T.B., A. Neumann, and R.P. Schwarzenbach. 2006. Reduction of nitroaromatic compounds by Fe(II) species associated with iron-rich smectites. *Environ. Sci. Technol.* 40:235–242.
- Hofstetter, T.B., R.P. Schwarzenbach, and S.B. Haderlein. 2003. Reactivity of Fe(II) species associated with clay minerals. *Environ. Sci. Technol.* 37:519–528.
- Houghton, R.P. 1979. *Metal complexes in organic chemistry*. Cambridge University Press, Cambridge, U.K.
- Hua, B., and B.L. Deng. 2008. Reductive immobilization of uranium(VI) by amorphous iron sulfide. *Environ. Sci. Technol.* 42:8703–8708.
- Huang, P.M. 1990. Role of soil minerals in transformation of natural organics and xenobiotics in soil, p. 29–115. *In* J.-M. Bollag and G. Stozky (eds.) *Soil biochemistry*, Vol. 6. Marcel Dekker, New York.
- Huang, P.M. 1991a. Ionic factors affecting the formation of short-range ordered aluminosilicates. *Soil Sci. Soc. Am. J.* 55:1172–1180.
- Huang, P.M. 1991b. Kinetics of redox reactions on surfaces of Mn oxides and its impact on environmental quality, p. 191–230. *In* D.L. Sparks and D.L. Suares (eds.) *Rates of chemical processes in soils*. SSSA Special Publication 27. SSSA, Madison, WI.
- Huang, P.M. 2004. Soil mineral–organic matter–microorganism interactions: Fundamentals and impacts. *Adv. Agron.* 82:391–472.
- Huang, P.M., and R. Fujii. 1996. Selenium and arsenic, p. 793–831. *In* D.L. Sparks (ed.) *Methods of soil analysis: Part 3. Chemical methods*. SSSA, Madison, WI.
- Huang, P.M., and A.G. Hardie. 2009. Formation mechanisms of humic substances in the environment, p. 41–109. *In* N. Senesi, B. Xing, and P.M. Huang (eds.) *Biophysico-chemical processes involving natural non-living organic matter in environmental systems*, Vol. 2. Wiley–IUPAC series in biophysico-chemical processes in environmental systems. John Wiley & Sons, Hoboken, NJ.
- Huang, P.M., M.K. Wang, and C.Y. Chiu. 2005. Soil mineral–organic matter–microbe interactions: Impacts on biogeochemical processes and biodiversity in soils. *Pedobiologia* 49:609–635.
- Hulth, S., R.C. Aller, and F. Gilbert. 1999. Coupled anoxic nitrification/manganese reduction in marine sediments. *Geochim. Cosmochim. Acta* 63:49–66.

- Huygens, D., P. Boeckx, P. Templer et al. 2008. Mechanisms for retention of bioavailable nitrogen in volcanic rainforest soils. *Nature Geosci.* 1:543–548.
- Ikan, R., Y. Rubinsztain, A. Nissenbaum, and I.R. Kaplan. 1996. Geochemical aspects of the Maillard reaction, p. 1–25. *In* R. Ikan (ed.) *The Maillard reaction: Consequences for the chemical and life sciences*. John Wiley & Sons, Chichester, U.K.
- Iler, R.K. 1979. *The chemistry of silica*. John Wiley & Sons, New York.
- Ilton, E.S., A. Haiduc, C.O. Moses et al. 2004. Heterogeneous reduction of uranyl by micas: Crystal chemical and solution controls. *Geochim. Cosmochim. Acta* 68:2417–2435.
- Ilton, E.S., and D.R. Veblen. 1994. Chromium sorption by phlogopite and biotite in acidic solutions at 25°C: Insights from X-ray photoelectron spectroscopy and electron microscopy. *Geochim. Cosmochim. Acta* 58:2777–2788.
- Jang, J.H., and B.A. Dempsey. 2008. Coadsorption of arsenic(III) and arsenic(V) onto hydrous ferric oxide: Effects on abiotic oxidation of arsenic(III), extraction efficiency, and model accuracy. *Environ. Sci. Technol.* 42:2893–2898.
- Jauregui, M.A., and H.M. Reisenauer. 1982. Dissolution of oxides of manganese and iron by root exudate components. *Soil Sci. Soc. Am. J.* 46:314–317.
- Jenne, E.A. 1977. Trace element sorption by sediments and soils-sites and processes, p. 425–553. *In* W.R. Chappell and K.K. Peterson (eds.) *Molybdenum in the environment*, Vol. 2. Marcel Dekker, New York.
- Jeon, B.H., B.A. Dempsey, and W.D. Burgos. 2003. Kinetics and mechanisms for reactions of Fe(II) with iron(III) oxides. *Environ. Sci. Technol.* 37:3309–3315.
- Jeon, B.H., B.A. Dempsey, W.D. Burgos, M.O. Barnett, and E.E. Roden. 2005. Chemical reduction of U(VI) by Fe(II) at the solid–water interface using natural and synthetic Fe(III) oxides. *Environ. Sci. Technol.* 39:5642–5649.
- Jernberg, K.M., and W.L. Philip. 1999. Fate of famoxadone in the environment. *Pestic. Sci.* 55:587–589.
- Jokic, A., A.I. Frenkel, and P.M. Huang. 2001a. Effect of light on birnessite catalysis of the Maillard reaction and its implication in humification. *Can. J. Soil Sci.* 81:277–283.
- Jokic, A., A.I. Frenkel, M.A. Vairavamurthy, and P.M. Huang. 2001b. Birnessite catalysis of the Maillard reaction: Its significance in natural humification. *Geophys. Res. Lett.* 28:3899–3902.
- Jokic, A., H.-R. Schulten, J.N. Cutler, M. Schnitzer, and P.M. Huang. 2004a. A significant abiotic pathway for the formation of *unknown* nitrogen in nature. *Geophys. Res. Lett.* 31:L05502.
- Jokic, A., H.-R. Schulten, J.N. Cutler, M. Schnitzer, and P.M. Huang. 2005. Catalysis of the Maillard reaction by  $\delta$ -MnO<sub>2</sub>: A significant abiotic sorptive condensation pathway for the formation of refractory N-containing biogeomacromolecules in nature, p. 127–152. *In* P.M. Huang, A. Violante, J.-M. Bollag, and P. Vityakon (eds.) *Soil abiotic and biotic interactions and impact on the ecosystem and human welfare*. Science Publishers Inc., Enfield, NH.
- Jokic, A., M.C. Wang, C. Liu, A.I. Frenkel, and P.M. Huang. 2004b. Integration of the polyphenol and Maillard reactions into a unified abiotic pathway for humification in nature: The role of  $\delta$ -MnO<sub>2</sub>. *Org. Geochem.* 35:747–762.
- Jokic, A., Z. Zimpel, P.M. Huang, and P.G. Mezey. 2001c. Molecular shape analysis of a Maillard reaction intermediate. *SAR QSAR Environ. Res.* 12:297–307.
- Jung, H., J.W. Kim, H. Choi, J.H. Lee, and H.G. Hur. 2008a. Synthesis of nanosized biogenic magnetite and comparison of its catalytic activity in ozonation. *Appl. Catal. B* 83:208–213.
- Jung, J.W., S. Lee, H. Ryu, K.H. Kang, and K. Nam. 2008b. Detoxification of phenol through bound residue formation by birnessite in soil: Transformation kinetics and toxicity. *J. Environ. Sci. Health. Part A Toxic/Hazard. Subst. Environ. Eng.* 43:255–261.
- Jung, Y., J. Choi, and W. Lee. 2007. Spectroscopic investigation of magnetite surface for the reduction of hexavalent chromium. *Chemosphere* 68:1968–1975.
- Kang, K.H., J. Dec, H. Park, and J.M. Bollag. 2004. Effect of phenolic mediators and humic acid on cyprodinil transformation in presence of birnessite. *Water Res.* 38:2737–2745.
- Kang, K.H., D.M. Lim, and H. Shin. 2006. Oxidative-coupling reaction of TNT reduction products by manganese oxide. *Water Res.* 40:903–910.
- Kappler, A., and S.B. Haderlein. 2003. Natural organic matter as reductant for chlorinated aliphatic pollutants. *Environ. Sci. Technol.* 37:2714–2719.
- Keeneykennicut, W.L., and J.W. Morse. 1985. The redox chemistry of Pu(V)O<sub>2</sub><sup>+</sup> interaction with common mineral surfaces in dilute solutions and seawater. *Geochim. Cosmochim. Acta* 49:2577–2588.
- Kemper, J.M., E. Ammar, and W.A. Mitch. 2008. Abiotic degradation of hexahydro-1,3,5-trinitro-1,3,5-triazine in the presence of hydrogen sulfide and black carbon. *Environ. Sci. Technol.* 42:2118–2123.
- Kersting, A.B., D.W. Efurud, D.L. Finnegan et al. 1999. Migration of plutonium in ground water at the Nevada test site. *Nature* 397:56–59.
- Ketelaar, J.A.A., H.R. Gersmann, and M.M. Beck. 1956. Metal-catalysed hydrolysis of thiophosphoric esters. *Nature* 177:392–396.
- Kim, D., and T.J. Strathmann. 2007. Role of organically complexed iron(II) species in the reductive transformation of RDX in anoxic environments. *Environ. Sci. Technol.* 41:1257–1264.
- Kirsch, R., A.C. Scheinost, A. Rossberg, D. Banerjee, and L. Charlet. 2008. Reduction of antimony by nano-particulate magnetite and mackinawite. *Mineral. Mag.* 72:185–189.
- Klier, K., and K. Kuchynka. 1966. Carbon monoxide oxidation and adsorbate-gas exchange reactions on MnO<sub>2</sub>-based catalysts. *J. Catal.* 6:62–71.
- Klupinski, T.P., and Y.P. Chin. 2003. Abiotic degradation of trifluralin by Fe(II): Kinetics and transformation pathways. *Environ. Sci. Technol.* 37:1311–1318.

- Klupinski, T.P., Y.P. Chin, and S.J. Traina. 2004. Abiotic degradation of pentachloronitrobenzene by Fe(II): Reactions on goethite and iron oxide nanoparticles. *Environ. Sci. Technol.* 38:4353–4360.
- Kodaka, R., T. Sugano, T. Katagi, and Y. Takimoto. 2003. Clay-catalyzed nitration of a carbamate fungicide diethofencarb. *J. Agric. Food Chem.* 51:7730–7737.
- Kolthoff, I.M. 1921. Iodometric studies. VII. Reactions between arsenic trioxide and iodine. *Anal. Chem.* 60:393–406.
- Kresge, A.J. 1975. Water makes proton transfer fast. *Acc. Chem. Res.* 8:354–360.
- Kriegman-King, M.R., and M. Reinhard. 1994. Transformation of carbon tetrachloride by pyrite in aqueous solution. *Environ. Sci. Technol.* 28:692–700.
- Krishnamurti, G.S.R., and P.M. Huang. 1987. The catalytic role of birnessite in the transformation of iron. *Can. J. Soil Sci.* 67:533–543.
- Krishnamurti, G.S.R., and P.M. Huang. 1988. Influence of manganese oxide minerals on the formation of iron oxides. *Clay Clay Miner.* 36:467–475.
- Kroll, H. 1952. The participation of heavy metal ions in the hydrolysis of amino acid esters. *J. Am. Chem. Soc.* 74:2036–2039.
- Kumada, K., and H. Kato. 1970. Browning of pyrogallol as affected by clay minerals. *Soil Sci. Plant Nutr.* 16:195–200.
- Kummert, R., and W. Stumm. 1980. The surface complexation of organic acids on hydrous- $\text{Al}_2\text{O}_3$ . *J. Colloid Interface Sci.* 75:373.
- Kung, K.-H., and M.B. McBride. 1988. Electron transfer processes between hydroquinone and hausmannite ( $\text{Mn}_3\text{O}_4$ ). *Clay Clay Miner.* 36:297–302.
- Kyuma, K., and K. Kawaguchi. 1964. Oxidative changes of polyphenols as influenced by allophone. *Soil Sci. Soc. Am. Proc.* 28:371–374.
- Laha, S., and R.G. Luthy. 1990. Oxidation of aniline and other primary aromatic amines by manganese dioxide. *Environ. Sci. Technol.* 24:363–373.
- Lee, J.S.K., and P.M. Huang. 1995. Photochemical effect on the abiotic transformation of polyphenols as catalyzed by Mn(IV) oxide, p. 177–189. *In* P.M. Huang, J. Berthelin, J.-M. Bollag, W.B. McGill, and A.L. Page (eds.) *Environmental impact of soil component interactions*, Vol. 1. Natural and anthropogenic organics. Lewis Publishers, Boca Raton, FL.
- Lee, W., and B. Batchelor. 2002a. Abiotic reductive dechlorination of chlorinated ethylenes by iron-bearing soil minerals. 1. Pyrite and magnetite. *Environ. Sci. Technol.* 36:5147–5154.
- Lee, W., and B. Batchelor. 2002b. Abiotic, reductive dechlorination of chlorinated ethylenes by iron-bearing soil minerals. 2. Green rust. *Environ. Sci. Technol.* 36:5348–5354.
- Lee, W., and B. Batchelor. 2003. Reductive capacity of natural reductants. *Environ. Sci. Technol.* 37:535–541.
- Lee, W.J., and B. Batchelor. 2004. Abiotic reductive dechlorination of chlorinated ethylenes by iron-bearing phyllosilicates. *Chemosphere* 56:999–1009.
- Lehmann, R.G., and H.H. Cheng. 1988. Reactivity of phenolic acids in soils and formation of oxidation products. *Soil Sci. Soc. Am. J.* 52:352–356.
- Lehmann, R.G., H.H. Cheng, and J.B. Harsh. 1987. Oxidation of phenolic acids by soil iron and manganese oxides. *Soil Sci. Soc. Am. J.* 51:352–356.
- Leuz, A.K., H. Monch, and C.A. Johnson. 2006. Sorption of Sb(III) and Sb(V) to goethite: Influence on Sb(III) oxidation and mobilization. *Environ. Sci. Technol.* 40:7277–7282.
- Li, F.B., C.S. Liu, C.H. Liang, X.Z. Li, and L.J. Zhang. 2008. The oxidative degradation of 2-mercaptobenzothiazole at the interface of beta- $\text{MnO}_2$  and water. *J. Hazard. Mater.* 154:1098–1105.
- Li, H., L.S. Lee, D.G. Schulze, and C.A. Guest. 2003. Role of soil manganese in the oxidation of aromatic amines. *Environ. Sci. Technol.* 37:2686–2693.
- Lide, D.R. 2008. *CRC Handbook of chemistry and physics*, 89th Ed. CRC Press, Boca Raton, FL.
- Liger, E., L. Charlet, and P. Van Cappellen. 1999. Surface catalysis of uranium(VI) reduction by iron(II). *Geochim. Cosmochim. Acta* 63:2939–2955.
- Lin, Y.T., and C.P. Huang. 2008. Reduction of chromium(VI) by pyrite in dilute aqueous solutions. *Sep. Purif. Technol.* 63:191–199.
- Liu, C., and P.M. Huang. 2000. Catalytic effects of hydroxy-aluminum and silicic acid on catechol humification, p. 37–51. *In* E. Ghabbour and G. Davies (eds.) *Humic substances: Components of plants, soil and water*. Royal Society of Chemistry, Cambridge, U.K.
- Liu, C., and P.M. Huang. 2001. The influence of catechol humification on surface properties of metal oxides, p. 253–270. *In* E. Ghabbour and G. Davies (eds.) *Humic substances: Structure, models and functions*. Royal Society of Chemistry, Cambridge, U.K.
- Liu, C., and P.M. Huang. 2002. Role of hydroxy-aluminosilicate ions (proto-imogolite sol) in the formation of humic substances. *Org. Geochem.* 33:295–305.
- Liu, S.-Y., R.D. Minard, and J.-M. Bollag. 1981. Oligomerization of syringic acid, a lignin derived derivative, by a phenoloxidase. *Soil Sci. Soc. Am. J.* 45:110–1105.
- Livens, F.R., M.J. Jones, A.J. Hynes et al. 2004. X-ray absorption spectroscopy studies of reactions of technetium, uranium and neptunium with mackinawite. *J. Environ. Radioact.* 74:211–219.
- Loganathan, P., R.G. Bureau, and D.W. Fuerstenau. 1977. Influence of pH on the sorption of  $\text{Co}^{2+}$ ,  $\text{Zn}^{2+}$ , and  $\text{Ca}^{2+}$  by a hydrous manganese oxide. *Soil Sci. Soc. Am. J.* 41:57–62.
- Loyo, R.L.D., S.I. Nikitenko, A.C. Scheinost, and M. Simonoff. 2008. Immobilization of selenite on  $\text{Fe}_3\text{O}_4$  and  $\text{Fe}/\text{Fe}_3\text{C}$  ultrasmall particles. *Environ. Sci. Technol.* 42:2451–2456.
- Luther, G.W., and J.I. Popp. 2002. Kinetics of the abiotic reduction of polymeric manganese dioxide by nitrite: An anaerobic nitrification reaction. *Aquat. Geochem.* 8:15–36.
- Luther, G.W., B. Sundby, B.L. Lewis, P.J. Brendel, and N. Silverberg. 1997. Interactions of manganese with the nitrogen cycle: Alternative pathways to dinitrogen. *Geochim. Cosmochim. Acta* 61:4043–4052.

- Madden, A.S., and M.F. Hochella. 2005. A test of geochemical reactivity as a function of mineral size: Manganese oxidation promoted by hematite nanoparticles. *Geochim. Cosmochim. Acta* 69:389–398.
- Maillard, L.C. 1913. Formation de matières humiques par action de polypeptides sur sucres. *C.R. Acad. Sci.* 156:148–149.
- Manning, B.A., and S. Goldberg. 1997. Adsorption and stability of arsenic(III) at the clay mineral–water interface. *Environ. Sci. Technol.* 31:2005–2011.
- Masscheleyn, P.H., R.D. Delaune, and W.H. Patrick. 1990. Transformations of selenium as affected by sediment oxidation reduction potential and pH. *Environ. Sci. Technol.* 24:91–96.
- Mazumdar, A., T. Goldberg, and H. Strauss. 2008. Abiotic oxidation of pyrite by Fe(III) in acidic media and its implications for sulfur isotope measurements of lattice-bound sulfate in sediments. *Chem. Geol.* 253:30–37.
- McBride, M.B. 1979. Reactivity of adsorbed and structural iron in hectorite as indicated by oxidation of benzidine. *Clay. Clay Miner.* 27:224–230.
- McBride, M.B. 1994. *Environmental chemistry of soils*. Oxford University Press, London, U.K.
- McCormick, M.L., and P. Adriaens. 2004. Carbon tetrachloride transformation on the surface of nanoscale biogenic magnetite particles. *Environ. Sci. Technol.* 38:1045–1053.
- McKenzie, R.M. 1981. The surface charge on manganese dioxides. *Aust. J. Soil Res.* 19:41–50.
- McKenzie, R.M. 1989. Manganese oxides and hydroxides, p. 439–465. *In* J.B. Dixon and S.B. Weed (eds.) *Minerals in soil environments*. SSSA, Madison, WI.
- Mill, T., and W. Mabey. 1988. Hydrolysis of organic chemicals, p. 71–111. *In* O. Hutzinger (ed.) *The handbook of environmental chemistry*, Vol. 2D. Reactions and processes. Springer-Verlag, Berlin, Germany.
- Mingelgrin, U., and S. Saltzman. 1979. Surface reactions of parathion on clays. *Clay. Clay Miner.* 27:72–78.
- Mingelgrin, U., S. Saltzman, and B. Yaron. 1977. A possible model for the surface-induced hydrolysis of organo-phosphorus pesticides on kaolinite clays. *Soil Sci. Soc. Am. J.* 41:519–523.
- Mitsunobu, S., Y. Takahashi, and Y. Sakai. 2008. Abiotic reduction of antimony(V) by green rust ( $\text{Fe}_4(\text{II})\text{Fe}_2(\text{III})(\text{OH})_2\text{SO}_4 \cdot 3\text{H}_2\text{O}$ ). *Chemosphere* 70:942–947.
- Moore, J.W., and R.G. Pearson. 1981. *Kinetics and mechanisms*. John Wiley & Sons, New York.
- Morgenstern, A., and G.R. Choppin. 2002. Kinetics of the oxidation of Pu(IV) by manganese dioxide. *Radiochim. Acta* 90:69–74.
- Mortland, M.M. 1970. Clay-organic complexes and interactions. *Adv. Agron.* 22:75–115.
- Mortland, M.M. 1986. Mechanisms of adsorption of nonhumic organic species by clays, p. 59–76. *In* P.M. Huang and M. Schnitzer (eds.) *Interactions of soil minerals with natural organics and microbes*. SSSA, Madison, WI.
- Mortland, M.M., and L.J. Halloran. 1976. Polymerization of aromatic molecules on smectites. *Soil Sci. Soc. Am. J.* 40:367–370.
- Murray, J.W., and J.G. Dillard. 1979. The oxidation of cobalt(II) adsorbed on manganese dioxide. *Geochim. Cosmochim. Acta* 43:781–787.
- Myneni, S.C.B., T.K. Tokunaga, and G.E. Brown. 1997. Abiotic selenium redox transformations in the presence of Fe(II,III) oxides. *Science* 278:1106–1109.
- Naidja, A., P.M. Huang, and J.-M. Bollag. 1998. Comparison of the reaction products from the transformation of catechol catalyzed by birnessite or tyrosinase. *Soil Sci. Soc. Am. J.* 62:188–195.
- Naidja, A., P.M. Huang, and J.-M. Bollag. 2000. Enzyme-clay interactions and their impact on transformations of natural and anthropogenic organic compounds in soil. *J. Environ. Qual.* 29:677–691.
- Naka, D., D. Kim, R.F. Carbonaro, and T.J. Strathmann. 2008. Abiotic reduction of nitroaromatic contaminants by iron(II) complexes with organothiol ligands. *Environ. Toxicol. Chem.* 27:1257–1266.
- Naka, D., D. Kim, and T.J. Strathmann. 2006. Abiotic reduction of nitroaromatic compounds by aqueous iron(II)—Catechol complexes. *Environ. Sci. Technol.* 40:3006–3012.
- Nakata, K., S. Nagasaki, S. Tanaka et al. 2004. Reduction rate of neptunium(V) in heterogeneous solution with magnetite. *Radiochim. Acta* 92:145–149.
- Nannipieri, P., and L. Gianfreda. 1998. Kinetics of enzyme reactions in soil environments, p. 449–479. *In* P.M. Huang, N. Senesi, and J. Buffle (eds.) *Structure and surface reactions of soil particles*, Vol. 4. IUPAC Ser. on Analytical and physical chemistry of environmental systems. John Wiley & Sons, New York.
- Nasser, A., G. Sposito, and M.A. Cheney. 2000. Mechanochemical degradation of 2,4-D adsorbed on synthetic birnessite. *Colloid Surf. A* 163:117–123.
- Negra, C., D.S. Ross, and A. Lanzirrotti. 2005. Oxidizing behavior of soil manganese: Interactions among abundance, oxidation state, and pH. *Soil Sci. Soc. Am. J.* 69:87–95.
- Nesbitt, H.W., G.W. Canning, and G.M. Bancroft. 1998. XPS study of reductive dissolution of 7 angstrom-birnessite by  $\text{H}_3\text{AsO}_3$ , with constraints on reaction mechanism. *Geochim. Cosmochim. Acta* 62:2097–2110.
- Nicholas, D.R., S. Ramamoorthy, V. Palace et al. 2003. Biogeochemical transformations of arsenic in circumneutral freshwater sediments. *Biodegradation*. 14:123–137.
- Nikalje, M.D., P. Phukan, and A. Sudalai. 2000. Recent advances in clay-catalyzed organic transformations. *Org. Prep. Proced. Int.* 32:1–32.
- O’Loughlin, E.J., S.D. Kelly, R.E. Cook, R. Csencsits, and K.M. Kemner. 2003a. Reduction of uranium(VI) by mixed iron(II/iron(III) hydroxide (green rust): Formation of  $\text{UO}_2$  nanoparticles. *Environ. Sci. Technol.* 37:721–727.
- O’Loughlin, E.J., S.D. Kelly, K.M. Kemner, R. Csencsits, and R.E. Cook. 2003b. Reduction of Ag-I, Au-III, Cu-II, and Hg-II by Fe-II/Fe-III hydroxysulfate green rust. *Chemosphere* 53:437–446.

- Osano, O., W. Admiraal, H.J.C. Klamer, D. Pastor, and E.A.J. Bleeker. 2002. Comparative toxic and genotoxic effects of chloroacetanilides, formamidines and their degradation products on *Vibrio fischeri* and *Chironomus riparius*. *Environ. Pollut.* 119:195–202.
- Oscarson, D.W., P.M. Huang, C. Defosse, and A. Herbillon. 1981a. Oxidative power of Mn(IV) and Fe(III) oxides with respect to As(III) in terrestrial and aquatic environments. *Nature* 291:50–51.
- Oscarson, D.W., P.M. Huang, U.T. Hammer, and W.K. Liaw. 1983a. Oxidation and sorption of arsenite by manganese dioxide as influenced by surface coatings of iron and aluminum oxides and calcium carbonate. *Water Air Soil Pollut.* 20:233–244.
- Oscarson, D.W., P.M. Huang, and W.K. Liaw. 1980. The oxidation of arsenite by aquatic sediments. *J. Environ. Qual.* 9:700–703.
- Oscarson, D.W., P.M. Huang, and W.K. Liaw. 1981b. The kinetics and components involved in the oxidation of arsenite by freshwater sediments. *Verh. Int. Ver. Theor. Angew. Limnol.* 21:181–186.
- Oscarson, D.W., P.M. Huang, and W.K. Liaw. 1981c. The role of manganese in the oxidation of arsenite by freshwater lake sediments. *Clay Clay Miner.* 28:219–225.
- Oscarson, D.W., P.M. Huang, W.K. Liaw, and U.T. Hammer. 1983b. Kinetics of oxidation of arsenite by various manganese dioxides. *Soil Sci. Soc. Am. J.* 47:644–648.
- Pal, S., J.-M. Bollag, and P.M. Huang. 1994. Role of abiotic and biotic catalysts in the transformation of phenolic compounds through oxidative coupling reactions. *Soil Biol. Biochem.* 26:813–820.
- Park, B., and B.A. Dempsey. 2005. Heterogeneous oxidation of Fe(II) on ferric oxide at neutral pH and a low partial pressure of O<sub>2</sub>. *Environ. Sci. Technol.* 39:6494–6500.
- Park, D., C.K. Ahn, Y.M. Kim, Y.S. Yun, and J.M. Park. 2008a. Enhanced abiotic reduction of Cr(VI) in a soil slurry system by natural biomaterial addition. *J. Hazard. Mater.* 160:422–427.
- Park, D., S.R. Lim, Y.S. Yun, and J.M. Park. 2007. Reliable evidences that the removal mechanism of hexavalent chromium by natural biomaterials is adsorption-coupled reduction. *Chemosphere* 70:298–305.
- Park, D., Y.S. Yun, H.W. Lee, and J.M. Park. 2008b. Advanced kinetic model of the Cr(VI) removal by biomaterials at various pHs and temperatures. *Bioresour. Technol.* 99:1141–1147.
- Park, D., Y.S. Yun, and J.M. Park. 2004. Reduction of hexavalent chromium with the brown seaweed *Ecklonia* biomass. *Environ. Sci. Technol.* 38:4860–4864.
- Park, D., Y.S. Yun, and J.M. Park. 2005. Studies on hexavalent chromium biosorption by chemically-treated biomass of *Ecklonia* sp. *Chemosphere* 60:1356–1364.
- Pearson, R.G. 1966. Acids and bases. *Science* 151:172–177.
- Pearson, R.G. 1976. Symmetry rules for chemical reactions. Wiley-Interscience, New York.
- Pecher, K., S.B. Haderlein, and R.P. Schwarzenbach. 2002. Reduction of polyhalogenated methanes by surface-bound Fe(II) in aqueous suspensions of iron oxides. *Environ. Sci. Technol.* 36:1734–1741.
- Penrose, W.R. 1974. Arsenic in the marine and aquatic sediments: Analysis, occurrence and significance. *CRC Crit. Rev. Environ. Contr.* 4:465–482.
- Pepper, S.E., D.J. Bunker, N.D. Bryan et al. 2003. Treatment of radioactive wastes: An X-ray absorption spectroscopy study of the reaction of technetium with green rust. *J. Colloid Interface Sci.* 268:408–412.
- Peretyazhko, T., J.M. Zachara, S.M. Heald et al. 2008a. Heterogeneous reduction of Tc(VII) by Fe(II) at the solid-water interface. *Geochim. Cosmochim. Acta* 72:1521–1539.
- Peretyazhko, T., J.M. Zachara, S.M. Heald et al. 2008b. Reduction of Tc(VII) by Fe(II) sorbed on Al (hydr)oxides. *Environ. Sci. Technol.* 42:5499–5506.
- Peterson, M.L., G.E. Brown, and G.A. Parks. 1996. Direct XAFS evidence for heterogeneous redox reaction at the aqueous chromium/magnetite interface. *Colloid Surf. A* 107:77–88.
- Petrie, R.A., P.R. Grossl, and R.C. Sims. 2002. Oxidation of pentachlorophenol in manganese oxide suspensions under controlled Eh and pH environments. *Environ. Sci. Technol.* 36:3744–3748.
- Pinnavaia, T.J., P.L. Hall, S.S. Cady, and M.M. Mortland. 1974. Aromatic radical cation formation on the intracrystal surfaces of transition metal layer silicates. *J. Phys. Chem.* 78:994–999.
- Pizzigallo, M.D.R., A. Napola, M. Spagnuolo, and P. Ruggiero. 2004. Mechanochemical removal of organo-chlorinated compounds by inorganic components of soil. *Chemosphere* 55:1485–1492.
- Pizzigallo, M.D.R., P. Ruggiero, C. Crecchio, and G. Mascolo. 1998. Oxidation of chloroanilines at metal oxide surfaces. *J. Agric. Food Chem.* 46:2049–2054.
- Plastourgou, M., and M.R. Hoffmann. 1984. Transformation and fate of organic esters in layered-flow systems: The role of trace metal catalysis. *Environ. Sci. Technol.* 18:756–764.
- Pohlman, A.A., and J.G. McColl. 1989. Organic oxidation and manganese and aluminum mobilization in forest soils. *Soil Sci. Soc. Am. J.* 53:686–690.
- Porterfield, W.W. 1983. Inorganic chemistry. A unified approach. Harper International SI Edition, London, U.K.
- Powell, B.A., M.C. Duff, D.I. Kaplan et al. 2006. Plutonium oxidation and subsequent reduction by Mn(IV) minerals in Yucca Mountain tuff. *Environ. Sci. Technol.* 40:3508–3514.
- Powell, B.A., R.A. Fjeld, D.I. Kaplan, J.T. Coates, and S.M. Serkiz. 2004. Pu(V)O-2(+) adsorption and reduction by synthetic magnetite (Fe<sub>3</sub>O<sub>4</sub>). *Environ. Sci. Technol.* 38:6016–6024.
- Power, L.E., Y. Arai, and D.L. Sparks. 2005. Zinc adsorption effects on arsenite oxidation kinetics at the birnessite-water interface. *Environ. Sci. Technol.* 39:181–187.
- Pracht, J., J. Boenigk, M. Isenbeck-Schroter, F. Keppler, and H.F. Scholer. 2001. Abiotic Fe(III) induced mineralization of phenolic substances. *Chemosphere* 44:613–619.

- Rai, D., and R.J. Serne. 1977. Plutonium activities in soil solutions and the stability and formation of selected plutonium minerals. *J. Environ. Qual.* 6:89–95.
- Rakshit, S., C.J. Matocha, and M.S. Coyne. 2008. Nitrite reduction by siderite. *Soil Sci. Soc. Am. J.* 72:1070–1077.
- Rakshit, S., C.J. Matocha, and G.R. Haszler. 2005. Nitrate reduction in the presence of wustite. *J. Environ. Qual.* 34:1286–1292.
- Ratasuk, N., and M.A. Nanny. 2007. Characterization and quantification of reversible redox sites in humic substances. *Environ. Sci. Technol.* 41:7844–7850.
- Ribault, L.L. 1971. Presence d'une pellicule de silice amorphe a la surface de cristaux de quartz des formations sableuses. *C.R. Acad. Sci. Paris Ser. D* 272:1933–1936.
- Ross, D.S., and R.J. Bartlett. 1981. Evidence for non-microbial oxidation of manganese in soil. *Soil Sci.* 132:153–160.
- Rubert, K.F., and J.A. Pedersen. 2006. Kinetics of oxytetracycline reaction with a hydrous manganese oxide. *Environ. Sci. Technol.* 40:7216–7221.
- Runde, W., S.D. Conradson, D.W. Efurud et al. 2002. Solubility and sorption of redox-sensitive radionuclides (Np, Pu) in J-13 water from the Yucca Mountain site: Comparison between experiment and theory. *Appl. Geochem.* 17:837–853.
- Russell, J.D., M. Cruz, and J.L. White. 1968a. The adsorption of 3-aminotriazole by montmorillonite. *J. Agric. Food Chem.* 16:21–24.
- Russell, J.D., M. Cruz, and J.L. White. 1968b. Model of chemical degradation of *s*-triazines by montmorillonite. *Science* 160:1340–1342.
- Russo, F., M.A. Rao, and L. Gianfreda. 2005. Bioavailability of phenanthrene in the presence of birnessite-mediated catechol polymers. *Appl. Microbiol. Biotechnol.* 68:131–139.
- Salbu, B., O.C. Lind, and L. Skipperud. 2004. Radionuclide speciation and its relevance in environmental impact assessments. *J. Environ. Radioact.* 74:233–242.
- Salvestrini, S., S. Capasso, and P. Lovino. 2008. Catalytic effect of dissolved humic acids on the chemical degradation of phenylurea herbicides. *Pest Manag. Sci.* 64:768–774.
- Salzman, S., B. Yaron, and U. Minglegrin. 1974. The surface-catalyzed hydrolysis of parathion on kaolinite. *Soil Sci. Soc. Am. Proc.* 38:231–234.
- Sanchez-Camazano, M., and M.J. Sanchez-Martin. 1983. Montmorillonite-catalyzed hydrolysis of phosmet. *Soil Sci.* 136:89–93.
- Sassman, S.A., and L.S. Lee. 2007. Sorption and degradation in soils of veterinary ionophore antibiotics: Monensin and lasalocid. *Environ. Toxicol. Chem.* 26:1614–1621.
- Sassman, S.A., A.K. Sarmah, and L.S. Lee. 2007. Sorption of tylosin A, D, and A-aldol and degradation of tylosin A in soils. *Environ. Toxicol. Chem.* 26:1629–1635.
- Scheffer, F., B. Meyer, and E.A. Niederbudde. 1959. Huminstoffbildung unter katalytischer Einwirkung natürlich vorkommender Eisenverbindungen im modelversuch. *Z. Pflanzenernähr. Dung. Bodenkd.* 87:26–44.
- Scheidegger, A.M., D. Grolimund, D. Cui et al. 2003. Reduction of selenite on iron surfaces: A micro-spectroscopic study. *J. Phys. IV* 104:417–420.
- Scheinost, A.C., and L. Charlet. 2008. Selenite reduction by mackinawite, magnetite and siderite: XAS characterization of nanosized redox products. *Environ. Sci. Technol.* 42:1984–1989.
- Schnitzer, M. 1977. Recent findings on the characterization of humic substances extracted from soils from widely differing climatic zones, p. 77–101. *In Proceedings of the symposium on soil organic matter studies II. IAEA Bulletin, Vienna, Austria.*
- Schnitzer, M. 1978. Humic substances: Chemistry and reactions, p. 1–64. *In M. Schnitzer and S.U. Khan (eds.) Soil organic matter. Elsevier, Amsterdam, the Netherlands.*
- Schnitzer, M. 1982. Quo vadis soil organic matter research. *Trans. 12th Int. Congr. Soil Sci.* 5:67–78.
- Schnitzer, M., and K. Ghosh. 1982. Characteristics of water-soluble fulvic acid-copper and fulvic acid-iron complexes. *Soil Sci.* 134:354–363.
- Schnitzer, M., and M. Levesque. 1979. Electron spin resonance as a guide to the degree of humification of peats. *Soil Sci.* 127:140–145.
- Scott, T.B., G.C. Allen, P.J. Heard, and M.G. Randell. 2005. Reduction of U(VI) to U(IV) on the surface of magnetite. *Geochim. Cosmochim. Acta* 69:5639–5646.
- Senesi, N., and M. Schnitzer. 1977. The effect of pH, reaction time, chemical reduction and irradiation on ESR spectra of fulvic acids. *Soil Sci.* 123:224–234.
- Shaughnessy, D.A., H. Nitsche, C.H. Booth et al. 2003. Molecular interfacial reactions between Pu(VI) and manganese oxide minerals manganite and hausmannite. *Environ. Sci. Technol.* 37:3367–3374.
- Shcherbina, N.S., S.N. Kalmykov, I.V. Perminova, and A.N. Kovalenko. 2007a. Reduction of actinides in higher oxidation states by hydroquinone-enriched humic derivatives. *J. Alloy. Comp.* 444:518–521.
- Shcherbina, N.S., I.V. Perminova, S.N. Kalmykov et al. 2007b. Redox and complexation interactions of neptunium(V) with quinonoid-enriched humic derivatives. *Environ. Sci. Technol.* 41:7010–7015.
- Shin, J.Y., C.M. Buzgo, and M.A. Cheney. 2000. Mechanochemical degradation of atrazine adsorbed on four synthetic manganese oxides. *Colloid Surf. A* 172:113–123.
- Shin, J.Y., and M.A. Cheney. 2004. Abiotic transformation of atrazine in aqueous suspension of four synthetic manganese oxides. *Colloid Surf. A* 242:85–92.
- Shin, J.Y., and M.A. Cheney. 2005. Abiotic dealkylation and hydrolysis of atrazine by birnessite. *Environ. Toxicol. Chem.* 24:1353–1360.
- Shindo, H. 1992. Relative effectiveness of short-range ordered Mn(IV), Fe(III), Al, and Si oxides in the synthesis of humic acids from phenolic compounds. *Soil Sci. Plant Nutr.* 38:459–465.

- Shindo, H., and P.M. Huang. 1982. Role of Mn(IV) oxide in abiotic formation of humic substances in the environment. *Nature* 298:363–365.
- Shindo, H., and P.M. Huang. 1984a. Catalytic effects of manganese(IV), iron(III), aluminium, and silicon oxides on the formation of phenolic polymers. *Soil Sci. Soc. Am. J.* 48:927–934.
- Shindo, H., and P.M. Huang. 1984b. Significance of Mn(IV) oxide in abiotic formation of organic nitrogen complexes in natural environments. *Nature* 308:57–58.
- Shindo, H., and P.M. Huang. 1985a. The catalytic power of inorganic components in the abiotic synthesis of hydroquinone-derived polymers. *Appl. Clay Sci.* 1:71–81.
- Shindo, H., and P.M. Huang. 1985b. Catalytic polymerization of hydroquinone by primary minerals. *Soil Sci.* 139:505–511.
- Shindo, H., and P.M. Huang. 1992. Comparison of the influence of Mn(IV) oxide and tyrosinase on the formation of humic substances in the environment. *Sci. Total Environ.* 117/118:103–110.
- Sinclair, C.J., and A.B.A. Boxall. 2003. Assessing the ecotoxicity of pesticide transformation products. *Environ. Sci. Technol.* 37:4617–4625.
- Skovbjerg, L.L., S.L.S. Stipp, S. Utsunomiya, and R.C. Ewing. 2006. The mechanisms of reduction of hexavalent chromium by green rust sodium sulphate: Formation of Cr-goethite. *Geochim. Cosmochim. Acta* 70:3582–3592.
- Smith, M.B., and J. March. 2001. March's advanced organic chemistry reactions, mechanisms, and structure. John Wiley & Sons, New York.
- Smith, B.A., W.E. Siems, A.L. Teel, and R.J. Watts. 2006. Pyrolusite (beta-MnO<sub>2</sub>)-mediated, near dry-phase oxidation of 2,4,6-trichlorophenol. *Environ. Toxicol. Chem.* 25:1474–1479.
- Smolen, J.M., and A.T. Stone. 1998. Organophosphorus ester hydrolysis catalyzed by dissolved metals and metal-containing surfaces, p. 157–171. *In* P.M. Huang, D.C. Adriano, T.J. Logan, and R.T. Checkai (eds.) *Soil chemistry and ecosystem health*. SSSA, Madison, WI.
- Solomon, D.H. 1968. Clay minerals as electron acceptors and/or electron donors in organic reactions. *Clay. Clay Miner.* 16:31–39.
- Solomon, D.H., and D.G. Hawthorne. 1983. *Chemistry of pigments and fillers*. John Wiley & Sons, New York.
- Sorensen, K.C., J.W. Stucki, R.E. Warner, and M.J. Plewa. 2004. Alteration of mammalian-cell toxicity of pesticides by structural iron(II) in ferruginous smectite. *Environ. Sci. Technol.* 38:4383–4389.
- Sorensen, K.C., J.W. Stucki, R.E. Warner, E.D. Wagner, and M.J. Plewa. 2005. Modulation of the genotoxicity of pesticides reacted with redox-modified smectite clay. *Environ. Mol. Mutagen.* 46:174–181.
- Sorensen, J., and L. Thorling. 1991. Stimulation by lepidocrocite (gamma-FeOOH) of Fe(II)-dependant nitrite reduction. *Geochim. Cosmochim. Acta* 55:1289–1294.
- Sposito, G. 1984. *The surface chemistry of soils*. Oxford University Press, Oxford, U.K.
- Stanton, D.T. 1987. Glass-catalyzed decomposition of oxycarboxin in aqueous solution. *J. Agric. Food Chem.* 35:856–859.
- Steelink, C. 1994. Application of N-15 NMR spectroscopy to the study of organic nitrogen and humic substances in the soil, p. 405–427. *In* N. Senesi and D. Miano (eds.) *Humic substances in the global environment*. Elsevier, Amsterdam, the Netherlands.
- Steinberger, R., and F.H. Westheimer. 1949. The metal ion catalyzed decarboxylation of dimethylxaloacetic acid. *J. Am. Chem. Soc.* 71:4158–4159.
- Steinberger, R., and F.H. Westheimer. 1951. Metal ion-catalyzed decarboxylation: A model for an enzyme system. *J. Am. Chem. Soc.* 73:429–435.
- Stepniewska, Z., K. Bucior, and R.P. Bennicelli. 2004. The effects of MnO<sub>2</sub> on sorption and oxidation of Cr(III) by soils. *Geoderma* 122:291–296.
- Stevenson, F.J., and M. Schnitzer. 1982. Transmission electron microscopy of extracted fulvic and humic acids. *Soil Sci.* 133:179–185.
- Stollenwerk, K.G., G.N. Breit, A.H. Welch et al. 2007. Arsenic attenuation by oxidized aquifer sediments in Bangladesh. *Sci. Total Environ.* 379:133–150.
- Stone, A.T. 1987. Reductive dissolution of manganese(III)/(IV) oxides by substituted phenols. *Environ. Sci. Technol.* 21:979–988.
- Stone, A.T., and J.J. Morgan. 1984a. Reduction and dissolution of manganese(III) and manganese(IV) oxides by organics. 1. Reaction with hydroquinone. *Environ. Sci. Technol.* 18:450–456.
- Stone, A.T., and J.J. Morgan. 1984b. Reduction and dissolution of manganese(III) and manganese(IV) oxides by organics. 2. Survey of the reactivity of organics. *Environ. Sci. Technol.* 18:617–624.
- Stone, A.T., and A. Torrents. 1995. The role of dissolved metals and metal-containing surfaces in catalyzing the hydrolysis of organic pollutants, p. 275–298. *In* P.M. Huang, J. Berthelin, J.-M. Bollag, W.B. McGill, and A.L. Page (eds.) *Environmental impact of soil component interactions*, Vol. 1. Natural and anthropogenic organics. CRC Press/Lewis Publishers, Boca Raton, FL.
- Strathmann, T.J., and A.T. Stone. 2002. Reduction of oxamyl and related pesticides by Fe-II: Influence of organic ligands and natural organic matter. *Environ. Sci. Technol.* 36:5172–5183.
- Stumm, W. 1992. *Chemistry of the solid-water interface*. John Wiley & Sons, New York.
- Stumm, W., R. Kummert, and L. Sigg. 1980. A ligand exchange model for the adsorption of inorganic and organic ligands at hydrous interfaces. *Croat. Chem. Acta* 53:291.
- Su, C.M., and R.W. Puls. 2008. Arsenate and arsenite sorption on magnetite: Relations to groundwater arsenic treatment using zero valent iron and natural attenuation. *Water Air Soil Pollut.* 193:65–78.



- Szecsody, J.E., D.C. Girvin, B.J. Devary, and J.A. Campbell. 2004. Sorption and oxic degradation of the explosive CL-20 during transport in subsurface sediments. *Chemosphere* 56:593–610.
- Tebo, B.M., H.A. Johnson, J.K. McCarthy, and A.S. Templeton. 2005. Geomicrobiology of manganese(II) oxidation. *Trends Microbiol.* 13:421–428.
- Tennakoon, D.T.B., J.M. Thomas, and M.J. Tricker. 1974. Surface and intercalate chemistry of layer silicates. Part II. An iron-57 Mossbauer study of the role of lattice-substituted iron in the benzidine blue reaction of montmorillonite. *J. Chem. Soc. Dalton Trans.* 1974:2211–2215.
- Theng, B.K.G. 1974. The chemistry of clay-organic reactions. John Wiley & Sons, New York.
- Theng, B.K.G. 1979. Formation and properties of clay-polymer complexes. Elsevier Science Publishing, New York.
- Theng, B.K.G. 1982. Clay-activated organic reactions, p. 197–238. *In* H. van Olphen and F. Veniale (eds.) *Proc. Int. Clay Conf.* 1981. Elsevier, Amsterdam, the Netherlands.
- Thompson, I.A., D.M. Huber, C.A. Guest, and D.G. Schulze. 2005. Fungal manganese oxidation in a reduced soil. *Environ. Microbiol.* 7:1480–1487.
- Thompson, T.D., and J.F. Moll. 1973. Oxidative power of smectites measured by hydroquinone. *Clay. Clay Miner.* 21:337–350.
- Thorn, K.A., and M.A. Mikita. 2000. Nitrite fixation by humic substances: Nitrogen-15 nuclear magnetic resonance evidence for potential intermediates in chemodenitrification. *Soil Sci. Soc. Am. J.* 64:568–582.
- Tokunaga, T.K., J. Wan, A. Lanzirotti et al. 2007. Long-term stability of organic carbon-stimulated chromate reduction in contaminated soils and its relation to manganese redox status. *Environ. Sci. Technol.* 41:4326–4331.
- Torrents, A. 1992. Hydrolysis of organic esters at the mineral/water interface. Ph.D. Thesis. Johns Hopkins University, Baltimore, MD.
- Torrents, A., and A.T. Stone. 1991. Hydrolysis of phenyl picolinate at the mineral/water interface. *Environ. Sci. Technol.* 25:143–149.
- Torres-Canabate, P., E. Davidson, E. Bulygina, R. Garcia-Ruiz, and J. Carreira. 2008. Abiotic immobilization of nitrate in two soils of relic *Abies pinsapo*-fir forests under Mediterranean climate. *Biogeochemistry.* 91:1–11.
- Tournassat, C., L. Charlet, D. Bosbach, and A. Manceau. 2002. Arsenic(III) oxidation by birnessite and precipitation of manganese(II) arsenate. *Environ. Sci. Technol.* 36:493–500.
- Twigg, M.V. 1989. *Catalyst handbook*. Wolfe Publishing Ltd., London, U.K.
- Ulrich, H.J., and A.T. Stone. 1989. Oxidation of chlorophenols adsorbed to manganese oxide surfaces. *Environ. Sci. Technol.* 23:421–428.
- USEPA (United States Environmental Protection Agency). 2009. Commonly encountered radionuclides. USEPA, Washington, DC. Available online with updates at <http://www.epa.gov/radiation/radionuclides/index.html> (accessed on August 17, 2009).
- Vairavamurthy, A., and S. Wang. 2002. Organic nitrogen in geo-macromolecules: Insights on speciation and transformation with K-edge XANES spectroscopy. *Environ. Sci. Technol.* 36:3050–3056.
- Vikesland, P.J., A.M. Heathcock, R.L. Rebodos, and K.E. Makus. 2007. Particle size and aggregation effects on magnetite reactivity toward carbon tetrachloride. *Environ. Sci. Technol.* 41:5277–5283.
- Voudrias, E.A., and M. Reinhard. 1986. Abiotic organic reactions at mineral surfaces, p. 462–486. *In* J.A. Davis and K.F. Hayes (eds.) *Geochemical processes at mineral surfaces*. ACS Symp. Ser. 323. American Chemical Society, Washington, DC.
- Walse, S.S., K.D. Shimizu, and J.L. Ferry. 2002. Surface-catalyzed transformations of aqueous endosulfan. *Environ. Sci. Technol.* 36:4846–4853.
- Wang, S., and W.A. Arnold. 2003. Abiotic reduction of dinitroaniline herbicides. *Water Res.* 37:4191–4201.
- Wang, T.S.C., J.-H. Chen, and W.-M. Hsiang. 1985. Catalytic synthesis of humic acids containing various amino acids and dipeptides. *Soil Sci.* 140:3–10.
- Wang, M.C., and P.M. Huang. 1986. Humic macromolecule interlayering in nontronite through interaction with phenol monomers. *Nature* 323:529–531.
- Wang, M.C., and P.M. Huang. 1987. Polycondensation of pyrogallol and glycine and the associated reactions as catalyzed by birnessite. *Sci. Total Environ.* 62:435–442.
- Wang, M.C., and P.M. Huang. 1991. Nontronite catalysis in polycondensation of pyrogallol and glycine and the associated reactions. *Soil Sci. Soc. Am. J.* 55:1156–1161.
- Wang, M.C., and P.M. Huang. 1992. Significance of Mn(IV) oxide in the abiotic ring cleavage of pyrogallol in natural environments. *Sci. Total Environ.* 113:147–157.
- Wang, M.C., and P.M. Huang. 1994. Structural role of polyphenols in influencing the ring cleavage and related chemical reactions as catalyzed by nontronite, p. 173–180. *In* N. Senesi and T.M. Miano (eds.) *Humic substances in the global environment and implications on human health*. Elsevier, Amsterdam, the Netherlands.
- Wang, M.C., and P.M. Huang. 1997. Catalytic power of birnessite in abiotic formation of humic polycondensates from glycine and pyrogallol, p. 59–65. *In* J. Drozł, S.S. Gonet, N. Senesi, and J. Webber (eds.) *Proc. 8th Conf. International Humic Substances Society*. Wroclaw, Poland.
- Wang, M.C., and P.M. Huang. 2000a. Characteristics of pyrogallol-derived polymers formed by catalysis of oxides. *Soil Sci.* 165:737–747.
- Wang, M.C., and P.M. Huang. 2000b. Ring cleavage and oxidative transformation of pyrogallol catalyzed by Mn, Fe, Al, and Si, oxides. *Soil Sci.* 165:934–942.
- Wang, M.C., and P.M. Huang. 2003. Cleavage and polycondensation of pyrogallol and glycine catalyzed by natural soil clay. *Geoderma* 112:31–50.
- Wang, M.C., and P.M. Huang. 2005. Cleavage of <sup>14</sup>C-labelled glycine and its polycondensation with pyrogallol as catalyzed by birnessite. *Geoderma* 124:415–426.

- Wang, T.S.C., P.M. Huang, C.-H. Chou, and J.-H. Chen. 1986. The role of soil minerals in abiotic polymerization of phenolic compounds and formation of humic substances, p. 251–281. *In* P.M. Huang and M. Schnitzer (eds.) Interactions of soil minerals with natural organics and microbes. SSSA, Madison, WI.
- Wang, T.S.C., M.M. Kao, and P.M. Huang. 1980. The effect of pH on the catalytic synthesis of humic substances by illite. *Soil Sci.* 129:333–398.
- Wang, T.S.C., and S.W. Li. 1977. Clay minerals as heterogeneous catalysts in preparation of model humic substances. *Z. Pflanzenernähr. Dung. Bodenkd.* 140:669–676.
- Wang, D.J., J.Y. Shin, M.A. Cheney, G. Sposito, and T.G. Spiro. 1999. Manganese dioxide as a catalyst for oxygen-independent atrazine dealkylation. *Environ. Sci. Technol.* 33:3160–3165.
- Wang, T.S.C., M.C. Wang, and P.M. Huang. 1983. Catalytic synthesis of humic substances by using aluminas as catalysts. *Soil Sci.* 136:226–246.
- Wang, T.S.C., K.L. Yeh, S.Y. Cheng, and T.K. Yang. 1971. Behavior of soil phenolic acids, p. 113–120. *In* Biochemical interaction among plants. National Academy of Science, Washington, DC.
- Waychunas, G.A., C.S. Kim, and J.F. Banfield. 2005. Nanoparticulate iron oxide minerals in soils and sediments: Unique properties and contaminant scavenging mechanisms. *J. Nanopart. Res.* 7:409–433.
- Weaver, R.M., M.F. Hochella, and E.S. Ilton. 2002. Dynamic processes occurring at the Cr-aq(III)–manganite (gamma-MnOOH) interface: Simultaneous adsorption, microprecipitation, oxidation/reduction, and dissolution. *Geochim. Cosmochim. Acta* 66:4119–4132.
- Wehrli, B. 1990. Redox reactions of metal ions at mineral surfaces. *In* W. Stumm (ed.) Aquatic chemical kinetics. Wiley-Interscience, New York.
- Wehrli, B., and W. Stumm. 1989. Vanadyl in natural waters: Adsorption and hydrolysis promote oxygenation. *Geochim. Cosmochim. Acta* 53:69–77.
- Wehrli, B., E. Wieland, and G. Furrer. 1990. Chemical mechanism in the dissolution kinetics of minerals: The aspect of active sites. *Aquat. Sci.* 52:3–31.
- Wei, J., G. Furrer, S. Kaufmann, and R. Schulin. 2001. Influence of clay minerals on the hydrolysis of carbamate pesticides. *Environ. Sci. Technol.* 35:2226–2232.
- White, A.F., and M.L. Peterson. 1996. Reduction of aqueous transition metal species on the surfaces of Fe(II)-containing oxides. *Geochim. Cosmochim. Acta* 60:3799–3814.
- Wigginton, N.S., K.L. Haus, and M.F. Hochella. 2007. Aquatic environmental nanoparticles. *J. Environ. Monit.* 9:1306–1316.
- Wilk, P.A., D.A. Shaughnessy, R.E. Wilson, and H. Nitsche. 2005. Interfacial interactions between Np(V) and manganese oxide minerals manganite and hausmannite. *Environ. Sci. Technol.* 39:2608–2615.
- Wilkins, R.G. 1991. Kinetics and mechanisms of reactions of transition metal complexes, 2nd Ed. VCH Publishers, Weinheim, Germany.
- Williams, L.P. 1965. Michael Faraday. Chapman & Hall, London, U.K.
- Williams, A.G.B., and M.M. Scherer. 2004. Spectroscopic evidence for Fe(II)–Fe(III) electron transfer at the iron oxide–water interface. *Environ. Sci. Technol.* 38:4782–4790.
- Wilson, M.A., and K.M. Goh. 1977. Proton-decoupled pulse Fourier-transform <sup>13</sup>C nuclear magnetic resonance of soil organic matter. *J. Soil Sci.* 28:645–652.
- Wilson, M.A., N.H. Tran, A.S. Milev, G.S.K. Kannangara, H. Volk, and G.Q.M. Lu. 2008. Nanomaterials in soils. *Geoderma* 146:291–302.
- Wolff, S.P. 1996. Free radicals and glycation theory, p. 73–88. *In* R. Ikan (ed.) The Maillard reaction. Consequences for the chemical and life sciences. John Wiley & Sons, Chichester, U.K.
- Wong, J.W., and T. Shibamoto. 1996. Genotoxicity of the Maillard reaction products, p. 129–159. *In* R. Ikan (ed.) The Maillard reaction. Consequences for the chemical and life sciences. John Wiley & Sons, Chichester, U.K.
- Yan, L.B., and G.W. Bailey. 2001. Sorption and abiotic redox transformation of nitrobenzene at the smectite–water interface. *J. Colloid Interface Sci.* 241:142–153.
- Yaylayan, V.A. 1997. Classification of the Maillard reaction: A conceptual approach. *Trends Food Sci. Technol.* 8:13–18.
- Zhang, H.C., W.R. Chen, and C.H. Huang. 2008. Kinetic modeling of oxidation of antibacterial agents by manganese oxide. *Environ. Sci. Technol.* 42:5548–5554.
- Zhang, H.C., and C.H. Huang. 2005a. Oxidative transformation of fluoroquinolone antibacterial agents and structurally related amines by manganese oxide. *Environ. Sci. Technol.* 39:4474–4483.
- Zhang, H.C., and C.H. Huang. 2005b. Reactivity and transformation of antibacterial N-oxides in the presence of manganese oxide. *Environ. Sci. Technol.* 39:593–601.
- Zhao, L., Z.Q. Yu, P.A. Peng et al. 2006. Oxidation kinetics of pentachlorophenol by manganese dioxide. *Environ. Toxicol. Chem.* 25:2912–2919.
- Ziechmann, W. 1959. Die Darstellung von Huminsäuren im heterogenen System mit neutraler Reaktion. *Z. Pflanzenernähr. Dung. Bodenkd.* 84:155–159.

# Soil pH and pH Buffering

19.1	Introduction .....	19-1
19.2	Definition and Determination of Soil pH.....	19-1
	Definition of pH • Determination of pH with Electrodes • Determination of Soil pH Using pH-Sensitive Dyes	
19.3	Acids and Bases in Soil Solutions.....	19-3
	Weak Acids • Weak Bases	
19.4	Overview of Reactions Controlling pH and pH Buffering .....	19-4
19.5	Buffering by Soil Organic Matter.....	19-5
19.6	Proton and Al Exchange in Silicate Clays.....	19-7
19.7	pH-Dependent Charge Buffering by Mineral Components .....	19-7
	Oxides and Hydroxides of Iron and Aluminum • pH-Dependent Charges on Silicate ClayEdges • Imogolite and Allophane	
19.8	Buffering by Dissolution and Precipitation of Carbonates .....	19-9
19.9	H <sup>+</sup> Consumption by Irreversible Weathering of Aluminous Minerals.....	19-9
	Weathering of Primary Silicates • H <sup>+</sup> Consumption by the Destruction of High-Activity Clay	
19.10	Determination of Buffer Capacities.....	19-10
	Total Titratable Acidity • Lime Requirement • Calcium Carbonate Concentrations in Soil • Determination of the Buffering of H <sup>+</sup> Inputs in Noncalcareous Soils	
19.11	Soil Acidification.....	19-11
	Natural Acidification • Acid Rain • Acid-Producing Fertilizers • Acidification by Sulfur Compounds	
	References.....	19-12

Paul R. Bloom  
*University of Minnesota*

Ulf Skjellberg  
*Swedish University of  
Agricultural Sciences*

## 19.1 Introduction

Soil pH is a measure of soil acidity or alkalinity and is probably the single most important chemical characteristic of a soil. In the past, soil acidity or alkalinity, reported in pH units, was also referred to as “soil reaction” (Mason and Obenshain, 1939), and this term is occasionally still used in some publications. However, “soil reaction” is no longer used by soil chemists (SSSA, 2008). Because of the importance of acidity and alkalinity in soils, pH has been called a master variable (McBride, 1994), with knowledge of soil pH required to understand many chemical processes including ion mobility, precipitation and dissolution equilibria and kinetics, and oxidation–reduction equilibria. Soil pH also affects nutrient availability to plants and the negative response of many plant species to soil acidity.

Soils are a complex mixture of solid-phase components that react to yield a measured pH value. These components also buffer soils against pH changes caused by natural and anthropogenic inputs of acids and bases. Knowledge of the reactions that buffer soil pH is necessary for an understanding of natural soil weathering and the response of a soil to inputs of lime, acid-forming N fertilizers, acid-mine wastes, and acid rain. The discussion in

this chapter focuses on the reactions of components that buffer soil pH in upland soils. Factors affecting pH and buffering in flooded soils are discussed in Chapter 14.

## 19.2 Definition and Determination of Soil pH

Because pH is a term that is only defined for solutions, in a strict sense, it cannot be applied to a solid-phase material like soil. However, the chemical properties of the solid-phase components in soil define the pH of the soil solution, the water in soil pores (Chapter 12).

### 19.2.1 Definition of pH

The term pH was defined by Sorensen (1909) to provide a convenient way of representing the H<sup>+</sup> or OH<sup>-</sup> concentrations in aqueous solutions. As currently defined, pH is the negative logarithm, base 10, of H<sup>+</sup> activity, log (H<sup>+</sup>), where activity is the concentration adjusted for nonideality caused by charge–charge interactions with other ions in solution. In all except saline soils, the ionic interaction correction is small and the difference between

$H^+$  concentration and activity is small. The determination of  $H^+$  also provides a measurement of  $OH^-$  in solution. At 25°C in pure water, the relation between  $OH^-$  activity, ( $OH^-$ ), and  $H^+$  activity, ( $H^+$ ), is given by

$$K_w = (H^+)(OH^-) = 1.0 \times 10^{-14} \quad (19.1)$$

where  $K_w$  is the ionization constant for water. Expressing Equation 19.1 as negative logarithms yields

$$pH + pOH = 14 \quad (19.2)$$

where pOH is the negative logarithm of the  $OH^-$  activity.

### 19.2.2 Determination of pH with Electrodes

Soil pH is determined by measuring the pH after equilibrating soil with pure water or a salt solution (SSSA, 2008). The pH of a solution in equilibrium with a soil varies with the composition and concentration of the salts in the solution because cations in solution displace  $H^+$  and  $Al^{3+}$ , an acidic cation, from soil surfaces. Three common standard methods for determining pH in soils involve the suspension in distilled water, 0.01 M  $CaCl_2$  or 1 M KCl solutions, and measurement of the solution pH in the solution (Thomas, 1996). In the United States, the most commonly reported pH measurements are in 1:1 (weight:volume) suspensions of air-dried soil in distilled water. A suspension of soil is prepared (e.g., 10 g of soil and 10 mL of distilled water), stirred vigorously, and then allowed to stand for 10 min. The suspension is stirred again and the pH is measured with a glass pH electrode and a pH meter (Thomas, 1996). The pH can also be measured with an ion-sensitive field-effect transistor (ISFET) electrode. These solid-state devices are more robust than glass electrodes, have a more rapid response, and are well adapted for making field measurements of soil pH (Rossel and Walter, 2004). However, the solid-state electrodes are more expensive than glass electrodes.

The determination of soil pH in a 1:1 water suspension is expected to give a higher pH value than the soil solution at field water contents. The quantity of water added results in a dilution of the salts in the soil solution and a lower-equilibrium salt concentration. This effect is illustrated by the 0.4 unit increase in pH obtained for an increase in water content in the soil suspension from 1:1 to 1:10 (Thomas, 1996). The 1:1 water determination of pH is influenced by the natural seasonal variation in soil solution salt concentrations and the effects of soil management; for example, recent fertilization. Soil pH measured in water is reported as  $pH_{(H_2O)}$  or  $pH_w$ .

At low salt concentrations, an error due to the junction potential effect can occur in determination of  $pH_{(H_2O)}$ . A pH measurement requires contact with the solution by a glass electrode and a porous liquid junction of a reference electrode. This is necessary to complete the circuit between the pH-sensitive glass electrode and the reference electrode, which is often built in the same

body as the glass electrode to form a combination electrode. The filling solution for the reference electrode is a concentrated KCl solution, which slowly leaks into the test solution through a porous liquid junction. Because soils are cation exchangers, they can have a disproportionate effect on the rate of  $K^+$  diffusion compared to  $Cl^-$  diffusion into solution, which sets up a potential across the junction (Coleman et al., 1951). This can cause a reduction in the measured pH (Thomas, 1996).

The method for measurement of pH in 0.01 M  $CaCl_2$  is the same as for measurement of pH in distilled water (Thomas, 1996). Because of the displacement of  $H^+$  and  $Al^{3+}$  from soil materials by  $Ca^{2+}$ , pH in 0.01 M  $CaCl_2$  [ $pH_{(CaCl_2)}$ ] is on an average about 0.3–0.4 units lower than in water (Essington, 2004). The measurement of pH in 0.01 M  $CaCl_2$  results in reduction or elimination of the problems due to variation in soil solution salt concentration and it eliminates the junction potential effect. Calcium is used in the determination of pH because it is the predominant soil solution cation in soils of temperate regions. The 0.01 M concentration, however, is somewhat higher than that found in most soil solutions.

The measurement of pH in 1 M KCl suspensions also generally yields lower pH values than in water. However, for some subsurface horizons of highly weathered soils of the tropics, pH in KCl can actually be greater than in water (van Raij and Peech, 1972). This occurs in subsoils low in permanent charge silicate clays and low in organic matter. Oxides and hydroxides of iron and aluminum are the predominant ion exchangers in these soils and at very acid pH values they are anion exchangers (Section 19.7). The addition of KCl results in a displacement of  $OH^-$  by  $Cl^-$  and an increase in pH (McBride, 1994).

### 19.2.3 Determination of Soil pH Using pH-Sensitive Dyes

Rapid determination of soil pH can be made colorimetrically with pH indicator dyes. Colorimetric methods are based on the change in color that takes place upon disassociation of a weak acid or a weak base organic dye. In solution, a weak acid dye molecule can dissociate:

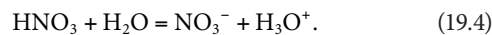


An increase in pH will cause a change in color as the undissociated dye, HI, changes to the dissociated form,  $I^-$ . Typically a mixture of dyes is used to yield color changes that take place over a wide range of pH. A dye solution is mixed with soil to make a slurry, and the dye is decanted from the soil so the color can be compared with a color chart. The pH measured in this manner corresponds with  $pH_{(H_2O)}$  measured with a glass electrode but is not as precise and can vary from the glass electrode results by as much as 0.4 units (Mason and Obenshain, 1939). Dye-impregnated pH papers also can be used to get quick pH measurement within 0.5 units of the true  $pH_{(H_2O)}$  (Thomas, 1996).

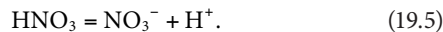
## 19.3 Acids and Bases in Soil Solutions

Soil solutions contain a mixture of weak acids and weak bases that buffer the pH of the solution. This buffering is small compared to the quantity of acidity or basicity (alkalinity) associated with the solid phases in soil and has little impact on soil pH buffering. However, the acid and base components in soil solutions directly impact plant roots and soil microbes and thus directly influence the vitality of the biotic community in a soil. Also, the acids and bases in soil solution directly impact mineral weathering and biogeochemical reactions involved in soil genesis.

In this chapter, we will use Brønsted's definition of acids and bases where an acid is a hydrogen ion ( $H^+$ ) donor and a base is an  $H^+$  acceptor (Stumm and Morgan, 1996). Because an  $H^+$  ion is just a proton, acids can be described as proton donors and bases as proton acceptors. According to this definition, reaction of an acid to lose a proton produces a conjugate base that can accept a proton; if the reaction is reversed. Conversely, a base that accepts a proton yields a conjugate acid. For example, when nitric acid donates protons to water, the base is  $H_2O$ . The reaction is

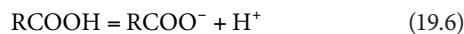


The nitrate anion is the conjugate base of nitric acid and the hydronium ion,  $H_3O^+$ , is the conjugate acid of water. Nitric acid is a strong acid because at all except very high  $H^+$  concentrations Reaction 19.4 goes all the way to the right and all of the  $HNO_3$  is ionized. The conjugate base of nitric acid, the nitrate anion, is a very weak base because it has very little tendency to accept protons. The above reaction in aqueous solution is often abbreviated to



### 19.3.1 Weak Acids

The weak acids in soil solutions include organic carboxylic acids,  $H_2CO_3$ , and  $Al^{3+}$ , a metal ion that undergoes hydrolysis. Carboxylic acids are organic compounds with one or more  $-COOH$  groups that have the potential to ionize to form the carboxylate anion,  $RCOO^-$ , according to the reaction



where

$RCOOH$  is any carboxylic acid

$R$  is an organic structure

Organic acids in soil solutions include simple acids like malic acid  $(COOH)CH_2CH(OH)CH_2(COOH)$  and citric acid  $(COOH)CH_2C(OH)(COOH)CH_2(COOH)$ , which are exuded from plant roots or by soil microbes. These acids generally have a short lifetime in soils because they are easily consumed by soil microbes. In addition, soil solutions contain macromolecular humified components produced by degradation of plant debris that can be operationally separated into humic and fulvic acids

(Chapter 11; Stevenson, 1994), with fulvic acids predominating in soil solutions. These natural organic acids are complex mixtures that contain carboxylic acid groups.

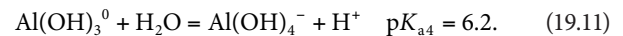
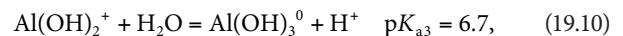
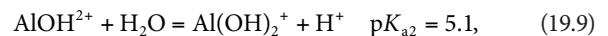
The strength (ability to donate protons) of a carboxylic acid is defined by the equilibrium constant:

$$K_a = \frac{(RCOO^-)(H^+)}{RCOOH} \quad (19.7)$$

where  $K_a$  is the acidity constant. Stronger acids have greater acidity constants. Often, the strength of a weak acid is given in terms of the negative log of the  $K_a$ , the  $pK_a$ . The lower the  $pK_a$  the greater the strength of the acid. At the pH equal to the  $pK_a$ , an acid is half ionized. At higher pH, it is more than half ionized, while at lower pH it is less than half ionized. Thus, at solution pH values less than the  $pK_a$ , a weak acid has a greater ability to donate protons than at higher pH values. Carboxylic acids in soil solution have  $pK_a$  values generally in the range of 3–5.

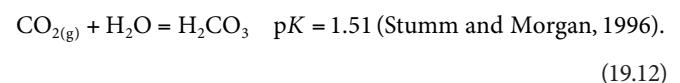
The soluble fulvic acids also contain phenolic groups,  $ArOH$ , where  $Ar$  is an aromatic six-carbon ring structure. Phenolic groups are generally much less concentrated than the carboxyl groups and they are much less acidic having  $pK$  values ranging from 7 to 11.

The  $Al^{3+}$  ion can be an important weak acid component in soil solutions of highly acid soils. This ion contributes to soil solution acidity and causes the acid toxicity response experienced by many plants in acid soils (Bloom et al., 2005; Fageria and Baligar, 2008). In water,  $Al^{3+}$  undergoes a series of hydrolysis reactions, which produce protons (Nordstrom and May, 1996):

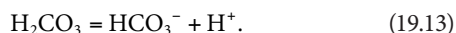


Although the second, third, and fourth hydrolysis reactions are important in determining the chemistry of  $Al$ , only the first hydrolysis reaction is a major source of protons in soil solution. The low solubility of solid  $Al(OH)_3$  limits the quantity of  $Al$  ions. At a pH of 5.0, a solution in equilibrium with  $Al(OH)_3$  has a total concentration of  $Al^{3+}$  of less than  $10^{-6}$  M (Nordstrom and May, 1996).

In soils, carbonic acid is also an important weak acid ( $H_2CO_3$ ) that is created by the dissolution of carbon dioxide:



When pH is increased, this acid ionizes to produce bicarbonate and  $H^+$ :



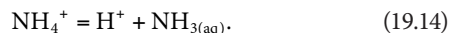
The  $pK_a$  for Reaction 19.13 is 6.35 (Stumm and Morgan, 1996) meaning that carbonic acid is a weaker acid than organic carboxylic acids or  $Al^{3+}$ . The concentrations of  $HCO_3^-$  in solution increase both with increase in pH and increase of concentration of  $CO_2$  in the air of soil pores. At a pH value above 6,  $HCO_3^-$  is often the predominant anion in soil solution.

For solutions in equilibrium with the earth's atmosphere,  $H_2CO_3$  is directly proportional to the partial pressure of atmospheric  $CO_2$ , which in 2007 was  $3.83 \times 10^{-4}$  atm. The concentration is increasing at the rate of  $0.014 \times 10^{-4}$  atm year<sup>-1</sup> (Anon, 2008). However, in soils where root and microbial respiration are active, the partial pressure can easily be 100 times greater (Fernandez and Kosian, 1987; Magnusson, 1992). This has a great effect on the content of  $HCO_3^-$  in soils (Andrews and Schlesinger, 2001).

### 19.3.2 Weak Bases

All of the anions of the weak acids above, as well as the hydrolyzed Al cations, are weak bases that can accept protons in the pH range found in soils. Because of the low  $pK_a$  values for organic acids and  $AlOH^{2+}$ , these ions are only important proton acceptors in very acid soils. For most neutral and alkaline soils, the concentration of bicarbonate determines the alkalinity of soil solutions, where alkalinity is defined as the quantity of strong acid needed to lower the pH of a solution to the end point for complete protonation of bicarbonate (about pH = 4.8) (Stumm and Morgan, 1996). The carbonate ion,  $CO_3^{2-}$ , is significant only in very high pH soils because the  $pK_a$  for the ionization of  $HCO_3^-$  to  $CO_3^{2-}$  is 10.33 (Stumm and Morgan, 1996).

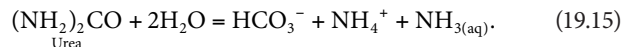
Under some conditions, solution ammonia,  $NH_{3(aq)}$ , is a significant base. These conditions are induced by the addition of fertilizer N as anhydrous ammonia [ $NH_{3(g)}$ ], or urea. When  $NH_{3(g)}$  is injected into a soil, it reacts with the soil solution to lower the  $H^+$  activity raising the pH. Ammonia is a conjugate base of  $NH_4^+$  and if the reaction in water is written like the weak acid reactions above:



The  $pK_a$  of this reaction is 9.5 (Stumm and Morgan, 1996) and in all except the highest pH soils, the reaction goes to the left consuming protons. This reaction creates localized pH values near anhydrous ammonia injection bands that can be >9.5 (Havlin et al., 2005).

Dissolution and hydrolysis of urea fertilizer in soils can also produce localized high concentrations of  $NH_{3(aq)}$  that can result in localized high pH. Fertilizer granules hydrolyze readily due

to the presence of urease enzymes in soils, resulting in an overall reaction:



The basicity effect of the  $NH_3$ -producing fertilizers is short-lived because biological oxidation of ammonium to nitrates produces two  $H^+$  ions, and the net effect is acidification.

## 19.4 Overview of Reactions Controlling pH and pH Buffering

Reactions of the solid-phase components control soil pH and are the reactions that buffer soil pH against rapid pH change with natural or anthropomorphic inputs of acids and bases (Bloom et al., 2005). Solid-phase soil materials have a much greater capacity to accept or donate protons than the soluble acids and bases in soil solution. Magdoff and Bartlett (1985) investigated the buffering in 51 surface soils of Vermont, USA by reacting these soils with  $H_2SO_4$  or  $CaCO_3$  for 30 days and determining the final pH in 0.01 M  $CaCl_2$ . They found maximal buffering (minimal slope of pH vs. added acid or  $CaCO_3$ ) to occur at both pH 3.5 or less and pH 7.5 or greater (Figure 19.1). The upper bound of the pH in the buffering shown in Figure 19.1 is fixed by the solubility of  $CaCO_3$  (Magdoff and Bartlett, 1985). They also showed that the buffer plot was generally linear in the pH range of 4.5–6.5, a range that encompasses most acid agricultural soils.

The pH-buffering reactions in soils include proton desorption and adsorption reactions with mineral and organic components as well as ion exchange, dissolution, and precipitation. Some of the soil components are effective in buffering over a wide range of pH values, while others are effective over a limited pH range (Table 19.1). The buffer ranges in Table 19.1 are those that were developed by Bloom et al. (2005) and are somewhat similar to those shown

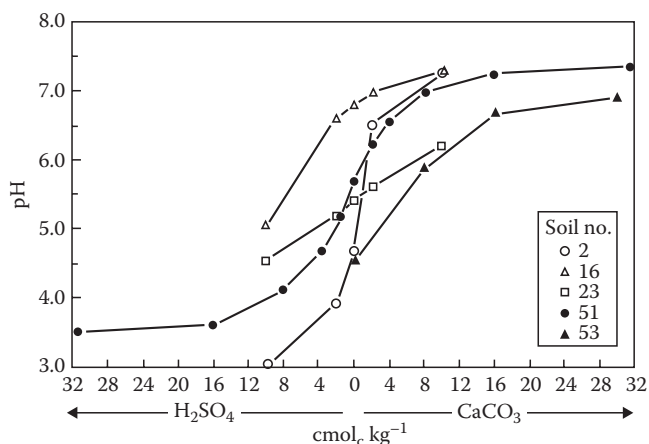


**FIGURE 19.1** Titration of surface soils from Vermont, U.S.A. with  $H_2SO_4$  and  $CaCO_3$ . The acid and base ( $CaCO_3$ ) additions are reported per gram of soils. The  $pH_{CaCl_2}$  was measured after a 30-day reaction at field capacity moisture content. (From Magdoff, F.R., and R.J. Bartlett, 1985. Soil pH buffering revisited. Soil Sci. Soc. Am. J. 49:145–148. With permission of Soil Science Society of America.)

**TABLE 19.1** Reactions of Solid-Phase Soil Components That Buffer pH in the Range of 3.5–9.5

pH Buffer Substance	pH Range	Proton Acceptor or Donation Reactions
Limestone, CaCO <sub>3</sub>	7–9.5	Dissolution and precipitation
Oxides and hydroxides of Fe and Al; silicate clay edges	Whole pH range	H <sup>+</sup> adsorption and desorption on surface hydroxyl sites
H <sup>+</sup> -SOM	Whole pH range	Dissociation and protonation of carboxyl and phenol groups
Al-SOM and Al(OH) <sub>3(s)</sub>	5–8	Precipitation of organic bound Al <sup>3+</sup> as Al(OH) <sub>3</sub> or dissolution of Al(OH) <sub>3</sub> by organic acids
Al <sup>3+</sup> /H <sup>+</sup> -exchange in SOM	Less than 4.5	H <sup>+</sup> exchange with Al <sup>3+</sup> on carboxyl and phenol groups
Al(OH) <sub>3</sub>	4–5.5	Al(OH) <sub>3</sub> dissolution/precipitation in soils with very low SOM content
Silicate clay interlayer Al(OH) <sub>n</sub> <sup>3-n</sup> in 2:1 clays	4.2–7	Hydrolysis and precipitation or dissolution of interlayer Al(OH) <sub>3</sub>
Permanent charge silicate clays	3.5–4.2	Ion exchange of H <sup>+</sup> and Al <sup>3+</sup>
Irreversible dissolution of high-activity 2:1 silicate clays and poorly ordered aluminosilicates	Less than 3.5	Consumes H <sup>+</sup> upon release of Al <sup>3+</sup> from reactive silicates
Very slow irreversible weathering primary silicate minerals	Whole pH range	Consumes H <sup>+</sup> upon dissolution of Ca <sup>2+</sup> , Mg <sup>2+</sup> , K <sup>+</sup> , and Na <sup>+</sup> from primary minerals

Source: Bloom, P.R., U.L. Skjellberg, and M.E. Sumner. 2005. Soil acidity, p. 411–460. In A. Tabatabai and D. Sparks (eds.) Chemical processes in soils. SSSA, Madison, WI.

by Ulrich (1991), with modifications and additions. For example, Ulrich did not include soil organic matter (SOM) and reactions on oxide and hydrous oxide surfaces. The buffer reactions in Table 19.1 will be discussed in more detail in Sections 19.5 through 19.9.

## 19.5 Buffering by Soil Organic Matter

Soil organic matter is a very important component of pH buffering in surface soils, even in typical upland soils that contain only a few percent organic matter. Like the soluble organic components in soil solution discussed in Section 19.3.1, SOM contains carboxyl and phenolic groups that can donate protons. Most of the acidity in SOM is contributed by the humidified components, operationally defined as humic and fulvic acid. In soils, some of the weak acid sites exchange protons with Al<sup>3+</sup>, which alters the proton donation behavior of SOM. Based on chemical analysis of humic and fulvic acids extracted from SOM (Chapter 11) various organic acids have been proposed to represent the acidity of carboxyl and phenolic sites in SOM. Most of the acidity is thought to arise from carboxyl and OH groups bound to aromatic ring structures, which can be represented by benzoic acid (Ar-COOH, pK<sub>a</sub> = 4.2) and phenol (Ar-OH, pK<sub>a</sub> = 10.0), where Ar is an aromatic ring (Smith et al., 2004).

Soil organic matter buffers pH over a wider range of pH values than predicted by a simple mixture of benzoic acid and phenol. The titration plots for two humic acids with an alkali metal hydroxide shown in Figure 19.2 illustrates that maximum buffering (minimal slope) is in the pH range of 4–6. At very low pH, the plots in Figure 19.2 have very low slopes because of the effect of dilution of acid on H<sup>+</sup> concentration as presented on a log (pH) scale. And at pH > 8.5, the buffering due to phenolic groups contributes to the low slope. A broadening of the buffering response occurs because the aromatic ring structures of the humic acid and fulvic acids are polysubstituted with carboxyl -COOH and phenolic -OH. This shifts the pK<sub>a</sub> values, resulting in aromatic ring structures with wide ranges of individual pK<sub>a</sub> values. Also, with the ionization of the acid sites, negative charges accumulate on

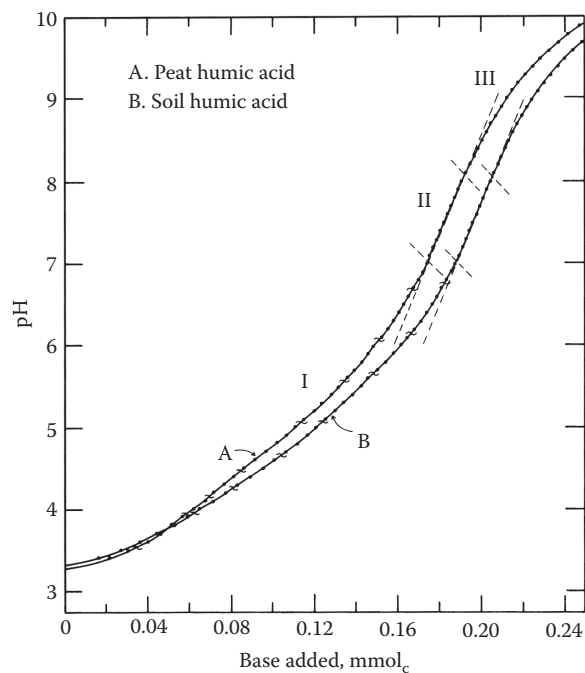


**FIGURE 19.2** Titration of 2 humic acids with strong base. (From Stevenson, F.J. 1994. Humus chemistry: Genesis, composition, reactions, 2nd Ed. Wiley, New York. Copyright Wiley-VCH Verlag GmbH & Co. KGaA. With permission.)

macromolecular structures and this charge reduces the proton donation ability of humic and fulvic acids at high pH values (McBride, 1994). The ionization of carboxyl groups is generally complete at pH 8 and the ionization of phenolic groups is complete at pH 11. Thus, common methods for determination of carboxyl acidity involve titrating to pH 8; and for the determination of the phenol titration to pH in excess of 11 (Stevenson, 1994). The negative charge sites produced by the ionization of the weak acid sites on humic and fulvic acids bind exchangeable cations. Organic matter contributes much of the pH-dependent cation exchange capacity (CEC) to soils (Chapter 16).

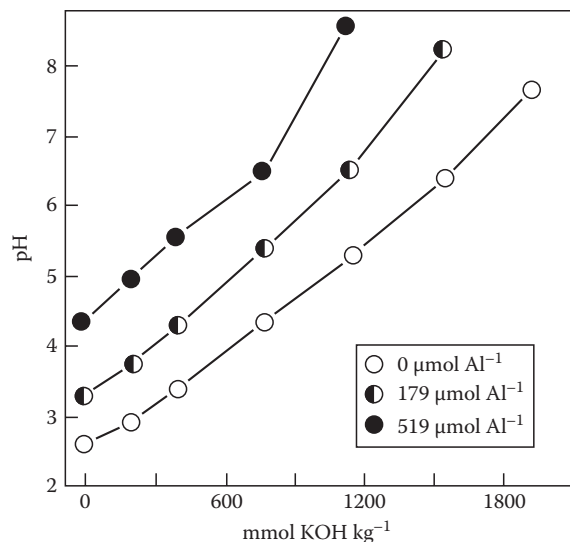
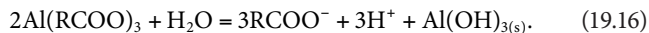


**FIGURE 19.3** Titration of Al-SOM containing different contents of Al<sup>3+</sup>. (From Hargrove, W.L., and G.W. Thomas. 1982. Titration properties of Al-organic matter. *Soil Sci.* 134:216–225. With permission of Wolters Kluwer Health.)

The binding of Al to acid functional groups in SOM is important both for Al chemistry and for pH buffering. In acid mineral soils, many of the carboxylate sites in SOM are bound to Al<sup>3+</sup>. This bonding is strong enough that only a small fraction of the Al can be extracted with 1 M KCl (Bloom et al., 1979), and most authors consider Al (and H<sup>+</sup>) bound to SOM to be nonexchangeable (Bertsch and Bloom, 1996). This strongly bound Al has a large effect on buffering. Hargrove and Thomas (1982) titrated SOM with varying Al<sup>3+</sup> contents and found that the pH buffering of the Al<sup>3+</sup>-treated SOM occurred at higher pH than for H<sup>+</sup>-saturated SOM (Figure 19.3). Aluminum-saturated SOM is a weaker acid than H<sup>+</sup>-saturated SOM.

As the pH of Al-SOM is raised to greater than about 5, the Al<sup>3+</sup> in solution exceeds the solubility of Al(OH)<sub>3</sub> and precipitation of amorphous Al(OH)<sub>3</sub> occurs (Walker et al., 1990). This can be illustrated by



This reaction is reversible and when the pH is lowered Al(OH)<sub>3</sub> dissolves and Al again becomes bound to organic matter. As with H<sup>+</sup>-SOM, increasing of pH by adding a base increases surface charge and the organic matter becomes more saturated with the cation of the base. In humic materials, except at very low pH, the pH is positively correlated with the saturation of cation exchange sites with the Ca<sup>2+</sup>, Mg<sup>2+</sup>, Na<sup>+</sup>, and K<sup>+</sup>; all cations of strong bases. In soil science, these are called “base cations” and a base saturation (BS) value, which is positively correlated to pH, can be calculated as a sum of charges of base cations divided by the CEC:

$$\text{BS} = \frac{2\text{Ca}^{2+} + 2\text{Mg}^{2+} + \text{Na}^+ + \text{K}^+}{\text{CEC}}. \quad (19.17)$$

In this calculation, the CEC value is determined at a reference pH of 7 or 8 (Bloom and Grigal, 1985; Ross et al., 2008). In less-acidic and neutral soils, the most abundant base cation is Ca<sup>2+</sup>.

As soils are acidified, base cations are displaced and the BS value decreases. At pH values less than 5, the BS is low and protons can displace soil adsorbed Al<sup>3+</sup> ions. This reaction results in a decrease in pH without a decrease in BS because H<sup>+</sup>-saturated SOM is a stronger acid than Al-saturated SOM. At pH less than 4.5, this exchange can add very significant quantities of Al<sup>3+</sup> to soil solution. At these low pH values, where hydrolysis of Al<sup>3+</sup> is not very significant Al<sup>3+</sup> is acting more like a base cation. In the high acid A and O horizons typical of many forest soils of northern temperate and humid tropical regions, plots of BS vs. pH show a better positive correlation with BS when Al<sup>3+</sup> is included as a base cation than if it is included as an acid cation (Skylberg, 1994, 1999; Ross et al., 2008).

SOM provides much of the pH buffering in most surface soils and much of the CEC. Helling et al. (1964) estimated the mean CEC of SOM in 60 mineral soils of Wisconsin, USA, at pH 8, to be 2000 mmol<sub>c</sub> kg<sup>-1</sup> of SOM. This value is the equivalent to the value for the titration of the acid form of organic matter with Ca(OH)<sub>2</sub> to pH 8 and provides a reasonable estimate for the capacity of SOM in mineral soils to buffer pH in the range of 3–8. With the exception of CaCO<sub>3</sub>, the pH-buffering capacity of SOM is equal or greater than other components in the soil (Table 19.2). Another indication of the importance of SOM for buffering in soils is the results after adding H<sub>2</sub>SO<sub>4</sub> and CaCO<sub>3</sub> to 51 surface soils (Magdoff and Bartlett, 1985). They took the data, including the four soils in Figure 19.1, and replotted it normalized to equivalent SOM contents. This yielded a single plot (Figure 19.4) for soils of differing organic matter contents suggesting that in these northern temperate region surface soils, the pH buffering is a function mostly of organic matter content.

**TABLE 19.2** Approximate Maximum Proton Donation or Adsorption Capacity of Soil Materials in the pH Range of 3.5–8

Soil Material	Capacity, mmol kg <sup>-1</sup>	References
Silicate clays		
Smectites	800–1,500	McBride (1994)
Vermiculite	1,500–2,000	McBride (1994)
Illite	200–400	McBride (1994)
Kaolinite	10–50	Thomas and Hargrove (1984)
SOM	2,000	Helling et al. (1964)
Allophane and imogolite	200–500	Wada (1989)
Hydroxides and oxides of Fe and Al <sup>a</sup>	50–400	Borggaard (1983)
CaCO <sub>3</sub> <sup>b</sup>	20,000	Stumm and Morgan (1996)

<sup>a</sup> Based on linear extrapolation between pH 8 and 3.5 of the data for hematite and goethite.

<sup>b</sup> The precipitation and dissolution of CaCO<sub>3</sub> takes place at pH 7 or greater.



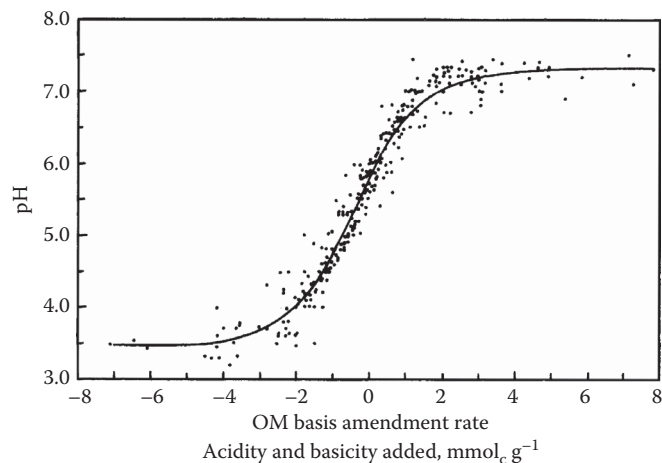


**FIGURE 19.4**  $pH_{CaCl_2}$  after a 30-day reaction of 51 soils from Vermont, U.S.A, with varying additions of  $H_2SO_4$  and  $CaCO_3$ . The acid and base addition are reported per gram of SOM. The data for all of the soils were adjusted along the x-axis to coincide with the zero addition pH for soil 51 (see Figure 19.1). (From Magdoff, F.R., and R.J. Bartlett. 1985. Soil pH buffering revisited. *Soil Sci. Soc. Am. J.* 49:145–148. With permission of Soil Science Society of America.)

## 19.6 Proton and Al Exchange in Silicate Clays

Ion exchange reactions on permanent charge sites in silicate clays can contribute to pH buffering (for a detailed discussion of ion exchange in clays see Chapter 16). The pH buffering by permanent charge on clays can involve exchange of hydronium ions,  $H_3O^+$ , but the exchange of  $Al^{3+}$  is much more significant.

High-activity clays; smectites, vermiculites, and illites, when saturated with  $H^+$  have very low pH values and are not stable. When montmorillonite, a smectite, is saturated with  $H^+$  the pH is less than 3.5. After 24 h of aging, acid dissolution of the clay structure produces  $Al^{3+}$  ions resulting in an increase in pH and replacement of the exchangeable  $H^+$  ions with  $Al^{3+}$  (Coleman and Craig, 1961). Aluminum clays are proton donors because of the ability of  $Al^{3+}$  on clay exchange sites to hydrolyze and to precipitate as  $Al(OH)_3$ , but they are weaker proton donors than  $H^+$  clays. Extraction of acid soils with neutral salt solutions, for example, 1 M KCl, yields mostly  $Al^{3+}$  not  $H^+$  (Thomas and Hargrove, 1984).

Titration of  $Al^{3+}$  montmorillonite (Figure 19.5) shows that at  $pH_{(H_2O)}$  values in the range of 5–6, the  $Al^{3+}$  on permanent charge sites strongly buffers pH (Turner and Nichol, 1962). Data in Figure 19.5 also show that as in soil, the measured pH in  $CaCl_2$  is lower than the pH in water.

When base is added to an  $Al^{3+}$ -saturated smectite or vermiculite, the initial reaction is the hydrolysis of Al cations on exchange sites (Bloom et al., 1977), but with sufficient addition of strong base, the  $Al^{3+}$  will eventually precipitate as  $Al(OH)_3$  in the interlayer space in the clay, accounting for much of the clay-mediated buffering at  $pH > 5$ . Because of  $OH^-$  deficiencies in interlayer  $Al(OH)_3$ , the interlayer can neutralize the negative charge on the clay. In the case of smectite, this produces hydroxy interlayer

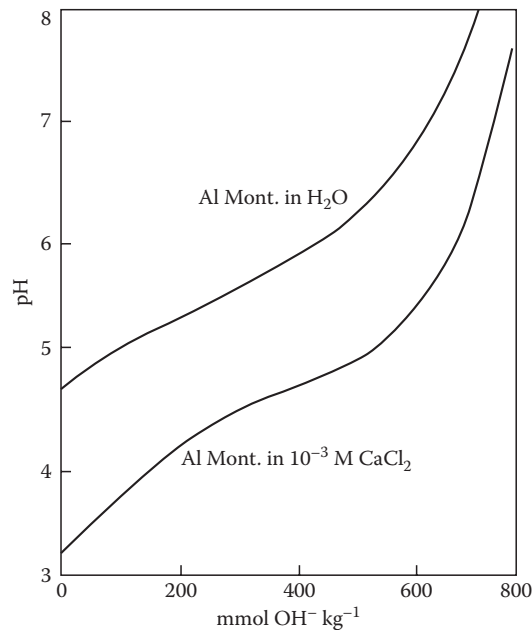


**FIGURE 19.5** Titration of an Al saturated montmorillonitic clay with NaOH with and without the addition 0.001 M  $CaCl_2$ . (From Turner, R.C., and W.E. Nichol. 1962. A study of the lime potential: 2. Relation between the lime potential and percent base saturation of negatively charged clays in aqueous salt suspensions. *Soil Sci.* 94:58–63. With permission of Wolters Kluwer Health.)

smectite (HIS), and in the case of vermiculite, this produces hydroxy interlayer vermiculite (HIV) (Chapter 21). Because the precipitation of interlayer  $Al(OH)_3$  blocks  $Al^{3+}$  in the interlayer from reacting with the base, the titration end point in Figure 19.5 is less than the CEC of the clay, which is  $800 \text{ mmol}_e \text{ kg}^{-1}$ .

As with SOM, buffering in  $Al^{3+}$ -saturated clays can be described as function of BS, assuming that both  $H^+$  and  $Al^{3+}$  are acid cations and that  $Al^{3+}$  cations represent 3 mol of acidity per mole of  $Al^{3+}$ . This is a usable generalization at pH values high enough for  $Al^{3+}$  to hydrolyze and act like an acid cation. In contrast, studies of very acidic surface soils from northern temperate forests have shown that at pH values less than 4.5,  $Al^{3+}$  should be treated as a base cation (Skylberg, 1994; Ross et al., 2008).

The capacity of silicate clays to buffer pH varies widely because of the large difference in the CEC of clays (Table 19.2). Kaolinite, a low-activity clay, has little or no permanent charge and has little capacity to buffer pH (Chapter 21). Illite has a much greater CEC and is a much more effective buffer of pH. Smectites and vermiculites are even more effective in buffering pH. Among the silicate clays, only the highest charge vermiculites approach the buffer capacity of SOM.

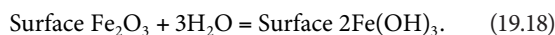
## 19.7 pH-Dependent Charge Buffering by Mineral Components

Like SOM, oxides and hydroxides of Fe(III) and Al, and poorly crystalline aluminosilicates, contribute to the pH-dependent charges in soil and to pH buffering. In addition, the edges of

crystalline silicate clays make a minor contribution to pH-dependent charge (Chapter 16.) Unlike SOM, these materials have surfaces that are both proton donors and proton acceptors.

### 19.7.1 Oxides and Hydroxides of Iron and Aluminum

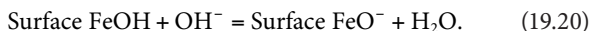
The oxides and hydroxides of Fe(III) and Al that accumulate in response to weathering are particularly important for pH buffering highly weathered soils (Uehara and Gillman, 1982). Common iron minerals in soil include hematite ( $\alpha\text{-Fe}_2\text{O}_3$ ), goethite ( $\alpha\text{-FeOOH}$ ), and ferrihydrite ( $\text{Fe}_3\text{O}_4 \cdot 4\text{H}_2\text{O}$ ) (Chapter 22). By far the most common aluminum hydroxide mineral is gibbsite,  $\text{Al}(\text{OH})_3$ . In water, the hydrated surfaces of these oxides and hydroxides contain strongly bound OH groups that can act both as proton donors and proton acceptors. For hematite, the surface hydration reaction is



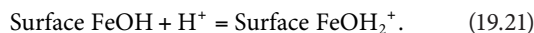
The strong bonding of the O atom to Fe(III) and Al weakens the bond of the proton to the O atom, making the surface-OH groups weakly acidic and at high pH, the metal-bound hydroxide groups can donate proton creating negative surface charges (McBride, 1994):



This reaction can also be written as an adsorption of  $\text{OH}^-$ :



Also these surface-OH groups can accept protons at low pH to become positively charged:



Surface adsorption of  $\text{H}^+$  and  $\text{OH}^-$  is quantified by titrating oxide suspensions in  $\text{Na}^+$  or  $\text{K}^+$  salts of anions that do strongly adsorb to the oxide surfaces (e.g.,  $\text{NO}_3^-$ ). The data of Parks and de Bruyn (1962) illustrate typical titrations for oxide suspensions (Figure 19.6). These data show the effects of increasing  $\text{KNO}_3$  concentration on the quantity of  $\text{H}^+$  or  $\text{OH}^-$  adsorbed. McBride (1994) explains this effect, in a  $\text{KNO}_3$  solution, as due to  $\text{K}^+$  displacement of  $\text{H}^+$  at high pH and the  $\text{NO}_3^-$  displacement of  $\text{OH}^-$  at low pH. At pH values less than 7, the oxides and hydroxides of Al and Fe are positively charged, and these surfaces are anion exchangers while at pH greater than 9 they are cation exchangers. At pH values in the range of 7–9, a point is found where the concentration of salt in solution has no effect on the pH. This is the point at which the net charge on the surface is zero; the point of zero net charge (pznc, also called the point of zero salt effect). For oxides and hydroxides of iron and aluminum, almost all measured pznc values are in the range of 7–9 (Chapter 15), meaning that

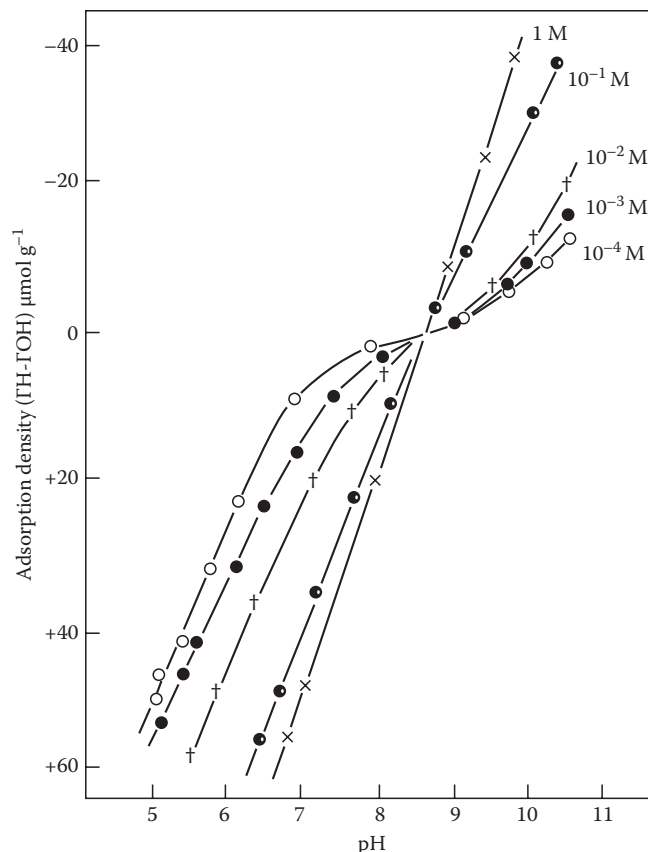


**FIGURE 19.6** Titration of  $\text{Fe}_2\text{O}_3$  with KOH and  $\text{HNO}_3$  in suspensions containing different concentrations of  $\text{KNO}_3$ . (With permission from Parks, G.A., and P.D. de Bruyn. 1962. The zero point of charge of oxides. *J. Phys. Chem.* 66:967–963. Copyright 1962 American Chemical Society.)

unlike silicate clays and organic matter the net surface charge of these materials is positive in all except alkaline pH soils.

### 19.7.2 pH-Dependent Charges on Silicate Clay Edges

The layer structure of silicate clays includes an  $\text{AlOH}$  layer with exposed hydroxyl groups on the edges of the structure (McBride, 1994). These Al hydroxyl groups can adsorb or desorb protons, but because of the influence of the  $\text{Si}^{4+}$  ions in the structure, the pznc is lower than for gibbsite. For example, a reported value for the pznc for the edge of kaolinite is 2.9 (Chapter 15). This means the edge charge can contribute to the negative charge in soils. For high-charged clays like smectites and vermiculite, this edge charge is small compared to the permanent structural charge. For example, for a smectite at pH 8, the pH-dependent negative charge is about  $50 \text{ mmol}_c \text{ kg}^{-1}$  compared to a permanent charge of about  $750 \text{ mmol}_c \text{ kg}^{-1}$  (McBride, 1994).

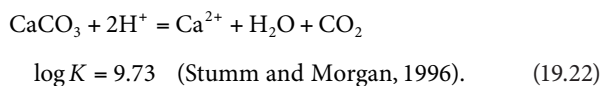
### 19.7.3 Imogolite and Allophane

Allophane and imogolite are aluminosilicates that like silicate clay edges have pH-dependent charge surfaces. Allophane is noncrystalline, not having long-range ordering in the structure,

and imogolite, which forms long tubes (Chapter 23; Wada, 1989) is a paracrystalline mineral with some disorder in the structure. Both of these materials are found in abundance in young volcanic soils. They are also found in some young soils in glacial parent material (e.g., spodosols in northern forests). Imogolite and allophane have  $p_znc$  values in the range of 5.5–7 (Clark and McBride, 1984; Wada, 1980).

## 19.8 Buffering by Dissolution and Precipitation of Carbonates

Carbonates are very important for pH buffering in nonacid soils. Calcite,  $\text{CaCO}_3$ , and dolomite,  $\text{CaMg}(\text{CO}_3)_2$ , are common components of soil parent materials in many soils. With sufficient rainfall and good drainage, these minerals weather from soils. In arid regions and in some areas in humid regions with poor drainage, however,  $\text{CaCO}_3$  can accumulate in soils (Chapter 30; Doner and Lynn, 1989). Under some conditions in arid regions,  $\text{MgCO}_3$ , which is much more soluble than calcite, can accumulate. Calcite acts as proton acceptor according to



The equilibrium equation for this reaction is

$$K = (\text{Ca}^{2+}) \frac{(P_{\text{CO}_2})}{(\text{H}^+)^2}. \quad (19.23)$$

Calculation of this equilibrium requires knowledge of the  $\text{CO}_2$  content in the soil atmosphere, expressed in units of partial pressure ( $P$ ). At 1 atm total pressure, the value of partial pressure is equivalent to the volume fraction in the air. This equilibrium, rewritten in a form that shows how  $\text{CaCO}_3$  weathers from calcareous soils, is



In soils, the  $\text{CO}_2$  produced by soil microbial and root respiration dissolves  $\text{CaCO}_3$  to produce calcium bicarbonate and over time  $\text{CaCO}_3$  will weather out of well-drained soils.

The pH in soils that contain calcite varies widely. In a  $\text{CaCO}_3$  suspension in distilled water in equilibrium with the ambient atmosphere ( $P_{\text{CO}_2} \approx 3.8 \times 10^{-4}$  atm) will contain two bicarbonate ions in solution for every  $\text{Ca}^{2+}$  ion and the pH will be 8.3 (Stumm and Morgan, 1996). Because the  $P_{\text{CO}_2}$  in soils is greatly increased due to microbial and root respiration, soil solution in equilibrium with calcite will have pH values considerably lower than 8.3 (Inskeep and Bloom, 1986). The effect of  $P_{\text{CO}_2}$  on soil pH varies due to differences in the rate of soil respiration and the rate of gas exchange with the atmosphere. Gas exchange varies with depth and quantity of air-filled pores in a soil, and  $P_{\text{CO}_2}$  increases with depth and after rainfall fills soil pores with water (Flechar et al., 2007).

Inskeep and Bloom (1986) showed that in pots with growing soybean plants the  $P_{\text{CO}_2}$  ranged from 0.0006 atm in drier soils to 0.031 atm at moisture contents approaching saturation. By the principle of Le Chatelier (the mass action principle), Reaction 19.22 will be shifted to the left when  $P_{\text{CO}_2}$  is raised, resulting in an increase in ( $\text{H}^+$ ) and a decrease in pH.

In soils, bicarbonate concentrations are commonly not equal to twice the concentration of  $\text{Ca}^{2+}$  because there can be other sources of  $\text{HCO}_3^-$  and  $\text{Ca}^{2+}$  than dissolution of calcite by carbonic acid. When the chemistry of a calcareous soil is dominated by calcium salts other than bicarbonate,  $2[\text{Ca}^{2+}]$  can be much greater than  $[\text{HCO}_3^-]$  and pH is much less than 8.3, even at low  $P_{\text{CO}_2}$ . Thus, calcareous soils containing gypsum ( $\text{CaSO}_4 \cdot 2\text{H}_2\text{O}$ ), where  $[\text{Ca}^{2+}]$  is elevated by gypsum solubility, pH can be as low as 7.0. In some arid regions, input of  $\text{Mg}^{2+}$ ,  $\text{Na}^+$ , and  $\text{HCO}_3^-$  results in concentrations of  $\text{HCO}_3^-$  much greater than twice  $[\text{Ca}^{2+}]$  and calcareous soils can have pH values as high as 9.5. In arid regions, where Mg accumulates, and hydrated  $\text{MgCO}_3$  forms, pH is greater than 8.5 because magnesium carbonate is much more soluble than  $\text{CaCO}_3$ .

Calcareous soils are very strongly buffered against acidification. One kilogram of  $\text{CaCO}_3$  can neutralize 20,000 mmol of  $\text{H}^+$  and hold pH at a value greater than 7 until all of  $\text{CaCO}_3$  is dissolved. Thus,  $\text{CaCO}_3$  is a much more effective buffer than SOM or any other component in soil (Table 19.2). If  $\text{CaCO}_3$  is compared with SOM on the basis of buffering against a decrease in pH from 8.0 to 7.0, the difference is even greater than shown in Table 19.2. This pH drop would result in the total dissolution of  $\text{CaCO}_3$  but would only neutralize about 200 mmol  $\text{c kg}^{-1}$  of SOM, about one-tenth of the total buffer capacity of SOM. Because of the high buffer capacity of the  $\text{CaCO}_3$ , calcareous soils are considered to be unaffected by acid rain and it is generally considered impractical to artificially lower the pH of calcareous soils to allow for the growth of acid-loving plants.

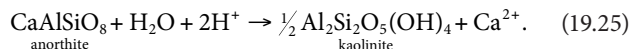
## 19.9 $\text{H}^+$ Consumption by Irreversible Weathering of Aluminous Minerals

The buffering reactions discussed above are all reversible and can to some degree be described using equilibrium equations. Some reactions that consume  $\text{H}^+$  in soils, however, are irreversible. These reactions include the weathering of primary aluminosilicate minerals and the destruction of high-activity clays in very low pH soils.

### 19.9.1 Weathering of Primary Silicates

Over the very long term, the weathering of primary aluminosilicate minerals from soil parent material consumes protons (Chapter 20). These reactions are irreversible for most primary minerals because these minerals only form at the high temperatures involved in rock-forming processes. An example of the weathering of a primary mineral is the reaction of the feldspar

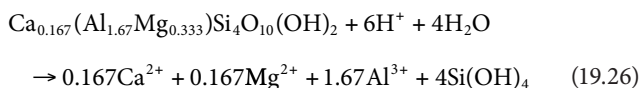
anorthite to form kaolinite in acid soils. This reaction consumes two protons for every mole of calcium mobilized:



The rates of weathering reactions depend on the type of primary mineral and the surface area exposed to soil solutions (Bloom and Nater, 1991). This means that, per unit mass, silt-sized particles weather much more rapidly than sand-sized particles. The rates of aluminosilicate dissolution reactions are pH dependent and at pH values typical in soils, aluminosilicates dissolve more rapidly at lower pH (Bloom and Nater, 1991; Sposito, 2004). Over time periods of less than decades, weathering of primary silicate minerals is generally not significant in buffering pH.

### 19.9.2 H<sup>+</sup> Consumption by the Destruction of High-Activity Clay

When the  $\text{pH}_{(\text{H}_2\text{O})}$  of a soil is decreased to values less than about 3.5, high-activity clays can dissolve quite rapidly consuming protons and releasing  $\text{Al}^{3+}$  into solution. As discussed in Section 19.6, H<sup>+</sup>-saturated high-activity clays have pH values less than 3.5 and dissolve to release  $\text{Al}^{3+}$ . At this pH,  $\text{Al}(\text{OH})_3$  is too soluble to form in soils and kaolinite forms slowly, so high-activity clays tend to dissolve congruently (no solid phase is formed in the reaction). For a Ca<sup>2+</sup> montmorillonite



where five of the six protons consumed are due to the release of  $\text{Al}^{3+}$  from the structure of the clay. This reaction likely accounts for much of the very strong buffering at pH 3.5 that was observed by Magdoff and Bartlett (1985) when they added  $\text{H}_2\text{SO}_4$  to soils (Figures 19.1 and 19.3).

## 19.10 Determination of Buffer Capacities

The determination of the capacity of soils to buffer pH has long been an interest of soil chemists. Many crops respond positively to the addition of lime to acid soils, but because of the differences in buffer capacity, soils of similar pH may require vastly different quantities of lime to yield the same increase in pH. Horticulturists have also been concerned with decreasing the pH of nonacid soils and they use aluminum sulfate or elemental S to allow for the vigorous growth of acidophilic plants (e.g., azaleas, rhododendron, and blueberries). As with liming, the quantity of acidifying agent necessary to lower the pH of a soil by a given amount depends on the buffer capacity. Also, acid rain can

negatively impact poorly buffered forest soils and the acidifying effects depend on the capacity of soils to buffer the long-term input of very dilute  $\text{HNO}_3$  and  $\text{H}_2\text{SO}_4$  (Bloom and Grigal, 1985; Ulrich, 1991; Watmough and Dillon, 2004).

### 19.10.1 Total Titratable Acidity

The total acidity in acid soils is operationally defined as consisting of two components, salt-replaceable (exchangeable) and residual (nonexchangeable) acidity (SSSA, 2008). Salt-replaceable acidity is the H<sup>+</sup> and  $\text{Al}^{3+}$  extractable with 1 M KCl, while the residual acidity is the acidity that is titratable in a soil suspension but is not easily replaceable with KCl (Bertsch and Bloom, 1996). In practice, the residual acidity is determined by the difference between the total acidity neutralized by raising the pH of a soil to a reference pH, usually 7.0 or 8.0, and the salt-replaceable acidity.

Total acidity can be determined by the titration of a soil suspension in a salt solution to the reference pH using a strong base or by the addition of increments of  $\text{CaCO}_3$  as shown in Figure 19.1. This produces a plot of the pH vs. the quantity of base consumed, but the response to titration with strong base and to  $\text{CaCO}_3$  additions is slow, and other laboratory methods are usually used. A standard method for relatively rapid determination of total acidity is to react a soil for several hours or overnight with a solution containing 0.5 M  $\text{BaCl}_2$  plus a triethanolamine (TEA) buffer adjusted to pH 8.0 or 8.2 (Thomas, 1982). TEA is well buffered at pH 8 and the solution contains  $\text{Ba}^{2+}$  to displace acidity from soil components. A reference pH of 8.0 or 8.2 is used to represent the pH attained when a soil is limed with excess lime. From a more fundamental point of view, pH 8 is a good choice because this is the end point for the titration of organic carboxyl acidity, as well as the  $\text{Al}^{3+}$  acidity bound to clays. With the  $\text{BaCl}_2$ -TEA method, the total acidity is calculated as the difference in the quantity of H<sup>+</sup> needed to titrate the  $\text{BaCl}_2$ -TEA solution to a pH of about 5, using a pH indicator dye, before and after reaction with a soil. This difference represents the quantity of acidity that reacts with the TEA buffer.

An alternative method for the calculation of total acidity is the difference between the CEC determined at pH 7.0 with ammonium acetate and the sum of exchangeable bases. Determination of CEC at pH 7.0 is the method most often used in the classification of soils (Burt, 2004). In this method, soil is reacted with an ammonium acetate solution at pH 7.0, the excess ammonium acetate is leached from the soil, and the  $\text{NH}_4^+$  ions bound to cation exchange sites are extracted with a salt solution and quantified (Sumner and Miller, 1996; Burt, 2004). Subtraction of the exchangeable bases from the pH 7.0 CEC represents the total acidity referenced to pH 7.0.

### 19.10.2 Lime Requirement

Development of the recommendations to growers for the liming of an acid soil with ground calcitic or dolomitic limestone (agricultural lime) requires a quick and easy method for the

determination of the quantity of base needed to raise the soil pH to an optimum value for a given crop (Bloom et al., 2005; Fageria and Baligar, 2008). Because crops differ in sensitivity to soil acidity, recommendations for liming may differ with crop. The most common methods used in the United States involve the reaction of a mixed buffer solution with a soil and after a period of reaction, measurement of the equilibrium pH (Godsey et al., 2007). The commonly used Mehlich method uses a mixed buffer solution containing acetate, glycerophosphate and TEA, in  $\text{BaCl}_2$ , that provides for a linear buffer response to acidity at pH values ranging from 4 to 6.5 (Mehlich, 1976; Hoskins and Erich, 2008). This solution has been modified by replacing the Ba with Ca to avoid the use of toxic substances (Godsey et al., 2007; Hoskins and Erich, 2008). The pH of the buffer mixture is adjusted to 6.5 and the lime requirement is determined from the pH after reaction with a soil using regression equations for different target pH values. At lower equilibrium pH, the lime requirement is greater. The regression equations are developed using the pH response of acid soils to known additions of  $\text{CaCO}_3$  (Hoskins and Erich, 2008). Hoskins and Erich (2008) showed that the inclusion of a soil  $\text{pH}_{(\text{H}_2\text{O})}$  term increased the correlation coefficient of the regression. The Shoemaker–McLean–Pratt (SMP) mixed buffer method is also commonly used (McLean et al., 1977), but this method is decreasing in acceptance because it contains two toxic buffers, *p*-nitrophenol and chromate, and tends to cause plugging of liquid junctions of pH electrodes (Hoskins and Erich, 2008). Other mixed buffer methods for determination of lime requirement include those of Adams and Evans (1962), Woodruff (1948), and Nõmmik (1983).

In areas of the world where highly weathered soils are dominant, it is common to base lime recommendations on the reduction of  $\text{Al}^{3+}$  saturation of the effective CEC, calculated as the sum of bases plus 1 M KCl extractable acidity (Fageria and Baligar, 2008). When lime is added,  $\text{Al}^{3+}$  precipitates to form insoluble  $\text{Al}(\text{OH})_3$ , decreasing  $\text{Al}^{3+}$  toxicity. To determine the lime requirement, the 1 M KCl replaceable  $\text{Al}^{3+}$  acidity is calculated as three times the molar quantity of extracted Al and this acidity, expressed in units of  $\text{cmol}_c \text{ kg}^{-1}$ , is multiplied by a factor to calculate the lime requirement in  $\text{Mg ha}^{-1}$ . The factor varies from 1, or less, in sandy soils to greater than 3 in very clayey soils. Also an adjustment for exchangeable  $\text{Ca}^{2+}$  and  $\text{Mg}^{2+}$  is used to yield a lime requirement, even for low acidity soils, if a soil is low in Ca and Mg. These two ions are often deficient for plant growth in highly weathered soils (Fageria and Baligar, 2008).

### 19.10.3 Calcium Carbonate Concentrations in Soil

The quantity of calcium carbonate in soils is generally determined by methods that measure the  $\text{CO}_2$  evolved after adding acid or the weight loss due to  $\text{CO}_2$  loss. In the weight loss method, carefully weighed soil samples are added to weighed flasks containing 3 M HCl and loosely covered with a rubber stopper (Loeppert and Suarez, 1996). The flask is swirled and uncovered periodically until all of the  $\text{CO}_2$  is evolved and the

flask is carefully reweighed. The content of carbonate is calculated assuming all of the carbonate is  $\text{CaCO}_3$  with a formula weight of  $100 \text{ g mol}^{-1}$ . For soils that have less than 2% or 3% carbonate, the weight loss method is not accurate (U.S. Salinity Laboratory Staff, 1954; Loeppert and Suarez, 1996).

Determination of the evolved  $\text{CO}_2$  provides a more accurate and precise measure of calcium carbonate (Loeppert and Suarez, 1996). Commonly used methods involve the determination of the pressure increase in a closed cell using an Hg manometer or pressure transducer  $\text{CO}_2$  (Williams, 1949; Martin and Reeve, 1955; Skinner et al., 1959; Evangelou et al., 1984) or the gravimetric determination of  $\text{CO}_2$  collected in a magnesium perchlorate trap (Loeppert and Suarez, 1996).

### 19.10.4 Determination of the Buffering of $\text{H}^+$ Inputs in Noncalcareous Soils

Routine laboratory methods have not been developed for the determination of the capacity of soils to buffer against acidification. However, addition of increments of acid with long-term incubation, as used by Magdoff and Bartlett (1985), can be used to determine the response of soils to acid additions (Figures 19.1 and 19.4). An alternative method is to equilibrate soil suspensions repeatedly with dilute acid. Bloom and Grigal (1985) suspended soils in  $2.5 \times 10^{-4} \text{ M H}_2\text{SO}_4$  for 24 h decanted and repeated 13 times. By measuring the pH of the equilibrated solutions, they were able to determine the quantity of protons adsorbed due to pH buffering in the soil. They were also able to determine the  $\text{Al}^{3+}$  and base cation losses in each treatment. This method much more closely simulates the response to acidic deposition (acid rain) with the resultant loss of bases and  $\text{Al}^{3+}$ . Bloom and Grigal (1985) used their plots of pH response to acid to test a numerical model for the response of soils to acidic deposition.

## 19.11 Soil Acidification

Soil acidification occurs as a natural process during soil formation. With sufficient inputs of acid rain to poorly buffered soils, natural acidification can be very significantly accelerated (Bloom and Grigal, 1985; Ulrich, 1991). Much more rapid acidification is produced by the addition of ammonium-forming nitrogen fertilizers. Even more rapid acidification is produced by the oxidation of sulfur and sulfur compounds added to soils or of sulfur compounds deposited by natural processes in coastal wetland soils that are exposed to oxidation when the water table is lowered by artificial drainage.

### 19.11.1 Natural Acidification

Under conditions of good drainage and rainfall sufficient to produce leaching,  $\text{H}_2\text{CO}_3$  and soluble organic acids cause the very slow acidification of soils that occurs during natural soil weathering. At pH values of about 6 and greater, the donation of protons by the reaction of  $\text{H}_2\text{CO}_3$  to produce  $\text{HCO}_3^-$  (Reaction 19.13) is the predominant acidifying reaction. As the pH is

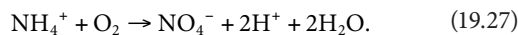
decreased to values much lower than the  $pK_a$  (6.35),  $H_2CO_3$  is a less effective proton donor and organic acids, having lower  $pK_a$  values, are the predominant proton donors. In calcareous soils,  $CaCO_3$  dissolution buffers the pH at values greater than 7 until it is all leached from the soil.

### 19.11.2 Acid Rain

The dry aerosol and wet acid deposition that makes up what is popularly called acid rain contains sulfuric and nitric acid plus  $NH_4^+$  that can be oxidized in soil to produce nitric acid (Sparks, 2003). Under preindustrial conditions, these acids were of minor importance in determining the composition of soil solutions. Industrialization has resulted in elevated strong-acid acidity in rainfall, which can have long-term negative impacts on poorly buffered soils in forests and other natural areas (Bloom and Grigal, 1985; Ulrich, 1991). Since the concentration of acidic components of acidic deposition is small compared to soil buffering, even in poorly buffered soils, soil acidification is difficult to document by field-based observations and contradictory results have been reported (Courchesne et al., 2005). One of the major difficulties is the spatial variability in soil properties (Likens et al., 1998). Studies that have shown significant soil acidification that appears to be due to acid rain include the work of Courchesne et al. (2005), who reported a statistically significant decrease in pH in the humus layer of soil collected from 1993 to 2002 and Watmough and Dillon (2004), who reported a depletion of exchangeable Ca for soil collected from 1983 to 1999. Both of these studies were conducted in forests of eastern Canada.

### 19.11.3 Acid-Producing Fertilizers

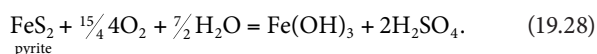
Nitrogen fertilizers that produce  $NH_4^+$  in soils; ammonium sulfate, ammonium nitrate, anhydrous ammonia, and urea, acidify soils. In soil, bacteria oxidize  $NH_4^+$  to nitrate producing  $H^+$  (Chapter 23; Havlin et al., 2005):



This reaction can produce sufficient acidification to require periodic addition of lime to cropland (Adams, 1984).

### 19.11.4 Acidification by Sulfur Compounds

Sulfuric acid produced in acid mine wastes or when the soils of coastal swamps are drained, can have a large impact on soils. When pyrite or iron sulfide associated with a seam of coal or a coastal organic soil is exposed to air, bacterial oxidation results in the production of sulfuric acid (McElnea et al., 2002; Sparks, 2003):



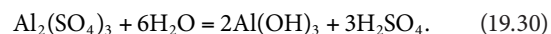
Under these conditions, soil pH values of less than 3 are possible. This reaction has produced large areas of acid sulfate soils in Vietnam, Malaysia, and Indonesia (Sanchez, 1976).

Acidification of nonacid soils for the growth of acid-loving (acidophilic) plants can be accomplished using elemental S. Bacterial oxidation produces a similar effect as for the oxidation of pyrite (Slaton, 2001):



Growers using elemental S must be very careful because pH values of 3.5 are easily attainable when excess sulfur produces too much sulfuric acid (Leitzke and Peterson, 1987) (Figure 19.4).

An alternative method is to add aluminum sulfate,  $Al_2(SO_4)_3$ , which produces acidity according to the reaction:



The lower pH generated by aluminum sulfate is limited by the solubility of  $Al(OH)_3$  and pH will not be decreased below about 4.5 but excessive aluminum sulfate can induce  $Al^{3+}$  toxicity problems for plant growth (Leitzke and Peterson, 1987).

## References

- Adams, F. 1984. Crop response to lime in the southern United States, p. 211–265. *In* F. Adams (ed.) Soil acidity and liming. No. 12 Agronomy. ASA, Madison, WI.
- Adams, F., and C.E. Evans. 1962. A rapid method for measuring of lime requirement of red–yellow podzolic soils. *Soil Sci. Soc. Am. Proc.* 26:355–357.
- Andrews, J.A., and W.H. Schlesinger. 2001. Soil  $CO_2$  dynamics, acidification, and chemical weathering in a temperate forest with experimental  $CO_2$  enrichment. *Global Biogeochem. Cy.* 15:149–162.
- Anon. 2008. State of the climate in 2007. *Bull. Am. Meteorol. Soc.* 89:S6–S102.
- Bertsch, P.M., and P.R. Bloom. 1996. Aluminum, p. 517–549. *In* D.L. Sparks (ed.) Methods of soil analysis. Part 3. Chemical methods. SSSA, Madison, WI.
- Bloom, P.R., and D.F. Grigal. 1985. Modeling soil response to acidic deposition in non-sulfate adsorbing soils. *J. Environ. Qual.* 14:481–495.
- Bloom, P.R., M.B. McBride, and B. Chadbourne. 1977. Adsorption of aluminum by smectite: I. Surface hydrolysis during  $Ca^{2+}$ – $Al^{3+}$  exchange. *Soil Sci. Soc. Am. J.* 41:1068–1073.
- Bloom, P.R., M.B. McBride, and R.M. Weaver. 1979. Aluminum organic matter in acid soils: Salt extractable aluminum. *Soil Sci. Soc. Am. J.* 43:813–815.
- Bloom, P.R., and E.A. Nater. 1991. Kinetics of dissolution of oxide and silicate minerals, p. 151–189. *In* D.L. Sparks and D.L. Suarez (eds.) The kinetics of physicochemical processes in soils. SSSA, Madison, WI.

- Bloom, P.R., U.L. Skyllberg, and M.E. Sumner. 2005. Soil acidity, p. 411–460. *In* A. Tabatabai and D. Sparks (eds.) Chemical processes in soils. SSSA, Madison, WI.
- Borggaard, O.K. 1983. Effect of surface area and mineralogy of iron oxides on their surface. *Clay. Clay Miner.* 31:230–232.
- Burt, R. (ed.). 2004. Soil survey laboratory methods manual. Soil survey investigations. Report No. 42. Version 4.0. Available at [ftp://ftp-fc.sc.gov.usda.gov/NSSC/Lab\\_Methods\\_Manual/SSIR42\\_2004\\_view.pdf](ftp://ftp-fc.sc.gov.usda.gov/NSSC/Lab_Methods_Manual/SSIR42_2004_view.pdf) (accessed on April 26, 2011)
- Clark, C.J., and M.B. McBride. 1984. Cation and anion retention by natural and synthetic allophane and imogolite. *Clay. Clay Miner.* 32:291–299.
- Coleman, N.T., and D. Craig. 1961. The spontaneous alteration of hydrogen clay. *Soil Sci.* 91:14–18.
- Coleman, N.T., D.E. Williams, T.R. Nielson, and H. Jenny. 1951. On the validity of interpretations of potentiometrically measured soil pH. *Soil Sci. Soc. Am. Proc.* 15:106–110.
- Courchesne, F., B. Cote, J.W. Fyles, W.H. Hendershot, P.M. Biron, A.G. Roy, and M.C. Turmel. 2005. Recent changes in soil chemistry in a forested ecosystem of Southern Quebec, Canada. *Soil Sci. Soc. Am. J.* 69:1298–1313.
- Doner, H.E., and Lynn, W.E. 1989. Carbonate, halide, sulfate, and sulfide minerals, p. 279–330. *In* J.B. Dixon and S.B. Weed (eds.) Minerals in soil environments. Soil Sci. Soc. Am., Madison, WI.
- Essington, M.E. 2004. Soil and water chemistry. CRC press, Boca Raton, FL.
- Evangelou, V.P., L.D. Whittig, and K.K. Tanji. 1984. An automated manometric method for the quantitative determination of calcite and dolomite. *Soil Sci. Soc. Am. J.* 48:1236–1239.
- Fageria, N.K., and V.C. Baligar. 2008. Ameliorating soil acidity of tropical oxisols by liming for sustainable crop production. *Adv. Agron.* 99:345–399.
- Fernandez, I.J., and P.A. Kosian. 1987. Soil air carbon dioxide concentrations in a New England spruce-fir forest. *Soil Sci. Soc. Am. J.* 51:261–263.
- Flechard, C.R., A. Neftel, M. Jocher, C. Ammann, J. Leifeld, and J. Fuhrer. 2007. Temporal changes in soil pore space CO<sub>2</sub> concentration and storage under permanent grassland. *Agric. For. Meteorol.* 142:66–84.
- Godsey, C.B., G.M. Pierzynski, D.B. Mengel, and R.E. Lamond. 2007. Evaluation of common lime requirement methods. *Soil Sci. Soc. Am. J.* 71:843–850.
- Hargrove, W.L., and G.W. Thomas. 1982. Titration properties of Al-organic matter. *Soil Sci.* 134:216–225.
- Havlin, J.L., J.D. Beaton, S.L. Tisdale, and W.L. Nelson. 2005. Soil fertility and fertilizers, 7th Ed. Prentice Hall, Upper Saddle River, NJ.
- Helling, C.S., G. Chesters, and R.B. Corey. 1964. Contribution of organic matter and clay to soil cation-exchange capacity as affected by the pH of the saturating solution. *Soil Sci. Soc. Am. Proc.* 28:517–520.
- Hoskins, B.R., and M.S. Erich. 2008. Modification of the Mehlich lime buffer test. *Commun. Soil Sci. Plant Anal.* 39:2270–2281.
- Inskeep, W.P., and P.R. Bloom. 1986. Kinetics of calcite precipitation in the presence of water soluble organic ligands. *Soil Sci. Soc. Am. J.* 50:1167–1172.
- Leitzke, D.A., and D.V. Peterson. 1987. Effects of soil acidification and chemical and mineralogical properties of a limed soil. *Soil Sci. Soc. Am. J.* 51:620–625.
- Likens, G.E., C.T. Driscoll, D.C. Buso, T.G. Siccama, C.E. Johnson, G.M. Lovett, W.A. Reiners, D.F. Ryan, C.W. Martin, and S.W. Bailey. 1998. The biogeochemistry of calcium at Hubbard Brook. *Biogeochemistry* 41:89–173.
- Loeppert, R.H., and D.L. Suarez. 1996. Carbonate and gypsum, p. 437–474. *In* D.L. Sparks (ed.) Methods of soil analysis. Part 3. Chemical methods. SSSA, Madison, WI.
- Magdoff, F.R., and R.J. Bartlett. 1985. Soil pH buffering revisited. *Soil Sci. Soc. Am. J.* 49:145–148.
- Magnusson, T. 1992. Studies of the soil atmosphere and related physical site characteristics in mineral forest soils. *J. Soil Sci.* 43:767–790.
- Martin, S.E., and R. Reeve. 1955. A rapid manometric method for the determining soil carbonate. *Soil Sci.* 79:187–197.
- Mason, D.D., and S.S. Obenshain. 1939. A comparison of methods for the determination of soil reaction. *Soil Sci. Soc. Am. Proc.* 3:129–137.
- McBride, M.B. 1994. Environmental chemistry of soils. Oxford University Press, New York.
- McElnea, A.E., C.R. Ahern, and N.W. Menzies. 2002. Improvements to peroxide oxidation methods for analysing sulfur in acid sulfate soils. *Aust. J. Soil Res.* 40:1115–1132.
- McLean, E.O., J.F. Terwiiler, and D.J. Eckert. 1977. Improved SMP buffer method for determination of lime requirement of acid soils. *Commun. Soil Sci. Plant Anal.* 8:667–675.
- Mehlich, A. 1976. A new buffer pH method for rapid estimation of exchangeable acidity and lime requirement of soils. *Commun. Soil Sci. Plant Anal.* 7:637–652.
- Nõmmik, H. 1983. A modified procedure for the rapid determination of titratable acidity and lime requirements in soils. *Acta Agric. Scand.* 33:337–348.
- Nordstrom, D.K., and H.M. May. 1996. Aqueous equilibrium data for mononuclear aluminum species, p. 30–80. *In* G. Sposito (ed.) The environmental chemistry of aluminum. Lewis Publishers, Boca Raton, FL.
- Parks, G.A., and P.D. de Bruyn. 1962. The zero point of charge of oxides. *J. Phys. Chem.* 66:967–963.
- Ross, D.S., G. Matschonat, and U. Skyllberg. 2008. Cation exchange in forest soils: The need for a new perspective. *Eur. J. Soil Sci.* 59:1141–1159.
- Rossel, R.A.V., and C. Walter. 2004. Rapid, quantitative and spatial field measurements of soil pH using an ion sensitive field effect transistor. *Geoderma* 119:9–20.
- Sanchez, P.A. 1976. Properties and management of soils in the tropics. Wiley, New York.
- Skinner, S.I.M., R.L. Halstead, and J.E. Brydon. 1959. Quantitative manometric determination of calcite and dolomite in soils and limestones. *Can. J. Soil Sci.* 39:197–204.

- Skyllberg, U. 1994. Aluminum associated with a pH-increase in the humus layer of a boreal haplic podzol. *Interciencia* 19:356–365.
- Skyllberg, U. 1999. pH and solubility of aluminium in acidic soils: A consequence of reactions between organic acidity and aluminium alkalinity. *Eur. J. Soil Sci.* 50:95–106.
- Slaton, N.A., R.J. Norman, and J.T. Gilmour. 2001. Oxidation rates of commercial elemental sulfur products applied to an alkaline silt loam from Arkansas. *Soil Sci. Soc. Am. J.* 65:239–243.
- Smith, R.M., A.E. Martell, and R.J. Motekaitis. 2004. NIST critically selected stability constants of metal complexes database. National Institute of Standards and Technology, U.S. Department of Commerce, Washington, DC.
- Sorensen, S.P.L. 1909. Enzyme studies: II. The measurement and importance of the hydrogen ion concentration in enzyme reaction. *Compt. Rend. Trav. Lab. (Carlsberg)* 8:1.
- Sparks, D.L. 2003. *Environmental soil chemistry*. Academic Press, New York.
- Sposito, G. 2004. *The surface chemistry of natural particles*. Oxford University Press, New York.
- SSSA (Soil Science Society of America). 2008. *Glossary of soil science terms*. SSSA, Madison, WI.
- Stevenson, F.J. 1994. *Humus chemistry: Genesis, composition, reactions*, 2nd Ed. Wiley, New York.
- Stumm, W., and J.J. Morgan. 1996. *Aquatic chemistry: Chemical equilibria and rates in natural waters*, 3rd Ed. Wiley, New York.
- Sumner, M.E., and W.P. Miller. 1996. Cation exchange capacity and exchange coefficients, p. 1201–1229. *In* D.L. Sparks (ed.) *Methods of soil analysis. Part 3. Chemical methods*. SSSA Book Series 5. SSSA, Madison, WI.
- Thomas, G.W. 1982. Exchangeable acidity, p. 159–165. *In* *Methods of soil analysis. Part 2. Chemical methods. Chemical and microbiological properties*. ASA Monograph 9. ASA, Madison, WI.
- Thomas, G.W. 1996. Soil pH and soil acidity, p. 475–490. *In* *Methods of soil analysis. Part 3. Chemical methods*. SSSA, Madison, WI.
- Thomas, G.W., and W.L. Hargrove. 1984. The chemistry of soil acidity, p. 3–56. *In* F. Adams (ed.) *Soil acidity and liming*. 2nd Ed. ASA, Madison, WI.
- Turner, R.C., and W.E. Nichol. 1962. A study of the lime potential: 2. Relation between the lime potential and percent base saturation of negatively charged clays in aqueous salt suspensions. *Soil Sci.* 94:58–63.
- Uehara, G., and G. Gillman. 1982. *The mineralogy, chemistry and physics of tropical soils with variable charge clays*. Westview Press, Boulder, CO.
- Ulrich, B. 1991. An ecosystem approach to soil acidification, p. 28–79. *In* B. Ulrich and M.E. Sumner (eds.) *Soil acidity*. Springer-Verlag, Berlin, Germany.
- U.S. Salinity Laboratory Staff. 1954. *Diagnosis and improvements of saline and alkali soils*. USDA Handbook 60. U.S. Government Printing Office, Washington, DC.
- Van Raij, B., and M. Peech. 1972. Electrochemical properties of some oxisols and alfisols of the tropics. *Soil Sci. Soc. Am. Proc.* 36:446–451.
- Wada, K. 1980. Mineralogical characteristics of andosols, p. 87–107. *In* B.K.G. Theng (ed.) *Soils with variable charge*. New Zealand Soil Science Society, Lower Hutt, New Zealand.
- Wada, K. 1989. Allophane and imogolite, p. 1051–1087. *In* J.B. Dixon and S.B. Weed (eds.) *Minerals in soil environments*. SSSA, Madison, WI.
- Walker, W.J., C.S. Cronan, and P.R. Bloom. 1990. Aluminum solubility in organic soil horizons from northern and southern forested watersheds. *Soil Sci. Soc. Am. J.* 54:369–374.
- Watmough, S.A., and P.J. Dillon. 2004. Major element fluxes from a coniferous catchment in central Ontario, 1983–1999. *Biogeochemistry* 67:369–398.
- Williams, D.E. 1949. A rapid manometric method of the determination of carbonate in soil. *Soil Sci. Soc. Am. Proc.* 13:127–129.
- Woodruff, C.M. 1948. Testing of lime requirement by means of a buffer solution and the glass electrode. *Soil Sci.* 66:53–63.